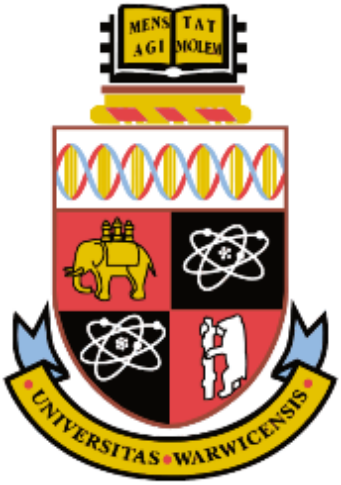

Dicarbonyl stress and dysfunction of the glyoxalase system in periodontal diseases

By

Amal Adnan Ashour

A thesis submitted in partial fulfilment of the requirements for the degree of

Doctor of Philosophy in Medicine

Warwick Medical School, University of Warwick

March 2016

Table of contents

Table of Figures

List of Tables

Acknowledgement

First and foremost all praise is due to almighty Allah; the most beneficial and the most merciful, for endowing me with health, patience, strength and knowledge to complete this project.

While my name may be alone on the front page of this thesis, I could not have persevered through the last few years without the support and understanding of the people I thank and acknowledge here.

To the inspiring and determined parents (Dr. Adnan Ashour and Dr. Salha Ashour), this PhD would not have been possible without your moral and emotional support. You always let me know that you are proud of me, which motivates me to work harder and do my best. I have never met anyone who believes in me more. It is the time to thank you for making me more than I am. I thank my brothers, sisters and parents in law for their unbelievable support and prayers.

I am forever indebted to my supervisors (Dr Naila Rabbani and Prof Paul Thornalley) for their enthusiasm, guidance, and unrelenting support throughout my research. Thank you for providing me with priceless advice, continuous support and help in shaping my research skills.

Most importantly, I would like to thank my fantastically supportive colleague and adored husband (Dr. Alaa Shafie). Your support, encouragement, patience and unwavering love have undeniably been the solid rock upon which the past twelve years of my life have been built. Furthermore, I thank my two princesses (Maria and Reema) for all the sacrifices they made to make me reach this goal. Thank you for sacrificing your favourite dinner meals and bedtime stories while I was in the lab pursuing my goals. Rather, you have always been there to cheer me up with your cards full of love and kisses. I owe my every achievement to both my daughters and husband.

I would also like to thank all of my friends for being supportive during my PhD, in particular Dr. Fozia Shaheen for her constant faith in me. Thank you to all the past and present members of the Protein Damage and Systems Biology Research

Group for their support and friendship during my PhD. It has been a great pleasure to work with such friendly and inspiring colleagues. Thank you everyone for brightening up the long research hours. In particular, thank you to Dr MingZhan Xue for sharing his expertise of various experimental methods. I am very grateful to him for his patience in answering all my questions. Special thanks go to Dr Attia Anwar for her technical support with the LC-MS/MS. Finally, I show extensive gratitude to all of the people who warmly contributed their stories, histories, and experiences. Carrying out my research would have been a totally different experience without having a supportive group and an excellent university.

Thank you to Taif University, Kingdom of Saudi Arabia for the financial support and my PhD scholarship and the Saudi Arabian Cultural Bureau in London for their supervision through my academic studies in UK.

Dedication

To my beloved parents Dr Adnan Ashour and Dr Salha Ashour, my beloved husband Dr Alaa Shafie and my lovely daughters who were, are and will always be the source of my strength.

Declaration

I am aware of the University of Warwick regulations governing plagiarism and I declare that all the work presented in this thesis, unless otherwise specifically stated, was original research performed by myself under the supervision of Dr Naila Rabbani and Prof Paul Thornalley. None of this work has been previously submitted to any other degree. The work presented (including data generated and data analysis) was carried out by the author except in the cases outlined below:

- GLO1-ARE transcriptional response reporter assay Glo1 inducers was performed by the host research team.

Amal Adnan Ashour

Abstract

Periodontal ligament inflammation or periodontitis is a common disease characterised by gradual destruction of connective tissue fibres that attach a tooth to the alveolar bone within which it sits. Diabetes and inflammation enhances periodontal bone loss through enhanced resorption and diminished bone formation. Periodontal ligament fibroblast attachment to collagen-I and function was impaired by methylglyoxal (MG) modification *in vitro.* The glyoxalase system is an anti-glycation defence in all cells that metabolises MG and thereby suppresses MG-mediated protein damage. Overexpression of Glo1 decreased the intracellular levels of MG The aim of this investigation was to improve the understanding of protein damage in PDL in diabetes, focusing on protein damage by MG in human periodontal ligament fibroblasts (hPDLFs) in hyperglycaemia and to evaluate the effects of high and low glucose concentrations on MG metabolism in hPDLFs with or without Glo1 inducers.

The effect of high glucose concentration on the formation and metabolism of MG was studied in hPDLFs *in vitro*. The ability of two small molecule Glo1 inducers, individually and in synergistic combination, to counter dicarbonyl stress in hPDLFs *in vitro* was studied. Interactions between hPDLFs to the extracellular matrix protein, collagen-I, were investigated and impairments in hPDLFs adhesion to MG-modified collagen-I coated plates were assessed. Protein susceptible to MG modification and inactivation in the cytosol of hPDLFs were identified by high resolution mass spectrometry proteomics. The effect of clinical periodontitis on plasma protein glycation, oxidation and nitration was also investigated in a pilot clinical investigation.

When hPDLFs were incubated with high glucose concentration *in vitro* there was a 45% decrease in Glo1 activity and 42% increase in D-lactate flux – surrogate indication of MG flux of formation, which contributed to increased cellular concentration of MG and increase in MG-H1 residue content of cell protein, compared to low glucose control. This indicated dicarbonyl stress was induced in hPDLFs by high glucose concentration *in vitro,* a model for hyperglycaemia *in vivo*. Decrease of Glo1 activity and increase in cellular MG concentration and MG-H1 residue content of cell protein was corrected with the addition of Glo1 inducers. The binding of hPDLFs to collagen-I was decreased by 30% in high glucose

concentration and was corrected by addition of Glo1 inducers. Proteomics analysis of cytosolic extracts of hPDLFs indicated that high glucose incubations produced changes in MG-modified proteins and also up-regulated and down-regulated unmodified proteins in hPDLFs. The pilot investigation of clinical periodontitis suggested a systemic effect of this local inflammation which was associated with changes in plasma protein glycation, oxidation and nitration.

This study reveals that dicarbonyl stress is a potential contributory pathogenic mechanism in hPDLFs in periodontitis and countering it may provide new treatment options to prevent and treat decline in periodontal health, particularly in diabetes. Small molecule inducers of Glo1 expression may in future contribute to improving periodontal health, particularly in diabetes.

Abbreviations

2-DE	2-Dimensional gel electrophoresis
3-DG	3-Deoxyglucosone
3DG-H	Hydroimidazolones derived from 3-DG
3-NT	3-Nitrotyrosine
4-ANI	4-Amino 1,8 naphthalimide
ACTB	β-actin gene
ADA	American diabetes association
AdipoR1	Adiponectin receptor 1
AGEs	Advanced glycation endproducts
AKR	Aldoketo reductase
ALDH	Aldehyde dehydrogenase
APEX	Absolute protein expression
ARE	Antioxidant response elements
AUC	Space under the curve
BAL	Broncho-alveolar lavage
BCA	Bicinchoninic acid
BMI	Body mass index
BSA	Bovine serum albumin
C.elegans	*Caenorhabditis elegans*
CaMKII	Calmodulin-dependent protein kinase II
cAMP	Cyclic adenosine monophosphate
CDK	Cyclin dependent kinases
cDNA	Complementary deoxyribonucleic acid
CDU	Collagen digestion unit
CEL	Nε-(1-carboxyethyl)lysine
CHX	Cycloheximide
cis-RSV	*cis*-Resveratrol
CMA	Nω-carboxymethyl-arginine
CML	Nε-carboxymethyl-lysine
CNV	Copy number variations
CRP	C-reactive protein
CTLA4	Cytotoxic t-lymphocyte antigen 4
DC	Detergent compatible assay
DCP	Dicarbonyl proteome
DHAP	Dihydroxyacetonephosphate
DMBA	Dimethylbenz(a)anthracene
DMEM	Dulbecco’s modified eagle's medium
DMSO	Dimethyl sulphoxide
DNTB	5,5'-Dithiobis (2-nitrobenzoic acid) or Ellman’s reagent
DT	Dityrosine
E2F4	Transcription factor E2F4
EC_{50}	Half maximal effective concentration

ECL	Enhanced chemiluminescence
ECM	Extracellular matrix
emPAI	Exponentially modified PAI
eNOS	Nitric oxide synthase
EPCs	Endothelial progenitor cells
ERK	Extracellular regulated
Erk1/2	Extracellular-signal-regulated kinases
ERM	Epithelial cell rests of Malassez
esRAGE	Endogenous secreted RAGE
F3K	Fructosamine-3-kinase
FBS	Fetal bovine serum
FFA	Free fatty acid
FFI	2-(2-Furoyl)-4(5)-(2-furanyl)-1H-imidazole
FL	Nε-fructosyl-lysine
FOXO	Forkhead box protein O
FOXO1	Forkhead box protein O1
FT-ICR	Fourier transform ion cyclotron resonance
G6P	Glucose-6-phosphate
GA3P	Glyceraldehyde-3-phosphate
GC_{50}	Median growth inhibitory concentration value
GCF	Gingival cervical fluid
GCS	γ-Glutamyl cysteine synthetase
GDM	Gestational diabetes mellitus
G-H	Hydroimidazolones derived from glyoxal
Glo1	Glyoxalase 1
Glo2	Glyoxalase 2
GLUT-2	Glucose transporter isoform-2
GOLD	Glyoxal-lysine dimer
GPx	Glutathione peroxidase
GR	Glutathione reductase
GS	Ground substance
GSH	Reduced glutathione
GS-MS	Gas chromatography with mass spectrometric detection
GSSG	Oxidised glutathione
GST	Glutathione-S-transferase
HAGH	Hydroxyacylglutathione hydrolase
HbA_{1C}	Glycosylated haemoglobin
HBO	Hyperbaric oxygen
HGFs	Human gingival fibroblasts
HIF1α	Hypoxia-inducible factor 1α
HK	Hexokinase
HLA	Human leukocyte antigen
HMGB1	High mobility group box-1 protein
HO-1	Hemoxygenase-1

hPDLFs	Human periodontal ligament fibroblasts
HPLC	High performance liquid chromatography
HSA	Human serum albumin
Hsd	Hesperidin
HSP	Hesperetin
ICAM	Intercellular adhesion molecule
ICAM-1	Intercellular adhesion molecule -1
ICAT	Isotope-coded affinity tags
ICPL	Isotope-coded protein labelling
IDF	International Diabetes Federation
IFIH1	Interferon-induced helicase
IGT	Impaired glucose tolerance
IL	Interleukins
IL2Ra	Interleukin 2 receptor alpha
IL-6	Interleukin-6
IP	Immunoprecipitation
IPA	Isopropanol
IPTL	Isobaric peptide termini labelling
IRAK	IL-1 Receptor-associated kinase
IRE	Insulin response element
IS	Internal standard
iTRAQ	Isobaric tags for relative and absolute quantification
JE	Junctional epithelium
JNK	c-Jun N-terminal kinase
LAL	Limulus amebocyte lysate
LBP	LPS-binding protein
LC-MS/MS	Liquid chromatography with tandem mass spectrometric detection
LDL	Low density lipoproteins
LPS	Lipopolysaccharides
MAPK	Mitogen activated protein kinases
MCP-1	Monocyte chemoattractant protein-1
MDA	Malondialdehyde
mDia-1	Mammalian diaphanous-1
MEM	Modified eagles medium
MetSO	Methionine sulfoxide
MG	Methylglyoxal
MG-H1	Hydroimidazolones derived from MG
MHC	Major histocompatibility complex
MMPS	Matrix metalloproteases
MNCV	Motor nerve conduction velocity
MODY	Maturity onset diabetes of the young
MOLD	MG derived lysine dimer
MRE	Metal responsive element

MRM	Multiple reaction monitoring
MSR	Macrophage scavenger receptor
MyD88	Myeloid differentiation protein 88
NBF	Nerve blood flow
NER	Nucleotide excision repair
NF- kB	Nuclear factor-kappa B
NFE2L2	Factor nuclear factor erythroid 2-related factor 2
NF-jB	Nuclear factor-jB
NFK	N-formylkynurenine
NHANES	National health and nutrition examination survey
NO	Nitric oxide
Nrf2	Nuclear erythroid factor E2 related factor-2
NSAF	Normalized spectral abundance factor
NSCLC	Non-small cell lung cancer
OBR	Obesity-related leptin and leptin receptor
ODS	Octadecyl silane
OPG	Osteoprotegerin
PAIs	Protein abundance indices
PBS	Phosphate buffer saline
PCA	Perchloric acid
PDL	Periodontal ligament
PGC-1α	PPAR gamma coactivator-1alpha
PGE2	Prostaglandin E2
PI3K	Phosphoinositol 3-kinase
PKC	Protein kinase C
PMNs	Polymorphonuclear neutrophils
PPAR- γ	Peroxisome proliferator-activated receptor γ
PTB	N-phenacylthiazolium bromide
PTMs	Post-translational modifications
PTPN22	Protein tyrosine phosphatase non-receptor type 22
PVDF	Polyvinyl difluoride
RAGE	Reseptor of advanced glycation endproducts
RANKL	Receptor activator of nuclear factor κB ligand
RIPA	Radioimmunoprecipitation
RNS	Reactive nitrogen species
ROX	Reactive oxygen species
RP-LC	Reversed-phase liquid chromatograph
RSV	Resveratrol
SCLC	Small cell lung cancer
SDF-1α	Stromal cell–derived factor–1α
SDS-PAGE	Sodium dodecyl sulfate polyacrylamide gel electrophoresis
SILAC	Stable isotope labelling by amino acids in cell culture
SILAM	Stable isotope labelling of mammals
SIN	Normalized spectral index

Sirt-1	Sirtuins-1
SOD	Superoxide dismutase
$SpBrBzGSHCp_2$	S-p-bromobenzylglutathione cyclopentyl diester
SR	Scavenger receptor
sRAGE	Soluble RAGE
SUR-1	Sulphonylurea receptor 1
T1DM	Type 1 diabetes mellitus
T2DM	Type 2 diabetes mellitus
TBS-T	Tris-buffered saline with Tween-20
TCA	Trichloroacetic acid
TFA	Trifloroacetic acid
THF	Tetrahydrofuran
TIR	Toll/IL-1 receptor homology domain
TIRAP	TIR domain containing adapter protein
TLR4	Toll-like receptor-4
TMT	Tandem mass tags
TNF-α	Tumour necrosis factor α
TOF	Time-of-flight
Tollip	Toll-interacting protein
TRAF6	Tumour necrosis factor receptor associated factor
tRSV	*trans*-Resveratrol
TSA	Trichostatin A
UPLC-MS/MS	Ultra-high performance liquid chromatography with tandem mass spectrometric detection
UV	Ultraviolet
VEGF	Vascular endothelial growth factor
WHO	World health organisation
XIC	Extracted ion chromatogram

1. Introduction

The periodontal ligament (PDL) is a specialized connective tissue, which occupies the space between the root of the tooth and the alveolar bone. In addition to its essential role in attaching the tooth to the alveolus, the PDL helps the tooth to withstand the substantial forces resulting from mastication and keeps it embedded in its socket. It also contributes to tooth sensation and nutrient supply to the surrounding structures (Palumbo, 2011). PDL inflammation, or periodontitis, is the commonest chronic inflammatory disease in the mouth, which characterised by breakdown of the supporting structures of the teeth including the periodontal ligament and alveolar bone. PDL inflammation can be caused by different factors; these causative factors can be external such as excessive plaque accumulation around the tooth (Selwitz et al., 2007), or systemic such as chronic systemic diseases like diabetes (Chang and Lim, 2012). Severe PDL inflammation affects 10–15% of adults and has several adverse effects on quality of life (Preshaw et al., 2013).

Diabetes is a common chronic metabolic condition that can cause PDL diseases. Such is the strong association with diabetes and development of a characteristic pathology that PDL disease has been called the "sixth complication of diabetes" along with retinopathy, nephropathy, neuropathy, macroangiopathy and delayed wound healing (Furukawa et al., 2007).

1.1 Periodontium and periodontal diseases

The periodontium is the tissue that surrounds and supports the teeth in their physical attachment and function. The formation of periodontal tissue occurs at the same time as formation and development of the tooth. The macroscopic components of periodontium are the gingiva, periodontal ligament (PDL), cementum and alveolar bone. These components maintain teeth in the maxillary and mandibular bones of the upper and lower jaw (Palumbo, 2011). Although the periodontium contains four different structures, each component interacts to co-operate dynamically and support each other (Bartold, 2006).

1.1.1 Components of periodontium

1.1.1.1 Gingiva

The gingiva is the soft tissue that overlies the mandible and maxilla inside the oral cavity and forms a seal around the base of tooth at its border with alveolar bone (Nanci and Bosshardt, 2006, Palumbo, 2011).

Macroscopic Anatomy of Gingiva

Gingiva is a coral pink tissue forms a scalloped outline around teeth cervices. It bonds to the underlying bone firmly and ascends apically to become alveolar mucosa. The alveolar mucosa is bounded to bone palatally but not labially (Weinberg et al., 2014). The gingival tissue is composed of two main parts: free gingiva and attached gingiva. The free gingiva extends by 2 mm from the gingival margin at tooth cervix to the free gingival groove which represents the level of cemento-enamel junction adjacent to the tooth (Newman et al., 2011) – Figure 1.

The gingival sulcus is the narrow space between the normal gingiva and the tooth surface. It extends from the free gingival margin coronally to the junctional epithelium apically. The normal depth of sulcus ranges between 0.5 to 3 mm with an average of 1.8 mm. More than 3 mm depth should be considered as a pathologic periodontal pocket (Miller, 2012) - Figure 1.

The gingiva is firmly attached to the underlying alveolar bone that extends apically from the gingival grove to the mucogingival junction. Stippling is the main feature of this part and it is defined as small depressions that can be clearly seen on the surface and gives the appearance of orange peel. The width of the attached gingiva varies according to the physiologic age and the location of the tooth in the oral cavity - whether it is an anterior or posterior, maxillary or mandibular location (Newman et al., 2011, Palumbo, 2011).

Microscopic anatomy of gingiva

The oral mucosa is composed of overlying epithelium and underlining connective tissue - the lamina propria. In free gingiva – the tissue that surrounds the tooth producing a cuff or collar of gingiva measured from the margin of the attached gingiva extending around the tooth at a width of *ca.* 1.5 mm, the epithelium is differentiated as follows: oral epithelium which faces the oral cavity; sulcular epithelium which is located in tooth side but not in contact to tooth surface; and

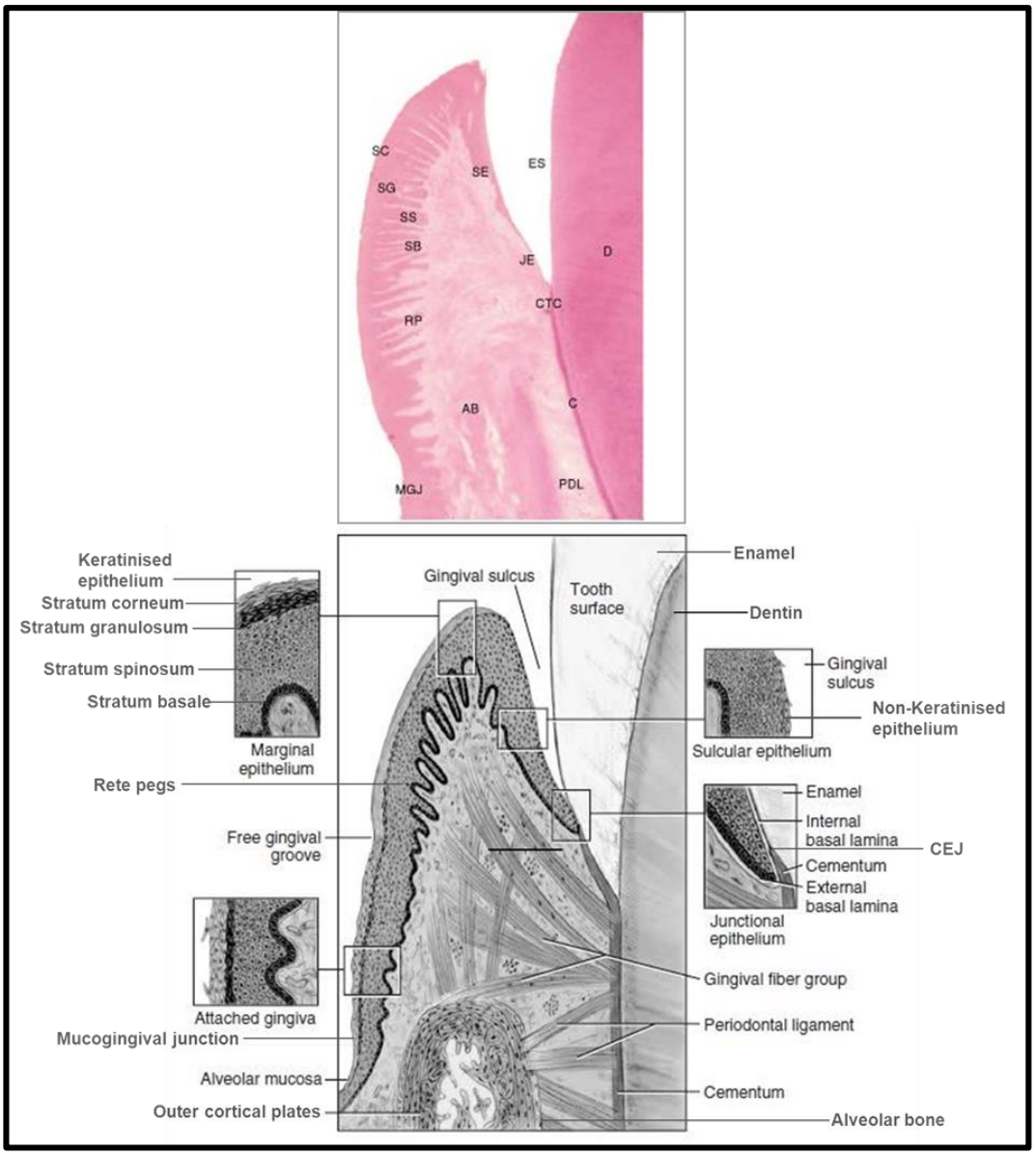

Figure 1: Anatomy of periodontium.
Modified from (Niemiec, 2012).

finally, the junctional epithelium which forms the connection between gingiva and tooth. The junctional epithelium is the base of the sulcus (Lang and Lindhe, 2015) - Figure 1.

The junctional epithelial cells are characterised by wide intercellular spaces acting as semi-permeable barrier and this facilitate the invasion of bacteria and their by-products into the tissue. In addition, it facilitates the passage of leukocytes (e.g. neutrophils) and immune components (e.g. complement), enzymes, and gingival cervical fluid (GCF) into gingival sulcus (Avery, 2011). This oral epithelium is a keratinised, stratified and squamous which is divided into four layers according to

the degree of differentiation of keratin producing cells. These four layers represent themselves as: stratum basale, stratum spinosum, stratum granulosum, and the stratum corneum (Palumbo, 2011).

1.1.1.2 Periodontal ligament (PDL)

The PDL is a specialised connective tissue that occupies the space between the root cementum and the alveolar bone. It is referred to as the lamina dura in radiographic analysis. Its width ranges between 0.15 mm to 0.25 mm. There are many vital functions of PDL. It acts as a cell reservoir for tissue homeostasis, repair and regeneration; as a sensory receptor required for accurate locating of the jaws during mastication; and as a supporting tissue for teeth in their place in the socket to permit them to withstand the extensive masticatory forces and distribute this force to the alveolar bone. In addition, the PDL is important in preventing the fusion and mineralisation of root cementum – the surface layer of the tooth root , with the surrounding bone by producing matrix gla protein – a vitamin-K-dependent protein containing γ-carboxyglutamatci acid (Gla) residues (Nanci and Bosshardt, 2006).

Components of PDL

The PDL consists of cells and extracellular components. The cell population is a heterogeneous and comprises fibroblasts, osteoblasts, cementoblasts, epithelial cell rests of Malassez and undifferentiated mesenchymal cells (Tomokiyo et al., 2008). The extracellular compartment is composed of well-defined collagen fibre bundles embedded in a ground substance which is amorphous background material (Nanci and Bosshardt, 2006). In the PDL there are three different types of fibre: elastic fibres, elaunin, and oxytalan fibres. The main constituents of the ground substance are glycosaminoglycans, glycoproteins and glycolipids (Miller, 2012).

Fibroblasts are the major cells of PDL. Although all fibroblasts look similar under the microscope, heterogeneity of the cell populations occurs between different connective tissues and within the same connective tissue. The periodontal ligament fibroblasts (PDLFs) are characterised by the rapid turnover of their extracellular compartment, specifically collagen (Miller, 2012). PDLFs are large cells with an extensive cytoplasm enclosing organelles related to protein synthesis and secretion. Reflecting the physical and hydrostatic pressure demands placed on the cells, PDLFs have a well-developed cytoskeleton and display numerous adherence and gap

junctions. The collagen fibrils in bundles of the periodontal ligament are constantly being remodelled by PDLFs due to the capability of PDLFs to simultaneously synthesize and degrade collagen (Nanci and Bosshardt, 2006).

Epithelial cells in PDL are called the epithelial cell rests of Malassez (ERM) which are fragments of Hertwig's epithelial root sheath the main progenitor of root formation. ERM occur adjacent to the cementum as a collection of cells and forming an epithelial network. The functional roles of the ERM are not completely understood and they may participate in periodontal repair and regeneration (Oka et al., 2012, Xiong et al., 2012).

A further important cellular constituent of PDL is the undifferentiated mesenchymal cell - progenitor cells of the PDL. In wound healing, the PDL donates cells for its own repair and to repair missing bone and cementum. Recently, from the human PDL, cells with stem cell features have been recognised and isolated (Maeda et al., 2012).

The major fibrils of the PDL are comprised of collagen-I, -III, and -XII. The single PDL fibrils have a comparatively smaller average width than tendon collagen fibrils, a difference assumed to reflect the short half-life of ligament collagen, and therefore less time for fibrillar assembly. Most of collagen fibrils in PDL are organised in definite and distinct fibre bundles which are called principal fibres. Every bundle resembles a joined cord; individual strands are continually remodelled whereas the whole fibre preserves its architecture and function. In this way, the fibre bundles have ability to adapt to the persistent stresses applied on them. The ends of collagen fibre bundles are implanted in cementum or bone. The implanted portion is named as Sharpey's fibres (Beertsen et al., 1997). Fibre bundles of PDL are illustrated in Figure 1 and 2.

There are also elastic fibres of the PDL. Three types of elastic fibres are present: elastic fibres, elaunin and oxytalan. Elastic fibres are comprised mainly of elsatin, elaunin – a deposition of elastin between oxytalan fibres, and oxytalan fibres – bundles of microfibrils composed of fibrillin-1 and fibrillin-2 crosslinked by transglutaminase. Oxytalan and elaunin fibres are associated with the gingival ligament (Newman et al., 2011).

Oxytalan fibres run in vertical direction from the cementum surface, making a three-dimensional branching meshwork that surroundings the root and ends in the apical arteries, veins, and lymphatics. Even though their role has not been completely

determined, they are assumed to adjust vascular flow with regard to tooth function. It is found that oxytalan fibres are thickened under stretching (Tsuruga et al., 2009).

Non-collagenous matrix proteins are also found in the PDL. Numerous non-collagenous matrix proteins, formed locally by occupier cells or transported by the blood flow, are present. These contain alkaline phosphatase (Oortgiesen et al., 2012), proteoglycans and glycoproteins as undulin, tenascin, and fibronectin (LeBlanc and Reisz, 2013). There is also extrafibrillar matrix or ground substance. It is amorphous matrix and has a substantial effect on the capacity of the tooth to tolerate stress. Ground substance increases in tissue fluids in areas of inflammation and injury (Nanci and Bosshardt, 2006).

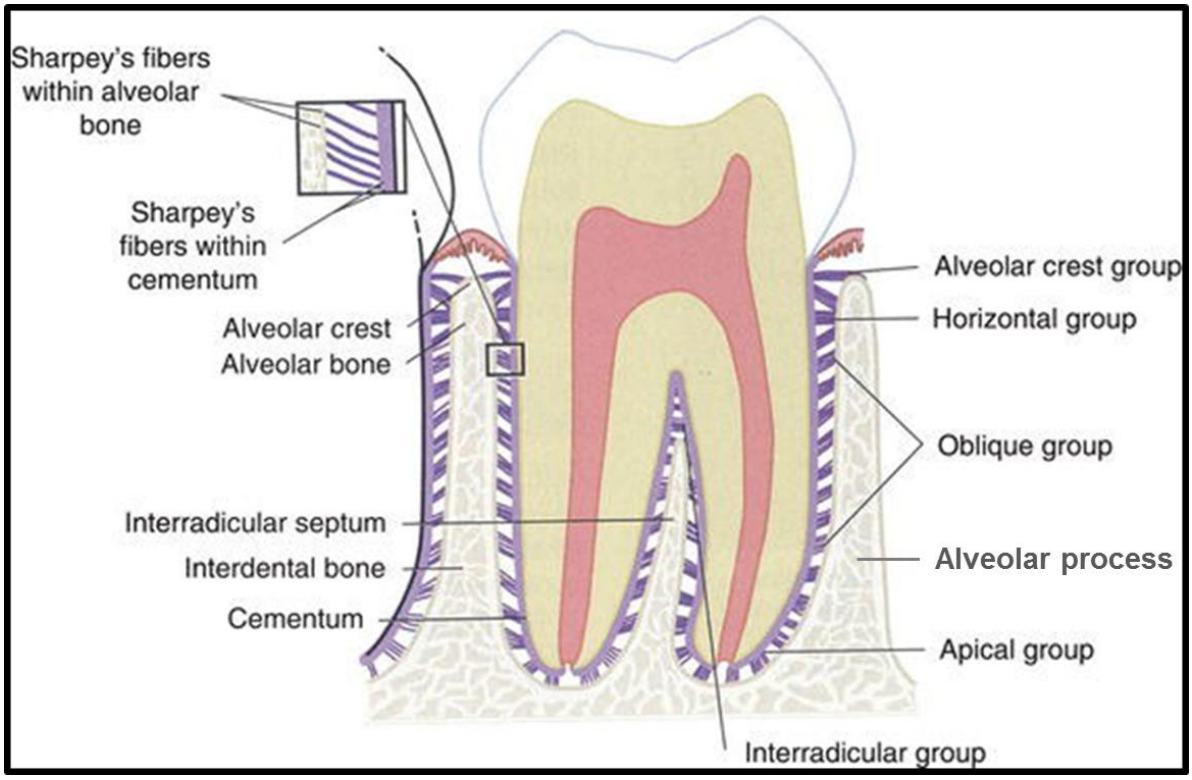

Figure 2: Periodontal ligament fibres groups.
This consists of two main groups: gingival fibre groups and the principal fibre groups. The principal fibre groups of the periodontal ligament are: **oblique fibres** - running from alveolar bone to tooth; **apical fibres** - radiating from the apex of the tooth to the adjacent alveolar bone; **horizontal fibres** - running from the cementum to the adjacent alveolar bone; and **inter-radicular fibres** - between the roots of multi-rooted teeth, running from the root to the adjacent alveolar bone. Modified from (Niemiec, 2012).

Periodontal ligament fibroblasts (PDLFs) - characteristics, physiological functions and interaction with the extracellular matrix

Periodontal ligament fibroblasts originate from the ectomesenchyme of the dental papilla. Fibroblasts are the predominant cell type in the periodontium (Beertsen et al., 1997). Viewed under electronic microscope, PDLFs have many cytoplasmic organelles - Golgi complexes, rough endoplasmic reticulum, mitochondria and secretory vesicles (Miller, 2012). PDLFs are connected by numerous types of junctions including gap and adherence junctions. PDLFs differ from other connective tissues cells in many aspects (Beertsen et al., 1997). The heterogeneity of PDLFs is based on the diversity of synthetic products, rate of synthesis, response to regulatory molecules and cellular turnover rates (Miller, 2012). PDLFs are oriented parallel to collagen fibres in longitudinal section. However, they may display a stellate appearance in cross-section. This orientation of PDLFs is caused by the cytoplasmic processes of PDLFs separating individual bundles of collagen fibres (Beertsen et al., 1997) - Figure 3.

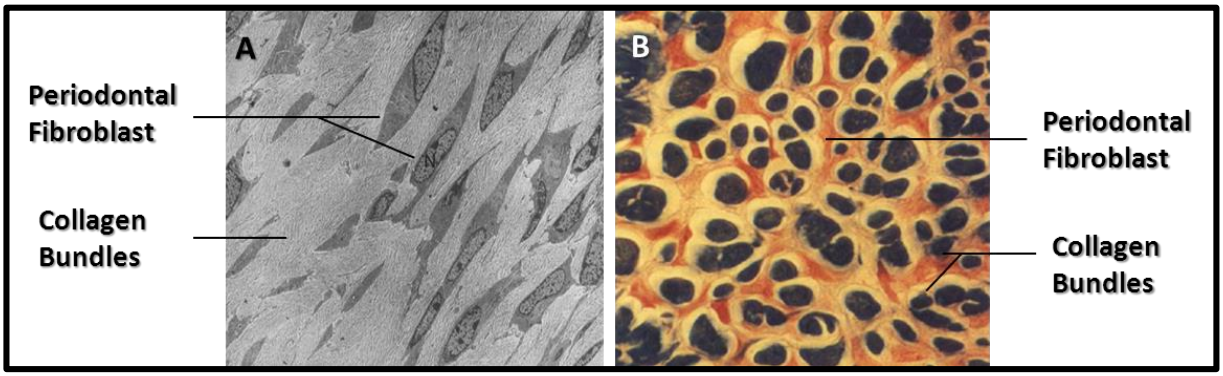

Figure 3: The orientation of fibroblasts in the periodontium.
A Longitudinal section shows parallel orientation of PDLFs to collagen fibres. B Cross-section shows the stellate appearance of PDLFs as the cytoplasmic processes separating bundles of collagen (Modified from (Beertsen et al., 1997).

Cell migration is an important function that has been detected in the periodontal ligament. It was observed in many cases including constantly erupting teeth, normal teeth function and PDL wound healing. PDLFs are relatively rich in cytoplasmic microfilament systems that are crucial for contraction and movement. Cell signalling pathways controlling the direction of migration and contractile actions are unknown. Structural polarity could be responsible for the directed migration of fibroblasts as the nucleus is usually in the trailing part of the cell, and

the Golgi complex and centrioles region are in front of the nucleus towards the leading edge of the cell, as is seen in migratory neutrophils (Beertsen et al., 1997).

PDLFs produce and maintain normal levels of ground substance. This forms the extracellular matrix by producing many components, including fibrous components such as collagen and elastin and non-fibrous components such as proteoglycans and glycoproteins (Miller, 2012). Characteristically, PDLFs have high alkaline phosphatase activity. Alkaline phosphatase is involved in phosphate metabolism, mineralization processes and acellular cementum creation. It is found along the PDLFs outer plasma membrane face. The extracellular collagenous fibre framework contains 10% of alkaline phosphatase. It is not known why the PDL does not undergo calcification in regular function in presence of the high expression of alkaline phosphatase activity. Periodontium regeneration is sustained by PDLFs proliferation after injury (Beertsen et al., 1997).

1.1.1.3 Cementum

Cementum is defined as the rigid, avascular connective tissue that covers the roots of teeth. It grabs the principal PDL fibres. The cementum composition is similar to composition of the bone. Cementum contains approximately 50% inorganic material, mostly hydroxyapatite, and 50% organic matter and water by weight. Two variants of cementum are recognised according to the source of the collagen fibres of the matrix and the presence or the absence of cells within cementum (Phillips, 2012). Acellular cementum is usually situated from the cementum-enamel junction (cervical region) to the root. It has a very slow developing rate. It is called acellular because it does not incorporate cells (Phillips, 2012), whereas, cellular cementum is found along the apical third of the tips of the roots and in furcation areas, branching point of the tooth root, in multi-rooted teeth. Cellular cementum is involved in repair of resorptive defects and root fractures. The cells involved, cementoblasts, are collagen-producing; when entrapped in lacunae within the matrix there are called cementocytes. Cementocytes are the characteristic components of cellular cementum (Phillips, 2012).

1.1.1.4 Alveolar bone

The alveolar process, or projections, is the bone of the jaw that holds the sockets, or alveoli, of the teeth. The development of alveolar process occurs at the

same time with the teeth development and eruption. It consists of outer cortical plates of compact bone, a central spongiosa, and bone lining the alveolus, or alveolar bone - Figures 1 and 2. The alveolar bone referred as bundle bone since it allows attachment of the periodontal ligament fibre bundles (Newman et al., 2011).

The alveolar bone is continuously remodelled as the tooth is constantly moving during mastication. Subsequently, alveolar bone must react to the functional demand positioned on it by the mastication forces. The process of remodelling of alveolar bone is similar to the remodelling of other types of bone. However, alveolar bone is unique because it turns over more rapidly than other bone processes. During the movement of the tooth, the force is distributed on the socket wall which result in bone resorption on one side of the tooth socket and balanced by formation of bone on the opposite side (Nanci and Bosshardt, 2006). In the case of tooth loss, the alveolar bone disappears (Trombelli et al., 2008).

1.1.2 Periodontal diseases

Periodontal disease is the inflammation and/or infection caused by dental plaque accumulation that destroys the tooth supporting tissues including gingiva, periodontal ligament, and tooth socket – the alveolar bone (Taylor and Borgnakke, 2008). Dental plaque is a soft pale-yellow sticky biofilm that develops naturally on the tooth surfaces. Plaque is made of bacteria, mucus, and food debris that deposit on the visible parts of the teeth and it is one of the most common causes of tooth decays. If plaque is not removed regularly, it hardens to form dental calculus, or tartar which is trapped at the tooth cervix (Selwitz et al., 2007). As a result of plaque and calculus accumulation, an irritation and inflammation of periodontal tissues occur due to acids resulting from degradation of fermentable sugars by bacteria (Lakschevitz et al., 2011).

1.1.2.1 Gingivitis

Gingivitis is defined simply as the inflammation of gingiva – Figure 4. It is a disease that affects the periodontium. Gingivitis is caused by continuous plaque accumulation on the surfaces of teeth. It shows the same clinical signs as any other soft tissue inflammation such as enlarged gingival outlines because of oedema or fibrosis, redness or bluish-redness, elevated temperature of sulcus, bleeding with probing and increased gingival exudate. However, these signs are not associated with

any periodontal attachment loss (Igic et al., 2012, Lang et al., 2009, Kasaj and Willershausen, 2013). Gingivitis is confined only to gingival tissue and it can be reversed once the cause is removed. If left untreated, gingivitis can progress to periodontitis (Igic et al., 2012).

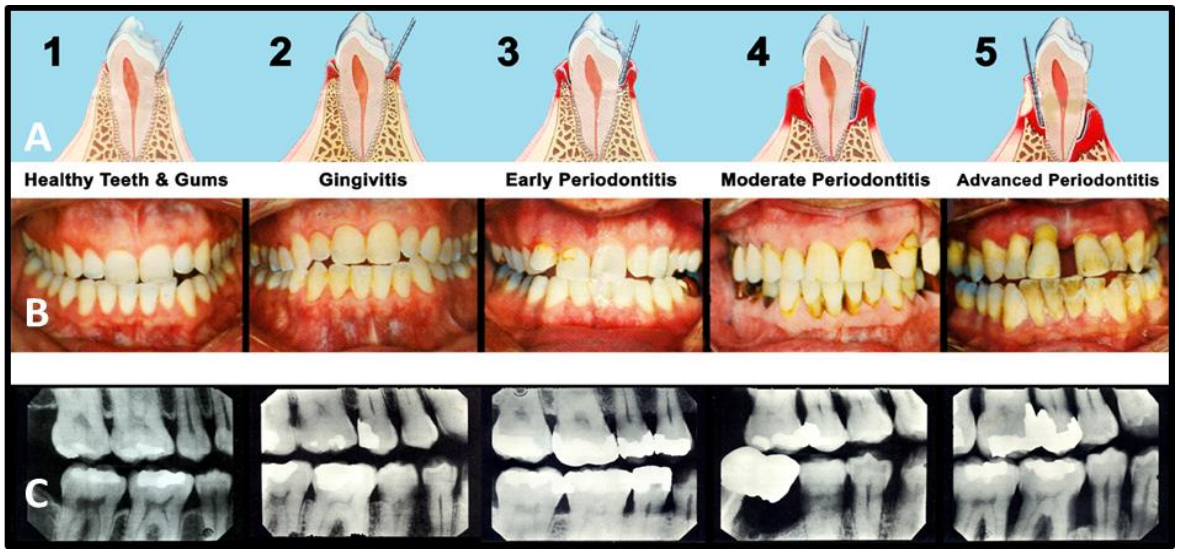

Figure 4: Periodontal dental diseases progression.
A. It shows the progression of periodontal pocket depth through the stages of the diseases. B. It shows the gradual recession of gum tissues that caused by periodontal inflammation. C. It shows X-rays in the space between the teeth, the supporting tissue gradually disappears as the disease progress. Modified from (Baker, 2000).

Classification of periodontal diseases is controversial issue. Many dental health experts suggest classification according to criteria such as etiologic factors, pathologic changes or clinical manifestations (van der Velden, 2005). One of the recommended classifications is based on the major causative factor of dental plaque. This classification categorizes gingivitis into two types: plaque-induced gingivitis, and plaque-induced gingivitis modified by particular systemic factors. These systemic factors include the following: hormonal imbalance – such as puberty, menstrual cycle and pregnancy; systemic drugs - anticonvulsants, immune-suppressants and calcium channel blockers; systemic diseases – such as diabetes and leukaemia; and malnutrition (Highfield, 2009).

1.1.2.2 Periodontitis

Periodontitis is one of the most common inflammatory diseases that affect the oral cavity. Periodontitis is a highly prevalent but largely hidden oral disease. It affects the quality of life negatively. In addition, it has been found that 15% of adults complain of sever periodontitis and about 40-60% have moderate periodontitis (O'Dowd et al., 2010). It is characterised by destroying the supporting structures of the tooth, or periodontium (Suvan et al., 2015, Preshaw et al., 2013) – Figure 4. In periodontitis, a destruction of periodontal ligament collagen fibres and alveolar bone resorption occurs along with a progressing attachment loss. Subsequently, a periodontal pocket is formed between the tooth and the gingiva. Periodontal pocket can be assessed by periodontal probe as it is difficult to be assessed visually (Borgnakke and Genco, 2015, Preshaw et al., 2013) – Figure 5.

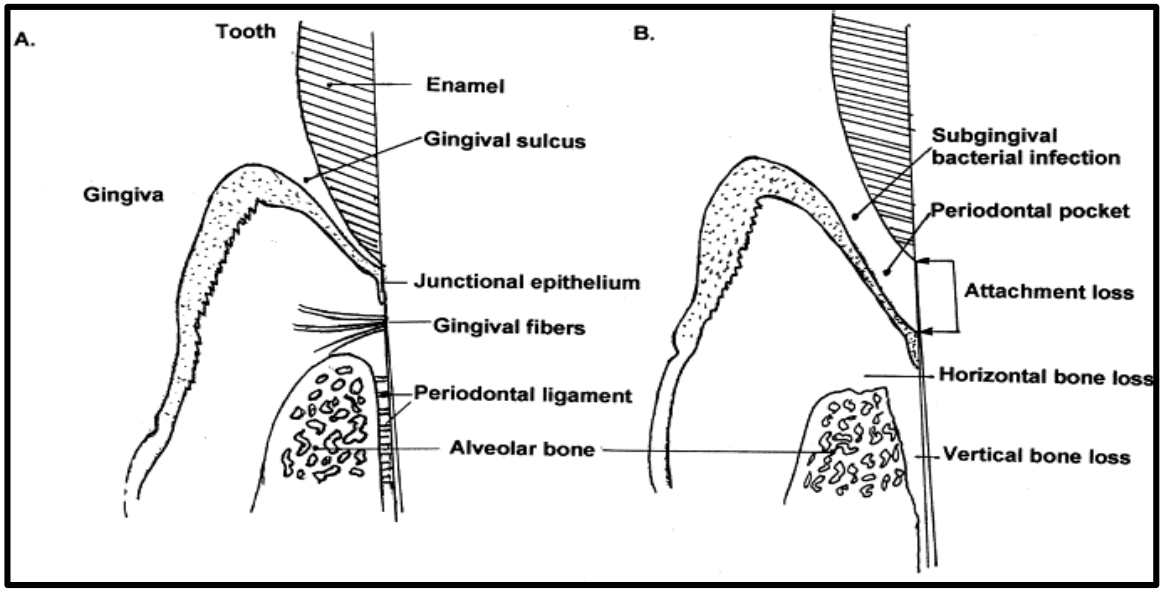

Figure 5: The periodontium in health and disease.
A. In health, the alveolar bone crest comes within 1 mm of the height of the cemento-enamel junction of the tooth. Gingival fibres connect the gingival soft tissue to the cementum of the tooth root, and periodontal ligament fibres connect the alveolar bone and cementum. B. In periodontal disease, Gram-negative bacterial infection occurs subgingivally. Soft tissue damage produces attachment loss and loss of the periodontal ligament fibres, deepening the sulcus into a periodontal pocket. Bone resorption lowers the height of the alveolar bone crest is called horizontal bone loss, and bone resorption moves the bone surface away from the tooth root is called vertical bone loss. Modified from (Baker, 2000).

Classification of the severity of periodontitis relates to the severe loss of periodontal ligament fibres, the so called clinical attachment loss (Wiebe and Putnins, 2000). According to the American Academy of Periodontology, the severity of periodontitis is classified as follows: mild, or early periodontitis when the tissue loss is approximately 1–2 mm; moderate periodontitis when the tissue loss is approximately 3–4 mm; and severe, or advanced periodontitis when the tissue loss is more than 5 mm (Wiebe and Putnins, 2000). Classification also relates to: the extent of the disease, the severity of the disease per tooth, the age of the patient and the clinical characteristics (van der Velden, 2005). Periodontitis classification is also affected by the same systemic factors which affect the classification of gingivitis with adding the genetic disorders such as familial and cyclic neutropenia (Highfield, 2009). Severe periodontitis is characterised by gingival erythema, gingival oedema, gingival bleeding, gingival recession, teeth mobility, drifting of teeth, discharge from periodontal pockets and teeth loss (Newman et al., 2011, (Smith et al., 2010). Tissue destruction in periodontitis is irreversible even if the progression of the disease is very slow (Borgnakke and Genco, 2015). Periodontitis is not painful and is often asymptomatic in its early stage. Thus, the condition progresses while the patient is unaware until the tooth mobility occurs.

The migration of the junctional epithelium (JE) alongside the root surface is considered one of the major changes found in tooth root structure in periodontitis. This causes changes in periodontium such as creation of gingival pocket and long junctional epithelium – Figure 5. Many functional changes accompany this structural modification. For example, the direction of crevicular exudate flow and neutrophil migration across the epithelium changes significantly as the free surface of the epithelium is now displaced from the sulcus bottom to the root surface. In addition, the free surface increases in size and is consequently exposed to more bacterial plaque. (Nanci and Bosshardt, 2006).

1.1.2.3 Pathology of periodontitis

Periodontitis is associated with mainly anaerobic gram-negative oral infection which cause gingival inflammation, damage of periodontal tissues, loss of alveolar bone, and eventual exfoliation of teeth in advanced cases (Liljenberg et al., 1994). Multiple strains of bacteria are considered the main etiological mediators of periodontitis. Lipopolysaccharides (LPS) or endotoxins found in the outer membrane

of gram-negative bacteria elicit strong immune responses in human subjects. The LPS inflammatory response is a key mediator of periodontitis (Offenbacher, 1996). LPS will be discussed in details later in this project.

History of the pathogenesis of periodontal disease

In early fifties, the interest in understanding the nature, classification and severity of periodontal diseases was started (Russell, 1956). In the mid-1960s, the modern era of the pathogenesis, prevention, and treatment of periodontal diseases began with human and animal experimental evidence indicating the key role of bacteria in the beginning of gingivitis and periodontitis (Lindhe et al., 1973, Slots, 1979). This led to the concept of pathogenesis mediated by bacterial infection as causative periodontal disease. This model involved bacterial plaque biofilm as the primary, direct cause in the development of periodontitis and led to the rejection of former concepts that involved non-bacterial factors, such as trauma from occlusion, systemic conditions, and diet. This theory of the key role of bacteria dramatically improved the prevention and treatment of periodontitis by targeting the bacteria with suitable antibodies. However, features included within the simple concept were for example, the hypothesis that bacterial plaque mass was the contributing factor and that bacterial products, such as collagenases, directly cause tissue destruction (Kornman, 2008). During the 1970s and early 1980s, research built on the simple concept of bacterial causation leading to great improvements in knowledge and understanding. Specific gram-negative, anaerobic or microaerophilic bacteria were implicated in the causation of periodontitis (Theilade, 1986), and the protective and destructive roles of the immune-inflammatory responses were defined in health and disease (Seymour, 1987).

By the 1980s the role of polymorphonuclear neutrophils (PMNs) in periodontal destruction in humans became widely accepted (Genco et al., 1986). Additionally, there was improvement in understanding that some clinical disease patterns or phenotypes had distinguishing bacteria and host responses. The extensive research over the mid-1980s directed to critical modifications in the pathogenesis theory.

In the late 1980s, the interaction of bacteria with host immune response with disease progression was investigated. Related connective tissue and bone damage was produced mainly by activated tissue mechanisms, such as those mediated by

matrix metalloproteinases, interleukin-1 and prostaglandins. The most important feature of the 1980s models is that a difference was now obvious between the role of the microbial challenge and immune-inflammatory mechanisms in the pathogenesis of periodontal disease. From 1985 - 1995 there was increased consideration that marked variations in host responses and clinical expression of disease occurred. In spite of a strong and reproducible correlation between plaque deposition and gingivitis development, the relationship was less clear on a patient-to-patient analysis and at different sites within the same patient. Epidemiological studies suggested exposure to plaque deposition for long periods caused periodontitis – with evidence gained from longitudinal studies in animal models and clinical investigations (Kornman, 2008). In a study in beagle dogs, plaque deposition was related with development of periodontitis; however, two of eight dogs did not develop periodontitis, regardless of substantial plaque and calculus deposition and extensive gingivitis (Lindhe et al., 1975). There was an unusual series of reports on longitudinal studies of tea plantation workers in Sri Lanka (Loe et al., 1978, Loe et al., 1986). Initially reports described failure to keep teeth clean regularly led to the development of extensive gingivitis and periodontitis of varying severity (Loe et al., 1978, Löe et al., 1978). Further analysis showed there were three different population subsets in relation to bacterial deposition-induced periodontitis development: all groups had poor oral hygiene and gingivitis but subsets developed no/minimal, moderate or severe periodontitis (Loe et al., 1986).

Further complexity to theoretical models of periodontitis was added when the effect of genetic polymorphism on the development and severity of periodontal disease emerged. Genetic effects were estimated to account for approximately 30% - 60% of the variability in the clinical severity of periodontitis (Corey et al., 1993, Michalowicz et al., 1991b). Twin studies revealed that greater variability in the risk for periodontal disease was found in dizygotic twins compared to monozygotic twins, assuming a similar home environment within families (Michalowicz et al., 1991a, Michalowicz et al., 2000). Genetic polymorphism is an important influence on individual risk of periodontal disease and its severity, and also relatedly host response to bacterial infection (Kornman et al., 1997).

In 1997, a new revised model of periodontitis emerged which accounted for engagement with key risk factors (Page and Kornman, 1997). In this model, bacterial products activated the host immune-inflammatory mechanisms. The initiation of the

host response induces soluble and cellular components of the host immune response to counter the microbial challenge in the gingival sulcus: induced expression of antibodies and recruitment and activation of PMNs. Furthermore, cytokines and prostaglandins, along with matrix metalloproteinases stimulated through the host response, may cause damage to connective tissue and bone and assume the disease clinical presentation (Kornman, 2008). Whilst the 1997 model of periodontal disease remains relevant today, there have been improvements in understanding about periodontal disease and related revisions of the model of pathogenesis.

One of the initial revisions came with recognition that microbial periodontal pathogens change in response to ecological alteration of the dental plaque. For example, change of diet to foods of different texture and low pH may lead to repopulation of dental plaques with bacteria with anaerobic and aciduric physiology (Socransky et al., 1998, Ximénez-Fyvie et al., 2000). Following this, several studies showed certain diseases, such as diabetes, genotype, and smoking, contribute strongly to the individual patient variance in the susceptibility to periodontitis. For example, in a recent study of young adults aged 26 - 32 years, *ca.* 70% new cases of periodontitis were smokers (Thomson et al., 2007). Finally, studies have defined the relationship between periodontitis and other diseases, such as cardiovascular disease, and clarified such interactions through bacterial seeding of dental plaques, studies of common inflammatory mechanisms and/or common modifying factors (Beck et al., 2000, Southerland et al., 2006). Recently, further advances were made in bacterial and immune-inflammatory mechanisms in periodontitis (Yamazaki et al., 2001, Popadiak et al., 2007).

1.1.3 Risk factors for periodontitis

1.1.3.1 Non-modifiable risk factors

Genetic factors

Although bacterial infection is the main etiologic mediator of periodontal disease, studies of identical twins found that 50% of the variability to periodontal disease is associated with host factors (Michalowicz et al., 2000). Indigenous and relatively isolated populations were also found to develop different characteristics of periodontal disease (Dowsett et al., 2001, Ronderos et al., 2001).

Host response

It is thought that pathogenesis in periodontal disease is caused by a dysfunctional immune response to bacterial infection rather than the damaging effects of bacterial pathogens directly (Van Dyke and Serhan, 2003). In localized aggressive periodontitis, it has been proposed that activated neutrophils mediate most of the tissue destruction detected (Van Dyke and Serhan, 2003). IL-1 genes (IL-1A and IL-1B) polymorphisms are related to periodontitis with particular IL-1 genotypes associated with the presence of pathogenic microorganisms (Socransky et al., 2000) to an increased risk of periodontitis in non-smokers and smokers (Meisel et al., 2002, Meisel et al., 2003). There is a potential relationship between IL-1 genotype and periodontal health in diabetics (Guzman et al., 2003). Currently, there is no definitive IL-1 genotype that confers sensitivity of individuals to high risk for periodontal disease. Current evidence suggests interactions of IL-1 genotypes with smoking and diabetes increase risk of periodontal disease (Van Dyke and Dave, 2005).

Aging

In ageing the collagen synthesis and the number of connective tissue cells are decreased. In addition, decrease in the number of PDLFs and related functional activities such as mitosis and biosynthetic activities occur. There is also a decrease in the formation of organic matrix and vascularization (Farias Gomes et al., 2010). Severe gingivitis is commonly seen in older adults with larger numbers of inflammatory cells – characterised by increased B cells and decreased PMNs, suggesting that the immunological response quality can be affected by aging (Farias Gomes et al., 2010). Biochemical, immunological and physiological changes occurring with aging may contribute to periodontal tissue damage in elderly people. However, the extent of aging effect on periodontal tissues is not well known and the periodontal tissue damage may arise as a consequence of other influences such as environmental factors, systemic diseases, medications and social modifications (Farias Gomes et al., 2010, Guiglia et al., 2010, Van Dyke and Dave, 2005). According to Van Dyke and Dave (2005), aging is not a risk factor for periodontal disease and rather tissue deterioration found in periodontal tissues of elderly people is a combination of that due to ageing and periodontal disease (Van Dyke and Dave, 2005).

1.1.3.2 Modifiable risk factors

Renal disease

Renal disease is an influential factor in periodontal disease. Some treatments for renal disease, such as calcium channel blockers and cyclosporine, are associated with increased risk of gingival enlargements. There is no clear evidence, however, that risk of periodontitis increases with renal failure (Proctor et al., 2005) although the prevalence of periodontitis in patients with renal disease was higher than in healthy subjects (Ioannidou and Swede, 2011, Ioannidou et al., 2011). There was increased serum C-reactive protein (CRP) in patients with periodontitis and renal disease, suggesting that periodontitis may contribute to the systemic inflammatory burden in renal disease cases (Ioannidou and Swede, 2011, Ioannidou et al., 2011, Chen et al., 2015)

Smoking

Smoking increases the risk of developing periodontitis and its severity (Pihlstrom et al., 2005). Smoking causes vasoconstriction of the blood vessels of periodontal tissues decreasing the blood flow (Zee, 2009). Recently, it was found that the immune response to pathogens in periodontal tissue is altered by tobacco use, especially tobacco smoking. Peripheral blood mononuclear phagocytes are increased but their function is compromised, diminishing activity against pathogens in the oral tissue and increasing risk of developing periodontal disease (Fokkema, 2012).

Obesity and overweight

There was a positive strong relationship between body mass index and diagnosis of periodontitis in an age-matched case–control study. This relationship was independent of gender, ethnicity, smoking status and dental plaque levels. Obesity was independently related to periodontitis when judged by a comprehensive, full-mouth clinical periodontal evaluation. Overweight and obese individuals have a greater risk of getting periodontitis in comparison with those who are within the category of BMI normal (Suvan et al., 2015).

Diabetes

The prevalence of periodontitis increases among patients with diabetes – type 1 and type 2. Poorly controlled hyperglycaemia in patients with diabetes tends to

cause more severe form of periodontitis than in non-diabetic subjects (Chang and Lim, 2012). It is thought that the systemic changes caused by diabetes reduce the host resistance to periodontal tissue breakdown. This alteration in host response may not be reversed by glycaemic control (Pacios et al., 2012). Additionally, it has been found that the long duration of diabetes with complications like retinopathy and nephropathy are correlated with worsening of periodontal states (Borgnakke and Genco, 2015, Preshaw et al., 2013).

1.2 Diabetes

1.2.1 Types of diabetes

1.2.1.1 Type 1 diabetes mellitus

Type 1 diabetes (T1DM) is due to absolute insufficiency of insulin production with little or no insulin being secreted (Holt et al., 2011). T1DM accounts for *ca.* 5-10% of diabetes cases globally (Haller et al., 2005). Approximately 10% of adults and 14% of children in UK with diabetes mellitus have T1DM. The prevalence of T1DM in children is 1 per 700-1000 and they are diagnosed in adolescence. Approximately 85% of patients with T1DM have no previous first-degree family history. However, the risk of getting the disease in cases of first degree relative increase to 15 times comparing with general population (IDF, 2015). The cause of T1DM autoimmune disease is still unidentified. The occurrence is mainly common in ages; 4-6 years and 10-14 years. The incidence rate reduces at time of puberty and is noticed to be stable between 15-29 years of age (Haller et al., 2005).

Many large studies have been performed to characterise the incidence of T1DM - for example, in the period 1990-1999, the WHO multinational project for childhood diabetes (DIAMOND study) and a collaborative European study (EURODIAB ACE) (Eurodiab, 2000, Karvonen et al., 2000).They found a geographical variation in the incidence of T1DM with highest incidence in Scandinavian and Mediterranean populations compared to oriental and equatorial populations (Karvonen et al., 2000). Although there was high genetic homogeneity in Scandinavian countries, T1DM incidence rates varied from 45 per 100,000 in Finland to 28 in Sweden and 20 in Denmark (Ali, 2010). A role of vitamin D levels and ultraviolet (UV) exposure was suggested in explanation of the strong North-South gradient in the incidence of T1DM and the fact that vitamin D is an immune regulator (Mohr et al., 2008). Some exceptions are Kuwait, Puerto Rico and Sardinia

- countries exposed to sun with high T1DM incidence, and Lithuania in the Northern latitude with low prevalence of T1DM. From these exceptions, it has suggested that vitamin D levels or sun exposure cannot be the only explanation of variation in the disease prevalence (Ali, 2010).

The incidence of diabetes in some studies showed seasonality (Willis et al., 2002, Levy-Marchal et al., 1995, Green and Patterson, 2001, Svensson et al., 2009). There are other studies where the seasonal influence was not found (Ye et al., 1998, Kida et al., 2000) which might have been masked by the genetic and environmental factors. Furthermore, no gender preference was noticed in T1DM (Gale and Gillespie, 2001).

Genetic factors

The etiology of T1DM is variable. In some individuals, the main cause can be various susceptibility genes such as human leukocyte antigen (HLA), insulin gene, protein tyrosine phosphatase non-receptor type 22 (PTPN22), interleukin 2 receptor alpha (IL2Ra), and cytotoxic t-lymphocyte antigen 4 (CTLA4) (Van Belle et al., 2011). Several gene loci are discovered to be linked with the risk of autoimmune T1DM. The major histocompatibility complex (MHC) or human leukocyte antigen (HLA) on chromosome 6, mainly at DR3/4 and DQ regions, is the genomic region that has the strongest association with risk of T1DM. The DR-DQ haplotype can be either influencing to or protecting against T1DM. For instance, the HLA DR3/4-DQ2/8 recognised as a high risk genotype for T1DM is found in more than 30% of children with T1DM but in only 2.3% of all new-borns in Colorado (Ali, 2010). The DR2 haplotype appears to be protective as it is found in 20% of the total population but only in 1% of the immune-mediated diabetes (Frohlich-Reiterer et al., 2008). Furthermore, other non-HLA gene loci have been suggested to be participated in T1DM risk: for example, the insulin gene IDDM2, the lymphoid tyrosine phosphatase gene PTPN22, the cytotoxic T lymphocyte associated-4 gene, the interleukin-2 receptor, the interferon-induced helicase (IFIH1) gene and the vitamin D 1 alpha hydroxylase gene CYP27B1 (Bennett and Todd, 1996, Bottini et al., 2004, Nistico et al., 1996, Lowe et al., 2007, Smyth et al., 2006, Bailey et al., 2007).

Environmental factors

Other triggers for T1DM could be environmental such as Cow's milk or enteroviruses such as coxsackieviruses (Van Belle et al., 2011). There is an increase in prevalence of T1DM in most populations, the monozygotic twins' discordance for the disease and the seasonality of T1DM occurrence all propose that environmental factors may have a role in the risk of T1DM. Several studies have indicated the role of viral infections in T1DM multiuse pathogenesis by direct demolition of β-cells or encouraging the release of islet antigens. In contrast, the hygiene hypothesis proposed a promising defending role of infectious agents against autoimmune mediated diabetes, even though this remedy lacks of enough clinical evidences. In addition, dietary factors have been involved in association with the risk of T1DM, for instance bovine protein, omega-3 fatty acids and several vitamins, environmental chemicals, and psychological stress, even if these theories are not convincing at meantime and needs additional investigation (Ali, 2010).

Pathogenesis of type 1 diabetes mellitus

T1DM is affected by autoimmune destruction of pancreatic beta-cells. Exogenous insulin administration is compulsory for survival. Pathogenesis is caused by cellular and humoral autoimmune response that generates destructive autoimmune antibodies. These are produced by macrophages and T lymphocytes and used against several antigens of beta-cells (Mallone and van Endert, 2008, Holt et al., 2011). Histologic appearance of insulitis with infiltration of the islets of Langerhans by immune cells containing T and B lymphocytes, monocytes/macrophages, and natural killer cells were detected in the pancreas of newly diagnosed T1DM patients (Gepts and Lecompte, 1981, Hanninen et al., 1992). Autoimmune antibodies cause beta-cell degradation: formation of autoimmune antibodies leads to beta-cell destruction. This causes inflammatory lesions in the pancreas with mononuclear cell infiltration of islets and decrease beta-cells mass, followed by diminished insulin production. Subsequently, many signs start to occur such as gradual reduction in the acute insulin response to circulatory glucose burden, impaired oral glucose tolerance and fasting hyperglycaemia (Holt et al., 2011, Eisenbarth, 1986). This is called 'autoimmune' T1DM. However, in some cases, insulin-dependent state without provable autoantibodies can be diagnosed. This is termed 'idiopathic' type 1 diabetes mellitus (Seino et al., 2010). It generally exists in African-Caribbean subjects and is

characterised by insulinopenia and/or ketoacidosis. The function of beta-cells may improve and normoglycaemia may be regained (Leu and Zonszein, 2010). The number and intensity of the autoantibodies in addition to genetic susceptibility and environmental triggers are influence the possibility of clinical T1DM development and progression (Ali, 2010).

T1DM can be either asymptomatic or mildly symptomatic; the majority is diagnosed with severe hyperglycaemia and/or ketoacidosis as a result of the fast development of the disease from β-cell destruction. After diagnosis of some T1DM patients, they show a short period when insulin treatment is not required. This could be caused by a transient recovery of β-cell function when achieving normoglycaemia (Martin et al., 1992). When the disease is diagnosed, however, patients usually lose all residual β-cell function within 1-3 years of diagnosis which necessitates exogenous insulin administration for survival (Ali, 2010).

The common clinical symptoms of type 1 diabetes noticed before diagnosis are: polyuria, polydipsia, abdominal pain and weight loss. Ketonuria and acidosis were identified in more than 75% and 40% of the cases respectively. In the younger age group, ketonuria and acidosis were significantly more frequent (Roche et al., 2005).

1.2.1.2 Type 2 diabetes mellitus

Type 2 diabetes mellitus (T2DM) has become an epidemic disease in the last decade. 91% of people with diabetes have T2DM (IDF, 2015). T2DM is mostly diagnosed at an age over 40 years because of a long period of an asymptomatic hyperglycaemic condition (Stumvoll et al., 2005). Patients with T2DM are characterised by insulin resistance or relative insulin insufficiency, which commonly do not need insulin for survival at start of the disease but may need insulin later once dietary control and other medications failures. Ketoacidosis is not common in T2DM and is generally limited to illness-triggered stress as infections. The risk factors for the development of T2DM is heterogeneous such as age, obesity, lack of exercise and genetic predisposition, however, exact aetiology remains unclear (ADA, 2015). The “common” type 2 diabetes has a multifactorial pathogenesis triggered by modifications in several gene products (Stumvoll et al., 2005).

Environmental and genetic risk factors

Insulin resistance is an early sign for T2DM. It is associated with obesity, sedentary lifestyle and unhealthy diet. Obesity itself is a major independent risk factor for T2DM. Central obesity which revealed by the waist-hip ratio is significantly related with insulin resistance and has been presented as predictor of T2DM in several studies (Narayan et al., 2007, Grundy, 2000, Groop, 1999).

Although lifestyle and overeating are the main causes of T2DM, genetic components also contribute to its pathogenesis. Genome-wide association studies have recognised multiple susceptibility gene loci for T2DM. Risk for T2DM increase 2.4 fold in cases of positive family history. Approximately 15–25% of the first-degree relatives of patients with T2DM have impaired glucose tolerance or diabetes. For subjects with one parent with T2DM, the lifetime risk of developing T2DM also is 38%. If the two parents have T2DM, the risk of developing T2DM by the age of 60 years is approximately 60% (Stumvoll et al., 2005).

Genetic mutations associated with T2DM are in high-affinity beta-cell sulphonylurea receptor 1 (SUR-1), glucose transporter isoform-2 (GLUT-2), glycogen synthase (GYS1) (Stumvoll et al., 2005), calpain-10 (CAPN10), potassium inward-rectifier 6.2 (KCJN11), peroxisome proliferator-activated receptor γ (PPAR γ), insulin receptor substrate-1 (IRS1), and others (Stumvoll et al., 2005).

Pathogenesis of type 2 diabetes mellitus

T2DM is insidious where clinical symptoms develop more slowly that for T1DM. Approximately 30% of the T2DM population is undiagnosed. Many T2DM patients suffer from vascular complications at time of diagnosis as a result of tissue damages by significant hyperglycaemia for 5-10 years before diagnosis (Fonseca and John-Kalarickal, 2010).

In T2DM there may be abnormalities of insulin action, insulin secretion or both. Epidemiological and clinical studies propose that T2DM is most commonly started with insulin resistance in the majority of population. Before the onset of T2DM, fasting glucose and glucose tolerance stay normal with increased response of fasting insulin and glucose-stimulated insulin. The latter resituates for insulin resistance. Impaired glucose tolerance (IGT) progresses and increased fasting and postprandial insulin levels try to recompense for insulin resistance (Thies et al., 1990, Cusi et al., 2000). Pancreatic β-cell function decreases steadily over time and

approaching increased hyperglycaemia diagnostic for diabetes. Contributing to this there is probably diminished metabolism and/or sensing of glucose, imperfect stimulatory molecules and amyloid deposition (Thies et al., 1990, Cusi et al., 2000). Mechanisms thought to contribute to this are: increased non-esterified fatty acids, inflammatory cytokines, adipokines, and mitochondrial dysfunction for insulin resistance, and glucotoxicity, lipotoxicity, and amyloid formation for beta-cell dysfunction.

Mechanisms of insulin resistance have been investigated. The insulin receptor substrates IRS-1 and IRS-2 are essential mediators in insulin signalling. Impaired IRS-1 phosphorylation in response to insulin was discovered in muscle tissues and adipocytes of T2DM patients. Phosphoinositide-3(PI3)-kinase, which contributes to the insulin-stimulated translocation of a glucose transporter GLUT-4 and glycogen synthase activation, is stimulated by binding to tyrosine phosphorylated IRS-1 and IRS-2. The activity of PI3-kinase was decreased in muscle of T2DM patients, (Thies et al., 1990, Cusi et al., 2000). Additional proposed mechanisms of insulin resistance are through the glucose transport system. Insulin stimulates glucose transport by stimulating the trafficking of GLUT4 from intracellular location to plasma membrane in tissues as adipocytes, skeletal muscle and cardiac muscle. Although the expression of GLUT4 is normal, decreased translocation of GLUT4 to the plasma membrane was found in patients with T2DM – suggesting impaired cell signalling for GLUT4 translocation (Kelley et al., 1996, Kruszynska and Olefsky, 1996).

Hyperglycaemia develops as a result of progressive loss of β-cell function. Usually this is accompanied by other metabolic abnormalities such as increased lipolysis and gluconeogenic precursors, lactate, pyruvate, alanine and glycerol. Increased lipolysis produces raised levels of fasting and postprandial plasma free fatty acid (FFA) and hepatic VLDL. Increased plasma FFA and hyperglycaemia are found when T2DM is established which further aggravate insulin resistance.

Skeletal muscle, liver and adipose tissue are the most important insulin-targeting tissues in the body. Defective insulin action and/or secretion on these tissues in T2DM drives metabolic disturbances such as decreased insulin-stimulated skeletal muscle glucose uptake, overproduction of hepatic glucose, and impaired suppression of plasma glucagon and adipocyte lipolysis, leading to fasting and postprandial hyperglycaemia (Fonseca and John-Kalarickal, 2010).

1.2.1.3 Other types of diabetes

There are several rarer forms of diabetes. Maturity onset diabetes of the young (MODY) is characterised by a group of disorders associated with monogenetic mutations affecting β-cell function or glucose sensing. Six genetic loci on various chromosomes have been recognised (Fajans et al., 2001). The main features of MODY are early onset (commonly before 25 years), family history of diabetes, slight hyperglycaemia and less chronic complications.

Genetic mutations of the insulin receptor lead to abnormal insulin action, causing hyperinsulinemia, hyperglycaemia and severe diabetes. Examples of this syndrome are: Leprechaunism and the Rabson-Mendenhall syndrome. These two syndromes have autosomal recessive inheritance (Longo et al., 2002). Injuries to pancreas such as pancreatitis, infection, trauma, pancreatectomy, and pancreatic cancer lead to diabetes if the damage to the pancreas is extensive. Extensive damage to β-cells and blocking of insulin secretion can caused by cystic fibrosis and hemochromatosis. Diabetes can be induced by drugs, hormones and toxins by interfering with insulin secretion or action. For example, Nicotinic acid and glucocorticoids disturb insulin action. Viral infections including coxsackievirus B, cytomegalovirus, adenovirus and mumps are assumed to prompt hyperglycaemia by damaging β-cells (Karjalainen et al., 1988, Pak et al., 1988). Additionally, some genetic syndromes including Down syndrome and Wolfram syndrome have been related with increased occurrence of diabetes. The etiology of the disturbance in glucose homeostasis in these diverse unrelated syndromes is still unclear (Triplitt et al., 2015).

1.2.1.4 Gestational diabetes mellitus (GDM)

Gestational diabetes mellitus is glucose intolerance immediately before or during pregnancy. Approximately 90% of all mothers with diabetes in pregnancy are of the GDM type (Engelgau et al., 1995). The incidence of GDM is approximately 8-9% of all pregnancies. Even though most of GDM terminates with delivery, the disease could continue after pregnancy. Glucose intolerance may happen before the start or at the beginning of pregnancy (Triplitt et al., 2015). In GDM, insulin resistance is initiated by interfering of pregnancy hormones with unidentified aetiology. GDM increases the possibility of new-born death and stillbirth, and having diabetes in future life. There are many risk factors of GDM such as obesity, history

of diabetes in the family, treatment of infertility, repetitive urinary tract infections, large size of infant, unclear neonatal death, pre-eclampsia, former GDM, and advanced maternal age (Bener et al., 2011).

1.2.1.5 Other diabetes complications

Complications of diabetes mellitus are microvascular disease (nephropathy, neuropathy and retinopathy) and increased risk of cardiovascular disease (CVD) and cerebrovascular disease. Patients with T2DM have 2 – 4 times greater risk of CVD than non-diabetic subjects (Stumvoll et al., 2005). Microvascular complications of diabetes may lead to blindness in advanced diabetic retinopathy, end stage renal failure in diabetic nephropathy, and sensory loss and nerve dysfunction in arms and legs with associated tissue damage in diabetic neuropathy such as ulcerated veins, gangrene and amputations (Donnelly et al., 2000).

1.3 Periodontitis in diabetes

1.3.1 Association of diabetes with periodontitis

Diabetes is a major risk factor for periodontitis (Salvi et al., 2008, Borgnakke and Genco, 2015). Risk of periodontitis is increased 3-fold in patients with diabetes compared with healthy subjects (Mealey and Ocampo, 2007). The glycaemic control status is vital in determining increased risk. For instance, in the US National Health and Nutrition Examination Survey (NHANES) III, patients with diabetes and HbA_{1c} >9% had a higher incidence of severe periodontitis after correcting for age, ethnicity, education, sex and smoking (Tsai et al., 2002). The importance of diabetes as a risk factor for periodontitis emerged in the 1990s in a number of cross-sectional and longitudinal studies examining the Pima Indian population. The incidence of periodontitis were higher in Pima Indians who had T2DM compared with healthy subjects (Taylor et al., 1998, Nelson et al., 1990, Emrich et al., 1991, Borgnakke and Genco, 2015). T1DM also increases risk of periodontitis. Approximately 10% of children (<18 years) with T1DM had greater attachment loss and bone loss compared with healthy controls, regardless of similar plaque scores (Cianciola et al., 1982). In a study includes 350 diabetic children (6 – 18 years old) vs 350 non-diabetic controls, the proportion of periodontal sites with sign of periodontitis was greater in the children with diabetes (Lalla et al., 2007).

One of the parameters frequently used to measure periodontal health is the attachment loss. Patients with poorly controlled T1DM or T2DM have poor periodontal health with increased attachment loss, bleeding from gums and increased tooth pocket depth (Mealey, 2000, Arrieta-Blanco et al., 2002). Other diabetes-associated factors influential contributing to tooth loss are: (1) duration of diabetes (Papapanou, 1996, Sandberg et al., 2000); and (2) presence of other complications (retinopathy, neuropathy, nephropathy and cardiovascular disease) (Borgnakke and Genco, 2015, Mealey and Ocampo, 2007, Chang and Lim, 2012). Some subjects with well-controlled diabetes still suffer from periodontal problems, indicating that diabetes-induced periodontal changes are not readily prevented with current treatments for glycemic control (Iacopino, 2001, Chang and Lim, 2012).

1.3.2 Factors contributing to development of periodontitis in patients with diabetes

1.3.2.1 Lipopolysaccharide (LPS), infection, pro-inflammatory mediators and polymorphnuclear neutrophils

LPS is one of the components of the cell wall of gram-negative anaerobic bacteria. LPS is a complex glycolipid. It stimulates the expression of pro-inflammatory cytokines, for instance interleukins IL-1β and IL-6, prostaglandin E2 (PGE2) and TNF-α, in macrophages and PDL cells. Cytokines then disturb the function of PDL cells by stimulating the production of matrix metalloproteases (MMPs), such as MMP-1, in PDL cells. MMP-1 is a major proteolytic enzyme, which cleaves natural type I and type III collagens, proposing its forceful contribution to PDL structure destruction (Maeda et al., 2012, Hatipoglu et al., 2015). In patients with diabetes with periodontitis, the elevation of many pro-inflammatory mediators was detected. These pro-inflammatory mediators include IL-1β, IL-6, prostaglandin E2 (PGE2), TNF-α, receptor activator of nuclear factor κB ligand (RANKL), matrix metalloproteinases (MMPs; particularly MMP-8, MMP-9 and MMP-13), T cell regulatory cytokines (e.g. IL-12, IL-18) and the chemokines (Preshaw et al., 2013). The nature of the inflammatory response among individuals is heterogeneous and is influenced by genetic, epigenetic and environmental factors. However, the pattern and rate of disease progression is determined by sum total of the inflammatory response in the periodontal tissues (Preshaw et al., 2013).

Patients with diabetes are usually more susceptible to severe infections than the non-diabetic individuals. Also, the severity of infections increases in the existence of diabetes. There is impaired host defence cell function, especially polymorphnuclear leukocyte and vascular changes in diabetic subjects (Mealey, 1999). Defects in polymorphonuclear neutrophil (PMN) activity such as impaired chemotaxis and phagocytosis are found in patients with diabetes. This is increased retention of PMNs in the periodontal tissue which increases the likelihood of tissue destruction by sustained release of MMPs and reactive oxygen species (ROS) (Mealey, 1999, Preshaw et al., 2013).

Acute viral and bacterial infections, especially those which continue for more than one month, increase insulin resistance in non-diabetic subjects. Furthermore, people who have periodontitis show an elevated levels of circulating pro-inflammatory cytokines which involve in increasing insulin resistance (Mealey and Oates, 2006, Lu et al., 2015, Mealey, 1999). Diabetic patients who have periodontitis had 6-fold higher risk of impaired glycaemic status compared to diabetic patients without periodontitis. Effective periodontal therapy such as scaling, root planning, localized gingivectomy and extraction of hopeless teeth adjunct with systemic tetracycline antibiotic therapy may improve glycaemic control and decreased HbA_{1c} (Mealey and Oates, 2006).

1.3.2.2 Collagen metabolism

Collagen homeostasis, synthesis and maturation are significantly affected by glucose level in the body. In patients with diabetes, there is a decrease in the collagen production with an increase in collagenase activity in gingival tissues. Gingival cervical fluid (GCF) collagenase activity was increased in patients with diabetes. This increase was inhibited by tetracycline despite the fact that collagenase is originated from PMNs and its production is not influenced by bacteria (Mealey, 1999).

Oral and extra oral diabetes-induced collagen abnormalities, such as a large decrease in synthesis and solubility of collagen in gingiva, skin and bone, and increased hydroxyproline excretion in urine - an amino acid marker of collagen degradation – have been found in diabetes. This suggest that the diabetes increases the breakdown of newly formed collagen in various connective tissues through the body (Golub et al., 1983). Increased GCF collagenase activity and decreased gingival

fibroblast collagen synthesis in diabetic patients have been detected. It was found that PMNs is the major cellular source of the increased collagenase activity in the GCF of patients with T1DM. PDLFs may also contribute to increased collagenase. Fibroblasts and other cells such as chondroblasts secrete the neutrophil collagenase - MMP8 (Ryan et al., 2003). MMP8 expression is inhibited by tetracycline although the production is not mediated by responses to bacteria (Mealey, 1999).

1.3.2.3 Wound healing

Wound healing is a cellular response to injury and includes activation of keratinocytes, fibroblasts, endothelial cells, macrophages, and platelets. These cell types release many growth factors and cytokines which are needed to organize and maintain healing. More than 100 known physiologic factors participate in wound healing insufficiencies in patients with diabetes. These include: impairment of production of growth factors, response of angiogenic factors, function of macrophages, accumulation of collagen, function of epidermal barrier, quantity of granulation tissue, migration and proliferation of keratinocyte and fibroblast, number of epidermal nerves, bone healing, and imbalance between the ECM components accumulation and their remodeling by MMPs (Brem and Tomic-Canic, 2007).

The normal acute wound healing is directed and preserved through multiple cell responsive factors, such as cytokines (including transforming growth factor beta (TGF-beta)), and chemokines (IL-10), released by keratinocytes, fibroblasts, endothelial cells, macrophages, and platelets. In wound-induced hypoxia, vascular endothelial growth factor (VEGF) released by macrophages, fibroblasts, and epithelial cells enhances the phosphorylation and activation of nitric oxide synthase (eNOS) in the bone marrow, causing an increase in nitric oxide (NO) levels, which prompts the mobilization of bone marrow endothelial progenitor cells (EPCs) to the circulation. The chemokine stromal cell–derived factor–1α (SDF-1α) direct these EPCs to the injury site, where they contribute in neovasculogenesis (Brem and Tomic-Canic, 2007). Gallagher et al. showed that in diabetic mice, eNOS phosphorylation in the bone marrow is compromised which directly restricts EPC mobilization from the bone marrow into the circulation. In addition, they found that SDF-1α expression is diminished in epithelial cells and myofibroblasts in the wound of diabetic, which inhibits EPC homing to wounds and thus confines wound healing. Furthermore, they show that hyperoxia in wound tissue with hyperbaric oxygen

therapy triggered increased NOS, increasing levels of NO and improved mobilization of EPC to the circulation. Though, administration of SDF-1α locally was essential to direct these cells to the wound site. This suggested that hyperbaric oxygen therapy with administration of SDF-1α provides an option of treatment to stimulate diabetic wound healing alone or in presence of current clinical protocols (Gallagher et al., 2007).

Impaired oral wound healing is a common problem in patients with diabetes. This is a result of the fibroblast dysfunction - the primary reparative cell in the periodontium (Willershausen-Zönnchen et al., 1991). Additionally, the collagen which is formed by fibroblasts is vulnerable to rapid degradation by MMPs and the production of MMPs is increased in diabetes (Golub et al., 1998). Accordingly, periodontal wound healing reacts poorly to chronic microbial stimuli in diabetes, causing increased bone loss and attachment loss (Mealey, 2006).

1.3.2.4 Oxidative Stress

The definition of oxidative stress is an imbalance of formation of reactive oxygen species (ROS) and antioxidants in favour of the former leading to cell and tissue damage. Increased formation of ROS occurs in diabetes through mitochondrial dysfunction, activation of NADPH oxidases and uncoupling of NO synthases (Bullon et al., 2009, Wright et al., 2006). There is an increase in the evidences which suggest that there is a strong relation between hyperglycemia, oxidative stress and diabetic complications. Increase in blood glucose levels cause overproduction of ROS by the mitochondria electron transport chain. In addition, high reactivity of ROS cause modification of DNA and protein and peroxidation of lipid (Piconi et al., 2003).

It was found that periodontitis is associated with oxidative stress and worsened by poor glycaemic status in patients with diabetes (Allen et al., 2011). ROS and oxidative stress are found up-regulated in the liver and adipose tissues of diabetic mice. In addition, ROS formation started before the elevation of TNF-α and FFA. Thus, reduction in antioxidant defence may lead to insulin resistance and insulin sensitivity improved by antioxidants (Bruce et al., 2003, Ceriello, 2000). Dysregulation of the oxidative balance by increased formation of ROS by PMN and metabolism in hyperglycaemia may contribute to periodontitis (Bullon et al., 2009). A recent study of chronic periodontitis found low-grade inflammation and systemic oxidative stress with decreased antioxidant capacity (Bullon et al., 2014).

1.3.3 Periodontitis and insulin resistance

Recently, there is an emphasis directed to the effect of chronic subclinical inflammation of periodontitis and insulin resistance on initiating and developing type 2 diabetes. As the oral infection is the main trigger of the inflammation, this leads to increase cytokine production. This causes insulin resistance lead to changes resulting in type 2 diabetes (Kim and Amar, 2006, Mealey and Oates, 2006, Preshaw et al., 2013).

1.3.4 Other oral manifestations of diabetes mellitus

In addition to periodontal diseases, there are many other oral manifestations of diabetes mellitus such as the decrease of salivary secretions or xerostomia, the enlargement of parotid gland and the increase of glucose level in gingival cervical fluid (GCF). Xerostomia can cause the feeling of burning mouth and tongue and increase the susceptibility of developing infection by opportunistic microorganisms such as Candida albicans. The elevation of glucose level in GCF may lead to alteration in plaque microflora and enhance the development of periodontal diseases and dental decays. These manifestations are frequently related to uncontrolled diabetes (Mealey, 1999).

1.3.5 Pathogenic mechanisms linking diabetes and periodontitis

Periodontitis is a chronic inflammatory disease in which inflammation in the periodontal tissues is caused by the long-term existence of the subgingival biofilm (dental plaque). The inflammatory response is recognised by alteration in the secretion of host-derived mediators of inflammation and tissue breakdown. Most studies recognised inflammatory mediators include IL-1β, IL-6, prostaglandin E2 (PGE2), TNF-α, receptor activator of nuclear factor κB ligand (RANKL), and the matrix metalloproteinases (MMPs; principally MMP-8, MMP-9 and MMP-13), as well as T cell regulatory cytokines (e.g. IL-12, IL-18) and the chemokines (Preshaw and Taylor, 2011). In periodontal pathogenesis, the complexity of cytokine networks is becoming progressively apparent, and it is obvious that there is significant heterogeneity in the inflammatory response nature between individuals. This heterogeneity is also influenced by genetic, epigenetic and environmental factors. The sum total of the inflammatory response in the periodontal tissues defines the form and rate of disease progress (Kinane et al., 2011).

Diabetes is characterised with hyperglycaemic state and this has several deleterious effects. It increases the formation of irreversible advance glycation end products (AGEs) and the expression of their signalling receptor RAGE. This relation, in turn, causes dysfunction of the immune cell, alteration of phenotype and function of other key cells in the periodontium, and imbalance of cytokine with increased generation of certain pro-inflammatory cytokines (Yan et al., 2009). Additionally, hyperglycaemia involved in increased levels of ROS and a state of oxidative stress, both directly and indirectly through the AGE/RAGE axis (will be discussed in details later in this project in section 1.4.5), stimulating quantitative and qualitative shifts in cytokine profiles (Bullon et al. 2009). Fourthermore, hyperglycaemia may modifies the RANKL/osteoprotegerin (OPG), again directly and indirectly via the AGE/RAGE axis, tipping the balance towards enhanced inflammation and destruction (Santos et al., 2010, Vieira Ribeiro et al., 2011). All the above, accompanied by the effects of ecological shifts in the subgingival biofilm and the circulating adipokines produced because of diabetes-associated adiposity and dyslipidaemia, direct this vicious cycle of cellular malfunction and inflammation - Figure 6. This cause loss of equilibrium where increased periodontal tissue destruction and impaired repair process, leading to accelerated and severe periodontitis (Taylor et al., 2015).

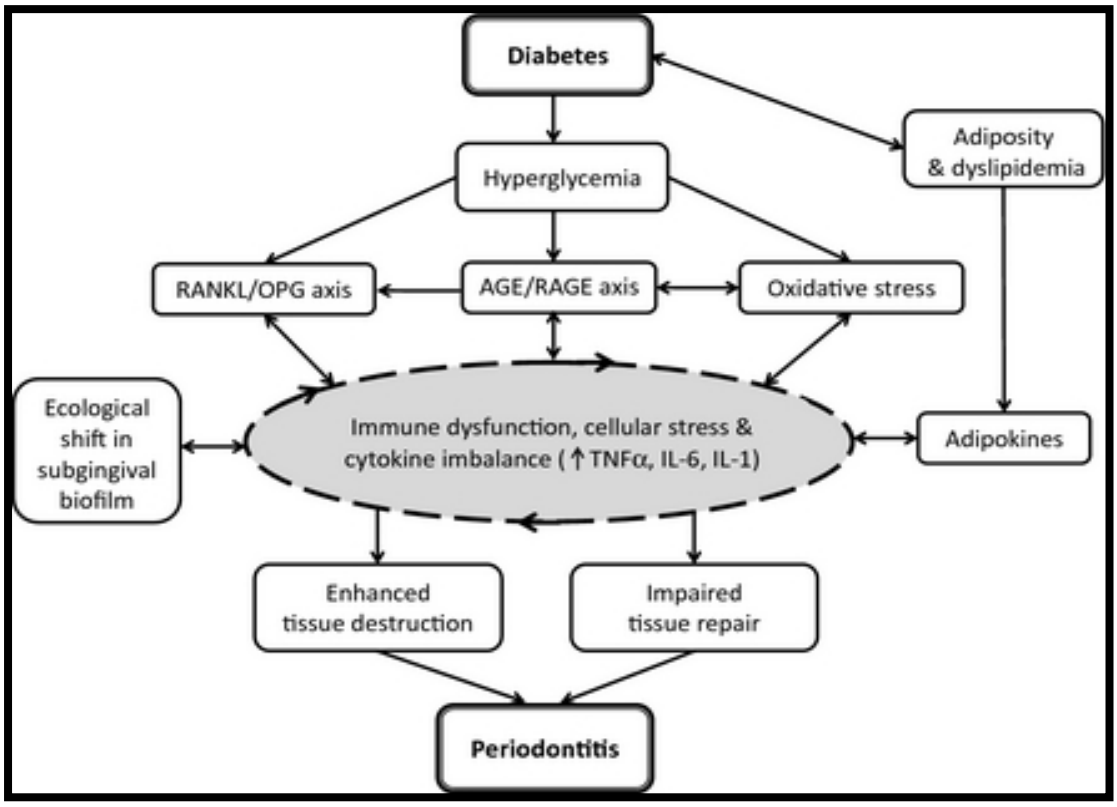

Figure 6: Explanation of potential mechanisms participated in the pathogenesis of periodontitis in diabetes.
Essentially, several connotations between different components in the figure are bidirectional, for instance, the pro-inflammatory state promote the generation of AGEs, ROS, and adipokines, elevated the RANKL/OPG ratio and helps pathogenic subgingival bacteria thrive. It is also essential to note the following; a) the quantity and quality of evidence supporting the various pathways varies, and b) even though the aim is to describe the major mechanisms and networks in the literature, other pathways and links between the various elements shown do exist, but cannot simply be illustrated in a single schematic. Finally, the processes outlined are possibly changed by several other factors, such as genetics, age, smoking, stress, all of which may contribute significantly to inter-individual variations in disease experience. Adopted from (Taylor et al., 2015).

1.3.6 Inflammation

Both T1DM and T2DM are associated with increased levels of systemic markers of inflammation (Dandona, 2004). Microvascular and macrovascular complications are partly driven by low-grade inflammation. Hyperglycaemia activates multiple pathways that increase inflammation, oxidative stress and apoptosis (Brownlee, 2005). In diabetes and obesity, there is elevation in serum levels of IL-6 and TNF-α. Future occurrence of T2DM is predicted by serum levels of IL-6 and C-reactive protein (CRP). There is an association with elevation of CRP

level and insulin resistance, T2DM and CVD. The main inducers of acute-phase proteins and CRP are TNF-α and IL-6. These both impair insulin signalling which potentially contributing to insulin resistance (Preshaw et al., 2013). In patients with periodontitis, serum levels of IL-6 and CRP are also elevated, with IL-6 levels associating with the degree of disease (Paraskevas et al., 2008). Periodontal disease may be exacerbated by the systemic low-grade inflammation of the diabetic state. In addition, adipokines and the proinflammatory properties of leptin may contribute to periodontal inflammation in obese subjects and patients with T2DM (Preshaw et al., 2007). Diabetes causes increased inflammation in periodontal tissues. For example, GCF, a fluid exudate that flows from the gingival margins, contains increased PGE2 and IL-1β in patients with T1DM with gingivitis or periodontitis compared with non-diabetic subjects with periodontal disease (Salvi et al., 1997). Patients with T2DM and poor glycaemic control, HbA_{1c} >8%, had higher IL-1β in GCF compared with patients with T2DM and HbA_{1c} <8%. Both HbA_{1c} and plasma glucose concentration were independently linked to increased IL-1β level in GCF (Engebretson et al., 2004).

When exposed to LPS, greater levels of TNF-α, IL-1β and PGE2 were produced from monocytes of patients with T1DM compared with monocytes from non-diabetic subjects. There is increased TNF-α in T2DM and extends the inflammatory reaction to *Porphyromonas gingivalis* (a periodontal pathogen normally found in the biofilm of patients with advanced periodontitis) (Naguib et al., 2004). Treatment of periodontal diseases showed a significant decrease in serum levels of inflammatory mediators, such as IL-6, TNF-α, CRP and MMPs, in patients with and without diabetes (O'Connell et al., 2008).

1.3.7 Biochemical mechanisms of periodontitis

1.3.7.1 Inflamatory signaling

Multiple pro-inflammatory cytokines are involved in the periodontitis immunopathology. Some of the most important cell signalling molecules involved in periodontium destruction are triggered by responses to TNF-α and IL-1β. These cytokines are increased in diseased periodontal sites throughout periods of active disease and tissue destruction. Furthermore, they are considerably decreased after periodontal treatment and return to the healthy tissues state (Iacopino, 2001).

IL-1β facilitates many processes, including recruitment of inflammatory cells, degranulation of PMNs, synthesis of inflammatory mediators PGE and MMPs, inhibition of collagen synthesis, and activation of both T and B lymphocytes. TNF-α is a major inducer of cell apoptosis, resorption of bone, secretion of MMPs, expression of intercellular adhesion molecule (ICAM), and production of IL-6. Once IL-6 produced, it promotes osteoclasts formation, osteoclastic bone resorption, and T-cell differentiation (Iacopino, 2001).

Increased serum proinflammatory cytokine levels occur in periodontitis. It has been hypothesized that periodontitis-induced proinflammatory cytokines elevations such as IL-1β and TNF-α. This elevation in cytokines can show a significant role in progress of many systemic diseases. Therefore, advanced periodontitis patients may be considered as systemically compromised even in the absence of obvious clinical symptoms of disease (Iacopino, 2001).

Destruction of the periodontal tissue detected in periodontitis is host-mediated by releasing pro-inflammatory cytokines. The pro-inflammatory cytokines are released by local tissues and immune cells as a response to the bacterial fragments, immunogenic factors and metabolites, specifically LPS. Key cell signalling by LPS is mediated by binding of CD14 and the Toll-like receptor-4 (TLR4) (Cohen, 2002) – Figure 7 .

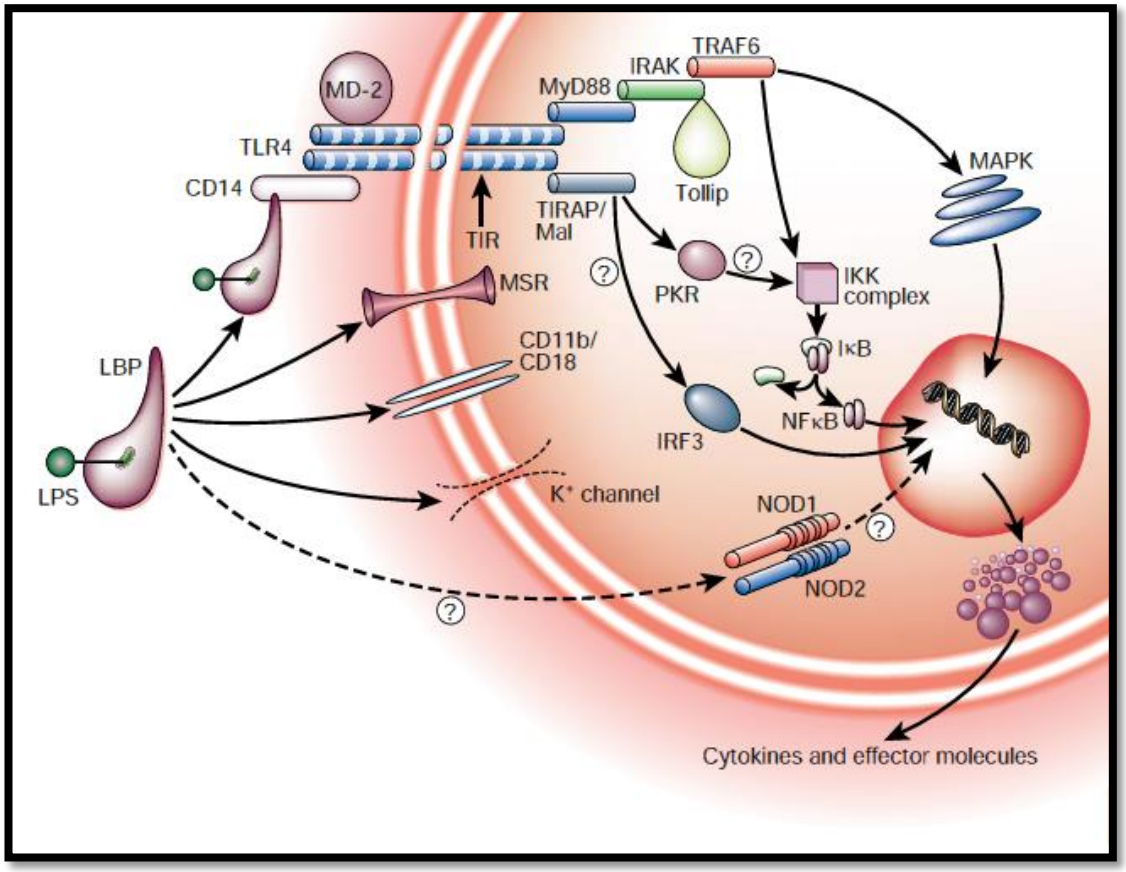

Figure 7: Cell-surface recognition of lipopolysaccharide (LPS).
From (Cohen, 2002). LPS is sensed via an LPS-binding protein (LBP)–LPS complex and then signalling through the Toll-like receptor 4 (TLR4)–MD-2 complex. Other cell surface molecules also sense LPS: macrophage scavenger receptor (MSR), CD11b/CD18 and ion channels. Intracellularly, TLR domain, TIR (Toll/IL-1 receptor homology domain), binds to IRAK (IL-1 receptor-associated kinase) facilitated by two adapter proteins, MyD88 (myeloid differentiation protein 88) and TIRAP (TIR domain containing adapter protein; also called MyD88-adapter-like protein or Mal), and inhibited by a third protein Tollip (Toll-interacting protein) (Cohen, 2002).

The mechanisms mediating inflammation driven periodontal ligament cell cytokine and chemokine expression are as follows. LPS binds to its receptor, TLR4, and this complex controls gene transcription of cytokine and chemokine genes through adaptor proteins and transcription factors (Dauphinee and Karsan, 2005, Covert, 2005). TLR4 signalling includes myeloid differentiation protein 88 (MyD88) -dependent and -independent pathways causing stimulation of nuclear factor-kappa-B (NF-kB). The MyD88-independent signalling includes stimulation of the adaptor molecule TRAM, which procedures a complex with TRIF. Then, this complex binds the adaptor protein tumor necrosis factor receptor associated factor-6 (TRAF6), causing stimulation of NF-kB. Both the MyD88-dependent and -independent

activation of NF-kB prompts inflammatory genes expression. Therefore, NF-kB is a promising drug target for anti-inflammatory treatment. In a murine periodontal ligament cell line, Patil et al have displayed that *Actinobacillus actinomycetemcomitans*- and *Escherichia coli*-derived LPS induced IL-6 expression is dependent on multiple MAPK pathways, invloving ERK and c-jun N-terminal kinase (JNK), representing that many intracellular signalling pathways control periodontal ligament cell cytokine gene activity (Patil et al., 2006, Jönsson et al., 2011).

1.4 Glycation

1.4.1 Definition of glycation

Glycation is the non-enzymatic reaction of sugars or related derivatives with proteins, nucleic acid and basic phospholipids. In this project, I focus on glycation of proteins in physiological systems. Protein glycation occurs by a sequence of successive and parallel reactions known as the Maillard reaction (Rabbani and Thornalley, 2012b). Early stage glycation adducts are those formed by reaction of glucose and other monosaccharides with N-terminal and lysine residue side-chain amino groups to form initially a Schiff's base intermediate which then undergoes a slow rearrangement, Amadori rearrangement, to from a ketoamine or Amadori product. For glycation of proteins by glucose, the Amadori products are N_{α}(1-deoxyfructos-yl)amino acid and N_{ε}(1-deoxyfructos-yl)lysine residues; these are often called trivially fructosyl-amino acid or fructosyl-lysine residues. These adducts may undergo reverse reaction, enzymatic repair initiated and catalysed by fructosamine 3-phosphokinase or slowly degrade to form stable end-stage products called advanced glycation endproducts (AGEs) (Rabbani and Thornalley, 2008a) (Rabbani and Thornalley, 2012a). α-Oxoaldehydes or dicarbonyls present in physiological systems such as methylglyoxal (MG), glyoxal and 3-deoxyglucosone (3-DG) react with proteins directly to form AGEs (Rabbani and Thornalley, 2008a) (Rabbani and Thornalley, 2012b). They react predominantly with arginine side-chain guanidino groups to form hydroimidazolone adducts.

Protein glycation leads to structural distortion, change in ionisation status and functional change or inactivation of proteins and thereby mediates cell and tissue dysfunction. The steady-state level of protein glycation is usually ≤ 5% of protein substrate and thereby may impact little on protein function. When the modified

protein has a different pathogenic function - for example increased binding of MG-modified low-density lipoprotein (LDL) to arterial walls or markedly decreased affinity of MG-modified collagen IV for surface integrin proteins of endothelial cells – then it is particularly insidious. Also, when glycation accelerates the degradation of proteins, it effectively decreases the half-life of the protein substrate and if there is no compensatory increase in protein synthesis then the steady-state concentration of the unglycated will decrease. By such mechanisms, glycation affects the concentrations of also unglycated proteins. Therefore, it is possibly that protein glycation may produce cell and tissue dysfunction, impairing normal physiological function and contributing to disease. For this reason, glycation is termed a type of protein damage (Thornalley and Rabbani, 2011b, Rabbani and Thornalley, 2015).

1.4.2 Historical background of glycation

In 1908, Arthur Robert Ling developed a process involving thermal drying of proteins with sugars, which produced a coloured and flavoured mixtures. He termed referred to the formation of browning pigments after heating the glucose with asparagine (Ling, 1908). These were the first documented adducts formed between amino acids and glucose. Louise Camille Maillard (1912) – considered the founder of glycation research - studied the reaction between glucose and glycine on heating. He suggested that brown pigments produced, melanoidins, were formed by an initial reaction between amines and saccharides that produced Schiff's base adducts. The name given to this reaction and related parallel and sequential reaction is the "Maillard reaction".

In 1913, the glyoxalase system was discovered. It is an important system catalysing MG to D-lactate in physiological systems (Dakin and Dudley, 1913, Neuberg, 1913).

Between 1925 and 1931, Mario Amadori discovered that the condensation of D-glucose with aromatic amines p-phentidine, p-anisidine or p-toluidine form two different structure of isomers which were not anomers (Amadori, 1929a). He found one of the isomers is more liable to hydrolysis and vulnerable to decomposition on standing in the solid state in air. He identified this as N-glycosylamine. Conversely, he incorrectly assumed that the Schiff's base was the more stable isomer, overlooking its resistance to hydrolysis by acid (Amadori, 1929b). Then, Kuhn and Dansi (1936) stated that the stable isomer was the product of a molecular

rearrangement instead of a Schiff's base. They also confirmed Amadori finding about the labile isomer, the N-substituted glycosylamine (Kuhn R and Dansi A, 1936). In 1937 Kuhn and Wegand found the structure of the stable isomer. It is the unbranched N-substituted 1-amino-1-deoxy-2-ketose (Kuhn R, 1937). Later, the reaction was called the Amadori rearrangement, involving the reaction of aldoses with amines. In 1953, Hodge suggested that formation of a Schiff's base followed by Amadori rearrangement is involved in the initial stages of the Maillard reaction. In addition, He suggested enolisation, oxidation and fragmentation reactions are contributed in fructosamine degradation to glucosone and other adducts (Hodge, 1953).

In 1958, Allan *et al*. described the first observation of glycation of a protein *in vivo*. They found a glycated variant of haemoglobin, HbA_{1c}, identifying it as a negatively charged component of human blood cell haemoglobin (Allen et al., 1958). Bookchin and Gallop (1968) studied glycated haemoglobin and described its elevation in diabetes (Bookchin and Gallop, 1968). Bunn et al (1975) described reactions which explain the creation of glycated haemoglobin (Bunn et al., 1975). In 1976, Anthony Cerami and his colleagues suggested the use of glycated haemoglobin HbA_{1c} as an indicator for the glycaemic control in patients with diabetes (Peterson et al., 1977). The value of HbA_{1c} is now a common clinical diagnostic marker of glycaemic control in diabetic patients (ADA, 2015).

Anet in 1960 described the degradation of a fructosamine (N,N-difructosylglycine) to 3-deoxyglucosone (Anet, 1960). Kato successfully isolated 3DG and 3-deoxypentosone from the browning reactions of amine with glucose and ribose (Kato, 1960, Kato et al., 1988). In biological systems, the reactive α-oxoaldehydes are essential precursors of formation of glycation adducts (Nass et al., 2014).

Bonsignore in 1973 reported the first indication of formation of MG by non-enzymatic degradation of triosephosphates to MG under physiological conditions and the degradation of glyceraldehyde-3-phosphate to MG (Bonsignore et al., 1973). In 1977, Takahashi described the reaction between amino-acids and glyoxal derivatives containing glyoxal and MG. Then, arginine was identified as the main amino acid altered and hydroimidazolone was one molecular structure suggested for adducts. However, no analytical data was presented to prove the suggestion (Takahashi, 1977). Later, the formation of hydroimidazolone adducts was confirmed. Then,

hydroimidazolones in the physiological systems and some foods found to be a principal AGE (Thornalley et al., 2003b, Henle et al., 1994). The formation of α-oxoaldehydes by fragmentation of saccharide moiety early in the Maillard reaction, this evidence was provided by Hayashi and Namiki (1980). This is called the Namiki pathway of the Maillard reaction, involving the formation of glyoxal and MG by saccharide fragmentation (Hayashi and Namki, 1980, Rabbani et al., 2010). Dicarbonyls are also formed by monosaccharide auto-oxidation as the slow oxidative degradation of monosaccharides under physiological conditions to form the respective α-oxoaldehydes and hydrogen peroxide (Wolff et al., 1984).

Nakayama et al (1980) defined the formation of 6-(2-formyl-5-hydroxymethylpyrrol-1-yl)-L-norleucine from 3-DG and lysyl residues in proteins known as AGE – pyrraline (Nakayama et al., 1980).

A product formed by degradation of Amadori product, 2-(2-furoyl)-4(5)-(2-furanyl)-1H-imidazole (FFI), was reported in 1984, (Pongor et al., 1984). This was later found to be an artefact – formed in pre-analytic processing (Obayashi et al., 1996).

The phrase "advanced glycation endproducts" (AGEs) was first used in 1986 by Cerami to refer them as "brown fluorescent pigments which cross link proteins" (Cerami, 1986). Brownlee and his colleagues found elevated collagen cross-linking in the arterial walls of diabetic rats and related fluorescence features of AGE compounds. The nucleophilic hydrazine derivative, aminoguanidine – later given the trademark name (Pimagedine^{TM}) - was studied as a prototype AGE inhibitor and diabetes-induced protein cross-linking (Brownlee et al., 1986).

Baynes and co-workers described the formation of N_{ε}(carboxymethyl)lysine (CML) and erythronic acid from degradation of proteins glycated by glucose and later the presence of both compounds in human urinary metabolite was reported (Ahmed et al., 1986). CML is also formed by the reaction of lysine residues with ascorbate and glyoxal formed in lipid peroxidation (Thorpe and Baynes, 2002).

Thornalley (1988) presented evidence of link between hyperglycaemia in diabetes, elevated flux of formation and concentration of MG and its potential involvement as main pathway causing the appearance of diabetic vascular complications (Thornalley, 1988) and reported 3 – 5 fold increase in MG concentration in blood samples of patients with T1DM and T2DM (McLellan et al., 1994a). In 2001 Brownlee included glycation by MG one of the major metabolic

pathways involved in the appearance of diabetic vascular complications (Brownlee, 2001). Between 1994 and 1998, clinical trials (ACTION I and ACTION II) for the avoidance of obvious nephropathy were conducted using the AGE inhibitor Pimagedine^{TM}. However, due to safety reasons and obvious absence of efficacy these trials were later terminated (Thornalley, 2003c).

In 1989, Sell and Monnier discovered an acid stable fluorescent compound formed by the glycation of collagen and called it pentosidine (Sell and Monnier, 1989). Pentosidine is a crosslink formed by a pentose moiety with lysine and arginine residues (Sell and Monnier, 1989).

Horiuchi and Kurokawa (1991) discovered the enzymatic metabolism of fructosamine adduct. It was reported that the fructosyl-amino acid oxidase catalysed the transformation of fructosyl-amino acids to free amino acid, glucosone and hydrogen peroxide (Horiuchi and Kurokawa, 1991). Later, Delpierre *et al*. (2000) discovered an enzyme that catalysed the phosphorylation of fructosamine and fructosamine residues forming fructosamine-3-phosphate (F3P). This enzyme called fructosamine 3-kinase. F3P fragments spontaneously resulting in de-glycation and repair of early glycated proteins.

Schmidt et al (1992) identified a cell surface protein that bound proteins highly modified by AGEs prepared *in vitro*. This was called an AGE receptor and was initially found in bovine lung endothelial cells and had a sequence molecular mass of 42 kDa (Schmidt et al., 1992). This is the best recognised AGE receptor called the receptor for advanced glycosylation end products (RAGE).

In 1996, Cerami *et al*. proposed the concept of AGE breakers, which were defined as compounds that may cleave glycation-derived crosslinks and reverse one of the damaging of glycation associated with ageing and disease. N-phenacylthiazolium bromide (PTB) was the prototype compound (Vasan et al., 1996). This and associated analogues had stability problems and the claimed complete breaking of crosslinks was rather slowing of the putative AGE breaker reaction by spontaneous degradation of PTB and acidification of incubations and cell cultures (Thornalley and Minhas, 1999, Price et al., 2001).

Shipanova and his colleagues (1997) identified argpyrimidine - a fluorescence AGE formed from MG (Shipanova et al., 1997). Vlassara and co-workers (1997) suggested the term “glycotoxins” to refer to highly reactive AGE

intermediates and created a series of current studies, assessing the physiological effects on AGEs in diet on health (Koschinsky et al., 1997).

Since 2000, there is a marked advances in glycation – particularly in relation to improved quantitation of glycation adducts and free adducts by stable isotopic dilution analysis LC-MS/MS (Thornalley et al., 2003b, Thornalley et al., 2010). Application of high resolution mass spectrometry proteomics was identified proteins susceptible to glycation by glucose and by MG (Rabbani and Thornalley, 2014a, Zhang et al., 2007, Schmidt et al., 2015). Pre-clinical models with genetically controlled increased exposure to glycation – F3K knockout mice and glyoxalase 1 (Glo1)-deficient mice (da-Cunha et al., 2006, El-Osta et al., 2008), and decreased glycation exposure – Glo1 transgenic mice (Inagi et al., 2002), have been developed and employed in studies of glycation in health and disease. The concept of "dicarbonyl stress" has emerged defined as the abnormal accumulation of dicarbonyl metabolites leading to increased protein and DNA modification contributing to cell and tissue dysfunction in ageing and disease. This explains the involvement of dicarbonyl glycation in health decline in ageing and in disease – particularly diabetes and its vascular complications, CVD, renal failure, schizophrenia, Parkinson's disease, carcinogenesis and mechanisms of action of anticancer drugs and Glo1 overexpression in multi-drug resistance – reviewed in (Rabbani and Thornalley, 2015)

The concept of AGE receptors has been well-investigated and role in health and disease has been best developed for RAGE. Even its involvement in responses to glycated porteins has been questioned and non-glycation ligands considered to be major phsyiological agonists. The link of RAGE to glycation was further complicated by suggestion that activaion of RAGE is linked to downregulation of Glo1, increasing sensitivity to dicarbonyl stress (Thornalley, 2007).

Roles for glycation in ageing, obesity and chronic disease have been advanced – particularly for diabetic complications (Ahmed et al., 2005a), renal failure (Agalou, 2005, Miyata et al., 2001), cardiovascular diseases, Alzheimer's, uremia, g (Ahmed et al., 2004, Chen et al., 2004, Rabbani et al., 2010), arthritis and cirrhosis (Ahmed et al., 2004), schizophrenia (Arai et al., 2010, Hambsch et al., 2010) Parkinson's disease (Kurz et al., 2010), carcinogenesis (Zender et al., 2008) and multidrug resistance (Santarius et al., 2010, Thornalley et al., 2010).

Treatments emerging from glycation research are dicarbonyl scavengers and Glo1 inducers. Treatments under current investigation are pyridoxamine as a dicarbonyl scavenger and small molecule Glo1 inducers (Lewis et al., 2012, Rabbani et al., 2014b) such as sulforaphane (Xue et al., 2012a) *trans*- resveratrol and hesperetin (Xue et al., 2016).

1.4.3 Molecular structures of advanced glycation end-products

AGEs are a heterogeneous collection of complex compounds (Thornalley et al., 2003b, Rabbani and Thornalley, 2008b). Examples are shown in Figure 8.

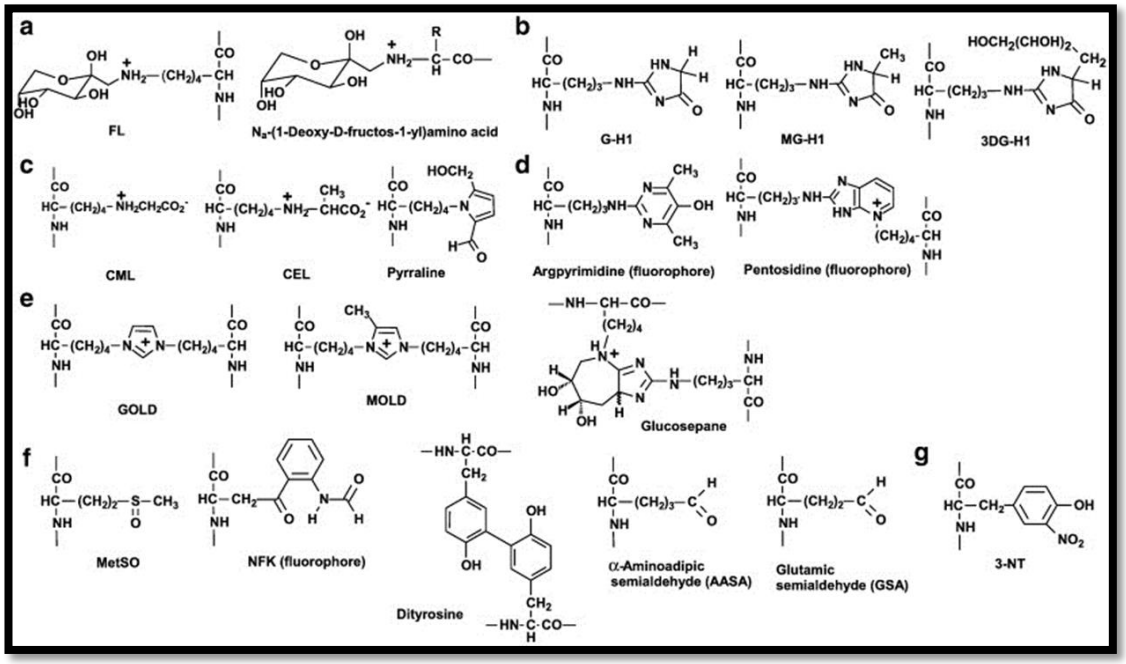

Figure 8: Protein glycation, oxidation and nitration adduct residues in physiological systems.
(a) Early glycation adducts - FL and Nα-(1-deoxy-D-fructos-1yl) amino acid residues. Advanced glycation endproducts: (b). Hydroimidazolones, (c). Monolysyl (d). Fluorophores, AGEs, (e). Non-fluorescent crosslinks, (f). Oxidation marker and (g). Nitration marker. From (Thornalley and Rabbani, 2014).

1.4.4 Biochemical and physiological effects of protein glycation

Glycation of proteins in physiological systems is generally minimal; that is, typically 0.5 – 10% proteins have one glycation adduct residue. Formation of FL residues increases steric demand on the immediate environment of the glycation site but does not change side positive charge (Röper et al., 1983). Formation of CML and CEL residues has a moderate increase in steric demand on the immediate

environment of the glycation and also adds a negative charge whilst preserving side chain positive charge. Hydroimidazolone formation increases steric demand and causes loss of positive charge. Arginine-derived hydroimidazolone formation is damaging because arginine residues have the highest probability of all amino acid residues types to be located at a functional site in a protein and loss of positive charge produces loss of functional interaction (Rabbani and Thornalley, 2012c). Functionally important arginine residues are also typically those reactive towards glycation as they are located at surface domains with polarisable electronic charge (Rabbani and Thornalley, 2012c).

Susceptible sites for lysine and arginine glycation are thought to be those with activating positive and negatively charge amino acid residues close, 3 – 4 residues distant, in the primary sequence but this has to be confirmed experimentally (Rabbani and Thornalley, 2012c). Protein glycation therefore usually causes minor loss of function of proteins. The physiological consequence of this is particularly important where this change in function of a minor fraction of total protein has a major physiological effect. Examples are:

(i) AGE modification of the integrin binding sites of vascular type IV collagen leading to endothelial cell detachment, exposure of the subendothelium and increased risk of thrombus formation (Dobler et al., 2006, Yamagishi et al., 2005).

(ii) AGE damage of mitochondrial proteins leading to increased ROS leakage from the mitochondria and increased oxidative stress (Morcos et al., 2008).

(iii) modification of the neural voltage gate sodium channels by methylglyoxal causing hyperalgesia in diabetic neuropathy (Bierhaus et al., 2012).

(iv) glycation of plasminogen in diabetes leading to reduction in plasmin generation and function (Ajjan, et. al, 2013), and

(v) methylglyoxal modification of LDL producing atherogenic small dense LDL (Rabbani et al., 2011).

(vii) methylglyoxal modification of HDL producing decrease concentration in plasma and loss of function of HDL (Godfrey et al., 2014).

A further effect of protein glycation is formation of non-sulfhydryl crosslinks. AGE-mediated cross-linking of proteins leads to decreased protein solubility and susceptibility to enzymatic digestion (Schnider and Kohn, 1981) which is particularly important when affected proteins such as connective tissues and extracellular matrix sustain such damage that leads to changes in their mechanical and structural

properties - increased rigidity and thickening of the capillary basement membrane. These changes are associated with ageing (Lee, 1993, Cardenas-Leon et al., 2008). Glycation inhibits the formation of soluble collagen fibrils *in vitro* and it does so without denaturing the collagen molecules. This was found to be accompanied by a decrease in lysyl oxidase-catalysed crosslink formation (Lien, et. al, 1984, Oliveira, et. al, 2011). X-Ray diffraction indicated that glycation caused an increase in intermolecular spacing in the collagen fibril, resulting in progressive expansion of the molecular packing and ultimate loss of the lattice structure (Tanaka et al., 1988, Brownlee, 2001). In contrast, glycation of insoluble tendon collagen resulted in the formation of intermolecular cross-links, leading to increased collagen rigidity (Kent, et. al, 1985, Couppé, et. al. 2009). This difference of effect of glycation may be due to the greater proximity of the peptide chains in tendon collagen, which are tightly cross-linked and susceptible to further cross-linking by glycation.

1.4.5 Receptor of advanced glycation end products (RAGE)

The observation of cell activation and dysfunction following exposure of cultured cells to proteins highly modified by AGEs led to the hypothesis of cell surface receptors that bind specifically AGE-modified proteins or AGE receptors – reviewed in (Thornalley, 1998a). Studies were often misleading for physiological function, however, because glycation proteins prepared *in vitro* had *ca*. 38 - 52 adducts per mol protein substrate and contained aggregates whereas proteins glycated *in vivo* are minimally modified with rarely more than one glycation adduct per mol protein and are not aggregated (Matsumoto et al., 2000, Westwood and Thornalley, 1995). Highly glycated proteins prepared *in vitro* have markedly different physiological interactions. For example, albumin glycated highly by glucose *in vivo* containing *ca.* 40 molar equivalents of glycation adducts had a plasma half-life of 1.2 h in rats and was mainly cleared from circulation in the liver (Matsumoto et al., 2000); whereas albumin glycated minimally glycated to the level found in diabetes had a half-life in rats of 47 h - similar to un-glycated albumin and is metabolized in the kidney and elsewhere by normal routes of albumin catabolism (Johnson et al., 1991) and analysis of glycation adduct content of plasma protein in blood flow into and out of the liver in human subjects gave no indication of glycated protein removal in the liver (Ahmed et al., 2004). This has prompted a reappraisal of putative AGE receptors. Proposed AGE receptors 1, 2 and 3 and scavenger receptors

are unlikely to have an AGE receptor function *in vivo* – as discussed (Ahmed and Thornalley, 2007). A further putative AGE receptor is RAGE.

RAGE is a cell surface receptor and has a well-substantiated role in vascular cell dysfunction (Schmidt et al., 1995, Yonekura et al., 2003, Chavakis et al., 2003). It is a member of the immunoglobulin superfamily of proteins and structurally has an extracellular V-shaped domain of 320 amino acids with two N-linked oligosaccharides, a membrane spanning domain of 21 amino acids and a short cytoplasmic domain of 41 amino acids. The V domain is responsible for most extracellular ligand binding. For intracellular signalling, the cytoplasmic tail is assumed to be essential and possibly mediate cellular migration (Sparvero et al., 2009). RAGE is associated with advance host responses in many pathological conditions such as diabetes, chronic inflammation, tumours, and neurodegenerative disorders (Sparvero et al., 2009).

Recent research indicated binding of albumin minimally modified with MG occurs to the V-domain of the RAGE with a binding constant K_D of 800 nM. There is a competitive binding by MG-H1 and related hydroimidazolone isomer-containing peptides which suggests MG-H1 is specifically recognised (Xue et al., 2014). In plasma of healthy human subjects, the concentration of MG-H1-albumin is *ca.* 4.5 μM (Ahmed et al., 2005b). In human monocytes *in vivo*, the RAGE protein copy number is 37,000 per cell (Hou et al., 2004), equivalent to a concentration of *ca.* 130 nM. Therefore, it is expected that RAGE be always saturated with MG-modified protein ligand which suggests this binding may be non-productive for activation of signal transduction. Recently, some studies indicate heparan sulfate-RAGE complexes are essential for mediating signal transduction (Xu et al., 2013) and heparan sulfate may decrease binding affinity for MG-modified protein such that there is limited binding in healthy subjects. In addition, RAGE has high affinity homophilic binding with K_D of 470 nM facilitating cell-cell interaction. This decreases the availability of the cellular RAGE for AGE-modified protein binding (Sessa et al., 2014).

RAGE was isolated initially from endothelial cells of bovine lung (Neeper et al., 1992). Human microvascular pericytes, endothelial cells and other cells express splice variants of RAGE: N-terminal truncated, C-terminal truncated and full length forms; only the latter two bound AGE-modified protein (Yonekura et al., 2003). The endogenous secreted C-terminal truncated RAGE, called endogenous secreted RAGE

(esRAGE), lacks the cytoplasmic and transmembrane domains of RAGE and is expressed in several human tissues (Cheng et al., 2005). Recombinant DNA techniques were used to produce a similar C-terminal truncated RAGE called soluble RAGE (sRAGE) (Park et al., 1998). esRAGE and sRAGE act as decoy receptors for RAGE ligands endogenously and experimentally, respectively, and thereby influence RAGE-ligand interactions and signalling. RAGE transgenic and knockout mice have provided functional genomic models to identify roles of RAGE in several disease states – particularly where an inflammatory mechanism is involved: atherosclerosis (Sakaguchi et al., 2003), sepsis (Liliensiek et al., 2004) and others - Figures 9 and10.

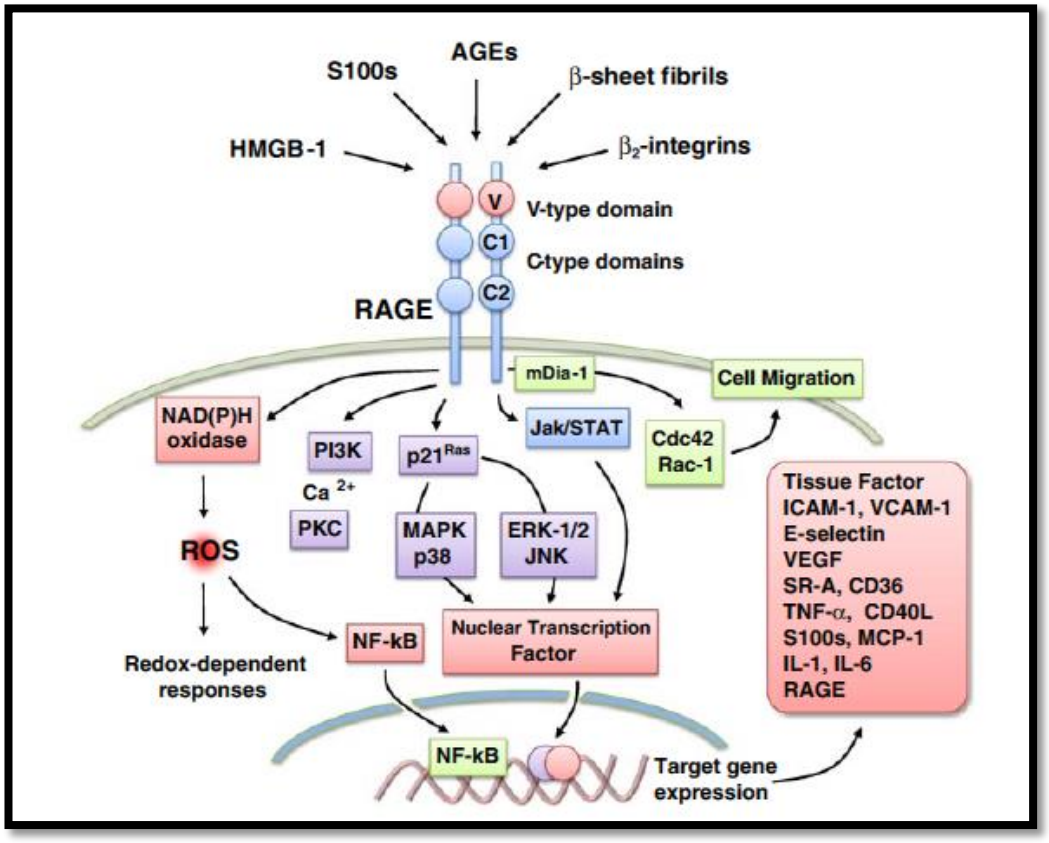

Figure 9: RAGE signal transduction pathways.
The engagement of RAGE stimulates the activation of a diverse array of signalling cascades, including mitogen activated protein kinases (MAPK), such as extracellular regulated (ERK)-1/2, p38 and c-Jun N-terminal kinase (JNK), Jak/STAT, phosphoinositol 3-kinase (PI3K), and members of the Rho GTPase signaling pathway (Cdc42 and Rac-1). RAGE activation may enhance the generation of ROS by activating NAD(P)H oxidase. RAGE-dependent responses converge to the activation of nuclear transcription factors, including nuclear factor (NF)-kB, and consequent target gene transcription. Other abbreviations: MCP-1 monocyte chemoattractant protein-1, mDia-1 mammalian Diaphanous-1, PKC protein kinase C, SR scavenger receptor. From (Vazzana et al., 2009).

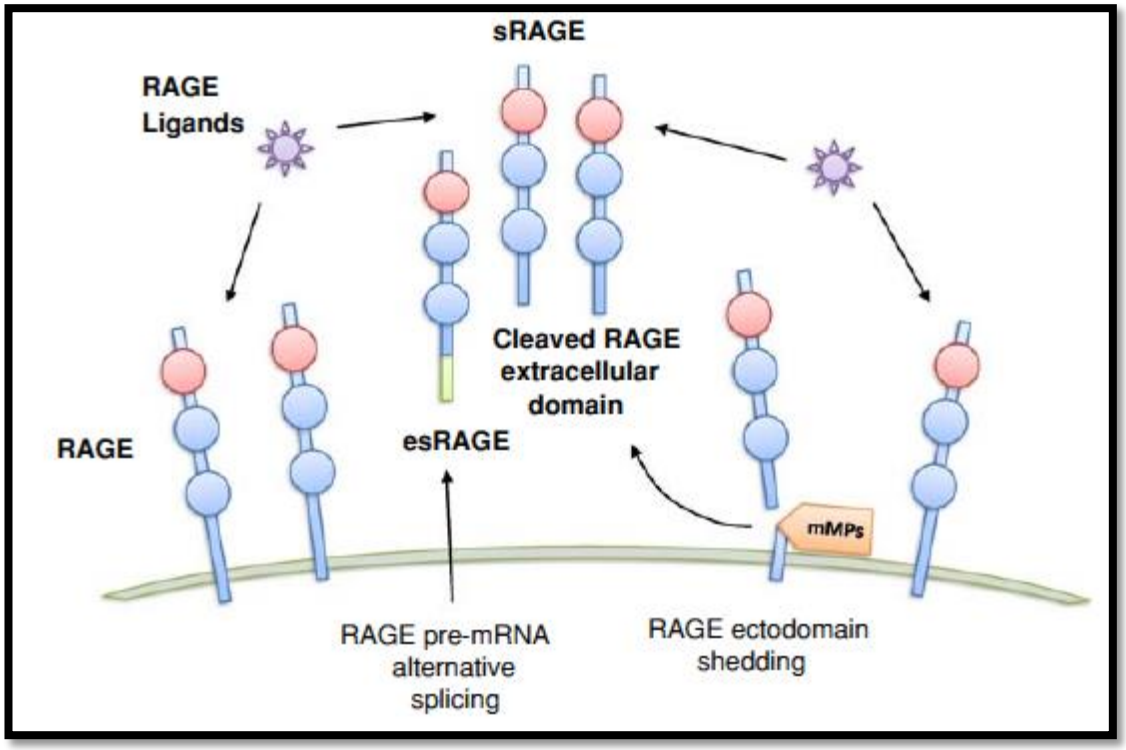

Figure 10: Soluble RAGE isoforms.
sRAGE consists in an heterogeneous population, comprising at least different isoforms: (1) the extracellular RAGE shedded form the surface receptor by the action of membrane-associated metalloproteinases (MMPs), such as ADAM-10 and MMP-9; (2) esRAGE, arising from RAGE pre-mRNA alternative splicing and characterised by a specific C-terminal sequence. Spanning the ligand-binding domain, sRAGE probably acts as a decoy for ligands, thus competitively inhibiting the engagement of cell-surface RAGE and other RAGE-ligand receptors. From (Vazzana et al., 2009).

The ligand(s) activating RAGE *in vivo* are less certain. It was initially thought that AGEs were the main activating ligands for RAGE. However, ligand binding activity is limited to only proteins highly-modified by AGEs and aggregated. Such proteins are rarely found in tissue and physiological fluids – but they are found in thermally processed foods and are ingested. Non-AGE ligands of RAGE are most likely agonist *in vivo*: high mobility group box-1 protein (HMGB1/amphoterin), and members of the S100/calgranulin protein family. RAGE binds members of the S100/calgranulin group of proteins: S100A12 (EN-RAGE) and S100b (Hofmann et al., 1999). Currently, cell activation by S100A12 and S100b appears to be a likely important function of RAGE *in vivo* – reviewed in (Thornalley, 2007). Activation of RAGE is linked to activation of the Ras/NF-kB signalling pathway (Yan et al. 1994, Huttunen, and Rauvala 1999).

1.4.6 Evidence for RAGE regulation of Glo1

The association of RAGE went a substantial revision following the work of Bierhaus and colleagues who found engagement of RAGE was associated with decreased expression of glyoxalase I (Glo1) (Bierhaus, 2006). Bierhaus found that induction of diabetes in wild-type mice decreased the expression of Glo1 whereas the induction of diabetes in RAGE (–/–) mice did not. Decreased Glo1 expression causes increased protein glycation (Thornalley, 2003b). The mechanistic interpretation of the association of RAGE expression and AGEs in tissues may, therefore, require reappraisal. The co-localization of RAGE and AGEs may be due to RAGE activation by S100 proteins (or other non-AGE agonists) decreasing the local expression of Glo1 and thereby increasing the local formation of AGEs. The functional role of decreasing Glo1 activity and increasing protein glycation by RAGE activation is not yet clear. This may be part of an inflammatory response leading to labelling proteins with dicarbonyl-derived hydroimidazolone AGE residues and directing these proteins to the proteasome for destruction. Methylglyoxal modification of proteins is thought to target proteins for proteasomal destruction (Du et al., 2006). If correct, this will link AGE formation to removal and destruction of proteins, at least for intracellular proteins – a "twist" or re-interpretation of the role originally attributed to the formation of AGE modified proteins by Cerami (Cerami, 1986).

The mechanism of down regulation of Glo1 expression by RAGE is unknown. It may occur by activation of NF-kB which then conflicts and blocks with signalling of transcription factor nuclear factor erythroid 2-related factor 2 (NFE2L2, or Nrf2) (Liu et al., 2008). Nrf2 regulates basal and inducible expression of Glo1 (Xue et al., 2012a) - Figure 11.

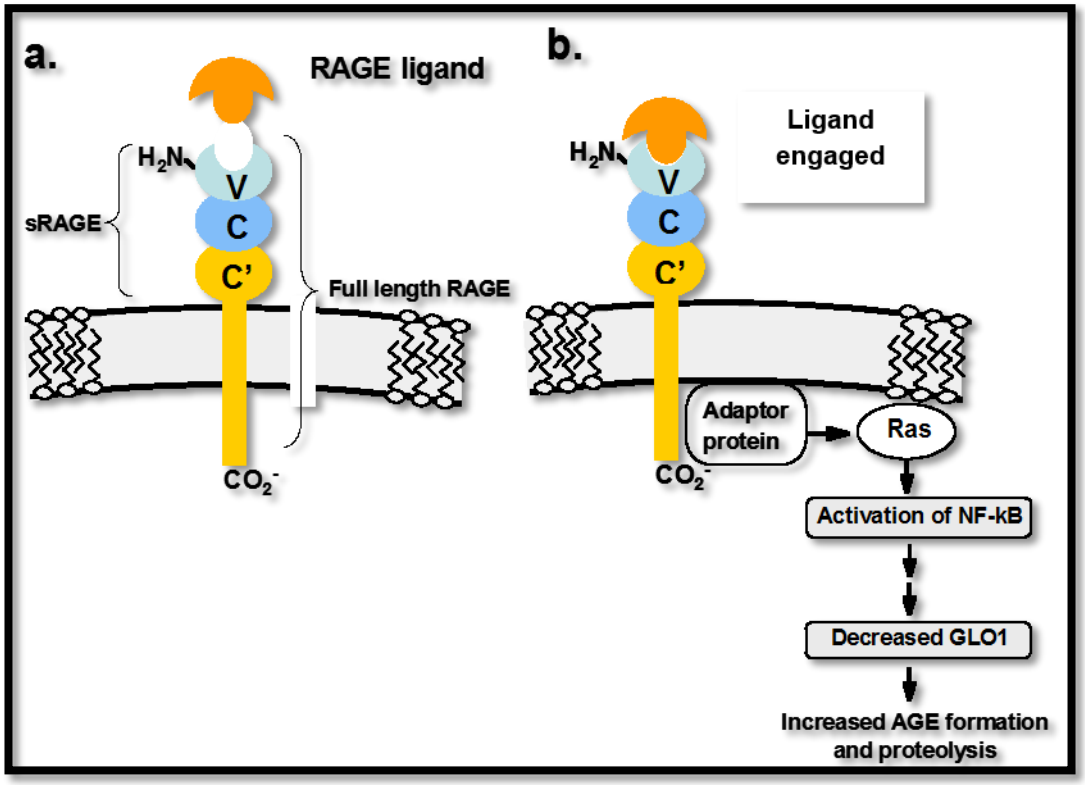

Figure 11: Model for down regulation of glyoxalase 1 by receptor for advanced glycation endproduct (RAGE).
(a.) Structure of RAGE and soluble RAGE (sRAGE). Key: V – variable region; C and C' conserved structural domains. (b.) RAGE signalling for down regulation of glyoxalase 1 (Xue et al., 2012a).

1.4.7 Evidence of involvement of glycation and RAGE in periodontal disease

The hyperglycaemic state of diabetes accelerates destruction of periodontal tissue. This destruction is caused by malfunction of polymorphonuclear leukocytes, changing of collagen metabolism and vascular permeability, reducing the viability and differentiation potential of cells within periodontium and shifting composition of microflora. In addition, hyperglycaemia increases the creation and accumulation of AGEs in plasma and tissues by oxidation and non-enzymatic glycation of proteins. AGEs can cause modification of matrix molecules cross-linking, impairment of the growth factors efficiency, elevation of oxidative stress in diabetic conditions, and exaggeration of inflammation significantly through interaction with the cellular RAGE (Chang et al., 2013). It has been found that glycation of collagen-I and fibronectin in PDL altered the PDL behaviour including reduction in cell migration which could contribute in impaired periodontal wound healing in diabetic individuals (Murillo et al., 2008).

Chang, et. al, (2012) found slight elevations of AGEs and RAGE with no histologic destruction in periodontium of animals with diabetes and without periodontitis. However, periodontal destruction in mice with diabetes and periodontitis was aggressive with evidence of AGE accumulation and increased RAGE expression. In addition, in healthy animals with periodontitis, increased AGEs and RAGE expression were found. The presence of the AGE-RAGE axis without diabetes implies that it is involved in the regulation of inflammation (Chang et al., 2013).

RAGE was found to be expressed in PDLF (Hasegawa, 2008). Hasegawa stimulated PDLF cells with HMGB1, with or without anti-RAGE, TLR2 and TLR4 antibodies, to measure IL-6 and IL-11 production using an enzyme-linked immunosorbent assay and mRNA expression was quantified by real-time PCR. PDLF cells expressed RAGE, TLR2 and TLR4 mRNA and production of IL-6 and IL-11 were augmented in PDLF cells stimulated with HMGB1. Hasegawa conclude that PDLF cells produce IL-6 and IL-11 in response to HMGB1 via RAGE, TLR2 and TLR4 (Hasegawa, 2008).

RAGE has a significant role in model periodontal disease. S100 proteins may be the most important activators and inflammatory mediators acting via RAGE *in vivo*. S100 has been proposed as important in periodontal disease and this may bind RAGE in PDL (Lalla et al., 2000). S100B was found to down regulate Glo1 in wild type fibroblasts cells but not in fibroblasts from RAGE knockout mice (Bierhaus et al., 2005a).

1.5 The Glyoxalase system

1.5.1 Enzymatic defence against glycation

The major enzymatic defence against MG glycation in physiological systems is provided by the glyoxalase system -Figure 12.

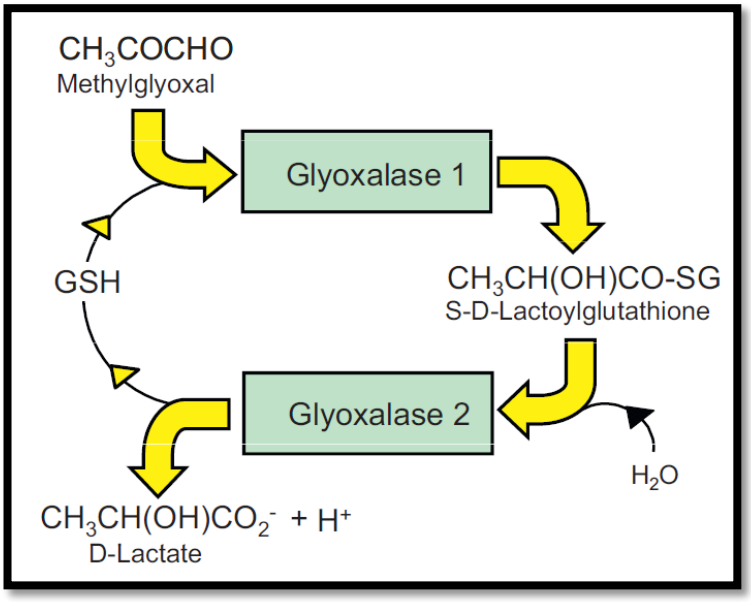

Figure 12: The Glyoxalase system and its metabolites.
From (Xue et al., 2011)

1.5.1.1 Glyoxalase system - definition and function

The glyoxalase system catalyses the metabolism of methylglyoxal (MG) to D-lactate via the intermediate S-D-lactoylglutathione. The glyoxalase system consists of two enzymes, glyoxalase 1 (Glo1) and glyoxalase 2 (Glo2) and a catalytic amount of reduced glutathione (GSH). The glyoxalase system is found in the cytosol or intracellular fluid of mammalian cells. It is present in animals, plants, bacteria, fungi and protoctista (Xue et al., 2011). The detoxification process of glyoxalase system contains two sequential reactions which follows the non-enzymatic construction of hemithioacetal from the MG CH_3COCHO reaction with GSH. Primarily, Glo1 influences the formation of S-D-lactoylglutathione $CH_3CH(OH)CO$-SG from the hemithioacetal.

$$\mathbf{CH_3COCHO + GSH \rightleftharpoons CH_3COCH(OH)\text{-}SG \rightarrow CH_3CH(OH)CO\text{-}SG}$$

For the methylglyoxal-glutathione hemithioacetal and human Glo1, the K_M is 71-130 µM and the k_{cat} is 7-11 x 10^4 min^{-1}. Secondly, Glo 2 catalyses S-D-lactoylglutathione to D-lactate and GSH. GSH will be consumed in the Glo1-catalyses reaction in the next circle (Xue et al., 2011).

$$\mathbf{CH_3CH(OH)CO\text{-}SG + H_2O \rightarrow CH_3CH(OH)CO_2^- + H^+ + GSH}$$

MG is the main physiological substrate for Glo1. MG significantly accumulates when Glo1 is suppressed *in situ* by decrease of GSH and in presence of cell permeable Glo1 inhibitors (Thornalley, 1993, Abordo et al., 1999, Thornalley et

al., 1996). Glyoxal, hydroxypyruvaldehyde $HOCH_2COCHO$ and 4,5-doxovalerate $H\text{-}COCOCH_2CH_2CO_2H$ are other substrates for Glo1 (Thornalley, 1993, Abordo et al., 1999, Thornalley et al., 1996, Thornalley, 1998c). The activity of Glo1 prevents the increase of these reactive α-oxoaldehydes and thus inhibits α-oxoaldehyde-mediated glycation reactions (Shinohara et al., 1998). Therefore, Glo1 is a main anti-glycation defence enzyme (Thornalley, 2003b, Thornalley, 2003a).

1.5.1.2 Histological development of glyoxalase system

The glyoxalase system was discovered in 1913 as an enzymatic system in physiological systems which catalysed the conversion of methylglyoxal to lactate (Neuberg, 1913, Dakin and Dudley, 1913). Later, the stereospecific formation of D-lactate appeared. Racker revealed in 1951 the presence of two consecutive steps catalysed by Glo1 and Glo2 were involved in the enzymatic system (Racker, 1951). Later in 1954, Racker proposed that D-lactate was the terminal product of metabolism of MG by glyoxalase system rather than L-lactate (Racker, 1954). Ekwall and Mannervik confirmed this later in 1974 (Ekwall and Mannervik, 1973). In 1960, studies on human arterial tissue showed decrease Glo1 activity with age (Kirk, 1960), which probably related with increased risk of cardiovascular disease with ageing.

Takahashi (1977) reported arginine-directed protein glycation by MG – the principal adduct found later to be a hydroimidazolone forming hydroimidazolone MG-H1 (Ahmed et al., 2002). In 1988, it was revealed that MG formation was increased in red blood cells incubated in high glucose concentrations *in vitro* (Thornalley, 1988). Thornalley and Atkins found an increase in Glo1 activity in STZ-induced diabetic and obese mice in 1989 (Atkins and Thornally, 1989). Then, Thornalley and his colleagues also noticed increased concentrations of MG, S-D-lactoylglutathione and D-lactate in patients with diabetes as compared to healthy controls (Thornalley et al., 1989).

In 1991, Wilson and his co-workers showed that Glo1 gene was a genetic factor related to body mass index (Wilson et al., 1991). Glo1 later was recognized as part of the human obesity genome.

In 1993, Philips and Thornalley measured the formation rate of the triosephosphates - GA3P and DHAP, under physiological conditions by using a specific MG assay. They found that *ca.* 0.1% glucotriose flux degraded to MG under

physiological conditions and this was the main source of MG formation in mammalian metabolism (Philips and Thornalley, 1993). In 1994, it was reported by Lo *et al*. that MG is a potent glycating agent forming AGEs (Lo et al., 1994b). In addition, it was shown that aminoguanidine was an effective MG scavenger and inhibited AGE formation to inhibit development of vascular complication of diabetes (Lo et al., 1994a).

In 1998, Shinohara reported a decrease in the accumulation of MG and associated AGEs as a consequence of overexpression of Glo1 in endothelial cells *in vitro* (Shinohara et al., 1998). In 1999, Abordo *et al.* described the accumulation of MG in cultured cells was linked with oxidative stress (Abordo et al., 1999). In the same year Beisswenger *et al*. reported a decrease in plasma concentration of MG in patients with T2DM receiving metformin therapy (Beisswenger et al., 1999).

Ranganathan *et al*. (1999) reported on GLO1 gene promoter analysis and revealed an insulin response element, displaying a possible association between expression of Glo1 and dysfunctions in diabetes (Ranganathan et al., 1999).

From 1989 to 2003, there were several studies describing a decrease in Glo1 and Glo2 activities and increase in MG and glyoxal derived AGEs with age in human and mouse tissues and cells (McLellan and Thornalley, 1989, Dunn et al., 1989, Dunn et al., 1991, Haik Jr et al., 1994, Ahmed et al., 1997, Sharma-Luthra and Kale, 1994). Pamplona *et al*. (2002) found a decrease in the MG-derived CEL residues in mitochondria of rat heart in case of long term caloric restriction (Pamplona et al., 2002). In 2003, Thornalley *et al*. developed stable isotopic dilution analysis LC-MS/MS methods for specific and sensitive measurement of MG-derived AGEs and found that MG-derived hydroimidazolone the major quantitative AGE in physiological systems (Thornalley et al., 2003b).

In 2006 Redon and his colleagues constructed a copy number variation (CNV) map. Glo1 was noticed to be positioned in one of the CNV regions (Redon et al., 2006). This was followed in 2009 by the finding that the non-transcribed region of Glo1 gene was a significant site of CNV in the genome of the mouse causing 4-fold alterations in expression of Glo1 (Cahan et al., 2009). In 2007 Zender *et al*. found in a genome-wide study of tumour suppressor genes that Glo1 was one of only 14 genes with tumour suppressor activity, likely linked to suppression of mutagenic MG-derived nucleotide AGEs, MGdG and CEdG (Zender et al., 2008, Thornalley et al., 2010). In 2008 Morcos *et al*. showed for the first time that Glo1 is a gene

influential on lifespan or "vitagene". Overexpression of Glo1 in *Caenorhabditis elegans* increased median and maximum lifespan by *ca.* 30% and silencing of Glo1 decreased lifespan by *ca.* 50% (Morcos et al., 2008).

In 2010, it was shown by Brouwers with his co-workers that Glo1 over-expression inhibited oxidative stress and endothelium dependent vaso-relaxation impairment in mesenteric arteries of diabetic rats. This implied to MG elevation in the diabetic state in initiation of vascular dysfunction and oxidative stress (Brouwers et al., 2010, Brouwers et al., 2011). Thornalley *et al*. presented that the major markers of physiological damage to genome is MG-derived DNA imidazopurinone MGdG adducts which are linked to DNA instability and mutagenesis *in vivo* (Thornalley et al., 2010). Santarius *et al*. discovered amplification of the GLO1 gene in human tumors. In 520 human tumours, amplification of Glo1 was noticed in *ca.* 8% with majority in breast cancer, 19%, small cell lung cancer (SCLC) 16% and non-small cell lung cancer (NSCLC) 11%. Glo1 amplification linked to increased Glo1 expression and multidrug resistance (Santarius et al., 2010).

In 2012, Xue *et al*. described the presence of a regulatory antioxidant-response element (ARE) in the 5'-untranslated region of exon 1 of the mammalian Glo1 gene. Transcription factor nuclear factor-erythroid 2 p45 subunit related factor 2 (Nrf2) binds to this ARE and increases basal and inducible expression of Glo1 (Xue et al., 2012a). Small molecule Nrf2 activators and Glo1 inducers are now providing the basis for development of Glo1 inducer functional foods to sustain healthy ageing and Glo1 inducer pharmaceuticals for treatment of vascular complications of diabetes and other diseases linked to dicarbonyl stress (Rabbani et al., 2014b).

1.5.1.3 Glyoxalase 1 - molecular properties, genetics and human polymorphism

Expression and activity of Glo1 is found in all human tissues. In fetal tissues, the specific activity of Glo1 is *ca.* 3 times higher than of similar adult tissues. In human tissues and blood cells there is approximately 0.2 μg Glo1 per gram of protein (Larsen et al., 1985).

The human GLO1 gene is located on chromosome 6 at band number 21.2. GLO1 gene is ~12.0kb in length and contains 6 exons and 5 introns (Gale and Grant, 2004). Expression of human GLO1 occurs at a diallelic genetic locus with alleles GLO^1 and GLO^2 in heterozygotes. These two alleles encodes for two related subunits

in heterozygotes. The enzyme of human Glo1 is a dimeric protein with 3 allozymes in heterozygotes designated as Glo1 1-1, Glo1 1-2 and Glo1 2-2. All allozymes have a molecular mass of 46 kDa (gel filtration) or 42 kDa (sequence), contain two zinc ions (one per subunit) and isoelectric point pI values of 4.8 - 5.1. Glo1 allozymes have unique charge densities and/or molecular shapes and may be resolved by ion exchange chromatography and non-denaturing gel electrophoresis resolved Glo1 allozymes (McLellan and Thornalley, 1991, Schimandle and Vander Jagt, 1979). Glo1 alleles are inherited in a simple co-dominant manner with the presence of characteristic expression of the phenotype (Thornalley, 2003b). The Glo1 translational product of human encloses 184 amino acids. There is a difference in amino acid sequence in the expression products of the two Glo1 alleles, only at position 111. There is an alanine residue in subunit Glo1-A, and there is a glutamic acid residue in subunit Glo1-E (Kim et al., 1995).

In post-translational processing, the N-terminal Met of Glo1 is removed and the N-terminal Ala is acetylated. Further phosphorylation and acetylation gives rise to several forms of differing pI (Xue et al., 2011). There is a vicinal disulphide bridge between cysteine residues 19 and 20. Cysteine-139 and cysteine-61 may also form of an intra-molecular disulphide. There is a mixed disulphide with glutathione on cysteine-139. N-terminal acetylation and C19/C20 disulphide formation did not affect Glo1 activity whereas glutathionylation on C139 strongly inhibited Glo1 activity *in vitro* (Birkenmeier et al., 2010). S-Nitrosylation by nitric oxide (NO) of Glo1 occurs on cysteine-139. C19 and C20 presence is important on S-nitrosylation which occurred on the acidic, α-form of Glo1 (De Hemptinne et al., 2007). The basic and reduced form of Glo1 is the NO-responsive, without intramolecular disulfide bonding (De Hemptinne et al., 2007). Glo1 is a substrate for calcium, calmodulin-dependent protein kinase II (CaMKII). Mainly but not exclusively, phosphorylation of Glo1 occurred on Thr-107 on the basic, reduced and NO-responsive form (Santarius et al., 2010, de Hemptinne et al., 2009, Xue et al., 2011, Birkenmeier et al., 2010).

The GLO1 promoter region contains binding sites for regulatory elements: insulin response element (IRE), metal responsive element (MRE) and glucocorticoid responsive element (GRE), positioned from -842 to -848bp, -647 to-654bp and -363 to -368bp respectively (Ranganathan et al., 1999), and activating enhancer binding protein 2 alpha (AP-2 alpha - also known as TFAP2A) positioned from -24 to -32

(Orso et al., 2010), E2F – binding to transcription factor E2F4 (Conboy et al., 2007) and ARE-1 positioned from -10 to -19, ARE-2 from -252 to -261 and ARE-3 from -1051 to -1060 (Xue et al., 2012a) – Figure 13. Glo1 was induced by oxidative stress in nematode *Onchocerca volvulus*, however the mechanism is still unidentified (Sommer et al., 2001) but may occur via the nematode orthologue of Nrf2.

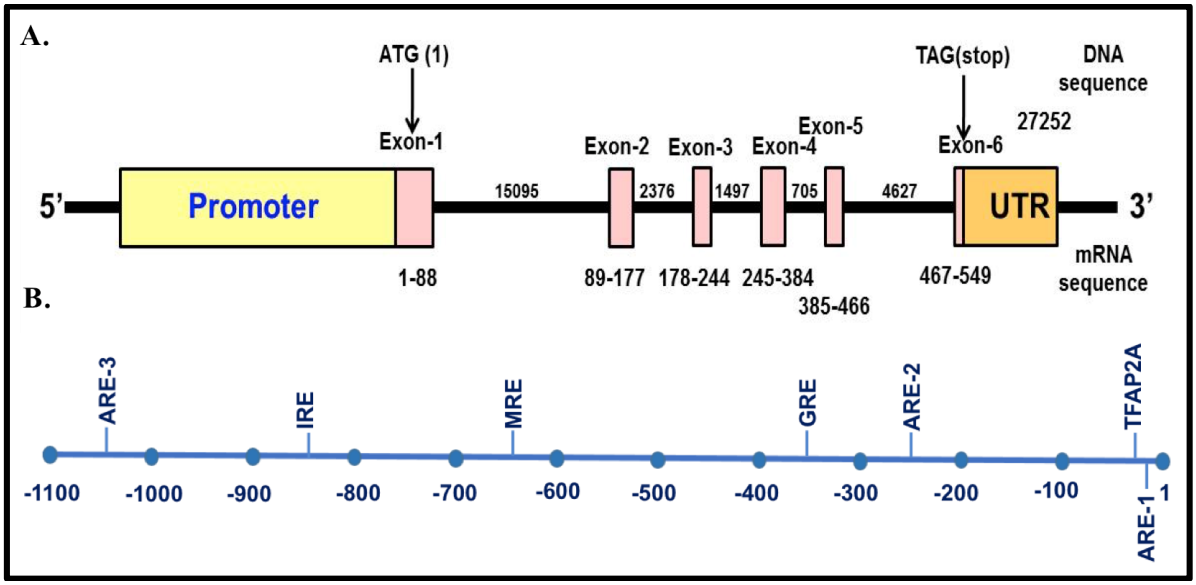

Figure 13: Human GLO1 gene structure.
A. Representation of human GLO1 gene (Yellow: promoter region, Pink: exon, Orange: untranslated region (UTR), Blue: regulatory elements). B. Promoter sequence of human GLO1 with positions of regulatory elements.

The crystal structure of human Glo1 in complex with competitive inhibitor S-benzylglutathione was determined using isomorphous replacement and 4-fold molecular averaging to 2.2 Å resolution (Cameron et al., 1997) – Figure 14. Each monomer consisted of two, structurally equivalent domains connected by a 20 connection of residue and anteceded by a long arm of N-terminal. The active site was located at the interface of the dimer, with the inhibitor and essential Zn^{2+} ion interacting with side chains from both subunits. The binding site of the zinc ions involved two residues from each subunit which are structurally equivalent from each domain: Gln-33A, Glu-99A, His-126B, Glu-172B plus two water molecules in octahedral coordination. (Cameron et al., 1997, Cameron et al., 1999a, Thornalley, 2003b).

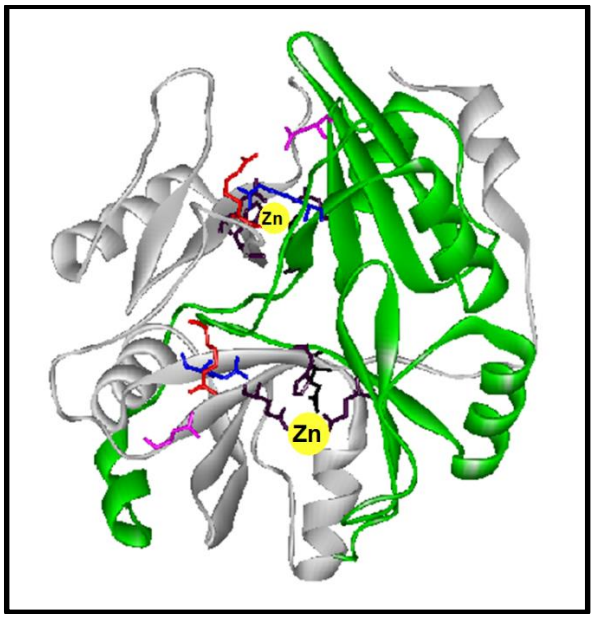

Figure 14: Glyoxalase 1 crystal structure.
Provided by Prof Paul Thornalley.

The catalytic mechanism suggested for the Glo1 reaction includes base-catalysed shielded proton transfer from C1 to C2 of the active site bound hemithioacetal. This creates an ene-diol intermediate with rapid, stereospecific reprotonisation and ketonisation to form the thioester product. The hemithioacetal forms are R- and S-forms. They are bound in the active site of Glo1 and are therein deprotonated; the subsequent reprotonation of the putative ene-diol intermediate happens stereo-specifically to produce the R-2-hydroxyacylglutathione derivative. Glu-172 and Glu-99 are the catalytic base for the S-substrate enantiomer and the R-substrate enantiomer respectively. These reaction mechanism produces a *cis*-ene-diol intermediate coordinated directly to the Zn^{2+} ion. This then is deprotonated to a *cis*-ene-diolate by Glu-172 which then reprotonates C2 stereo-specifically to create the product of R-2-hydroxyacylglutathione (Himo and Siegbahn, 2001). Glyoxal, methylglyoxal and hydroxypyruvaldehyde formed S-glycolylglutathione, S-D-lactoylglutathione and S-L-glyceroylglutathione by glyoxalase I respectively. They are hydrolysed by glyoxalase II respectively to glycolate, D-lactate and L-glycerate (Clelland and Thornalley, 1991).

Glo1 of other mammalian species has similar molecular characteristics to those of the human enzyme. Glo1 enzymes of mammalian, bacterial and plant origins are usually dimeric. However, Glo1 of yeast is a monomer of 32 and 37 kDa for

Saccharomyces cerevisae and *Schizosaccharomyces pombe*, respectively. These monomers have two copies of a segment corresponding to the monomer of Glo1 in humans. The sequence identity of Glo1 of human with Glo1 of bacterial *Pseudomonas putida* is 55% and with Glo1 of yeast *Saccharomyces cerevisiae* among residues 1-182 and 183-326 is 47% (Thornalley, 2003b). This may suggest that different origins of Glo1 may have arisen by divergent evolution from a common ancestor (Xue et al., 2011).

1.5.1.4 Glyoxalase 2 - molecular properties, genetics and human polymorphism

Glyoxalase 2 (Glo2) activity occurs in all cells of eukaryotic and prokaryotic organisms (Thornalley, 1993). Glo2 has been identified in yeast - *Saccharomyces cerevisiae* and *Hansenula mrakii* (Murata et al., 1986, Inoue and Kimura, 1992), protozoans - malaria parasite *plasmodium falciparium* (Vander Jagt, 1993) and *Leishmania braziliensis* (Darling and Blum, 1988), helminths including cestodes, digeneans and nematodes (Brophy et al., 1990, Pemberton and Barrett, 1989) and fungus; *Candida albicans* (Talesa et al., 1989).

There are two major forms of human Glo2: isoform 1 which is the mitochondrial form and its molecular mass 33,806 Da (sequence) and isoelectric point of 8.3 (predicted) and the isoform 2 which is the cytosolic form and its molecular mass 29,200 Da (SDS-PAGE; sequence 28,860 Da) and isoelectric point of 8.3 (Allen et al., 1993a, Ridderstrom et al., 1996, Cordell et al., 2004). Glo2 is a thiolesterase and has extensive substrate specificity for glutathione thiol esters favourably with S-2-hydroxyacylglutathione derivatives (Thornalley, 1991).

The cytosolic Glo2 of human contains two domains: a four-layered β sandwich and a mostly α-helical domain. The active site consist of a binuclear metal ion-binding site inclosing zinc (II) and iron (II) ions and a substrate-binding site covering the domain interface (Xue et al 2011). Additionally, there is a hydroxide ion attached to both metal ions and is located at 2.9 Å from the carbonyl carbon of the substrate in a site that may perform as the nucleophile during catalysis (Cameron et al., 1999b). The binding of metal ion in Glo2 is important for activity (Dragani et al., 1999, Limphong et al., 2009). The hydrolysis rate of S-D-lactoylglutathione to GSH and D-lactate catalysed by Glo2 followed Michaelis-Menten kinetics where the k_{cat} and K_M values were estimated as 727 s^{-1} and 146 μM respectively (Allen et al., 1993a). Acetylation of Glo2 is found at lys-229 (Choudhary et al., 2009).

The gene of human Glo2 is hydroxyacylglutathione hydrolase (HAGH). It is situated on chromosome 16 in region 16p13.3. Glo2 genetic polymorphism is extremely rare. Usually, only one phenotype- HAGH1 is expressed. Also, a rare second form named HAGH2 has been detected (Thornalley, 1993). The gene of Glo2 consists of 10 exons and is transcribed to two different mRNA species from 9 and 10 exons, respectively. The 9-exon-derived transcript encodes both the mitochondrial and cytosolic Glo2 forms. The Glo2 targeted to mitochondria originates from an AUG codon in the mRNA sequence, and cytosolic Glo2 is produced by internal ribosome entry at a downstream AUG codon. The 10-exon derived transcript contains an in-frame termination codon among the two initiating AUG codons and only encodes the cytosolic Glo2. The glyoxalase II form of mitochondria is directed to the mitochondrial matrix (Cordell et al., 2004).

1.5.1.5 D-Lactate

L-Lactate is the main stereoisomer of lactate made in the human intermediary metabolism (Drury and Wick 1965). D-Lactate is the other enantiomer which is generally about 1-5% of the L-lactate concentration in plasma. D-Lactate of exogenous sources is found at relatively high concentration in fermented food; for example, yogurt, sauerkraut and pickles. Furthermore, in the gut, D-lactate is absorbed from microbial fermentation (Mortensen et al., 1991, Hove, 1998, Ewaschuk et al., 2005, De Vrese and Barth, 1991). D-Lactate is formed endogenously in intermediary metabolism by the glyoxalase pathway and metabolised by 2-hydroxyacid dehydrogenase to pyruvate (Thornalley, 1993). In humans, D-lactate is well metabolised, however, it has higher fractional renal clearance than L-lactate (Connor et al., 1983). Infusion of D-lactate in humans at 1.0-1.3 mmol sodium D-lactate/kg/hr lead to nearly 90% of the D-lactate to metabolised whereas the residual 10% is excreted in urine (Oh et al., 1985). The D-lactate metabolism is reduced to nearly 75% of the overall clearance with higher infusion rates of 3.0-4.6 mmol/kg/hr (Oh et al., 1985). Its concentrations in blood plasma rises approximately 2-3 fold after meal and exercise (Ohmori and Iwamoto, 1988, Kondoh et al., 1992b). Permeability of D-lactate to cell membranes occurs via transporters, the inorganic anion exchange system and the specific lactate transporter, and also by ionic diffusion. Excretion of D-lactate occurs mainly in urine and with minor

excretions in stool and sweat (Oh et al., 1985, Kondoh et al., 1992b, Kondoh et al., 1992a).

Increased D-lactate can be used as an indicator of the elevated flux of formation of MG in cells where D-lactate is unable to metabolised; for example, red blood cells and lens fibre cells (Thornalley, 1993). D-lactate concentration increases in median of cultures of endothelial cells and red blood cells when cultured in high glucose conditions, and in plasma and urine of STZ-induced diabetic rats and patients with diabetes (Thornalley, 1988, Phillips and Thornalley, 1993, Karachalias N, 2005, McLellan et al., 1994a). The D-lactate levels in plasma in healthy adults is approximately 2 – 20 nM (Thornalley, 1988, Phillips and Thornalley, 1993, Karachalias N, 2005, McLellan et al., 1994a). Higher values may be reached when the analytical method does not avoid even limited racemisation of L-lactate which is normally existing in >100 folds excess over D-lactate (De Vrese and Barth, 1991, McLellan et al., 1992, Ohmori and Iwamoto, 1988, Brandt et al., 1980).

Endpoint enzymatic assay is used for measuring D-lactate with either absorbance or fluorescence detection of NADH formed in presence of D-lactic dehydrogenase. The amount of D-lactate in the sample is equivalent to the amount of NADH formed from NAD+ at endpoint, occurring concomitant with oxidation of D-lactate to pyruvate (McLellan et al., 1992). In addition, D-lactate may be detected from the amount of pyruvate formed where pyruvate is detected after derivatisation with 1,2-diaminobenzene to 2-hydroxy-3-methylquinoxaline by high performance phase liquid chromatography (HPLC) with fluorescent detection (Ohmori and Iwamoto, 1988, Ohmori et al., 1991).

1.5.1.6 S-D-Lactoylglutathione

S-D-Lactoylglutathione is a physiological intermediate of the glyoxalase system. It is formed from the hemithioacetal adduct of MG and GSH in a reaction catalysed by Glo1. Then, in the reaction catalysed by Glo2, S-D-Lactoylglutathione is hydrolysed to GSH and D-lactate (McLellan et al., 1993).

$$\mathbf{MeCOCHO + GSH \rightleftharpoons MeCOCH(OH)\text{-}SG \xrightarrow{Glyoxalase\ 1} MeCH(OH)CO\text{-}SG}$$

S-D-Lactoylglutathione is formed in the cytosol of cells and does not freely cross membranes of the cell. However, when it leaks from cells by the GSH conjugate transporter, γ-glutamyltransferase - found on the external surface of

plasma membrane of cells - cleaves S-D-lactoylglutathione to S-D-lactoylcysteinylglycine. Then, S-D-lactoylcysteinylglycine rearranges to N-D-lactoylcysteinylglycine spontaneously (Tate, 1975) and this may be cleaved by dipeptidase to N-D-lactoylcysteine.

In the 1980s, Thornalley and his colleagues found remarkable biological properties of S-D-lactoylglutathione added to cells in culture i.e. in the extracellular compartment. They revealed that S-D-lactoylglutathione prompted toxicity and growth arrest in human leukaemia cells *in vitro* (Thornalley and Tisdale, 1988). Moreover, in human neutrophils, S-D-Lactoylglutathione influence the percentage of stimulus-activated granule secretion, where at low concentrations it potentiated secretion (2 - 5µM) and while at higher concentrations (100 µM - 5mM) it inhibited secretion (Thornalley et al., 1990). These effects were found to be mediated by N-D-lactoylcysteine which enters cells by passive diffusion as it has a major solution species which is unionised. It is an inhibitor of dihydro-oratase of the *de novo* pyrimidine synthesis pathway. Inhibition of pyrimidine synthesis accounted for the anticancer activity of S-D-lactoylglutathione and all the effects of granule secretion through effects of metabolic channelling of pyrimidine metabolites into nucleotide conjugates influencing cell signalling for degranulation (Edwards et al., 1993, Edwards and Thornalley, 1994, Edwards et al., 1996).

1.5.1.7 Non-glyoxalase detoxification of MG

When the glyoxalase system is impaired or inhibited, glyoxal is metabolised to glycolaldehyde by aldoketo reductase (AKR) isozymes 1B1 (aldose reductase), 1B3 and MG is metabolised to mainly hydroxyacetone by 1B8 and AKR isozymes 1A4, 1B1 and 1B3 (Baba et al., 2009). Metabolism of glyoxal and MG by AKR 1B1 probably occurs mainly in the renal medulla where high expression of AKR 1B1 outcompetes Glo1 (Larsen et al., 1985, Nishimura et al., 1993). Concentrations of glyoxal and MG may be elevated in renal failure as a result of impaired Glo1 activity. Glo1 activity in renal and vascular cell may be reduced in renal failure by many factors including decreased concentration of GSH in oxidative stress, decreased Glo1 expression and glutathionylation of Glo1. Expression of Glo1 may be reduced by stimulation of RAGE and by suppression of signalling by Nrf2. Glo1 and AKRs 1A4, 1B1, 1B3 and 1B8 are ARE-linked genes with basal and inducible

expression controlled by Nrf2 (Xue et al., 2012a, Kwak et al., 2003, MacLeod et al., 2009, Nishinaka and Yabe-Nishimura, 2005, Thimmulappa et al., 2002).

Aldehyde dehydrogenase may also contribute in the degradation of MG in case of impairment or absence of the glyoxalase system. MG is oxidized to pyruvate by methylglyoxal dehydrogenase in an NAD+ dependent reaction (Nemet et al., 2006). There are more than 17 known functional aldehyde dehydrogenase genes (Vander Jagt and Hunsaker, 2003). The most significant genes: aldehyde dehydrogenase 1 (ALDH1), aldehyde dehydrogenase 2 (ALDH2) and aldehyde dehydrogenase 3 (ALDH3). They commonly show wide specificity and detoxify many aldehydes in humans (Vander Jagt et al., 2001). Unhydrated aldehydes are the preferred substrates of these genes (Vander Jagt et al., 2001, Nemet et al., 2006). Consequently, MG-a fully hydrated α-oxoaldehyde- is not readily reduced by ALDH1 and ALDH2 (Vander Jagt et al., 2001, Nemet et al., 2006, Izaguirre et al., 1998).

1.5.2 Regulation of Glo1 gene expression

Initial Glo1 inhibitors were developed based on GSH conjugates which were Glo1 substrate analogues. S-bromobenzylglutathione was a prototype of Glo1 inhibitor. Other Glo1 inhibitors include S-p-bromobenzylglutathione, Bis[(S-N-4-chlorophenyl-N-hydroxycarbamoyl)glutathione-hexa(β-alanyl)] suberate diamide, γ-Glutamyl-γ-(N-4-bromophenyl-N-hydroxycarbamoyl)glutamylglycine and S-p-bromobenzylglutathione cyclopentyl diester. Methotrexate, anti-cancer drug known as amethopterin, was a weak inhibitor of Glo1 (Thornalley and Rabbani, 2011a). Glo1 expression and activity may be decreased in some abnormal physiological conditions. Glo1 activity was decreased in the sciatic nerves of STZ-induced diabetic mice causing diabetic neuropathy (Stoyanov et al., 2007). This was related to the RAGE activation in diabetic mice with knock-out RAGE, Glo1 down regulation and development of diabetic neuropathy did not occur (Stoyanov et al., 2007). Neuropathy was re-established in RAGE knockout mice by dosing mice with a cell permeable Glo1 inhibitor, S-p-bromobenzylglutathione cyclopentyl diester ($SpBrBzGSHCp_2$) (Stoyanov et al., 2007). This implicated RAGE mediated down regulation of Glo1 in diabetic neuropathy and may increase MG concentration in development of neuropathy. Other mechanisms of Glo1 expression suppression in diabetes may be through hypertonic stress as mouse embryonic stem cells revealed reduced expression of Glo1 in hypertonic stress (Mao et al., 2008).

Glo1 found to be induced by small molecule inducers (Lewis et al., 2012, Rabbani et al., 2014b) such as sulforaphane (Xue et al., 2012a) *trans*- resveratrol and hesperetin (Xue et al., 2016). It has recently been shown that basal and inducible expression of Glo1 is regulated by Nrf2 by binding to a functional ARE (Xue et al., 2012a). Inflammatory signalling of LPS and TNFα may contribute to obesity and insulin resistance (Cani et al., 2007). In the nucleus and cytosol of macrophages, LPS inflammatory signalling stimulate the expression of Glo1 via the Tol-4 receptor (Du et al., 2010). RAGE and LPS activate pro-inflammatory signalling through NF-kB. It may thereby represses the Nrf2/ARE pathway: p65 of the NF-kB pathway deprives CREB-binding protein from Nrf2 and thereby suppresses Nrf2-activated transcriptional activity (Liu et al., 2008) – including Glo1 expression. NF-kB signalling activated by TNF-α may also produce competition with Nrf2 for CREB-binding protein and down regulate expression of Glo1 – Figure 15. This and other mechanisms could drive decrease of Glo1 expression by inflammatory signalling.

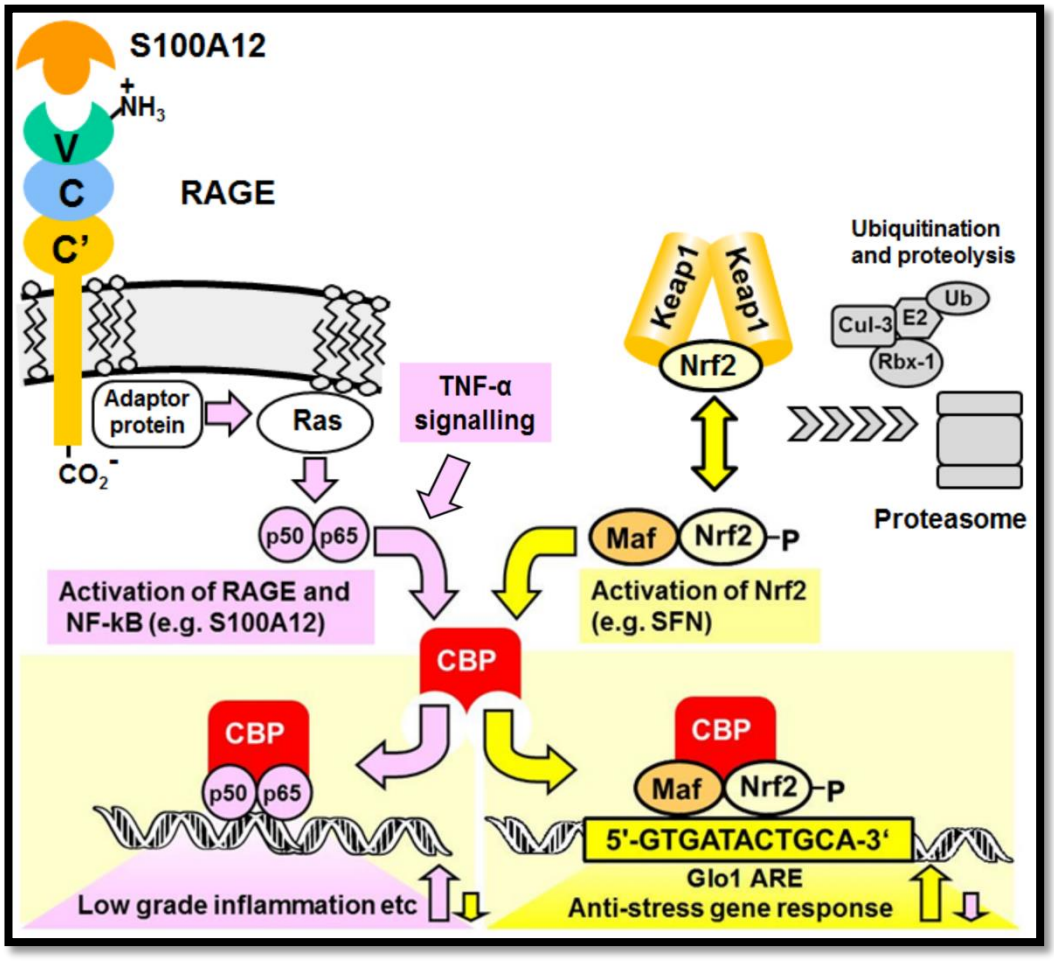

Figure 15; Receptor for advanced glycation endproduct (RAGE).
Proposed signalling for conflict with Nrf2.

1.5.3 Copy number variation of GLO1 gene

There is a newly recognised source of genetic diversity which is copy number variations (CNV). It defined as segregating duplications and deletions in the DNA which caused by genetic diversity and may result in increased susceptibility to specific diseases (Williams IV et al., 2009). Approximately 75% of CNV is found at a frequency of less than 3% in human populations, suggesting a stochastic origin and maintenance of most of this variation (Hastings et al., 2009). Some CNVs maybe more prevalent, however, GLO1 CNV increase was common to all three tissues examined - hypothalamus, hematopoietic and adipose (Cahan et al., 2009).

Williams *et al*. analysed gene copy number in mice strain using a Hidden Markov Model (HMM) approach and Affymetrix exon arrays. This assigns probabilities to hybridisation probes for three states: duplicated, deleted or ground, relative to the B6 reference strain. They identified the GLO1 locus as a hotspot for CNV in mice with particular strains undergoing duplications (Williams IV et al., 2009). Presence of the duplication is related with 4-fold increased in GLO1 expression (Williams IV et al., 2009, Cahan et al., 2009).

Furthermore, GLO1 CNV was found in the human genome (Redon et al., 2006). Redon *et al*. constructed a first-generation CNV map of the human genome by investigating 270 subjects from four populations with ancestry in Europe, Africa or Asia. A total of 1,447 CNV regions were detected covering 12% of the genome. The only gene found in a copied region of *ca.* 122 kb was GLO1. There were 5 copy number increases, suggesting a normal GLO1 CNV prevalence *ca*. 2% (Redon et al., 2006). GLO1 CNV was confirmed in the human population (Wong et al., 2007) and also found in other primates (Perry et al., 2008).

1.5.4 Glyoxalase 1 - a critical role in enzymatic defence against glycation

Glycation of proteins leads to protein modification which can cause structural derangement, impaired function and loss of side chain charge. Increase of the glycation adducts have been associated to chronic diseases. In physiological systems, glycation of protein is prevented and repaired by elements of the enzymatic defence against glycation. The concept of this enzymatic defence against glycation was established by Thornalley in 2003 and includes activities of enzymes that prevent the glycation adducts formation and also repair sites of early glycation (Thornalley, 2003b, Thornalley, 2003a). These include Glo1, aldehyde reductase, aldehyde

dehydrogenase, amadoriase and fructosamine 3-kinase. Detoxification of reactive α-oxoaldehydes - specifically MG, glyoxal and 3-DG - is performed by Glo1, aldehyde reductases and aldehyde dehydrogenase. Fructosamine 3-kinase catalyse the removal of fructosamine glycation adducts which formed by glucose protein glycation. The enzymatic defence against glycation decreases the damage to the proteome. However, it does not totally prevent it as glycation of proteins, nucleotides and basic phospholipids still occurs but it is suppressed to a low tolerable level (Thornalley, 2003b). In disease states, such as diabetes and chronic and acute renal failure, the enzymatic defence against glycation is overwhelmed and hence glycation adducts increase. Glo1 is the major defence against glycation by MG and glyoxal. The decline of Glo1 expression with age may contribute to the development of ageing and ageing associated disease (Morcos et al., 2005).

1.5.5 Glyoxalase inhibitors

Chemical inhibitors of Glo1 and Glo2 have been applied experimentally to observe the effects of endogenous elevation in dicarbonyls. Earlier studies revealed that glutathione thioether S-conjugate are substrate analogue inhibitors of Glo1 and may find use as anticancer drugs (Vince and Daluge, 1971, Vince et al., 1971). Early studies failed to demonstrate antitumour activity of glutathione thioether S-conjugates because prodrug modifications are required to facilate cell permeability and stabilise them from degreadation in the extracellular compartment. Inhibitors of Glo1 and Glo2 were developed by Lo and Thornalley (1992). Substrate analogue inhibitors of Glo1 had some residual inhibitory activity towards Glo1 (Bush and Norton, 1985). The problem of cell permeability and extracellular stability of glutathione thioether S-conjugates was solved by Lo and Thornalley who prepared diester derivataives. Glutathione thioether S-conjugate diesters, such as the prototype Glo1 cell permeable inhibitor S-p-bromobenzylglutathione cyclopenyl diester ($BrBzGSHCp_2$), were permeable to cells as they have a major solution species which is unionised and were also stable in the extracellular compartment as esterified glutathion derivatives are poor substrates for γ-glutamyl transferase. Once inside cells, glutathione thioether S-conjugate diesters are de-esterified by cell non-specific esterase and the Glo1 inhibitor is produced and trapped in the cell cytosol wherein lies the Glo1 receptor (Thornalley, 2003b). The effects of different S-conjugates of glutathione on growth and viability of cells were examined (Lo and Thornalley,

1992). This showed that unesterfied inhibitors probably did not enter cells and are degraded and no cytotoxicity was found. Ester derivatives were found to be unaffected to cleavage by the enzyme γ-glutamyltransferase and so more capable to enter cells, where the ester groups would be cleaved, representing the inhibitor in active form. Accordingly, $BrBzGSHCp_2$ was found to be a cell permeable inhibitor of Glo1 appropriate for use in cell based trials and also proposed to be of use in inhibiting tumour growth and prompting apoptosis (Thornalley et al., 1996).

1.6 Dicarbonyls

1.6.1 Dicarbonyl stress

Dicarbonyl stress is the abnormal accumulation of α-oxoaldehyde metabolites causing increased protein and DNA modification leading to cell and tissue dysfunction. This contributes to cell and tissue dysfunction in ageing and disease (Rabbani and Thornalley, 2014b). There are many examples including the elevation of MG in ageing plants, elevation of MG-protein modification in ageing human lens, elevation of plasma and tissue concentration of MG in diabetes, and elevation of MG, glyoxal, 3-DG concentrations and other dicarbonyls in renal failure (Rabbani and Thornalley, 2015). Dicarbonyl stress is a result of an imbalance between the formation of dicarbonyl metabolites and the enzymatic metabolism of them and also by increased exposure to exogenous dicarbonyls (Mingzhan et al., 2012). Normal levels of glyoxal, MG and 3-DG in human plasma are 50 - 150 nM and 1 - 4 μM in plant and mammalian cells. When dicarbonyl concentrations increase beyond this, dicarbonyl stress arises and contributes to impaired health and disease (Rabbani and Thornalley, 2015)

1.6.2 Dicarbonyl glycation and protein damage

1.6.2.1 Physiological dicarbonyl and historical aspects

Dicarbonyl compounds are intermediates of the Maillard reaction. The complexity of the Maillard reaction appears from multiple fragmentation reactions of sugar moiety, creating branch points in the reaction network. Saccharides may suffer dehydration, oxidation and fragmentation reactions before attaching to an amine substrate and therefore many equivalent reaction pathways may happen. Moreover, there are reactive dicarbonyls in the physiological systems. These reactive dicarbonyls – particularly α-oxoaldehydes - are important reactive intermediates of

Maillard reaction as they redirect minor but important part of the flux of glycation reaction intermediates to form AGEs on functional arginine residues (Thornalley, 2005).

In 1898, Pinkus discovered degradation of glucose to reactive α-oxoaldehydes. Since then their contribution to glycation in physiological systems and food has been extensively investigated. α-Oxoaldehydes are important saccharide derivatives as they make major quantitative and functional contributions in physiological systems. α-Oxoaldehydes are potent glycating agents, being 200 - 20,000 times more reactive than glucose and form AGEs directly. For example, incubation of human *plasma ex vivo* at 37 ^{o}C with 1 μM [^{14}C]MG led to complete and irreversible binding of MG to plasma protein within 24 h (Thornalley, 2005). Dicarbonyl concentrations in physiological systems are 10,000 - 50,000 times lower than glucose. Nevertheless, reactive dicarbonyls remain important AGEs precursors. MG, glyoxal and 3-DG are the main dicarbonyls – Figure 16. The most important dicarbonyl is MG as it has high reactivity, relatively high flux of formation *in vivo* and undergoes glycation directed mostly but not exclusively to functional arginine residues to form the most quantitatively predominant AGE, MG-H1 (Thornalley, 2005). An example of MG modification of protein is glycation of mitochondrial proteins. Glycation of mitochondrial protein by MG was associated with increased ROS and protein damage by oxidation and nitration (Thornalley, 2008).

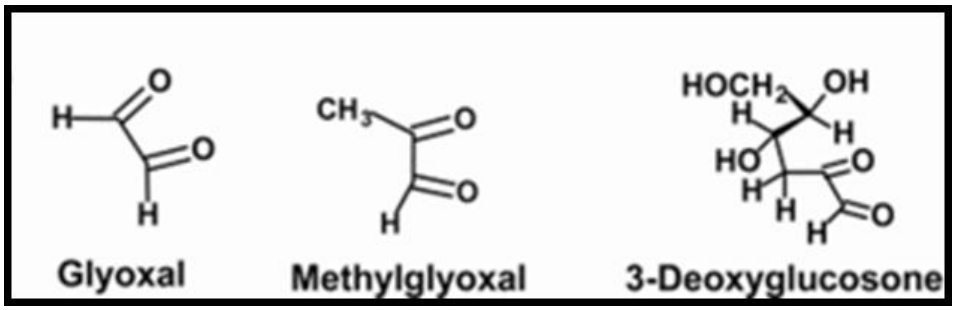

Figure 16: Physiological dicarbonyl metabolites.

1.6.2.2 Metabolic sources and reactions

MG is formed *in vivo* by non-enzymatic elimination of phosphate from the triosephosphates - glyceraldehyde-3-phosphate (GA3P) and dihydroxyacetonephosphate (DHAP) (Philips and Thornalley, 1993). GA3P is more reactive than DHAP in degradation to MG but this is countered by the concentration

ratio of DHAP/GA3P in cells *in situ* such that the contributions of GA3P and DHAP degradation to MG formation are similar (Philips and Thornalley, 1993). Triosephosphates are intermediates of anaerobic glycolysis (Embden-Meyerhof pathway) and also gluconeogenesis and glyceroneogenesis pathways – the latter is increased in obesity by cycling of triglycerides and free fatty acids from the liver to adipose tissue. MG is also formed by cytochrome E4502 E1-catalysed oxidation of acetone from ketone bodies, degradation of threonine via aminoacetone, degradation of monosaccharides and by degradation of proteins glycated by glucose (Thornalley, 2005).

There are three forms of MG in aqueous solution under physiological settings: dihydrate $CH_3C(OH)_2CH(OH)_2$ (28%), monohydrate $CH_3COCH(OH)_2$ (71%) and the reactive unhydrated form CH_3COCHO (1%) (Rabbani and Thornalley, 2012a). MG reacts with arginine residues to produce the quantitatively dominant AGE which is known in physiological systems as MG-H1 (Thornalley et al., 2003b, Ahmed et al., 2005a) and a minor fluorescent AGE argpyrimidine. There are other minor adducts formed with lysine residues and arginine and lysine residues: CEL, MOLD and MODIC (Ahmed et al., 2005a, Thornalley et al., 2003b). Increase of glucose level cause increased MG production in cultured endothelial cells (Shinohara et al., 1998, Queisser et al., 2010, Dobler et al., 2006), rats (Queisser et al., 2010) and human subjects with prediabetes and diabetes (Beisswenger et al., 2001). Cellular glucose uptake is controlled by GLUT1 receptors in endothelial cells; increased glucose uptake by GLUT1 leads to cytosolic hyperglycaemia and increased glucose metabolism (Dobler et al., 2006). This increases flux of MG formation. Decrease in Glo1 activity also occurs (Phillips et al., 1993, McLellan et al., 1994a) and this synergises with increased MG flux to increase the concentration of MG (Rabbani et al., 2014b). When MG concentration increases, the rate of formation and steady-state concentration of AGEs (Dobler et al., 2006), apoptosis of retinal pericytes (Liu et al., 2004a) and oxidative stress is enhanced (Rabbani and Thornalley, 2008a). AGE formation is induced by MG leads to modification of protein which can cause structural derangement, impaired function and loss of side chain charge (Thornalley, 2008). Some MG protein modifications studied includes: human serum albumin (Ahmed et al., 2005c), haemoglobin (Chen et al., 2005), vascular basement membrane of type IV collagen (Dobler et al., 2006), low density lipoproteins (LDL) (Rabbani et al., 2010, Rabbani et al., 2011) and high density lipoproteins (HDL)

(Godfrey et al., 2014). There are several pathological changes increased such as: angiopoietin-2 transcription (Yao et al., 2007), increased superoxide formation (Rosca et al., 2005), and alteration of fibroblast activity (Giardino et al., 1994).

Physiological formation of glyoxal occurs by auto-oxidation of glucose and by lipid peroxidation (Thornalley, 2005). Glyoxal targets arginine and lysine protein residues to form hydroimidazolone G-H1, CMA, CML, GOLD and GODIC (Nangia-Makker et al., 1993, Lo et al., 1994b). Protein glycation by glyoxal also causes structural distortion and functional impairment.

3-DG is a glucose and fructosamine derived α-oxoaldehyde and glycating agent. It is *ca.* 100-fold less reactive than MG. 3-DG reacts with lysine and arginine proteins residues to form particular AGEs – hydroimidazolones 3DG-H1 and associated structural isomers and pyrraline (Beisswenger et al., 2003, Thornalley et al., 2003b). The enzymatic activity of fructosamine-3-kinase (F3K) is a major source for 3-DG. F3K phosphorylates fructoselysine to 3-phospho fructoselysine which degrades spontaneously to lysine, phosphate and 3-DG (Thornalley, 2005, Beisswenger et al., 2003). Raised levels of 3-DG have been found with diabetes (Beisswenger et al., 2003). Important association has been found between increased 3-DG concentrations and glomerular hyperfiltration and diabetic nephropathy (Beisswenger et al., 2003). High levels of 3DG-H were found in the kidneys of diabetic patients and animals (Niwa et al., 1996, Karachalias et al., 2010). Additionally, 3-DG causes foetal malformation which is a feature of diabetic embryopathy (Eriksson et al., 1998).

1.6.3 DNA glycation by dicarbonyls

DNA has susceptibility to glycation by MG and glyoxal. Deoxyguanosine (dG) is the most reactive nucleotide towards dicarbonyl glycation under physiological conditions. The main nucleotide AGEs include imidazopurinone derivatives 3-(2′-deoxyribosyl)-6,7-dihydro-6,7-dihydroxyimidazo[2,3-b]purin-9(8)one (GdG) derivative of glyoxal and 3-(2′-deoxyribosyl)-6,7-dihydro-6,7-dihydroxy-6-methylimidazo[2,3-b]purin-9(8)one (MGdG) derivative of MG (Thornalley et al., 2010). There are other adducts formed by glyoxal including: N_2-carboxymethyl-deoxyguanosine (CMdG) and 5-glycolyldeoxycytidine (gdC). A further minor adduct formed by MG is N_2-(1-carboxyethyl)-deoxyguanosine (CEdG) (Thornalley et al., 2010). These are nucleotide AGEs. DNA glycation is related to

mutagenesis, DNA strand breaks and cytotoxicity (Thornalley, 1999). Nucleotide excision repair (NER) suppress glycation of nucleotide and its detrimental effects (Murata-Kamiya et al., 1998, Murata-Kamiya et al., 1999, Pischetsrieder et al., 1999). Mutation by MG-derived nucleotide AGEs leading to carcinogenesis may underlie why Glo1 is considered a tumour suppressor protein (Zender et al., 2008).

1.6.4 Measurement of dicarbonyls

A problem in this research area is to perform a reliable estimation of the MG and glyoxal concentrations in physiological systems. MG and glyoxal may be produced by degradation of monosaccharides, glycated proteins, glycolytic intermediates and derivatising agents during pre-analytic processing. Therefore, physiological concentrations of MG and glyoxal have often been overestimated. Chemical derivatisation of α-oxoaldehydes is important for required assay sensitivity. Best methods have been: (i) derivatisation with 1,2-diaminobenzene and gas chromatography with mass spectrometric detection (GC-MS) (Beisswenger et al., 1999), and (ii) liquid chromatography with tandem mass spectrometric detection (LC-MS/MS) with stable isotopic dilution analysis (Dobler et al., 2006, Kurz et al., 2011). A reference protocol has been published (Rabbani and Thornalley, 2014c). The concentrations of MG and glyoxal in human blood plasma are in between 100 – 120 nM and cellular concentrations of MG (1 – 5 μM) and glyoxal (0.1 – 1 μM) (Dobler et al., 2006, Kurz et al., 2011). This is corroborated by independent predictions from metabolic models of MG glycation (Rabbani and Thornalley, 2014c). Failure to control interferences during sample processing has led to 10 – 1000-fold overestimates.

Following from this, experiments to study effects of glyoxal and MG on cultured cells and tissues have used concentrations 10- 1000- fold higher than found physiologically. These are likely to be only applicable for acute intoxication and cytotoxicity. The use of MG at millimolar concentrations to show insulin signalling impairment, for example, is of unlikely physiological relevance (Riboulet-Chavey et al., 2006). Extreme overestimates of MG concentration lead to exaggeration of the physiological and toxicological role of MG in physiological setting and thus to the uncertainty of the health risks posed by endogenous exposure to MG in aging and disease, in healthcare products (such as thermally sterilized dialysis fluids), in foods and beverages, and in the environment. A well-validated reference protocol for MG

assay and systems modelling corroboration of estimates will hopefully decrease risk of overestimation in the future (Rabbani and Thornalley, 2014c).

1.6.5 Dicarbonyl proteome

Proteins vulnerable to glycation by dicarbonyls with associated functional impairment are called as the 'dicarbonyl proteome' (DCP) (Rabbani and Thornalley, 2008b). Proteomic applications have been conducted to recognise the DCP (Ahmed et al., 2005c, Dobler et al., 2006). Proteins include albumin (Ahmed et al., 2005c), haemoglobin (Chen et al., 2005), type IV collagen (Dobler et al., 2006), LDL (Rabbani et al., 2011), HDL (Godfrey et al., 2014), co-repressor protein sina3A (Yao et al., 2007), αA lens crystallin (Gangadhariah et al., 2010), HIFIα co-activator protein p300 (Thangarajah et al., 2009) and 20S proteome subunits (Queisser et al., 2010) are recognised to be susceptible to MG glycation and hotspot sites for modification by MG within them have been identified.

In human serum albumin, MG produced hotspot modification of Arg-410 *in vitro* and *in vivo* (Ahmed et al., 2005c). Arg-410 is located in the drug-binding site II and the active site of albumin-associated esterase activity. The MG-H1 residue formed inhibited drug binding and esterase activity.

MG modified vascular basement membrane collagen-IV, forming MG-H1 residues at hotspot modifications sites in arginine-glycine-aspartate (RGD) glycine-phenylalanine-hydroxyproline-glycine-glutamate-arginine (GFOGER) integrin binding sites of collagen (Dobler et al., 2006). This caused detachment of endothelial cells, anoikis and decreased angiogenesis. MG modification of collagen-IV *in vivo* likely contributes to the increased number of circulating endothelial cells found in diabetes and renal failure which is a risk predictor of CVD.

MG reacts with lipoproteins, low-density lipoprotein (LDL) and high-density lipoprotein (HDL). LDL minimally modified by MG (MG_{min}-LDL) contained mostly hydroimidazolone MG-H1 and accounted for 3 – 10% LDL *in vivo*. MG_{min}-LDL had decreased particle size, increased binding to proteoglycans and increased aggregation *in vitro*. Cell culture studies showed that MG_{min}-LDL was bound by the LDL receptor but not by the scavenger receptor, and had increased binding affinity for cell surface heparan sulfate-containing proteoglycan. Radiotracer studies in rats showed that MG_{min}-LDL had similar fractional clearance rate in plasma to unmodified LDL but increased partitioning onto the aortal wall. Mass spectrometry peptide mapping

identified the arginine hotspot site of apolipoprotein B100 modification in MG_{min}-LDL. A computed structural model predicted that methylglyoxal modification of apolipoprotein B100 induces distortion, increasing exposure of the N-terminal proteoglycan binding domain on the surface of LDL. Methylglyoxal modification of LDL forms small, dense LDL with increased atherogenicity. This non-oxidative process may explain escalation of cardiovascular risk in diabetes and renal failure, and resistance of early stage atherosclerosis to antioxidant therapy. Quantitation of methylglyoxal-modified LDL may improve cardiovascular disease risk models and therapeutics to decrease methylglyoxal may improve preventive treatment of cardiovascular disease (Rabbani et al., 2011).

MG-modified HDL was also found *in vivo*. Major fractions of HDL were isolated from healthy human subjects and patients with T2DM and fractions modified by MG and related dicarbonyl metabolites quantified. HDL modified by MG and related dicarbonyl metabolites accounted for 2.6% HDL and increased to 4.5% in patients with T2DM. HDL fractions were glycated by MG to minimum extent *in vitro* and molecular, functional and physiological characteristics determined. MG modification induced re-structuring of the HDL particles, decreasing stability and plasma half-life *in vivo*. It occurred at sites of apolipoprotein A-1 linked to membrane fusion, intramolecular bonding and ligand binding. Kinetic modelling of methylglyoxal modification of HDL predicted a negative correlation of plasma HDL-C with methylglyoxal-modified HDL which could be validated clinically. It also predicted dicarbonyl modification produces 2 - 6% decrease in total plasma HDL and 5 - 13% decrease in functional HDL clinically. MG modification of HDL may accelerate HDL degradation and impairs its functionality *in vivo*, likely contributing to increased risk of cardiovascular disease (Godfrey et al., 2014).

Recent application of high resolution mass spectrometry proteomics has attempted to identify globally the dicarbonyl proteome. In pilot studies using nanoflow liquid chromatography-Orbitrap Fusion^{TM} mass spectrometry with peptide HCD fragmentation, we analysed cytosolic protein extracts of human aortic endothelial cells in primary culture. In control samples, cell cytosolic protein had a total MG-H1 residue content of *ca.* 0.4 mmol/mol arg measured by LC-MS/MS analysis of exhaustive enzymatic digests; while in tryptic digests, Orbitrap Fusion analysis detected 1027 proteins of which 12 contained MG-H1 or MG-derived dihydroxyimidazolidine residues. After incubation of cytosolic protein extracts with

exogenous MG to increase the MG-H1 content *ca.* 20-fold, we then detected total MG-H1 residue content of *ca.* 8 mmol/mol arg and identified 1366 proteins of which 344 now contained MG-H1 or MG-derived dihydroxyimidazolidine residues (Rabbani and Thornalley, 2014a). In a recent report (Schmidt et al., 2015), plasma digests were analysed by nanoflow chromatography-LTQ Orbitrap XL ETD mass spectrometry and tryptic peptides scanned for m/z 152.1 and 166.1 indicative of glyoxal and MG modified proteins. Forty-four peptides representing 42 proteins were annotated. Arginine modifications were mostly represented by glyoxal-derived hydroimidazolones (34 peptides/39 sites) and MG-derived dihydroxyimidazolidine (8 peptides/8 sites) and MG-H1 (14 peptides/14 sites). Use of high temperature and pH processing in this study may have compromised the outcome; many glyoxal modified proteins were detected whereas LC-MS/MS analysis typically shows very low amounts of glyoxal-derived-AGEs, hydroimidazolone and N_{ω}-carboxymethylarginine, in plasma protein (Ahmed et al., 2005b).

Protein modification by MG is damaging because it is directed to arginine residues and arginine residues have the highest probability of any amino acid residue to be located at functional sites in proteins - sites of protein-protein, enzyme-substrate or protein nucleotide interaction (Gallet et al., 2000). MG modification causes loss of charge of the arginine residue and functional inactivation of the protein. MG modification tends to be directed to functional arginine residues because the accessibility and depolarisability of the electronic charge that confers the functional role is also activates the residue for MG modification (Rabbani and Thornalley, 2014a).

1.6.6 Clinical implications of dicarbonyls

Reactive dicarbonyls and the related glycation adducts with nucleotides and proteins are implicated in ageing and number of pathological processes and diseases such as diabetes, tumourigenesis and multi-drug resistance, and neurodegenerative diseases (Brownlee, 2005, Kuhla et al., 2005, Morcos et al., 2008, Rabbani et al., 2011, Thornalley, 2008).

1.6.7 Repair of glycated proteins

The main early stage glycation adduct of glucose, FL, can be de-glycated. Therefore, glycated proteins can be repaired by a pathway catalysed by fructosamine

3-kinase (Delpierre et al., 2000, Pascal et al., 2009). However, currently there is no recognised de-glycation mechanism for hydroimidazolone-modified proteins (Rabbani and Thornalley, 2012c). Proteins having hydroimidazolone adducts contain distorted and damaged structures and possibly as a result are directed to the proteosome for proteolysis (Dobler et al., 2006, Hernebring et al., 2006). MG-H1 free adducts are thereby released from proteins for urinary excretion. MG-H1 free adducts are found in plasma and urine in both laboratory rodents and human subject (Karachalias et al., 2010, Thornalley et al., 2003a).

1.7 Project-specific background

1.7.1 Measurement of protein glycation, oxidation and nitration

1.7.1.1 Advances in measurement of protein glycation, oxidation and nitration adducts

The analysis of protein glycation, oxidation and nitration adducts involves the detection and quantitation of trace amounts (fmol – pmol) of multiple glycated, oxidised and nitrated amino acids with the presence of 10^3 - 10^6 fold excess of associated unmodified amino acids. This provides a profound challenge for the analytical methodology employed. Many adducts are also unstable in pre-analytic processing at high pH and temperature. Protein glycation, oxidation and nitration adducts have been analysed by immunoassay (Wu and Steward, 1991, Yamamoto et al., 1989) and fluorescence (Vishwanath et al., 1986). The gold standard reference method for quantification is stable isotopic dilution analysis LC-MS/MS.

1.7.1.2 Immunoassay

Immunoassays were used initially for quantifying protein glycation, oxidation and nitration adduct analytes. Immunoassays have good analytical performance for specific and high affinity binding for peptide and protein analytes. However, there may be poor and insufficient antigen specificity in detection of protein glycation, oxidation and nitration adducts. For example, monoclonal antibody 6D12 was initially thought to bind CML residues specifically but later it was revealed that it binds both CML and CEL residues; indeed, it binds CEL preferentially over than CML (Ikeda et al., 1996, Koito et al., 2004). There are other interferences in pre-analytic processing of immunoassays: introduction of analyte into the assay matrix in blocking proteins to reduce non-specific binding of the antibody, creation of analyte during sample processing and effects of complex sample matrix on antibody function. Examples of interferences include: use of physiological proteins as blocking proteins which contain protein glycation, oxidation and nitration adduct residues – this may be avoided by use of synthetic polyamino acids lacking amino acid residue substrates of glycation, oxidation and nitration adducts (Rabbani et al., 2011), processing samples having FL residues at high pH for CML measurement where CML residues are formed from FL residues during the high pH processing step, and use of AGE immunoassays for food analysis when calibration, development and validation of the immunoassay was performed in a diluted plasma or serum

sample matrix. Thus, immunoassays have frequently given variable and overestimated values of analyte content and poor reproducibility. Nevertheless, immunoassays have analytical advantages: assessment of spatial localisation of antigen in immunohistochemistry, high throughput and relatively low cost. Therefore, if immunoassays can be validated and corroborated to LC-MS/MS reference methods they stay a very valuable analytical source.

1.7.1.3 Fluorescence

Assays based on fluorescence are limited to the minor number of protein glycation and oxidation adduct analytes that are fluorescent. A chromatographic resolution step is required for quantitative measurement. AGEs have been measured by "total AGE fluorescence", determining fluorescence with excitation and emission wavelengths of 350 nm and 450 nm, respectively (Šebeková et al., 2001). Later, the method of measuring total AGE fluorescence has been improved to detect low molecular mass AGE peptides or free adducts (Thomas et al., 2004, Wróbel et al., 1997). These methods have several analytical difficulties: (1) the major quantitative AGEs are not fluorescent and hence are not detected (Rabbani and Thornalley, 2009), (2) the oxidative adduct and fluorophore, N-formylkynurenine cause significant interference (Buxton and Guilbault, 1974), and (3) there are different fluorophores contribute to the global measure of fluorescence each with a different specific fluorescence, therefore, no quantitation can be achieved – Table1. Estimates of "total AGE fluorescence" provide a qualitative measure of damage made by both glycation and oxidation adduct fluorophores.

Oxidation of tryptophan produces fluorophores NFK and kynurenine (Fukunaga et al., 1982). Interaction of proteins with the lipid peroxidation product malondialdehyde produces fluorophores such as 3,5-diformyl-1,4-dihydropyridin-4-yl-pyridinium derivatives (Yamada et al., 2001) and related crosslinks (Itakura et al., 1996). These and other compounds such as retinoid derivatives in retinal tissue (Eldred and Lasky, 1993, Sparrow et al., 1999) may contribute to the fluorescence of the ageing pigment "lipofuscin" – although the mixture of fluorophores is complex (Li et al., 2006).

Table 1: Fluorophores associated with protein damage by glycation and oxidation.

Fluorophore	Structure	Fluorescence characteristics: λexcitation, λemission	Reference
	Glycation		
Pentosidine	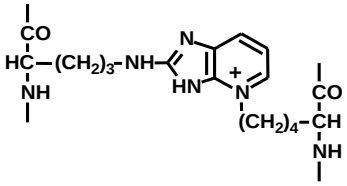	335 nm, 385 nm	(Sell and Monnier, 1989)
Argpyrimidine	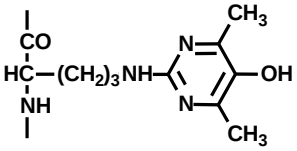	320 nm, 385 nm	(Shipanova et al., 1997)
Vesperlysine A (LM-1)	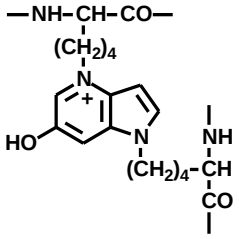	345 nm, 405 nm	(Tessier et al., 1999)
"AGE fluorescence"	Multiple	350 nm, 440 nm	(Monnier et al., 1984)
	Oxidation		
N-Formylkynurenine	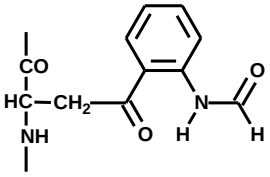	325 nm, 434 nm	(Fukunaga et al., 1982)
Kynurenine	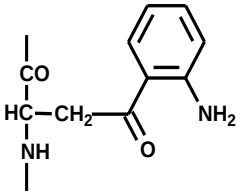	365 nm, 480 nm	(Fukunaga et al., 1982)
2-Amino-6-(3,5-diformyl-1,4-dihydro-4-methyl-pyridin-1-yl)hexanoic acid	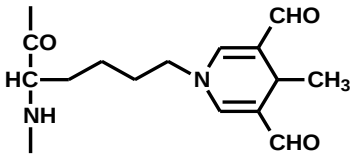	387 nm, 455 nm	(Yamada et al., 2001)
"Fluorescent oxidation products"	Multiple fluorophores	360 nm, 430 nm	(Shimasaki, 1994)
Lipofuscin	Multiple fluorophores	340 – 390 nm, 430 – 490 nm	(Li et al., 2006, Sohal, 1981)

Modified from (Xue, 2009).

1.7.1.4 Stable isotopic dilution analysis liquid chromatography with tandem mass spectrometric detection (LC- MS/MS)

Isotopic dilution analysis liquid chromatography with tandem mass spectrometric detection (LC-MS/MS) is the gold standard reference method used for analysis of protein glycation, oxidation and nitration adducts - as described (Thornalley et al., 2003b). Protein glycation, oxidation and nitration adduct residues in protein samples can be determined after exhaustive enzymatic hydrolysis. Protein glycation, oxidation and nitration free adducts are determined in ultrafiltrate of physiological fluids, typically prepared using a 3 kDa or 12 kDa cut-off microspin filter. This technology was developed in our group and many research teams are now using it. Other techniques – especially immunoassay - are useful for high sample throughput but the protocol and use in a particular sample matrix should be corroborated to the reference LC- MS/MS method before use. Ultra-high performance liquid chromatography with tandem mass spectrometric detection (UPLC-MS/MS) and robotic automation of enzymatic hydrolysis techniques are now used. Some examples of protein glycation, oxidation and nitration adducts markers by isotopic dilution analysis LC-MS/MS are illustrated in Table 2.

Table 2: Protein glycation, oxidation and nitration adducts markers determined by stable isotopic analysis LC-MS/MS

Analyte group	Analyte
Early glycation adduct	FL
Advance glycation adduct AGEs	
Hydroimidazolones	MG-H1, G-H1, 3DG-H
Monolysyl AGEs	CEL, CML, pyrraline
Imidazolium AGEs	MOLD, GOLD, DOLD
Fluorescent AGEs	Pentosidine, argpyrimidine
Other	Nδ-carboxymethylarginine
Oxidation adducts	S-carboxymethylcysteine, ornithine MetSO, dityrosine, NFK, alpha-aminoadipic semialdehyde, glutamic semialdehyde
Nitration adducts	3-NT

1.7.2 Therapeutic approaches to counter dicarbonyl stress

Investigational therapeutic interventions to counter dicarbonyl stress have mainly been based on scavenging by chemical agents. Aminoguanidine or Pimagedine^{TM} is a dicarbonyl scavenger that inhibits AGE formation (Thornalley, 2003c). The first report of use of aminoguanidine was by Brownlee *et al*. to suppress AGE formation in diabetes-induced arterial wall protein crosslinking (Brownlee et al., 1986). Aminoguanidine reacts with dicarbonyls such as glyoxal, MG and 3-DG and produce 3-amino-1,2,4-triazine derivatives (Thornalley et al., 2000). It was evaluated as a potential therapeutic agent for vascular complications of diabetes. However the clinical use of aminoguanidine was halted due to toxicity and poor clinical efficacy (Thornalley, 2003c). Dicarbonyl scavengers require high intrinsic chemical reactivity and hence toxicity may be expected.

Other dicarbonyl scavengers under development are *N*-terminal 2,3-diamino-propionic acid peptides (Sasaki et al., 2009), 3,3-dimethyl-D-cysteine (Wondrak et al., 2002), functionalised polymer beads with dicarbonyl scavenging has been proposed for dialysis fluid (Yamamoto et al., 2007) and phenacylthiazolium compounds (Ferguson et al., 1999). The latter compound exhibited a further problem of reactive scavengers – it was unstable in aqueous solution and degraded with acidification of cell cultures used in experimental evaluations (Thornalley and Minhas, 1999).

Supplementation with high dose of thiamine and related derivatives may decrease MG formation by activating the reductive pentosephosphate pathway and suppressing triosephosphate concentrations. Increased oxidative pentosephosphate pathway activity increases NADPH formation to sustain activities of aldoketo reductases and indirectly preserve Glo1 activity by GSH reductase activity and GSH levels. Supplementation with high dose of thiamine prevented and reversed early-stage diabetic nephropathy in experimental and clinical diabetes (Babaei-Jadidi et al., 2003, Rabbani et al., 2009). S-Benzoylthiamine-monophosphate (Benfotiamine) supplementation in experimental peritoneal fluid decreased peritoneal fibrosis, markers of inflammation and neovascularisation causing improvements in characteristics of peritoneal transport (Kihm et al., 2011). These beneficial effects may be related to decrease of dicarbonyl stress (Babaei-Jadidi et al., 2003).

Metformin, or N,N-dimethylbiguanide, is a extensively recommended drug for the treatment of type 2 diabetes and other metabolic syndromes. Moreover,

metformin shows antioxidant properties and it has been exhibited in neurogenesis, spatial memory formation and reduce the risk of Parkinson's disease (Solís-Calero et al., 2015). Previously, it has been suggested that metformin scavenges α-dicarbonyl compounds and inhibiting the subsequent creation of AGEs. Metformin reacted with MG and glyoxal and led to triazepinone derivatives formation (Ruggiero-Lopez et al., 1999) and more recently hydroimidazolone derivatives (Kinsky et al., 2016)– although the amounts of adducts formed are too low to account for marked suppression of plasma MG concentration. Thornalley and co-worker investigated the kinetics of reaction of metformin with MG and concluded that it is not kinetically competent to be an effective MG scavenger *in vivo* (Battah et al., 2002)– this corroborates with the findings of low levels of MG adducts. Metformin has the advantage of as drug which is safe and a good tolerability profile (Solís-Calero et al., 2015).

A recent advances in approaches to decline dicarbonyls is the potential use of Nrf2 activators that may stimulate expression of Glo1, aldoketo reductase and aldehyde dehydrogenase isozymes to enhance the metabolism of dicarbonyls (Xue et al., 2012a). Methyl 2-cyano-3,12-dioxo-oleana-1,9(11)dien-28-oate (Bardoxolone methyl) recently shows benefits for treatment of diabetic patients with stage 3-4 renal disease (GFR= 20-45 ml/min/1.73m^2 of body surface area) (Pergola et al., 2011). However, bardoxolone methyl is a weak inducer of Glo1 expression (Xue et al., 2012a). Its development was halted due to adverse effects (Chin et al., 2014). Small molecule activators of Nrf2 increase expression of different ARE-linked gene subsets (Xue et al., 2015a, Xue et al., 2015c)- likely due to the ability of Nrf2 activators to recruit the requisite accessory proteins and increase nuclear concentration of functionally active Nrf2 to the level required for increased expression of the ARE-linked gene of interest. A specific functional screen for GLO1-ARE transcriptional activation was therefore required. Thus developing of Glo1 inducers to enhance dicarbonyls metabolism is required. Dicarbonyls metabolism by Glo1 inducers as a pharmacologic strategy for therapeutic intervention has a superior advantage over other methods like chemical scavenging. Resveratrol (RSV) was found to be a Glo1 inducer (Chen et al., 2012).

1.7.3 Resveratrol

RSV (3,5,4'-trihydroxylstilbene; RSV) is a natural polyphenol with 2 aromatic rings linked by a methylene bridge (Baur and Sinclair, 2006). It exists in two geometric isomer forms - *trans* (tRSV) and the *cis* (*cis*-RSV) isomers; inter-conversion of *trans*- to *cis*- isomer is promoted by exposure to UV light (Constant, 1997). Normally, RSV is found in grapes, red wine, certain other red berries, Japanese knotweed, peanuts, roots of rhubarb and other plants from trace to mg/g contents. RSV content increases 2 - 10 fold when grapes are exposed to UV light (Shakibaei et al., 2009) - Table 3. tRSV is the major form found naturally in plants and has the significant biological activity. It is a phytoallexin that defends plants against fungal infection – such as the grey mould fungus *Botrytis cinerea*. RSV was discovered in 1940 as a phenolic element of the medicinal herb hellebore-Veratrum grandiflorum (Takaoka, 1940). In 1992, Siemann and Creasy suggested RSV may have a role in the cardioprotective effects of red wine (Siemann and Creasy, 1992). It is considered to be one of the wine components which responsible for the French paradox. The French paradox is the phenomena of low mortality related to coronary heart disease despite a lifestyle containing a high-fat diet and smoking (Yu et al., 2012). The skin and seeds of grape varieties Vitis vinifera, Labrusca, and Muscadine may contain 50-100 µg RSV per gram fresh weight and the concentration in wine varies between 0.1 to 14 mg/l for red wine and from 0.04 to 3.5 mg/l for white wine (with the greatest concentrations observed in wines from Pinot noir grapes) (Mark et al., 2005, Pervaiz, 2003, Lekli et al., 2010). Subsequently, RSV has been widely studied and claims of protective effects against a variety of chronic diseases - mainly cardiovascular atherosclerosis, cancer, diabetes and hypertension (Bradamante et al., 2004, Jang et al., 1997, Fröjdö et al., 2008, Baur and Sinclair, 2006). A large number of pharmacological targets for RSV have been claimed - Table 4. Most potent activity is found for tRSV.

Table 3: Dietary sources of tRSV

Source	tRSV content	Comments
Red wines	0.1-14.3 mg l^{-1}	*cis*-RSV, *trans*-piceid* and *cis*-piceid* also present, typically at slightly lower concentrations
White wines	<0.1–2.1 mg l^{-1}	Generally tRSV found at concentrations of <0.1 mg l^{-1}, exceptions include Swiss, Portuguese and German Riesling wines, *cis*-RSV, *trans*-piceid and *cis*-piceid also present
Ports and sherries	Generally <0.1 mg l^{-1}	
Grapes	0.16–3.54 μg g^{-1}	Contents are similar for wine or table grapes, and black or white grapes. *trans*-Piceid is predominant at concentrations of 1.5–7.3 μg g^{-1}
Dry grape skins	24.1 μg g^{-1} (average)	*trans*-Piceid and *cis*-piceid found at concentrations of 42.19 μg g^{-1} and 92.33 μg g^{-1}, respectively
Red grape juices	0.50 mg l^{-1} (average)	*trans*-Piceid, *cis*-piceid and *cis*-RSV found at concentrations of 3.38 mg l-1, 0.79 mg l^{-1} and 0.06 mg l^{-1}, respectively
White grape juices	0.05 mg l^{-1} (average)	*trans*-Piceid and *cis*-piceid found at concentrations of 0.18 mg l^{-1} and 0.26 mg l^{-1}, respectively
Cranberry raw juice	~0.2 mg l^{-1}	*cis*-RSV also found at a concentration of ~0.03 mg l^{-1}
Blueberries	Up to ~32 ng g^{-1}	
Bilberries	Up to ~16 ng g^{-1}	
Other Vaccinium berries	7–5,900 ng g^{-1} (dry sample)	Highest concentrations in lingonberries
Peanuts	0.02–1.92 μg g^{-1}	
Roasted peanuts	0.055 μg g^{-1}	
Boiled peanuts	5.1 μg g^{-1}	
Peanut butters	0.3–0.4 μg g^{-1} (average)	*trans*-Piceid also found at a concentration of 0.13 μg g^{-1}
100% Natural peanut butters	0.65 μg g^{-1} (average)	*trans*-Piceid also found at a concentration of 0.14 μg g^{-1}
Pistachios	0.09–1.67 μg g^{-1}	
Groundnuts (Arachis hypogaea)	ND	
Rhubarb	ND	
Hops	0.5–1 μg g^{-1}	*trans*-Piceid and *cis*-piceid found at concentrations of 2–9 μg g^{-1} and 0.9–6 μg g^{-1}, respectively
Itadori (Polygonum	0.68 mg l^{-1}	*trans*-Piceid also found at a concentration of 9.1 mg l^{-1}

cuspidatum) tea		
Herbal Veratrum (Lily)	ND	
Cassia quinquangulata	ND	
Gnetum klossii	ND	
Polygonum cuspidatum	0.524 mg g^{-1}	*trans*-Piceid also found at a concentration of 1.65 mg g^{-1}
Rhubarb (Rheum rhaponticum) dry root	3.9 mg g^{-1}	
Yucca schidigera bark	ND	

Modified from (Baur and Sinclair, 2006).
*Piceid, stilbenoid glucoside, is the major resveratrol derivative in grape juices (Romero-Pérez et al., 1999).

Table 4: Molecular targets of tRSV

Target	Effect
Metabolism and Aging	Sirtuin-1 (Sirt1) ↑, AMP-activated protein kinase (AMPK) ↑, Glucose transporter (GLUT-4) ↑, PDEs ↓,
Cytokines	Transforming growth factor β2 (TGFβ2) ↑, Transforming growth factor α (TGFα) ↓, Epidermal growth factor (EGF) ↓, Tumour necrosis factor (TNF) ↓, Interleukin (IL)-1β ↓, Interleukin (IL)-6 ↓, Vascular epithelial growth factor (VEGF) ↓, Insulin like growth factor 1 receptor (IGF-1R) ↓.
Transcription Factors	Activator protein-1 (AP-1) ↓, Nuclear factor-kappa B (NF-κB) ↓, Beta catenin (β-catenin) ↓, Early growth response (erg)-1 ↑, Androgen receptor (AR) ↓.
Cell Cycle Proteins	Cyclin D1 ↓, Retinoblastoma (Rb) ↓, Cyclin A ↓, Cyclin-dependent kinase (cdk)-2 ↑, Cyclin B1 ↓, $P21^{CIp1/WAF1}$ ↑, $P27^{kip1}$ ↑.
Invasion and Metastasis	Cyclooxygenase (COX)-2 ↓, 5-Lipoxgenase (5-LOX) ↓, Inducible nitric oxide synthase (iNOS) ↓, Vascular cell adhesion molecules (VCAM-1) ↓, Intercellular adhesion molecule (ICAM-1) ↓, Tissue factor ↓, NADPH:quinone oxidoreductase (NQO)-1 ↑.
Apoptosis	FasL ↑, Bax ↑, Bel-2 ↓, Surviving ↓, P53 ↑.
Kinases	Protein kinase C (PKC) ↓, Syk ↓, Protein kinase D (PKD) ↓, Casein kinase II (CKII) ↓, Extracellular signal-regulated kinase (ERK) ½ ↓.
Others	Ribonucleotide reductase↓, DNA polymerase↓, CYP1A1↓, Nonsteroidal anti-inflammatory drug-activated gene (NAG-1) ↑.

Modified from (Aggarwal and Shishodia, 2006).

Pharmacological mechanisms of action of tRSV *in vivo* are controversial because many cell-based studies *in vitro* have studied response to 10 – 50 µM tRSV and the upper limit of plasma concentration in human subjects is 2 µM (Boocock et al., 2007). Not the least of the concerns is the apparent activation of SIRT1 by tRSV has an EC_{50} of 22 µM (Lakshminarasimhan et al., 2013). This has led to the proposal that the basis for the apparent "activation" of SIRT1 by tRSV *in vivo* is through effects on increased availability of NAD+ co-factor rather than direct activation of SIRT1 enzyme (Cantó et al., 2009).

1.7.3.1 Effect of tRSV on diabetes

Anti-diabetic effects of tRSV

Management of T2DM focuses on three main features of metabolic regulating: glycaemic control, protection of pancreatic β-cells and improvement of insulin action for T2DM.

Glycaemic control

Studies of Zucker obese rats treated orally with 5 mg/kg/day tRSV showed a modest decrease in blood glucose: 6.1 mM versus 7.1 mM (Lekli et al., 2008). In ob/ob obese mice, oral doses of 5 and 15 mg/kg/day tRSV were ineffective and 50 mg/kg/day tRSV decreased blood glucose from *ca.* 14 mM to *ca.* 10 mM (Sharma et al., 2011). In STZ-diabetic rats and milder insulinopenic STZ-nicotinamide diabetic rats, orally administered 0.75 mg/kg/day tRSV decreased plasma glucose by 30 – 50% (Su et al., 2006). Thirunavukkarasu *et al*. found similar effects in STZ-diabetic rats with oral 2.5 mg/kg/day tRSV and Palsamy and Subramanian, 2008 found similar effects in STZ-nicotinamide-diabetic rats with oral 5 mg/kg/day tRSV. Moreover, reduced levels of glycosylated haemoglobin (HbA_{1C}) was detected in tRSV treated diabetic rats. This suggests prolonged reduction of glycaemia (Palsamy and Subramanian, 2010, Palsamy and Subramanian, 2008). Key enzymes of carbohydrate metabolism (hexokinase, glucose-6-phosphatase, fructose-1,6-bisphosphatase, glucose-6-phosphate dehydrogenase, glycogen synthase and glycogen phosphorylase, pyruvate kinase and lactate dehydrogenase) were increased in kidney and liver of STZ-nicotinamde diabetic rats treated with oral 2.5 mg/kg/day tRSV (Palsamy and Subramanian, 2009).

In contrast, Silan reported more modest decrease in blood glucose by *ca.* 10% with i.p. administration of 5 mg/kg/day tRSV to STZ-diabetic rats (Silan, 2008). Also Schmatz *et al*. (2009a,b) found no decrease in blood glucose of STZ diabetic rats with i.p. administration of 10 and 20 mg/kg/day. It appears that in obese and chemically-induced diabetes tRSV is less effective when administered i.p. rather than orally (Schmatz et al., 2009b, Schmatz et al., 2009a).

tRSV has also been studied in the prevention of chemically-induced diabetes where tRSV administration is initiated soon after STZ injection. The protection against insulinopenic activity depends on how soon after STZ injection the tRSV treatment is initiated; the longer the delay, the weaker the effect of tRSV – showing that tRSV is improving blood glucose by disturbing the toxicity of STZ to pancreatic beta-cells. In mild diabetes model of STZ-nicotinamide, the anti-hyperglycaemic effect of tRSV may relate to a stimulatory effect on intracellular glucose transport. Increased glucose uptake in cells including hepatocytes, adipocytes, and skeletal muscle cells isolated from STZ induced diabetic rats was found to be enhanced in the absence of insulin. This suggests that the anti-hyperglycaemic effect of tRSV may be insulin independent (Su et al., 2006). Studies on models of diabetic rat displayed amplified expression of GLUT-4 with tRSV treatment (Penumathsa et al., 2008, Chi et al., 2007).

Enhancement of insulin action

There are a number of animal studies which have proposed tRSV as a beneficial compound for improving insulin action in T2DM. Baur and his colleagues (2006) revealed that when high fat diet mice were administered orally 22 mg/kg/day tRSV there was improved insulin sensitivity (Baur et al., 2006). Furthermore, fasting and random insulin and glucose levels in plasma were decreased as compared to high fat diet fed mice without tRSV. Stimulation of phosphorylated AMP-activated protein kinase (AMPK), a metabolic controller that stimulates insulin sensitivity and fatty acid oxidation, by tRSV was suggested as the mechanism of action – finding evidence for phosphorylation and two downstream indicators of activity-phosphorylation of acetyl-CoA carboxylase at Ser79 and reduced expression of fatty acid synthase (Baur et al., 2006). Related findings of decreased plasma insulin in tRSV treated high fat diet-fed mice were also noticed by other research groups: Lagouge *et al*. with an oral dose of 200 – 400 mg/kg tRSV, Sun *et al*. with oral dose

of 2.5 mg/kg tRSV and Um *et al*. with an oral dose of 400 mg/kg tRSV (Lagouge et al., 2006, Sun et al., 2007, Um et al., 2010). The higher doses of tRSV used are not clinically translatable and benefits of tRSV clinically have not been confirmed in meta-analysis of clinical studies (Liu et al., 2014).

Oral treatment of genetically obese, hyperphagic, diabetic KKAy mice with 2 and 4 mg/kg/day tRSV improved insulin resistance, and oral treatment of genetically obese Zucker rats with 10 mg/kg tRSV per day prevented insulin resistance but not obesity (Lagouge et al., 2006, Chen et al., 2012, Rivera et al., 2009). Several studies in mice and rats have reported anti-obesity effects: Sprague-Dawley rats given 6, 30 or 60 mg/kg/day tRSV showed no, 24% and 19% decrease in body fat, respectively; Wistar rats fed orally 100 mg/kg/day tRSV had decreased body weight; mice fed orally 400 mg/kg/day tRSV had decreased body weight (Macarulla et al., 2009, Um et al., 2010, Shang et al., 2008, Rocha et al., 2009). Anti-obesity effects of tRSV are only apparent at very high doses that are not clinically translatable and tolerable (Vang et al., 2011).

Treatment with tRSV has been claimed to produce effects similar to those induced by caloric restriction - such as decreased age-related cardiac dysfunction, decrease in blood glucose levels and inhibition of gene expression profiles related with cardiac and skeletal muscle ageing. tRSV dosing of mice decrease in signs of aging - including decreased albuminuria, inflammation and apoptosis in the vascular endothelium, increased aortic elasticity, reduced cataract formation, greater motor coordination, and preserved bone mineral density. This achieved, however, at doses of 100 – 400 mg/kg/day (Pearson et al., 2008). A lower dose of tRSV, 4.9 mg/kg/day orally, initiated in middle age (14 months old mice) led to change in gene expression similar to caloric restriction (CR) without decrease in body weight found with CR. (Barger et al., 2008, Pearson et al., 2008).

In vitro studies have presented similar effects but there *in vivo* relevance is doubtful because of high supraphysiological concentrations. tRSV (6 – 50 µM) treatment of rat adipocytes showed decreased ATP content, decreased accumulation of triglyceride, decreased lipogenesis and decreased lipolytic response to epinephrine, and ES (62.5 – 250 µM) treatment of rat adipocytes decreased leptin secretion (Szkudelska et al., 2011, Szkudelska et al., 2009). Human adipocytes cultured with conjugated linoleic acid and 10, 25 and 50 µM tRSV had decreased insulin resistance, increased insulin-stimulated glucose transport and reduced

inflammation when compared to cells exposed to conjugated linoleic acid only (Kennedy et al., 2009). This was proposed to be caused by decrease of cellular stress, prevention of activation of extracellular signal related kinase, inhibition of inflammatory gene expression, increase in peroxisome proliferator-activated receptor γ (PPAR- γ) activity (Szkudelska et al., 2011, Szkudelska et al., 2009).

AMPK and Sirt-1 activation have been connected to tRSV induced enhancement in insulin action. There were several studies on animals which demonstrated the activation of AMPK and Sirt-1 by tRSV (Baur et al., 2006, Lagouge et al., 2006, Lee et al., 2009, Shang et al., 2008, Hausenblas et al., 2015). In AMPK deficient high fat diet mice, tRSV was unsuccessful in decreasing body fat and improving insulin action. Sirtuins participate in NAD(+)-dependent protein deacetylation and are key controllers of transcription, apoptosis, metabolism, and aging (Um et al., 2010). Seven human sirtuins (SIRT1-7) are found, and Sirt1 has been involved significantly as a mediator of the pathways downstream of calorie restriction that have been presented to defer the onset and decrease the occurrence of age-related diseases such as type 2 diabetes (Pacholec et al., 2010, Baur et al., 2006). Sirt1 action is directed to histone proteins in addition to several transcription factors such as p53, the forkhead box protein (FOXO) family, PPAR-γ, co-activator 1α and PPAR gamma coactivator-1alpha (PGC-1α). Sirt1 enhances function of mitochondria, induces genes for mitochondrial and fatty acid oxidation and increases potential of mitochondrial membrane (Lagouge et al., 2006). In human endothelial cells *in vitro*, 10 – 100 μM tRSV increased the mRNA expression of Sirt1 (Kao et al., 2010). In a different study, 3 – 30 μM tRSV human coronary artery endothelial cells presented up-regulation of MnSOD expression and increased cellular levels of GSH in a concentration dependent manner (Ungvari et al., 2009). These effects were diminished by knocking down Sirt1 and mimicked by Sirt1 overexpression-presenting the action of tRSV via Sirt1 activation. However, the thought of tRSV being the main activator of Sirt1 was challenged recently (Dolinsky and Dyck, 2011, Pacholec et al., 2010). Therefore, even though the exact tRSV mechanism of action is uncertain, it has a significant role in improving insulin action.

Protection of β-cells

In T2DM, hyperglycaemia occurs in the presence of hyperinsulinemia – insulin resistance leading to increased glucose concentration drives the pancreas to secret a compensatory release of insulin. Prolonged overstimulation of β-cells lead to their exhaustion and degradation causing inadequate insulin secretion (Hansen et al., 2004). Normally, glucose-induced insulin secretion is mediated by a sequence of actions: intracellular glucose transport by GLUT2 transporter, glucose metabolism by oxidative glycolysis, hyperpolarisation of inner mitochondrial membrane, increased formation of ATP, increased ATP/ADP ratio, closure of the ATP-sensitive potassium channels, depolarisation of plasma membrane, opening of voltage-operated Ca2+ channels and increase in cytosolic Ca^{2+}. The increase in cytosolic Ca^{2+} activates secretion of insulin. Constant insulin-secretory response is preserved by intensifying signal generation in the β-cells (Henquin, 2000, Maechler, 2002). In rat pancreatic islets, treatment with 1 – 100 μM tRSV caused increased L-lactate, reduced oxidation of glucose, diminished hyperpolarisation of the inner mitochondrial membrane and decreased levels of ATP (Szkudelski, 2007). Since the ATP/ADP ratio is important for insulin secretion, reduced formation of ATP with tRSV led to decreased secretion of insulin from the pancreatic islets. However, insulin secretion inhibition by tRSV was noticed to be reversible and were not because permanent changes in the β-cells (Kennedy et al., 2009, Szkudelski, 2006). Inhibition of insulin secretion by tRSV may decrease β-cells degradation as a consequence of their chronic overstimulation but this hypothesis needs confirmation and requires further investigation.

Other mechanisms activated by tRSV may protect pancreas islets. When isolated pancreatic islets of rat were exposed to cytokines, there was increased DNA binding of NF-κB, increased production of NO and expression of eNOS (Lee et al., 2009). Conversely, when treated with 10 and 50 μM tRSV all these damaging effects were inhibited. Moreover, the viability of islets exposed to cytokines and tRSV was increased and compared to ones exposed only to cytokines. tRSV was found to repair β-cells secretory function; disturbed by cytokine action. Furthermore, the reduction in glucose induced insulin secretion as a consequence of cytokine exposure was restored completely after pre-treated the pancreatic islets with tRSV. These concentrations of tRSV, however, are not achievable clinically.

The protective role of tRSV from cytokine action on pancreatic β-cells was also present in experimental animals. In rat models of experimental diabetes, oral tRSV administration decreased plasma TNF-α, IL-1β and IL-16 as compared to non tRSV treated diabetic rats (Palsamy and Subramanian, 2010).

tRSV has been proposed to inhibit diabetes through its anti-oxidant effects. Beta-cells are more vulnerable to oxidative damage as a result of significantly lower anti-oxidant defence as compared to other cells (Lenzen, 2008). Levels of lipid peroxides, hydroperoxides and protein carbonyls were increased in STZ-induced diabetic rats, compared to controls (Palsamy and Subramanian, 2010). Activities of antioxidant enzymes, including superoxide dismutase, catalase, GSH, peroxidase and glutathione-S-transferase were decreased in the diabetic rats. These were corrected by tRSV treatment. Oxidative stress is considered to be a key factor causing β-cell dysfunction in T2DM (Robertson, 2006).

1.7.3.2 Role of tRSV in diabetic cardiovascular complications

Several studies had suggested protective effects of tRSV on the vasculature and heart in experimental diabetes. STZ-diabetic rats treated i.p. with 0.75 mg/kg tRSV 3 times daily had decreased thickening of vascular wall, the deposition/cross-linking of collagen, and vascular permeability as compared to the untreated diabetic rodents (Jing et al., 2010). Vascular smooth muscle cells of the tRSV-treated rats were showed less proliferation, lower NF-κB, and extracellular-signal-regulated kinases (Erk1/2) activation and diminished proliferation. Additionally, tRSV was found to decrease expression of RAGE in diabetic rats (Jing et al., 2010) and improve the vasorelaxant ability of the diabetic aorta (Silan, 2008). tRSV-induced decreased RAGE and NF-κB signalling pathway may suppress DM-induced vasculopathy (Jing et al., 2010).

In STZ-induced diabetic rats, tRSV presented cardio-protective effects on the myocardium by up-regulation of thioredoxin, NO, heme-oxygenase, and VEGF (Thirunavukkarasu et al., 2007). Also, 10 mg/kg/day tRSV was found to restore normal vascular function and prevent oxidative stress in T1DM in rats via increasing eNOS (Arrick et al., 2011). Moreover, tRSV enhanced left ventricular diastolic relaxation in diabetes by stopping TNF-α-induced NF-κB activation, consequently inhibiting the expression and activation of NADPH oxidase along with increasing eNOS (Zhang et al., 2010). Therefore, tRSV protects against cardiac dysfunction in

diabetes via preventing oxidative stress and improving NO availability. The positive effects of tRSV have been related with Sirt1 activation. tRSV activates Sirt1 which improves the expression of sarcoplasmic calcium ATPase (SERCA2a) and cardiac function in diabetic mice (Sulaiman et al., 2010). tRSV (10 μM) increased mitochondrial content in endothelial cells by Sirt1 activation and eNOS up-regulation; tRSV (20 mg/kg/day) produced a similar response in aortas of db/db diabetic mice (Csiszar et al., 2009). The heart in diabetes is also vulnerable to ischemia-reperfusion injury. tRSV has also been considered for its capability to protect the diabetic heart from ischemia- reperfusion injury. In Zucker obese rats, oral 5 mg/kg/day tRSV decreased in cardiac apoptosis in ischemia-reperfused hearts in presence or absence of glucose uptake (Lekli et al., 2008).

1.7.3.3 Role of tRSV in other diabetic complications

The effect of tRSV has been studied in other diabetic complications including nephropathy, retinopathy and neuropathy. To assess the effect of tRSV on diabetic nephropathy, db/db mice were treated with 20 mg/ kg/day of resveratrol for 12 weeks. The results showed a decrease in albuminuria, improvement in the glomerular matrix expansion and inflammation. tRSV also increased the phosphorylation of AMPK and the activation of SIRT1–PGC-1α signalling in db/db mice (Kim et al., 2013b). In STZ induced diabetic rats with nephropathy, treatment with tRSV (20 μmol/l) increased activity of FoxO1 and a significantly up regulated the expression of AdipoR1- down-regulation of AdipoR1 is a cause of diabetic nephropathy (Ji et al., 2014). Wu and his colleagues also found that tRSV has protective effects against diabetic nephropathy by modifying the SIRT1/FOXO1 pathway. Their findings showed that activity of FOXO1 is decreased, with a parallel decrease in the catalase expression, a FOXO1 target gene, and expression of SIRT1 reduced in the renal cortex of STZ induced diabetic rats, improving renal oxidative stress (Wu et al., 2012). Palsamy and Subramanian found that tRSV (5 mg/kg orally for 30 days) resulted in normalization of the clearance of creatinine and the plasma levels of adiponectin, C-peptide, and renal oxidative stress and inflammation in STZ nicotinamide induced diabetic rats. Furthermore, tRSV treatment ameliorated the antioxidant enzymes [superoxide dismutase (SOD), catalase, glutathione peroxidase (GPx), glutathione-S-transferase (GST), and glutathione reductase (GR)] dysfunction and decreased levels of vitamin C, vitamin E and reduced glutathione (GSH) in

diabetic nephropathy. Moreover, they found that the expression levels of Nrf2 and its downstream enzyme, involving γ-glutamyl cysteine synthase (GCS), m-GST, and hemoxygenase-1 (HO-1) were significantly reduced in the renal tissues of diabetic rats (Palsamy and Subramanian, 2011) and tRSV corrected this. Zhang et al. reported that high levels of glucose increased mesangial cell proliferation and fibronectin expression through the c-Jun N-terminal kinase JNK/NF-κB/NADPH oxidase/ROS pathway, which was inhibited by tRSV (5 µM; 10 µM) *in vitro* (Zhang et al., 2012).

Few studies were conducted to investigate the effect of tRSV on diabetic retinopathy. Soufi et al. reported that oral administration of tRSV (5 mg/kg/day) for four-month in STZ induced diabetic rat significantly alleviated hyperglycaemia, weight loss, enhancement of oxidative markers, lipid peroxidation index. tRSV also improved oxidized to reduced glutathione ratio, and superoxide dismutase activity in both blood and retinas of the diabetic rats. Furthermore, tRSV treatment to diabetic rat reduced the increased levels of retinas NF-κB activity and apoptosis rate (Soufi et al., 2012). Ciddi and Dodda found that in sugar-induced lens opacity model, tRSV (10 µg/ml) displayed a significant protective effect inhibiting opacification and polyols formation in cattle lens (Ciddi and Dodda, 2014).

The diabetic neuropathy caused mainly by oxidative stress, AGE formation, lipid peroxidation (Vinik, 2008). Using of tRSV in diabetic neuropathy as a potent antioxidant was established by Kumar et al. STZ induced diabetic rats developed neuropathy assessed by reduction in motor nerve conduction velocity (MNCV), nerve blood flow (NBF) and increased thermal hyperalgesia. After 2-week of treatment with tRSV (10 and 20 mg/kg), it significantly ameliorated the alterations in MNCV, NBF, and hyperalgesia. In addition, tRSV reduced enhanced levels of malondialdehyde (MDA), peroxynitrite and increased the catalase levels in diabetic rats. This study suggested the potential of tRSV as a treatment of diabetic neuropathy, its protective effect may be mediated by reducing oxidative stress (Kumar et al., 2007). Another study investigated whether combination of tRSV and 4-amino 1,8 naphthalimide (4-ANI) is effective in the development of diabetic neuropathy. STZ induced diabetic rats were treated for 2 weeks with tRSV (10 mg/kg) and 4-ANI (3 mg/kg). Combination of tRSV and 4-ANI enhanced nerve conduction and nerve blood flow and improved diabetic neuropathic pain (Sharma et al., 2009). STZ induced diabetic rats were treated for 2 weeks with tRSV (10 and 20 mg/kg). The results showed that tRSV decreased the expression of p65 and IκB-α in

treated rats. In addition, tRSV ameliorated the elevated levels of TNF-α, IL-6 and COX-2. These findings suggest that tRSV also prevent neuropathy through inhibiting NF-κB activity and inflammation apart from its antioxidant effect (Kumar and Sharma, 2010).

1.7.3.4 Role of *trans*-resveratrol in periodontal diseases

tRSV has an antioxidant and anti-inflammatory properties which can decrease oxidative stress and inflammation. Direct scavenging of ROS is unlikely to explain these effects as tRSV and *cis*-RSV have equal direct scavenging activity of ROS but tRSV has more potent effects in physiological systems. Antioxidants activities of tRSV are, therefore, likely due to indirect effects of inducing increased expression of antioxidant enzymes. There are few studies were conducted to identify the effect of tRSV on counteract the periodontal tissue breakdown in inflammatory status. A recent study found that administration to rats of tRSV, 10 mg/kg/day by gavage for 30 days – 19 days before induction of periodontitis and 11 days after, decreased periodontal tissue breakdown and alveolar bone loss; periodontitis was induced by cotton ligature in a cervical position secured sub-marginally. Lower levels of IL-17 were found in the tRSV treatment group but no change in IL-1β and IL-4 levels were found (Casati et al., 2013).

Tamaki and his colleagues studied tRSV-containing extracts from the melinjo plant. Oral dose of 10 mg/kg/day limited alveolar bone loss in ligature-induced periodontitis and activated the SIRT1/AMPK and the Nrf2/antioxidant defence pathways in inflamed gingival tissues. Additionally, tRSV-containing extracts intake decreased urinary levels of 8-hydroxydeoxyguanosine and dityrosine, serum nitrite/nitrate and nitrotyrosine, and proinflammatory cytokines. Hence, oral administration of tRSV-containing extracts may suppress the development of ligature-induced periodontitis and enhance systemic oxidative and nitrosative stress (Tamaki et al., 2014).

The effects of tRSV on human gingival fibroblasts (HGFs) *in vitro* under oxidative stress prompted by hydrogen peroxide were studied. tRSV (25 – 75 μM) improved cell proliferation under oxidative stress. Moreover, tRSV was effective at preventing ROS production. HGFs treated with tRSV (50 μM) up-regulated collagen-I gene transcription after 3 h and continued for 24 h (Orihuela-Campos et

al., 2015). It is doubtful if these effects of supraphysiological concentrations of tRSV can be translated *in vivo*.

Recently, it is found that tRSV given after induction of periodontitis by daily subcutaneous injection to rats at a dose of 5 mg/kg body weight for 2 weeks protected from periodontal tissue breakdown by inhibiting inflammatory responses and by stimulating antioxidant defence systems. The effect of tRSV on HGF growth and variability *in vitro* was studied. tRSV increased growth at 25 – 100 μM and decreased growth and viability at >100 μM (Bhattarai et al., 2016).

1.7.4 Hesperetin

Hesperetin (HSP) is a member of a group of phenolic compounds called flavanones – derivatives of a core 2,3-dihydro-2-phenylchromen-4-one structure. Flavanones originated from plants and are used as traditional remedies (Sun et al., 2013). HSP closely-related to the glycoside derivative, hesperidin (hesperetin 7-rutinoside, hesperetin 6-O-α-L-rhamnosyl-D-glucose), found in oranges and other citrus fruits (Khan and Dangles, 2014). Hesperidin was first extracted from citrus peel by the French chemist Lebreton (Pietta, 2000).

Hesperidin is found particularly lemon, limes and sweet oranges (Khan and Dangles, 2014). Hesperidin is absorbed poorly after de-glycosylation by gut bacteria in the small intestine and colon which likely contributes to high variability of exposure to HSP from the diet. HSP, however, is absorbed efficiently without enteral metabolism (Kanaze et al., 2007). The concentration of HSP and hesperidin (mostly the latter) in a typical serving of commercial orange juice was *ca.* 22 mg per 100 ml (Erlund et al., 2001) but specific varieties of citrus fruits may have levels 10 – 20 fold higher (Khan and Dangles, 2014). HSP is absorbed effectively, metabolised to glucuronide and sulfate derivatives and excreted in urine. Conjugates of hesperetin are widely detected in urine of clinical studies as markers of consumption of oranges, orange juice or related citrus fruits. The peak plasma concentration of HSP achieved in healthy subjects after bolus dose of 135 mg was 2.7 μM (Erlund et al., 2001); *cf.* peak plasma concentration of HSP after consumption of one litre of orange juice, 1.3 μM. The plasma half-life of HSP in healthy people is 1.3 – 2.2 h (Erlund et al., 2001). HSP is an approximately equal mixture of R- and S-stereoisomers with similar pharmacokinetic properties (Lévèques et al., 2012).

There was no adverse effects of dosing with 135 mg HSP per day in healthy adults (Kanaze et al., 2007). HSP is considered extremely safe (Garg et al., 2001); the LD_{50} of hesperetin in rats was estimated to be >2000 mg/kg (Vaeth, 2006). In mouse embryonic stem cells in culture there was no effect of HSP on cell viability up to and including 100 μM (Choi et al., 2006). Hesperidin can be fully deglycosylated to HSP by hesperidin 6-*O*-α-L-rhamnosyl-β-D-glucosidase – which has been recently isolated and cloned from bacteria (Neher et al., 2015) and by chemical processing (Seitz and Wingard Jr, 1978).

1.7.4.1 Antioxidant properties of hesperetin

Flavanones have several biological properties, including antioxidant, anticancer, cancer chemopreventive, and anti-inflammatory properties (Harborne and Williams, 2000). Garg *et al*. reviewed the physicochemical and biological activities of Hesperidin and HSP, concluding they displayed antioxidant, anti-inflammatory, anticarcinogenic, and antiallergic properties (Garg et al., 2001). However, most of these studies use high concentration of HSP (50 μM) *in vitro* to identify benefits of this flavanone such as anti-obesity (Kim et al., 2013a). In addition, large number of studies have been published describing its new pharmacological activities, molecular targets, and mechanisms of action (Romano et al., 2013, Chiba et al., 2014). Recent findings show that the antioxidant activity of Hesperidin includes free radical scavenging activity and increased antioxidant cellular defences via the ERK/Nrf2 signalling pathway but has very weak activity (Chen et al., 2010a, Elavarasan et al., 2012). Recent research on flavonoids has focused on the protective properties of Hesperidin and HSP against several oxidants, such as peroxynitrite and hydrogen peroxide, and several other chemicals and toxins that cause damage to tissues via oxidative stress or other mechanisms (Kamaraj et al., 2010, Kalpana et al., 2009, Shrivastava et al., 2013).

The antioxidant properties of Hesperidin and HSP are achieved by at least two mechanisms: direct radical scavenging and augmenting cellular antioxidant defences. Studies have shown that Hesperidin and HSP have ability to neutralise reactive oxygen species (ROS), including superoxide anions, hydroxyl radicals, peroxynitrite, and nitric oxide radicals (Garg et al., 2001, Kim et al., 2004, Wilmsen et al., 2005, Choi, 2008). Wilmsen *et al*. incubated suspensions of yeast *S. cereyisiae* cells contain 2 $x10^6$ cells/ml with and without Hesperidin (25 and 50 μM) and

stressing agents (1 mM) for 6 h at 28 °C. Hesperidin increased activities of catalase and superoxide dismutase (Wilmsen et al., 2005). Choi (2008) administrated HSP to mice in which oxidative stress had been induced by dimethylbenz(a)anthracene (DMBA). HSP was administered orally to two of the three groups at 10 and 50 mg/kg body weight for 5 weeks (Choi, 2008). Thiobarbituric acid reactive substances (TBARS) and carbonyl content were measured as biomarkers of lipid peroxidation and protein oxidation, respectively. Treatment with HSP resulted in a normal level of lipid peroxidation in DMBA-treated groups, representing the protective effects of HSP. Hesperidin and HSP decreased tissue damage induced by hydrogen peroxide, peroxynitrite, CCl4, nicotine, DMBA, cadmium, LPS, acetaminophen, tert-butyl hydroperoxide, technetium (99m Tc, a radioactive element), gamma radiation, cyclophosphamide, benzo[α]pyrene, and acrylonitrile (neurotoxin) (Ahmad et al., 2012, Arafa et al., 2009, Balakrishnan and Menon, 2007b, Balakrishnan and Menon, 2007a, Chen et al., 2010b, Sahu et al., 2013, Hosseinimehr et al., 2009)

1.7.4.2 Role of hesperetin in glycation

There are few publications on the effects of Hesperidin and HSP on early glycation and AGEs. Li *et al*. reported an *in vitro* inhibitory effect of Hesperidin and HSP against glycation reaction when RNase was incubated with MG (100 mM) and bovine serum albumin (BSA) was incubated with glucose (100 mM) (Li et al., 2012a, Li et al., 2012b). These results are not translatable in physiological system and the study also suffers with technical flaws.

1.7.4.3 Anti-inflammatory effects of hesperetin

Flavanone have been used for their anti-inflammatory properties as either simple plant extracts or purified flavanone fractions (Kang et al., 2011, Ramelet, 2001). There are many *in vitro* and *in vivo* studies have been conducted to investigate Hesperidin and HSP (1 mM) ability in decreasing the inflammatory reactions. Wei et al., administrated Hesperidin orally at 5, 10 and 30 mg/kg to mouse allergic asthma model where the mice were sensitized and challenged by 100 µg of ovalbumin (OVA) to induce chronic airway inflammation and airway remodelling. The administration of Hesperidin significantly lowering the number of infiltrating inflammatory cells and Th2 cytokines in bronchoalveolar lavage (BAL) fluid

compared with the OVA-induced group of mice. Hesperidin decreased OVA-specific IgE serum levels (Wei et al., 2012). Yeh and his colleges used Hesperidin to investigate its modulation of lung local immune responses. Mice were treated with intratracheal LPS (100 μg) 30 min before Hesperidin oral administration (200 mg/kg). After 4 and 24 h, proinflammatory (TNF-α, IL-1β, IL-6), anti-inflammatory (IL-10, IL-4, IL-12) cytokines, chemokines (KC, MCP-1 and MIP-2), total cell counts, nitric oxide production, and proteins were measured in bronchoalveolar lavage fluid. The results showed that Hesperidin downregulate the LPS-increased expression of TNF-α, IL-1 α, IL-6, KC, MIP-2, MCP-1, and IL-12. Also, it enhanced the production of IL-4, IL-10 (Yeh et al., 2007). In the OVA-induced inflammation model, levels of cytokines such as IL-4 in BAL fluid increased more than in LPS-induced inflammation models (Wei et al., 2012, Yeh et al., 2007). Therefore, flavanone immunomodulatory effects may translate to immunosuppression in the OVA model but immunopotentiation in the LPS model (Wei et al., 2012, Yeh et al., 2007). Hesperidin has been proposed as a food supplement to treat complication of obesity but it did not improve glycaemic control nor insulin resistance in overweight and obese subjects (Rizza et al., 2011). Table 5 presents the anti-inflammatory effects of Hesperidin, HSP and related compounds.

Table 5: The anti-inflammatory effects of Hesperidin, HSP and related compounds.

Study model	Compound (s)	Major findings	References
	Hesperidin (30 μM)	↓ Prostaglandin E_2 (PGE_2)	(Sakata et al., 2003)
LPS-stimulated RAW 264.7 cells	Flavonoid mixture (nobiletin, naringin, and Hesperidin) (10, 50, 100 and 150 μg/ml)	↓ COX-2 and iNOS at both the protein and mRNA levels in a dose-dependent manner and probably via blocking NF-κB and the MAPK signaling pathway.	(Kang et al., 2011)
	Hesperidin and HSP and other flavonoids (10 -100 μM)	↓ NO, ↓ COX-1 and ↓ COX-2.	(Lee and Kim, 2010)
LPS-stimulated RAW 264.7 and A7r5 cells	Hesperidin and HSP (40 – 100 μM) and HSP metabolites (2.5 - 20 μM)	↓ iNOS and COX-2	(Yang et al., 2011)
H_2O_2-stimulated rat endothelial cells	HSP glucuronide metabolites, i.e. HSP-7G and HSP-3′G (100 μM)	↓ ICAM-1 and MCP-1	(Yamamoto et al., 2013)
HMC-1 cells, a human mast cell line	Hesperidin (0.1 mg/ml) and *Citrus unshiu* peel water extract (1 mg/ml)	↓ Inflammatory cytokine, HIF-1α and ↓ extracellular signal-regulated kinase (ERK) phosphorylation.	(Choi et al., 2007)
Human umbilical vein endothelial cells (HUVECs)	Hesperidin and other active compounds were extracted from *P. trifoliata* (Rutaceae) (1 -50 μM)	↓ TNF-α-induced VCAM-1 protein expression.	(Nizamutdinova et al., 2008)
Rat model of rheumatoid arthritis, AA	Hesperidin (40, 80 and 160 mg/ kg)	↑ IL-1β, IL-6, TNF-α and ↑ IL-10 secretion from synoviocytes. ↑ T-lymphocyte proliferation and ↑ IL-2 production.	(Li et al., 2008, Li et al., 2010)
	7,3′-dimethoxy HSP (20, 40, and 80 mg/ kg)	↓ TNF-α, IL-1β, IL-6. ↓	(Li et al., 2012c,

		antiapoptotic Bcl-2 expression and ↑ pro-apoptotic Bax expression.	Li et al., 2012b, Li et al., 2012a)
Murine OVA-induced airway inflammation	Hesperidin (5, 10 and 30 mg/kg)	↓ B cell-dependent production of OVA-specific IgE. ↓ OVA-induced total cell and ↓ cytokines such as IL-4, IL-5, and IL-13 in bronchoalveolar lavage fluid (BALF).	(Wei et al., 2012, Kim et al., 2011)
Xylene-induced ear oedema	Hesperidin and HSP (150 and 75 mg/kg respectively)	↓ Ear swelling in this model	(Rotelli et al., 2003)
Rat air pouch model of inflammation	Hesperidin (50 mg/kg) and naringin (30 mg/kg)	↓ Lipid peroxidation, ↓ superoxide dismutase (SOD), ↓ catalase (CAT), ↓ reduced glutathione (GSH) and ↓ NO in tissue.	(Jain and Parmar, 2011)
Murine dextran sulfate sodium-induced ulcerative colitis	Hesperidin (10, 40 and 80 mg/kg)	↓ IL-6	(Xu et al., 2009)
Murine LPS-induced acute lung inflammation model	Hesperidin (200 mg/kg)	↓ TNF-α, IL-1β, IL-6, and MCP-1, and ↑ anti-inflammatory cytokines such as IL-4 and IL-10 by its immunomodulatory effect.	(Yeh et al., 2007)
Healthy human beings	Orange juice (500 ml daily) and Hesperidin (292 mg in a capsule)	No marked effect on leukocyte activation, cytokine production (IL-2 and IL-4), or NK-cell lytic activity.	(Perche et al., 2014)

Modified from (Parhiz et al., 2015).

1.7.5 Proteomics

Proteomics is one focus of study in post-genomic science where all proteins in the whole or fractional proteome are detected, post-translational modifications (PTMs) and turnover are studied. Proteomics studies can thereby address the amount of gene products from gene expression in cells under basal and experimentally manipulated states and study interactions and subcellular distributions of proteins. Proteomics has thereby helped define protein composition of organelles, systematic explanation of protein-protein interactions and the large-scale mapping of PTMs – especially protein phosphorylation - as response to a stimulus. It is allied with gene expression studies measuring whole transcriptome mRNA levels, translational rates and turnover in 'transcriptomics' using oligonucleotide chips, and all metabolites in samples in metabolomics studies (Ong and Mann, 2005).

The term 'proteomics' was initially used to describe studies using two-dimensional gel electrophoresis (2-DE) of proteins with following gel excision of protein spots and protein identification by mass spectrometry – usually after limited proteolysis by trypsin. In 2-DE experiments, the pattern of staining of proteins from two samples revealed changes of up or down regulation of protein subsets. Staining of proteins was used to determine relative amounts of each protein within the sample. Limitations of the 2-DE approach are low resolution and bias against membrane proteins. The dynamic range of protein detection was also limited and could not accommodate the 7 - 12 orders of magnitude within a biological sample. Consequently, 2-DE gel studies have been superseded by nanoflow liquid chromatography-high resolution mass spectrometry (MS) in proteomics studies (Anderson and Anderson, 1998, Aebersold and Mann, 2003).

The principal workflow in MS proteomics sample analysis involves limited proteolysis by trypsin and/or lys-C to digest proteins to peptides (Fang et al., 2002), partial resolution of peptides by nanoflow liquid chromatography and detection and fragmentation of peptides by positive ion electrospray ionisation mass spectrometer. Subsequent fragment ion series mass spectra, MS_n spectra, are employed to sequence peptides and identification the protein(s) from which they were derived. Bioinformatics analysis tools are required for data analysis and threshold criteria for protein identification have been set by consensus. A minimum of two unique peptides are required for protein identification. Excellent detection and identification of protein-specific peptides approve their existence within the sample. Nevertheless,

inability to identify or detect a peptide does not certainly mean that the protein is absent, as the peptides possibly be under the threshold of recognition. As a result, the Boolean nature of MS protein identification schemes (present or absent by set threshold criteria) delivers an inadequate picture of protein abundance in a sample. Sensitive MS-based proteomic methods simply recognise 1000s of proteins in each samples but robust quantitation is challenging (Aebersold and Mann, 2003)

Quantitative data of protein have two forms: the absolute amount of the protein in the sample or the relative change in the amount of protein between two conditions. Absolute quantification is the measurement of the amount of the substance under investigation; for example, ng ml^{-1} of a protein or the copy number of a protein per cell. In relative quantification, the amount of a substance is measured in relative to another measure of the same substance, for example a fold change of protein abundance caused by drug treatment. Theoretically, absolute quantification includes relative comparisons; if the absolute amounts of the proteins are identified in two samples, their comparative ratios can be easily calculated (Ong and Mann, 2005, Sadygov et al., 2004).

Protein identification scores from commonly used algorithms (e.g. Mascot) cannot be used for quantitative measure of protein abundance. Rather quantitation is based on 'protein abundance indices' (PAIs). In order to low to high level of surety of quantitation, an initial approach is based on the number of peptides used in protein detection: this increases with increasing the amount of protein, and a greater protein will produce more quantifiable peptides than a low abundance protein. This is a simple PAI approach in which the number of observed peptides is normalized to the number of observable peptides for the protein in question (Rappsilber et al., 2002, Sanders et al., 2002). Ishihama et al. have detected that the relationship between the number of peptides detected and the amount of protein within a given sample is logarithmic, producing the concept of an exponentially modified PAI (emPAI) (Ishihama et al., 2005).

A range of experimental techniques and related protocols have been developed for protein isolation, separation, digestion, enrichment, depletion, identification and absolute and relative quantification of proteins. Currently, there are two main approaches to quantify protein by LC-MS/MS one including chemical labelling and the other one is label free (Wong and Cagney, 2010).

1.7.5.1 Labelling-based quantification

Most quantitative proteomic approaches depend on the samples labelling from different conditions with stable isotopes (^{2}H, ^{13}C, ^{15}N, ^{18}O) and a subsequent quantitative analysis by mass spectrometry with deduction of analyte amount by stable isotopic dilution analysis. Isotopic labelling is achieved by metabolic, chemical or enzymatic labelling. Methods applying stable-isotope labelling include: stable isotope labelling by amino acids in cell culture (SILAC), stable isotope labelling of mammals (SILAM), isotope-coded affinity tags (ICAT), isotope-coded protein labelling (ICPL), isobaric tags for relative and absolute quantification (iTRAQ), tandem mass tags (TMT), isobaric peptide termini labelling (IPTL), dimethyl labelling as well as several variants of these techniques. Interbatch coefficients of variation by this method are typically <10% (Megger et al., 2013).

1.7.5.2 Label-free quantification

Label-free quantitative approaches of proteomics can be divided into two different strategies of quantification that are briefly described in the following. The first approach is called spectral counting and involves a counting and a comparison of the number of fragment-ion spectra (MS/MS) attained for peptides of a certain protein. Because of the experimental findings that the number of tandem mass spectra of a specific peptide increases with an increasing amount of the equivalent protein, a relative proteins quantification between different samples is possible (Liu et al., 2004b). However, as the quantification in this method depend on a simple counting of resultant spectra rather than on quantifying physical data, the spectral counting method is debateable (Bantscheff et al., 2007, Bantscheff et al., 2012). Nevertheless, spectral counting is extensively employed and was more developed over the years. For instance, improved approaches of spectral counting have been reported that take into consideration aspects inducing the number of spectral counts, such as physicochemical properties of peptides and the lengths of the corresponding proteins. These approaches are identified as absolute protein expression (APEX) (Lu et al., 2007) and normalized spectral abundance factor (NSAF) (Florens et al., 2006, Zybailov et al., 2006). Recently, normalized spectral index (SIN) was presented which associates three MS abundance features, specifically peptide count, spectral count and fragment-ion intensity. This approach has revealed to eradicate discrepancies between measurements of replicate and permits quantitative

reproducibility and significant quantification in replicate MS measurements (Griffin et al., 2010).

The second approach of label-free quantitative proteomics measures the chromatographic peak areas of peptide precursor ions (molecular ions) - also called mass spectrometric signal strengths. Depending on the chromatographic technique (e.g. reversed-phase liquid chromatography), the peptides are separated according to their specific physical properties (e.g. hydrophobicity, charge) and are then ionized and identified by mass spectrometric analysis. In acquiring the mass spectrum, each peptide of a specific mass/charge ratio creates one mono-isotopic mass peak. The intensity of this peak as a function of the retention time can be visualized in an extracted ion chromatogram (XIC) and the area under the curve (AUC) can be determined. The areas of chromatographic peaks have been found to associate linearly in a wide range with the abundance of protein which makes their measurement achievable for quantitative studies (Bondarenko et al., 2002, Chelius and Bondarenko, 2002). This approach is straightforward and very convenient; however to achieve reliable results numerous experimental and technical features have to be considered. Additionally, raw LC–MS data produced in the experiments have to be post-processed (e.g. detection of features, alignment of retention times, normalization of MS intensities, peak picking, and noise reduction) for quantitative analysis (Megger et al., 2013). Interbatch coefficients of variation by this method are typically ≥30% (Megger et al., 2013).

1.7.5.3 Sample preparation, purification and separation for label-free quantification

Proteomic analysis may be made for different sample types varying from body fluids (e.g. serum, plasma, urine, bile) to cell lines or isolated cell types and tissue samples (Megger et al., 2013). Cell lysis, protein isolation and digestion is then performed. Cell lysis buffers and conditions are chosen depending on the whole or fractional proteome to be investigated e.g. membrane proteins, organelle proteins, cytosolic proteins, extracellular proteins and others (Shevchenko et al., 2012).

Digestion protocols involve trypsin and /or lys-C or other proteases (Wiśniewski et al., 2009). Trypsin is the most prevalent protease used in mass spectrometry as a result of its high proteolytic activity and cleavage specificity. However, trypsin has certain weaknesses, which is incomplete digestion.

Furthermore, trypsin activity is resisted by tightly folded proteins and inhibited by many reagents used in protein preparation (Saveliev et al., 2013). Lys-C overcomes the proteolytic resistance of tightly folded proteins and cleaves lysine sites with exceptional efficiency and specificity. Supplementing trypsin with Lys-C overcomes trypsin weaknesses (Saveliev et al., 2013). Additionally, spin columns are progressively used for sample purification (Antharavally et al., 2011) and corresponding on-filter digestion procedures are also available (Shevchenko et al., 2012). In-solution digestion procedures for small sample amounts were developed by Vékey and co-workers (Turiák et al., 2011).

Determination of total protein concentration in samples is also vital, particularly in the case of label-free quantification. Protein determination after extraction of protein from a sample is mandatory to check the successful protein isolation and to deduce the amount of protease required in the digestion step (Megger et al., 2013). Protein content may be determined by colorimetric methods, such as Bradford (Bradford, 1976), bicinchoninic acid (BCA) (Smith et al., 1985), biuret, Lowry (Lowry et al., 1951) or Popov assay (Popov et al., 1974). Alternatively, concentration of protein can be determined by amino acid analysis (Tyler, 2000).

Peptides achieved from a tryptic digestion are partially resolved by reversed-phase liquid chromatography (RP-LC) prior to and hyphenated with mass-spectrometric analysis. For label-free quantitative analysis by peptide ion intensities, the reproducibility of this stage is important (Megger et al., 2013). To confirm chromatographic reproducibility within a label-free study, it is advantageous to use an internal standard containing stable-isotope coded peptides. The retention times of these standard peptides can be used to observe the performance of LC–MS over a period of time and can be used as landmarks for the chromatographic alignment through following data analysis. Sickmann *et al.* obtained an internal standard of synthetic stable-isotope coded peptides that can act to assess several parameters on LC and MS level (Burkhart et al., 2011).

Several high-resolution mass analysers have been used for label-free proteomics analyses: time-of-flight (TOF), Fourier transform ion cyclotron resonance (FT-ICR) or Orbitrap analysers (Panchaud et al., 2008, Aebersold and Mann, 2003).

Bioinformatics and biostatistical tools have become necessary to handle and interpret the massive amount of data created in a single proteomic analysis. Useful open-source software is available (Megger et al., 2013). The dominant mass analyser used in proteomics studies is currently the Orbitrap mass spectrometer, mainly because of its high mass resolution, relatively easy analysis of output data and applicability to multiple types of peptide fragmentation (collision-induced dissociation CID, electron-transfer dissociation ETD and higher-energy collisional dissociation HCD).

1.7.6 Human periodontal ligament fibroblasts

Primary cultures of mammalian cells provide good similarity with tissue *in vivo* although they have limited growth potential and life span (Khojasteh et al., 2010).

1.7.6.1 Collection of hPDLFs

Primary hPDLFs collection techniques were described in 1985 by Ragnarsson and co-workers. Clinically healthy pre-molars or third molars were extracted. They are washed with sterile phosphate buffer saline (PBS) three times. The gingival attachment is carefully removed by surgical sharp scalpel. The crown is dipped in a 5.25% sodium hypochlorite solution for 2 min to eliminate bacteria and any remaining gingival cells. Each tooth is placed in sterile 15 ml centrifuge tube with 5 ml 0.125% trypsin and 0.1% collagenase and incubated at 37 ^{O}C for one hour. After incubation, the tooth was removed and the tube was centrifuged at 100 g for 2 min and cells collected by centrifugation. Cell were washed in complete medium (MEM, 10% FBS, containing 50 µg /ml gentamicin, 3 µg /ml fungazone) and plated into 60-mM culture dishes. The cells are incubated and replenished everyday with complete medium (Ragnarsson et al., 1985).

Another further technique was based on obtaining PDL explants by scraping the middle third of the root surface using a sterile surgical blade. Care was applied to avoid contamination from gingival or periapical granulation tissues. Then the explanted PDL is rinsed in sterile phosphate buffer saline (PBS) containing 2% penicillin–streptomycin solution (100 U/ml and 100 µg/ml). Next, the cells are sterilized in biopsy media: Dulbecco's Modified Eagle's Medium (DMEM) with glucose (4500 mg/ml), 10% foetal bovine serum (FBS), 2% penicillin–streptomycin,

250 µg/ml gentamicin sulfate and 2.5 µg/ml amphotericin B (Chou et al., 2002, Khojasteh et al., 2010, Somerman et al., 1990, Nizam et al., 2014) .

1.7.6.2 Separation of fibroblasts and epithelial cells

The periodontal ligament fibroblasts cells start to grow out from the explants within about ten days (Jönsson et al., 2011). When confluence is obtained, the cells are subcultured by differential trypsinisation. The dishes are rinsed with PBS and the cells are removed with 0.15% trypsin. The removal of cells should be closely observed by phase microscopy. The trypsin will remove the fibroblasts earlier and faster than the epithelial cells. The early and late removed cell are collected separately and plated into clean culture dishes (Ragnarsson et al., 1985).

1.7.6.3 Characteristic of primary hPDLFs

The teeth used for collecting explants are generally extracted for orthodontic reasons from subjects between 12 and 18 years of age. The hPDLFs viability is high, probably because of the fact that the cells originate from young and healthy individuals. After passage, the cells are re-seeded and then used for experimentations in passages two to eight. It was found that in passages 3 to 5, cells respond in a similar way to stimulation with hormones and growth promoters (Jönsson et al., 2005). This suggests that their phenotype is preserved, even though some osteogenic markers such as alkaline phosphatase activity, have been shown to be reduced at later (passage 6) compared with earlier passages (Itaya et al., 2009). Cell viability decreases beyond passage 7 which suggest that the periodontal ligament fibroblasts then undergo senescence (Jönsson et al., 2011).

1.7.7 Human periodontal ligament fibroblasts as a model for periodontitis

Periodontal ligament fibroblasts are used in research to investigate inflammation, disease process and tissue breakdown in periodontal diseases. Human periodontal ligament fibroblasts **(**hPDLFs) have an important role in modulating the inflammatory process in periodontium (Özdemir et al., 2014).

1.7.7.1 Inflammation promoters enhance hPDLFs cytokine and chemokine mRNA and protein production

In addition to their fibroblast and osteoblast-like properties, hPDLFs have functional characteristics comparable to those of leukocytes and leukocyte-derived cells such as macrophages involved in essential immunity (Özdemir et al., 2014). hPDLFs express and secrete cytokines and chemokines in response to stimulation of inflammation promoter – Table 6. The cytokine and chemokine transcript and protein levels were found low or below the level of detection in unstimulated hPDLFs but they increase markedly with stimulation by inflammation promoters, such as bacterial lipopolysaccharide (LPS) (Jönsson et al., 2011). LPS prompts cytokine production in human gingival fibroblasts (HGFs) (Souza et al., 2010, Almasri et al., 2007). This suggests that hPDLFs and HGFs work together to promote proinflammatory actions.

Cytokine and chemokine production by hPDLFs was detected in response to stimulation with 1 ng/ml to 10 ng/ml LPS (Jönsson et al., 2008, Jönsson et al., 2009). LPS prompted hPDLFs cytokine/chemokine expression, was detected within hours but also after several days (3–21 day) of treatment. This is presenting that both acute and long-term stimulation with inflammation promoters stimulate cell-signalling pathways causing cytokine/chemokine production (Jönsson et al., 2008).

Inflammation promoter-induced cytokine and chemokine production is detected in hPDLFs in passages 3 to 5. This is found in both acute (24 hour) and chronic (3–21 day) LPS stimulation responses (Jönsson et al., 2008).

Table 6: A review of papers presenting data on pro-inflammatory stimulus-induced cytokine/chemokine expression in hPDLFs.

Proinflammatory stimulus	Cytokine/ chemokine	Transcript/protein level	Reference
***Escherichia coli* LPS**	IL-6, MCP-1	Protein	(Jönsson et al., 2008)
***E. coli* LPS**	GROα	mRNA and protein	(Jönsson et al., 2009)
TNF-α	IL-6	Protein	(Okada et al., 1997)
Porphyromonas gingivalis, P. intermedia	IL-1β, IL-6, IL-8	mRNA	(Yamamoto et al., 2006)
***P. endodontalis* LPS**	IL-6	mRNA and protein	(Ogura et al., 1994)
***Actinobacillus actionomycetem-comitans* LPS, *E. coli* LPS**	IL-1β, IL-6, IL-8	mRNA and protein	(Agarwal et al., 1998)
***E. coli* LPS**	TNFα, IL-1β, IL-6, RANKL	mRNA and protein	(Shu et al., 2008)
***P. gingivalis* LPS, *E. coli* LPS**	IL-6, IL-8	mRNA and protein	(Yamaji et al., 1995)
Streptococcus mutans	IL-6, IL-8	Protein	(Engels-Deutsch et al., 2003)
TNFα, IL-1β	MCP-1	mRNA and protein	(Ozaki et al., 1996)
Reactive oxygen species (H_2O_2)	IL-8	mRNA and protein	(Lee et al., 2008)
***P. gingivalis* LPS**	IL-6	Protein	(Morandini et al., 2010)
***E. coli* LPS**	IL-1β, TNFα	mRNA	(Wada et al., 2004)

Adapted from (Jönsson et al., 2011).

Leptin has powerful effects on immunity and inflammation. Recent evidence suggests a role of leptin in periodontitis as judged by the effect of leptin on the level of serum interleukin IL-1β, IL-6, and TNF-α, as well as clinical markers of periodontal breakdown (Zimmermann et al., 2013, Meng et al., 2015). Li and co-workers (2015) studied this in hPDLFs. High dose of leptin can induce the expression of mRNA and protein of IL-6 and IL-8 in hPDLFs through binding with obesity related leptin receptor-b (OBRb) and triggering different intracellular signalling pathways (Li et al., 2015).

In hPDLFs, IL-17 upregulated the production of IL-6 and MMP-1 sequentially. IL-6/sIL-6R (soluble IL-6 receptor) may improve the effects of IL-1β on MMP-1 production. IL-17 likely induces MMP-1 production directly and also indirectly by stimulating IL-6 production, thus causing in the degradation of collagens in the PDL (Shibata et al., 2014).

The effect of high mobility group box 1 (HMGB1) on cultured hPDLFs was investigated. hPDLFs expressed RAGE, TLR2 and TLR4 mRNA. Production and mRNA expression of IL-6 and IL-11 were increased in hPDLFs cells stimulated with HMGB1. Furthermore, they were inhibited by anti-RAGE, TLR2 and TLR4 antibodies. This suggested that hPDLFs cells produce IL-6 and IL-11 in response to HMGB1 via RAGE, TLR2 and TLR4 (Hasegawa, 2008). A further study conducted to investigate the effects of different concentrations of high glucose on apoptosis in hPDLFs and the potential mechanisms involved. hPDLFs were cultured and subjected to glucose of different concentration (5.5, 15, 25, and 35 mM) for 24 hours. The data show that high glucose prompts a concentration- and caspase-3-dependent increase of apoptosis in hPDLFs *in vitro*. Stimulation of caspase-3 triggered by high glucose is independent of Fas/FasL signalling pathways system. A mechanism for the regulation of hPDLFs apoptosis by high glucose was proposed (Liu et al., 2013).

1.8 Aims and objectives

In this project I hypothesised that increased concentration of MG is produced in hPDLFs by exogenous MG, hyperglycaemia associated with diabetes and inflammatory signalling leading to increased extracellular matrix modification causing human PDL fibroblast (hPDLFs) dysfunction and extracellular matrix detachment. The aim of this study is to test this hypothesis and characterise the activity of glyoxalase system and the influence of dicarbonyls on hPDLFs growth and function *in vitro* – including under stress of high glucose concentration as a model of hyperglycaemia in diabetes. The major experimental model for this hPDLFs cells in primary culture. This is a widely used cell culture model of mechanisms of cell dysfunction and injury leading to periodontitis (Mariotti and Cochran, 1990). hPDLFs are key cells mediating dysfunction in periodontitis in diabetes (Somerman et al., 1990).

Objective 1: To characterise the glyoxalase system and dicarbonyl metabolism in hPDLFs cells *in vitro* and dicarbonyl stress induced by high glucose concentration

There is no previous research on the glyoxalase system and the associated dicarbonyl metabolism in hPDLFs or related cell lines. There was a report describing increased MG in gingival crevicular fluid (GCF) of subjects with periodontitis but since the study estimated MG in "pmol per site" without assessment of site volume, it is not clear what the concentration of MG was nor if the change in periodontitis relates to a change in concentration (Kashket et al., 2003). If the GCF volume was < 1 μl, as is usual (Teles et al., 2010), MG estimates were > 100 μM which is typically of profound overestimates of MG (Rabbani and Thornalley, 2014c). There is emerging evidence that dicarbonyl stress contributes to pathogenesis in inflammation and diabetes. Therefore, it is important to characterise the glyoxalase enzymatic system using well-validated analytical techniques in a relevant cell type, hPDLFs cells, and assess how it response to stress of inflammatory stimuli and high glucose concentration.

To achieve this objective, hPDLFs cells will be used as a model in which to characterise the glyoxalase system in both low concentration of glucose, 8 mM, and high concentration of glucose, 25 mM. The glyoxalase enzymes activities and the associated metabolites concentrations, dicarbonyls, D-lactate and glutathione, will be

measured. The glyoxalase pathway flux will be measured and the glucose consumption will be used to estimate the proportional flux from triosephosphates in cells cultured in low and high glucose. Cellular protein will be examined for damage marker adducts to identify whether exposure to higher concentrations of glucose has an influence on the level of cellular protein damage. In hPDLFs model, dicarbonyls, glutathione and cell thiols will be determined, as well as the RNA expression of glyoxalase 1 to characterise alterations in dicarbonyl metabolism and hPDLFs function.

Objective 2: To study the effect of Glo1 inducers on the formation and metabolism of methylglyoxal in hyperglycaemia in hPDLFs *in vitro* and cell function

High glucose concentration in hyperglycaemia associated with diabetes and downregulation of Glo1 expression in inflammation is likely to cause dicarbonyl stress in hPDLFs lead to cell dysfunction and contribute to periodontal disease. The most effective strategy to counter this is to increase the expression of Glo1. This may be achieved through the functional ARE and activators of Nrf2 which induce Glo1 (Xue et al., 2012a).

To achieve this objective, the effect of recently discovered small molecule Glo1 inducers on the formation and metabolism of MG will be studied in hPDLFs. Glo1 inducers have been screened from libraries of dietary bioactive compounds known to activate transcription factor Nrf2 and may thereby increase Glo1 expression through Nrf2 binding to a functional antioxidant response element (Xue et al., 2012a). This was done on a commercailisation project in the host research team. The best Glo1 induction was achived with a binary, 2-compound co-formulation. This has been applied in this project. Levels of glyoxalase 1 activity, protein, mRNA expression and concentration of dicarbonyls and protein damage markers will be determined in cell extracts to assess the effect of Glo1 inducers on production of dicarbonyls and the markers of protein damage and the impact on cell function in high glucose. Levels of glucose consumption, D-lactate and L-lactate production will be measured in medium obtained from same culture. Glutathione and cell thiols will be determined to characterise changes in dicarbonyl metabolism and hPDLFs function.

The functional activity of hPDLFs may be changed in dicarbonyl stress. One target for dicarbonyl glycation affecting functionality is modification of RGD and GFOGER integrin binding sites by MG and detachment of hPDLFs from collagen-I in the extracellular matrix; *cf*. detachment of endothelial from collagen type IV modified by MG (Dobler et al., 2006). The sites of modification were specific arginine residues within integrin binding sites, essential for cell-ECM binding in both endothelial cells and periodontal cells. To achieve this objective hPDLFs cells will be cultured on control and MG-modified collagen-I coated plates and adhesive ability will be assessed colorimetrically. Then, the effect of Glo1 inducer on the attachment ability of hPDLFs to collagen will be determined.

Objective 3: To study the dysfunction of hPDLFs exposed to AGE-modified proteins *in vitro*

hPDLFs have been shown to activate RAGE which is thought to bind proteins highly modified by AGEs (Neeper et al., 1992, Kislinger et al., 1999) – although there is concern whether it binds proteins modified minimally by AGEs found in cells and tissues of physiological systems (Thornalley, 2007, Buetler et al., 2008, Thornalley, 1998b). If AGE-modified proteins bind and activate RAGE in hPDLFs it may lead to activation of the NF-kB system, inflammatory signalling and tissue cell dysfunction. It has also been claimed that RAGE activation down regulates Glo1 (Bierhaus et al., 2005a) – although this has to be further confirmed. This would produce and exacerbate dicarbonyl stress in hPDLFs.

To achieve this objective, the effect of human serum albumin glycated to low and high extent by CML (CML_{min}-HSA and CML-HSA), albumin glycated by glucose to form FL and a mixture of glucose-derived AGEs and unglycated albumin as control will be prepared *in vitro*. Then, hPDLFs will be treated with the modified human serum albumin and activation of NF-kB and Glo1 activity and expression in hPDLFs *in vitro* will be investigated.

Objective 4: To study the mechanism of down regulation of glyoxalase protein in hPDLFs *in vitro*

When endothelial cells and other cells are incubated in high glucose concentration and develop dicarbonyl stress (Dobler et al., 2006), a contributing factor is decrease in activity of Go1 protein. If this occurs in hPDLFs the mechanism

of Glo1 down regulation will be investigated. Assay of Glo1 mRNA, protein and activity will be performed to assess if the loss of Glo1 activity is due to decreased expression, increased degradation or inhibitory PTM. Glo1 is a target for acetylation (Li et al., 2012) and deacetylation by sirtuins (Rauh et al., 2013). In addition, tRSV corrects decreased SIRT1 activity in cells exposed to high glucose concentration *in vitro* (Mortuza et al., 2013). Sirtuin are protein deacetylases - mediated deacetylation reaction by coupling lysine deacetylation to NAD hydrolysis (Guarente, 2013). To further pursue this objective, I will investigate putative acetylation and other PTMs of Glo1 in hPDLFs by high resolution mass spectrometry proteomics and immunoblotting. I will assess if there is a link between Glo1 acetylation and Glo1 protein content, as may occur in acetylation-directed ubiquitination (Xiong and Guan, 2012). I will also investigate sirt1 and sirt2 protein level and mRNA expression in hPDLFs incubated in low and high glucose concentrations with or without Glo1 inducers. In addition, the effect of deacetylase inhibitors and activators on Glo1 activity and mRNA expression level in hPDLFs incubated in low and high glucose will be determined.

Objective 5: To study the dicarbonyl proteome in the cytosol of hPDLFs incubated in low and high glucose *in vitro*

Dysfunction of hPDLFs in dicarbonyl stress is mediated by protein modification by MG and related dicarbonyls. MG is formed and accumulates in the cell cytoplasm where it modify proteins. Change in the total level of the major MG-derived AGE, MG-H1, in cytosolic extracts of cell protein has been determined in Objective 1. To identify which proteins suffer MG-H1 modification, I will apply high resolution mass spectrometry proteomics analysis to cytosolic extracts of cell protein from hPDLFs cultured in low (8 mM) and high (25 mM) glucose for three days. I will use as positive control a cytosolic extract of cell protein from hPDLFs that has been incubated in cell-free system with exogenous MG to increase MG-H1 content *ca.* 10-fold. Samples were prepared for proteomic analysis, mass spectrometric analysis performed on a nanoflow-Orbitrap platform and unmodified and MG-H1-modified proteins identified by MS/MS sequencing. Data analysis will include bioinformatics pathway analysis to assess which metabolic pathways in the cell cytosol are most sensitive to dicarbonyl stress.

Objective 6: To characterise glycation, oxidation and nitration adduct residue content of plasma protein of healthy people, patient with periodontitis and patients with periodontitis and end stage renal disease

To achieve this objective, plasma will be collected from healthy people as control subjects, patient with periodontitis and patients with periodontitis and chronic kidney disease (CKD) stage 3 or 4. All of the latter group also had diabetes mellitus. The glycation, oxidation and nitration adduct residue content of plasma protein was determined by stable isotopic dilution analysis LC-MS/MS.

2. Materials and Methods

2.1 Materials

2.1.1 Cells and tissues

Primary human periodontal ligament fibroblasts (hPDLFs) were purchased from ScienCell, Carlsbad, USA; cat. no. 2630. hPDLFs were isolated from human periodontal tissue of healthy individuals which is located between the cementum of the teeth and the alveolar bone of the mandible.

2.1.2 Cell culture reagents

Primary hPDLFs were maintained in Modified Eagles Medium (MEM) (cat. no. M8042, ScienCell) supplemented with 10% Foetal Bovine Serum (FBS) and penicillin-streptomycin (cat. nos. F7524 and P0781 respectively; Sigma Aldrich, Gillingham, Dorset UK) and L-glutamine (200 mM solution; cat. no. 25030-024, Gibco Life Technology, Paisley, UK). Tissue culture grade plastic polystyrene T75 flasks was purchased from Fisher Scientific (Nunclone™, Loughborough, UK). Trypsin/EDTA (0.25%; a solution, sterile-filtered, containing 2.5 g porcine trypsin and 0.2 g EDTA. $4Na^+$ per liter of Hanks' Balanced Salt Solution with phenol red) was purchased from Invitrogen Life Technologies (Paisley, UK; cat. no. 25200-072). Trypan blue dye was purchased from Sigma Aldrich (cat. no. 302643).

2.1.3 Enzymes, substrates, cofactors, and consumables

Proteases, peptidases, D-lactic dehydrogenase, L-lactic dehydrogenase and other enzymes were purchased from Sigma-Aldrich. L-Lactic dehydrogenase (EC 1.1.1.27) was from bovine heart, type III with activity of ≥ 500 units/mg protein. D-Lactic dehydrogenase (EC 1.1.1.28), lyophilised powder, was from Staphylococcus epidermidis and had activity of ≥ 80 units/mg protein. Pepsin (EC 3.4.23.1) was from porcine stomach mucosa with a specific activity of 3460 units/mg protein (1 unit hydrolysed haemoglobin with an increase in A280 of 0.001 AU per min of trichloroacetic acid-soluble products, at pH 2 and 37 ^oC); prolidase (EC 3.4.13.9) was from porcine kidney and had a specific activity of 145 units/mg protein, where 1 unit of activity hydrolyses 1.0 μmol of Gly-Pro per min, at pH 8 at 40 ^oC; leucine aminopeptidase (EC 3.4.11.2), type VI, was from porcine kidney microsomes with a specific activity of 22 units/mg protein (1 unit of activity hydrolysed 1.0 mol of L-

leucine-p-nitroanilide to L-leucine and p-nitroaniline per min at pH 7.2 and 37 ^{o}C); pronase E (EC 3.4.24.31), type XIV, was from bacterial *Streptomyces griseus* with a specific activity of 4.4 units/mg protein (1 unit of activity hydrolysed casein forming 1.0 mmol of tyrosine per min at pH 7.5 and 37 ^{o}C); and collagenase (EC.3.4.24.3) was from bacterial *clostridium histolyticum* with specific activity of 125 Collagen Digestion Unit (CDU)/mg protein (CDU definition – one unit liberates peptides from collagen equivalent in ninhydrin colour to 1.0 μmol L-leucine in 5 h at pH 7.4 at 37 °C in the presence of calcium ions).

2.1.4 Primers and antibodies

Primers

Glo1 and β-actin primers were designed using OligoPerfect^{TM} designer software and purchased from Invitrogen. Primers for SIRT1, SIRT2, COL1, COL3 and COL12 genes were purchased from Sigma Aldrich (Gillingham, Dorset, UK). Primers were used to amplify cDNA for mRNA of GLO1, β-actin, SIRT1, SIRT2, COL1, COL3 and COL12 are summarised in Table 7**.**

Table 7: The primers sequences used for amplification

Primers	Forward	Reverse
GLO1	5'-ATGCGACCCAGAGTTACCAC-3'	5'-CCAGGCCTTTCATTTTACCA-3'
ACTB	5'-GGACTTCGAGCAAGAGATGG-3'	5'-AGCACTGTGTTGGCGTACAG-3'
SIRT1	5′-AGGATAGAGCCTCACATGCAA-3′	5′-TCGAGGATCTGTGCCAATCATA-3′
SIRT2	5′-ATCCCCGACTTTCGCTCTC-3′	5′- GGTTGGCTTGAACTGCCCA -3′
CLO1	5' GTGCTAAAGGTGCCAATGGT-3'	5'- ACCAGGTTCACCGCTGTTAC-3'
CLO3	5'- CCAGGAGCTAACGGTCTCAG-3'	5'- CAGGGTTTCCATCTCTTCCA-3'
CLO12	5'- CTCCTTGGGCATTAAAGCTG-3'	5'- GCTTCCAATTCTGAGCGAAC-3'

Antibodies

Anti-Glo1 rabbit polyclonal antibody (cat. no. H00002739-D01) used for immunoprecipitation experiments was purchased from VWR International Ltd (Lutterworth, UK). Monoclonal anti-Glo1 antibody produced in rat (cat. no. SAB4200193), anti-rabbit IgG antibody (cat. no. A9169), anti-mouse IgG antibody (cat. no. A9917) and anti-rat IgG antibody (cat. no. B7139) were purchased from Sigma-Aldrich. Anti-β-actin mouse monoclonal antibody (cat. no. ab6276) and anti-acetyl lysine rabbit polyclonal antibody (cat. no. ab80178) were purchased from

Abcam (U.K). Anti-SIRT1 (cat. no. ab32441) and anti-SIRT2 (cat. no. ab51023) rabbit monoclonal antibodies were purchased from Abcam (U.K).

2.1.5 Other analytical reagents

Methanol, acetonitrile, isopropanol (IPA) and tetrahydrofuran (THF) (all HPLC grade) were purchased from Fisher Scientific. Trifluoroacetic acid (TFA, ≥ 99% HPLC grade), Trifluoroacetic acid (TCA, BioUltra, ≥ 99.5%) and formic acid (FA, ≥ 98%) were purchased from Sigma-Aldrich. All other reagents, salts, acids and bases for buffers were analytical grade reagents and purchased from Sigma-Aldrich and Fisher Scientific. D-Lactate, D-glucose, reduced glutathione (GSH) and glycine were purchased from Sigma-Aldrich. Methylglyoxal (MG) for cell culture was prepared by the hydrolysis of methylglyoxal dimethylacetal in dilute sulphuric acid and purified by fractional distillation under reduced pressure, as previously described (McLellan and Thornalley, 1992)

Human serum albumin solution (Zenalb^{TM} 20; 200 g/l of which >95% is human albumin, endotoxin free) was purchased from Bio Products Laboratory Limited (Hertfordshire, UK). Nicotinamide adenine dinucleotide, oxidised form, (NAD^+; cat. no. N6522), aminoguanidine hydrochloride (cat. no. 369494), D-lactic acid (cat. no. L0625), L-lactic acid (cat. no. L6402) pyruvate (cat. no. P2256), and glyoxal (cat. no. 43612; 40% aqueous solution) were purchased from Sigma-Aldrich. Lipopolysaccharides, LPS (cat. no. L6143; from *Salmonella enterica* serotype typhimurium, γ-irradiated), tumour necrosis factor-α, TNF-α (cat. no. T0157) – human recombinant, expressed in yeast and had activity of ≥2 × 107 U/mg, buffered aqueous solution, were purchased from Sigma Aldrich. Trichostatin A (TSA), [R-(E,E)]-7-[4-(dimethylamino)phenyl]-N-hydroxy-4,6-dimethyl-7-oxo-2,4-heptadienamide from *Streptomyces species* (cat. no. T8552), sirtuin-1 (SIRT1) inhibitor 6-chloro-2,3,4,9-tetrahydro-1H-carbazole-1-carboxamide (EX-527; cat. no. E7034), and sirtuin-2 (SIRT2) inhibitor 2-cyano-3-[5-(2,5-dichlorophenyl)-2-furanyl]-N-5-quinolinyl-2-propenamide (AGK2; cat. no. A8231), were purchased from Sigma Aldrich.

2.1.6 Other consumables

Sodium phosphate monobasic (cat. no. 71505), hydrochloric acid (analytical grade, 1 N; HCl) (cat. no. H1758) bovine serum albumin, EDTA, triton-X100,

Tween-20, diethylenetriaminepentaacetic acid (DETAPAC) (cat. no. D6518), mannitol and *trans*-resveratrol (tRSV, cat. no. R5010), ammonium persulphate (ACS reagent grade, cat. no. 248614), N,N,N',N'-tetramethylethylene-1,2-diamine (TEMED, ≥ 99% electrophoresis grade), β-mercaptoethanol, 3',3",5',5"-tetrabromophenol sulfonphthalein sodium salt (bromophenol blue, electrophoresis grade) were purchased from Sigma-Aldrich. Protease inhibitor cocktail (cat.no. 04693159001) and phosphatase inhibitor cocktail (cat. no. 04906845001) tablets were purchased from Roche Diagnostics (Mannheim, Germany). 10 x RIPA lysis buffer (cat. no. 20-188) (0.5 M Tris-HCl, pH 7.4, 1.5 M NaCl, 2.5% deoxycholic acid, 10% NP-40, 10 mM EDTA) was purchased from Millipore, UK. Coomassie Brilliant Blue G-250 (analytical grade) and hydrazine hydrate (cat. no. 18412) was purchased from Fluka (Poole, Dorset, UK). Tris(hydroxymethyl)aminomethane (Tris), Tris-HCl base, perchloric acid, sodium chloride and potassium bicarbonate were purchased from Fisher Scientific (Loughborough, UK).

The 10 x premixed electrophoresis Tris-glycine buffer (cat. no. 1610732; 1 x dilution contains 25 mM Tris, 192 mM glycine, pH 8.3), 10 x Tris-buffered-saline TBS (cat. no. 1706435 ; 1 x dilution gives 20 mM Tris, 500 mM NaCl, pH 7.4), Criterion™ TGX™ stain-free gel 4–20% precast polyacrylamide gel (cat. no. 3450412, 3450418, 3450426), *Trans*-Blot® Turbo™ PVDF pre-cut blotting transfer pack (cat. no. 1704157), including filter paper, buffer, polyvinyl difluoride (PVDF) membrane for use with *Trans*-Blot Turbo transfer system (cat. no. 1704155) were purchased from Bio-Rad (Hertfordshire, UK). Photographic film was purchased from GE Healthcare (Little Chalfont, UK). Spectro^{TM} multicolor broad range protein ladder (10-260 kDa, for 4 – 20% Tris-glycine SDS-PAGE), enhanced chemiluminescence (ECL) reagent kit (cat. no. 32106) and sodium dodecyl sulphate (SDS) (cat. no. 28312B) were purchased from Fisher Scientific.

Concentrated protein assay dye and reagents for Bradford assay (cat. no. 5000201) and DC assay (cat. no. 5000111) were purchased from Bio-Rad Laboratories. BCA protein assay was purchased from Fisher Scientific.

Microplate U bottom polystyrene 96-well Sterilin plate, HPLC vials, inserts and plastic supports, caps and microspin filters "Spin-X" (0.2 μm pore size) were purchased from Fisher Scientific. Amicon ultrafiltration microcentrifuge tubes and filter inserts (0.5 ml, 3 kDa and 10 kDa cut-off) were purchased from Merck-Millipore (Watford, UK).

2.1.7 Analytical and preparative kits

The glucose assay kit - hexokinase method (cat. no. GAHK20) - was purchased from Sigma-Aldrich. The RNAse mini kit (cat .no. 74106) was from Qiagen, UK. Nuclear extraction kit (cat. no. 40010) and TransAM® Flexi NF-κB p65 kits (cat. no. ab133128) were purchased from Abcam as UK supplier of products for Active Motif (La Hulpe, Belgium). Pierce™ Limulus Amebocyte Lysate (LAL) chromogenic endotoxin quantitation kit (cat. no. 88282), Direct magnetic IP/Co-IP kit and Dynabeads® Protein G immunoprecipitation kit (cat. no. 10007D) were purchased from Fisher Scientific (Loughborough, UK). CytoSelect™ 48-well cell adhesion assay (collagen I, colorimetric) (cat. no. CBA-052) was purchased from Cambridge Bioscience Ltd (Cambridge, UK).

2.1.8 Chromatographic materials

For dicarbonyl assay the column-BEH C18, 1.7 µm particle size column (100 x 2.1 mm) fitted with a (5 x 2.1mm) pre-column was purchased from Waters (Elstree, Herts, UK). The two columns used for protein damage markers and glutathione analysis - 5 µm particle size Hypercarb™ columns (column 1, 2.1 x 50 mm; and column 2, 2.1 mm x 250 mm) were purchased from Fisher Scientific. Analytical microcentrifuge tube filter inserts (0.2 µm) were purchased from Alltech Associates Applied Science Ltd (Carnforth, Lancs, U.K.). For proteomics analysis the column used was: an Acclaim PepMap ODS µ-precolumn cartridge, 300 µm i.d. x 5 mm, 5 µm particle size, 100 Å pore size, fitted to an Acclaim PepMap ODS RSLC 75 µm i.d. x 50 cm, 2 µm particle size, 100 Å pore size main column (Thermo Scientific).

2.1.9 Analytical standards

2.1.9.1 Calibration standards for protein glycation, oxidation and nitration adduct analysis

The standards for protein damage markers were prepared by current and previous members of host research team, as described previously (Thornalley et al., 2003b, Ahmed et al., 2003). [*guanidino*-$^{15}N_2$]-L-Arginine, 4,4,5,5-[$^{2}H_4$]L-lysine and [$^{13}C_6$]L-lysine, [*methyl*-$^{2}H_3$]-L-methionine and *ring*-[$^{2}H_4$]-L-tyrosine (all >98% isotopic purity) were purchased from Cambridge Isotope Laboratories (Andover,

MA, USA). [*guanidino*-$^{15}N_2$]MG-H1, [*guanidino*-$^{15}N_2$]3DG-H and [*guanidino*-$^{15}N_2$]G-H1 were prepared in house from [*guanidino*-$^{15}N_2$]-L-arginine after conversion to the Nα-t-butoxycarbonyl derivative (Thornalley et al., 2003b, Meldal and Kindtler, 1986). [$^{2}H_8$]MOLD was prepared from 4,4,5,5-[$^{2}H_4$]-L-lysine after conversion to the Nα-formyl derivative (Finot and Mauron, 1969). [$^{13}C_6$]CEL, [$^{13}C_6$]CML and [$^{13}C_6$]pentosidine were prepared from [$^{13}C_6$]-L-lysine after conversion to the Nα-formyl derivative. The synthetic methods for the preparation, purification and characterisation of all AGE calibration standards were as described for their non-isotopically substituted analogues (Ahmed et al., 2003). [*methyl*-$^{2}H_3$]MetSO was prepared from [*methyl*-$^{2}H_3$]-L-methionine, and [$^{2}H_6$]dityrosine and [$^{2}H_3$]3-nitrotyrosine (3-NT) were prepared from *ring*-[$^{2}H_4$]-L-tyrosine, using previously described methods (Lapp and Dunn, 1955, Huggins et al., 1993, Sokolovsky et al., 1966).

2.1.9.2 Dicarbonyl calibration standards

Glyoxal (40% aqueous solution) from Sigma-Aldrich was used without purification. High purity MG and 3-deoxyglucosone (3-DG) were prepared in-house by the host research team. MG was prepared as mentioned before and described by McLellan (McLellan and Thornalley, 1992). 3-DG was prepared from glucose and toluidine by method of Madson and Feather (Madson and Feather, 1981) with modifications described by Henle and Bachmann (Henle and Bachmann, 1996). The concentration of stock solutions of dicarbonyls was calibrated by conversion to 1,2,4-triazine derivatives by incubation with aminoguanidine hydrochloride and spectrophotometric detection, deducing concentrations of the 1,2,4-triazine derivatives and thereby dicarbonyl precursors from known extinction coefficients (Thornalley et al., 2000).

2.1.10 Instrumentation

A Nikon Eclipse TE2000-S inverted microscope (Kingston-Upon-Thames Surrey, U.K.) was used to view cells and record micrographs. Neubauer haemacytometer was used for cell counting (Model no. 0630410, Marienfeld-Superior, Paul Marienfeld GmbH & Co. KG, Lauda-Königshofen, Germany). A FLUOstar OPTIMA microplate reader from BMG Labtech (Aylesbury, U.K) was used for microplate spectrophotometry and fluorimetry. Other spectrophotometry

was performed with UVICON UV/VIS spectrophotometer (Northstar Scientific Limited, Leds, U.K.). The Vibra-Cell sonicator, used to disrupt cells, was from Jencons Scientific (Leighton Buzzard, UK). A Criterion™ Cell electrophoresis chamber (Model no. 1656020), *Trans*-Blot® Turbo™ Transfer System (Model no. 170-4155) and PowerPac™ Basic Power Supply (Model no. 164-5050) were purchased from Bio-Rad. Applied Biosystems™ 7500 Real-time PCR machine was from Life Technologies. Quantification of RNA stock solutions was performed using a ND-1000 Nanodrop spectrophotometer (Nanodrop, Wilmington, USA). A gel imaging system for fluorescence and chemiluminescence, G:BOX Chemi XX6 system, was purchased from Syngene (Cambridge,UK).

Liquid chromatography-tandem mass spectrometry (LC-MS/MS) analysis was performed using two different instruments from Waters (Manchester, U.K.): (i) an Acquity™ UPLC system with a Quattro Premier XE tandem mass spectrometer, and (ii) and an Acquity™ UPLC system with a Xevo-TQS tandem mass spectrometer. Enzymatic hydrolysis was performed using a CTC-PAL Automation System (CTC-Analytics, Zwingen, Switzerland). The centrifugal evaporator was a Savant Instruments SpeedVac (Thermo Scientific, Waltham MA). For high resolution mass spectrometry proteomics analysis, The UltiMate® 3000 RSLCnano LC system was used coupled with Thermo Orbitrap Fusion mass spectrometer (Thermo Scientific).

2.1.11 Software

Microplate assays were analysed using Optima software version 2.10 R2 (BMG Labtech). Real-time PCR analysis was performed using 7500 Fast System Software version 1.4.0. ImageQuant densitometry software (GE Healthcare Life Sciences, Amersham, U.K.) was used for quantification of Western blot protein levels. RNA primers were designed using the OligoPerfect™ design tool (Invitrogen Life Technologies). Masslynx software, version 4.1 (Waters), was used to integrate the tandem mass spectrometry metabolomics data. The proteomics raw data was processed using Proteome Discoverer (version 1.4.0.288, Thermo Scientific), Progenesis QI™ (Nonlinear Dynamics, Newcastle upon Tyne, U.K.) and Scaffold™ version 4.4.3 (Proteome Software, Portland, Oregon, USA). Molecular ion fragmentation mass spectra, MS^2, were searched with SEQUEST and Mascot engine against a human protein database, Uniprot (http://www.uniprot.org June-July 2015).

The programme EnzFitter (Biosoft, Cambridge, U.K.) was used for non-linear regression in data fitting to dose-response curves.

2.2 Cell culture methods

2.2.1 Human periodontal fibroblasts cells culture

hPDLFs cells were maintained in Modified Eagles Medium (MEM) supplemented with L-alanyl-L-glutamine (2 mM), 10% FBS and 100 Units/ml penicillin and 100 µg/ml streptomycin at 37 ^{o}C under aseptic conditions and an atmosphere of air/5% carbon dioxide/100% humidity. Cells were passaged approximately every 3 days with a seeding density of *ca.* 5,000 cells/cm^2. Cells were harvested using 0.25% trypsin-EDTA, subsequently neutralised by addition of culture media. For experiments performed in low and high glucose conditions, culture media was supplemented with β-D-glucose to a final concentration of 8 mM and 25 mM using a concentrated sterile aqueous stock solution of β-D-glucose. Unless stated otherwise, all experimental cultures were performed for 3 days on cells between passages 3 and 5. Cells were collected by trypsinisation and sedimentation by centrifugation; and media samples were centrifuged prior to storage to sediment any detached cells. Cell and media samples were stored at – 80 ^{o}C until subsequent analysis. Cell viability was ≥ 98% at the start of all experiments determined using Trypan blue dye exclusion.

2.2.2 Cell culture experimentation

Assessment of human periodontal fibroblasts viability

Primary hPDLFs were cultured in 6 well plates (5000 cells/cm²) in triplicate in MEM media supplemented with three different glucose concentrations (5.5 mM, 8.0 mM and 25.0 mM). Total cell number and viable cell number was counted every day for 6 days and a cell growth curve constructed.

The effect of exogenous methylglyoxal on hPDLFs growth – dose-response study

Primary hPDLFs were cultured in low glucose concentration (8 mM) in 6 well plates at a cell density of 5000 cells/cm² in triplicate. In the second day of culturing the cells, the cells were incubated in fresh media containing 8 mM glucose with variable MG concentrations, 0, 25, 50, 100 and 200 µM MG, for 2 days. Cells

were counted after 48 h using a Neubauer haemocytometer. Viable and non-viable cell numbers were recorded to produce a MG concentration-response curve. Data were fitted to the dose-response equation $V=100 \times (GC_{50})^n / ((GC_{50})^n + ([MG])^n)$ where V is the viable cell number as a percentage of control cultures without MG, GC_{50} is the median growth inhibitory concentration value, [MG] is the concentration of MG and n is the logistic regression coefficient (also known as the Hill coefficient). Experimental data of V and [MG] were fitted by non-linear regression of V on [MG] using the programme EnzFitter solving for GC_{50} and n.

Effect of methylglyoxal on hPDLFs growth – time course study

Primary hPDLFs were cultured at a cell density of 5000 cells/cm^2 in 6-well plates in MEM in low and high glucose concentration, 8 mM and 25 mM respectively, in triplicate. After 24 h, the cells were incubated in fresh media with 8 mM or 25 mM glucose and with and without 200 μM MG. The number of viable and non-viable cells were counted every day for three days.

Characterisation of glyoxalase system and dicarbonyls metabolism in hPDLFs in model hyperglycaemia

Primary hPDLFs cells were cultured in MEM in low and high glucose concentration, 8 mM and 25 mM respectively, for 3 days in triplicate. Cell extracts were analysed for Glo1 activity, total protein, MG-H1 residue content of cell protein and MG concentration. Medium was analysed for concentrations of glucose, MG, MG-H1 free adduct and D-lactate.

Effect of Glo1 inducers on the glyoxalase system and dicarbonyl metabolism in hPDLFs *in vitro*

Primary hPDLFs cells were cultured in MEM with low and high glucose concentration, 8 mM and 25 mM respectively, with and without tRSV (10 μM), HSP (10 μM) or tRSV+HSP (tRSV, 10 μM and HSP, 10 μM) for 3 days in triplicate. Cells were analysed for Glo1 activity, protein and mRNA, MG and cell protein MG-H1 residue content. Medium was analysed for concentrations of glucose, MG, MG-H1 free adduct and D-lactate. Aldose reductase and MG reductase activities were also measured. The attachment of hPDLFs to collagen-I was also measured (see below).

Glo1 half-life experiment

Primary hPDLFs cells were cultured in MEM with low and high glucose concentration, 8 mM and 25 mM respectively, in 6 well plates. After 24 h, fresh MEM was added to each well with cycloheximide (CHX, 10 µM) and with and without tRSV (10 µM) for 2 days in triplicate. Cell viability test was assessed. Cell protein extracts were analysed for Glo1 protein content after a further 24, 48 and 72 h.

Glo1 acetylation

Primary hPDLFs cells were cultured in MEM with low and high glucose concentration, 8 mM and 25 mM respectively, with and without tRSV (10 µM). Glo1 protein was pulled down by immunoprecipitation technique and the acetylation of Glo1 protein was detected by immunoblotting method.

Primary hPDLFs cells were cultured in MEM with low glucose and high glucose concentration, 8 mM and 25 mM respectively. After 24 h, fresh MEM was added to each flask with and without SIRT1 inhibitor EX 527 (100 nM), SIRT2 inhibitor AGK2 (4 µM) or class I and II mammalian histone deacetylase inhibitor TSA (300 nM) and incubated for a further 2 days in triplicate. Dose response curve was constructed. Cell viability was assessed. Cells were analysed for Glo1 activity and mRNA.

Proteomics analysis of primary human periodontal fibroblasts

Primary hPDLFs cells were cultured in MEM with low and high glucose concentration, 8 mM and 25 mM respectively, for 3 days in triplicate. A cytosolic protein extract was prepared and analysed by high resolution mass spectrometry proteomics – see below.

Effect of highly glycated protein/RAGE interaction on inflammatory signalling and Glo1 expression in hPDLFs *in vitro*

To assess if glycated protein activate inflammatory signalling activated in hPDLFs *in vitro,* cells were incubated for 3 days in triplicate in MEM with 8 mM glucose supplemented with various preparations of glycated protein: AGE_{min}-HSA, AGE-HSA, CML_{min}-HSA and CML-HSA (50 µg/ml or 100 µg/ml final concentration). Low level of endotoxin in the glycated protein preparations had been

confirmed beforehand by measurement by Limulus Amebocyte Lysate (LAL) assay. Cell viability assessment was performed. Cells were analysed for Glo1 activity and Glo1 mRNA. Transcription factor p56/NFκB activation status was measured on nuclear extracts.

2.2.3 Preparation of glycated derivatives of human serum albumin

Aliquots of Zenalb^{TM} HSA solution (250 µl, 20% w/v) were washed four times with sodium phosphate buffer (1.25 ml, 100 mM, pH 7.4) by diafiltration using microspin ultrafilters (10 kDa), centrifuged at 4000 g for 15 min and 4 ^{o}C under sterile conditions. Concentration of the washed HSA aliquots were determined by Bradford assay.

2.2.3.1 Preparation of human serum albumin modified minimally and highly by glucose-derived glycation adducts (AGE_{min}-HSA and AGE-HSA, respectively)

Minimally glycated HSA (AGE_{min}-HSA) was prepared by incubation of HSA (50 mg/ml) with β-D-glucose (40 mM) in sodium phosphate buffer (100 mM, pH 7.4) at 37 ^{o}C for 5 weeks. Highly glycated HSA (AGE-HSA) was prepared by incubation of HSA (50 mg/ml) with β-D-glucose (1.67 M) in sodium phosphate buffer (100 mM, pH 7.4) at 37 ^{o}C for 60 days. These incubations were prepared and incubated under aseptic and endotoxin-free conditions. Unmodified HSA control was incubated without glucose and treated similarly. The modified protein was then dialysed against ammonium bicarbonate buffer (30 mM, pH 7.9) at 4 ^{o}C for 24 h. The modified protein was lyophilised to dryness and stored at -20 ^{o}C until use (Ahmed and Thornalley, 2002).

2.2.3.2 Preparation of modified human serum albumin modified minimally and highly by N^{ε}-carboxymethyl-lysine residues (CML_{min}-HSA and CML-HSA, respectively)

CML_{min}-HSA was prepared by incubation of HSA (0.66 mM) with glyoxylic acid (2.15 mM) and sodium cyanoborohydride (56 mM in 200 mM sodium phosphate buffer, pH 7.8) at 37 ^{o}C for 24 h. CML-HSA was prepared by incubation of HSA (0.66 mM) with glyoxylic acid (21.5 mM) and sodium cyanoborohydride (56 mM in 200 mM sodium phosphate buffer, pH 7.8) at 37 ^{o}C for 24 h. The

modification experiments were performed under aseptic and endotoxin free conditions. The modified protein was dialysed against phosphate buffer saline (PBS), pH 7.4 and 4 ^{o}C, and stored at –20 ^{o}C (Ahmed and Thornalley, 2002).

2.2.4 Effect of glycated human serum albumin on activation of NF-κB in hPDLFs *in vitro*

2.2.4.1 Limulus amebocyte lysate LAL assay

LPS may activate NF-kB in hPDLFs (Preshaw et al., 2013) and hence LPS contamination of glycated proteins is a potential interference in assessing activation of NF-κB in hPDLFs *in vitro* by glycated proteins. Glycated proteins were prepared form endotoxin-free HSA of clinical HSA infusion solutions and under aseptic conditions. Endotoxin content of the glycated HSA preparations was assessed by chromogenic LAL assay (Unger et al., 2014). The reporter chromophore of samples was measured in a microplate reader at 405 nm. A standard curve was created using the *E. coli* LPS standard from 0.1 – 1.0 endotoxin unit (EU) per ml. One EU is approximately equivalent to 100 pg endotoxin *E. coli* LPS – Figure 17.

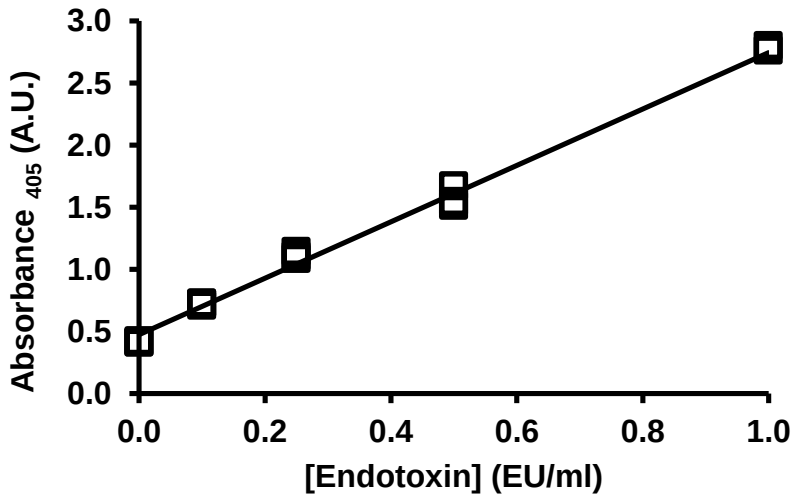

Figure 17: Calibration curve for E. coli endotoxin.
Linear regression equation: Absorbance= (2.41 ± 0.08) x endotoxin (EU/ml) + (0.0339 ± 0.0403); R^2 = 0.997; (n = 15).

The assay microplate was maintained in a heating block for 10 min at 37 ^{o}C. An aliquot of blank, standard or test sample (50 µl) was added into the appropriate microplate well then covered with lid and incubated for 5 min at 37 ^{o}C. An aliquot of LAL was added (50 µl) to each well then microplate was covered by lid and gently

shacked for 10 s and incubated at 37 ºC for 10 min. An aliquot of chromogenic substrate solution (100 µl) was then added to each well, samples mixed for 10 s and incubated at 37 ºC for 6 min. Finally, an aliquot of stop reagent (25% (v/v) acetic acid, 50 µl) was added to each well and samples mixed for 10 s. The absorbance at 405 nm of standard and test samples was recorded by microplate reader.

2.2.4.2 Nuclear extraction protocol

Principle of assay

Nuclear extraction is the process of obtaining non-denatured and active proteins from nuclear compartment of the cell by using high-salt extraction method. The extracted nuclear proteins are used to monitor NF-kB activation (Singh et al., 2012)

Cell cultures

hPDLFs were cultured at a cell density of 5000 cells/cm^2 in T175 flasks in MEM with 8 mM glucose. After 24 h, the media was changed and the fresh media was added supplemented with glycated protein (AGE_{min}-HSA, AGE-HSA, CML_{min}-HSA or CML-HSA; 50 µg/ml or 100 µg/ml) and cell cultures continued for a further 2 days. Cell pellets were then collected by as follow. The cells were washed by ice cold PBS/ phosphatase inhibitors (5ml) and was aspirated. Aliquot of ice cold PBS/ phosphatase inhibitors (3ml) was added to the cells (8×10^6) and cells were collected by scraping from culture flasks with cell lifter and transferred to pre-chilled 15ml conical tubes. Cell suspension was centrifuged for 5 min at 200 x g in a pre-cooled centrifuge at 4˚C and supernatant was removed.

Nuclear extraction

The cell pellet was gently resuspended in 1X hypotonic buffer (250 µl) by pipetting up and down and incubated on ice for 15 min. The cells were transferred into a pre-chilled microcentrifuge tube and an aliquot of NP40 detergent (10%, 25 µl) was added. The homogenate was vortexed for 10 s then centrifuged (14,000 g, 1 min, 4 ºC). The supernatant was transferred and retained (cytosolic fraction). The nuclear pellet was re-suspended in complete cell extraction buffer (50 µl; 10 mM DTT (5 µl), lysis buffer (44.5 µl) and protease inhibitor cocktail (0.5 µl)) by pipetting the solution in and out of the pipette tip 5 times. The suspension was

incubated for 40 min on ice on a rocking platform shaker, 150 rpm, then vortexed for 30 s. The suspension was centrifuged (10 min, 14,000 g, 4 °C) and the supernatant retained (nuclear fraction) and stored in -80 ^{o}C. The protein level in nuclear fraction was measured by the Bradford method.

2.2.4.3 Assay of NF-κB system activation status

The transcription factor nuclear factor κB (NF-κB) is a key transcriptional system for activation of a battery of pro-inflammatory genes (Ghosh and Hayden, 2008). Measurement of NF-κB activation status in cells is an indicator of cell inflammation. Herein the TransAM^{TM} activation assay is used (ActiveMotif, La Hulpe, Belgium). In NF-κB activation, the p50/p65 heterodimer moves into cell nucleus and binds NF-κB consensus motifs to activate inflammatory gene expression. The method involves adding a stimulated cell nuclear extract with biotinylated oligonucleotide NF-κB consensus motif to capture activated NF-κB binding. The binding reaction is then transferred to the wells of a 96-well streptavidin coated plate and is quantified using an antibody specific for the bound p50/p65 heterodimer. A second anti-IgG-horseradish peroxidase antibody is added to enable chromogenic detection in an ELISA protocol. The assay was performed with assay reagents and protocol provided by the manufacturer.

An aliquot of nuclear extract of test samples (10 µg) and biotinylated oligonucleotide (1 pmol) were diluted to 50 µl with complete binding buffer in a microcentrifuge tube. For positive control, Jurkat nuclear extract (2 µl; 5 µg) and biotinylated oligonucleotide (1 pmol) were diluted to 50 µl in complete binding buffer. For blank assay, biotinylated oligonucleotideto (1 pmol) was diluted to 50 µl in complete binding buffer. Each tube was vortex mixed and incubated in room temperature for 30 min. An aliquot (50 µl) of the mixture was transferred in to the well on the 96-well streptavidin-coated assay plate. The plate was covered with adhesive cover and incubated for 1 h at room temperature with mild agitation. After incubation, each well was washed three times with 200 µl washing buffer. An aliquot (100 µl) diluted p50/p65 heterodimer antibody (1:1000) was added to each well, covered with adhesive cover and incubated for 1 h at room temperature without agitation. Each well was washed three times with 200 µl washing buffer and an aliquot of diluted anti-IgG-HRP antibody conjugate (100 µl; 1:1000) was added to each well, the plate was covered with adhesive cover and incubated for 1 h at room

temperature. The wells were washed three times with 200 µl washing buffer and an aliquot (100 µl) of developing solution was added to each well, incubated for 10 min at room temperature in the dark and then an aliquot (100 µl) of stop solution was added. The absorbance at 450 nm of wells was recorded.

2.2.5 GLO1-ARE, mutant non-functional stable ARE and NQO1-ARE transfectant reporter cells lines

These were produced by transfection of a pGL4.22[luc2CP/puro] reporter vector containing GLO1-ARE (ARE-1 from our previous notation), mutated functionally inactive GLO1-ARE (ARE1m, negative control) and quinone reductase ARE (NQO1-ARE) – a conventional ARE-related marker gene (Xue et al., 2012b, Xue et al., 2015b). Transfected HepG2 cells were selected with puromycin (1 µg/ml). After culture for 3 weeks, puromycin-resistant cells were screened for luciferase activity after treatment with 4 µM SFN for 6 h. After validation of positive clones by measuring luciferase activity, the stable cell line was expanded in selection media and thereafter used in studies for screening of bioactive compounds and synergism. Briefly, stable transfectant cell lines were incubated with and without bioactive compounds and combination of tRSV and HSP (0.625 – 5.0 µM) for 6 h in MEM medium with 10% fetal calf serum and 2 mM glutamine under an atmosphere of 5% CO_2 in air, 100% humidity and 37 ^oC. This incubation period was optimum to judge initial rate of increase in transcriptional response in cells treated with compounds without increase in untreated controls. For the reporter assay, 100 µl Cell Culture Lysis Reagent (CCLR, Promega, Southampton, UK) was added to cell and shaken gently for 30 min. The mixture of cell lysate was centrifuged (12,000 g, 5 min, 4 ^oC) and an aliquot (20 µl) of supernatant used in the reporter assay. The luciferase activity was determined using a Luciferase Assay System (Promega). The luciferase response is given in Relative Light Units (RLU). Data are corrected for blank response and normalised to the highest effect (100%) achieved with 10 µM tRSV. Data of normalised responses (blank = 0%, 10 µM tRSV = 100%) for varied bioactive concentrations are fitted by non-linear regression to a dose-response curve, $E = E_{max} \times [Bioactive]^n/(EC_{50}^n + [Bioactive]^n)$, solving for EC_{50} and n (logistic regression coefficient - also called the Hill coefficient). Nrf2-dependent transcriptional response was verified by siRNA silencing of Nrf2, as described (Xue et al., 2012b). This experiment was performed by the host research team.

2.2.6 Cell adhesion assay – unmodified collagen-I

Primary hPDLFs were incubated with high and low glucose media in triplicate for 3 days with or without Glo1 inducers (i.e. tRSV, HSP or tRSV+HSP). Cells (0.1-1.0 x 10^6 cells/ml) were then suspended in serum free media containing 10 µM of either tRSV, HSP or tRSV+HSP. An aliquot of cell suspension (150 µl) was added to each well of a 48-well plate where walls of the wells were coated with collagen-I (CytoSelect™ cell adhesion assay plate, Cambridge Bioscience Ltd). The plate was incubated at 37 °C for 3 h. All steps were performed under sterile conditions. The unattached cells were then carefully removed by aspirating the media. After washing the plate 5 times with PBS (250 µl), an aliquot of cell stain solution (200 µl, 0.5% (w/v) crystal violet, 30% (v/v) ethanol and 3% (w/v) formaldehyde) was added to fix and stain the attached cells and incubated for 10 min at room temperature. The stain solution was aspirated, and the plate was then washed 5 times with deionized water (500 µl) and dried in air. Finally, an aliquot of extraction solution (200 µl, 10% (w/v) citric acid) was added to each well and incubated for 10 min on an orbital shaker to dissolve crystal violet stain. The absorbance of the wells at 595 nm was recorded.

2.2.7 Cell adhesion assay – modified collagen

Primary hPDLFs were incubated with 8 mM glucose and 25 mM glucose media for 3 days with or without tRSV, HSP or tRSV+HSP. The media from these cell cultures were then incubated for 3 h in 37 ^{o}C with or without aminoguanidine (500 µM) under sterile conditions. Aminoguanidine is a potent MG scavenger and derivatised MG completely in the time (Thornalley et al., 2000). An aliquot of these conditioned media samples (200 µl) was then added to the wells of a collagen-I adhesion plate and incubated for 24 h at 37 ^{o}C. The collagen-I plates were then washed 3 times with PBS (250 µl). hPDLFs cells grown under normal conditions (8 mM glucose, 0.1-1.0 x 10^6 cells/ml) were then added to wells of preconditioned collagen plate. The plates were incubated for 3 h at 37 ^{o}C. The unattached cells were then carefully removed by aspirating the media. After washing the plate 5 times with PBS (250 µl), an aliquot of cell stain solution (200 µl, 0.5% crystal violet, 30% ethanol and 3% formaldehyde) was added to fix and stain the attached cells and incubated for 10 min at room temperature. The stain solution was aspirated from the wells. The wells were washed 5 times with deionized water (500 µl) and left to dry

in air. Finally, an aliquot of extraction solution (200 µl, 10% citric acid) was added to each well and incubated for 10 min on an orbital shaker to dissolve crystal violet stain. The absorbance of the wells at 595 nm was recorded.

2.3 Analytical methods

2.3.1 Total protein assay

2.3.1.1 Bradford method to measure total protein

The concentration of protein in cell lysates was quantified by Bradford protein assay (Bradford, 1976, Compton and Jones, 1985). Stock solutions of bovine serum albumin (BSA) was calibrated by UV absorption spectrophotometry using the extinction coefficient at 279 nm for a 1% (10 mg/ml) solution; ε_{279} (1%) = 6.9 cm^{-1} (Peters, 1962). Protein samples were diluted in the range 0.05 to 0.3 mg/ml. Test samples, BSA standards and blanks in triplicate (20 µl per well) were mixed with 200 µl of Bradford reagent in a 96-well microplate and incubated for 15 min on a shaker at room temperature. Absorbance was read at 595 nm. The concentration of protein in test samples was calculated by interpolation of the calibration curve.

2.3.1.2 Detergent compatible lowry method

For immunoblotting and proteomics experiments, the detergent compatible assay (DC assay) was used to measure protein concentration of hPDLFs cell extracts containing 0.5% SDS (RIPA buffer). This is a colorimetric assay for detergent solubilised protein based on the Lowry assay (Lowry et al., 1951).

2.3.2 Enzymatic activity assay

2.3.2.1 Preparation of samples

Primary hPDLFs cells were cultured under condition described above and then collected by trypsinisation, counted and sedimented by centrifugation (150 g, 5 min). Cell pellets were washed with ice-cold PBS three times. The cell pellets (*ca.* 1 x 10^6 cells) were re-suspended in sodium phosphate buffer (10 mM, pH 7.0, 200 µl), sonicated on ice (110 W, 30 s) and the membranes sedimented by centrifugation (20,000 g, 30 min, 4 ^oC). The supernatant was retained and stored at -80 ^oC for later use as lysate in enzymatic activity assays.

2.3.2.2 Activity of Glo1

The activity of Glo1 is assayed by measuring the initial rate of formation of S-D-lactoylglutathione from the MG-GSH hemithioacetal formed non-enzymatically from MG and GSH. The reaction is followed spectrophotometrically at 240 nm; $\Delta_{\varepsilon 240}$ = 2.86 mM^{-1} cm^{-1} (Allen et al., 1993b). Hemithioacetal was prepared by pre-incubation of MG (2 µmol) with GSH (2 µmol) at 37 °C for 10 min in sodium phosphate buffer (50 mM, pH 6.6, 980 µl). The cell lysate (20 µl) was added and the absorbance at 240 nm was monitored with time for 5 min. The activity of Glo1 was calculated from the initial increase in absorbance, corrected for buffer blank. Glo1 activity is given in units per mg protein where one unit of Glo1 activity is the amount of enzyme which catalyses the formation of 1 µmol of S-D-lactoylglutathione from the hemithioacetal substrate per minute under assay conditions (Allen et al., 1993b). The activity of Glo1 may be assayed in the presence of Glo2 because the high concentrations of the MG-GSH hemithioacetal used inhibits Glo2 activity (Uotila, 1973).

2.3.2.3 Activity of glyoxalase 2

The activity of Glo2 is determined by measuring the initial rate of hydrolysis of S-D-lactoylglutathione to GSH and D-lactate – Figure 18. The hydrolysis of S-D-lactoylglutathione is followed spectrophotometrically at 240 nm for which $\Delta_{\varepsilon 240}$ = -3.10 $mM^{-1}cm^{-1}$ (Clelland and Thornalley, 1991, Allen et al., 1993a).

S-D-lactoylglutathione (0.3 mM, 100 µl) was incubated in Tris/HCl (50 mM, pH 7.4, 850 µl) and 37 ^{o}C, and the cell lysate or lysate buffer for the blank (50 µl) was added and followed the absorbance at 240 nm for 5 min at 37 ^{o}C. The initial rate of change in absorbance was deduced. One unit of Glo2 activity equals the volume of enzyme that catalyses the hydrolysis of 1 µmol of S-D-lactoylglutathione per minute under assay conditions (Allen et al., 1993b). Cytosolic cell extracts were performed by sonication as described above.

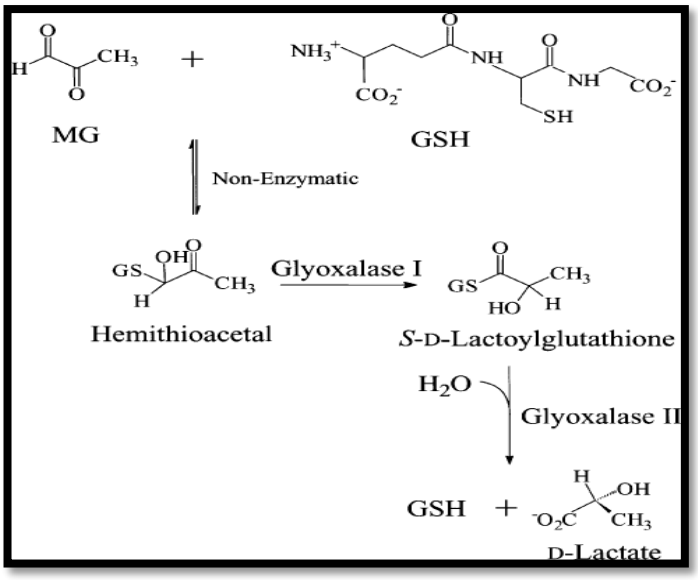

Figure 18: The catalytic reactions of the glyoxalase system.
From (Clugston et al., 2004).

2.3.2.4 Methylglyoxal reductase activity

NADPH-dependent aldoketo reductase provides an alternative metabolic fate for MG and converts it to hydroxyacetone. AKR isozymes 1A4, 1B1 (aldose reductase) and 1B3 metabolise MG (Baba et al., 2009). MG reductase activity is determined by measuring the initial rate of oxidation of NADPH by cell lysates in the presence of MG and NADPH, followed spectrophotometrically at 340 nm; $\Delta\varepsilon_{340}$ = - 6.20 $mM^{-1}cm^{-1}$.

MG reductase

$$\mathbf{CH_3COCHO + NADPH + H^+ \longrightarrow CH_3COCH_2OH + NADP^+}$$

MG (1 mM) was incubated with NADPH (0.1 mM) in sodium phosphate buffer (50 mM pH 7.4 and 37 ^oC) and cell lysate, or lysate buffer for blank, added to a final volume of 1 ml. The solution was mixed by inversion and the absorbance at 340 nm measured for 5 min. The activity of MG reductase is measured in units where one unit catalyses the reduction of 1 µmol of MG per min under assay conditions.

2.3.2.5 Methylglyoxal dehydrogenase activity

NAD^+-dependent MG dehydrogenase converts methylglyoxal to pyruvate (Monder, 1967). The methylglyoxal dehydrogenase activity is determined by

measuring the initial rate of reduction of NAD^+ by cell lysates in the presence of MG and NAD^+, followed spectrophotometrically at 340 nm; $\Delta\varepsilon_{340} = 6.20\ mM^{-1}cm^{-1}$.

$$CH_3COCHO + NAD^+ + H_2O \xrightarrow{\text{MG dehydrogenase}} CH_3COCO_2^- + NADH + 2H^+$$

Cell lysate, or lysate buffer for blanks, is added to MG (1 mM) and NAD^+ (0.1 mM) in sodium phosphate buffer (50 mM, pH 7.4 and 37 ^oC) and the sample mixed well by inversion. The reaction was monitored for absorbance at 340 nm for 5 min. The activity of MG dehydrogenase is measured in units where one unit catalyses the oxidation of 1 µmol of MG per minute under assay conditions.

2.3.3 Total cell thiol assay

The concentration of cell thiol – protein thiol + non-protein thiol (mainly GSH) – was determined by measuring the absorbance produced by the reaction of cell extract with 5,5'-dithiobis (2-nitrobenzoic acid) (DTNB) or Ellman's reagent. DTNB is reacts with thiols to from the yellow chromophore, 5-mercapto-2-nitrobenzoic acid – Figure 19. 5-Mercapto-2-nitrobenzoic acid is detected by absorbance with λ_{max} at 412 nm (Hansen et al., 2007, Hansen and Winther, 2009). It can also be monitored by a 405 nm, 10 nm bandwidth, filter on an absorbance mode microplate reader, as used herein.

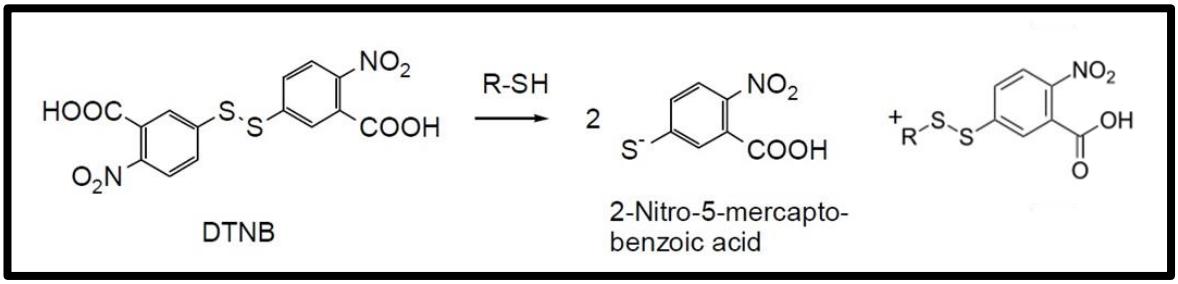

Figure 19: Reaction of DTNB with thiol R-SH.

Cell cytosol extract was prepared by re-suspending *ca.* 1 x 10^6 cells in sodium phosphate buffer (10 mM, pH 7.0), sonicating the cell suspension on ice (110 W, 30 s), and sedimenting the cell membranes by centrifugation (20,000 g, 30 min, 4 °C). The supernatant was retained and stored at – 80 ^oC until analysis. An aliquot of DTNB solution (125 µl, 1 mM DTNB in 100 mM sodium phosphate buffer, pH 7.4, with 0.2 mM DETAPAC) was added to the wells (96-well

microplate) followed by distilled water (100 µl). Cell cytosol extract (25 µl) was then added to the well and the absorbance at 405 nm was monitored until a stable maximum value was reached – after 20 min. The absorbance increase at 405 nm was used to calculate the level of cellular thiols. Using GSH as an analytical standard thiol, the assay was calibrated in the range of 0 - 30 nmol GSH- Figure 20.

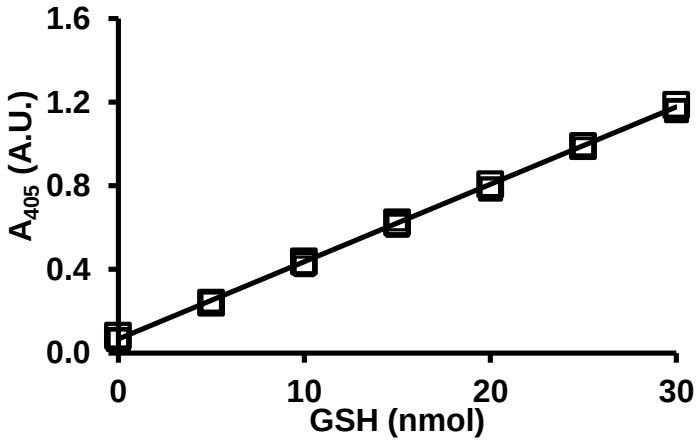

Figure 20: Calibration curve for GSH.
Linear regression equation: A_{412} (A.U.) (0.037 ± 0.0003) x thiols (nmol) + (0.063 ± 0.0047); R^2 = 0.999 (n = 21).

2.3.4 D-Glucose assay

The glucose concentration in culture media was measured using commercially available an end-point enzymatic assay. Assay mixtures contained: 1.5 mM NAD^+, 1 mM ATP, 1 unit/ml hexokinase (HK) and 1 unit/ml glucose-6-phosphate (G-6-P) dehydrogenase (Sigma Aldrich). The enzymatic basis of the assay is illustrated in - Figure 21.

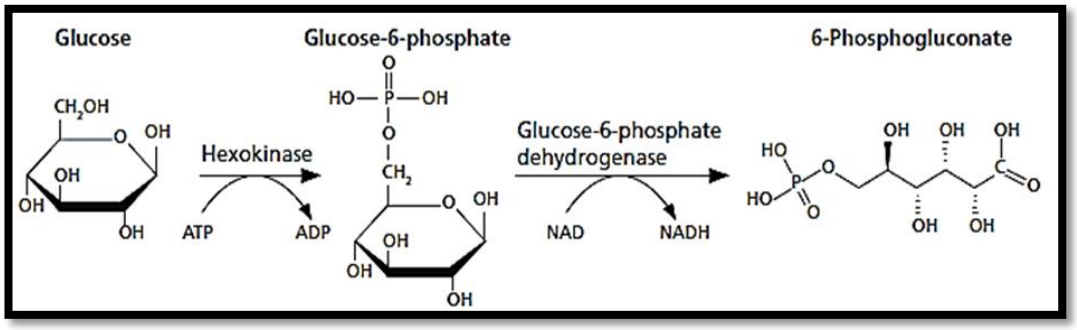

Figure 21: Detection of glucose via hexokinase (HK) and glucose-6-phosphate dehydrogenase.

Glucose is converted to 6-phosphogluconate via glucose-6-phosphate using hexokinase and glucose-6-phosphate dehydrogenase catalytic enzymes. The NADH formed in the reaction mixture is measured by absorbance at 340 nm. As equimolar amounts of glucose is phosphorylated in this reaction as NAD^+ is reduced to NADH. The increase in absorbance at 340 nm is directly proportional to the concentration of NADH and hence to concentration of glucose in the sample.

2.3.4.1 Preparation of sample

A standard curve was constructed in the range of 0.25 – 1.50 mM glucose - Figure 22. An aliquot of standard or diluted sample (25 µl) was added to each well of a microplate then the assay reagent (225 µl) was added. The plate was incubated at room temperature for 15 min before the absorbance at 340 nm was read using a spectrophotometer.

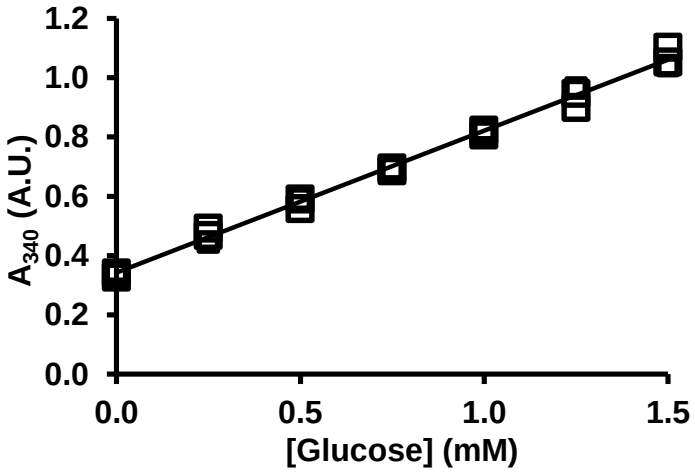

Figure 22: Calibration curve for D-glucose.
Linear regression equation: A_{340} (A.U.) = (0.479 ± 0.009) x D-glucose (mM) + (0.0008± 0.008); R^2 = 0.996 (n = 21).

2.3.5 Assay of D-lactate

The flux of formation of D-lactate by hPDLFs was determined by measuring the concentration of D-lactate in the culture medium at baseline and end of the culture period. D-Lactate crosses cell membranes by the specific lactate transporter, the inorganic anion exchange system and by non-ionic passive diffusion. An end-point enzymatic fluorometric assay was used (McLellan et al., 1992). D-lactate is converted to pyruvate by the enzyme D-lactic dehydrogenase. The enzymatic reaction occur during the incubation at 37 ^oC. The increase in NADH concentration is measured by fluorescence ($\lambda_{excitation}$ = 340 nm, $\lambda_{emission}$ = 460 nm).

D-Lactate + NAD^+ ⇌ pyruvate + NADH

2.3.5.1 Preparation of sample

An aliquot of ice-cold perchloric acid (PCA) (1 ml, 0.6 M) was added to culture medium (500 µl) for deproteinisation. The mixture was vortexed and left on ice for 10 min to complete protein precipitation. The samples were centrifuged (7000 g, 4 ^oC, 5 min) to sediment the protein precipitate. An aliquot of the supernatant (700 µl) was neutralised to pH 7 by adding potassium bicarbonate (200 µl, 2 M), mixed and centrifuged again (7000 g, 4 ^oC, 10 min) to sediment the precipitate of potassium perchlorate. Samples were then saturated in CO_2 and were degassed by placing in a centrifugal evaporator at room temperature for 5 min under reduced pressure (20 mmHg). An aliquot of degassed deproteinised extract or D-lactate standard solution (100 µl) was added in duplicate to the 96-well black microplate containing glycine-hydrazine buffer (100 µl; 1.2 M glycine, 0.5 M hydrazine hydrate, 2.5 mM DETAPAC, pH 9.2) and NAD^+ (4 mM, 25 µl). The reaction was started on the addition of D-lactic dehydrogenase enzyme (25 µl, 250 units per ml). The microplate was incubated at 37 ^oC in the dark for 2 h. Each sample has its own control without the enzyme and used as a blank. The fluorescence of NADH was monitored at $\lambda_{excitation}$ 340 nm and $\lambda_{emission}$ 460 nm. A standard curve for calibration was constructed in the range of 0 – 6 nmol D-lactate/ well – Figure 23.

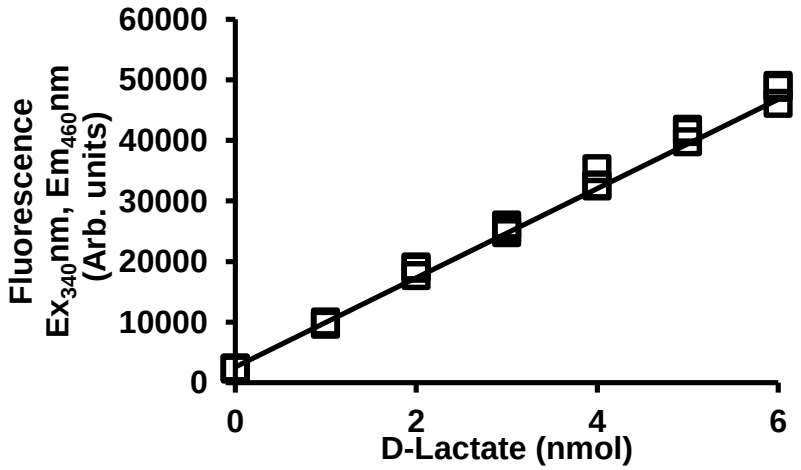

Figure 23: Calibration curve for D-lactate assay.
Linear regression equation: Fluorescence (arb. units) = (7648 ± 88) x D-lactate (nmol) + (2523 ± 317); R^2 = 0.999 (n = 21).

2.3.6 Assay of L-lactate

The method to measure the concentration of L-lactate in culture medium was similar to that of D-lactate – see above. A standard curve was produced using L-lactate standards and the enzyme L-lactate dehydrogenase was used instead of the D-lactate dehydrogenase used for the D-lactate assay. The standard curve range was selected to ensure that the range used was linear and a time-course achieved to establish the optimal incubation length. Since cellular level of L-lactate is higher than D-lactate, media samples were diluted 10-fold with water to ensure that concentrations measured were within the standard curve range – Figure 24.

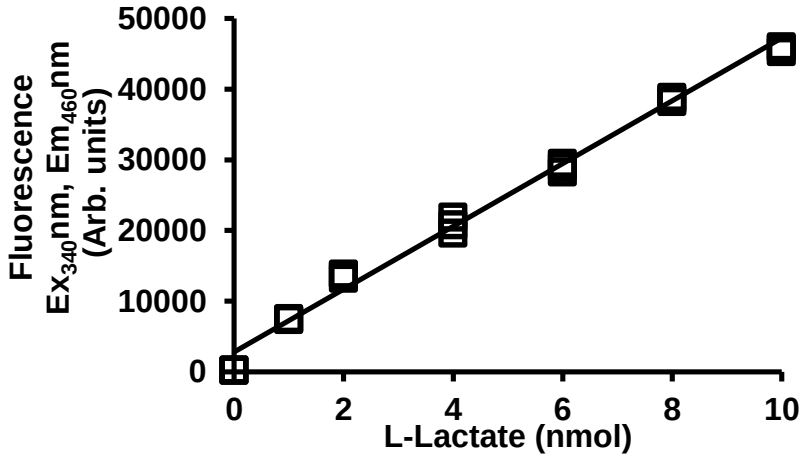

Figure 24: Calibration curve for L-lactate.
Linear regression equation: Fluorescence = (4176 ± 178) x L-lactate (nmol) + (2919 ± 603); R^2 = 0.991 (n = 21).

2.3.7 Real-Time PCR quantitation

The relative copy number of specific gene mRNA in hPDLFs cells was measured by real-time quantitative PCR. This method includes the extraction of mRNA with subsequent reverse transcription to cDNA. The cDNA is then quantified by measuring fluorescence in a PCR reaction. SYBR green dye was used to produce the fluorescence. This dye is highly fluorescent when bound to double-stranded DNA.

2.3.7.1 Primer design and testing

Primers were designed using the OligoPerfect^{TM} designer software by using mRNA and genomic DNA sequences found in the UCSC genome browser. Multiple primer pairs were designated for each gene. Amplicon length (optimal 100-150 bp) was considered and primers spanning exon-exon junctions were selected when possible. Dissociation plots were implemented for all primers to test performance. $MgCl_2$ concentration was optimised when necessary. Example dissociation plots are shown in – Figure 25. Dissociation plots were constructed for each assay plate. This guaranteed that the primers performed constantly.

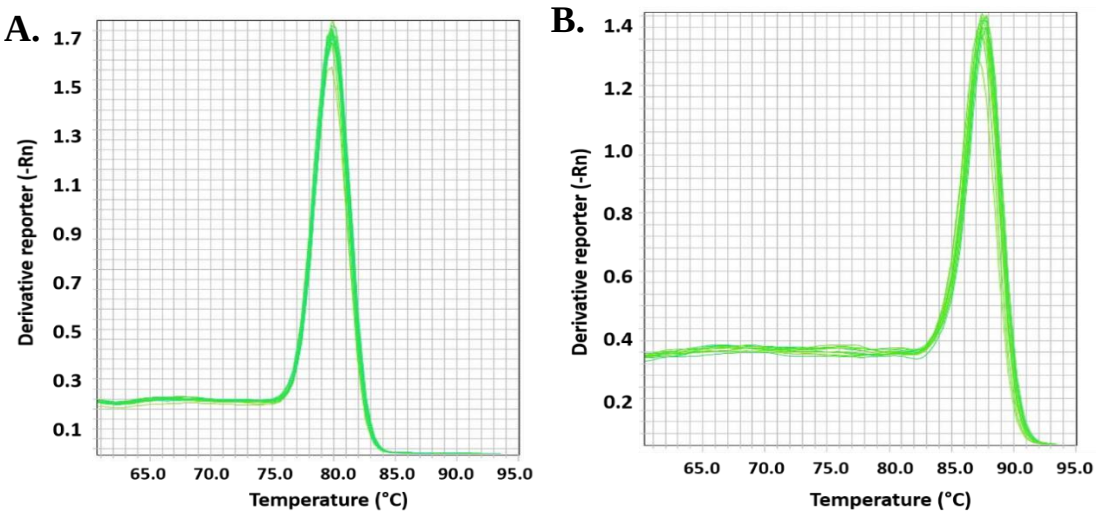

Figure 25: Dissociation plots for primers.
(A) GLO1 dissociation curve. (B) COL1 dissociation curve.

2.3.7.2 RNA extraction and purification

Sample preparation

Primary hPDLFs cells were cultured in 8 mM glucose and 25 mM glucose with or without Glo1 inducers as described in cell culture section. After incubation for desired experimental period, RNA extracts of cells were prepared.

Total RNA was extracted using the Qiagen RNeasy mini kit according to the manufacturer's instructions. Briefly, the samples were lysed by addition of a lysis buffer (350 µl) containing β-mercaptoethanol and pipetting the suspension in and out of a pipette 10 times. The lysis buffer contained a high concentration of guanidine-thiocyanate which acted as a chaotropic agent promoting cell lysis. Lysed samples were mixed with 70% (v/v) ethanol to improve binding conditions to the silica-based spin-column. The sample was washed with multiple buffers to eliminate impurities

and finally RNA was eluted by addition of RNAse-free water. The quality and concentration of RNA was determined spectrophotometrically using a NanoDrop 1000 spectrophotometer. RNA sample (2 µl) was used to measure the concentration of RNA at A_{260}, given that value of 1.0 at A_{260} is equal to 40 µg/ml of RNA. The quality of the RNA was determined by ratio between A_{260} and A_{280}. Pure RNA was expected to give a ratio of 1.9 - 2.1. Each sample was diluted to 50 ng nucleic acid and concentration confirmed using NanoDrop 1000.

2.3.7.3 Reverse transcription

cDNA was synthesised from the RNA using reverse transcription. A total of 0.2 µg RNA (12 µl in 20 µl reaction) from cells was annealed with oligo (dT) (1 µl) at 70 ^{o}C for 5 min before chilling on ice. Subsequently, 8 µl of master mix containing 10 U/µl RNase inhibitor (1 µl), 10 mM dNTPs (1 µl), 5 X Bioscript reaction buffer (4 µl) and Bioscript reverse transcriptase (1 µl) mix in nuclease-free water were added to each sample. Samples were heated at 42 ^{o}C for 60 min. The reaction was stopped by heating to 70 ^{o}C for 10 min. The synthesised cDNA was mixed with 40 µl (3 X dilution) of nuclease-free water and stored at –20 ^{o}C repeated freeze-thawing was avoided before analysis.

2.3.7.4 Analysis of gene mRNA expression by SYBR green

This method was used to measure the expression of mRNA of specific genes and normalised to housekeeping gene. The mRNA was firstly transcribed to cDNA as described in previous section. The synthesised cDNA was used for standard and for analyses.

2.3.7.5 Preparation of standards

Samples with the highest mRNA concentration were used to create the standard curve. RNA volume (1 µg) was used to extract cDNA using the same method described formally. The formed cDNA was used to custom standards 0 - 1000,000 pg using serial dilutions. A typical standard curve is shown in Figure 26.

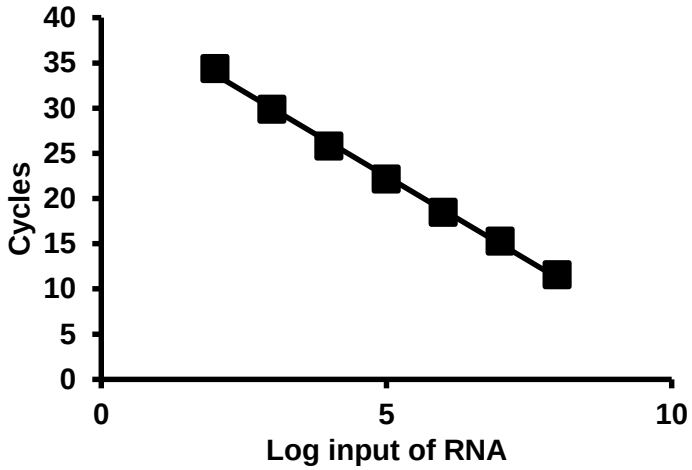

Figure 26: RT-PCR calibration curve.
Linear regression equation: Threshold cycle = (-3.748 ± 0.083) x log input amount of mRNA + (41.6 ± 0.447); R^2 = 0.999 (n = 21).

2.3.7.6 Data analysis

In a clear 96 well plate, sample (2 µl) was mixed with Master Mix SYBR Green (10 µl), primer (0.5 µl) and nuclease free water (7.5 µl). Then, the plate was sealed and centrifuged for few seconds; mRNA expression was measured using a 7500 Fast-Real time PCR machine. Plates were heated to 95 °C for 10 min to activate the hot-start DNA polymerase, 40 cycles of 95 °C x 15 s and 60 °C x 60 s. A standard curve of serially diluted pooled cDNA over the range 0 - 1000,000 pg was run alongside assay samples and used for quantification using β-actin as a reference gene.

2.4 Immunoblotting for Glo1

Expression level of Glo1 protein in primary hPDLFs was measured by Western blotting and normalised to β-actin.

2.4.1 Sample preparations

Primary hPDLFs were cultured in 8 mM glucose and 25 mM glucose with or without 10 µM tRSV, HSP or tRSV+HSP. After treatment, cells were trypsinised, washed and collected as described in cell culture section. Cell pellets were resuspended in RIPA buffer with phosphatase inhibitor and protease inhibitor and incubated on ice for 10 min. Cell lysate suspension was centrifuged (20,000 g, 30 min, 4 ^{o}C) and supernatant was collected and stored at -80 ^{o}C until the analysis.

The protein concentration was measured by DC assay. According to DC assay readings, the protein samples were prepared for loading onto the gel wells. Loading buffer containing β-mercaptoethanol (4x Laemmli sample buffer, Bio-rad) and the protein samples were mixed to make the total concentration 20 µg. Samples were heated at 95 ^{o}C for 5 min to denature the protein and loaded onto the gel.

2.4.2 Western blotting

Cell protein extract (20 µg) was separated using 4–20% precast polyacrylamide gel (4-20% criterion™ TGX stain-free™ gel), gel was inserted into the Criterion electrophoresis cell (Bio-rad). Premixed electrophoresis buffer (25 mM Tris, 192 mM glycine, 0.1% SDS, pH 8.3) following 1 fold dilution was poured into the electrophoresis cell to separate protein samples by SDS-PAGE. An aliquot of the prestained protein ladder (10 µl) and the test sample (15 µl) was loaded into the wells. Finally, samples were electrophoresed at 150 V for 1 h.

The sandwich layer of semi-dry transfer consisted of paper, gel and membrane was prepared by using pre-cut blotting transfer pack that included filter paper, PVDF membrane. These were used with *Trans*-Blot Turbo transfer system (Bio-rad) to transfer proteins from gel to membrane – Figure 27. Semi-dry transfer was performed at 2.5A; 25V constant for 15 min.

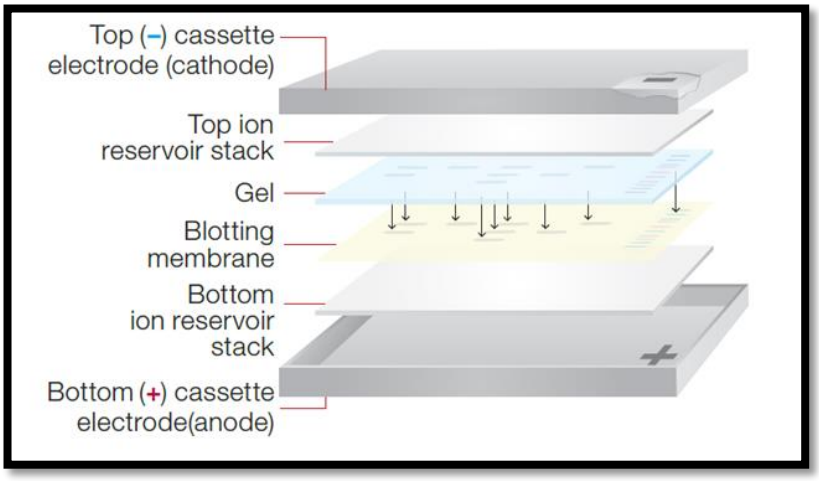

Figure 27: Gel and membrane setup for electrophoretic transfer (bio-rad).

The transfer membrane was firstly blocked with 5% (w/v) dried milk protein in Tris-buffered saline with Tween-20 (TBS-T buffer; 150 mM NaCl, 10 mM Tris/HCl pH 7.6 and 0.05% Tween-20). The membrane was then probed using pre-

determined concentrations of primary antibody (anti Glo1 rat, 1/3000; anti β-actin mouse, 1/1000) overnight in 4 ^{o}C in 1% (w/v) dried milk protein in TBS-T buffer. After blotting with primary antibody, the membrane was washed three times with TBS-T buffer for 10 min. Membrane was then probed with secondary antibody (anti-rat, 1/10000; anti-mouse, 1/10000) at room temperature for 1 h followed by rinsing three times with TBS-T and developed with ECL reagent. Photographic image was taken by G:BOX Chemi systems (Syngene). The intensity of the Glo1 protein band was normalised to β-actin (protein loading control). Membranes was scanned and quantified with ImageQuant densitometry software.

2.4.3 Immunoprecipitation (IP)

2.4.3.1 Preparing cells for immunoprecipitation

Cell pellets were suspended in 1x RIPA buffer, phosphatase inhibitor and protease inhibitor and incubated on ice for 10 min. Cell lysate suspension was centrifuged (20,000 g, 30 min, 4 ^{o}C). Supernatants were transferred to new microcentrifuge and stored at -80 ^{o}C until further analysis.

2.4.3.2 Pre-clear lysate

Pre-clear the lysate is a way to remove potentially reactive components from the cell lysate prior to the immunoprecipitation of desired protein to prevent a non-specific binding of these components to the IP beads or antibody. Pre-clear the sample by passing the sample over the beads alone. Lysate was incubated with beads only for 1 h at 4 ^{o}C. Beads are then removed and discarded prior to the immune-precipitation. The protein concentration of remaining lysate was measured by DC assay.

2.4.3.3 Immunoprecipitation (IP) protocol

Dynabeads G was re-suspended in the vial by vortexing for 30 s and aliquots (50 µl, 1.5 mg) were transferred to microcentrifuge tubes. Tubes were placed on the magnetic stand and the supernatants were removed. An aliquot of Glo1 rabbit antibody (5 µg) was added to the beads, diluted in TBS buffer (300 µl) and mixed. The beads and the antibody mixture were incubated with rotation for 10 min at room temperature to allow the Ab-conjugated Dynabeads to be formed. Aliquots of cell

lysate containing the required protein concentration (100 µg) of each sample were added to the Ab-conjugated Dynabeads.

To immunoprecipitate the target antigen, the mixture was incubated at 4 ºC with gentle end-over-end mixing overnight to form the immune complex. The next day, tubes were placed on the magnetic stand and the supernatant was discarded. The beads were washed with TBS buffer (200 µl) three times; after each wash, the supernatant was removed.

An aliquot (5 µl) of SDS sample loading buffer containing β-mercaptoethanol in 4 x Laemmli sample buffer and TBS (15 µl) was added to the beads. The beads were incubated at 95 ºC for 5 min then tubes were placed on the magnetic stand and eluents were collected. The samples were allowed to cool to room temperature before applying to SDS-PAGE gel.

2.4.3.4 Western blotting for immunoprecipitate samples

IP samples (20 µl) were separated using 8–16% Mini-PROTEAN® TGX™ gel using the Mini-ProteanR Tetra cell system (Bio-rad) as described above. Membranes were probed using pre-determined concentrations (rabbit, 1/1000) of anti-acetyl-lysine antibody (primary antibody) overnight in 4 ºC in 1% milk in TBS-T. Membranes were then probed with secondary antibody (anti-rabbit, 1/10000) at room temperature for 1 h and photographic image was taken by G:BOX Chemi systems (Syngene).

2.4.3.5 Stripping of the membrane

The membrane was incubated in a stripping buffer for 45 min at 37 ºC on shaker. The membrane was washed with water then washed 3 times with TBS-T buffer for 10 min. The membrane was then blocked with 5% dried milk protein in TBS-T for 1 h. Membranes were then probed using pre-determined concentrations of anti-Glo1 (rat, 1/3000) antibody (primary antibody) overnight in 4 ºC in 1% dried milk protein in TBS-T. After blotting with primary antibody the membranes were washed three times with TBS-T buffer for 10 min. Membrane was then probed with secondary antibody (anti-rat, 1/10000) at room temperature for 1 h. Membranes were washed three times with TBS-T and developed with ECL reagent and photographic image was taken by G:BOX Chemi systems (Syngene). Membrane was scanned and quantified with Image Quant densitometry software.

2.5 LC-MS/MS methodology

2.5.1 Assay of protein glycation, oxidation and nitration adducts by LC-MS/MS

Protein glycation, oxidation and nitration adducts residues in cell protein were analysed by LC-MS/MS after exhaustive enzymatic hydrolysis, and free adducts in the media were quantified by stable isotopic dilution analysis liquid chromatography with tandem mass spectrometric detection (LC-MS/MS) (Rabbani et al., 2014a, Thornalley et al., 2003b). This is a gold standard technique with high specificity and sensitivity developed by the host team.

Analytes tested were: early glycation adduct N_{ε}-fructosyl-lysine (FL); AGEs N_{ε}-(1-carboxyethyl)lysine (CEL), N_{ε}-carboxymethyl-lysine (CML), hydroimidazolones derived from glyoxal (G-H1), MG (MG-H1) and 3-DG (3DG-H and related structural isomers), N_{ω}-carboxymethyl-arginine (CMA), MG derived lysine dimer (MOLD) and oxidation adducts - methionine sulfoxide (MetSO), dityrosine (DT) and N-formylkynurenine (NFK); and nitration adduct 3-nitrotyrosine (3-NT).

2.5.1.1 Sample preparation, filtration and washing

An aliquot (300 µl) of cell culture medium from hPDLFs cultures was filtered by microspin ultrafiltration (3 kDa cut-off) at 14,000 g for 20 min at 4 ºC until around 200 µL of ultrafiltrate was collected and stored at -80 ºC until further analysis. The hPDLFs cell lysate (100 µl) was washed by 4 cycles of concentration to 40 µL and dilution to 500 µl with water over microspin ultrafilter (10 kDa cut-off) at 4 ºC. The protein concentration was determined by Bradford method. For the hydrolysis, an aliquot of washed protein sample containing 100 µg of protein was diluted to 20 µl with water in a glass vial and flushed with argon in preparation for enzymatic hydrolysis.

2.5.1.2 Enzymatic hydrolysis of soluble protein

The reagents and test samples were placed in a robotic processor (PAL HTS9, CTC Analytics, Switzerland) ready for automated enzymatic hydrolysis – Figure 28. All steps were performed under argon to inhibit the oxidative degradation of protein substrate. The processor was programmed to perform series of additions as follows: aliquots of 100 mM HCl (10 µl), pepsin solution (2 mg/ml in 20 mM HCl; 5

µl), and thymol solution (2 mg/ml in 20 mM HCl; 5 µl) were added, and the samples were incubated at 37 ºC for 24 h. The samples were then neutralized and buffered at pH 7.4 by the addition of 12.5 µl 100 mM potassium phosphate buffer, pH 7.4, and 5 µl 260 mM KOH. Pronase E solution (2 mg/ml in 10 mM KH_2PO_4, pH 7.4; 5 µl) and penicillin/streptomycin (1000 units/ml and 1 mg/ml respectively; 5 µl) was added, and the samples were incubated at 37 ºC for 24 h. Finally, aminopeptidase solution (2 mg/ml in 10 mM KH_2PO_4, pH 7.4; 5 µl) and prolidase solution (2 mg/ml in 10 mM KH_2PO_4, pH 7.4; 5 µl) were added, and the samples were incubated at 37 ºC for 48 h. This gave the final enzymatic hydrolysate (77.5 µl) for the LC-MS/MS assay - Table 8. It is important that addition of reagents used should be in the correct order to prevent pH overshoot. Hydrolysed sample (5 µl) and water (20 µl) was mixed with internal standard mixture (25 µl) in HPLC vials to be analysed for protein glycation, oxidation and nitration adducts and related amino acids by LC-MS/MS.

Figure 28: CTC PAL HTS9 processor

Table 8: Protocol for enzymatic hydrolysis of protein using CTC-PAL automated sample processor.

Addition	Volume added (µl)
Day 0	
100 mM HCl	10.0
Pepsin solution (2 mg/ ml)	5.0
Thymol (1 mg/ml)	5.0
Incubate for 24 hours at 37 ºC	
Day 1	
100 mM KH_2PO_4/K_2HPO_4 buffer, pH 7.4	12.5
260 mM KOH	5.0
Pronase E solution (2 mg/ml)	5.0
Penicillin (100 units/ml) and streptomycin (1 mg/ml)	5.0
Incubate for 24 h at 37 ºC	
Day 2	
Aminopeptidase solution (2 mg/ml)	5.0
Prolidase solution (2 mg/ml)	5.0
Incubate for 48 h at 37 ºC	

Adapted from (Rabbani et al., 2014a).

2.5.1.3 Preparation of standard curve

Standard curves for LC-MS/MS analysis were prepared in the range shown in Table 9, using a cocktail of normal and isotopic standards prepared as described in Tables 10. Seven calibration samples were prepared from 0 to 6 using stock calibration solutions with water. The solution (50 µl) was applied directly to LC-MS/MS for detection of each analyte. Figure 29 shows typical calibration curves for arginine and MG-H1.

Table 9: Preparation of calibration standard solutions from cocktails of normal and stable isotopic standards for protein glycation assay, oxidation and nitration adduct residues of hPDLFs protein extracts.

Cal no	Normal standards solution (µl)	Water (µl)	Stable isotopic standard solution (µl)	Total volume (µl)
0	0.00	25.00	25	50
1	1.25	23.75	25	50
2	2.50	22.75	25	50
3	6.25	18.75	25	50
4	12.50	12.50	25	50
5	18.75	6.25	25	50
6	25.00	0.00	25	50

Table 10: Analyte content of calibration standard solutions for protein glycation assay, oxidation and nitration adduct residues of hPDLFs protein extracts.

	Analytical standard (nmol)							Internal standard	
Cal no	0	1	2	3	4	5	6	(nmol)	
Lys	0	0.05	0.10	0.25	0.50	0.75	1.00	[$^{13}C_6$]Lys	0.25
Arg	0	0.05	0.10	0.25	0.50	0.75	1.00	[$^{15}N_2$]Arg	0.25
Met	0	0.05	0.10	0.25	0.50	0.75	1.00	[$^{2}H_3$]Met	0.25
Tyr	0	0.01	0.02	0.05	0.10	0.15	0.20	[$^{2}H_4$]Tyr	0.1
Trp	0	0.01	0.02	0.05	0.10	0.15	0.20	[$^{15}N_2$]Trp	0.05
	Analytical standard (pmol)							Internal standard	
Cal no	0	1	2	3	4	5	6	(pmol)	
FL	0	0.250	0.50	1.250	2.50	3.750	5.00	[$^{2}H_4$]FL	0.30
Orn	0	0.125	0.25	0.625	1.25	1.875	2.50	[$^{2}H_6$]Orn	2.50
G-H1	0	0.025	0.05	0.125	0.25	0.375	0.50	[$^{15}N_2$]G-H1	0.25
MG-H1	0	0.125	0.25	0.625	1.25	1.875	2.50	[$^{15}N_2$]MG-H1	1.25
3DG-H	0	0.125	0.25	0.625	1.25	1.875	2.50	[$^{15}N_2$]3DG-H	1.25
CML	0	0.125	0.25	0.625	1.25	1.875	2.50	[$^{13}C_6$]CML	0.25
CEL	0	0.025	0.05	0.125	0.25	0.375	0.50	[$^{13}C_6$]CEL	0.25
CMA	0	0.025	0.05	0.125	0.25	0.375	0.50	[$^{13}C_2$]CMA	0.25
MOLD	0	0.025	0.05	0.125	0.25	0.375	0.50	[$^{2}H_8$]MOLD	0.25
MetSO	0	0.125	0.25	0.625	1.25	1.875	2.50	[$^{2}H_3$]MetSO	1.25
DT	0	0.025	0.05	0.125	0.25	0.375	0.50	[$^{2}H_6$]DT	0.25
3-NT	0	0.025	0.05	0.125	0.25	0.375	0.50	[$^{3}H_2$]3-NT	0.25
NFK	0	0.025	0.05	0.125	0.25	0.375	0.50	[$^{15}N_2$]NFK	0.25

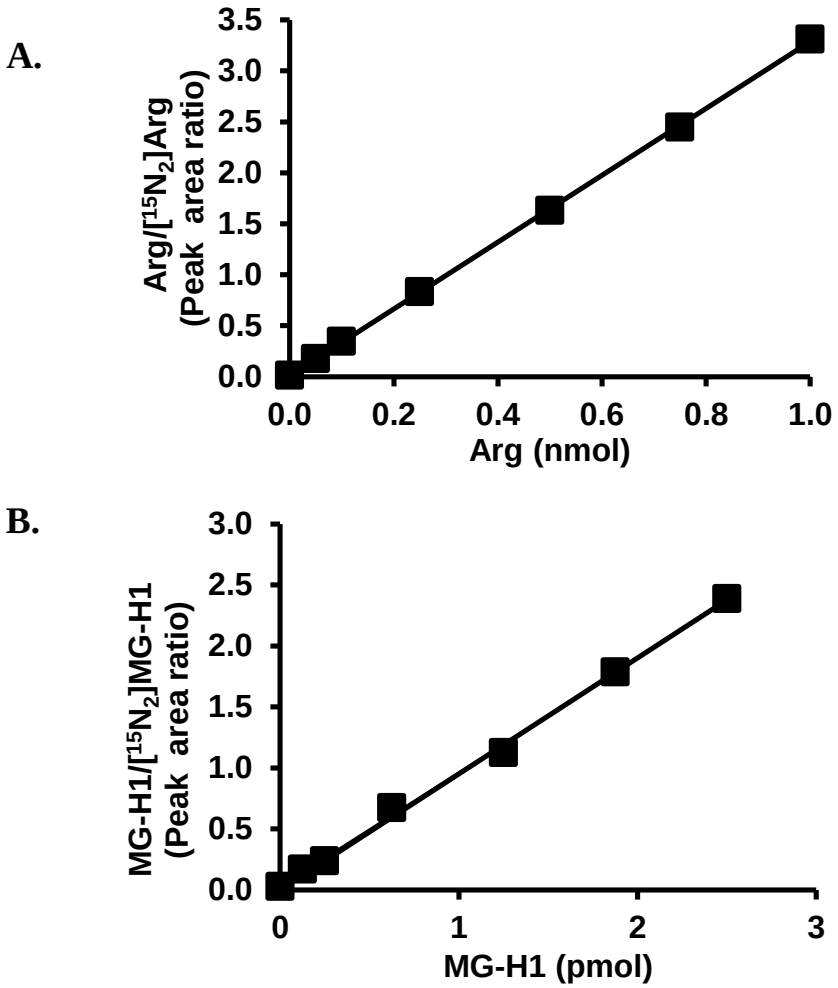

Figure 29: Typical calibration curves for arginine and MG-H1 in stable isotopic dilution analysis LC-MS/MS.
A. Calibration curve of arginine. Linear regression equation: arg/[$^{15}N_2$]arg peak area ratio = (3.49 ± 0.02) x arg (nmol) + (0.028 ± 0.009); R^2 = 0.999 (n = 7). B. Calibration curve of MG-H1. Linear regression equation: MG-H1/[$^{15}N_2$]MG-H1 peak area ratio = (0.934 ± 0.019) x MG-H1 (pmol) + (0.031± 0.025); R^2 = 0.998 (n = 7).

2.5.1.4 LC-MS/MS (Xevo-TQS system) conditions

For chromatographic conditions of the LC-MS/MS analyses, two 5 µm particle size Hypercarb columns were used in series (column 1: 2.1 x 50 mm; and column 2: 2.1 mm x 250 mm). The mobile phase was: solvent A - 0.1% TFA in water, and solvent B - 0.1% TFA in 50% acetonitrile (ACN). Solvents for the post-run method for column washing were: solvent A - 0.1% TFA in water, and solvent C - 0.1% TFA in 50% tetrahydrofuran (THF). The elution profiles for assay run and column washing and re-equilibration are given in Table 11. Flow from the column in the interval 4 to 35 min was directed to the MS/MS detector. Electrospray positive ionisation mass spectrometric multiple reaction monitoring (MRM) was used to

detect all protein damage analytes. The ionisation source temperature and desolvation temperature were 120 °C and 350 °C, respectively. The cone gas and desolvation gas flow were 99 l/h and 901 l/h, respectively. Optimised molecular ion and fragment ion masses and collision energies for MRM detection are given in – Table 12. Masslynx software was used to integrate the chromatographic peaks. Analyte amounts were normalised to amount of related unmodified amino acid in protein hydrolysates to deduce content of glycation, oxidation and nitration adduct residues in hPDLFs cell protein and to volume to deduce concentrations of glycation, oxidation and nitration free adducts in culture media. A similar elution profile was used for the Acquity^{TM}-Quattro Premier LC-MS/MS system.

Table 11: Elution profile for stable isotopic dilution analysis liquid chromatography with tandem mass spectrometric detection analysis of protein glycation, nitration addaucts and oxidation (Acquity^{TM}-Xevo-TQS system).

Time (min)	Flow rate (ml/min)	Solvent A (%)	Solvent B (%)	Gradient
0	0.2	100	0	----
5	0.2	100	0	Isocratic
8	0.2	97	3	Linear
12	0.2	97	3	Isocratic
15	0.2	83	17	Linear
18	0.2	83	17	Isocratic
24	0.2	20	80	Linear
24	0.2	97	3	Immediate
35	0.2	97	3	Isocratic
		Post-run		
0	0.4	0	100	-----
10	0.4	0	100	Isocratic
20	0.2	0	100	Isocratic
20	0.2	100	0	Immediate
25	0.2	100	0	Isocratic
40	0.4	100	0	Isocratic

Table 12: Chromatographic retention times and MRM detection conditions for detection of glycation, oxidation and nitration adducts by (LC-MS/MS) (AcquityTM-Xevo-TQS system).

Analyte	Rt (min)	Molecular ion (Da)	Fragment ion (Da)
Lys	5.6	147.1	84.1
[$^{13}C_6$]Lys	5.6	153.1	89.1
Val	8.6	117.8	72.0
[$^{2}H_8$]Val	8.6	125.8	80.0
MetSO	8.7	166.1	56.2
[$^{2}H_3$]MetSO	8.7	169.1	56.2
3DG-H	11.7	319.1	70.1
[$^{15}N_2$]3DG-H	11.7	321.1	70.1
MG-H1	11.9	229.2	114.1
[$^{15}N_2$]MG-H1	11.9	231.2	116.1
CMA	12.3	233.1	70.1
[$^{13}C_2$]CMA	12.3	235.1	70.1
G-H1	12.7	215.2	100.1
[$^{15}N_2$]G-H1	12.7	217.2	102.1
MOLD	15.0	341.2	83.9
[$^{2}H_8$]MOLD	15.0	349.2	87.9
Tyr	18.4	182.9	137.0
[$^{2}H_4$]Tyr	18.4	186.9	141
NFK	23.7	237.1	191.1
[$^{15}N_2$]NFK	23.7	239.1	193.1
3-NT	23.4	227.1	181.1
[$^{2}H_3$]3-NT	23.4	230.1	184.1
Trp	23.7	205.1	158.8
[$^{15}N_2$]Trp	23.7	205.1	160.8
CML	32.1	205.1	84.1
[$^{13}C_6$]CML	32.1	211.1	89.1
FL	32.1	291.1	84.1
[$^{2}H_4$]FL	32.1	295.1	88.1
CEL	32.2	219.2	130.0
[$^{13}C_6$]CEL	32.2	225.2	136.0
Arg	32.2	176.2	70.1
[$^{15}N_2$]Arg	32.2	178.2	70.1
Met	32.2	150.0	104.0
[$^{2}H_3$]Met	32.2	153.0	107.0

2.5.2 Assay of dicarbonyls by stable isotopic dilution analysis LC-MS/MS

Methylglyoxal, glyoxal and 3-DG amount in cultured hPDLFs and media were determined by using 1,2-diaminobenzene for derivatisation and quantification of the subsequent quinoxaline compounds – Figure 30 – by stable isotopic dilution analysis LC-MS/MS (Rabbani and Thornalley, 2014c).

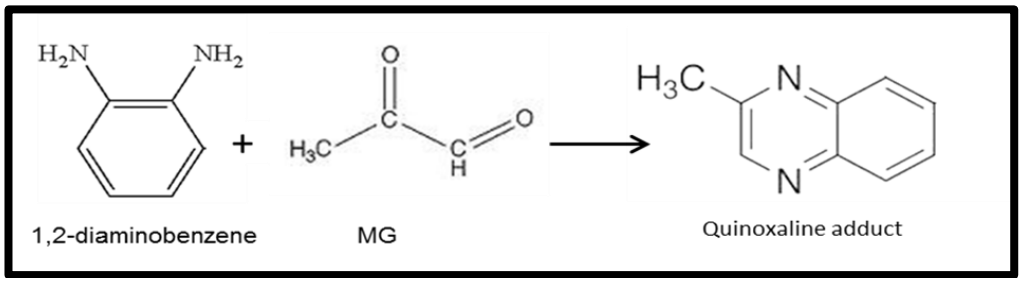

Figure 30: Derivatisation used in the dicarbonyl assay.

2.5.2.1 Sample preparation

Primary hPDLFs were cultured in experimental conditions described previously. For sample collection for analysis of media, culture medium was removed, centrifuged (250 g, 5 min) to sediment any detached cells and the supernatant removed and stored at – 80 ^{o}C until analysis. For the cell samples, remaining medium was aspirated and the cells washed with a minimum volume of PBS to remove any residual media. Then, the cells were trypsinised, trypsin neutralised, and the detached cells were counted and pelleted by centrifugation (250 g, 5 min). The supernatant was removed and cell pellets were frozen at -80 ^{o}C immediately.

For analysis of cell pellets, 10 µl of cold 20% trichloroacetic acid (TCA) containing 0.9% sodium chloride solution (NaCl) (TCA-saline) was added to cell pellets to de-proteinise the samples then samples were vortex mixed well. An aliquot of water (40 µl) was added. For media samples, an aliquot of culture medium (20 µl) was used, and 10 µl of TCA-saline and 20 µl of water were added. Subsequent preparation was similar for both sample types: an aliquot of 3% sodium azide in water (5 µl) was added to inhibit peroxidase activity and isotopic standard cocktail (5 µl; 2 pmol stable isotopic dicarbonyl) then added to each sample. The samples were vortex mixed and centrifuged (6,000 g, 10 min, 4 °C). Supernatant (45 µl) was removed and added to 10 µl derivatisation agent solution (0.5 mM diaminobenzene in 200 mM HCl containing 0.5 mM DETAPAC). Samples and standards were kept

at room temperature in the dark for 4 h for derivatisation to quinoxaline adducts to go to completion and then analysed by LC-MS/MS. Standards (2 - 20 pmol) were derivatised at the same time with the samples for calibration of the analyte/internal standard response ratio.

2.5.2.2 Preparation of calibration standards

Cocktails of dicarbonyls which contain MG, glyoxal and 3DG at 800 nM and [^{13}C]dicarbonyls at 400 nM were prepared and used to prepare standards over the range 2 - 20 pmol glyoxal, MG and 3-DG as shown in Table 13 and 14 and Figure 31.

Table 13: Calibration standards for dicarbonyls

Calibration no	MG (pmol)	Glyoxal (pmol)	3-DG (pmol)	Isotopic standard (IS)
0	0	0	0	2
1	2	2	2	2
2	4	4	4	2
3	8	8	8	2
4	12	12	12	2
5	16	16	16	2
6	20	20	20	2

Table 14: Preparation of calibration standards from stock solution

	Volume Added (µl)						
	Cal0	Cal1	Cal2	Cal3	Cal4	Cal5	Cal6
10%TCA-0.9%NaCl	10.0	10.0	10.0	10.0	10.0	10.0	10.0
Water	25.0	22.5	20.0	15.0	10.0	5.0	0.0
3% Sodium azide	5.0	5.0	5.0	5.0	5.0	5.0	5.0
Dicarbonyl standard (800pmol/ml)	0.0	2.5	5.0	10.0	15.0	20.0	25.0
[^{13}C]Dicarbonyls (400 pmol/ml)	5.0	5.0	5.0	5.0	5.0	5.0	5.0
0.5 mM DB	10.0	10.0	10.0	10.0	10.0	10.0	10.0

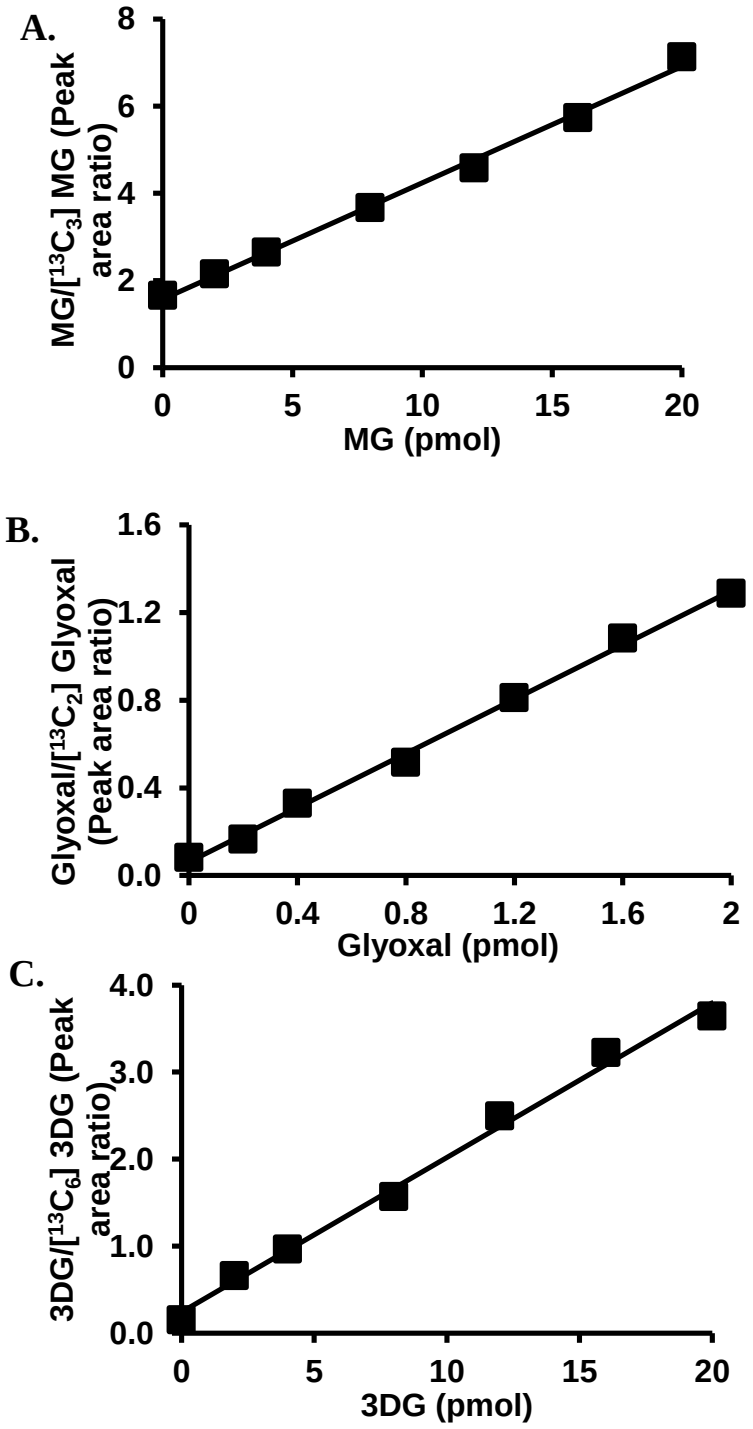

Figure 31: Standard curve for dicarbonyls.
(A) Methylglyoxal. Regression equation: Peak area ratio = ((0.267 ± 0.008) x MG [pmol]) + (1.58 ± 0.09); R^2 = 0.996 (n = 7). (B) Glyoxal. Regression equation: Peak area ratio = ((0.062 ± 0.002)x glyoxal [pmol]) + (0.062 ± 0.017); R^2 = 0.997 (n = 7). (C) 3-DG. Regression equation: Peak area ratio = ((0.169 ± 0.005)x 3-DG [pmol]) + (-0.052 ± 0.056); R^2= 0.996 (n = 7).

2.5.2.3 LC-MS/MS conditions

LC was performed by using a reverse phase octadecylsilica (ODS) BEH C18, 1.7 µm particle size column (100 x 2.1 mm) fitted with a 5 x 2.1 mm pre-column. The temperature of column was 30 °C. Solvents used were 0.1% TFA in water (solvent A) and 0.1% TFA in 50:50 acetonitrile (MeCN) in water (solvent B). The gradient used is displayed in Table 15 below.

Table 15: The gradient used for dicarbonyl analysis on LC-MS/MS.

Method phase	Time (min)	Flow rate (mL/min)	Solvent A (%)	Solvent B (%)	Curve
Analysis	0.0	0.2	100	0	0
	10.0	0.2	0	100	Linear
	15.0	0.2	0	100	Isocratic
Re-equilibration	15.0	0.2	100	0	
	30.0	0.2	100	0	Isocratic

Analysis was performed by using Acquity™ UPLC system with eluate directed into the electrospray source of a Quattro Premier XE tandem mass spectrometer. Optimised mass spectrometer settings were: capillary voltage was 0.6 kV, ion source temperature 120 °C, desolvation gas temperature 350 °C and cone and desolvation gas flows 140 and 900 l/h respectively. Table 16 shows the optimised multiple reaction monitoring (MRM) conditions used in mass spectrometric detection, along with their retention times, cone voltage and collision energy. Data analysis was performed using MassLynx software. Calibration curves were constructed by plotting peak area ratio of analyte/isotopic standard against analyte concentration.

Table 16: Optimised MRMs used for dicarbonyls analysis.

Analyte	Retention time (min)	Parent ion (Da)	Fragment ion (Da)	Cone voltage (V)	Collision energy (eV)
MG	7.8	145.1	77.1	24	24
Glyoxal	7.1	131.0	77.1	24	23
3-DG	5.6	235.2	199.0	21	15
[$^{13}C_3$]MG	7.8	148.1	77.1	24	24
[$^{13}C_2$]glyoxal	7.1	133.0	77.1	24	23
[$^{13}C_6$]3DG	5.6	241.2	205.0	21	15

2.5.3 Glutathione assay by LC-MS/MS

The amount of reduced glutathione (GSH), oxidised glutathione (GSSG) and S-D-lactoylglutathione in cultured hPDLFs cells and media samples was measured by stable isotopic dilution analysis LC-MS/MS.

2.5.3.1 Sample preparation

Primary hPDLFs were cultured in 8 mM glucose and 25 mM glucose as described previously. After 3 days of incubation, the media was removed and cells were washed with PBS. Cells were trypsinised, counted and pelleted by centrifugation (150 g, 5 min). An aliquot (40 µl) of a solution including 10% TCA, 0.15% NaCl and 0.25% sodium azide in water was added to each cell pellet sample. This solution aids in protein precipitation and acts as a preservative by inhibiting peroxidase enzymes. Samples were then centrifuged (20,000 g, 30 min, 4 ^{o}C) and supernatant (10 µl, equivalent to 0.5 million cells) was mixed with internal standard (10 µl), made up to 50 µl by the addition of 0.1% TFA (aq) and analysed by LC-MS/MS for detection of each analyte.

2.5.3.2 Preparation of calibration standards

Stock solutions (1 mg/ml) of GSH hydrochloride and GSSG were prepared in water. Further dilutions of these stocks were made using 0.1% TFA (solvent A). Calibration standards were prepared for sample analysis over the range 100-8000 pmol and 5-100 pmol for GSH and GSSG respectively - Table 17. Standards were prepared as shown in Table 18 and Figure 32. S-D-lactoylglutathione was not routinely included in calibration standards since the quantities in test samples were below the limit of detection for the assay.

Table 17: Standard curve concentrations.

	GSH (pmol)	GSH IS (pmol)	GSSG (pmol)	GSSG IS (pmol)
S1	0	100	0	25
S2	200	100	5	25
S3	400	100	10	25
S4	1000	100	20	25
S5	2000	100	50	25
S6	4000	100	80	25
S7	6000	100	100	25
S8	8000	100	-	-

Table 18: Standard curve preparation.

	GSH (µl)	GSSG (µl)	0.1% TFA (µl)	12.5% TCA (µl)	IS cocktail (µl)
S1	0	0	20	20	10
S2	0.5 (400 µM)	2.5 (2 µM)	15	20	10
S3	1.0 (400 µM)	5.0 (2 µM)	10	20	10
S4	2.5 (400 µM)	10 (2 µM)	0	20	10
S5	5.0 (400 µM)	5.0 (10 µM)	10	20	10
S6	10 (400 µM)	8.0 (10 µM)	4	20	10
S7	15 (400 µM)	10 (10 µM)	0	20	10
S8	20 (400 µM)	-	-	20	10

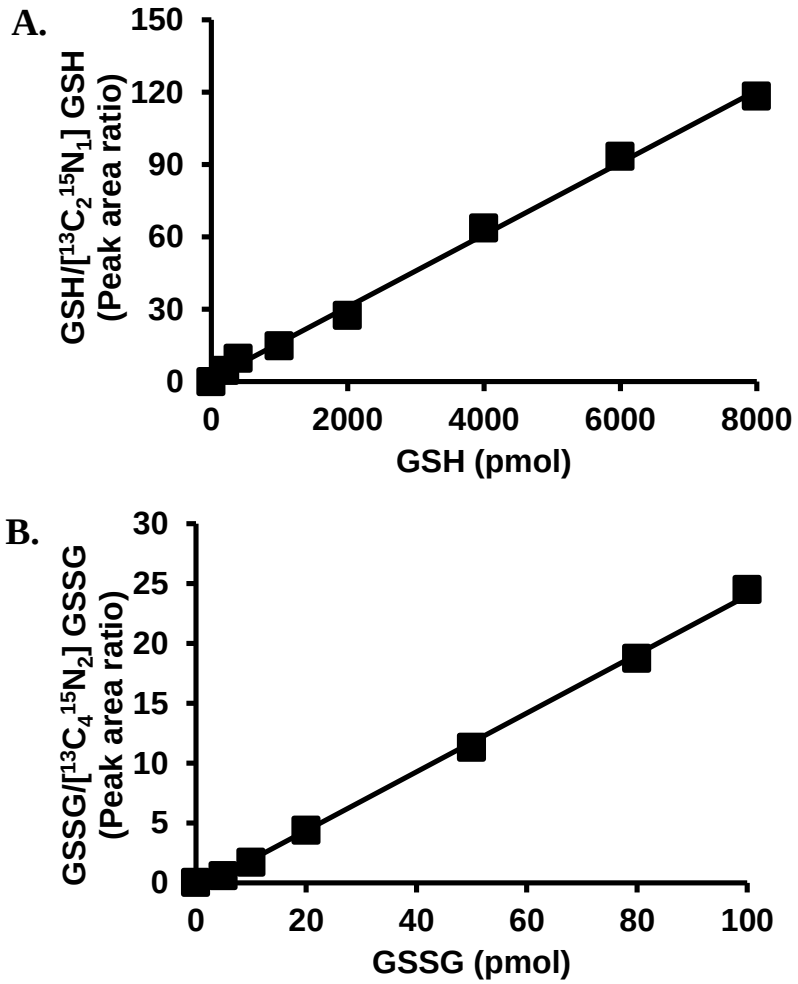

Figure 32: Standard curve for glutathione.
(A) GSH. Regression equation: Peak area ratio = ((0.015 ± 0.0003)x GSH [pmol]) ± (1.13± 1.30); R^2 = 0.997 (n = 8). (B) GSSG. Regression equation: Peak area ratio = ((0.245± 0.004)x GSSG [pmol]) ± (-0.556 ± 0.231); R^2 = 0.998. (n=7).

2.5.3.3 LC-MS/MS conditions

GSH, GSSG and S-D-lactoylglutathione were detected in hPDLFs cells by LC-MS/MS. Two graphite Hypercarb HPLC columns were used in series (50 x 2.1 mm and 250 x 2.1 mm, particle size 5 µm) with a column temperature of 30 ºC. Solvents used were: 0.1% TFA in water (solvent A); 0.1% TFA in 50:50 MeCN (solvent B); and 0.1% TFA in 50% THF (solvent C). The gradients used during the run and post run are presented in Tables 19.

Table 19: Gradient used for glutathione assay on liquid chromatography with tandem mass spectrometric detection.

Time (min)	Flow rate (mL/min)	Solvent A (%)	Solvent B (%)	Gradient
Sample analysis				
0	0.2	100	0	0
1	0.2	100	0	Isocratic
15	0.2	40	60	Linear
		Column wash and re-equilibration		
0	0.4	0.0	100	---
10	0.4	0.0	100	Isocratic
10	0.4	100	0	---
25	0.4	100	0	Isocratic

LC-MS/MS was performed on the AcquityTM UPLC-Premier XE tandem mass spectrometer system, as described above. For mass spectrometric detection, the capillary voltage was 0.6 kV. The source ionisation temperature was 120 ^{o}C. The desolvation gas flow and cone gas flow was 549 l/h and 146 l/h. The optimised MRMs used for detection, along with their retention times, cone voltage and collision energy are given in Table 20.

Table 20: Optimised MRMs used for glutathione assay.

Analyte	Retention time (min)	Parent ion (Da)	Fragment ion (Da)	Cone voltage (V)	Collision Energy (eV)
GSH	11.7	308.16	179.1	30	13
GSSG	11.7	613.20	483.7	52	18
S-D-Lactoyl-glutathione	12.7	380.21	76.2	32	35
[$^{13}C_2{}^{15}N_1$]GSH	14.3	311.16	182.1	30	13
[$^{13}C_4{}^{15}N_2$]GSSG	14.4	619.20	489.7	52	18

Data analysis was performed using MassLynx software. Calibration curves were constructed by plotting peak area ratio of analyte/isotopic standard against analyte concentration. Total glutathione levels were also calculated by formula: Total GSH = GSH + (2 x GSSG). Estimates of cellular GSH, GSSG and total GSH are given as nmol per million cells.

2.6 Statistical Analysis

Experiments were performed using analysis in replicates of triplicates or greater. Difference between normally distributed experimental groups was tested using Student's t-test assuming equal or unequal variance. The data generated here is normally distributed and assessment of statistical differences between two study groups were required. Therefore, t-test is applied in this assessments. Significance was defined as $p \leq 0.05$.

2.7 Proteomics analysis of cytosolic protein

hPDLFs were cultured in MEM with 8 mM glucose and 25 mM glucose for 3 days. Lysate was prepared by sonication. Cell pellets were suspended in aliquots of 10 mM sodium phosphate buffer, pH 7.0 (400 µl) and sonicated on ice (110 W, 30 s). Samples were centrifuged (20,000 g, 30 min, 4 ^{o}C) to sediment membranes. The supernatant was transferred and stored at -80 ^{o}C until analysis. The protein concentration was measured using Bradford assay. Lysate (500 µg) was washed by 4 cycles of concentration to 40 µl and dilution to 400 µl with water over microspin ultrafilter (10 kDa cut-off) at 4 ^{o}C. The final washed protein concentration determined by Bradford method. For a positive control sample of MG-modified proteins, cell protein (100 µg) was incubated with MG (467 µM) for 24 h at 37 ^{o}C – Figure 33.

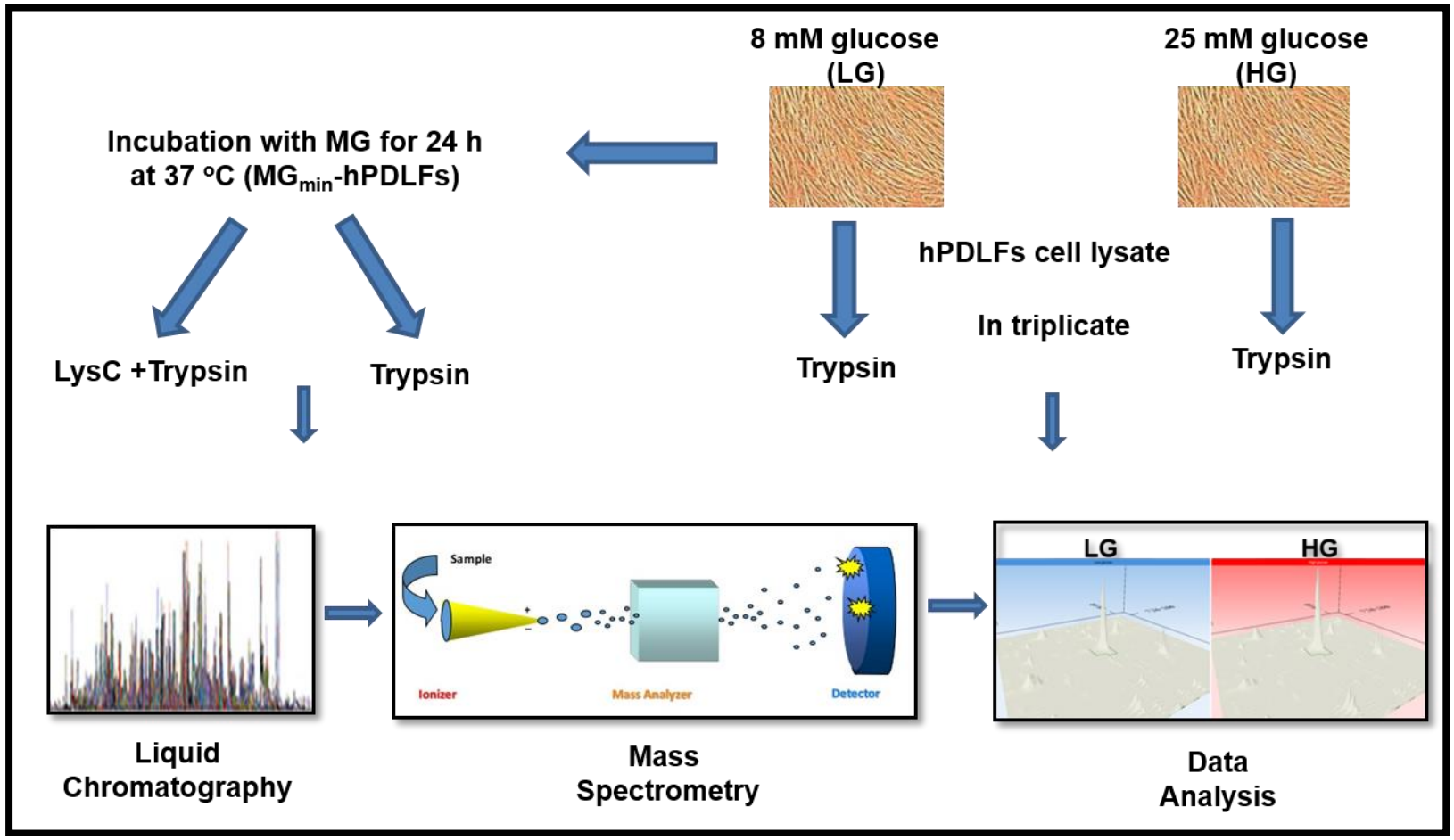

Figure 33: Proteome analysis of hPDLFs cell lysate.

2.7.1 Protocol of tryptic digestion of cytosolic protein

To an aliquot of cytosolic protein extract (100 µg) was dissolved in dithiothreitol (6 µl, 6 mM) and incubated at 37 ºC in the dark for 30 min to reduce disulphide bonds in the protein. Then, thiol groups were modified by addition of iodoacetamide (5.9 µl, 10.8 mM) and incubated at 37 ºC in the dark for 30 min. Residual iodoacetamide was quenched by further addition of dithiothreitol (5.9 µl, 6 mM) and incubated at 37 ºC in the dark for 30 min. An aliquot of TPCK-treated trypsin (1 mg/ml, 5 µl) in 1 mM calcium chloride/500 mM ammonium bicarbonate, pH 8.0, was then added and the sample was incubated at 37 ºC for 5 h in the dark. Finally, the reaction was stopped by adding 10% TFA (5 µl) in water. The sample was lyophilised to dryness to remove volatile salts and re-suspend in an aliquot (100 µl) 0.1% formic acid in water and analysed by nanoflow liquid-chromatography-Orbitrap mass spectrometry.

2.7.2 Protocol of Lys-C-Trypsin protease digestion of cytosolic protein

A Lys-C protease digestion protocol similar to the previous one for tryptic digestion was used; instead of adding TPCK-treated trypsin to the cytosolic protein, an aliquot of Lys-C protease (1 mg/ml, 5 µl) in 500 mM ammonium bicarbonate, pH 8.0, was added and incubated for 1 h at 37 ºC. Then TPCK-treated trypsin (1 mg/ml, 5 µl) in 1 mM calcium chloride/500 mM ammonium bicarbonate, pH 8.0, was added and samples were incubated at 37 ºC for 5 h in the dark.

2.7.3 Peptide separation, protein identification and quantitation

The processed cell lysate samples were submitted to the Mass Spectrometry and Proteomics Facility at Warwick University for a label-free proteomic quantitation analysis. Reversed phase nanoflow liquid chromatography- mass spectrometry for global protein identification was performed on an Orbitrap mass spectrometer equipped with a microspray source operating in positive ion mode. For proteomics analysis the column used was: an Acclaim PepMap µ-pre-column cartridge (trap), 300 µm i.d. x 5 mm, 5 µm particle size, 100 Å pore size, fitted to an Acclaim PepMap RSLC 75 µm i.d. x 50 cm, 2 µm particle size, 100 Å pore size main column (Thermo Scientific). It was installed on an Ultimate 3000 RSLCnano system (Dionex). An aliquot (5 µl) of each sample was injected. After injection, the peptides were eluted off of the trap onto the analytical column. Mobile phases were:

A - 0.1% formic acid in water, and B - 0.1% formic acid in acetonitrile. The flow rate was programmed at 0.3 µl/min. Mobile phase B was increased from 3% to 35% in 125 to 220 min, depending on the complexity of the sample, in order to separate the peptides. Mobile phase B was then increased from 35% to 80% in 5 min before being brought back quickly to 3% in 1 min. The column was equilibrated at 3% of mobile phase B for 15 min before the next sample. Peptides were eluted directly (300 nl min^{-1}) via a Triversa Nanomate nanospray source (Advion Biosciences, NY) into a Thermo Orbitrap Fusion (Q-OT-qIT, Thermo Scientific) mass spectrometer. Survey scans of peptide precursors from 350 to 1500 *m*/*z* were performed at 120K resolution (at 200 *m*/*z*) with automatic gain control (AGC) 4×10^5. Precursor ions with charge state 2 - 7 were isolated (isolation at 1.6 Th [Thomson units; m/z =1] in the quadrupole) and subjected to high energy collision dissociation (HCD) fragmentation. The collusion-induced dissociation fragmentation energy was programmed to 35%. It was used rapid scan MS analysis in the ion trap, the AGC was set to 1 x 10^4 and the max injection time was 200 ms. Dynamic exclusion duration was set to 45 s with a 10 ppm tolerance around the selected precursor and its isotopes. Monoisotopic precursor selection was turned on. The instrument was run in top speed mode with 2 s cycles. Sequence information from the MS/MS data was managed by converting the raw (.raw) files into a merged file (.mgf) using MSConvert in ProteoWizard Toolkit (version 3.0.5759) (Kessner et al., 2008). The resulting .mgf files were searched, and the database was searched against protein sequence databases.

2.7.4 Data analysis

Database search. MS^2 spectra were searched with Mascot engine (Matrix Science, version 2.5.0) against *Homo sapiens* database (http://www.uniprot.org/). Mascot was set up to search the human_uniprot_18June2015 database assuming the digestion enzyme trypsin to determine levels of false-positive peptide identifications, spectra were also searched against the corresponding reverse database, the common Repository of Adventitious Proteins Database (http://www.thegpm.org/cRAP/index.html). Search parameters for precursor mass and product ions tolerance were, respectively, ± 5 ppm and ± 0.8 Da, with allowance made for two missed trypsin cleavages, fixed modification of cysteine through

carbamidomethylation and methionine oxidation. Only fully tryptic peptide matches were allowed.

Validation. Scaffold (version Scaffold 4.3.2, Proteome Software Inc.) was used to validate MS/MS based peptide and protein identifications from MS/MS sequencing results. Peptide identifications were accepted if they could be established at greater than 95.0% probability by the Scaffold Local FDR algorithm. Protein identifications were accepted if they could be established at greater than 95.0% probability and contained at least 3 identified peptides. Protein probabilities were assigned by the Protein Prophet algorithm (Nesvizhskii et al., 2003). Proteins that contained similar peptides and could not be differentiated based on MS/MS analysis alone were grouped to satisfy the principles of parsimony. Proteins sharing significant peptide evidence were grouped into clusters.

2.7.5 Protein function and ontology

Protein ontology was evaluated using literature reports of protein roles as well as Web-based tools (http://www.reactome.org/) to identify functional annotation to characterise molecular functions and biologic processes that were used in reporting the potential relationships and interconnecting ontologies for proteins determined to show differential expression in hPDLFs.

2.7.6 Statistical analyses

The mean, standard deviation, confidence score and ANOVA test for all proteins were determined using the datasets of the three matched hPDLFs pellets using bioinformatics software and statistical program analysis by Progenesis QI for proteomics 2.0 (Nonlinear Dynamics, Newcastle upon Tyne. Algorithms for calculating protein probabilities from peptide probabilities were performed using Progenesis. A relative quantification of protein concentration was performed using non-conflicting peptides in Progenesis (see http://www.nonlinear.com/progenesis/qi-for-proteomics/v2.0/faq/which-quantitation-method-should-i-choose-for-my-experiment.aspx#relative-all for further details). Briefly, this method considers non conflicting peptides identified as part of the protein for quantification.

The following graphs show the experiment matrices calculated and visualised in Progenesis. The graph below shows mean abundance of peptides found in each experiment, identified peptide ions shown in yellow – Figure 34. Peptide ion abundance was calculated using the current experiment design. The levels of peptides identified was similar in both condition about 5% identified in LG and 4.8% in HG. Small decrease in peptide identification in HG suggests more peptide may have been glycated and not identified. Total and identified peptide ions are heavily skewed towards right in the histogram indicating that low abundance peptides were missed identifications and saturation at high abundance may compromise the accuracy of quantification.

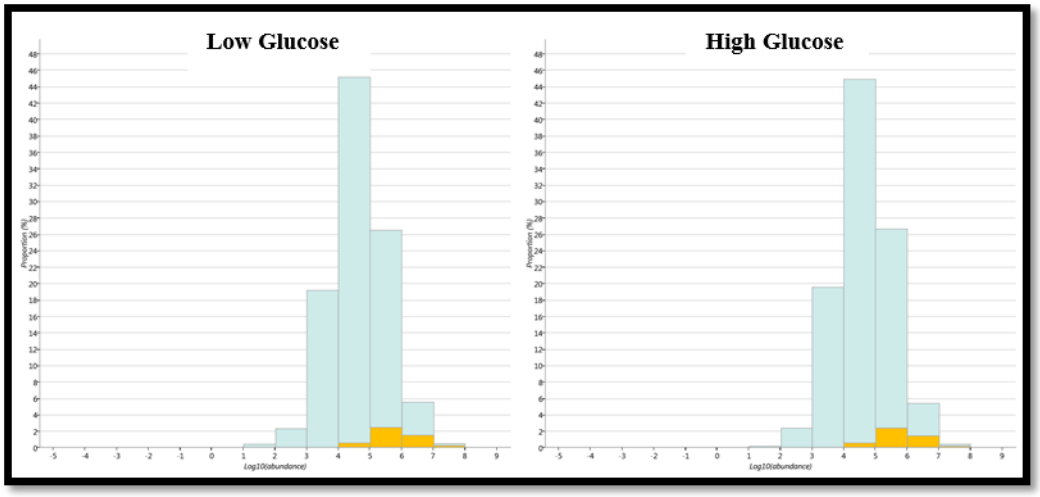

Figure 34: relative abundance of protein in low and high glucose hPDLFs proteomics samples.
Data are mean ± SD, n = 3.

The efficiency of tryptic digestion was high – *ca.* 70% protein was digested, 20% peptides contained one missed cleavage and *ca.* 2% peptides contained 2 missed cleavages. The mean number of missed cleavage per peptide ions by trypsin was very low in all preparations as indicated in the graph below – Figure 35.

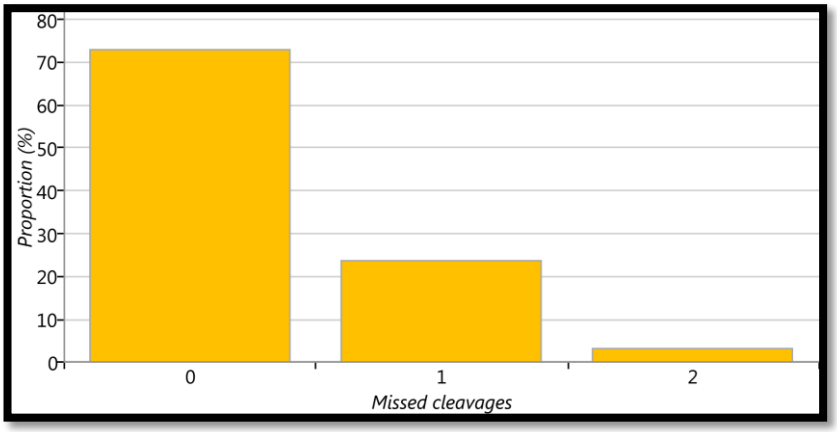

Figure 35: The mean number of missed cleavage per peptide ions by trypsin.

Figure 36 below shows the scan rate variation within the experimental condition run on the mass spectrometer. The variability between run was low indicating high quantification accuracy of the proteome concentration in low and high glucose.

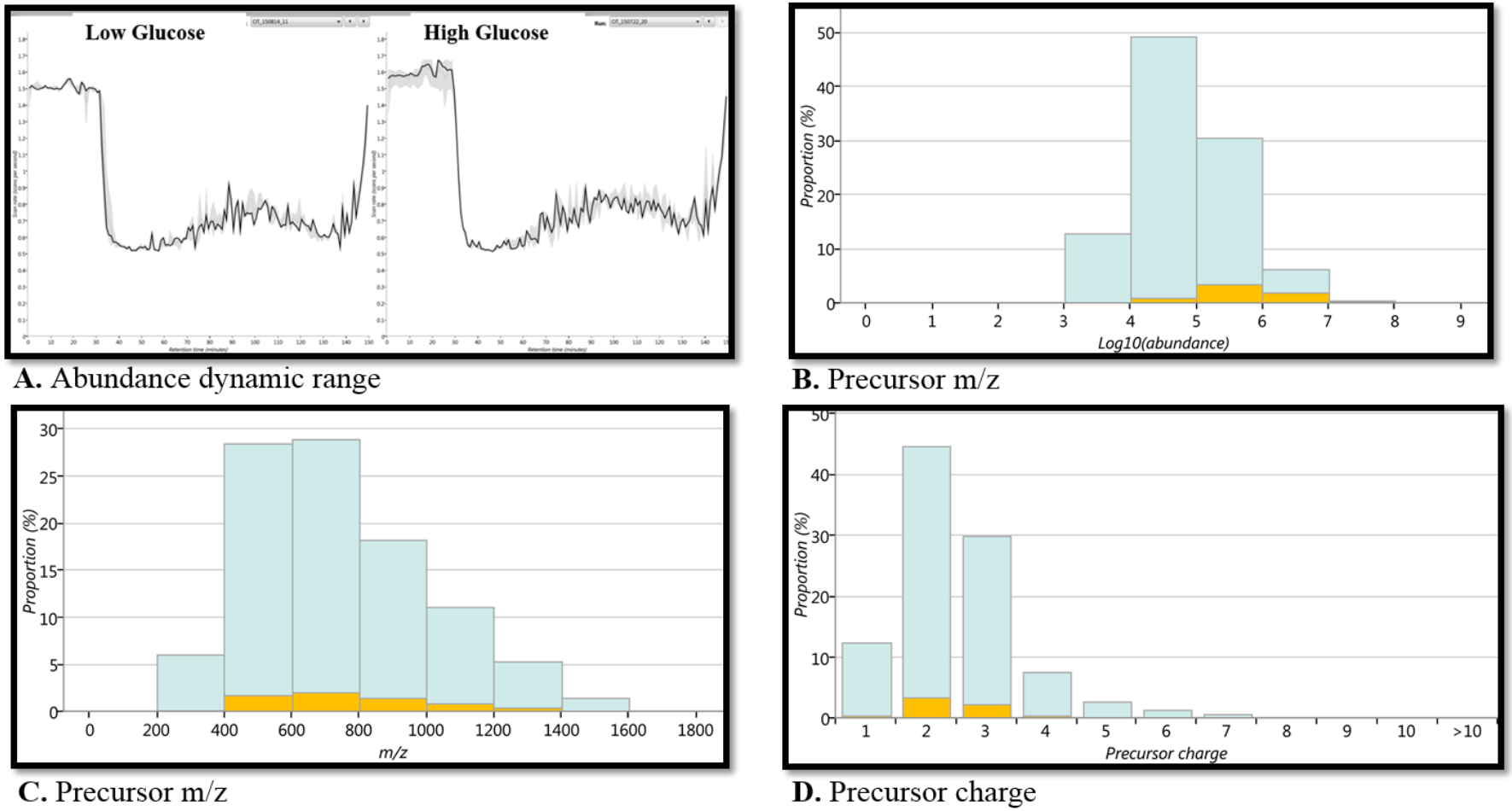

Figure 36: The scan rate variation within the experimental condition run on the mass spectrometer.

2.8 Characterisation of protein glycation, oxidation and nitration markers in plasma of healthy people, periodontitis patients and periodontitis patients with Co-morbidities

2.8.1 Study groups

2.8.1.1 Control group

Age- and gender-matched periodontally healthy control subjects (*n* =17, 11 males and 6 females; mean age = 49 ± 6 years, range = 32–60 years) were recruited from staff of the University Hospital, Coventry and Warwickshire. Normal healthy control subjects were recruited with no history of periodontitis, diabetes or renal failure suggestive of any pathology. Venous blood samples were collected after consent was obtained from the subject.

2.8.1.2 Periodontitis without any co-morbidity

Samples of blood plasma used in this study came from ENERGISE study (NCT00952536). Subjects with chronic periodontitis from the placebo arm (n= 17, 9 males and 7 females; mean age = 43 ± 11 years, range = 38–60 years) were recruited from patients referred to the periodontal department of Birmingham's Dental Hospital (Birmingham, U.K.). Volunteers were both non-smokers and medically healthy by medical history questionnaire. Volunteers had chronic periodontitis as defined by a minimum of two sites per quadrant with pocketing or interproximal attachment loss of >6 mm and one-third radiographic bone loss. The exclusion criteria were: patients with aggressive disease, patients with physical or mental disability, pregnant women, patients whose medical history may place them at risk of complications from periodontal therapy (e.g. need for antibiotic prophylaxis, Warfarinised patients), patients taking long-term antimicrobial or anti-inflammatory drugs, patients unable to swallow capsules, patients unable to provide informed consent, current smokers (or within 5 years), patients taking regular vitamin supplementation (Chapple et al., 2012). The clinical characteristics of patients with periodontitis is presented in Table 21.

2.8.1.3 Periodontitis with co-morbidities

The plasma sample of patients with comorbidities such as chronic periodontitis, diabetes and chronic kidney disease (CKD) were from the RIISC (Renal impairment in secondary care) cohort (n = 5, 4 males and 1 female; mean age

= 58 ± 9 years, range = 52–74 years) were recruited at Birmingham Hospital NHS Trust. The inclusion criteria for these patients were: patients with, CKD stage 3 or 4, diabetes with a HbA1c at >58 mmols/mol and severe periodontitis as defined by Page and Eke (Page and Eke, 2007).

Ethical approval for this work was sought and obtained from local ethics committees at Birmingham Hospital NHS Trust, Birmingham, U.K., South Birmingham Local Research Ethics Committee, U.K (the REC numbers are: 10/H1207/109 and 10/H1207/6). The collection of samples from patients and healthy subjects with informed consent and use of them were approved by the NRES Committee West Midlands – South Birmingham (REC No: 13/WM/0097) and were conducted in accordance with the Declaration of Helsinki. The clinical characteristics of the study groups is presented in Table 21.

Table 21: Clinical characteristics of healthy people and patients with periodontitis

Clinical characteristics	Control	Periodontitis	Co-morbidities and periodontitis
N	16	17	5
Age (yr)	43 ± 11	49 ± 6	58 ± 9
Gender M/F	9/7	11/6	4/1
Co-morbidities	None	None	Diabetes, CKD
eGFR (ml/min/1.72m^2)	None	None	19 ± 10
HbA_{1c} (mmol/mol)	None	None	87.2 ± 25.9

2.8.2 Plasma sample preparation, filtration, washing and delipidation

Plasma (100 µl) was diluted 5-fold with water and washed by 4 cycles of concentration to 50 µl and dilution to 500 µl with water over a microspin ultrafilter (10 kDa cut-off) at 4 ^{o}C. The final washed protein (100 µl) was delipidated by extraction 3-times with an equal volume of water-saturated ether. Residual ether was removed in a centrifugal evaporator and protein concentration determined by Bradford method. Please see section 2.5.1 in material and methods for details.

2.8.3 Hydrolysis of sample protein

For the hydrolysis, an aliquot of washed protein sample containing 100 µg of protein was diluted to 20 µl with water in a glass vial and flushed with argon in preparation for enzymatic hydrolysis as described above in section 2.5.1.

2.8.4 Statistical Analysis

Experiments were performed using analysis in replicates of triplicates or greater. Difference between normally distributed experimental groups was tested using Student's t-test assuming equal or unequal variance. The data generated here is normally distributed and assessment of statistical differences between two study groups were required. Therefore, t-test is applied in this assessments. Significance was defined as $p \leq 0.05$. Non-parametric data were analysed using Mann Whitney-U test (2 groups).

3. Results

3.1 Characterisation of the glyoxalase system in human periodontal ligament fibroblasts *in vitro*

3.1.1 Growth and viability of hPDLFs incubated in 5.5 mM, 8.0 mM and 25.0 mM glucose *in vitro*

Growth and viability of hPDLFs incubated in 5.5 mM, 8.0 mM and 25.0 mM glucose was studied. The viable cell number increased progressively throughout the period of culture. At day 6 the viable cell number had increased from 0.048 x10^6 at seeding to: 1.35 ± 0.26 x10^6 cells in 5.5 mM glucose, 1.83 ± 0.14 x10^6 cells in 8.0 mM glucose and 3.37 ± 0.17 x10^6 cells in 25.0 mM glucose. The cell viability, as judged by Trypan blue exclusion test, was > 98.5% in the three culture conditions. Cell growth curves were plotted of viable cell number against time over 6 days - Figure 37. The growth of hPDLFs was higher in medium containing 8.0 mM glucose and growth tended to slow beyond 3 days in 5.5 mM glucose and 5 days in 8.0 mM glucose. The mean growth rate from day 1 – day 3 was 27% higher in in 8.0 mM glucose, compared to in 5.5 mM glucose cultures. The rate of hPDLFs growth in 8.0 mM glucose and 25.0 mM glucose was similar until the day 5 when cell growth stopped in 8.0 mM glucose cultures and continued in 25.0 mM glucose.

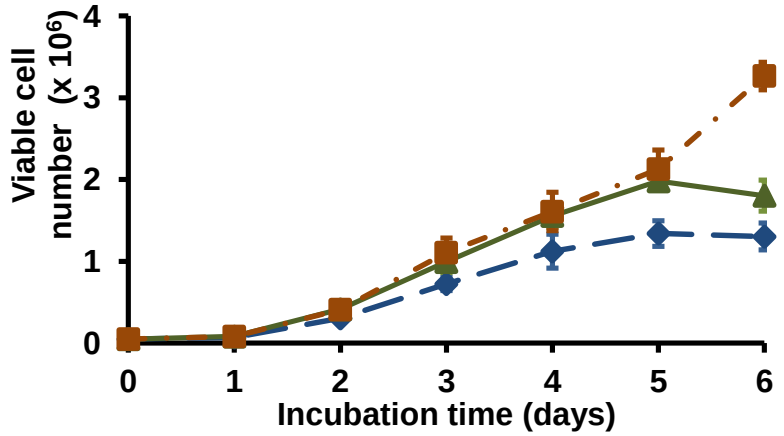

Figure 37: Growth curve of hPDLFs cells in media containing 5.5 mM, 8.0 mM and 25.0 mM glucose *in vitro*.
Primary hPDLFs cells (5000 cells/cm^2) were incubated in MEM media with 10% FBS and the glucose concentrations indicated for 6 days. Data are mean ± SD (n = 3). Key: 5.5 mM glucose, 8.0 mM glucose and 25.0 mM glucose

To further examine hPDLFs growth kinetics, the growth curves are shown with log transformation of cell number estimates. This shows that the rate of cell growth was highest from day 1 to day 2 when the doubling time was *ca.* 0.43 – 0.47 days. Beyond this, in all culture conditions the rate of cell growth slowed progressively until stopping at day 5 for cultures with 5.5 mM and 8.0 mM glucose with slow, extended growth to day 6 occurring in cultures with 25.0 mM glucose – Figure 38. In subsequent sub-cultures of these hPDLFs cell growth was stimulated again, suggesting that the slowing of cell growth was linked to depletion of nutrients rather than a cumulative cell doubling limited growth – known as the Hayflick limit (Effros and Walford, 1984). In subsequent experiments hPDLFs sub-cultured and grown for up to 3 days were used where mean population doubling time was: 5.5 mM glucose, 0.69 ± 0.10 days, 8.0 mM glucose, 0.63 ± 0.08 days, and 25.0 mM glucose, 0.61 ± 0.08 days (n = 12).

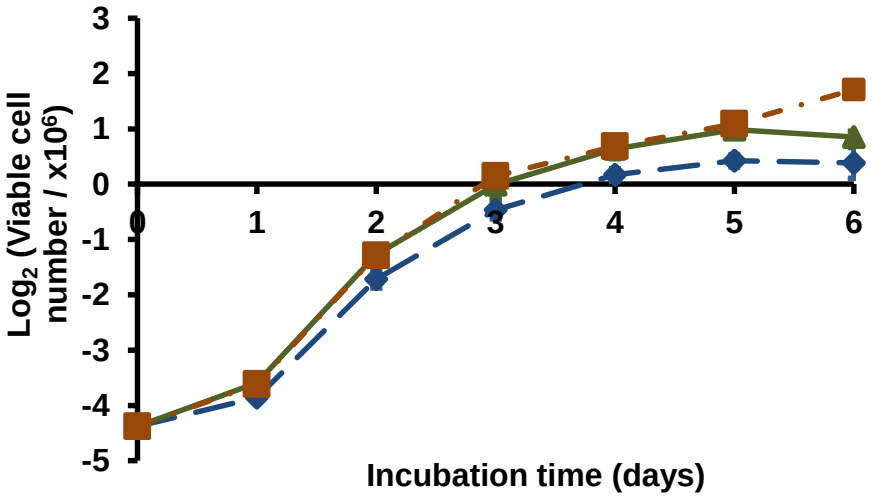

Figure 38: Growth curve of hPDLFs cells in media containing 5.5 mM, 8.0 mM and 25.0 mM glucose *in vitro* – logarithm transformation of cell number. Log_2 transformation. Primary hPDLFs cells (5000 cells/cm^2) were incubated in MEM media with 10% FBS and the glucose concentration indicated for 6 days. Data are mean ± SD (n = 3). Key: 5.5 mM glucose, 8.0 mM glucose, and 25.0 mM glucose.

In subsequent experiments to study effects of low and high glucose on metabolism and function of hPDLFs, cultures with 8.0 mM glucose were employed as the "low glucose concentration" (LG) conditions and cultures with 25.0 mM glucose were employed as the "high glucose concentration" (HG)

conditions. The 5.5 mM glucose culture was not used so that hPDLFs with similar growth rate were compared in LG and HG conditions. Moreover, the normal salivary glucose level in a healthy subject is *ca.* 8.0 mM glucose and in patients with diabetes is typically *ca.* 25.0 mM (Aydin, 2007). Primary hPDLFs were maintained in 8.0 mM glucose and 25.0 mM glucose for three days without change of medium.

3.2 Characterisation of the glyoxalase system of hPDLFs incubated in high and low glucose concentration conditions *in vitro*

3.2.1 The activity of glyoxalase 1 and glyoxalase 2 of hPDLFs cells incubated in high glucose concentration *in vitro*

Activities of Glo1 and Glo2 were measured in hPDLFs cells incubated in low glucose and high glucose concentrations. The activity of Glo1 in low glucose culture was 985 ± 148 mU per mg protein (n = 5). This was decreased *ca.* 45% after 3 days incubation under high glucose conditions (P<0.001) – Table 22 and Figure 39. The activity of Glo2 in low glucose culture was 4.20 ± 2.71 mU per mg protein (n = 5). This was not changed after 3 days incubation under high glucose conditions – Table 22 and Figure 39.

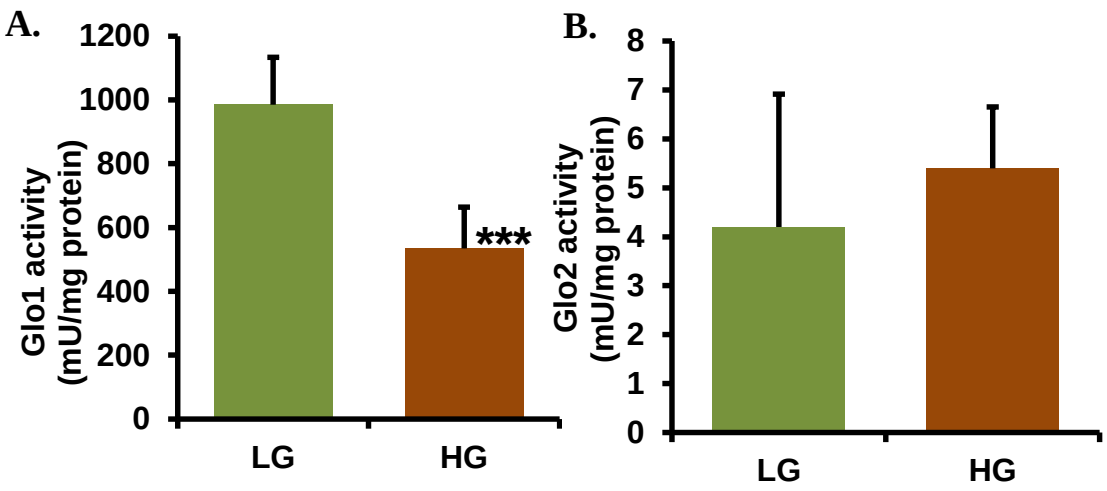

Figure 39: Enzymatic activities of the glyoxalase system in hPDLFs cells *in vitro*.
Activities of (A) Glo1, (B) Glo2 in hPDLFs cells were cultured in medium containing low glucose concentration (8 mM) and high glucose concentration (25 mM) for 3 days. Data are mean ± SD (n = 5). Significance: * and ***, P<0.05 and P<0.001, respectively (*t-test*) with respect to low glucose control.

3.2.2 Glyoxalase 1 protein content of hPDLFs cells incubated in low and high glucose concentration *in vitro*

The level of the Glo1 protein in the hPDLFs cells cultured in low and high glucose conditions was determined by Western blotting. Glo1 proteins was decreased by *ca.* 19% in high glucose cultured cells, compared to low glucose cultured controls – Figure 40.

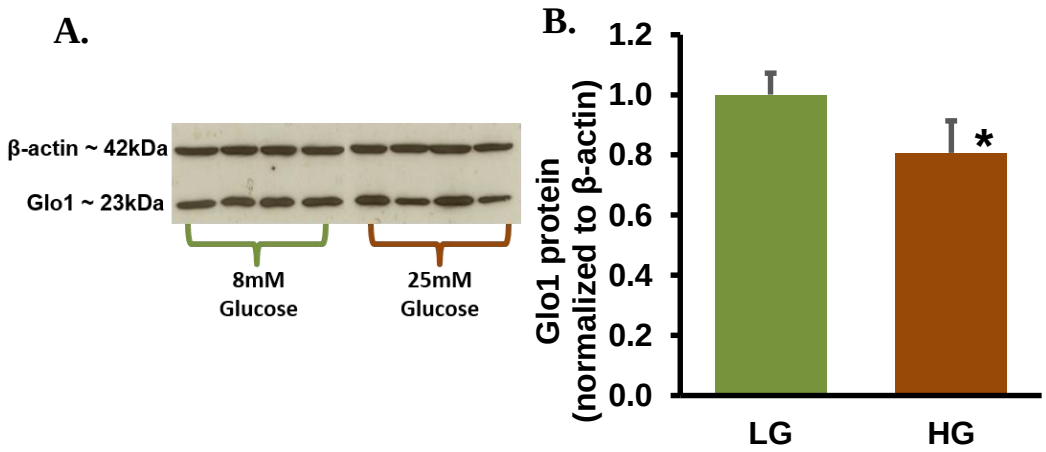

Figure 40: Glyoxalase 1 protein content of hPDLFs incubated in high glucose concentration *in vitro*.
(A) Glo1 protein blot, (B) Glo1 protein blot interpretation. hPDLFs were cultured in medium containing 8 mM and 25 mM glucose for 3 days. Data are mean ± SD (n = 4). Significance: * P<0.05 (*t-test*) with respect to low glucose control. Key: LG, low glucose concentration (8 mM); HG, high glucose concentration (25 mM).

3.2.3 Glyoxalase 1 gene expression in hPDLFs incubated in high glucose concentration *in vitro*

Expression of Glo1 of hPDLFs cells incubated in low and high glucose conditions was measured by RT-PCR. There was no significant change in the Glo1 gene expression in hPDLFs cultured in low and high glucose. This suggests that the high glucose may affect the Glo1 protein stability and functionality either by modification by reactive dicarbonyls and followed by acetylation leading to proteasomal degradation or inactivation by glycation damage to the catalytic site.

Table 22: Values of Glo1 and Glo2 activity and GLO1 gene expression in hPDLFs cells incubated in media contains high and low glucose *in vitro*

Analyte	LG	HG
Glo1 activity (mU/mg protein)	985 ± 148	534 ± 129***
Glo2 activity (mU/mg protein)	4.20 ± 2.71	5.40 ± 1.25
GLO1 mRNA (normalized to β-actin mRNA)	0.792 ± 0.002	0.791 ± 0.003

Data are mean ± SD, n = 5. Significance: ***, P<0.001 *(t-test)* respectively, with respect to low glucose control.

3.2.4 Dicarbonyl concentration in hPDLFs cells incubated in low and high glucose concentrations *in vitro*

High glucose concentration decreased Glo1 activity in hPDLFs and hence it is likely that dicarbonyl stress is induced under these conditions. This was investigated by assay of the levels of MG, glyoxal and 3-DG in cell culture medium and hPDLFs cells following culture for 3 days in medium containing 8 mM glucose and 25 mM glucose. MG concentration of the medium and MG content of cells was increased significantly by *ca.* 60% and 41%, respectively, in the high glucose conditions, compared to low glucose control (P<0.01). The concentration of 3-DG in the medium was increased 4-fold (P<0.001) and the cell content of 3-DG was increased 3-fold (P<0.001) in the high glucose conditions, compared to low glucose control. Glyoxal level did not change with high glucose treatment in the cell and medium – Figure 41 and Table 23.

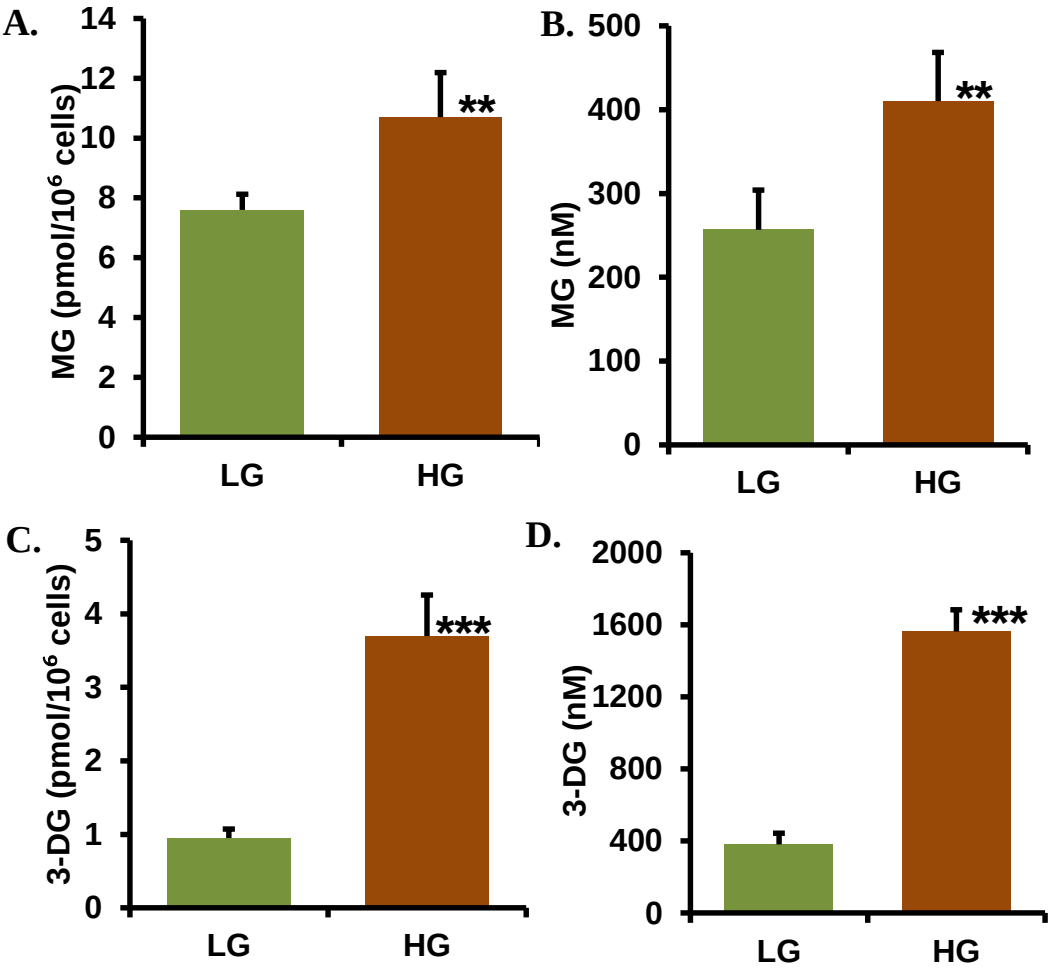

Figure 41: Effect of high glucose concentration on cellular content and medium concentration of dicarbonyl levels in hPDLFs *in vitro*.
hPDLFs were cultured in medium containing 8 mM and 25 mM glucose for 3 days. (A) Cellular MG. (B) MG in culture medium. (C) Cellular 3-DG. (D) 3-DG in culture medium. Data are mean ± SD, n = 5. Significance: ** and ***, P<0.01 and P<0.001, respectively *(t-test)*, with respect to low glucose control. Key: LG, low glucose (8 mM); HG, high glucose (25 mM).

Table 23: Effect of high glucose concentration on dicarbonyls assay measurement in hPDLFs cells and medium *in vitro*

		Methylglyoxal	Glyoxal	3-DG
Human PDLFs (pmol/10⁶cells)	LG	7.59 ± 0.53	9.11 ± 1.45	0.949 ± 0.128
	HG	10.7 ± 1.5**	9.04 ± 1.24	3.70 ± 0.56***
Media (nM)	LG	257 ± 47	909 ± 81	382 ± 61
	HG	410 ± 58**	1028 ± 118	1562 ± 121***

Data are mean ± SD, n = 5. Significance: ** and ***, P<0.01 and P<0.001, respectively *(t-test)*, with respect to low glucose control. Key: LG, low glucose (8 mM); HG, high glucose (25 mM).

3.2.5 Flux of formation of D-lactate and concentration of L-lactate in hPDLFs cells cultured in low and high glucose conditions *in vitro*

The flux of D-lactate produced by human cells often approximates to flux of MG formation as >99% of MG formed is metabolised by the glyoxalase system, metabolism of D-lactate by human cells is often limited and in cultured cells the only source of D-lactate is the glyoxalase system (Rabbani and Thornalley, 2012c). To establish if D-lactate is metabolised in the hPDLFs, D-lactate was measured in culture medium of hPDLFs with and without addition of exogenous D-lactate (10 nmol). Media alone was also analysed for D-lactate with or without exogenous D-lactate. D-Lactate concentration increased in the culture medium from baseline after culture for 3 days. Incubations of hPDLFs with added 10 nmol D-lactate showed a similar increase and maintained the differential of + 10 nmol after 3 days and set at baseline – Table 24. From this study it can be inferred that D-lactate was not metabolised significantly by hPDLFs cells *in vitro* under the conditions studied and accumulation of D-lactate in hPDLFs cultures is therefore a measure of flux of formation of MG.

Primary hPDLFs cells were cultured in low and high glucose concentration for 3 days. The concentration of D-lactate was determined in the media samples collected on baseline and at day 3. The flux of D-lactate was determined by subtracting the amount of D-lactate at baseline from that at day 3 and normalising to final cell number and days in culture – presenting D-lactate flux as nmol per million cells per day. The production of D-lactate was increased 42% in hPDLFs cultured in high glucose, compare to low glucose ($P<0.001$) - Figure 42 and Table 25. This suggests that the flux of formation of MG in hPDLFs is increased in high glucose concentration conditions.

L-Lactate is the terminal product of anaerobic glycolysis and it is readily metabolised. Similar measurement of the flux of L-lactate as for D-lactate above is a qualitative marker of glycolytic activity and underestimate of L-lactate formation since it is readily metabolised. Nevertheless, apparent L-lactate has been assumed to be qualitative marker of glycolytic activity (Forristal et al., 2013). When apparent flux of L-lactate formation was measured over 3 days of hPDLFs cultured in high glucose concentration there was no significant change in

apparent flux of L-lactate formation, compared to low glucose control. As expected, apparent flux of L-lactate formation was markedly higher than the flux of D-lactate formation - Figure 42 and Table 25.

Table 24: D-lactate metabolism in the hPDLFs

	D-Lactate production (nmol)
Control media	5.67 ± 0.33
Media + exogenous D-lactate (10 nmol)	15.6 ± 0.34
Difference	9.88 ± 0.71

Data are mean ± S.D, n = 3.

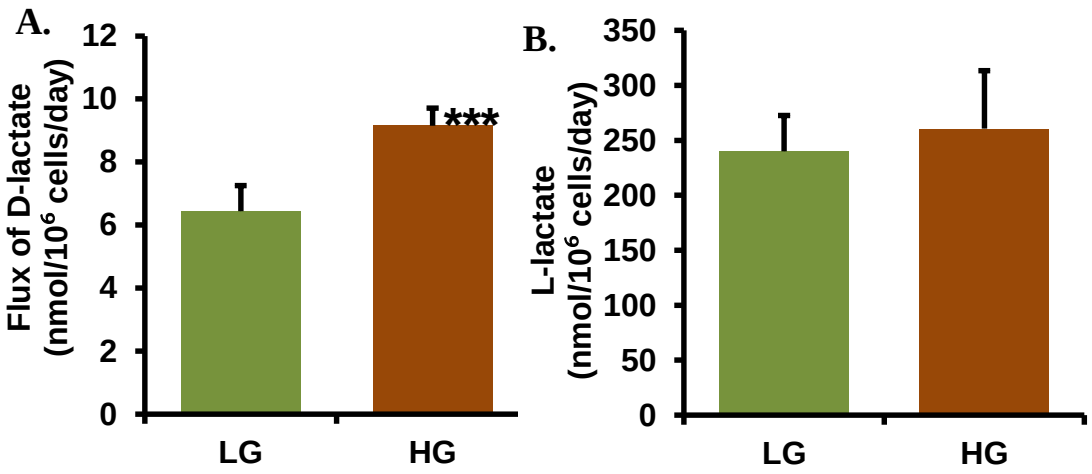

Figure 42: Flux of formation of D-lactate and concentration of L-lactate in hPDLFs cells cultured in low and high glucose conditions *in vitro*.
hPDLFs cells were cultured in medium containing 8 mM and 25 mM glucose for 3 days. (A) D-lactate production in hPDLFs cells, (B) L-lactate production in hPDLFs cells. Data are mean ± S.D, n = 5. Significance: ***, P<0.001 (*t-test*) with respect to low glucose control. Key: LG, low glucose (8 mM); HG, high glucose (25 mM).

3.2.6 Consumption of D-glucose by hPDLFs cells incubated in low and high glucose *in vitro*

Net glucose consumption by hPDLFs may be readily assessed by measuring the decrease in glucose concentration in the culture medium over 3 days. When glucose consumption was measured over 3 days of hPDLFs cultured in high glucose concentration there was a 93% increase in glucose consumption, compared to low glucose control (P<0.001) – Figure 43. Increased glucose metabolism through anaerobic glycolysis increases the flux of triosephosphate

formation and thereby the flux of MG formation. To assess if there is increased proportion of flux of glucotriose (2 x flux of glucose consumption) degrading to MG in high glucose conditions, the flux of D-lactate was calculated as a percentage of flux of glucotriose. The flux of formation of D-lactate as a percentage of flux of glucotriose was decreased *ca.* 24% in high glucose cultures, compared to low glucose control, suggesting that glucose may be diverted or consumed in other pathways e.g. pentosephosphate pathway in high glucose conditions - Figure 43 and Table 25.

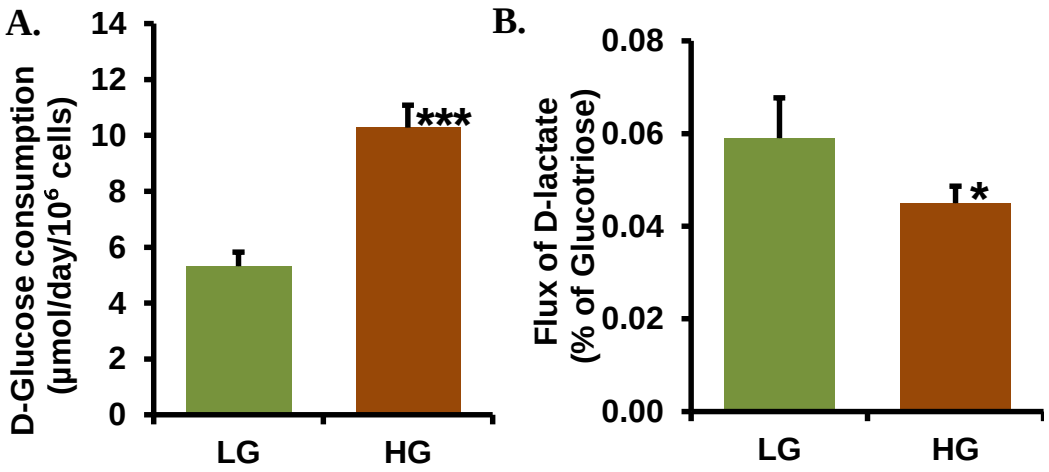

Figure 43: Consumption of D-glucose by hPDLFs cells incubated in high glucose *in vitro*.
hPDLFs cells were cultured in medium containing 8 mM and 25 mM glucose for 3 days. (A) D-Glucose consumption in hPDLFs cells. (B) Percentage flux of D-lactate from glucotriose in hPDLFs cells. Data are mean ± SD, n = 5. Significance: *, P<0.05 and ***, P<0.001 (*t-test*) with respect to low glucose control. Key: LG, low glucose (8 mM); HG, high glucose (25 mM).

Table 25: Values of different analytical assays performed on hPDLFs medium contains high and low glucose *in vitro*

	Culture Medium	
Analyte	LG	HG
L-Lactate production (nmol/day/10^6 cells)	240 ± 33	261 ± 53
D-Glucose consumption (µmol/day/10^6 cells)	5.32 ± 0.50	10.3 ± 0.80***
D-Lactate production (nmol/day/10^6 cells)	6.43 ± 0.81	9.15 ± 0.55**
D-lactate flux (% Glucotriose)	0.059 ± 0.009	0.045 ± 0.004**

Data are mean ± SD, n = 5. Significance: *, P<0.05, **, P<0.01 and ***, P<0.001 *(t-test)* with respect to low glucose (control). Key: LG, low glucose (8 mM); HG, high glucose (25 mM).

3.2.7 Thiols and glutathione in hPDLFs cultured in low and high glucose conditions *in vitro*

GSH is a cofactor in the glyoxalase system. The cellular contents of reduced and oxidised glutathione (GSH and GSSG) and total thiols were measured in hPDLFs cells following a 3 days culture supplemented with low and high glucose. The cell thiol level was increased *ca.* 24% in high glucose comparing with the control. Protein thiols were determined by subtracting GSH level from the samples. In low glucose cultures, the protein thiols content of hPDLFs was 16.0 ± 1.6 nmol/10^6 cells. Protein thiols were increased *ca.* 43% in hPDLFs cells with high glucose, compare to low glucose control (P<0.001) - Figure 44 and Table 26. The levels of GSH and GSSG decreased with high glucose conditions by 22% and 24% respectively. Total glutathione levels were also calculated: Total GSH = GSH + (2 x GSSG). Total GSH level was decreased by 22% in high glucose compare to low glucose control - Figure 45 and Table 26.

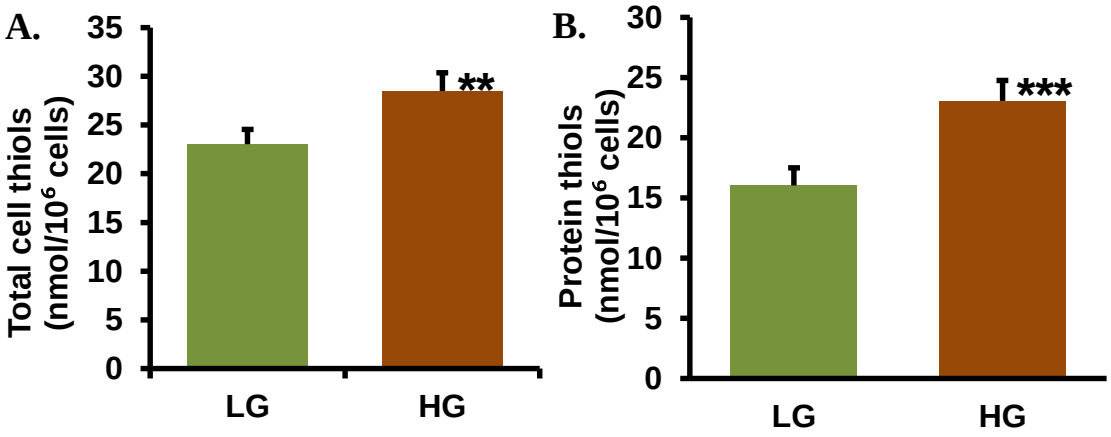

Figure 44: Effect of high glucose concentration on the total cell thiols in hPDLFs *in vitro*.
hPDLFs cells were cultured in medium containing 8 mM and 25 mM glucose for 3 days. (A) Total cell thiols. (B) Protein thiols. Data are mean ± SD, n = 5. Significance: ** and ***, P<0.01 and P<0.001, respectively (*t-test*) with respect to low glucose (control). Key: LG, low glucose (8 mM); HG, high glucose (25 mM).

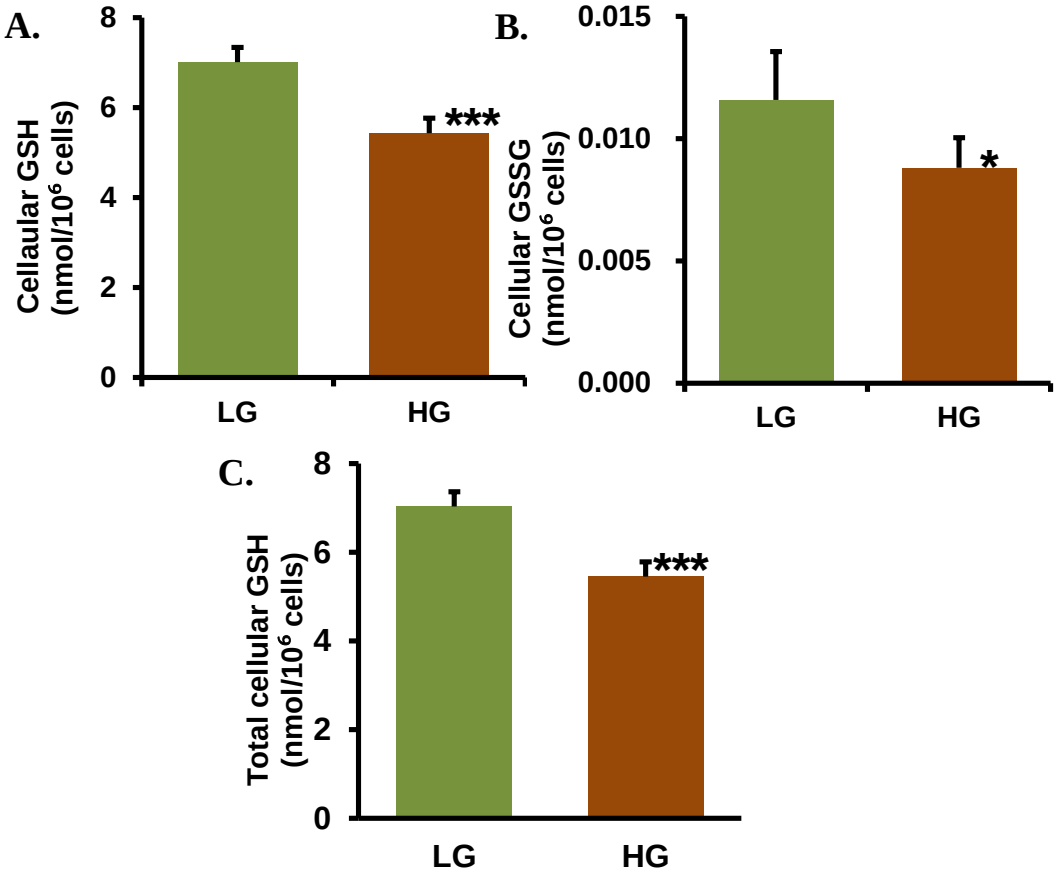

Figure 45: Effect of high glucose concentration on the glutathione level in hPDLFs *in vitro*.

hPDLFs cells were cultured in medium containing 8 mM and 25 mM glucose for 3 days. (A) Reduced glutathione, (B) oxidized glutathione and (C) total glutathione. Data are mean ± SD, n = 5. Significance: * and ***, P<0.05, and P<0.001, respectively (*t-test*) with respect to low glucose (control). Key: LG, low glucose (8 mM); HG, high glucose (25 mM).

Table 26: Effect of high glucose concentration on thiols and glutathione level in hPDLFs *in vitro*

Analyte (nmol/10^6 cells)	LG	HG
Total protein thiols	23.1 ± 1.5	28.5 ± 1.86**
Protein thiols	16.0 ± 1.6	23.1 ± 1.9***
Cellular GSH	7.01 ± 0.33	5.43 ± 0.33 **
Cellular GSSG	0.0116 ± 0.0020	0.0088 ±0.0012***
Cellular total GSH	7.03 ± 0.33	5.45 ± 0.33 *
% Total GSH as GSH	99.7	99.7
% Total GSH as GSSG	0.3	0.3
S-D-Lactoylglutathione	< LOD	<LOD

Data are mean ± SD, n = 5. Significance: *, ** and ***, P<0.05, P<0.01 and P<0.001, respectively (*t-test),* with respect to low glucose control. Key: LG, low glucose (8 mM); HG, high glucose (25 mM). LOD for S-D-Lactoylglutathione was 1.1 (pmol/10^6 cells).

3.2.8 Effect of high glucose concentration on protein glycation, oxidation and nitration adduct content of hPDLFs cellular protein and flux of free adduct formation *in vitro*

Protein glycation, oxidation and nitration adducts were measured as adduct residues of hPDLFs cell protein and as flux of free adduct formation released in the cell culture by cell proteolysis of glycated, oxidised and nitrated protein after 3 days of culture. Results are shown in Table 27.

The cellular content of MG-H1 and FL increased in high glucose by 85% and 64% ($P<0.01$ and $P<0.05$) respectively comparing with the level in low glucose. FL degrades oxidatively to CML, level of CML was increased two fold in high glucose compare to low glucose ($P<0.05$) – Figure 46. The level of CML/FL showed no change in high glucose culture and which indicate no change in the oxidative stress. Dicarbonyls are reactive glycating agents and target specifically arginine residues but not exclusively. It is expected to find a significant increase in protein glycation markers.

The free adduct found in the media are mainly formed by proteolysis of cellular proteins – Table 28. The free adducts MG-H1 and FL increased 2 folds in high glucose compared to control ($P<0.001$ and $P<0.01$ respectively). The level of free adducts 3DG-H1 was increased more than three folds in high glucose ($P<0.001$). CMA free adduct was increased by 45% in high glucose ($P<0.05$) – Figure 47. The significant increase of glycation free adducts is indicative of increased flux of protein damage by glycation and effective clearance of damaged cell proteome by proteolysis in the proteasomes. Oxidation and nitration markers did not change between the two conditions

The changes in glyoxalase pathway and its metabolites in hyperglycaemic condition in hPDLFs indicate a significant role of dicarbonyls in periodontal inflammation and diseases.

Table 27: Effect of high glucose concentration on cellular protein glycation, oxidation and nitration adduct content of hPDLFs cells *in vitro*

Protein adduct residue	LG	HG
FL (mmol/mol lys)	1.78 ± 0.33	3.34 ± 0.553***
CML (mmol/mol lys)	0.100 ± 0.036	0.186 ± 0.028**
CEL (mmol/mol lys)	0.026 ± 0.016	0.041 ± 0.017
MOLD (mmol/mol lys)	0.003 ± 0.002	0.004 ± 0.003
CMA (mmol/mol arg)	0.068 ± 0.034	0.081 ± 0.037
MG-H1 (mmol/mol arg)	0.330 ± 0.163	0.763 ± 0.201**
G-H1 (mmol/mol arg)	0.018 ± 0.014	0.023 ± 0.007
3DG-H (mmol/mol arg)	0.225 ± 0.123	0.227 ± 0.135
3NT (mmol/mol tyr)	0.0031 ± 0.0011	0.0019 ± 0.0009
DT (mmol/mol tyr)	0.080 ± 0.055	0.046 ± 0.037
NFK (mmol/mol trp)	0.109 ± 0.042	0.091 ± 0.03
MetSO (mmol/mol met)	1.66 ± 1.53	1.14 ± 0.43
CML/FL	0.059 ± 0.026	0.058 ± 0.017

Data are mean ± SD, n = 4. Significance: *, P<0.05 and **, P<0.01 (*t-test*) with respect to low glucose (control). Key: LG, low glucose (8 mM); HG, high glucose (25 mM).

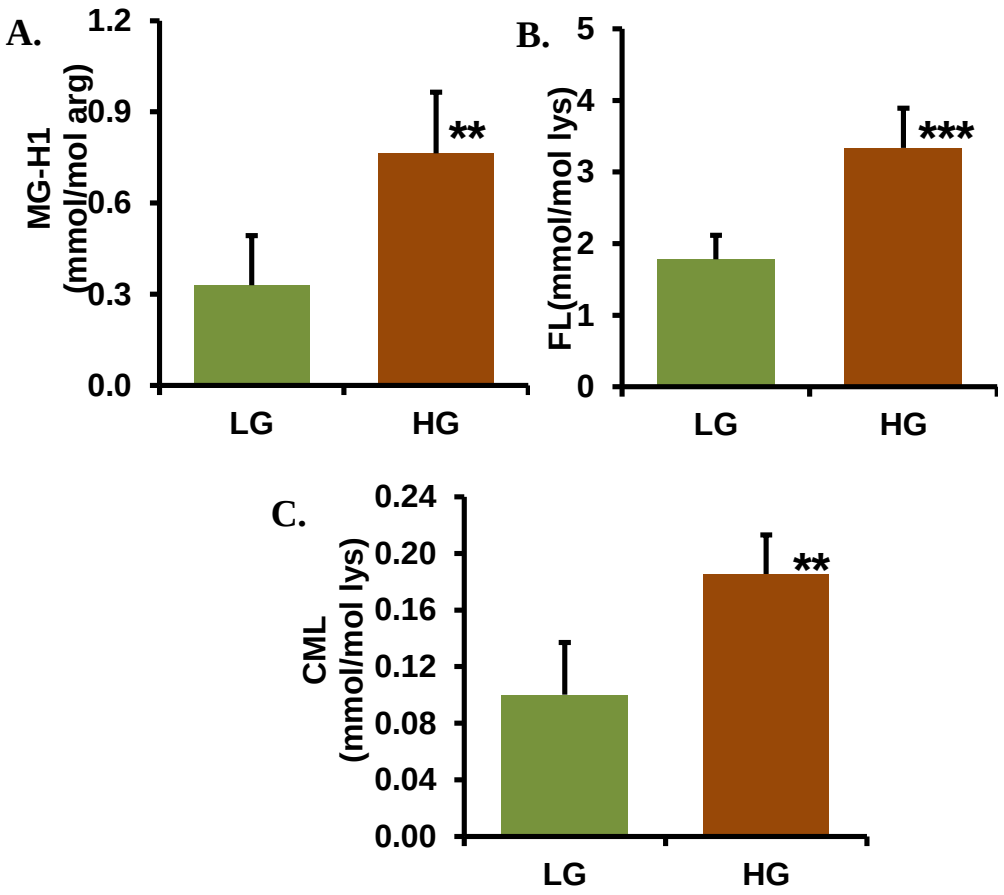

Figure 46: Effect of high glucose concentration on cellular protein glycation, oxidation and nitration adduct residue content of hPDLFs cells *in vitro*. hPDLFs cells were cultured in medium containing 8 mM and 25 mM glucose for 3 days. (A) MG-H1 (B) FL. (C) CML. Data are mean ± SD, n = 4. Significance: * and **, P<0.05 and P<0.01 (*t-test*) with respect to low glucose (control). Key: LG, low glucose (8 mM); HG, high glucose (25 mM).

Table 28: Effect of high glucose concentration on flux of protein glycation and oxidation free adducts of hPDLFs cells *in vitro*.

Free adduct production (pmol/10^6 cells/day)	LG	HG
FL	404 ± 203	882 ± 281*
CML	38.3 ± 11.2	44.8 ± 14.8
CEL	2.80 ± 1.58	3.94 ± 2.02
CMA	5.42 ± 0.60	7.89 ± 1.56*
MG-H1	2.87 ± 0.43	5.66 ± 0.73***
G-H1	2.44 ± 1.53	0.906 ± 0.433
3DG-H	1.61 ± 0.44	5.07 ± 0.89***

Data are mean ± SD, n = 4. Significance: *, P<0.05, **, P<0.01 and ***, P<0.001 (*t-test*) with respect to low glucose (control). Key: LG, low glucose (8 mM); HG, high glucose (25 mM).

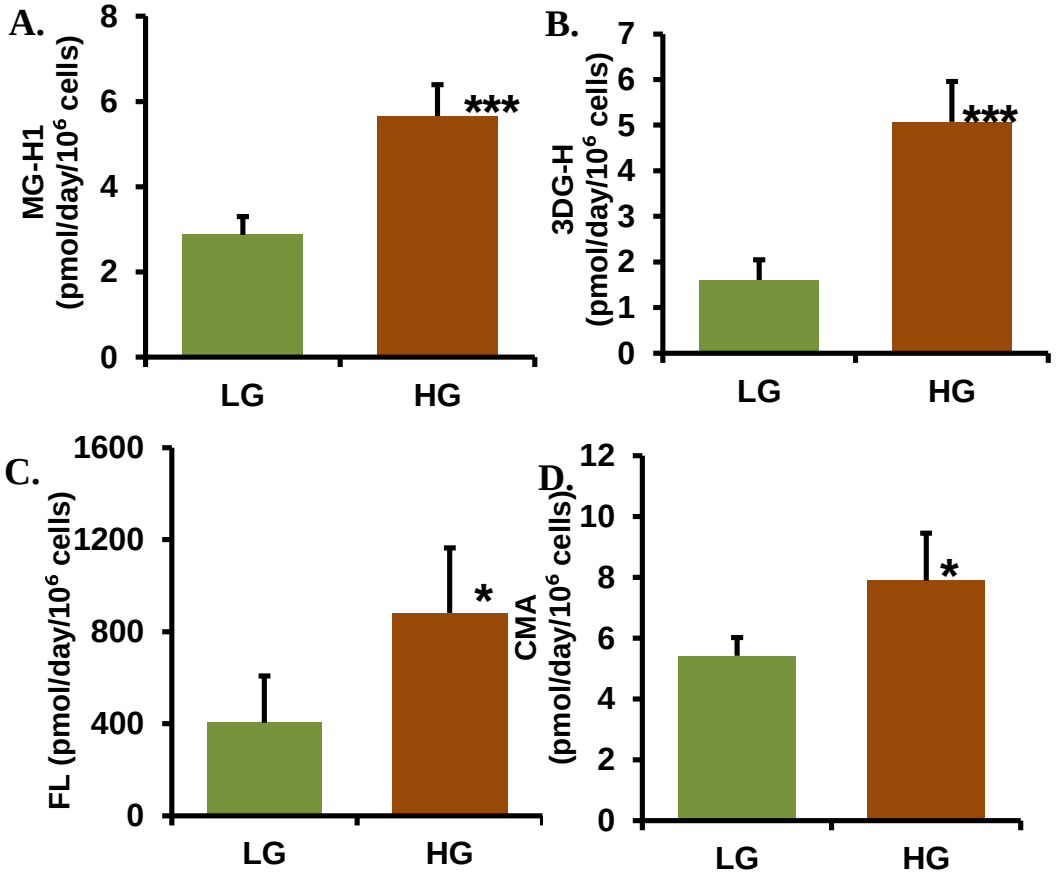

Figure 47: Effect of high glucose concentration on flux of protein glycation and oxidation free adducts of hPDLFs cells *in vitro*.
hPDLFs cells were cultured in medium containing 8 mM and 25 mM glucose for 3 days. (A) MG-H1. (B) 3DG-H1. (C) FL. (D) CMA. Data are mean ± SD, n = 4. Significance: *, ** and ***, P<0.05, P<0.01 and P<0.001, respectively (*t-test*) with respect to low glucose (control). Key: LG, low glucose (8 mM); HG, high glucose (25 mM).

3.2.9 Effect of exogenous methylglyoxal on the growth and viability of hPDLFs *in vitro*

Primary hPDLFs were incubated with and without 25 - 1000 µM MG for 48 h and cell growth and viability assessed. At ≥ 50 µM MG there was a decrease in hPDLFs viable cell number and ≥ 200 µM MG there was decrease in cell viability. This suggestes that with addition of exogenous MG of progressively increased concentration, there is initially growth arrest of hPDLFs and the both growth arrest and cytotoxicity at ≥ 200 µM MG. The MG concentration – cell growth response curve is shown in Figure 48 and the MG concentration – cell viability response is given in Figure 49. From this the median growth inhibitory

concentration GC_{50} value of MG was 250 ± 3 µM and n, the logistic regression coefficient (also known as the Hill coefficient) was 1.23 ± 0.17. A growth curve of hPDLFs with and without 200 µM MG was studied over 4 days.

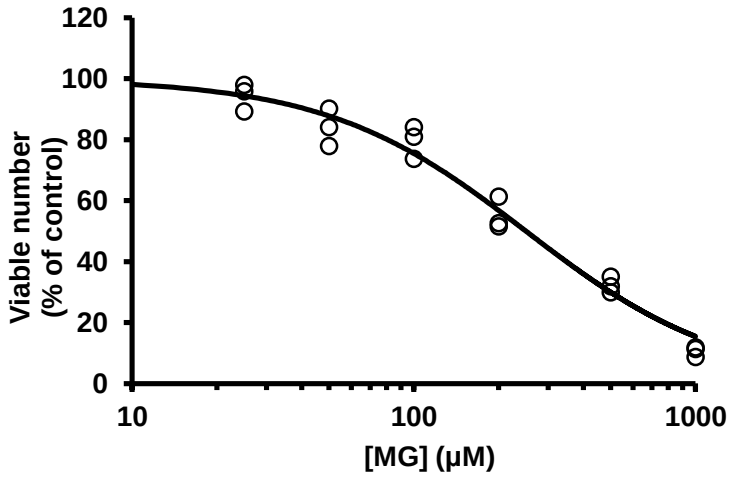

Figure 48: The MG concentration – cell growth response curve for hPDLFs *in vitro.*
Data were fitted to the MG concentration - response equation and solved for GC_{50} and n by non-linear regression. GC_{50} = 250 ± 3 µM, n = 1.23 ± 0.17 (N = 18).

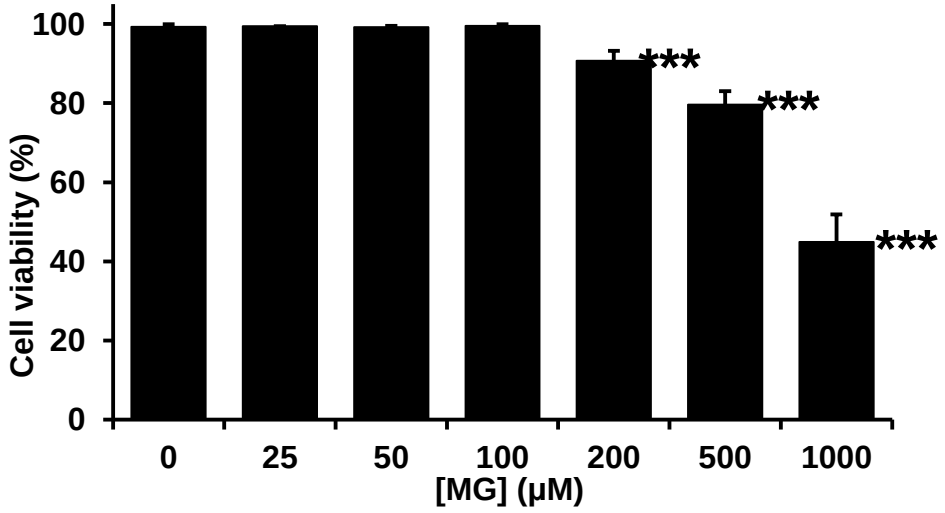

Figure 49: The MG concentration – cell viability response for hPDLFs *in vitro*.
Data are mean ± SD (n = 3). Significant: ***, P<0.001; (*t-test).*

3.2.10 Effect of 200 µM methylglyoxal on the growth and viability of human periodontal ligament fibroblasts in low and high glucose concentration *in vitro*

Primary hPDLFs were seeded in 6-well plate and incubated with 8 mM glucose, 8 mM glucose + 200 µM MG and 25 mM glucose + 200 µM MG. Viable and non-viable cells were counted every day for 4 days. Addition of MG decreased cell growth and viability to similar extent in both low and high glucose conditions - Figure 50 and 51.

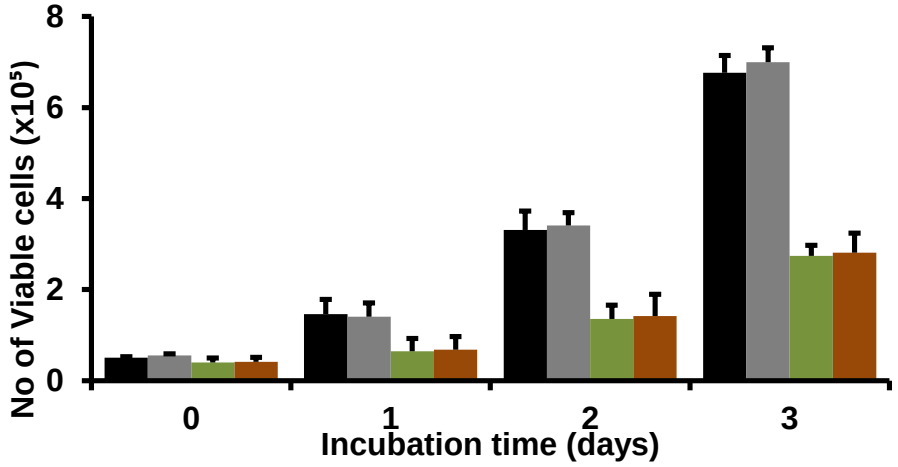

Figure 50: Effect of 200 µM methylglyoxal on growth and viability of hPDLFs in low and high glucose conditions *in vitro*.
Primary hPDLFs were seeded at a density of 5000 cells per cm². Key: , 8 mM glucose; , 25 mM glucose; , 8 mM glucose + 200 µM MG; and , 25 mM glucose + 200 µM MG. Data are mean ± SD (n = 3).

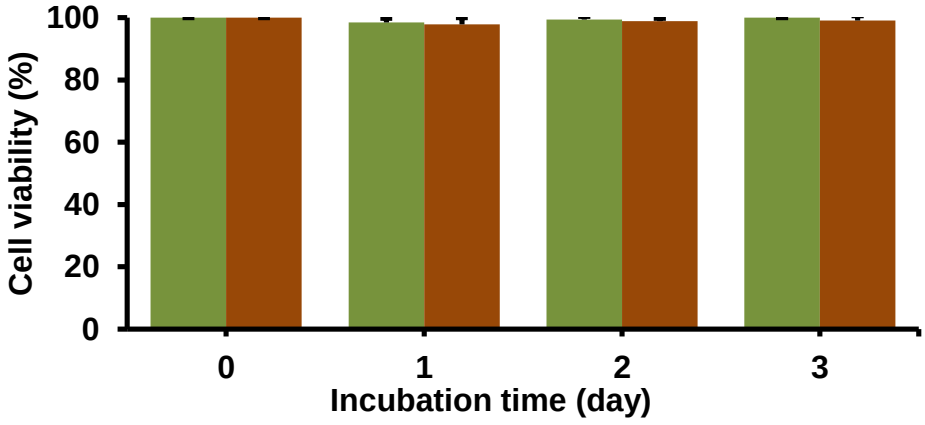

Figure 51: Effect of 200 µM methylglyoxal on cell viability for hPDLFs *in vitro*.
Key: , 8 mM glucose + 200 µM MG; and , 25 mM glucose + 200 µM MG. Data are mean ± SD (n = 3).

3.3 Effect of glyoxalase 1 inducers on the glyoxalase system and MG metabolism in hPDLFs *in vitro* in low and high glucose concentrations

The host research team identified tRSV as an inducer of Glo1. A stable transfectant luciferase reporter cell line with transcriptional regulatory elements was developed from human HepG2 cells, as described for quinone reductase ARE (NQO1-ARE) (Xue et al., 2015a), incorporating regulatory elements: GLO1-ARE or functionally inactive mutant as negative control - ARE-1 and ARE1m in previous work (Xue et al., 2012a). Nrf2-dependent transcriptional response was verified by siRNA silencing of Nrf2. After screening of *ca.* 100 dietary bioactive compounds with Nrf2 activator activity, the highest E_{max} was produced by tRSV. In corroboration of this, Cheng *et al*. reported that 10 µM tRSV induced increased Glo1 protein in HepG2 cells *in vitro* (Cheng et al., 2012). The lowest EC_{50} for GLO1-ARE transcriptional activity was found with HSP. For tRSV, EC_{50} = 2.52 ± 0.19 µM and E_{max} 100 ± 2%; and for HSP, EC_{50} = 0.59 ± 0.01 µM and E_{max} 24.4 ± 0.1%. In previous clinical studies, dietary supplementation of 150 mg HSP achieved a peak plasma concentration of 6.7 µM (Takumi et al., 2012), suggesting that HSP may be a competent Glo1 inducer for clinical use but with low maximal effect; and dietary supplementation of 500 mg tRSV achieved a peak plasma concentration of *ca.* 0.3 µM (Takumi et al., 2012), 8-fold lower than the EC_{50} for GLO1-ARE response. To enhance efficacy we studied the pharmacological synergism of tRSV and HSP together. Study of the GLO1-ARE transcriptional response of 5 µM HSP with 0.625 – 10 µM tRSV showed that HSP combined synergistically with tRSV, decreasing the EC_{50} of tRSV *ca.* 2-fold to 1.46 ± 0.10 µM whilst maintaining the E_{max} – Figure 52C). The predicted increase of GLO1-ARE transcriptional response from concentration response curves of 0.1 – 1.0 tRSV in the presence of 5 µM HSP was 3 – 79 fold, including up to 80% increase over additive effects - Figure 52D. This suggests marked benefits may accrue from use of tRSV+HSP co-formulation.

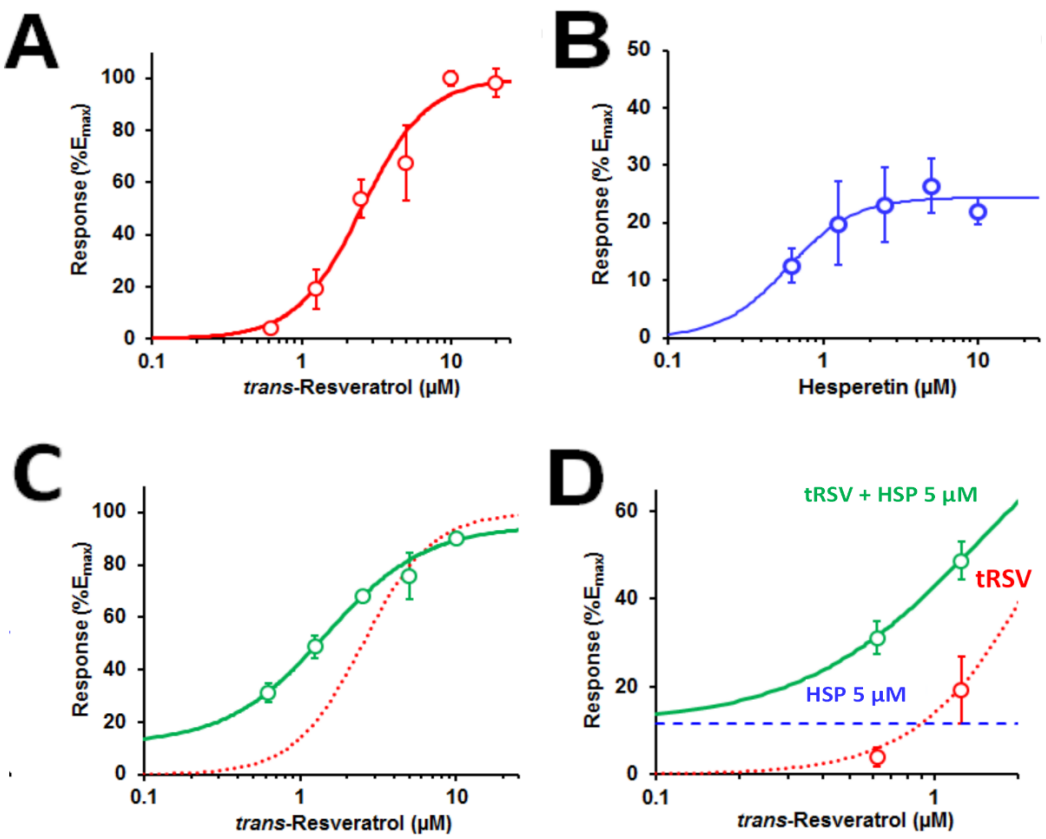

Figure 52. Induction of glyoxalase 1 expression by *trans*-resveratrol and hesperetin.

GLO1-ARE transcriptional response reporter assay. Data of normalised responses for varied bioactive concentrations were fitted by non-linear regression to the equation $E = E_{max} \times [Bioactive]^n/(EC_{50}^n + [Bioactive]^n)$, solving for E_{max}, EC_{50} and n (Hill coefficient). A: Concentration-response curve for tRSV. Data are mean ± SD (n = 3) for 5 concentrations. Non-linear regression (red curve): $E (\%) = 100 \times [tRSV]^{3.92}/(2.52^{3.92} + [tRSV]^{3.92})$. B: Concentration-response curve for HSP. Data are mean ± SD (n = 3 - 8) for 6 concentrations. Non-linear regression (blue curve): $E (\%) = 24.4 \times [HSP]^{2.01}/(0.59^{2.01} + [HSP]^{2.01})$. C: Concentration-response curve for tRSV in the presence of 5.0 μM HSP. Data are mean ± SD (n = 3 - 6) for 5 concentrations. Non-linear regression (red curve): $E (\%) = (83.4 \times [tRSV]^{1.36}/(1.46^{1.36} + [tRSV]^{1.36})) + 11.6$; green curve – tRSV+ 5.0 μM HSP, red dotted curve – tRSV only (as for A:).

One of the objectives of this project is to evaluate effect of Glo1 inducers on the glyoxalase system and MG metabolism in hPDLFs cultured in low and high glucose concentrations *in vitro*. To achieve this objective, hPDLFs were cultured in low glucose concentration (8 mM glucose) and high glucose concentration (25 mM glucose) with and without 10 µM tRSV, HSP and 10 µM tRSV and HSP in combination with (tRSV+HSP). Cells were incubated for three days.

3.3.1 The viability of hPDLFs grown in media containing 8 mM and 25 mM glucose with Glo1 inducers *in vitro*

Primary hPDLFs (5000 cells/cm^2) were seeded in 6 well plates and incubated for 3 days in MEM medium containing 8 mM glucose or 25 mM glucose with and without 10 µM Glo1 inducer for 3 days and the viable cell number was counted in all the study groups. The viable cell number increased throughout the culture period and show a steady increase in all the groups with no significant change in the viability under any condition – Figure 53. The cell viability was $0.813 \pm 0.133 \times 10^6$ in control cultures and was unchanged with treatments.

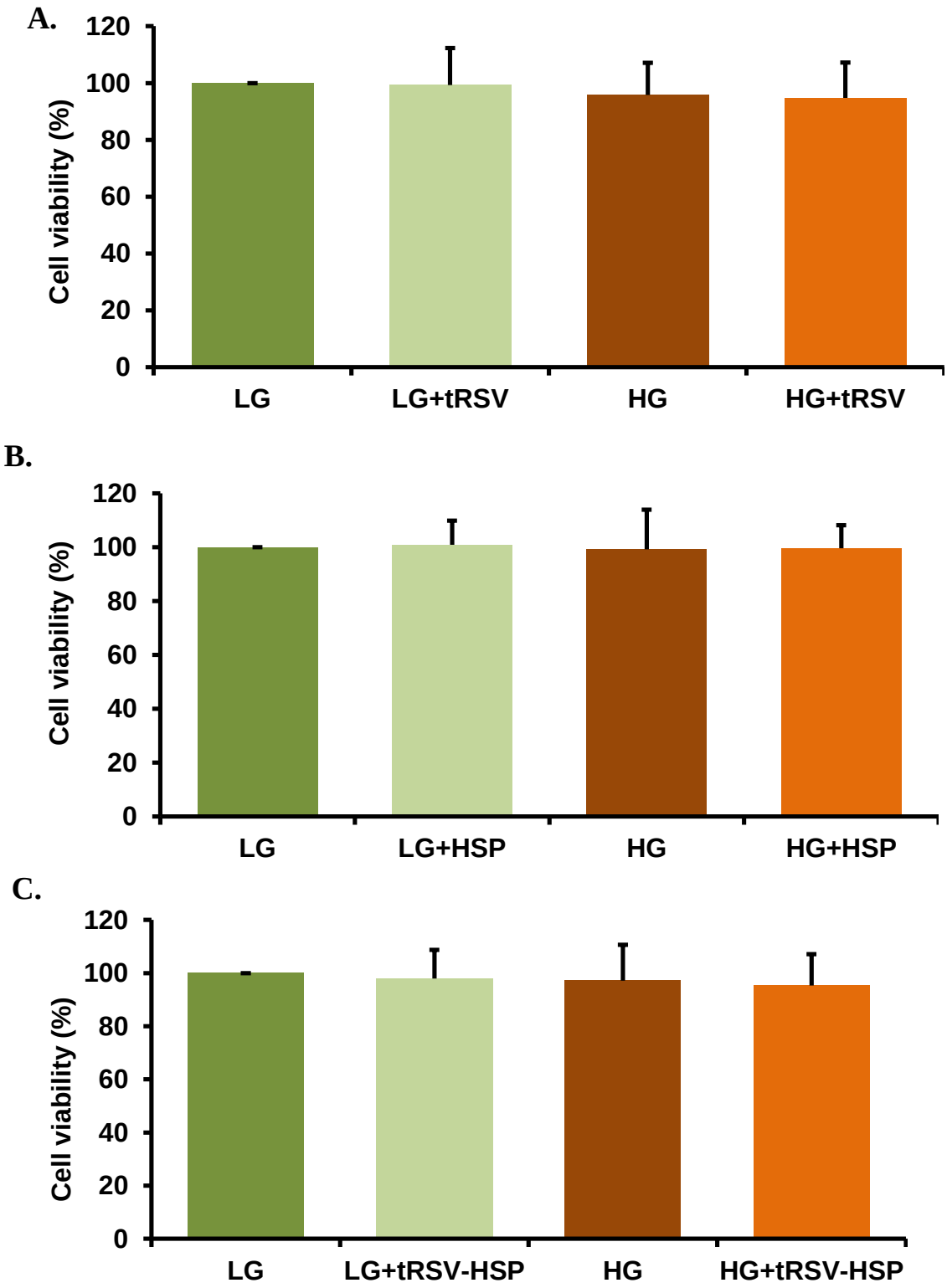

Figure 53: The viability of hPDLFs grown in media containing 8 mM glucose and 25 mM glucose with and without Glo1 inducers *in vitro*.
hPDLFs cells were cultured in 8 mM glucose and 25 mM glucose-containing medium for 3 days with or without: (A) tRSV (10 µM); (B) HSP (10 µM); and (C) tRSV+HSP (10 µM)**.** Data are mean ± SD, n = 3.

3.3.2 Effect of Glo1 inducers on the enzymatic activities of glyoxalase system in hPDLFs cells *in vitro*

3.3.2.1 Effect of Glo1 inducers on the activity of glyoxalase 1 in hPDLFs cells *in vitro*

Primary hPDLFs cells were cultured in low and high glucose concentrations for 3 days with and without 10 µM tRSV, 10 µM HSP and 10 µM tRSV+HSP. Incubation of hPDLFs with Glo1 inducers in LG conditions produced different effects: incubation with tRSV did not increase Glo1 activity significantly where incubation with HSP increased the activity of Glo1 *ca.* 22% ($P<0.05$) and incubation with tRSV+HSP increased the activity of Glo1 *ca.* 20% ($P<0.05$). When hPDLFs were incubated in HG culture conditions, the activity of Glo1 was decreased by *ca.* 43% ($P<0.001$), compared to LG controls. This decrease in activity of Glo1 was prevented by incubation with tRSV, HSP and with tRSV+HSP combined ($P'<0.001$ with respect to HG control). With tRSV+HSP combined treatment under HG conditions, there was a 15% increase in activity above LG control value which approached significance ($P = 0.061$, *t-test*). This suggests that Glo1 inducers may increase Glo1 activity in normal glycaemic conditions and prevent a deficit of Glo1 activity in model hyperglycaemia - Figure 54 and Table 29.

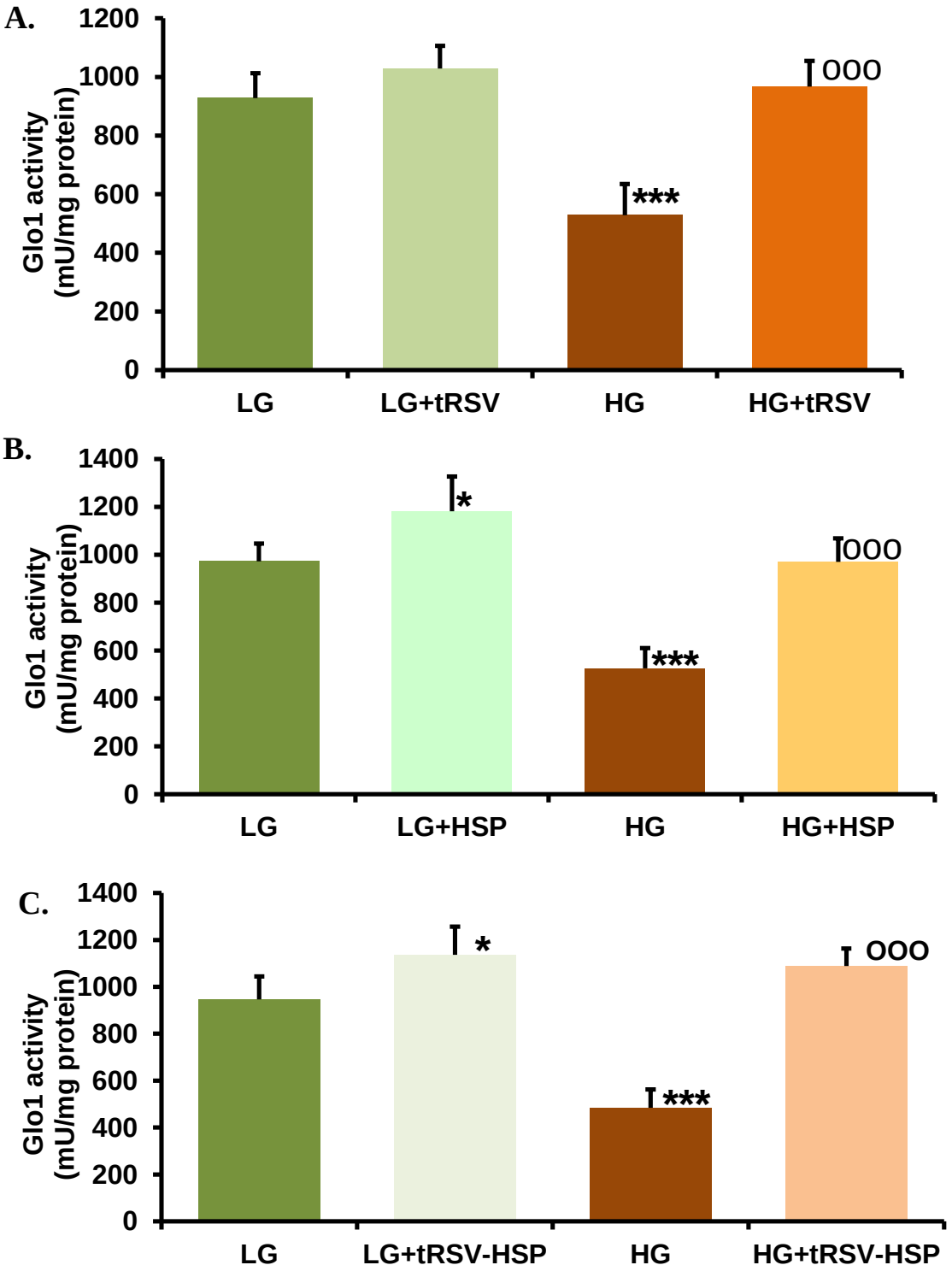

Figure 54: Effect of Glo1 inducers on enzymatic activity in hPDLFs grown in media containing 8mM and 25mM glucose *in vitro*.
Panels A, B and C show Glo1 activity in hPDLFs cells incubated for 3 days with 10 µM tRSV, 10 µM HSP and 10 µM tRSV+HSP, respectively. Data are mean ± SD, n = 4. Significance: *, P<0.05 and ***, P<0.001 *(t-test)* with respect to low glucose control; and ^{ooo}, P<0.001 *(t-test)* with respect to high glucose control.

Table 29: Effect of Glo1 1 inducers on Glo1 activity in hPDLFs *in vitro*

Glo1 activity (mU/mg protein)	LG	LG + Glo1 inducer	HG	HG+ Glo1 inducer
10 µM tRSV	928 ± 84	1028 ± 78	529 ± 106**	967 ± 88 ᵒᵒᵒ
10 µM HSP	972 ± 74	1181 ± 146*	526 ± 84.5***	971 ± 99 ᵒᵒᵒ
10 µM tRSV+HSP	946 ± 99	1137 ± 120*	485 ± 77.6***	1089 ± 75 ᵒᵒᵒ

Data are mean ± SD, n = 4. Significance: *, ** and ***, P<0.05, P<0.01 and P<0.001 *(t-test)* with respect to low glucose control; ᵒᵒᵒ, P<0.001 *(t-test)* with respect to high glucose control.

3.3.2.2 Effect of Glo1 inducers on glyoxalase 1 protein content of hPDLFs *in vitro*

Primary hPDLFs cells were cultured in 8 mM and 25 mM glucose for 3 days with and without 10 µM tRSV, 10 µM HSP and 10 µM tRSV+HSP combined. Glo1 protein content of cell protein was assessed by immunoblotting. In LG conditions, there was no significant increase in Glo1 protein with Glo1 inducers. Data dispersion in the estimate of Glo1 protein of LG control cultures (coefficient of variation 13%, n = 3) indicated a change of *ca.* 29% is just detectable at the 5% significance level. In HG conditions, there was a decrease in Glo1 protein of 30% (P<0.05). tRSV, HSP and tRSV+HSP combined prevented the decrease in Glo1 protein (+tRSV, P<0.047; + HSP, P<0.041; tRSV+HSP, P'<0.012 with respect to HG control) – Figure 55.

3.3.2.3 Effect of *trans*-resveratrol on glyoxalase 1 expression in hPDLFs cells *in vitro*

Cells were treated with *trans*-resveratrol (10 µM) for 3 days in low and high glucose. Glo1 gene expression was quantified in all four study groups by RT-PCR and normalized to β-actin mRNA. The levels of Glo1 mRNA did not change as before and tRSV has no affect either. Normalized GLO1 mRNA to β-actin mRNA level was: low glucose control, 0.771 ± 0.007, high glucose control 0.768 ± 0.005, low glucose with tRSV, 0.786 ± 0.007 and high glucose with tRSV 0.773 ± 0.018.

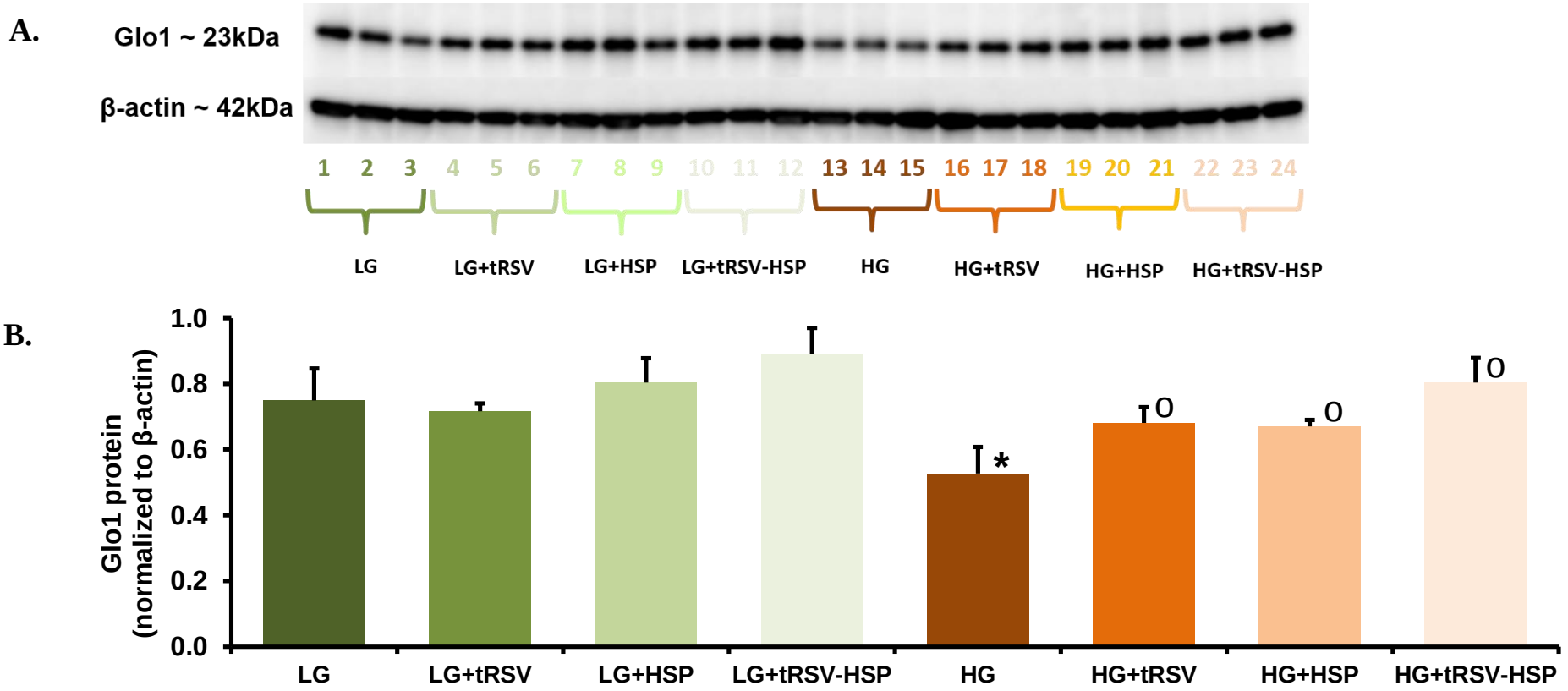

Figure 55: Effect of Glo1 inducers on Glo1 protein content of hPDLFs *in vitro*.
(A) Glo1 protein blot, (B) Glo1 protein blot interpretation. hPDLFs cells were cultured in 8 mM glucose medium (LG) and 8 mM glucose medium with 10 µM tRSV (LG+tRSV), 10 µM HSP (LG+HSP) and 10 µM tRSV and HSP (LG+tRSV-HSP), and 25 mM glucose medium (HG) and 25 mM glucose medium with 10 µM tRSV (HG+tRSV), 10 µM HSP (HG+HSP) and 10 µM tRSV and HSP (HG+tRSV-HSP) for 3 days. Data are mean ± SD, n = 3. Significance: *, P<0.05 *(t-test)* with respect to low glucose control; ^{o}, P<0.05 *(t-test)* with respect to high glucose control.

3.3.3 The effect of *trans*-resveratrol on the half-life of Glo1 protein *in vitro*

A possible explanation for the prevention of decrease in Glo1 activity and protein without change in Glo1 expression by tRSV in hPDLFs incubated in high glucose concentration is an effect on Glo1 stability. To test this I planned a conventional experiment to measure the half-life of Glo1 protein in hPDLFs with high glucose concentration cultures with and without tRSV. This uses cycloheximide to block protein synthesis and then quantify the rate of decrease in Glo1 protein.

3.3.3.1 Time course curve for hPDLFs treated with cycloheximide *in vitro*

In preparation for the Glo1 protein half-life study, the effect of cycloheximide on hPDLFs growth and viability was assessed. hPDLFs were cultured in MEM in low glucose concentration. After 24 hours, new MEM medium was added to each well with 10 µM cycloheximide (CHX) for 2 days. Addition of CHX induced growth arrest and toxicity in hPDLFs: viable cell number decreased by 48% at day 1 and 75% at day 2, compared to the control - Figure 56.

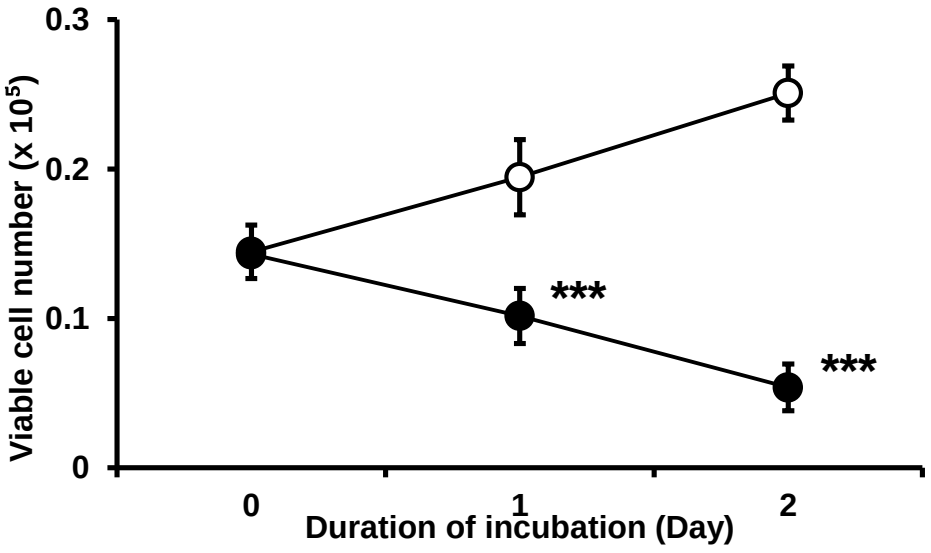

Figure 56: Effect of cycloheximide on the growth and viability of hPDLFs *in vitro*.
Data are mean ± SD (n = 3). Key: ○-○, control; ●-●, + 10 µM cycloheximide.

3.3.3.2 Effect of cycloheximide on glyoxalase 1 protein expression in the presence of *trans*-resveratrol in hPDLFs *in vitro*

Primary hPDLFs cells were cultured in MEM in low and high glucose concentration. After 24 h, the medium was replaced with the fresh medium supplemented with CHX (10 µM) with and without tRSV (10 µM) and incubated for 2 days. Immunoblotting was performed as described in the method section. Glo1 protein band intensity was decreased with addition of CHX in low and high glucose treated cells however, it was stabilised by tRSV treatment - Figure 57A. The intensity value of each sample of each treatment group was fitted to first-order exponential decay - Figure 57B and Table 30. The rates of Glo1 protein degradation and half-life indicated that high glucose concentration de-stabilised Glo1 protein and tRSV corrected this.

Table 30: the effect of tRSV on the half-life of Glo1 protein in hPDLFs *in vitro*.

	8mM (CHX, 10 µM)	**25mM (CHX, 10 µM)**	**25mM (CHX 10µM, tRSV 10 µM)**
k_{Deg} (Day^{-1})	0.302 ± 0.048	0.531 ± 0.059	0.188 ± 0.047
$T_{1/2}$ (days)	2.30	1.31	3.66

Data are mean ± SD, n = 3

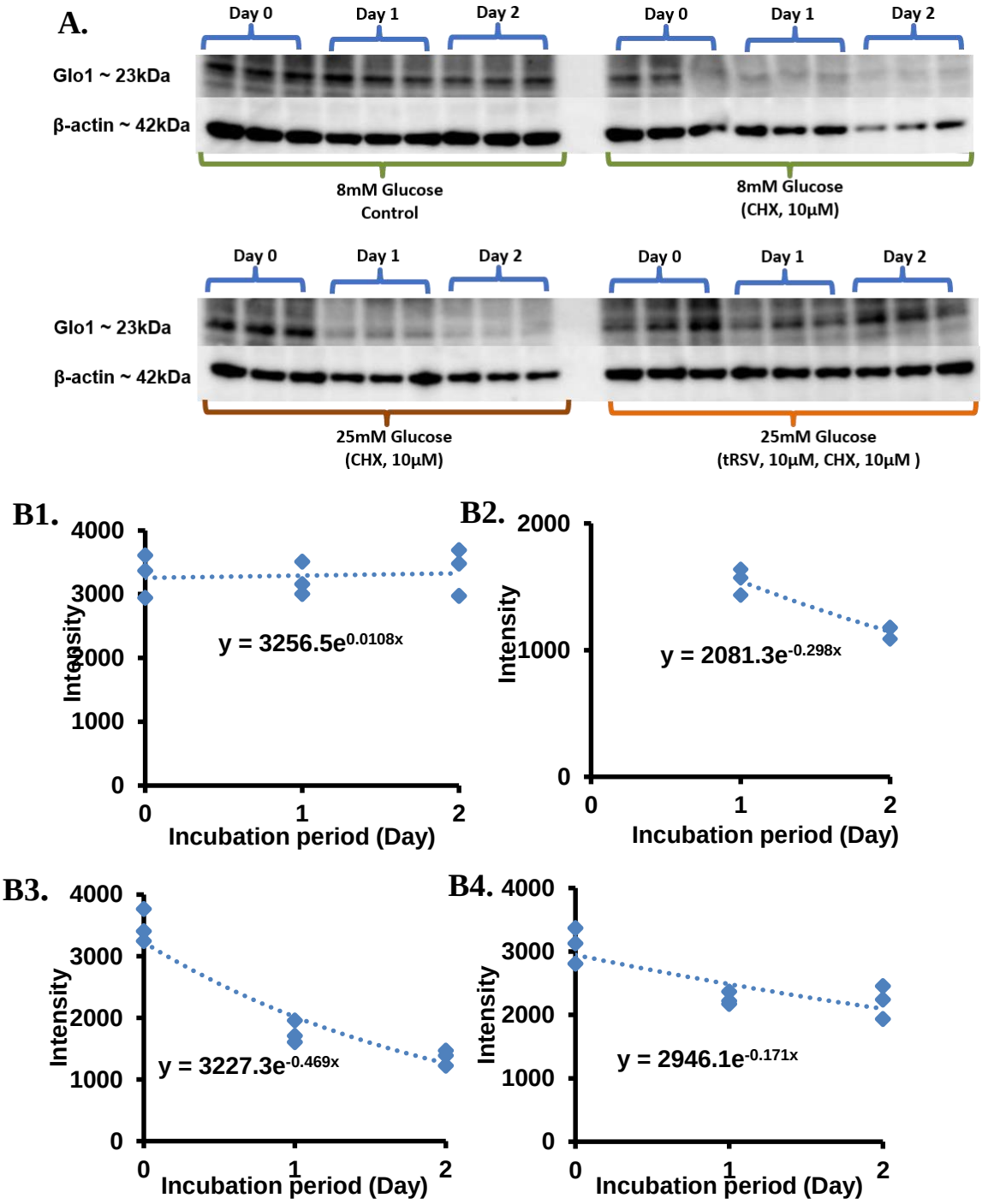

Figure 57: Time course of Glo1 protein intensity.
(A) Protein expression, (B1) 8 mM glucose control, (B2) 8 mM glucose + CHX, (B3) 25 mM glucose + CHX and (B4) 25 mM glucose + tRSV + CHX.

3.3.4 Effect *trans*-resveratrol on other enzymatic activity related to dicarbonyl metabolism in hPDLFs cells *in vitro*

The effects of the Glo1 inducer, tRSV, on other enzymatic activities related to dicarbonyl metabolism in hPDLFs cells was studied. The activity of the second enzyme of the glyoxalase pathway, Glo2, was not affected by tRSV.

Metabolism by MG reductase and MG dehydrogenase are alternative fates to the glyoxalase pathway for MG metabolism. There was low activity of MG reductase in hPDLFs which was not changed by tRSV or in HG conditions. The activity of MG dehydrogenase was below the limit of detection. The glyoxalase pathway is, therefore, likely the major pathway for MG metabolism in hPDLFs – Table 31.

Table 31: Values of different enzymatic activities of the glyoxalase system performed on hPDLFs cells incubated in media contains high and low glucose with Glo1 inducers *in vitro*

Analyte	LG	LG + tRSV	HG	HG + tRSV
Glo1 activity (mU/mg protein)	928 ± 84	1028 ± 78	529 ± 106**	967 ± 88 ^{ooo}
Glo2 activity (mU/mg protein)	4.63 ± 0.67	4.03 ± 0.99	4.64 ± 0.99	3.36 ± 1.21
MG reductase (mU/mg protein)	0.09 ± 0.02	0.07 ± 0.02	0.08 ± 0.01	0.06 ± 0.03
MG dehydrogenase (mU/mg protein)	<LOD	<LOD	<LOD	<LOD

Data are mean ± SD, n = 4. Significance: **, P<0.01 respect to low glucose control (8 mM glucose) *(t-test)*. ^{ooo}, P<0.001 *(t-test)* with respect to high glucose control (8 mM glucose). LOD for MG dehydrogenase was 0.0005 mU/mg protein.

3.3.5 Effect of Glo1 inducers on flux of formation of D-lactate and L-lactate in hPDLFs cells *in vitro*

Primary hPDLFs cells were cultured in 8 mM glucose and 25 mM glucose for 3 days with and without 10 µM tRSV, 10 µM HSP and 10 µM tRSV+HSP. The flux of formation of D-lactate was increased significantly in hPDLFs cells in high glucose without tRSV by 41% (P<0.01) and also in high glucose with tRSV by 40% (P<0.01) – Figure 58 and Table 32. However in the presence of HSP, the flux of D-lactate formation in low glucose concentration was decreased 13% (P<0.05); and in high glucose concentration cultures, the flux of D-lactate

formation was increased by + 53% (P<0.01) with respect to low glucose control in the absence of HSP and this increase was lowered to + 22% in the presence of HSP (P<0.01 with respect to low glucose control; P'<0.05 with respect to high glucose control) – Figure 58 and Table 32. These effects were sustained in low glucose and further enhanced in high glucose with tRSV+HSP combined supplementation. The flux of D-lactate formation in low glucose concentration was decreased 12% (P<0.05); and in high glucose concentration cultures, the flux of D-lactate formation was increased by + 44% (P<0.001) with respect to low glucose control in the absence of tRSV+HSP combined supplementation and this increase was prevented in the presence of tRSV+HSP combined supplementation (P'<0.001 with respect to high glucose control) – Figure 58 and Table 32. The formation of L-lactate did not change in high glucose compare to low glucose cultures and the treatment with Glo1 inducers had no effect on the formation of L-lactate - Table 33.

Table 32: Effect of Glo1 inducers on formation of D-lactate in hPDLFs cells *in vitro*

D-Lactate production (nmol/day/10^6 cells) in culture medium				
	LG	**LG + Glo1 inducer**	**HG**	**HG + Glo1 inducer**
10 µM tRSV	7.00 ± 0.36	6.82 ± 0.63	9.90 ± 1.08**	9.78 ± 0.78**
10 µM HSP	6.57 ± 0.54	5.72 ± 0.31*	10.1 ± 1.03***	7.99 ± 0.59$^{**, o}$
10 µM tRSV+HSP	6.79 ± 0.47	5.99 ± 0.39*	9.74 ± 0.42***	6.91 ± 0.69 ^{ooo}

Data are mean ± SD, n = 4. Significance: *, **, and ***, P<0.05, P<0.01 and P<0.001, respectively, compared to low glucose control; ^{o} and ^{ooo}, P<0.05 and P<0.001, respectively, compared to high glucose control *(t-test)*.

Table 33: Effect of Glo1 inducers on L-lactate concentration in hPDLFs cells *in vitro*

L-Lactate production (nmol/day/10^6 cells) in culture medium				
	LG	**LG + Glo1 inducer**	**HG**	**HG + Glo1 inducer**
10 µM tRSV	276 ± 34	275 ± 54	252 ± 17	248 ± 33
10 µM HSP	277 ± 28	302 ± 33	256 ± 26	252 ± 41
10 µM tRSV+HSP	277 ± 28	243 ± 33	256 ± 26	234 ± 33

Data are mean ± SD, n = 4.

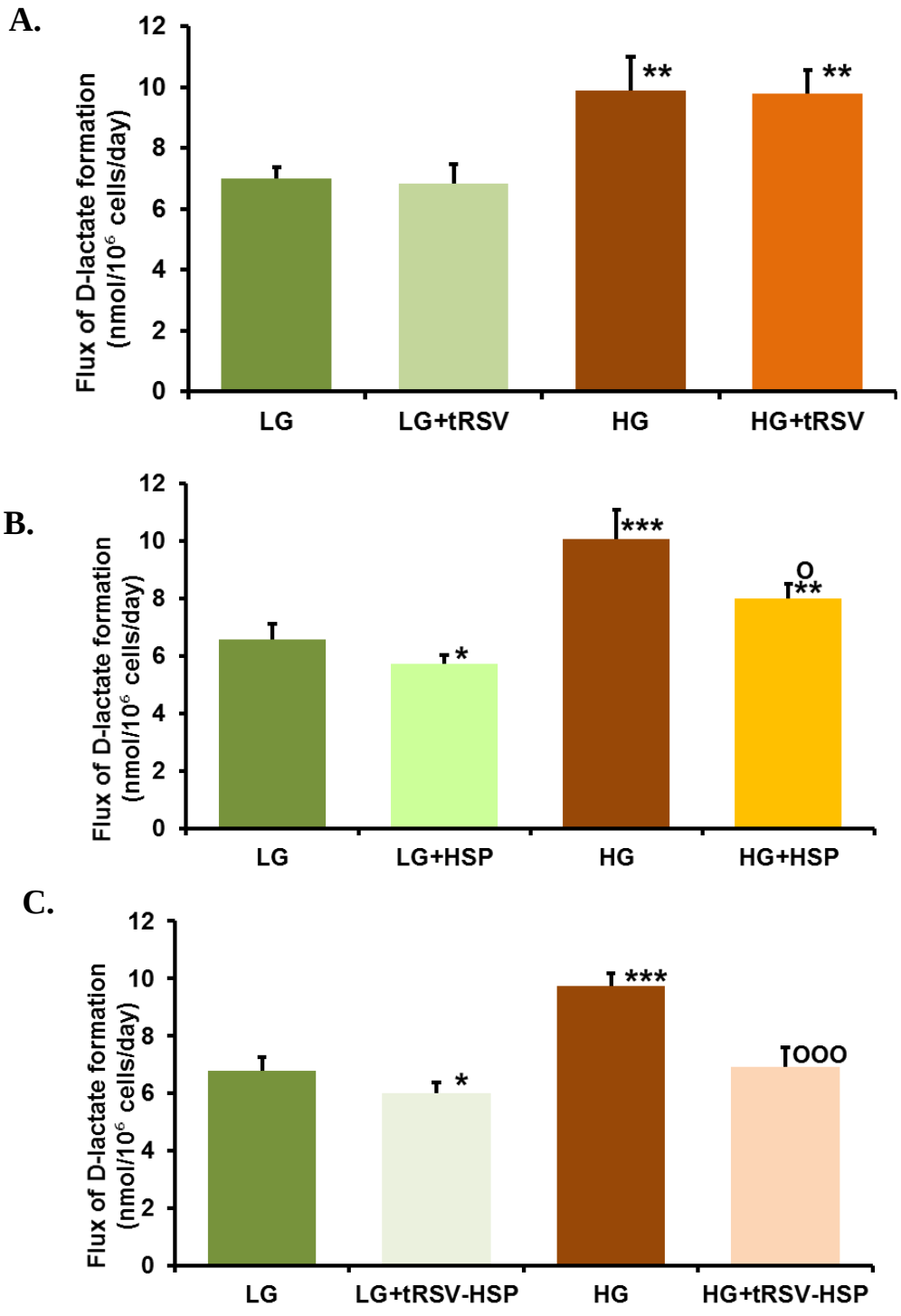

Figure 58: Effect of Glo1 inducers on flux of formation of D-lactate in hPDLFs cells *in vitro*.

hPDLFs cells were cultured in 8 mM glucose (LG) and 25 mM glucose (HG) medium with or without: (A) 10 µM tRSV, (B) 10 µM HSP and (C) 10 µM tRSV+HSP for 3 days. Data are mean ± SD, n = 4. Significance: *, **, and ***, P<0.05, P<0.01 and ***, P<0.001, respectively, compared to low glucose control; ^{o} and ^{ooo}, P<0.05 and P<0.001, respectively, compared to high glucose control *(t-test)*.

3.3.6 Effect of Glo1 inducers on consumption of D-glucose by hPDLFs cells *in vitro*

Glucose consumption was measured in hPDLFs cultures. Cells were cultured as before in low and high glucose with and without the Glo1 inducers (10 µM tRSV, HSP and tRV+HSP combined). In experiments with tRSV supplementation, in low glucose cultures addition of 10 µM tRSV did not change glucose consumption. In high glucose cultures, glucose consumption was increased 95% with respect to low glucose control (P<0.001) and this was not changed by tRSV (P<0.001 with respect to low glucose control) – Figure 59 and Table 34. In experiments with HSP supplementation, in low glucose cultures, 10 µM HSP decreased glucose consumption by 20% (P<0.05). In high glucose cultures, glucose consumption was increased 89% with respect to low glucose control (P<0.01) and this was lowered to an increase 56% with HSP (P<0.01 with respect to low glucose control; P'<0.05 with respect to high glucose control) – Figure 59 and Table 34. In experiments with tRSV+HSP combined supplementation, in low glucose cultures, 10 µM tRSV+HSP combined decreased glucose consumption by 24% (P<0.05). In high glucose cultures, glucose consumption was increased 80% with respect to low glucose control (P<0.01) and this was corrected by tRSV+HSP combined supplementation – Figure 59 and Table 34.

Table 34: Effect of Glo1 inducers on D-glucose consumption in hPDLFs cells *in vitro*

D-Glucose Consumption (µmol/day/10^6 cells) in culture medium				
	LG	**LG + Glo1 inducer**	**HG**	**HG + Glo1 inducer**
10 µM tRSV	5.16 ± 0.39	4.90 ± 0.31	10.1 ± 0.37***	9.29±0.77***
10 µM HSP	5.83 ± 0.58	4.67 ± 0.27*	11.0 ± 0.86**	9.12±0.68**,o
10 µM tRSV+HSP	5.92 ± 0.71	4.49 ± 0.49*	10.7 ± 1.14**	7.53 ± 1.10 o

Data are mean ± SD, n = 4. Significance: *, ** and ***, P<0.05, P<0.01 and P<0.001, respectively, compared to low glucose control; o, P<0.05 with respect to high glucose control *(t-test).*

The flux of D-lactate formation as percentage of glucotriose was also calculated as described previously. This was decreased 16 – 30% in high glucose cultures, compared to low glucose control. Glo1 inducers did not change this derived compound variable - Table 35.

Table 35: Effect of Glo1 inducers on D-lactate flux in hPDLFs cells *in vitro*

D-lactate flux (% glucotriose)				
	LG	**LG + Glo1 inducer**	**HG**	**HG + Glo1 inducer**
10 µM tRSV	0.068 ± 0.006	0.070 ± 0.010	0.048 ± 0.006**	0.053 ± 0.006*
10 µM HSP	0.057 ± 0.004	0.061 ± 0.002	0.048 ± 0.002*	0.044 ± 0.003**
10 µM tRSV+HSP	0.058 ± 0.007	0.067 ± 0.005	0.046 ± 0.002*	0.046 ± 0.008

Data are mean ± SD, n = 4. Significance: *, ** and ***, P<0.05, P<0.01 and P<0.001, respectively, compared to low glucose control *(t-test)*).

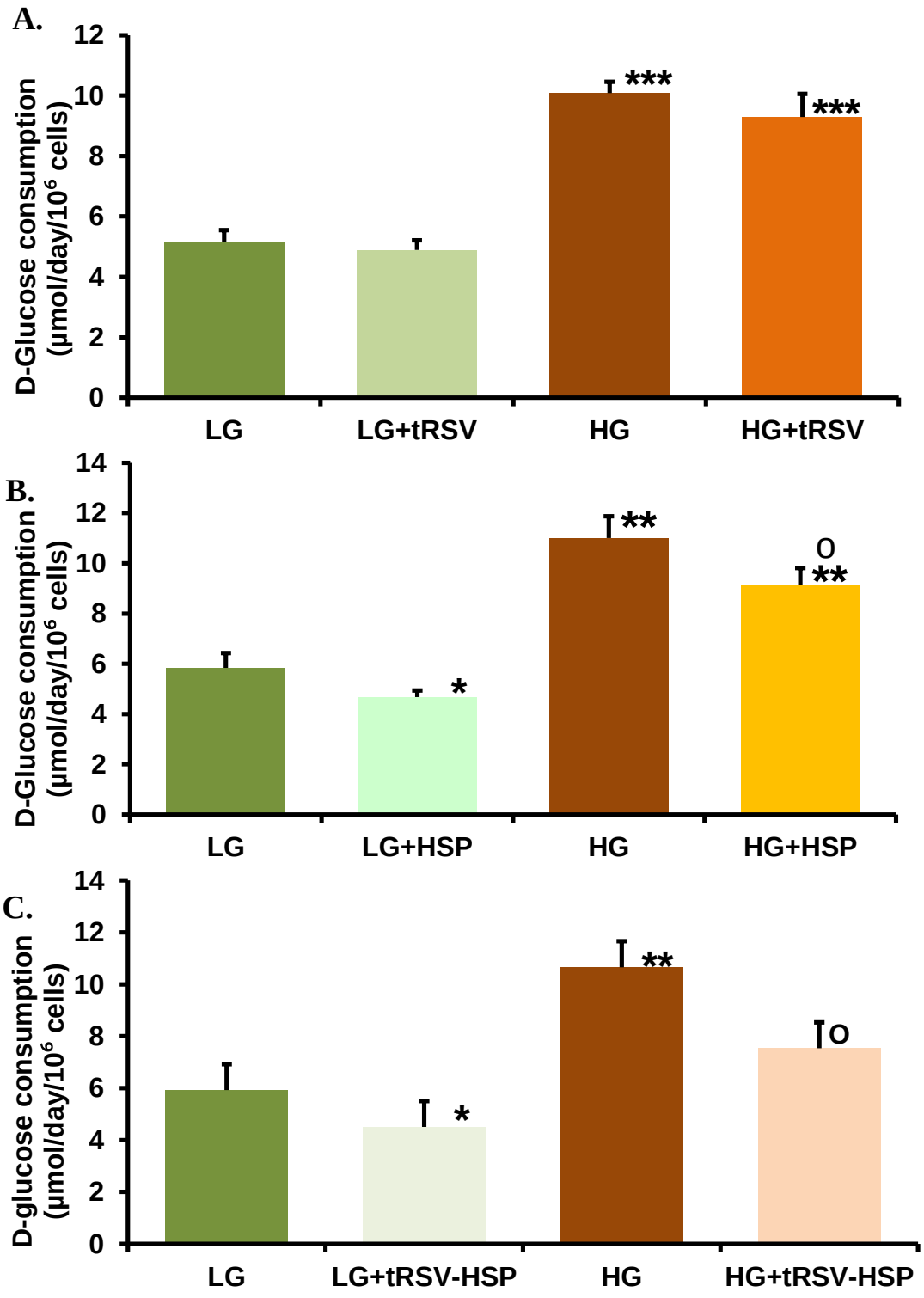

Figure 59: Effect of Glo1 inducers on consumption of D-glucose by hPDLFs cells *in vitro.*

hPDLFs cells were cultured in 8 mM glucose medium (LG) and 25 mM glucose medium (HG) for 3 days without or with: (A) 10 µM tRSV, (B) 10 µM HSP, and (C) 10 µM tRSV+HSP. Data are mean ± SD, n = 4. Significance: *, ** and ***, P<0.05, P<0.01 and P<0.001, respectively, compared to low glucose control; °, P<0.05 with respect to high glucose control *(t-test)*).

3.3.7 Effect of *trans*-resveratrol on the concentration of dicarbonyls in hPDLFs incubated in low and high glucose *in vitro*

Primary hPDLFs cells were incubated in either 8 mM glucose or 25 mM glucose with or without 10 μM tRSV for 3 days. Cellular and culture medium levels of dicarbonyls were evaluated by the LC-MS/MS.

The cellular content of MG was not changed by addition of tRSV in low glucose cultures. The cellular content of MG was increased by 160% in high glucose culture ($P<0.001$) and 100% in high glucose culture with tRSV ($P<0.05$), with respect to low glucose control. There was a trend for addition of tRSV to decrease cellular concentration of MG (-60%) but this did not reach significance ($P = 0.07$). The cellular content of glyoxal in low glucose culture was decreased 56% by addition of tRSV ($P<0.001$). The cellular content of glyoxal was not increased in high glucose culture and was decreased 57% by addition of tRSV ($P<0.001$, with respect to low glucose control; $P'<0.01$ with respect to high glucose control) – Figure 60. The cellular content of 3-DG in low glucose culture was not decreased by addition of tRSV. The cellular content of 3-DG was increased 82% in high glucose culture ($P<0.05$) and was unchanged by addition of tRSV – Table 36.

The concentration of MG in the culture medium was not changed by addition of tRSV in low glucose cultures. The concentration of MG in the culture medium was increased by 62% in high glucose culture ($P<0.05$), with respect to low glucose culture control, and was corrected by addition of tRSV ($P<0.05$ with respect to high glucose control. The concentration of glyoxal in the culture medium was decreased 42% by addition of tRSV in low glucose cultures ($P<0.05$). The concentration of glyoxal in the culture medium was not increased in high glucose culture, with respect to low glucose culture control, but was decreased 45% by addition of tRSV ($P<0.05$ with respect to low glucose control; $P<0.01$ with respect to high glucose control) - Figure 61. The concentration of 3-DG in the culture medium was not changed by addition of tRSV in low glucose cultures. The concentration of 3-DG in the culture medium was increased 110% in high glucose culture ($P<0.001$), with respect to low glucose culture control, and

was not decreased by addition of tRSV (P'<0.001 with respect to low glucose control) – Table 36.

Table 36: Effect of *trans*-resveratrol on dicarbonyls levels in human periodontal ligament fibroblasts and medium *in vitro*

		Methylglyoxal	Glyoxal	3-DG
		(pmol/10^6cells)	(pmol/10^6cells)	(pmol/10^6cell)
hPDLFs	**LG**	3.98 ± 1.00	7.79 ± 2.43	1.94 ± 0.70
	LG+tRSV	4.47 ± 0.95	2.31 ± 0.83 ***	1.41 ± 0.65
hPDLFs	**HG**	10.4 ± 0.6***	6.29 ± 0.93	3.53 ± 0.60*
	HG+tRSV	7.97 ± 2.10*	1.77 ± 0.92***,^{oo}	3.98 ± 1.08*
		(nM)	**(nM)**	**(nM)**
Medium	**LG**	276 ± 82	362 ± 46	313 ± 51
	LG+tRSV	269 ± 81	210 ± 58*	290 ± 72
Medium	**HG**	449 ± 38*	422 ± 78	658 ± 66***
	HG+tRSV	351 ± 36^{o}	234 ± 43^{oo}	723 ± 95***

Data are mean ± SD, n = 4. Significance: * and ***, P<0.05 and P<0.001, respectively, compared to low glucose control; ^{o} and ^{oo}, P<0.05 and P<0.01, respectively, compared to high glucose control (*t-test*).

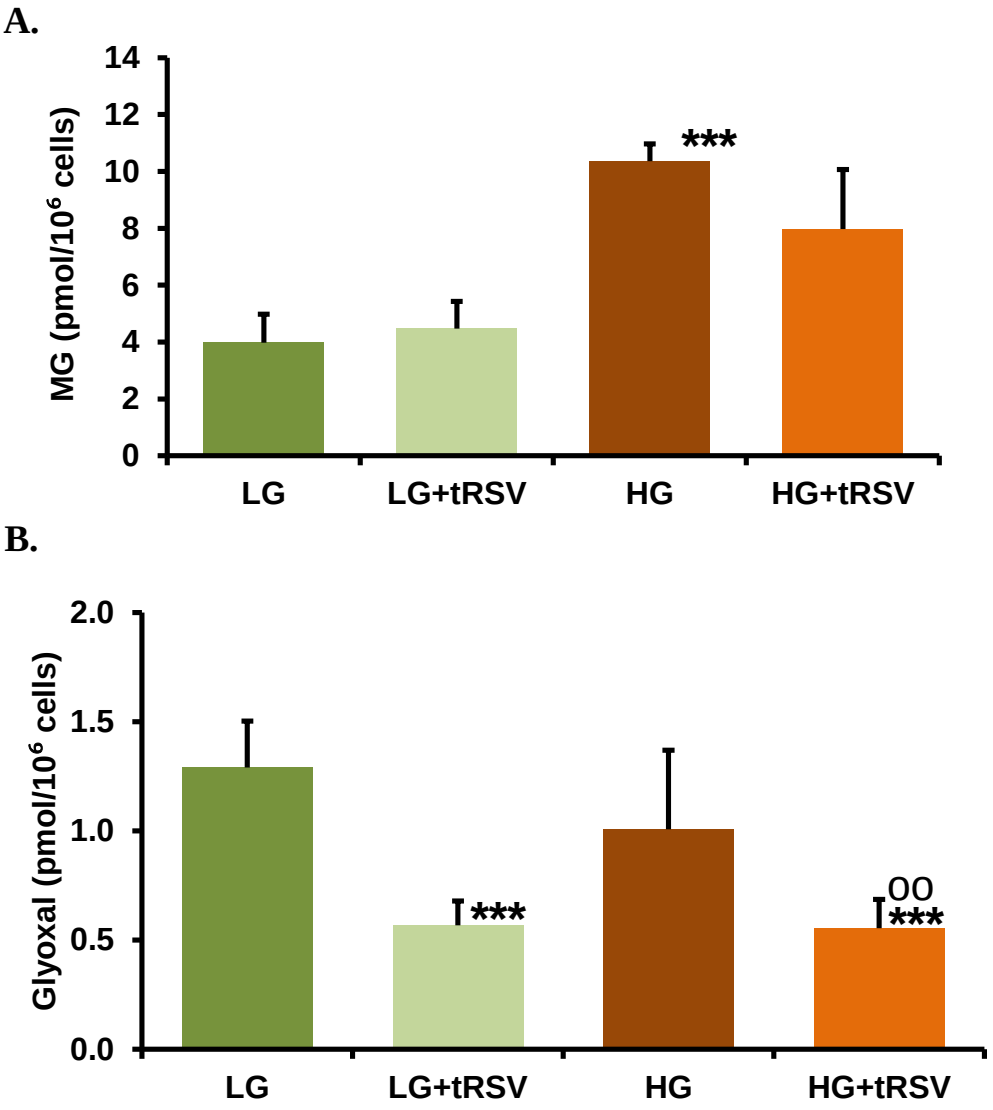

Figure 60: Effect of *trans*-resveratrol on cellular levels of dicarbonyls in hPDLFs cells *in vitro*.
hPDLFs cells were cultured in 8 mM and 25 mM glucose medium with or without tRSV (10 µM) for 3 days. (A) MG. (B) Glyoxal. Data are mean ± SD, n = 4. Significance: *, ** and ***, P<0.05, P<0.01 and P<0.001, respectively, compared low glucose control; ^{oo}, P<0.01 with respect to high glucose control *(t-test).*

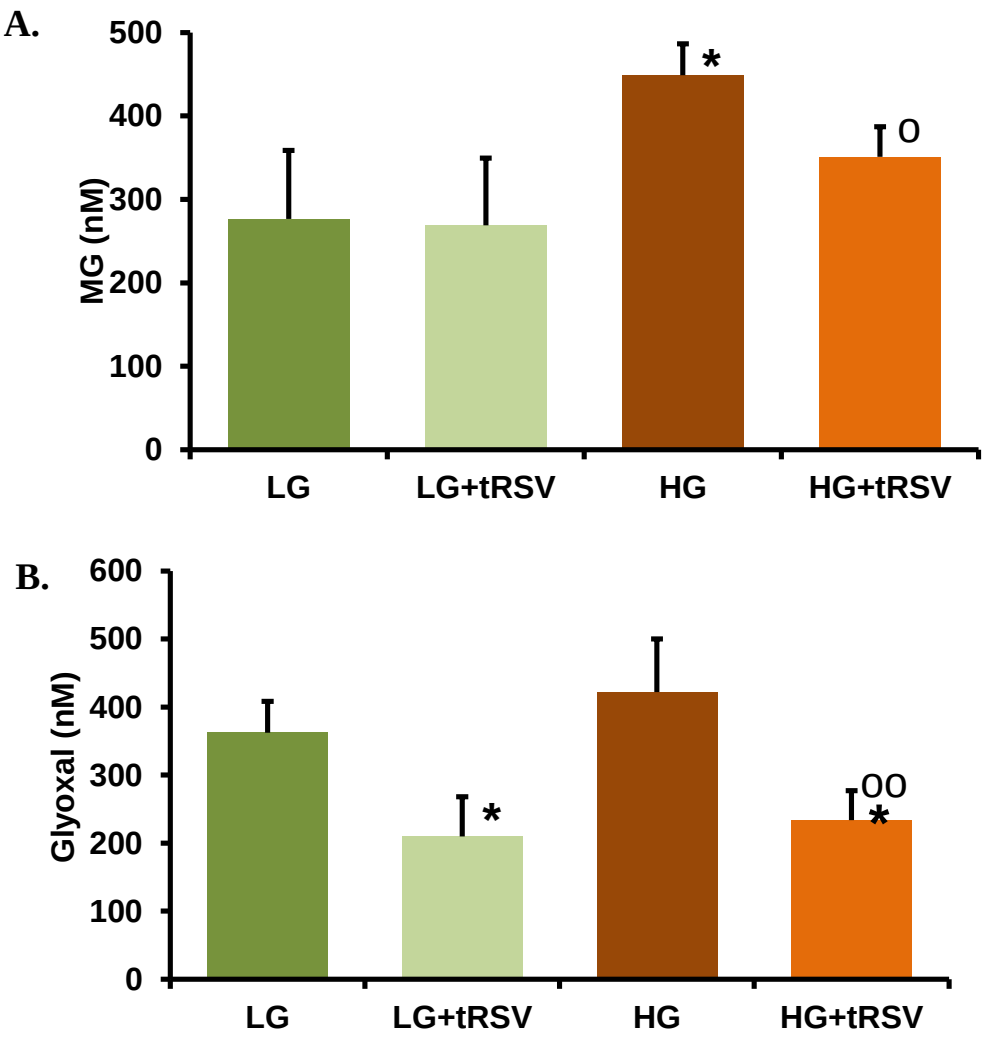

Figure 61: Effect of *trans*-resveratrol on levels of dicarbonyls in the medium of hPDLFs cells *in vitro*.
hPDLFs cells were cultured in 8 mM and 25 mM glucose medium with or without tRSV (10 µM) for 3 days. (A) MG. (B) Glyoxal. Data are mean ± SD, n = 4. Significance: *, P<0.05 compared low glucose control; ^{o} and ^{oo}, P<0.05 and P<0.01, respectively, compared to high glucose control *(t-test).*

3.3.8 Effect of hesperetin and *trans*-resveratrol and hesperetin combined on the concentration of dicarbonyls in hPDLFs incubated in low and high glucose with tRSV *in vitro*

In further experiments primary hPDLFs cells were incubated in either 8 mM glucose or 25 mM glucose with or without 10 µM HSP and 10 µM tRSV+HSP for 3 days. Cellular dicarbonyls were evaluated by the LC-MS/MS.

The cellular content of MG was not changed by addition of HSP and tRSV with HSP combined in low glucose cultures. The cellular content of MG was increased by 128% in high glucose culture ($P<0.001$), 78% in high glucose culture with HSP and corrected to low glucose control levels tRSV with HSP combined. The cellular content of glyoxal in low glucose culture was not changed by addition of HSP and tRSV with HSP combined. The cellular content of glyoxal was not increased in high glucose culture and was not changed by additions of HSP and tRSV with HSP combined – Figure 62 and Table 37. The cellular content of 3-DG in low glucose culture was not changed by addition of HSP and tRSV with HSP combined. The cellular content of 3-DG was increased 33% in high glucose culture ($P<0.05$) and this was corrected by addition of HSP and tRSV+HSP combined - Figure 62 and Table 37.

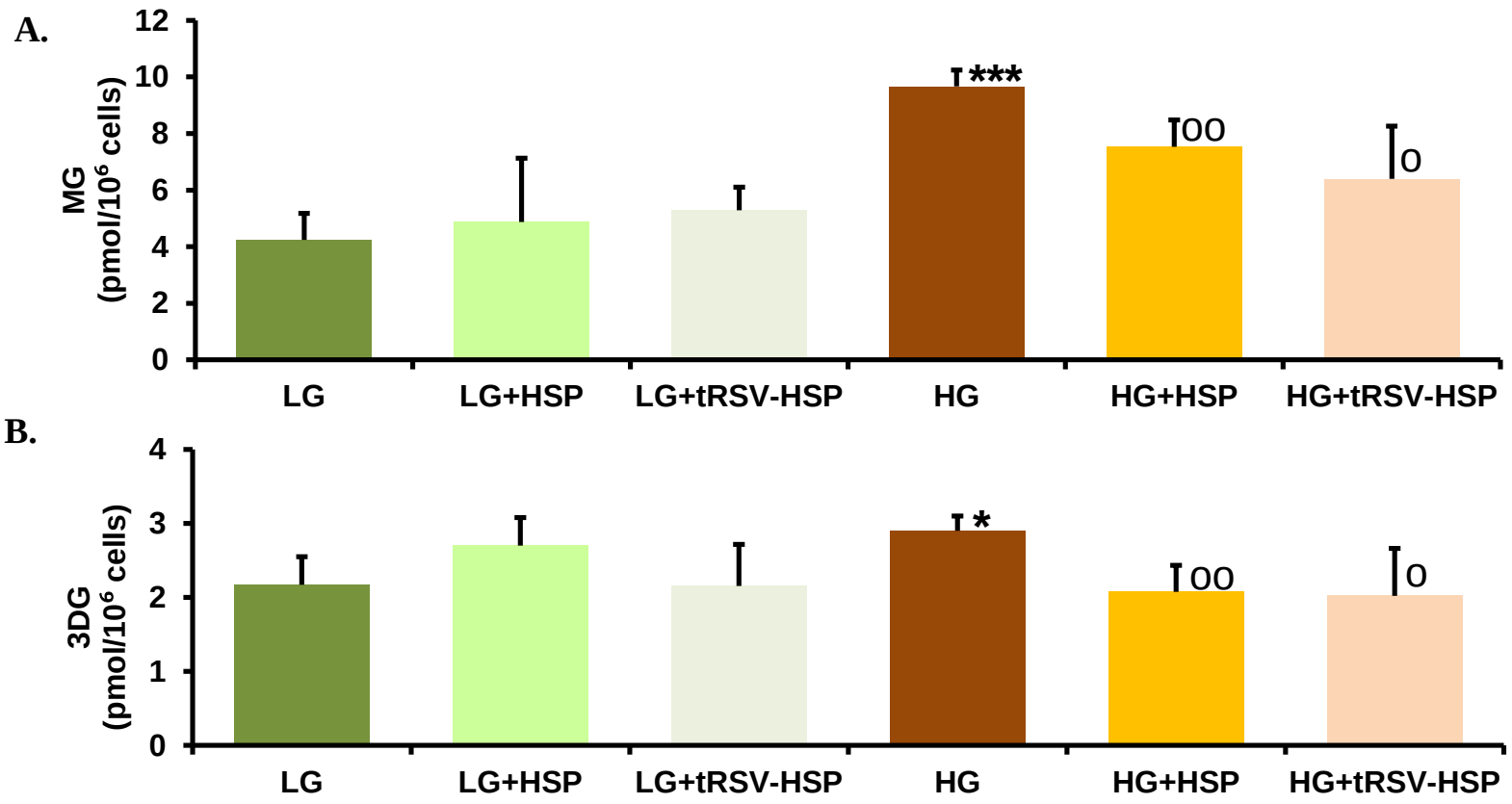

Figure 62: Effect of hesperetin and *trans*-resveratrol and hesperetin combined on cellular levels of dicarbonyls in hPDLFs cells *in vitro*.

hPDLFs cells were cultured in 8 mM glucose (LG) and 25 mM glucose medium (HG) with or without 10 µM HSP and 10 µM tRSV + HSP for 3 days. Key: (A) MG. (B) 3-DG. Data are mean ± SD, n = 4. Significance: * and ***, P<0.05 and P<0.001, respectively. compared to low glucose control; ^{o} and ^{oo}, P<0.05 and P<0.01, respectively. compared to high glucose control *(t-test).*

Table 37: Effect of Glo1 inducers on dicarbonyls levels in human periodontal ligament fibroblasts and medium *in vitro*

Glucose	Methylglyoxal (pmol/10^6cells)	Glyoxal (pmol/10^6cells)	3-DG (pmol/10^6cell)
LG	4.24 ± 0.94	6.74 ± 2.14	2.17 ± 0.38
LG+HSP	4.88 ± 2.25	6.72 ± 0.82	2.70 ± 0.38
LG+tRSV+HSP	5.28 ± 0.82	5.86 ± 1.61	2.16 ± 0.56
HG	9.67 ± 0.57***	6.02 ± 2.34	2.90 ± 0.20*
HG+HSP	7.54 ± 0.94^{oo}	5.77 ± 1.18	2.08 ± 0.36^{oo}
HG+tRSV+HSP	6.40 ± 1.86^{o}	4.25 ± 1.92	2.02 ± 0.64^{o}

Data are mean ± SD, n = 4. Significance: * and ***, P<0.05 and P<0.001, respectively. compared to low glucose control; ^{o} and ^{oo}, P<0.05 and P<0.01, respectively. compared to high glucose control *(t-test).*

3.3.9 Effect of *trans*-resveratrol on the availability of thiols and glutathione in hPDLFs cells *in vitro*

Most of the reactive dicarbonyls, glyoxal and MG, detected in cells are bound reversibly to protein and non-protein thiols which limits their reactivity to produce other irreversible protein modifications. In low glucose cultures, the total cell thiols in hPDLFs, mainly protein cysteine thiols + GSH, was 27.5 ± 0.9 nmol/10^6 cells. This was unchanged by addition of tRSV. Surprisingly total cell thiols were increased *ca,* 13% in hPDLFs cells with high glucose, compare to low glucose control (P<0.001). This was prevented by addition of 10 µM tRSV – Figure 63 and Tabl 38. Protein thiols were determined by subtracting GSH level from the samples. In low glucose cultures, the protein thiols content of hPDLFs was 20.2 ± 1.3 nmol/10^6 cells. Protein thiols were increased *ca,* 25% in hPDLFs cells with high glucose, compare to low glucose control (P<0.01). Protein thiols of hPDLFs were decreased by addition of 10 µM tRSV. In low glucose culture, protein thiols decreased *ca.* 15%, with respect to low glucose control. In high glucose culture, protein thiols decreased *ca,* 12%, with respect to low glucose control (P<0.05 with respect to low glucose control and P'<0.001 with respect to high glucose control) - Figure 63 and Tabl 38.

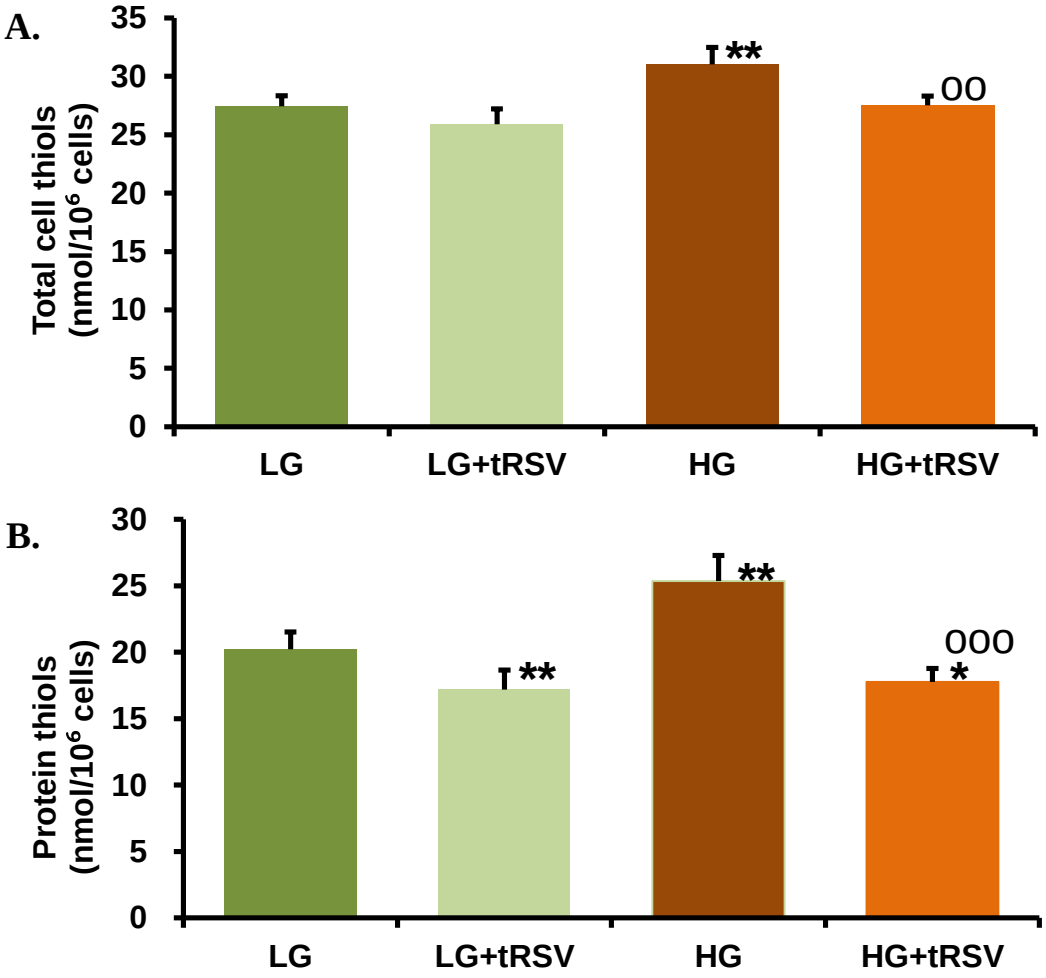

Figure 63: Effect of *trans*-resveratrol on the cell thiols in hPDLFs cells *in vitro*.
hPDLFs cells were cultured in 8 mM and 25 mM glucose medium with or without 10 µM tRSV for 3 days. Data are mean ± SD, n = 4. Significance: *, P<0.05, **, P<0.01 and ***, P<0.001 with respect to low glucose control; ^{oo}, P<0.01 and ^{ooo}, P<0.001 with respect to high glucose control (*t-test*).

To explore the changes in GSH metabolism, GSH and GSSG were measured and also total GSH deduced. In low glucose cultures, the GSH content of hPDLFs was 7.21 ± 0.93 nmol/10^6 cells. This was increased 21% by tRSV (P<0.05). In high glucose cultures, the GSH content of hPDLFs was decreased by 21% (P<0.05). Addition of tRSV corrected the decrease in GSH of hPDLFs and, moreover, increased GSH by 35%, with respect to low glucose control (P<0.01 with respect to low glucose control; P'<0.001 with respect to high glucose control). In low glucose cultures, the GSSG content of hPDLFs was 0.00814 ±

0.00054 nmol/10^6 cells. This was unchanged by tRSV. In high glucose cultures, the GSSG content of PDLFs was decreased by 20% (P<0.01). Addition of tRSV did not correct this decrease (P<0.05 with respect to low glucose control). In low glucose cultures, the total GSH content of hPDLFs was 7.23 ± 0.94 nmol/10^6 cells. This was increased 21% by tRSV (P<0.05). In high glucose cultures, the total GSH content of hPDLFs was unchanged. Addition of tRSV increased total GSH by 35% with respect to the low glucose control (P<0.01) - Figure 64 and Table 38.

Table 38: Effect of *trans*-resveratrol on glutathione levels in primary hPDLFs cells *in vitro*.

Analyte	LG	LG+tRSV	HG	HG+tRSV
Total thiols (nmol/10^6 cells)	27.5±0.90	25.9±1.31	31.1±1.45*	27.5±0.79 ^{oo}
Protein thiols (nmol/10^6 cells)	20.2 ± 1.3	17.2 ± 1.47	25.4 ± 1.93	17.8 ± 1.0
GSH (nmol/10^6 cells)	7.21 ± 0.94	8.71 ± 0.65*	5.68 ± 1.28*	9.75 ± 0.63**,^{oo}
GSSG (nmol/10^6 cells)	0.00814 ± 0.00054	0.00760 ± 0.0010	0.00648 ± 0.00053**	0.00692 ± 0.00047*
Total GSH (nmol/10^6 cells)	7.23 ± 0.94	8.72 ± 0.65*	5.70 ± 1.28*	9.76 ± 0.63**,^{ooo}
% Reduced (GSH)	99.8	99.8	96.7	99.9
% Oxidised (GSSG)	0.2	0.2	3.3	0.1

Data are mean ± SD, n = 4. Significance: * and **, P<0.05 and P<0.01 with respect to low glucose control; ^{oo} and ^{ooo}, P<0.01 and P<0.001 with respect to high glucose control (*t-test*).

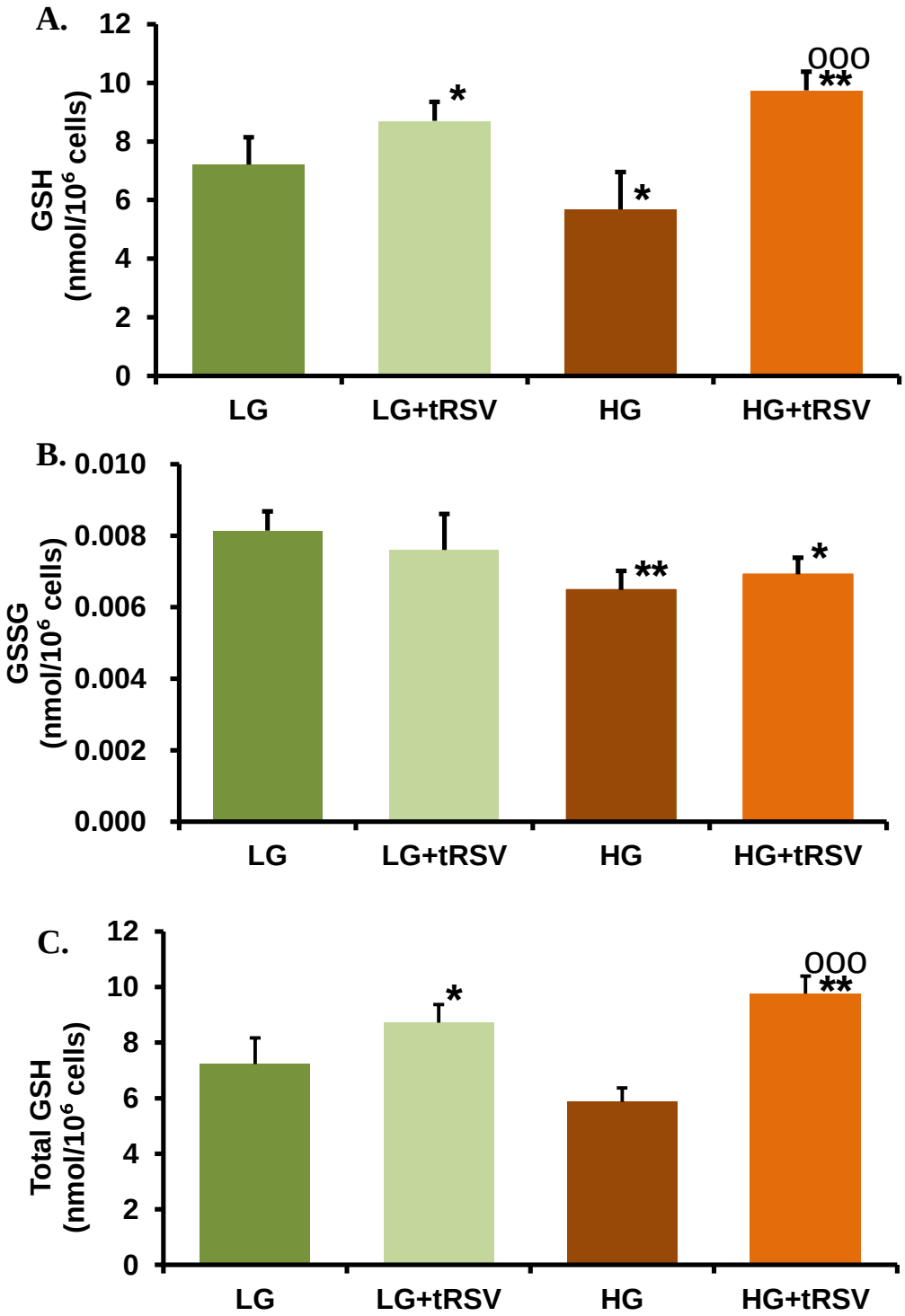

Figure 64: Effect of *trans*-resveratrol on glutathione metabolism in hPDLFs cells *in vitro*.

hPDLFs cells were cultured in 8 mM glucose (LG) and 25 mM glucose (HG) medium with or without 10 µM tRSV for 3 days. (A) GSH, (B) GSSG, and (C) Total GSH. Data are mean ± SD, n = 4. Significance: * and **, P<0.05 and P<0.01, respectively, compared to low glucose control; ᵒᵒᵒ, P<0.001 with respect to high glucose control (*t-test*).

3.3.10 Effect of *trans*-resveratrol on glycation, oxidation and nitration adduct residue content of cytosolic protein extracts of hPDLFs cells *in vitro*

Primary hPDLFs were cultured for 3 days in low and high glucose with or without 10 µM tRSV and glycation, oxidation and nitration adduct residue content of cytosolic protein extracts analysed. In low glucose cultures, the MG-H1 residue content of cell protein was 0.416 ± 0.059 mmol/mol arg. This was unchanged by addition of tRSV. In high glucose cultures, the MG-H1 residue content of cell protein was increased 74% compared to low glucose control ($P<0.01$) which was corrected by addition of tRSV. In low glucose cultures, the FL residue content of cell protein was 0.123 ± 0.022 mmol/mol lys. This was unchanged by addition of tRSV. In high glucose cultures, the FL residue content of cell protein was increased by 242% compared to low glucose control ($P<0.001$). This increase was decreased to +108 by addition of tRSV ($P<0.05$ with respect to low and high glucose controls). In low glucose cultures, the CML residue content of cell protein was 0.076 ± 0.007 mmol/mol lys. This was unchanged by addition of tRSV. In high glucose cultures, the CML residue content of cell protein was increased by 51% compared to low glucose control ($P<0.01$). This increase was unchanged by addition of tRSV ($P<0.01$ with respect to low glucose control). In low glucose cultures, the CMA residue content of cell protein was 0.062 ± 0.011 mmol/mol arg. This was decreased 46% by addition of tRSV ($P<0.01$). In high glucose cultures, the CMA residue content of cell protein was unchanged but it was decreased 51% in high glucose by addition of tRSV ($P<0.01$ with respect to low and high glucose controls).

The level of CML/FL in low glucose cultures is 0.085 ± 0.025. This was unchanged in high glucose culture or with addition of tRSV to hPDLFs in low and high glucose culture. This indicated no change in the oxidative stress with addition of tRSV hPDLFs in low or high glucose culture. The glycation and oxidation adduct residue content of cell protein are presented in Figure 65 and Table 39.

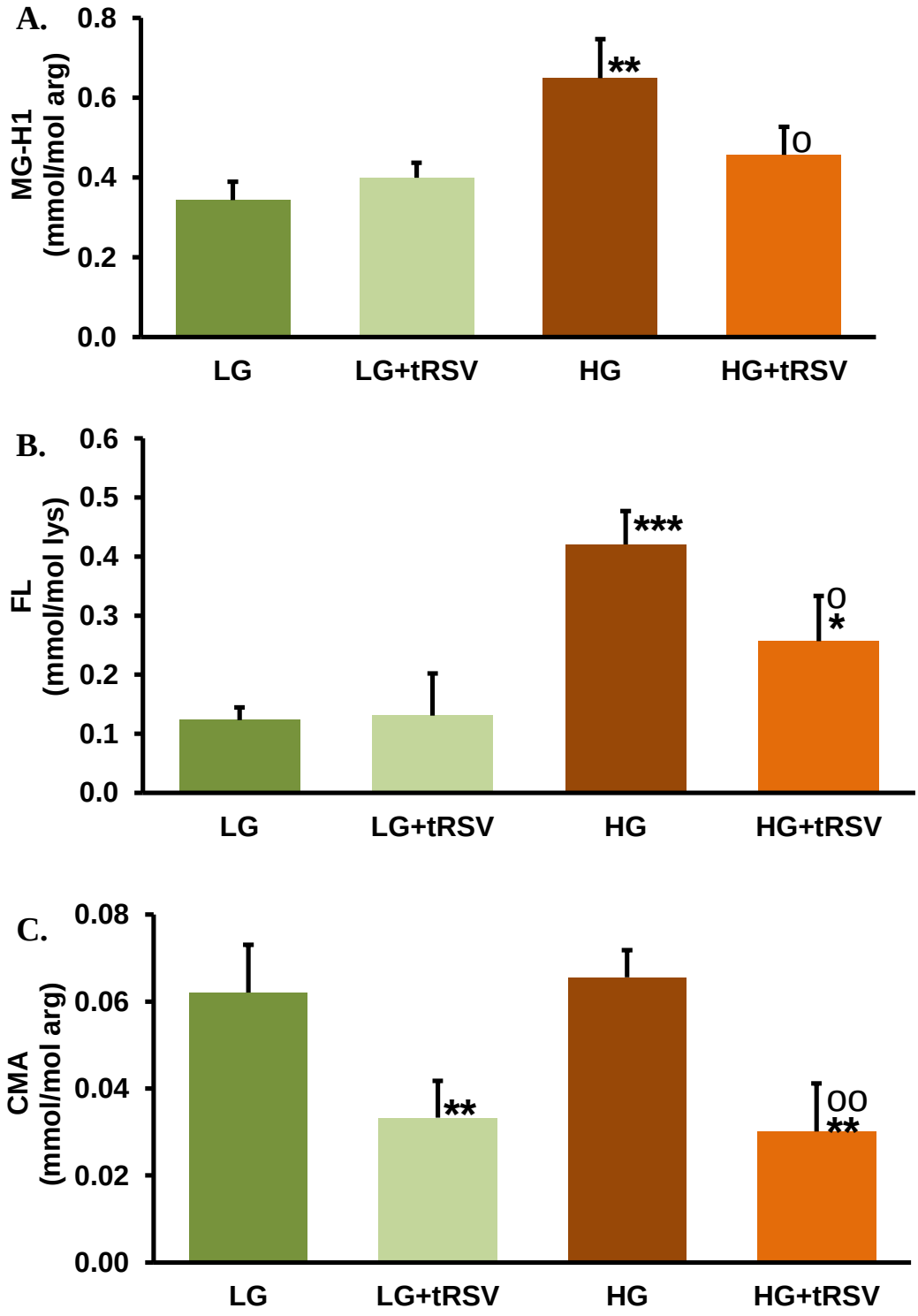

Figure 65: Effect of *trans*-resveratrol on cellular protein glycation adduct content of hPDLFs cells *in vitro*.
(A) MG-H1. (B) FL. (C) CMA. Data are mean ± SD, n = 4. Significance: *, ** and ***, P<0.05, P<0.01 and P<0.001, respectively, compared to low glucose control; ^{o} and ^{oo}, P<0.05 and P<0.01 respectively, compared to high glucose control (*t-test*).

Table 39: Effect of *trans*-resveratrol on cellular protein content of protein glycation and oxidation adduct residues of hPDLFs cells *in vitro*

Protein adduct residue	LG	LG+tRSV	HG	HG+tRSV
FL (mmol/mol lys)	0.972 ± 0.390	0.867 ± 0.628	3.40 ± 0.96**	1.76 ± 0.553^{oo}
CML (mmol/mol lys)	0.076 ± 0.007	0.085 ± 0.004	0.114 ± 0.015**	0.114 ± 0.013**
CEL (mmol/mol lys)	0.030 ± 0.009	0.027 ± 0.006	0.035 ± 0.010	0.034 ± 0.010
MOLD (mmol/mol lys)	0.0055 ± 0.0038	0.0045 ± 0.0026	0.0043 ± 0.0021	0.0032 ± 0.0016
CMA (mmol/mol arg)	0.062 ± 0.011	0.033 ± 0.008**	0.066 ± 0.006	0.030 ± 0.011^{oo}
MG-H1 (mmol/mol arg)	0.416 ± 0.059	0.462 ± 0.037	0.727 ± 0.122**	0.540 ± 0.085^{o}
G-H1 (mmol/mol arg)	0.012 ± 0.007	0.019 ± 0.009	0.015 ± 0.013	0.027 ± 0.015
3DG-H (mmol/mol arg)	0.182 ± 0.100	0.123 ± 0.045	0.148 ± 0.032	0.132 ± 0.082
3NT (mmol/mol tyr)	0.0013 ± 0.0002	0.0017 ± 0.0003	0.0013 ± 0.0005	0.0014 ± 0.0002
DT (mmol/mol tyr)	0.036 ± 0.008	0.033 ± 0.009	0.037±0.007	0.046 ± 0.019
NFK (mmol/mol trp)	0.199 ± 0.044	0.209 ± 0.052	0.217 ± 0.095	0.232 ± 0.036
MetSO (mmol/mol met)	2.09 ± 0.28	1.72 ± 0.49	2.13±0.55	2.01 ± 0.21
CML/FL	0.085 ± 0.025	0.107 ± 0.061	0.086 ± 0.010	0.069 ± 0.023

Data are mean ± SD, n = 4. Significance: *, ** and ***, P<0.05, P<0.01 and P<0.001 with respect to low glucose control; ^{o} and ^{oo}, P<0.05 and P<0.01 with respect to high glucose control *(t-test).*

3.3.11 Effect of *trans*-resveratrol on flux of glycation, oxidation and nitration free adducts of hPDLFs cells *in vitro*

Primary hPDLFs were cultured for 3 days in low and high glucose with or without 10 µM tRSV. The concentration of glycation, oxidation and nitration free adducts were measured in culture medium at baseline and at 3 days and the flux of free adduct increase deduced.

In low glucose cultures, the flux of MG-H1 free adduct formation was 2.10 ± 0.67 pmol/10^6 cells/day. This was unchanged by addition of tRSV. In high glucose cultures, the flux of MG-H1 free adduct formation was increased 52% compared to low glucose control ($P<0.05$) which was corrected by addition of tRSV. In low glucose cultures, the flux of CML free adduct formation was 10.0 ± 7.2 pmol/10^6 cells/day. This was unchanged by addition of tRSV. In high glucose cultures, the flux of MG-H1 free adduct formation was increased 196% compared to low glucose control ($P<0.01$). This increase was lowered to + 121% by addition of tRSV ($P<0.05$ with respect to low glucose control; $P'<0.01$ with respect to high glucose control) – Figure 66 and Table 40.

In low glucose cultures, the flux of 3DG-H free adduct formation was 0.678 ± 0.559 pmol/10^6 cells/day. This was increased by + 617% in high glucose incubation ($P<0.001$). In low glucose cultures, MetSO free adduct formation was 0.678 ± 0.559 pmol/10^6 cells/day. This was increased by 527% in high glucose incubation ($P<0.001$). In low glucose cultures, the flux of CMA free adduct formation was 0.678 ± 0.559 pmol/10^6 cells/day. This was increased by 25% in high glucose incubation ($P<0.05$). 3DG-H, MetSO and CMA free adduct formation levels were unchanged by addition of tRSV in low or high glucose incubations - Table 40.

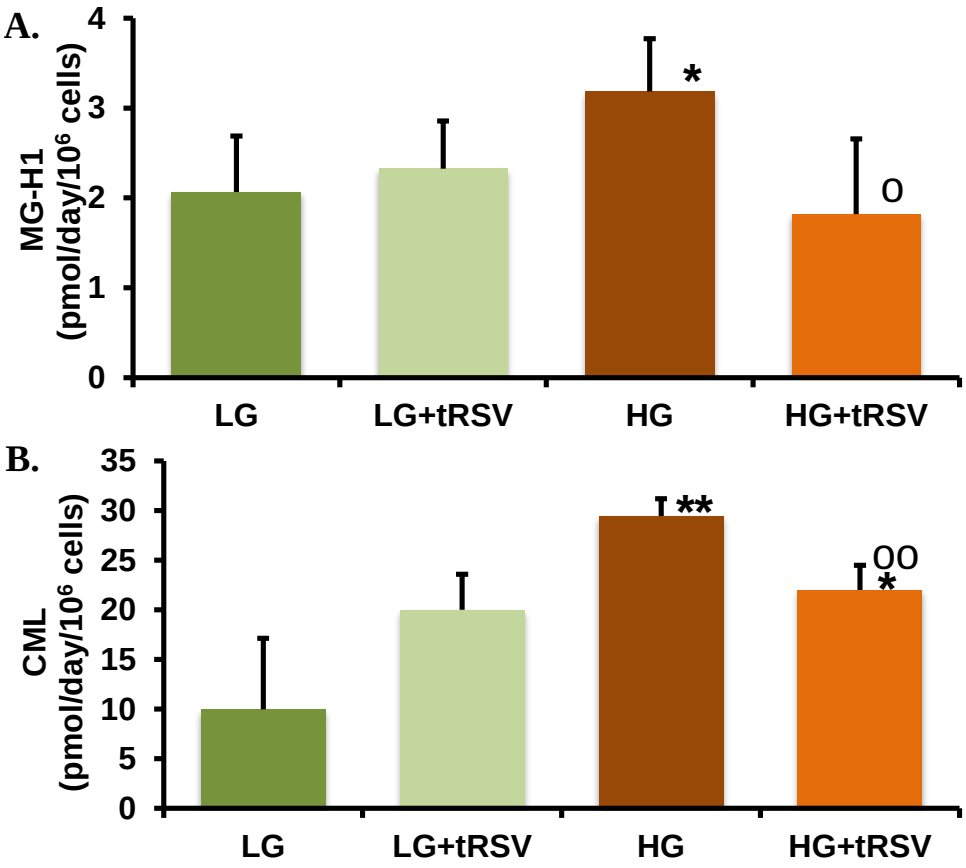

Figure 66: Effect of *trans*-resveratrol on flux of protein glycation free adducts formed by hPDLFs cells in culture *in vitro*.
(A) MG-H1. (B) CML. Data are mean ± SD, n = 4. Significance: * and **, P<0.05 and P<0.01, respectively, compared to low glucose control; ^{o} and ^{oo}, P<0.05 and P<0.01 respectively, compared to high glucose control *(t-test).*

Table 40: Effect of *trans*-resveratrol on flux of protein glycation and oxidation free adducts formed by hPDLFs cells *in vitro*

Free adduct	LG	LG+tRSV	HG	HG LG+tRSV
FL	323 ± 110	312 ± 102	1032 ± 425*	1133 ± 429**
CML	10.0 ± 7.2	19.9 ± 3.6	29.5 ± 1.7**	22.0 ± 2.5 ^{oo}
MetSO	0.506 ± 0.160	0.514 ± 0.151	3.17 ± 0.56***	3.10 ± 0.88***
CMA	4.55 ± 0.29	4.22 ± 0.54	5.66 ± 0.61*	6.36 ± 0.50**
MG-H1	2.09 ± 0.67	2.33 ± 0.53	3.18 ± 0.59*	1.82 ±0.83 ^{o}
GH1	1.25 ± 0.85	1.73 ± 0.99	0.479 ± 0.339	0.756 ± 0.580
3DG-H	0.678 ± 0.559	0.697 ± 0.263	4.77 ± 0.30***	4.59±1.37***

Data are mean ± SD (pmol/day/10^6 cells; n = 4). Significance: *, ** and ***, P<0.05, P<0.01 and P<0.001, respectively, compared to low glucose control; ^{o} and ^{oo}, P<0.05 and P<0.01, respectively, compared to high glucose control *(t-test).*

3.3.12 Studying the effect of highly and minimally glycated protein on inflammatory signalling activated by RAGE in hPDLFs *in vitro*

Bierhaus and colleagues published preliminary evidence that activation of RAGE by proteins highly modified by AGEs decreased expression of Glo1 (Bierhaus, 2006). Studies in OVE26 mice with and without RAGE expression had change in Glo1 expression supporting this (Reiniger et al., 2010). The mechanistic details are still unclear. It now seems unlikely that protein glycated minimally by AGEs as found *in vivo* do not bind RAGE (Thornalley, 2007) and the claim that CML-modified proteins bind RAGE contested (Kistinger et al., 1999, Buetler et al., 2008). Albumin highly modified by AGEs and aggregated, however, does bind RAGE (Valencia et al., 2004). Since the hPDLFs may be exposed to the highly glycated protein from food with epithelial barrier breakdown in periodontitis, the effect of albumin highly modified by CML (CML-HSA) and glucose-derived AGEs (AGE-HSA) was investigated. I hypothesised that the decrease in Glo1 activity may occur in hPDLFs when RAGE binds CML-HSA and AGE-HSA and activates NF-κB. Crosstalk between NF-κB and Nrf2 (Liu et al., 2008) is expected to downregulated basal and inducible expression of Glo1 (Xue et al., 2012a). This was investigated in this project.

3.3.12.1 Effect of AGE-HSA and CML-HSA on the viability of hPDLFs *in vitro*

Primary hPDLFs were incubated for 3 days in MEM medium containing 8 mM glucose with unmodified HSA (100 µg/ml), AGE-HSA (50 – 100 µg/ml) and CML-HSA (50 – 100 µg/ml). In day 3 the viable cell number was counted in all the study groups. The viable cell number increased throughout the culture period and shows a steady increase in all the groups with no significant change in the vitality under any condition – Figure 67.

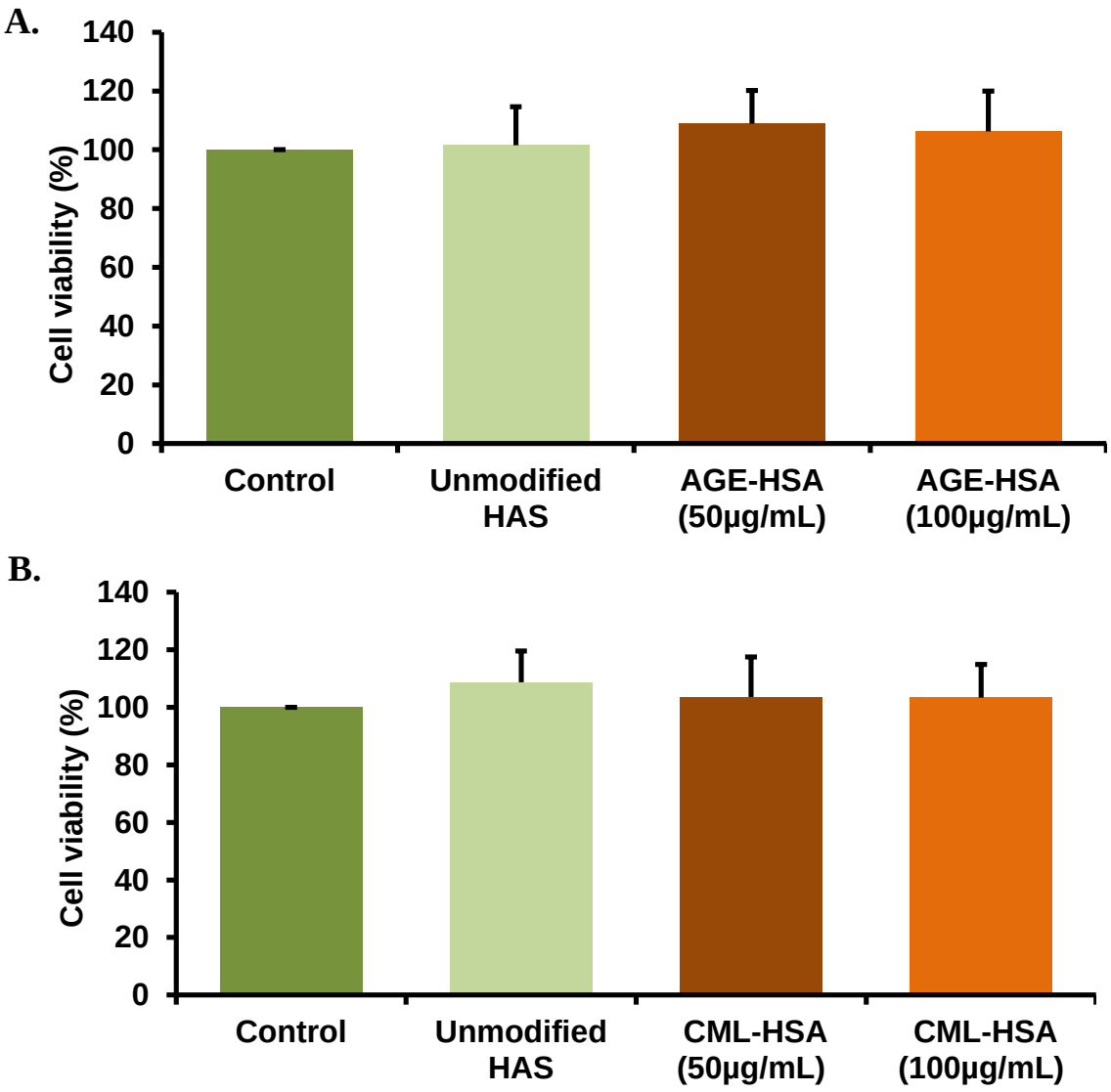

Figure 67: Effect of AGE-HSA and CML-HSA on the viability of hPDLFs *in vitro*.
(A) The viability of hPDLFs treated with AGE-HSA (50 – 100 µg/ml). (B) The viability of hPDLFs treated with CML-HSA (50 – 100 µg/ml). Data are mean ± SD, n = 3.

3.3.12.2 Endotoxin content of albumin derivatives highly modified AGEs

The concentration of endotoxin in the modified albumin was measured by a quantitative chromogenic limulus assay. The data shows low levels of endotoxins in modified albumin proteins which are lower than level of endotoxin in body plasma (0.5 EU/mL) - Table 41.

Table 41: The levels of endotoxin in modified albumin derivatives.

Sample	Endotoxin (EU/mg)
CML-HSA	0.112 ± 0.040
CML_{min}-HSA	0.127 ± 0.028
Unmodified HSA control (CML-HSA)	0.153 ± 0.031
AGE-HSA	0.170 ± 0.077
Unmodified HSA control (AGE-HSA)	0.216 ± 0.027
AGE_{min}-HSA	0.143 ± 0.018
Unmodified HSA control (AGE_{min}-HSA)	0.198 ± 0.021

Data are mean ± SD, n = 3.

3.3.12.3 Effect of highly glycated albumin derivatives on activation of transcription factor NF-κB in hPDLFs *in vitro*

Primary hPDLFs were cultured for 3 days in cultures with 8 mM glucose in presence of highly glycated albumin derivatives proteins (100 µg/ml). Cell nuclear extracts were prepared and an aliquot of nuclear extract (10 µg) was tested for activated p65. The outcome showed no significant activation of NF-kB, as indicated by level of nuclear DNA bound p65. This suggests that highly AGE-modified albumin did not activate inflammatory signalling in hPDLFs. Previous studies may have endotoxin contamination in the protein preparation that caused activation of the RAGE receptor. In this study a great care was taken to avoid endotoxin contamination (see Table 41). Table 42 shows average of the expression in 10 µg of hPDLFs nuclear extract.

Table 42: The effect of modified albumin protein derivatives on the activation of transcription factor NF-κB in hPDLFs *in vitro.*

Sample	DNA-bound p65 (% of control)
Control	0.801 ± 0.035
Positive control (Jurkat nuclear extract)	1.25 ± 0.017
TNFα (100 nM)	0.818 ± 0.053
CML-HSA	0.824 ± 0.047
CML_{min}-HSA	0.831 ± 0.095
Unmodified HSA control (CML-HSA)	0.822 ± 0.027
AGE-HSA	0.865 ± 0.037
Unmodified HSA control (AGE-HSA)	0.834 ± 0.062
AGE_{min}-HSA	0.844 ± 0.013
Unmodified HSA control (AGE_{min}-HSA)	0.800 ± 0.059

Data are mean ± SD, n = 3.

3.3.12.4 The effect of modified albumin proteins on the Glo1 gene expression in hPDLFs *in vitro*

Primary hPDLFs were incubated for 3 days in MEM medium in low glucose containing highly glycatyed and unglycated control HSA derivatives (50 and 100 µg/ml). Glo1 gene expression was quantified in all study groups. The levels of Glo1 mRNA showed no change in response to glycated and unglcated albumin derivatives - Table 43.

Table 43: The effect of modified albumin proteins on the Glo1 gene expression in hPDLFs *in vitro.*

Analyte	**Control**	**Unmodified HSA control (100 µg /ml)**	**AGE-HSA (50 µg/ml)**	**AGE-HSA (100 µg/ml)**
GLO1 mRNA (normalized to β-actin mRNA)	0.740 ± 0.006	0.749 ± 0.006	0.735 ± 0.011	0.732 ± 0.018
	Control	**Unmodified HSA control (100µg /ml)**	**CML-HSA (50 µg/ml)**	**CML-HSA (100 µg/ml)**
GLO1 mRNA (normalized to β-actin mRNA)	0.737 ± 0.006	0.746 ± 0.003	0.735 ± 0.007	0.730 ± 0.024

Data are mean ± SD, n = 3.

3.4 Effect of Glyoxalase 1 inducers on the adhesion and function of hPDLFs to collagen and modified collagen *in vitro*

3.4.1 The expression of collagen-I, collagen-III and collagen-XII in hPDLFs cells *in vitro*

Primary hPDLFs were cultured for 3 days in 8 mM glucose and 25 mM glucose supplemented with or without tRSV (10 µM). Expression of collagen-I, collagen-III and collagen-XII genes (COL1, COL3 and COL12) was measured by RT-PCR in hPDLFs cells. The expression of COL1 was decreased significantly in high glucose treatment by 11% ($P<0.05$) compared to low glucose and *trans*-resveratrol (10 µM) corrected the decrease - Figure 68. tRSV supplementation increased the expression of COL1 by 12% ($P<0.01$) and the expression of COL3 and COL12 by 5% ($P<0.001$) in high glucose treated hPDLFs with respect to controls - Table 44.

Table 44: The effect of *trans*-resveratrol and high glucose on collagen gene expression in hPDLFs *in vitro.*

	COL1 mRNA	COL3 mRNA	COL12 mRNA
LG	0.799 ± 0.007	1.19 ± 0.008	1.44 ± 0.014
LG + tRSV	0.787 ± 0.021	1.21 ± 0.012*	1.45 ± 0.016
HG	0.714 ± 0.054*	1.20 ± 0.014	1.46 ± 0.020
HG + tRSV	0.814 ± 0.007$^{*,\#,o}$	1.26 ± 0.013***,^{ooo}	1.54 ± 0.038**,^{oo}

Data are mean ± SD, n = 4. Significance: *, **, and ***, $P<0.05$, $P<0.01$ and $P<0.001$ with respect to low glucose control; ^{oo} and ^{ooo}, $P<0.01$ and $P<0.001$ with respect to high glucose control; $^{\#}$ $P<0.05$ with respect to low glucose with tRSV *(t-test).*

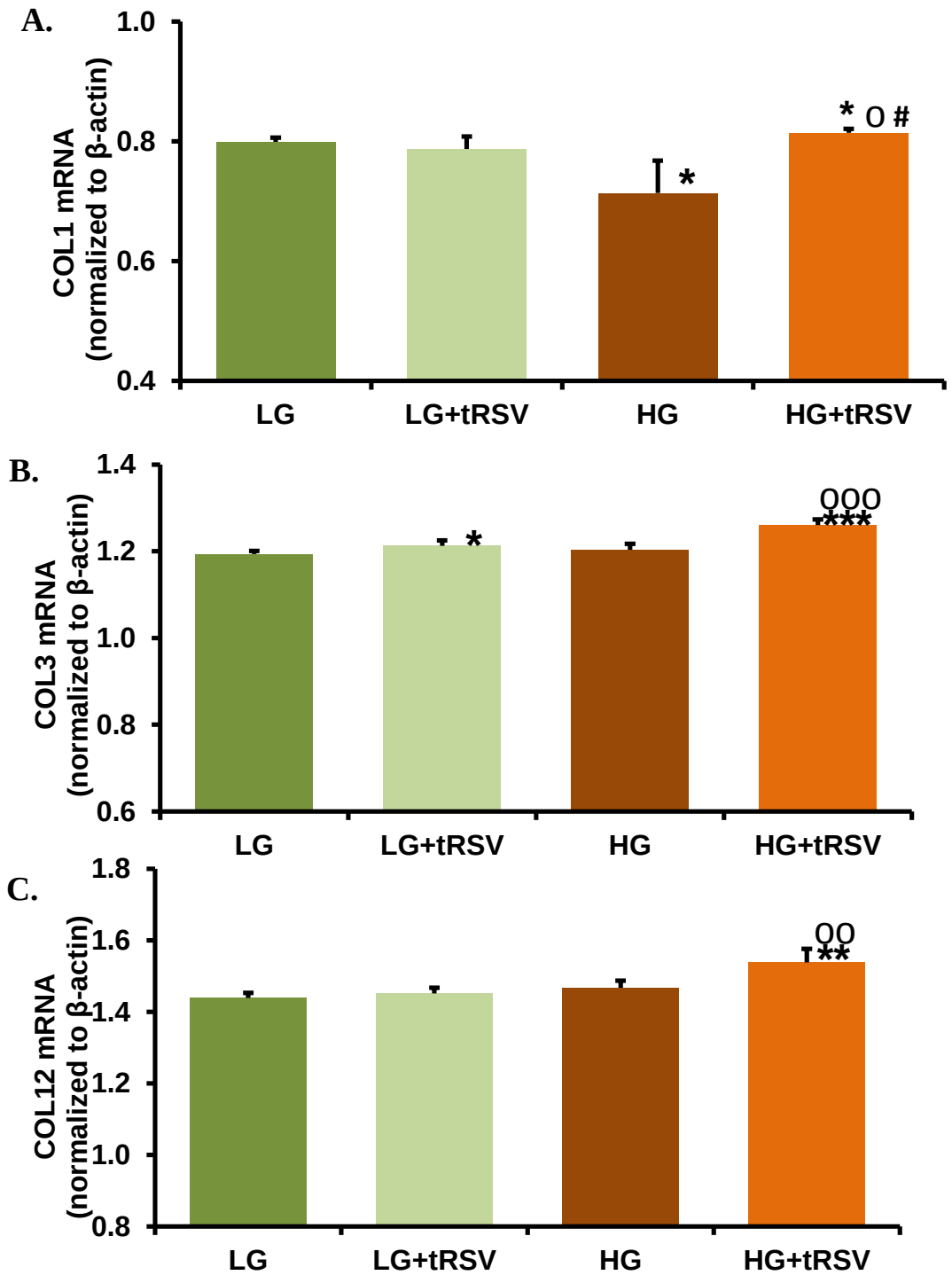

Figure 68: The effect of *trans*-resveratrol and high glucose on collagen genes expression in hPDLFs *in vitro*.
(A) COL1 expression, **(B)** COL3 expression and **(C)** COL12 expression. Data are mean ± SD, n = 4. Significance: *, **, and ***, P<0.05, P<0.01 and P<0.001 with respect to low glucose control; ^{oo} and ^{ooo}, P<0.01 and P<0.001 with respect to high glucose control; $^{\#}$ P<0.05 with respect to low glucose with tRSV *(t-test)*.

3.4.2 Effect of glyoxalase 1 inducers on the adhesion efficiency of hPDLFs to collagen-I *in vitro*

Cell adhesion assay was performed on previously treated hPDLFs which were cultured for 3 days in MEM with low glucose and high glucose with or without tRSV, HSP and tRSV+HSP (10 µM). The ability of hPDLFs adhesion to ECM collagen-I was assessed.

When hPDLFs were incubated in high glucose concentration, there was a *ca.* 30% decrease in adhesion of the cells to collagen, compared to low glucose concentration control ($P<0.05$). Glo1 inducers both individually, tRSV and HSP, and in combination, tRSV+HSP, increased adhesion of hPDLFs to collagen-I by *ca.* 52%, 40% and 57%, respectively, when incubated in the low glucose concentration conditions ($P<0.05$). In high glucose concentration, Glo1 inducers increased the adhesion to Collagen-I *ca*. 3-fold, compared to high glucose control and 2-fold compared to low glucose control – Figure 69.

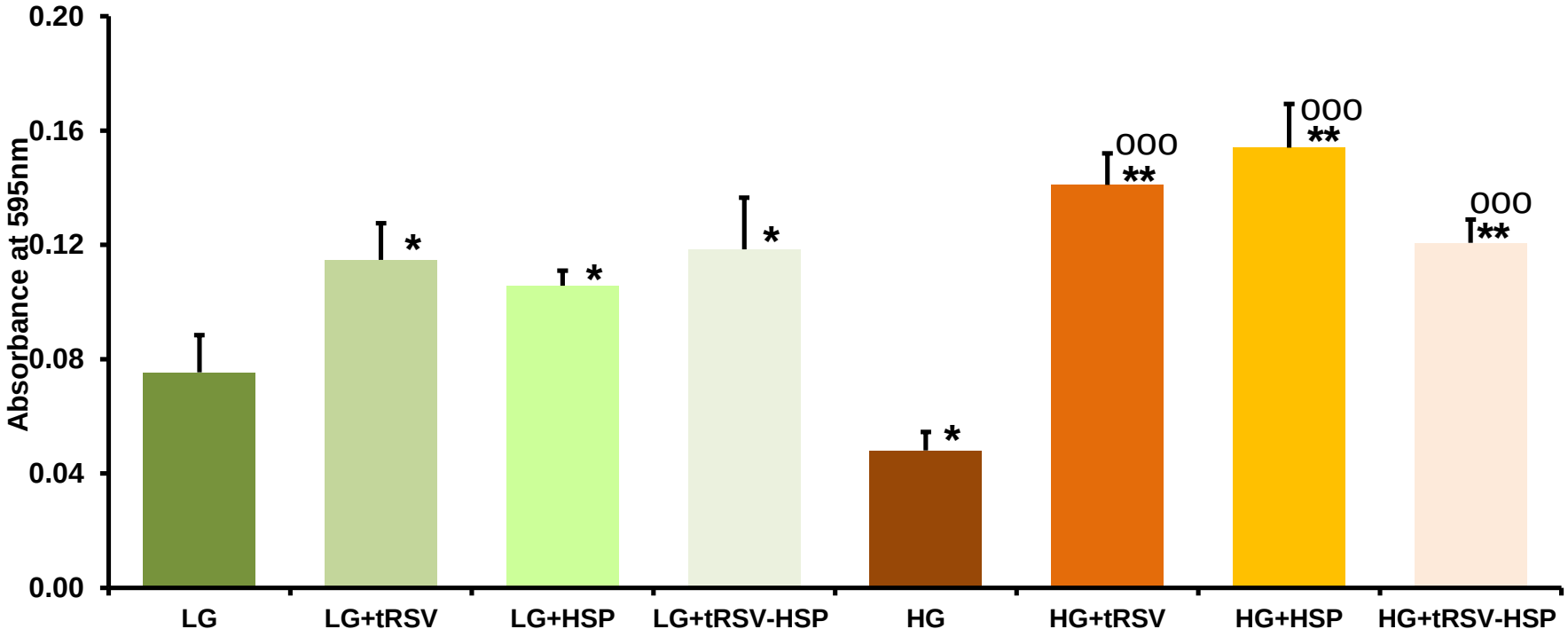

Figure 69: Effect of glyoxalase 1 inducer on the adhesion efficiency of hPDLFs to collagen-I *in vitro*.
Data are mean ± SD, n = 3. Significance: * and **, P<0.05 and P<0.01, respectively, compared to low glucose control; ^{ooo}, P<0.001 compared to high glucose control (*t-test*).

3.4.3 Effect of glyoxalase 1 inducers on the adhesion efficiency of hPDLFs to collagen-I modified by conditioned media *in vitro*

Culture medium from PDLFs incubated with and without tRSV, HSP and tRSV+HSP for 3 days was collected. This was incubated with and without 500 μM aminoguanidine (AG) for 3 h in 37 ^{O}C to scavenge dicarbonyls with AG. Collagen-I coated plates were incubated with the conditioned media for 24 h and adhesion of hPDLFs to the collagen-I was studied.

The results of incubating cells on to pre-conditioned collagen coated plates gave similar trend in adhesion as found in the section above. The only difference was that the level of attachment to collagen was lower in all study groups when preconditioned with media without AG. The cell adhesion was decreased *ca.* 60% to collagen incubated with high glucose medium without AG compared to with AG ($P<0.01$). Glyoxalase 1 inducers alone or in combination (tRSV, HSP and tRSV+HSP) increased the attachment of hPDLFs to collagen-I by *ca*. 30% in low glucose groups ($P<0.05$). In high glucose concentration, the attachment capability increased more than 2-fold with the addition of the Glo1 inducers with respect to high glucose control - Figure 70 and 71. Table 45 shows the difference in attachment level of hPDLFs to the preconditioned collagen with or without aminoguanidine (AG, 500μM).

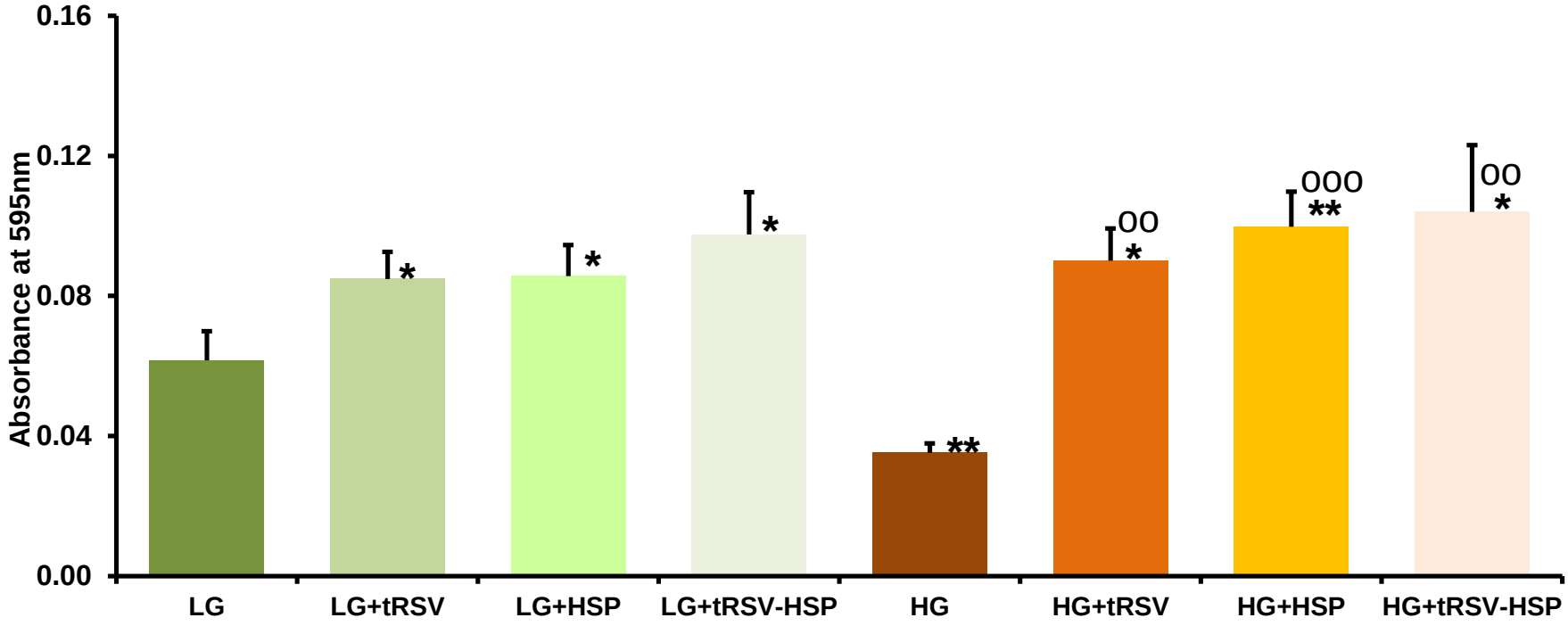

Figure 70: Effect of glyoxalase 1 inducer on the adhesion efficiency of hPDLFs to modified collagen-I *in vitro*.
Data are mean ± SD, n = 3. Significance: *and **, P<0.05 and P<0.01, respectively, compared to low glucose control; ^{oo} and ^{ooo}, P<0.01 and P<0.001, respectively, compared to high glucose control (*t-test*).

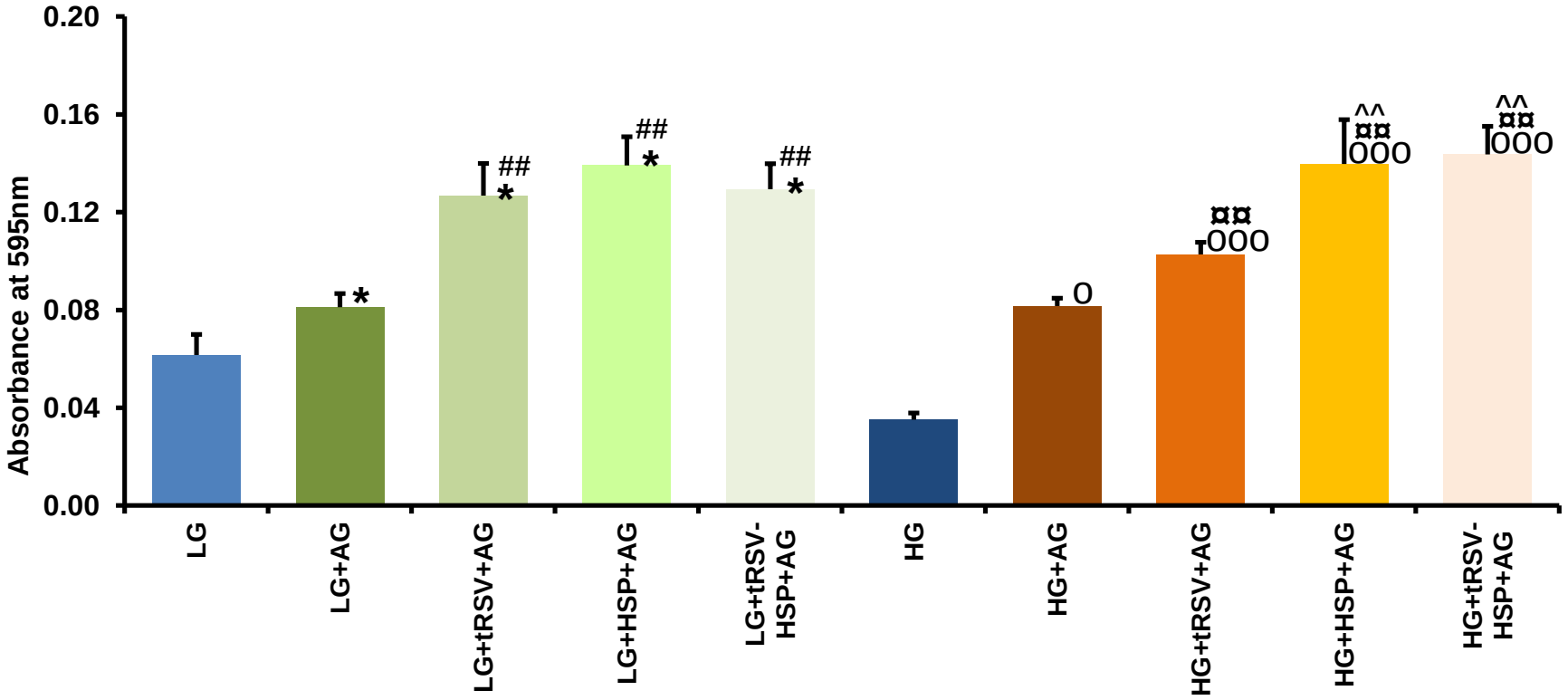

Figure 71: Effect of glyoxalase 1 inducer on the adhesion efficiency of hPDLFs to modified collagen-1 incubated with aminoguanidine *in vitro.*

Data are mean ± SD, n = 3. Significance: * and **, P<0.05 and P<0.01, respectively, compared to low glucose control without AG; ##, P<0.01 with respect to low glucose with AG; º and ººº, P<0.05 and P<0.001, respectively, compared to high glucose control without AG; ¤¤, P<0.01 with respect to high glucose with AG;^^^, P<0.001 with respect to high glucose with tRSV (*t-test*). Key: LG, low glucose (8 mM); HG, high glucose (25 mM); tRSV, *trans*-resveratrol (10 µM); HSP, Hesperetin (10 µM) and tRSV+HSP, HSP in combination with tRSV (10 µM); AG, aminoguanidine (500 µM).

Table 45: The difference in attachment level of hPDLFs to the preconditioned collagen with or without aminoguanidine

	Adhesion of hPDLFs to the preconditioned collagen		
Conditions	**Media**	**Media + AG**	**P.Value**
LG	0.062 ± 0.008	0.081 ± 0.006	<0.05
LG+tRSV	0.085 ± 0.008	0.127 ± 0.013	<0.01
LG+HSP	0.086 ± 0.009	0.139 ± 0.012	<0.01
LG(tRSV+HSP)	0.098 ± 0.012	0.129 ± 0.011	<0.05
HG	0.035 ± 0.003	0.082 ± 0.003	<0.001
HG+tRSV	0.080 ± 0.011	0.103 ± 0.005	<0.05
HG+HSP	0.100 ± 0.010	0.140 ± 0.018	<0.05
HG(tRSV+HSP)	0.104 ± 0.019	0.144 ± 0.012	<0.05

Data are mean ± SD, n = 3.

3.5 Study of the Glo1 protein acetylation in hPDLFs in vitro

The prevention of decline of Glo1 in hPDLFs incubated in high glucose concentration by tRSV may be related to the activation of sirtuins by tRSV and prevention of acetylation of Glo1. Acetylation of human Glo1 at K148 is known (Lundby et al., 2012) and this likely undergoes de-acetylation by cytosolic sirtuin-2 (Rauh et al., 2013). tRSV may activate both SIRT1 and SIRT2 in situ through increased provision of NAD+ cofactor (Guarente, 2013). Our latest research indicates that cell dysfunction driven by high glucose involves decreased Glo1 protein and activity driven by acetylation-activated ubiquitination and proteolysis (Thornalley et al., 2014).

I hypothesised that the effect of tRSV on Glo1 to counter dicarbonyl stress in hPDLFs, therefore, is likely stabilisation of Glo1 protein to degradation, probably by suppressing acetylation-linked ubiquitination. In order to test this hypothesis, acetylation of Glo1 protein by immunoblotting, SIRT1 and SIRT2 protein level and mRNA expression were examined in hPDLFs, which were incubated in low and high glucose concentrations with or without tRSV (10 μM) for three days. In addition, I determined the effect of inhibitors of deacetylases on Glo1 activity in hPDLFs. The half life of Glo1 protin is 60 h (Xue et al., 2012a)., therefore incubating the hPDLFs for 72 h is reasonable time to detect any change in Glo1 activity by acetylation or deacetylation.

3.5.1 Effect of low and high glucose on Glo1 acetylation *in vitro*

Primary hPDL fibroblasts were incubated with MEM containing low glucose and high glucose with or without tRSV (10 μM) for three days. Glo1 protein was precipitated by Dynabeads as described in the method section. The pulled down Glo1 was blotted and the acetylation was determined and normalized by Glo1 level – Figure 72. There was no change in the acetylation through all samples under any condition.

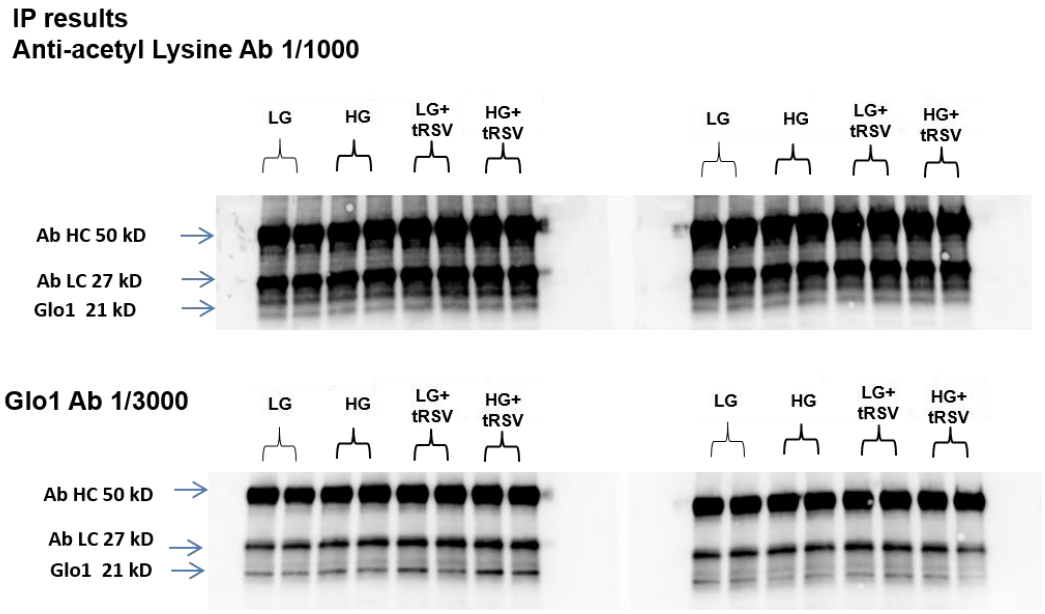

Figure 72: the effect of *trans*-resveratrol and high glucose on Glo1 acetylation *in vitro*.
Glo1 protein was precipitated by Dynabeads. The pulled down Glo1 was blotted and the acetylation was determined and normalized by Glo1 level. Kys: LG, low glucose (8 mM); HG, high glucose (25 mM); tRSV, trans-resveratrol (10 µM); Ab HC, antibody high chain; Ab LC, antibody low chain.

3.5.2 The effect of inhibitors of deacetylases compound and high glucose on hPDLFs *in vitro*

3.5.2.1 The viability of hPDLFs treated with different concentrations of acetylation compound (Trichostatin A, TSA) *in vitro*

Primary hPDLFs were treated for 48 hours with or without 100, 150, 200 and 300 nM TSA. After 48 h the viable cell number was counted. The viable cell number increased throughout the culture period and show a steady increase in all the groups with no significant change in the viability with any concentration. However, there is a tendency of decrease in the viability when the concentration increase. The cell viability response for hPDLFs *in vitro* is shown in Figure 73. A growth curve of hPDLFs with and without 300 nM TSA was studied over 4 days in LG and HG.

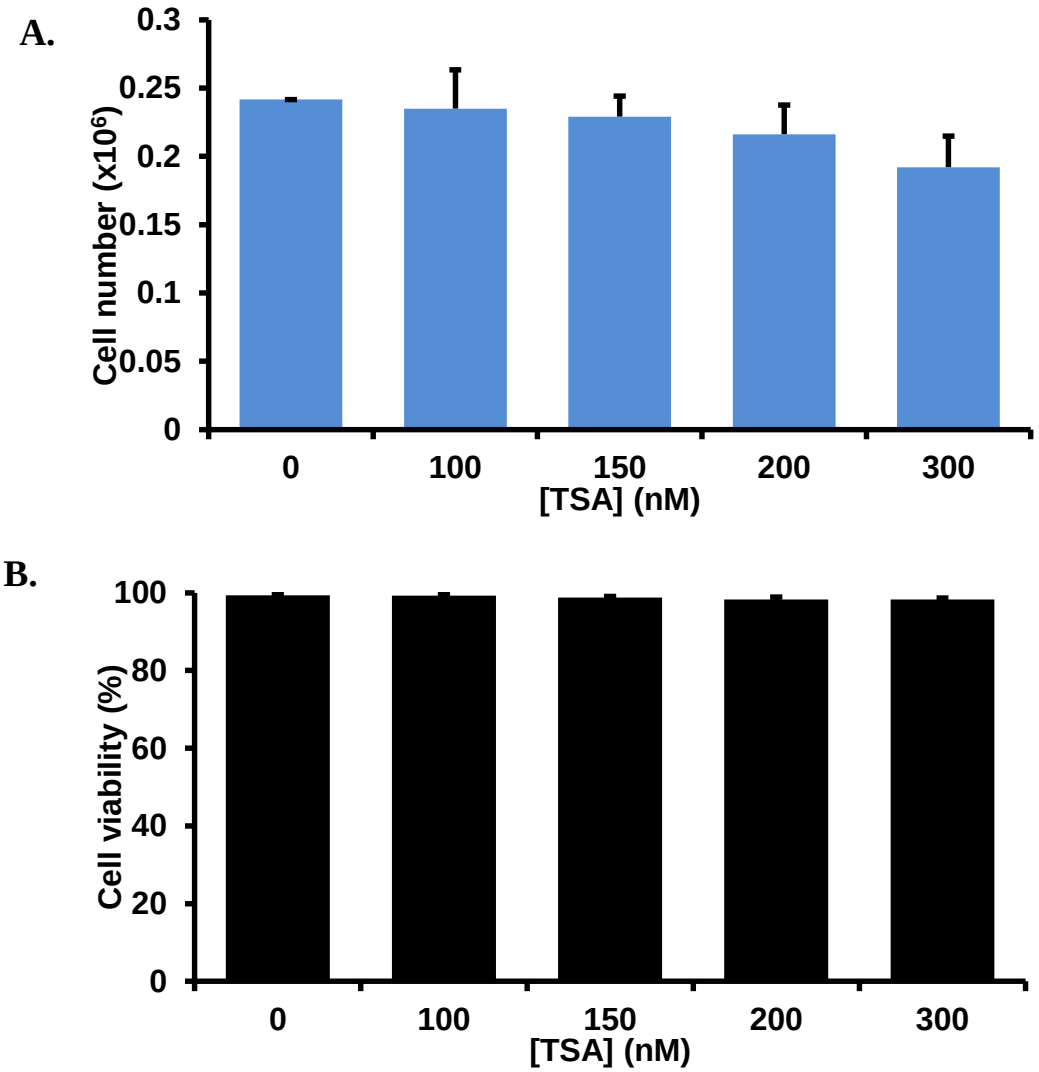

Figure 73: The TSA concentration – cell viability response for hPDLFs *in vitro*.
Data are mean ± SD (n = 3).

3.5.2.2 Time course curve for hPDLFs treated with 300 nm trichostatin A *in vitro*

Primary hPDLFs were treated for four days with (300 nm) trichostatin A. TSA causes no significant changes in the growth of the cells. After 24 hours, the growth of treated hPDLFs was stable compared with the control group. In day three and four, the growth started to decline by 10% compare to the controls but this was not significant - Figure 74.

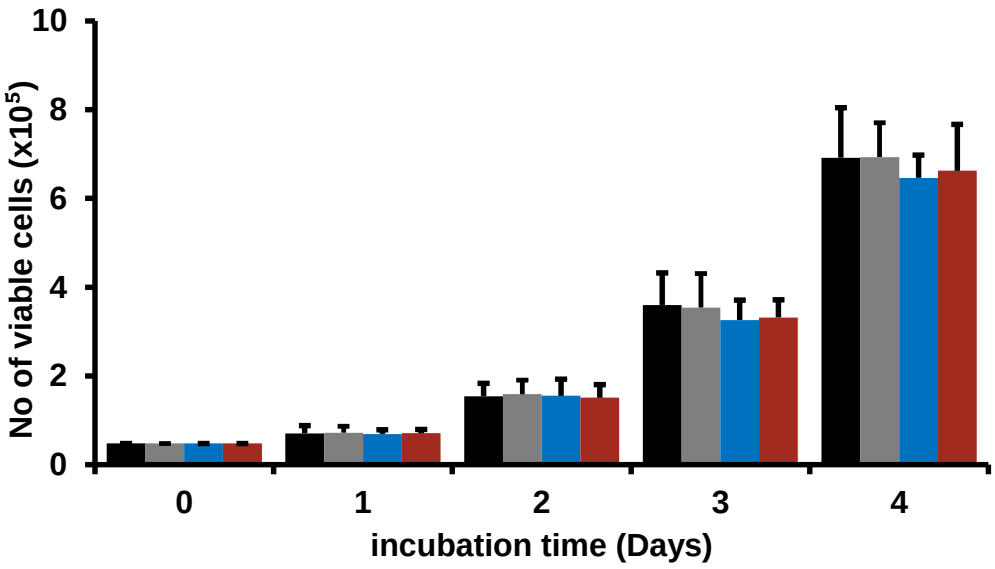

Figure 74: The viable cell number of treated and untreated hPDLFs with 300 nM of TSA over four days *in vitro*.
Key: , 8 mM glucose; , 25 mM glucose; , 8 mM glucose + 300 nM TSA and , 25 mM glucose + 300 nM TSA. Data are mean ± SD (n = 3).

3.5.3 The effect of inhibitors of deacetylases and high glucose on hPDLFs *in vitro*

3.5.3.1 The viability of hPDLFs treated with different concentrations of sirtuin 1&2 inhibitors *in vitro*

Sirt 1 inhibitor (EX-527)

Primary hPDLFs were incubated with and without 10 - 1000 nM EX-527 for 48 h and cell growth and viability assessed. At ≥ 100 nM EX-527 there was a decrease in PDLFs viable cell number and cell viability. This suggested that with addition of exogenous EX-527 of progressively increased concentration, there is initially growth arrest of hPDLFs and both growth arrest and cytotoxicity at ≥ 100 nM EX-527. The EX-527 concentration – cell growth response curve is shown in Figure 75 and the EX-527 concentration – cell viability response is given in Figure 76. From this the median growth inhibitory concentration GC_{50} value of EX-527 was 364 ± 38 nM and n, the logistic regression coefficient (also known as the Hill coefficient) was 2.04 ± 0.36. A growth curve of hPDLFs with and without 100 nM EX-527 was studied over 4 days in LG and HG.

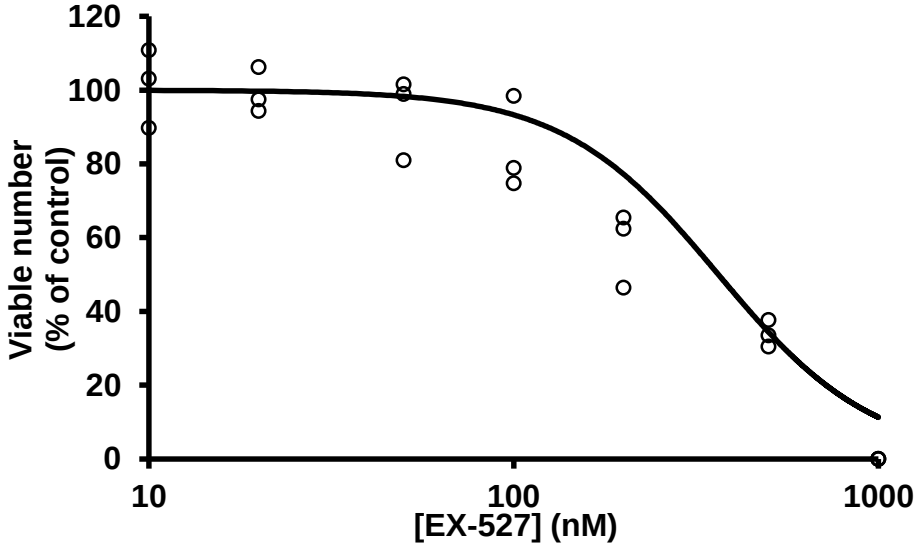

Figure 75: The EX-527 concentration – cell growth response curve for hPDLFs *in vitro.*
Data were fitted to the EX-527 concentration - response equation and solved for GC_{50} and n by non-linear regression. GC_{50} = 364 ± 38 nM, n = 2.04 ± 0.36 (N = 21).

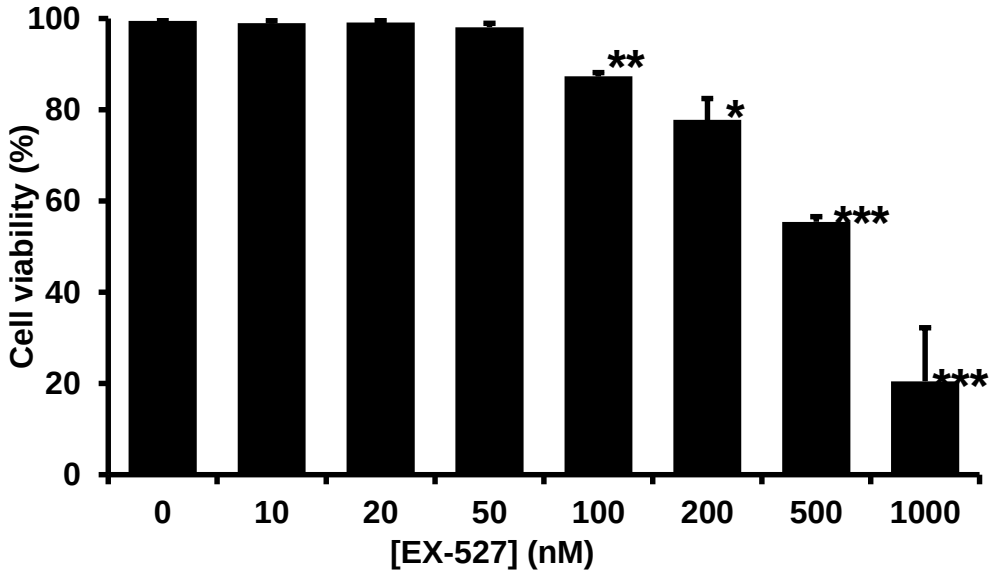

Figure 76: The EX-527 concentration – cell viability response for hPDLFs *in vitro.*
Data are mean ± SD (n = 3). Significant: *, P<0.05, **, P<0.01 and ***, P<0.001; *t-test.*

Sirt 2 inhibitor (AGK-2)

Primary hPDLFs were incubated with and without 0.5 - 20 µM AGK-2 for 48 h and cell growth and viability assessed. At ≥ 4 µM AGK-2 there was a decrease in PDLFs viable cell number and ≥ 8 µM AGK-2 there was decrease in cell viability. This suggested that with addition of exogenous AGK-2 of progressively increased concentration, there is initially growth arrest of hPDLFs and both growth arrest and cytotoxicity at ≥ 8 µM AGK-2. The AGK-2 concentration – cell growth response curve is shown in Figure 77 and the AGK-2 concentration – cell viability response is given in Figure 78. From this the median growth inhibitory concentration GC_{50} value of AGK-2 was 7.21 ± 0.38 µM and n, the logistic regression coefficient (also known as the Hill coefficient) was 2.24 ± 0.26. A growth curve of hPDLFs with and without 4 µM AGK-2 was studied over 4 days in LG and HG.

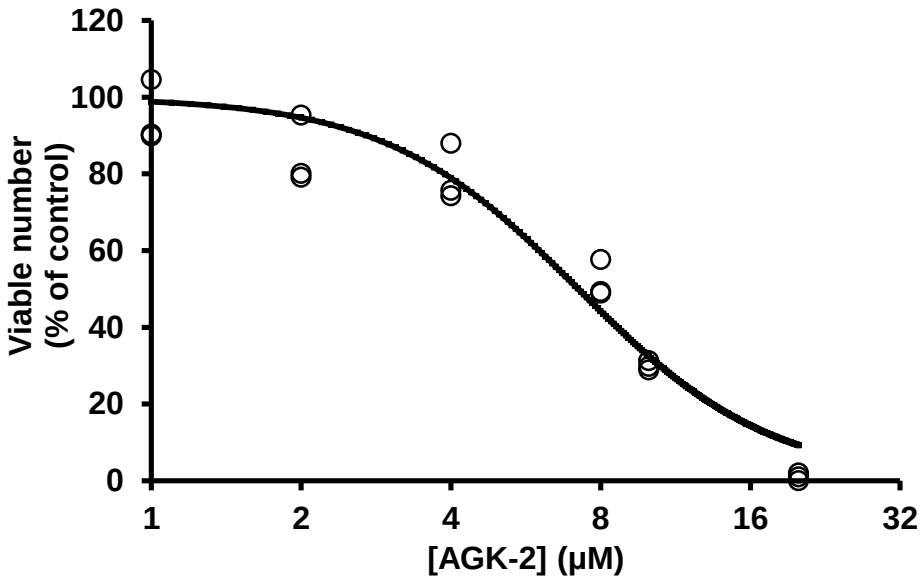

Figure 77: The AGK-2 concentration – cell growth response curve for hPDLFs *in vitro.*
Data were fitted to the EX-527 concentration - response equation and solved for GC_{50} and n by non-linear regression. GC_{50} = 7.21 ± 0.38 µM, n = 2.24 ± 0.26 (N = 24).

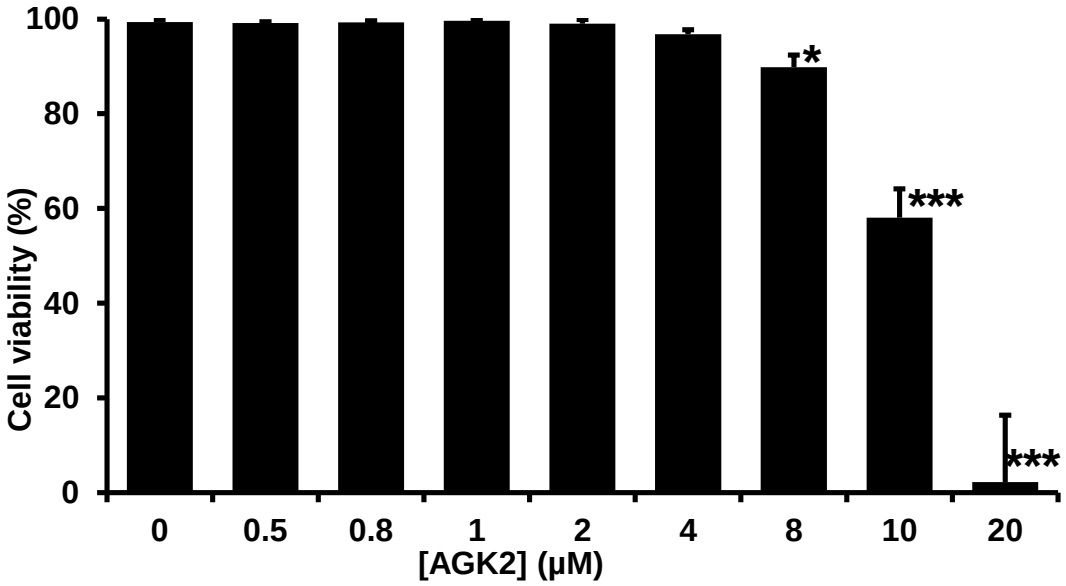

Figure 78: The AGK-2 concentration – cell viability response for hPDLFs *in vitro*.
Data are mean ± SD (n = 3). Significant: *, P<0.05 and ***, P<0.001; *t-test.*

3.5.3.2 Time course curve for hPDLFs treated sirtuin 1&2 inhibitors *in vitro*

Sirtuin 1 inhibitors EX-527

Primary hPDLFs were treated for 4 days with (100 nM) EX-527. EX-527 causes a no significant changes in the growth of the cells. After 24 hours, the growth of treated hPDLFs was stable compared with the control group. In day four the growth started to decline by *ca.* 15% compare to the controls but this was not significant - Figures 79.

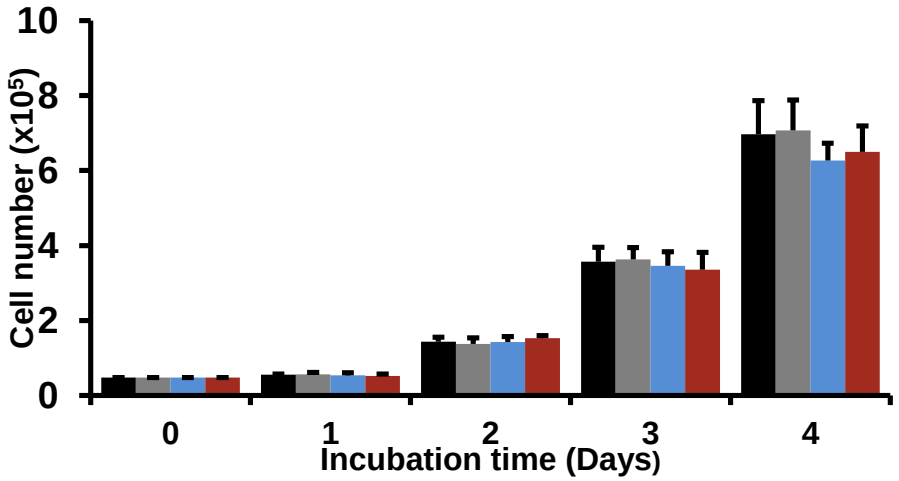

Figure 79: The viable cell number of treated and untreated hPDLFs with 100 nM of EX-527 over four days *in vitro*.
Key: , 8 mM glucose; , 25 mM glucose; , 8 mM glucose + 100 nM of EX-527 and ,25 mM glucose + 100 nM of EX-527. Data are mean ± SD (n = 3).

Sirtuin 2 inhibitors AGK-2

Primary hPDLFs were treated for four days with (4 µM) AGK-2. AGK-2 causes a no significant inhibition in the growth of the cells. The growth of treated hPDLFs was stable compared with the controls over 4 days of incubation with 4 µM AGK-2 – Figure 80.

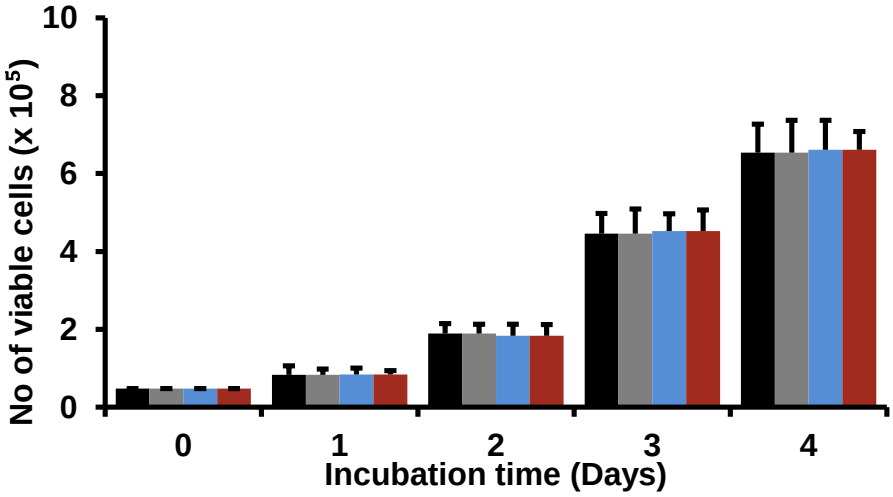

Figure 80: The viable cell number of treated and untreated hPDLFs with 4 µM of AGK-2 over four days *in vitro*.
Key: , 8 mM glucose; : , 25 mM glucose; , 8 mM glucose + 4 µM of AGK-2 and , 25 mM glucose + 4 µM of AGK-2. Data are mean ± SD (n = 3).

3.5.4 Effect of acetylation and deacetylation compound on glyoxalase 1 activity and gene expression in hPDLFs *in vitro*

No changes were found in SIRT1 and SIRT2 mRNA and protein levels in hPDLFs incubated in high glucose concentration, with respect to low glucose concentration control, and no effects of added tRSV – Table 46. Furthermore, the deacetylase and SIRT inhibitors had no effect on Glo1 activity and mRNA expression level in hPDLFs incubated in low and high glucose – Table 47, 48 and 49.

Table 46: the effect of *trans*-resveratrol and high glucose on SIRT1 and SIRT2 genes expression in hPDLFs *in vitro*.

Analyte	SIRT1 mRNA (normalized to β-actin mRNA)	SIRT2 mRNA (normalized to β-actin mRNA)
LG	0.653 ± 0.009	0.587 ± 0.032
LG+tRSV	0.642 ± 0.026	0.584 ± 0.010
HG	0.645 ± 0.012	0.586 ± 0.014
HG+tRSV	0.647 ± 0.013	0.602 ± 0.020

Data are mean ± SD, n = 4.

Table 47: Effect of TSA on glyoxalase 1 activity and gene expression in hPDLFs *in vitro*.

Analyte	Glo1 activity (mU/mg protein)	GLO1 mRNA (normalized to β-actin mRNA)
LG	914 ± 50	1.25 ± 0.002
LG + (TSA, 300 nM)	826 ± 87	1.27 ± 0.015
HG	538 ± 72**	1.27 ± 0.014
HG + (TSA, 300 nM)	484 ± 33**	1.27 ± 0.014

Data are mean ± SD, n = 4. Significance: **, P<0.01 (*t-test*) with respect to low glucose control.

Table 48: Effect of sirtuin 1 inhibitor on glyoxalase 1 activity and expression in hPDLFs *in vitro*

Analyte	Glo1 activity (mU/mg protein)	GLO1 mRNA (normalized to β-actin mRNA)
LG	920 ± 60	1.24 ± 0.021
LG + (EX-527, 100 nM)	817 ± 42	1.24 ± 0.013
HG	529 ± 39**	1.24 ± 0.035
HG + (EX-527, 100 nM)	466 ± 52**	1.22 ± 0.035

Data are mean ± SD, n = 4. Significance: ***, P<0.001 with respect to low glucose control *(t-test).*

Table 49: Effect of sirtuin 2 inhibitor on glyoxalase 1 activity and expression in hPDLFs *in vitro*

Analyte	Glo1 activity (mU/mg protein)	GLO1 mRNA (normalized to β-actin mRNA)
LG	989 ± 47	1.24 ± 0.021
LG + (AGK-2, 4 µM)	858 ± 88	1.24 ± 0.002
HG	531 ± 75**	1.24 ± 0.009
HG + (AGK-2, 4 µM)	475 ± 46**	1.24 ± 0.009

Data are mean ± SD, n = 4. Significance: **, P<0.01 with respect to low glucose control *(t-test)*.

3.6 Studying the modification of cytosolic proteins in hPDLFs: high mass resolution proteomics analysis

Primary hPDLFs cells were cultured in low and high glucose in triplicate for 3 days. Cytosolic protein was subjected to trypsin and tryptic peptides were analysed in high resolution mass spectrometer Orbitrap for identification of the protein and the changes occurring to the proteome in high glucose concentration. Reproducibility of the biological replicates was examined and found high correlation within the low and high glucose groups. In this study two proteomic software programmes were used to analyse and quantify proteomics data.

1. Scaffold

This is a bioinformatics tool for validation of proteomics data. The scaffold analysis workflow combines several peptides and protein validation methods after an initial data-base search engine analysis using MASCOT and SEQUEST. The search engine analyses peptide molecular ion and fragment ion series spectra to produce probability scores of peptide and protein identification (Searle, 2010). The total identified proteins by Scaffold in all 3 replicates of hPDLFs cultures in low and high glucose are given in Figure 81A. Mascot searches based on MS^2 data is required to identify peptides and protein in Scaffold. This analysis cannot quantify peptide ion responses and related amounts of peptides and proteins in the samples.

2. Progenesis

This is a second software programme used in this study to quantify peptides and proteins that requires both MS^1 and MS^2 data. Progenesis is a simple and more popular software for label free quantification compare to MaxQuant software. Non-conflicting peptides were used for label-free quantification in Progenesis. A total of 1105 cytosolic protein were quantified and identified in hPDLFs. There are 1077 proteins were found in the cytosol of hPDLFs in both low and high glucose concentration conditions - Figure 81B. The spectra of 16 proteins were found only in low glucose and 12 proteins only in high glucose culture of hPDLFs suggesting a relatively low abundance of these proteins in low and high glucose cultures – Figure 81.

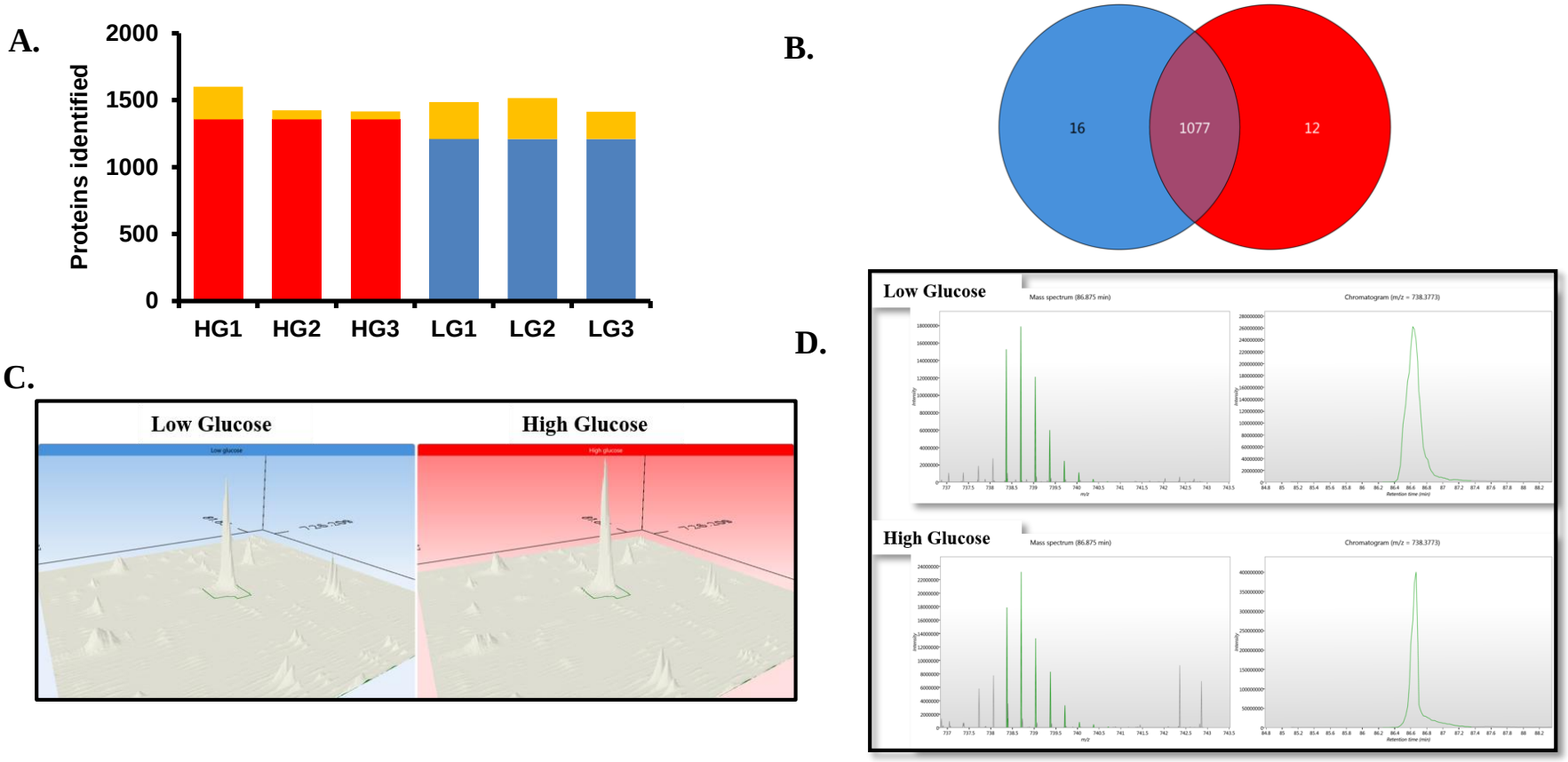

Figure 81: Proteome analysis of hPDLFs cell lysate cultured in low and high glucose.
Cell lysate (triplicate) from low and high glucose culture was digested, each sample was analysed by LCMS on Orbitrap. (A) Number of protein identification (in Scaffold) without match between runs (yellow) and with match between runs option (red and blue). (B) Total proteome identified and quantified in Progenesis. (C)3D and (D)1D image of a peptide of GAPDH. The peptide sequence of GAPDH is IISAPSADAPMFVMGVNHEK. Data are mean ± SD, n = 3. Blue colour indicates low glucose and red colour indicates high glucose

A specimen of 3D and 1D image of a peptide of GAPDH - VIISAPSADAPMFVMGVNHEK - found in low and high glucose conditions is given in Figure 81. The cluster of all identified proteins in two conditions is shown in Figure 82.

The level of *ca.* 39 of 1077 proteins identified in low and high glucose concentration conditions were changed significantly: 18 proteins in hPDLFs cytosol were up regulated in high glucose - including Putative adenosylhomocysteinase involved in 143 molecular and biological pathways identified using Reactome.org for ontology analysis. This protein is also involved in many signalling pathways e.g. signalling by VEGF and FGFR1- 4, innate immunity system, muscle contraction and regulation of insulin signalling. Other protein like Hexokinase was expected to be up regulated in high glucose because of its roles in glycolysis, glucose transport and metabolism, regulation of gene expression in beta cells and beta cells development etc. Twenty one proteins were down regulated in hPDLFs cell lysate from cells incubated in high glucose concentration. Only 13 proteins were identified by the Reactome pathway analysis programme and placed these proteins in 116 pathways. HMGB1, involved in inflammation, was found to be decreased in the hPDLFs cell lysate when cultured in high glucose concentration. A list of the down- regulated and up-regulated proteins is given in Table 50.

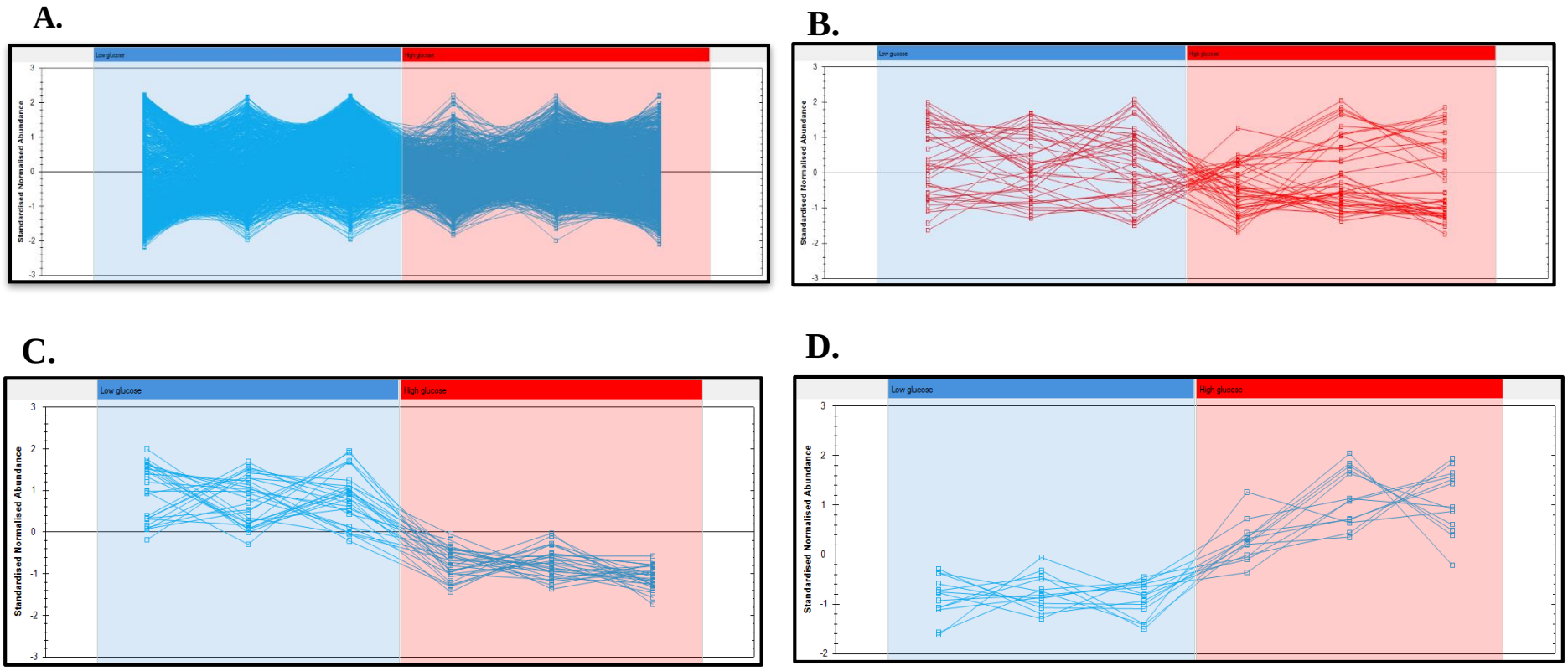

Figure 82: Protein cluster.
(A) All identified proteins in two conditions (B) 39 protein change significantly in low and high glucose. (C) down and (C) up regulated in HG. Blue colour indicates low glucose and red colour indicates high glucose.

Table 50: Cytosolic proteins down and up regulated significantly in hPDLFs incubated in high glucose concentration.

Protein accession numbers	Protein name	Gene accession numbers	Log 2 (change)	Unique peptide	Percentage sequence coverage	Anova (p)
CND1	Condensin complex subunit 1	NCAPD2		2	5.4%	0.016
Q99707	Methionine synthase	MTR		2	2.5%	0.016
P43034	Platelet-activating factor acetylhydrolase IB subunit alpha	PAFAH1B1		5	32.2%	0.000
Q12797	Aspartyl/asparaginyl beta-hydroxylase	ASPH		1	2.4%	0.027
A8MTY9	Down syndrome critical region protein 3	DSCR3		2		0.033
Q32Q12	Nucleoside diphosphate kinase	NME1-NME2		2	30.7%	0.036
HMGB1	High mobility group protein B1	HMGB1		4	26.5%	0.023
O14617	Isoform 5 of AP-3 complex subunit delta-	AP3D1		7	10.1%	0.046
I3L459	Phosphatidylinositol transfer protein alpha isoform	PITPNA		1	29.6%	0.050
ARC1B	Actin-related protein 2/3 complex subunit 1B	ARPC1B		6	32.8%	0.021
Q9BRP8-2	Isoform 2 of Partner of Y14 and mago	WIBG		2	25.0%	0.014
Q96HC4	PDZ and LIM domain protein 5	PDLIM5		6	15.9%	0.027
O95816	BAG family molecular chaperone regulator 2	BAG2		3	33.6%	0.021
Q9H3H3-2	Isoform 2 of UPF0696 protein C11orf68	C11orf68		2	14.4%	0.036
HOOK3	Protein Hook homolog 3	HOOK3		4	10.3%	0.046
C9J0J7	Profilin-2	PFN2		2	49.5%	0.041
Q9UHD8-2	Isoform 2 of Septin-9	SEPT9		19		0.048
Q9NUQ8-2	Isoform 2 of ATP-binding cassette sub-family F member 3	ABCF3		2	5.4%	0.044
P63241-2	Isoform 2 of Eukaryotic translation initiation factor 5A-1	EIF5A		11	32.1%	0.017
COMD8	COMM domain-containing protein 8	COMMD8		2	8.2%	0.012
MOES	Moesin	MSN		25	40.6%	0.012
A0A087X0S5	Collagen alpha-1(VI) chain	COL6A1		20	28.5%	0.017
LYPA2	Acyl-protein thioesterase 2	LYPLA2		2	22.1%	0.033
E5RIH5	TELO2-interacting protein 2	TTI2		2	4.4%	0.019

P98082-3	Isoform 3 of Disabled homolog 2	DAB2		4		0.048
O43865	Putative adenosylhomocysteinase 2	AHCYL1		2	11.7%	0.040
Q14240-2	Isoform 2 of Eukaryotic initiation factor 4A-II	EIF4A2		6	34.6%	0.017
TBL1R	F-box-like/WD repeat-containing protein TBL1XR1	TBL1XR1		4	15.4%	0.012
Q05519-2	Isoform 2 of Serine/arginine-rich splicing factor 11	SRSF11		2	6.0%	0.036
G3XAI2	Laminin subunit beta-1	LAMB1		3	3.5%	0.033
Q14697-2	Isoform 2 of Neutral alpha-glucosidase AB	GANAB		3	36.1%	0.030
Q9UMX0	Ubiquilin-1	UBQLN1		2	14.1%	0.031
E9PB90	Hexokinase	HK2		2	3.4%	0.024
O15085-2	Isoform 2 of Rho guanine nucleotide exchange factor 11	ARHGEF11		2		0.043
A0A087X0I4	Coatomer subunit epsilon	COPE		3	48.2%	0.034
P38117-2	Isoform 2 of Electron transfer flavoprotein subunit beta	ETFB		2	25.5%	0.026
Q96BJ3	Axin interactor, dorsalization-associated protein	AIDA		2	17.6%	0.027
Q7Z6Z7	E3 ubiquitin-protein ligase HUWE1	HUWE1		4	9.2%	0.026
ABCE1	ATP-binding cassette sub-family E member 1	ABCE1		2	19.0%	0.012

Data are mean ± SD, n = 3. Down regulated proteins upregulated proteins.

Sixteen proteins were found only in hPDLFs in low glucose incubations – Table 51. One of these proteins is isoform 2 of glycogen synthase kinase-3 beta which is involved in many molecular functions. It contributes to NF-κB binding and p53 binding which function as dimeric transcription factors that regulate the expression of genes influencing a broad range of biological processes including innate and adaptive immunity, inflammation, stress responses, B-cell development, and lymphoid organogenesis (Perkins, 2006). In addition, aldehyde dehydrogenase, dimeric NADP-preferring is found in low glucose incubation. It catalyzes oxidation-reduction (redox) reaction in which an aldehyde or ketone (oxo) group acts as a hydrogen or electron donor and reduces NAD or NADP (Ko et al., 2012).

On the other hand, twelve proteins were detected uniquely in hPDLFs incubated in high glucose – Table 52. Isoform 3 of E3 ubiquitin-protein ligase is one of the identified proteins and it involves in NF-κB signaling pathway. As it mentioned previously, NF-κB signaling pathway influences a broad range of biological processes. In addition, isoform 5 of glycogen debranching enzyme was detected in high glucose incubation. It has a role in glucose metabolism and glycogen breakdown.

Table 51: Proteins detected in cytosolic extracts of hPDLFs only when incubated in low glucose concentration.

Protein accession numbers	Protein name	Gene accession numbers	GO: molecular function
O15085-2	Isoform 2 of Rho guanine nucleotide exchange factor 11	ARHGEF11	G-protein coupled receptor binding, GTPase activator activity and Rho guanyl-nucleotide exchange factor activity
H0YBD7	Heterogeneous nuclear ribonucleoprotein H	HNRNPH1	Nucleic acid binding and nucleotide binding
Q9UKV8-2	Isoform 2 of Protein argonaute-2	AGO2	Core promoter binding, double-stranded RNA binding, endoribonuclease activity, endoribonuclease activity, cleaving miRNA-paired mRNA, endoribonuclease activity, cleaving siRNA-paired mRNA, metal ion binding, miRNA binding, mRNA binding, poly(A) RNA binding, protein C-terminus binding, RNA 7-methylguanosine cap binding, RNA polymerase II core binding, single-stranded RNA binding, siRNA binding and translation initiation factor activity
Q5SSJ5	Heterochromatin protein 1-binding protein 3	HP1BP3	DNA binding and nucleosome binding
Q99879	Histone H2B type 1-M	HIST1H2BM	DNA binding
P61764-2	Isoform 2 of Syntaxin-binding protein 1	STXBP1	Identical protein binding, poly(A) RNA binding, SNARE binding, syntaxin-1 binding and syntaxin binding
E9PNN6	Aldehyde dehydrogenase, dimeric NADP-preferring	ALDH3A1	3-chloroallyl aldehyde dehydrogenase activity
A0A0A0MRM8	Unconventional myosin-VI	MYO6	ATP binding and motor activity
A0A087WWE2	DNA-directed RNA polymerase	POLR2A	Core promoter binding and DNA-directed RNA polymerase activity
K7EMW4	Nicalin	NCLN	Protein destabilization, regulation of protein complex assembly and regulation of signal transduction
O94992	Protein HEXIM1	HEXIM1	7SK snRNA binding, cyclin-dependent protein serine/threonine kinase

			inhibitor activity and snRNA binding
O15344-2	Isoform 2 of E3 ubiquitin-protein ligase Midline-1	MID1	Identical protein binding, ligase activity, microtubule binding, phosphoprotein binding, protein heterodimerization activity, protein homodimerization activity, ubiquitin protein ligase binding and zinc ion binding
C9JEJ2	Choline-phosphate cytidylyltransferase A	PCYT1A	Catalytic activity
Q5JSL3	Dedicator of cytokinesis protein 11	DOCK11	Rho guanyl-nucleotide exchange factor activity
A0A087WWM0	Trafficking protein particle complex subunit 3	TRAPPC3	ER to Golgi vesicle-mediated transport
P49841-2	Isoform 2 of Glycogen synthase kinase-3 beta	GSK3B	ATP binding, beta-catenin binding, kinase activity, NF-κB binding, p53 binding, protein kinase A catalytic subunit binding, protein kinase binding, protein serine/threonine kinase activity, RNA polymerase II transcription factor binding, au-protein kinase activity and ubiquitin protein ligase binding

Data are mean ± SD, n = 3.

Table 52: Proteins detected in cytosolic extracts of hPDLFs only when incubated in high glucose concentration.

Protein accession numbers	Protein name	Gene accession numbers	GO: molecular function
Q05519-2	Isoform 2 of Serine/arginine-rich splicing factor 11	SRS11	RNA splicing, Transport of Mature Transcript to Cytoplasm etc
A0A0C4DGQ5	Calpain small subunit 1	CAPNS1	Ca2+ binding, Proteolysis
E7EMW7	E3 ubiquitin-protein ligase UBR5	UBR5	Ligase, Ubl conjugation pathway, Ubiquitin-protein transferase activity
Q96EP0-3	Isoform 3 of E3 ubiquitin-protein ligase	RNF31	TNFR1-induced NFκB signalling pathway death Receptor Signalling, Regulation of TNFR1 signalling
P35222	Catenin beta-1	CTNNB1	Cell-cell communication, developmental biology, disease, immune system, metabolism of proteins and signal transduction, apoptosis etc.
Q9NS86	LanC-like protein 2	LANCL2	ATP binding, catalytic activity, Positive regulation of absciasic acid activated signalling etc.
P33991	DNA replication licensing factor MCM4	MCM4	Cell cycle and DNA replication
P35573-2	Isoform 5 of Glycogen debranching enzyme	AGL	Glucose metabolism, Glycogen breakdown
P23634-6	Isoform XB of Plasma membrane calcium-transporting ATPase 4	ATP2B4	Platelet calcium homeostasis, Platelet and ion homeostasis, Cardiac conduction, etc
Q52LW3	Rho GTPase-activating protein 29	ARHGAP29	Signal transduction, Rho GTPase cycle
Q9NQZ2	Something about silencing protein 10	UTP3	Chromatin regulator, Developmental protein
P49750-4	Isoform 4 of YLP motif-containing protein 1	YLPM1	Repressor, transcription, transcription regulation

Data are mean ± SD, n = 3.

Thirty proteins were found modified in hPDLFs. Ten of these proteins were found modified in hPDLFs in low glucose incubation and twenty proteins were detected in high glucose incubations – Table 53 and 54. A total of 173 proteins were modified by MG-H1 were detected in the positive control, where hPDLFs cell lysate incubated with MG – Table 55. Vimentin protein is found modified in the positive control, low incubation and high incubation. There are two other proteins found modified in positive control and in high incubation includes the following; isoform SV of 14-3-3 protein epsilon and actin cytoplasmic 2. Isoform SV of 14-3-3 protein epsilon was modified by CEL in peptide k3. Actin cytoplasmic 2 protein share the same modified peptide (r21) with the positive control. This protein involves in the following biological process: ATP binding, protein binding, structural constituent of cytoskeleton and ubiquitin protein ligase binding. There is one protein was modified by MG-H1 in low and high incubation which is echinoderm microtubule-associated protein-like 1.

Table 53: Modified proteins in cytosolic extracts of hPDLFs incubated in low glucose concentration.

Protein accession numbers	Protein name	Gene accession numbers	Percentage sequence coverage	Variable modifications identified by spectrum
P62310	U6 snRNA-associated Sm-like protein LSm3	LSM3	20.6%	MG-H1:r1
E9PEB9	Dystonin	DST	4.79%	MG-H1:r9
Q6UXN9	WD repeat-containing protein 82	WDR82	8.95%	MG-H1:r8
P08670	Vimentin	VIM	62.7%	FL:k1 and k2
Q9P2R6	Arginine-glutamic acid dipeptide repeats protein	RERE	3.00%	MG-H1:r16, r7 and FL:k5
F8W717	Echinoderm microtubule-associated protein-like 1	EML1	4.73%	MG-H1:r12
P19525	Interferon-induced, double-stranded RNA-activated protein kinase	EIF2AK2	9.07%	FL:k10 and k11
P23921	Ribonucleoside-diphosphate reductase large subunit	RRM1	10.4%	FL:k8
Q5SW96	Low density lipoprotein receptor adapter protein 1	LDLRAP1	8.77%	MG-H1:r13
Q8IVF2	Protein AHNAK2	AHNAK2	0.86%	MG-H1:r11

Data are mean ± SD, n = 3

Table 54: Modified proteins in cytosolic extracts of hPDLFs incubated in high glucose concentration.

Protein accession numbers	Protein name	Gene accession numbers	Percentage sequence coverage	Variable modifications identified by spectrum
Q04446	1,4-alpha-glucan-branching enzyme	GBE1	27.8%	CML:K9
Q60FE5	Filamin A	FLNA	45.0%	CML:k13 and MG-H1:r8
Q2TAL8	Glutamine-rich protein 1	QRICH1	3.35%	MG-H1:r5
Q01780-2	Isoform 2 of Exosome component 10	EXOSC10	3.60%	FL:k6
Q96KG9-2	Isoform 2 of N-terminal kinase-like protein	SCYL1	8.22%	CML:k3, k9 and r8
P35659-2	Isoform 2 of Protein DEK	DEK	14.4%	CEL:k21
P08237	Isoform 3 of ATP-dependent 6-phosphofructokinase, muscle type	PFKM	16.2%	FL:k7
P62258-2	Isoform SV of 14-3-3 protein epsilon	YWHAE	64.4%	CEL:k3
E7EVA0	Microtubule-associated protein	MAP4	14.7%	CEL:k8
P27816	Microtubule-associated protein 4	MAP4	33.1%	CEL:k8
A0A0A0MT60	Peptidyl-prolyl *cis*-trans isomerase	FKBP15	7.72%	CEL:k11
Q5TZA2	Rootletin	CROCC	0.000%	CEL:k6
P63313	Thymosin beta-10	TMSB10	50.0%	CML:k3
P60709	Actin, cytoplasmic 1	ACTB	64.0%	MG-H1:r21
Q9UL25	Ras-related protein Rab-21	RAB21	22.7%	MG-H1:r10
P23921	Ribonucleoside-diphosphate reductase large subunit	RRM1	7.95%	FL:k8
P08670	Vimentin	VIM	64.2%	FL:k1, k4 and k2
P63261	Actin, cytoplasmic 2	ACTG1	64.0%	MG-H1:r21
F8W717	Echinoderm microtubule-associated protein-like 1	EML1	1.49%	MG-H1:r12
Q9H2D6	TRIO and F-actin-binding protein	TRIOBP	1.99%	MG-H1:r2, r6 and r10

Data are mean ± SD, n = 3.

Table 55: Proteins with MG-H1 residues modification in cytosolic extracts of hPDLFs incubated with exogenous methylglyoxal (MG modification positive control).

Protein accession numbers	Protein name	Gene accession numbers	Percentage sequence coverage	RMG-H1 (+54.01) identified
P62857	Ribosomal protein S28	RPS28	46.4%	r11
P60468	Protein transport protein Sec61 subunit beta	SEC61B	30.2%	r28
P06703	Protein S100-A6	S100A6	88.9%	r8, r15, r8 and r15
P61604	10 kDa heat shock protein, mitochondrial	HSPE1	53.9%	r6 and r7
P60903	Protein S100-A10	S100A10	76.3%	r4
Q15836	Vesicle-associated membrane protein 3	VAMP3	24.0%	r7
Q99584	Protein S100-A13	S100A13	25.5%	r6
P05387	60S acidic ribosomal protein P2	RPLP2	93.0%	r13
P31949	Protein S100-A11	S100A11	85.7%	r7 and r9
P09382	Galectin-1	LGALS1	82.2%	r10, r12 and r4
P07737	Profilin-1	PFN1	35.0%	r14
P08708	40S ribosomal protein S17	RPS17	17.0%	r1
Q14019	Coactosin-like protein	COTL1	41.5%	r16
A0A0A0MTI5	Acyl-CoA-binding protein	DBI	32.2%	r11
Q8NI22	Multiple coagulation factor deficiency protein 2	MCFD2	68.5%	r24
P63241	Eukaryotic translation initiation factor 5A-1	EIF5A	50.6%	r1
F5H265	Polyubiquitin-C	UBC	45.0%	r9, r11 and r6
P61088	Ubiquitin-conjugating enzyme E2 N	UBE2N	38.2%	r4
P62937	Peptidyl-prolyl *cis*-trans isomerase A	PPIA	47.9%	r15
P63208	S-phase kinase-associated protein 1	SKP1	55.8%	r1
P14209	CD99 antigen	CD99	31.9%	r14
P49006	MARCKS-related protein	MARCKSL1	69.2%	r3
A0A087X271	Calponin	CNN2	33.5%	r5

Q99497	Protein deglycase DJ-1	PARK7	57.1%	r7
P30086	Phosphatidylethanolamine-binding protein 1	PEBP1	61.0%	r2
Q8WZA0	Protein LZIC	LZIC	23.7%	r8
O00264	Membrane-associated progesterone receptor component 1	PGRMC1	57.9%	r3
E7EMB3	Calmodulin	CALM2	47.4%	r13 and r44
P37802	Transgelin-2	TAGLN2	61.8%	r9
Q01995	Transgelin	TAGLN	43.3%	r7and r6
E9PK25	Cofilin-1	CFL1	49.5%	r3
P04792	Heat shock protein beta-1	HSPB1	46.3%	r17
P52565	Rho GDP-dissociation inhibitor 1	ARHGDIA	50.5%	r16
P23284	Peptidyl-prolyl *cis*-trans isomerase B	PPIB	55.1%	r11 and r9
Q9H299	SH3 domain-binding glutamic acid-rich-like protein 3	SH3BGRL3	14.6%	r8
O15173	Membrane-associated progesterone receptor component 2	PGRMC2	34.1%	r2
P09936	Ubiquitin carboxyl-terminal hydrolase isozyme L1	UCHL1	44.8%	r18
P49755	Transmembrane emp24 domain-containing protein 10	TMED10	35.6%	r4
P30041	Peroxiredoxin-6	PRDX6	53.1%	r9
Q8TEA8	D-tyrosyl-tRNA(Tyr) deacylase	DTD1	32.7%	r5
F8W1A4	Adenylate kinase 2, mitochondrial	AK2	41.4%	r17
O00299	Chloride intracellular channel protein 1	CLIC1	56.4%	r27
Q9BVK6	Transmembrane emp24 domain-containing protein 9	TMED9	25.5%	r2
P78417	Glutathione S-transferase omega-1	GSTO1	32.0%	r3
P30048	Thioredoxin-dependent peroxide reductase, mitochondrial	PRDX3	29.7%	r4
P63104	14-3-3 protein zeta/delta	YWHAZ	71.0%	r5, r6 and r4
P67936	Tropomyosin alpha-4 chain	TPM4	53.6%	r11
P30040	Endoplasmic reticulum resident protein 29	ERP29	44.4%	r1
P06753-2	Isoform 2 of Tropomyosin alpha-3 chain	TPM3	33.1%	r10
P62258	14-3-3 protein epsilon	YWHAE	62.7%	r10
B1AK87	Capping protein (Actin filament) muscle Z-line, beta,	CAPZB	67.3%	r2

	isoform CRA_a			
P09651-3	Isoform 2 of Heterogeneous nuclear ribonucleoprotein A1	HNRNPA1	50.2%	r20, r10 and r1
P22392-2	Isoform 3 of Nucleoside diphosphate kinase B	NME2	46.1%	r2
O15260	Surfeit locus protein 4	SURF4	7.81%	r18
P21796	Voltage-dependent anion-selective channel protein 1	VDAC1	58.0%	r2, and r19
Q07021	Complement component 1 Q subcomponent-binding protein, mitochondrial	C1QBP	40.8%	r14
P30084	Enoyl-CoA hydratase, mitochondrial	ECHS1	47.9%	r11
P29966	Myristoylated alanine-rich C-kinase substrate	MARCKS	47.6%	r7
P45880	Voltage-dependent anion-selective channel protein 2	VDAC2	47.3%	r16
P06748	Nucleophosmin	NPM1	37.8%	r14
Q9P0L0-2	Isoform 2 of Vesicle-associated membrane protein-associated protein A	VAPA	19.7%	r2
Q99623	Prohibitin-2	PHB2	27.1%	r9
P00387	NADH-cytochrome b5 reductase 3	CYB5R3	45.2%	r17 and r19
P40926	Malate dehydrogenase, mitochondrial	MDH2	52.4%	r6 and r7
P09525	Annexin A4	ANXA4	36.7%	r15 and r27
P08758	Annexin A5	ANXA5	72.5%	r3 and r15
P04406	Glyceraldehyde-3-phosphate dehydrogenase	GAPDH	66.3%	r14
P07195	L-lactate dehydrogenase B chain	LDHB	70.1%	r9 and r22
P00338	L-lactate dehydrogenase A chain	LDHA	63.0%	r9
P51665	26S proteasome non-ATPase regulatory subunit 7	PSMD7	57.1%	r17
P22626	Heterogeneous nuclear ribonucleoproteins A2/B1	HNRNPA2B1	37.1%	r10 and r16
Q96D15	Reticulocalbin-3	RCN3	48.5%	r13
P37837	Transaldolase	TALDO1	42.4%	r9
P07355	Annexin A2	ANXA2	65.8%	r24
P04083	Annexin A1	ANXA1	64.5%	r11 and r16
Q15293	Reticulocalbin-1	RCN1	62.8%	r12 and r4

B4DY09	Interleukin enhancer-binding factor 2	ILF2	54.0%	r23
P04075	Fructose-bisphosphate aldolase A	ALDOA	66.2%	r8 and r1
B4DFG0	Protein DEK	DEK	15.6%	r8
Q15019	Septin-2	SEPT2	19.9%	r14
P63261	Actin, cytoplasmic 2	ACTG1	83.7%	r21 and r13
Q70UQ0-4	Isoform 4 of Inhibitor of nuclear factor kappa-B kinase-interacting protein	IKBIP	38.7%	r1 and r15
Q6NZI2	Polymerase I and transcript release factor	PTRF	27.2%	r18
Q13561	Dynactin subunit 2	DCTN2	62.8%	r15
P00558	Phosphoglycerate kinase 1	PGK1	63.1%	r7, r15 and r10
E9PBS1	Multifunctional protein ADE2	PAICS	17.2%	r12
P52597	Heterogeneous nuclear ribonucleoprotein F	HNRNPF	21.9%	r3
O60664-4	Isoform 4 of Perilipin-3	PLIN3	36.7%	r15 and r14
G5E972	Lamina-associated polypeptide 2, isoforms beta/gamma	TMPO	18.1%	r16
P05455	Lupus La protein	SSB	29.2%	r6
Q9BS26	Endoplasmic reticulum resident protein 44	ERP44	26.8%	r15 and r8
P06733	Alpha-enolase	ENO1	70.5%	r4
Q8NBS9	Thioredoxin domain-containing protein 5	TXNDC5	55.8%	r16
Q15084	Protein disulfide-isomerase A6	PDIA6	47.7%	r11, r24, r10 and r2
P27797	Calreticulin	CALR	79.1%	r13, r9 and r15
P36957	Dihydrolipoyllysine-residue succinyltransferase component of 2-oxoglutarate dehydrogenase complex, mitochondrial	DLST	38.9%	r11
P68104	Elongation factor 1-alpha 1	EEF1A1	48.1%	r12
P07954-2	Isoform Cytoplasmic of Fumarate hydratase, mitochondrial	FH	45.8%	r18
A0A087WSV8	Nucleobindin 2, isoform CRA_b	NUCB2	41.7%	r2
B4DJV2	Citrate synthase	CS	22.7%	r2 and r16
P50395	Rab GDP dissociation inhibitor bet	GDI2	54.8%	r3
E9PAM4	Uncharacterized protein	E9PAM4	4.55%	r1

Q01518	Adenylyl cyclase-associated protein 1	CAP1	37.9%	r12
P07099	Epoxide hydrolase 1	EPHX1	24.6%	r23
P52209	6-phosphogluconate dehydrogenase, decarboxylating	PGD	39.1%	r5
P08670	Vimentin	VIM	77.7%	r2, r5, r10, r16, r37, r22, r8, r7, r5 and r9
C9J813	Caldesmon	CALD1	26.8%	r7
P50995	Annexin A11	ANXA11	25.1%	r15
P06576	ATP synthase subunit beta, mitochondrial	ATP5B	28.7%	r24
P30101	Protein disulfide-isomerase A3	PDIA3	52.5%	r15 and r10
P07237	Protein disulfide-isomerase	P4HB	70.9%	r6, r15, r1 and r16
P49257	Protein ERGIC-53	LMAN1	32.9%	r1
P14618	Pyruvate kinase PKM	PKM	42.4%	r16
C9JIZ6	Prosaposin	PSAP	12.7%	r7
P25705	ATP synthase subunit alpha, mitochondrial	ATP5A1	32.2%	r17 and r1
K7ELL7	Glucosidase 2 subunit beta	PRKCSH	38.5%	r2, r19 and r13
P13674	Prolyl 4-hydroxylase subunit alpha-1	P4HA1	43.6%	r4 and r1
P10809	60 kDa heat shock protein, mitochondrial	HSPD1	53.2%	r25 and r1
P00367	Glutamate dehydrogenase 1, mitochondrial	GLUD1	45.9%	r13, r4 and r6
P31948	Stress-induced-phosphoprotein 1	STIP1	34.1%	r4
A0A0A0MTS2	Glucose-6-phosphate isomerase	GPI	33.9%	r7 and r9
Q07065	Cytoskeleton-associated protein 4	CKAP4	63.0%	r6, r1, r24, r18 and r16
P26038	Moesin	MSN	52.5%	r10, r17 and r21
P04843	Dolichyl-diphosphooligosaccharide--protein glycosyltransferase subunit1	RPN1	38.7%	r12
O60506	Heterogeneous nuclear ribonucleoprotein Q	SYNCRIP	35.5%	r3, r18 and r5
E7EX17	Eukaryotic translation initiation factor 4B	EIF4B	13.5%	r28
P12956	X-ray repair cross-complementing protein 6	XRCC6	44.3%	r1
P49748	Very long-chain specific acyl-CoA dehydrogenase,	ACADVL	23.5%	r13

	mitochondrial			
P11142	Heat shock cognate 71 kDa protein	HSPA8	56.8%	r12, r5, r14 and r18
P11021	78 kDa glucose-regulated protein	HSPA5	64.1%	r12, r6, r2, r18, r17, r9, r15, r5 and r14
P13667	Protein disulfide-isomerase A4	PDIA4	56.4%	r6, r10, r12 r2 and r4
P38646	Stress-70 protein, mitochondrial	HSPA9	45.7%	r12, r9, r2, r4, r3, r14, r19 and r11
P02545	Prelamin-A/C	LMNA	42.3%	r12, r4, r11, r5, r1 and r14
P08133	Annexin A6	ANXA6	70.0%	r5, r4, r9, r6 and r15
P19338	Nucleolin	NCL	26.6%	r10 and r8
P16070-7	Isoform 7 of CD44 antigen	CD44	9.68%	r13
P06396-2	Isoform 2 of Gelsolin	GSN	26.9%	r11
P13010	X-ray repair cross-complementing protein 5	XRCC5	42.9%	r12
P08238	Heat shock protein HSP 90-beta	HSP90AB1	47.5%	r13 and r15
P07900	Heat shock protein HSP 90-alpha	HSP90AA1	46.9%	r5
Q9UHB6	LIM domain and actin-binding protein 1	LIMA1	14.1%	r11
A2A274	Aconitate hydratase, mitochondrial	ACO2	36.0%	r2
P05556	Integrin beta-1	ITGB1	21.2%	r11
P14625	Endoplasmin	HSP90B1	56.7%	r10, r9, r14, r2, r11, r12, r1 and r7
Q12906	Interleukin enhancer-binding factor 3	ILF3	22.9%	r16
P13639	Elongation factor 2	EEF2	30.7%	r9
Q9Y2J2-2	Isoform 2 of Band 4.1-like protein 3	EPB41L3	14.3%	r5
P35221	Catenin alpha-1 s	CTNNA1	29.6%	r2
P12814	Alpha-actinin-1	ACTN1	51.9%	r13
O43707	Alpha-actinin-4	ACTN4	53.5%	r13, r11, r2 and r12
P12110	Collagen alpha-2(VI) chain	COL6A2	8.24%	r27

Q9Y4L1	Hypoxia up-regulated protein 1	HYOU1	24.9%	r7
O95197	Reticulon-3	RTN3	3.29%	r11
Q5JRX3	Presequence protease, mitochondrial	PITRM1	17.1%	r6
P82094	TATA element modulatory factor	TMF1	3.84%	r13
P18206	Vinculin	VCL	47.3%	r21 and r3
Q16531	DNA damage-binding protein 1	DDB1	12.9%	r21
A0A087WTA8	Collagen alpha-2(I) chain	COL1A2	16.5%	r16
A0A087WYK8	Nardilysin	NRD1	6.71%	r11
P02452	Collagen alpha-1(I) chain	COL1A1	26.2%	r4, r3, r16 and r10
E7EQT4	Apoptotic chromatin condensation inducer in the nucleus	ACIN1	2.92%	r7
A0A0A0MRV0	Ribosome-binding protein 1	RRBP1	27.9%	r6, r2 and r18
P42704	Leucine-rich PPR motif-containing protein, mitochondrial	LRPPRC	17.6%	r14
P11047	Laminin subunit gamma-1	LAMC1	11.4%	r8
E9PAV3	Nascent polypeptide-associated complex subunit alpha, muscle-specific form	NACA	2.55%	r4
Q9Y490	Talin-1	TLN1	31.0%	r26 and r14
P46821	Microtubule-associated protein 1B	MAP1B	31.6%	r19 and r1
P21333	Filamin-A	FLNA	39.1%	r2, r18, r5, r14 and r6
Q14315	Filamin-C	FLNC P	17.5%	r5
P12111	Collagen alpha-3(VI) chain	COL6A3	12.2%	r13
A0A087WV66	Antigen KI-67	MKI67	0.768%	r12
Q15149	Plectin	PLEC	27.0%	r6, r9, r8, r12, r5, r10, r2 and r3
Q09666	Neuroblast differentiation-associated protein	AHNAK	35.4%	r15, r13, r3 and r11

Data are mean ± SD, n = 3.

3.7 Characterisation of protein glycation, oxidation and nitration markers in plasma protein of healthy subject, subjects with chronic periodontitis and periodontitis patients with co-morbidities

Plasma protein collected from patients with periodontitis and patients with periodontitis and other comorbid diseases such as diabetes and CKD was analysed for protein damage markers using gold standard analytical technique LC-MS/MS with stable isotope dilution analysis.

In healthy people, FL residue content of plasma protein was 4.67 ± 1.50 mmol/mol lys. This was significantly decreased in periodontitis patients *ca.* 61% compared to healthy patients ($P<0.001$). In addition, the residue content of FL in plasma of diabetic, CKD and periodontitis was decreased *ca.* 33% compared to healthy people ($P<0.001$) however, FL level was increased significantly by72% ($P<0.001$) compared to patients with periodontitis only. CML residue content of plasma protein in health people was 0.121 ± 0.062 mmol/mol lys. This was markedly decrease in periodontitis patients and patient with diabetic, CKD and periodontitis by 64% and 54% respectively compared to healthy people ($P<0.001$). The level of CEL residue in health people was 0.019 ± 0.007 mmol/mol lys. This was increased significantly 149% ($P<0.001$) in the plasma protein of patient with comorbidities only. In healthy people, G-H1 residue was decreased 70% in periodontitis patients ($P<0.01$) and 60% in patient with diabetic, CKD and periodontitis compared to healthy people ($P<0.05$). MG-H1 residue content of plasma protein was unchanged in periodontitis patients and patient with diabetic, CKD and periodontitis compare to control group. However, 3DG-H residue content of plasma protein was increased significantly in plasma protein of patients with periodontitis by 93% ($P<0.001$) and in patient with diabetic, CKD and periodontitis by 154% ($P<0.01$ with respect to health people) and by 31% ($P<0.01$ with respect to periodontitis patients). Level of MOLD residue was increased significantly in plasma protein of patients with periodontitis by 36 folds ($P<0.001$ with respect to health people) and in patient with diabetic, CKD and periodontitis by 49 folds ($P<0.01$ with respect to health people). The increase of MetSO residue content was highly significant in both groups, patients with periodontitis ($P<0.001$) and in patient with diabetic, CKD and periodontitis

(P<0.001) compared to health control group. In healthy people, NFK residue content of plasma protein was 0.360 ± 0.378 mmol/mol trp. This was increased significantly in plasma protein of patients with periodontitis by 716% (P<0.001) and in patient with diabetic, CKD and periodontitis by 613% (P<0.01) with respect to health people. 3-NT residue content of plasma protein was also increased in plasma protein of patients with periodontitis by 96% (P<0.01) and in patient with diabetic, CKD and periodontitis by 97% (P<0.05) with respect to health people. CMA residue content of plasma protein was decreased 27% in periodontitis patients (P<0.01) with respect to health people. The protein glycation, oxidation and nitration markers in plasma of healthy people, periodontitis patients and periodontitis patients with Co-morbidities are presented in Table 56 and Figure 83.

Table 56: Protein glycation, oxidation and nitration markers in plasma of healthy people, periodontitis patients and periodontitis patients with Co-morbidities

mmol/mol amino acid modified			
	Control subjects	**Periodontitis subjects**	**Diabetic, CKD and periodontitis subjects**
FL	4.67 ± 1.50	1.81 ± 0.29***↓	3.13 ± 0.42***↓^{ooo}↑
CML	0.075 (0.043 – 0.135)	0.041 (0.031 - 0.051)***↓	0.051 (0.049 - 0.066)***↓
CEL	0.019 ± 0.007	0.019 ± 0.009	0.047 ± 0.012**↑^{ooo}↑
G-H1	0.019 (0.033 – 0.006)	0.011 (0.008 - 0.013)**↓	0.016 (0.009 - 0.019)*↓
MG-H1	0.213 ± 0.115	0.261 ± 0.038	0.272 ± 0.059
3DG-H	0.054 ± 0.039	0.104 ± 0.018***↑	0.137 ± 0.035**↑^{oo}↑
MOLD	0.0007 ± 0.0004	0.026 ± 0.015***↑	0.034 ±0.012**↑
MetSO	0.015 ± 0.029	3.72 ± 0.70***↑	9.67 ± 1.91***↑^{oo}↑
NFK	0.205 (0.076 – 0.593)	2.83 (2.58 - 3.24)***↑	2.63 (2.42 - 2.68)***↑
3-NT	0.0053 ± 0.0033	0.010 ± 0.002**↑	0.010 ± 0.004*↑
CMA	0.024 ± 0.007	0.018 ± 0.005**↓	0.020 ± 0.016

Data are means ± SD or median (lower – upper quartile) Statistical analysis was performed using independent samples *t-test.* *, **, and ***, P<0.05, P<0.01 and P<0.001 with respect to healthy people; ^{oo} and ^{ooo}, P<0.01 and P<0.001 with respect to periodontitis patients.

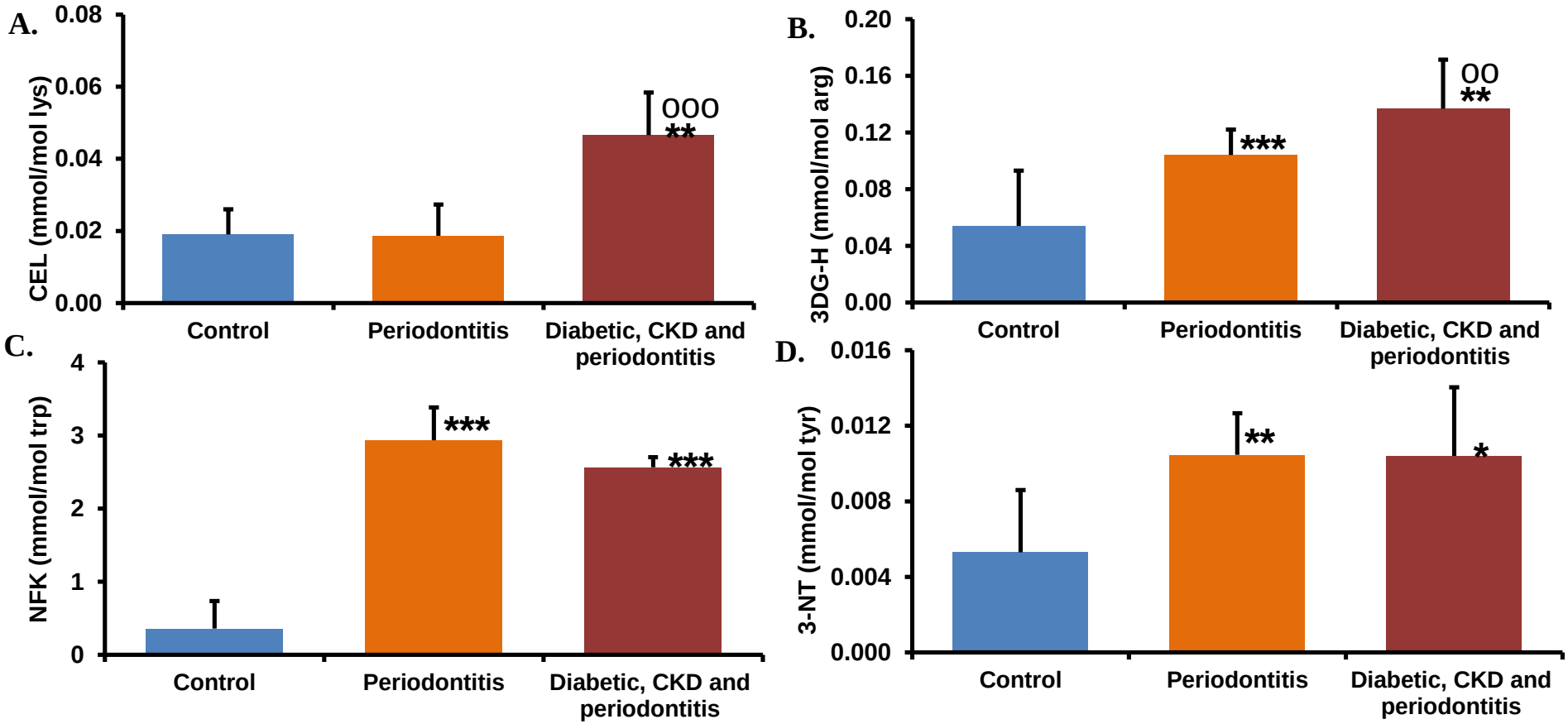

Figure 83: Protein glycation, oxidation and nitration markers in plasma of healthy people, periodontitis patients and periodontitis patients with Co-morbidities.

(A) CEL. (B) 3DG-H. (C) NFK. and (D) 3-NT. Data are means ± SD or median (lower – upper quartile) Statistical analysis was performed using independent samples *t-test.* *, **, and ***, P<0.05, P<0.01 and P<0.001 with respect to healthy people; ^{oo} and ^{ooo}, P<0.01 and P<0.001 with respect to periodontitis patients.

4. Discussion

Periodontal ligament (PDL) inflammation, or periodontitis, is the most common chronic inflammatory disease in the oral cavity. It is characterised by breakdown of the supporting structures of the teeth including the periodontal ligament. Many factors contributes in PDL inflammation can be external such as excessive plaque accumulation around the tooth (Selwitz et al., 2007), or systemic such as chronic systemic diseases as diabetes (Chang and Lim, 2012). Epidemiological data confirm that diabetes is a major risk factor for periodontitis – with risk of periodontitis increased *ca.* 3-fold in diabetes. Increased hyperglycaemia is linked to increased severity of periodontitis. The mechanisms that link hyperglycaemia to periodontitis are not clearly understood but are thought to involve disturbance of immune function, neutrophil responses to infection and soluble immune response mediators such as cytokines. There is also evidence to suggest that periodontitis influences glycaemia control – with treatment of periodontitis improving HbA_{1c} by 0.4%. The presence of diabetic nephropathy also exacerbates periodontitis and CVD in the presence of diabetic nephropathy is exacerbated by periodontitis (Preshaw et al., 2013). Mechanisms underlying the link of glycaemia control to periodontitis are likely similar to those linking hyperglycemia to vascular complications. A key driver in this relationship that has emerged in the last decade is dicarbonyl stress – particularly the accumulation of the reactive metabolite, MG (Rabbani and Thornalley, 2015).

Methylglyoxal is the precursor of quantitatively major AGEs. MG-derived AGE modification of proteins is functionally damaging whereas glycation by glucose has less marked functional effect. Increased MG in diabetes is driven by increased formation with increased flux of glucose metabolism in hyperglycemia in cells with GLUT1 glucose transport and by down regulation of Glo1 expression and protein stability by inflammation and other mechanisms. Increased levels of MG-derived AGEs and decreased Glo1 activity are found in the kidney, retina and nerve in diabetes and are associated with the development of diabetic nephropathy, retinopathy and neuropathy. Overexpression of Glo1 prevents the development of nephropathy, retinopathy and neuropathy in experimental diabetes (Rabbani and Thornalley, 2015).

In this project I hypothesised that increased concentration of MG is produced in hPDLFs by exogenous MG, hyperglycaemia associated with diabetes and inflammatory signalling leading to increased extracellular matrix modification causing hPDLFs dysfunction and extracellular matrix detachment. The aim of this study is to test this hypothesis and to study MG metabolism by the glyoxalase system in hPDLFs primary cell culture. The major experimental model for this hPDLFs cells in primary culture. This is a widely used cell culture model of mechanisms of cell dysfunction and injury leading to periodontitis (Mariotti and Cochran, 1990). hPDLFs are key cells mediating dysfunction in periodontitis in diabetes (Somerman et al., 1990).

4.1 Effect of glucose concentration on growth and viability of hPDLFs *in vitro*

I investigated the effect of glucose concentration on the growth of hPDLFs in primary culture. When hPDLFs incubated in medium containing 5.5 mM, 8.0 and 25.0 mM glucose, there was similar rapid growth in 8.0 and 25.0 mM glucose over 3 days but partial growth arrest without decrease in viability in 5.5 mM glucose. Subculture with new medium restored high cell growth and hence, over the passage range studied, hPDLFs maintained reproducible growth kinetics. The normal salivary glucose level in a healthy subject is *ca.* 8.0 mM glucose and in patients with diabetes mellitus the plasma concentrations of glucose is often 25.0 mM or higher (Aydin, 2007). In subsequent experiments to study effects of low and high glucose on metabolism and function of hPDLFs, cultures with 8.0 mM glucose were employed as the “low glucose concentration” (LG) conditions and cultures with 25.0 mM glucose were employed as the “high glucose concentration” (HG) conditions. hPDLFs with similar growth rate were compared in LG and HG conditions but the 5.5 mM glucose culture was not used. Primary hPDLFs were maintained in 8.0 mM glucose and 25.0 mM glucose for 3 days without change of medium. Use of 8.0 and 25.0 mM glucose was chosen for these conditions as cultures gave similar growth kinetics and hence differences found in cell function were not due to low glucose concentration-induced growth arrest.

The recommended growth conditions for hPDLFs in primary culture from a commercial supplier was medium containing 25 mM glucose. This is likely to provide a medium rich in nutrient for culture up to 6 days but does not provide

optimum function – see below. hPDLFs maintained rapid growth characteristics and the hPDLFs phenotype over the passages used herein (passages 3 - 5). hPDLFs growth was stimulated again in subsequent sub-cultures and this suggests that the slowing of cell growth was linked to depletion of nutrients rather than a cumulative cell doubling limited growth – known as the Hayflick limit (Effros and Walford, 1984). In subsequent experiments hPDLFs sub-cultured and grown for up to 3 days. The population doubling time was *ca.* 0.62 days in medium containing 8 and 25 mM glucose which is relatively rapid and similar to human foetal fibroblasts: *cf.* population doubling time for human dermal BJ fibroblasts, *ca.* 4 days, and of lung foetal fibroblasts 0.8 days (Sitte et al., 2000, Chen et al., 1995).

Culture of hPDLFs herein for 3 days at an initial density of 5000 cells/cm^2 in 8 mM and 25 mM glucose did not produce a decrease in cell viability. Previous studies seeding hPDLFs at 20,000 cells/cm^2 and incubating cells for 3 days and then exposure to different glucose concentrations for 24 h found increased apoptosis with 25 mM glucose (Liu et al., 2013). However, this was likely due to the high cell density used by the authors and rapid confluence conditions achieved by day 3 where after there is confluence-driven apoptosis (Yasaka et al., 1996). Other studies did not find decreased viabiluity of hPDLFs when cultured at 20 and 25 mM gluocse, as found herein (Nishimura et al., 1996, Ohgi and Johnson, 1996).

4.2 The glyoxalase system and dicarbonyl metabolism in hPDLFs cells *in vitro*

To my knowledge, this is the first time the glyoxalase system has been studied in hPDLFs. The activity of Glo1 in low glucose concentration was 985 ± 148 mU per mg protein; *cf.* 110 mU per mg protein in human RBCs (McLellan et al., 1994b) and *ca.* 1,500 mU per mg protein in human aortal endothelial cells in primary culture (Thornalley et al., 2014). hPDLFs, therefore, have a relatively high activity of Glo1 – similar to that of vascular cells. Glo1 activity markedly exceeded activities of MG reductase and dehydrogenase, so the glyoxalase pathway is the major route for detoxification of MG. The activity of Glo2 in hPDLFs in low glucose concentration was relatively low at 4.20 ± 2.71 mU per mg protein; *cf. ca.* 64 mU per mg protein in human RBCs (McLellan et al., 1994b). However, the relative activities of Glo1 and Glo1 *in situ* with physiological concentrations of substrate, taking into account K_M and k_{cat} for the reactions catalysed, are such that the intermediate S-D-

lactoylglutathione is <0.1% of total cell GSH (Rabbani et al., 2014b) and this was also found for hPDLFs – see below.

The concentration of MG in hPDLFs in low glucose concentration was *ca.* 8 pmol per 10^6 cells. Fibroblast cell volume is *ca.* 2.5 pl per cell (Mitsui and Schneider, 1976). This suggests the concentration of MG in hPDLFs is *ca.* 3 µM. This is keeping with the concentration of MG in other human cells of 2 - 4 µM (Rabbani and Thornalley, 2014c). The cellular concentration of glyoxal was similar and that of 3-DG was *ca.* 10-fold lower. MG is more reactive than glyoxal towards protein glycation and hence poses the greatest threat to cell protein modification and dysfunction. The flux of D-lactate in hPDLFs in low glucose concentration was *ca.* 6 nmol/10^6 cells/day, equivalent to *ca.* 0.06% flux of glucotriose. This is similar to flux of D-lactate found previously in human RBCs and endothelial cells (Thornalley, 1988, Thornalley et al., 2014, Shinohara et al., 1998) and is consistent with MG mainly being formed by non-enztymatic degradration of triosephosphates (Phillips and Thornalley, 1993). There was no significant metabolism of exogenous D-lactate added to primary hPDLFs cultures, suggesting that D-lactate formation by the glyoxalase system in this case represents the flux of MG formation.

The concentration of GSH and GSSG in hPDLFs was *ca.* 7 and 0.012 nmol per 10^6 cells, respectively, suggesting only 0.3% of GSH is oxidised under low glucose condistions. A previous estimate of GSH in hPDLFs was *ca.* 30 nmol per mg protein (Chang et al., 2003), equivalent to *ca.* 6 nmol GSH and in reasonable agreement with the estimate here. The concentration of GSH in hPDLFs was therefore *ca.* 3 mM and GSSG *ca.* 5 µM, suggesting hPDLFs have a strongly reducing cytosol. The glyoxalase system intermediate, S-D-lactoylglutathione, was <1.1 pmol per 10^6 cells, equivalent to < 0.4 µM or < 0.02% total GSH.

4.3 The effect of high glucose and dicarbonyl stress on the glyoxalase system and dicarbonyl metabolism in hPDLFs cells *in vitro*

In high glucose concentration media, there is expected increased uptake and metabolism of glucose by hPDLFs. Cell of the fibroblast lineage express GLUT1, GLUT3 and GLUT4 glucose transporters (Longo et al., 1989). When incubated medium containing 25 mM glucose (HG), the flux of glucose metabolism was increased *ca.* 2-fold but the flux of net L-lactate formation was unchanged. This is

consistent with increased uptake and metabolism of glucose in HG medium. Methylglyoxal made mainly from triphosphate intermediates of glycolysis process. Hence, increased glucose consumption is reflected in increased triphosphate intermediates, increased degradation to MG and increased flux of D-lactate formation. The increase in flux of D-lactate was less than the increase in glucose consumption, however, and may indicate increased metabolism of glucose by the pentosephosphate pathway in HG cultures. There was no indication of oxidative stress in hPDLFs incubated in high glucose concentration as the concentration of cellular total cell thiols and protein thiols were both increased in HG cultures. The cellular concentration of GSH and GSSG were both decreased by 22% and 23%, suggesting GSH synthesis may be modestly impaired. The cellular activity of Glo1 was decreased 45% in HG cultures. The increased flux of MG formation, as indicated by increased flux of D-lactate, the decreased activity of Glo1 and decreased cellular GSH concentration synergise to increase MG concentration in HG cultures. MG concentration of the medium and MG content of cells was increased by *ca.* 60% and 41%, respectively, in HG cultures. The concentration of glyoxal was unchanged in cells and medium of HG cultures. As glyoxal is mainly produced by oxidative processes, this is also indicative of no increase in oxidative stress in HG cultures. The cellular and medium concentration of 3-DG was increased *ca.* 4-fold in HG cultures and this is likely originating mainly from the glucose in the medium undergoing slow dehydration to 3-DG. It does not pose a great threat to hPDLFs since its reactivity towards glycation and AGE formation is *ca.* 200-fold lower than MG and the cellular and medium concentrations are *ca.* 8-fold lower and 2-fold higher than MG, respectively.

The glycation status of hPDLFs was assessed by quantifying the content of glycation adducts of a cytosolic protein extract and flux of increase of glycation free adducts increasing in the cell culture medium with time. FL and MG-H1 were major early glycation and AGE of cell protein, respectively. Both were increased *ca.* 2-fold in the high glucose culture, reflecting increase in glucose and MG exposure in the HG culture. Oxidative markers were unchanged in cell protein of HG cultures – CML/FL ratio, MetSO, NFK, DT and 3-NT, suggesting HG conditions did not increase cellular oxidative stress. This was supported by increased cell thiols and unchanged GSH/GSSG ratio. Fluxes of FL and AGE free adducts, CMA, MG-H1

and 3DG-H, were increased in HG cultures, suggesting increased proteolysis of glycated proteins; with a minor contribution from increased direct formation by glycation of arg and lys in the culture medium. This indicates that hPDLFs in HG culture suffer increased glycation by glucose and dicarbonyl stress and not increased oxidative or nitrative stress.

I investigated the likely mechanism of decrease in Glo1 activity of hPDLFs in HG medium. Decrease in Glo1 protein has been found previously in cells in HG culture where it has been claimed to be due to decreased Glo1 expression or increased Glo1 degradation (Bierhaus, 2006, Giacco et al., 2014, Thornalley et al., 2014). In hPDLFs, with decreased Glo1 activity in HG culture there was no related decrease in Glo1 mRNA but there a related decrease in Glo1 protein, suggesting increased proteolysis of Glo1 in the HG cultures. I investigated the possible acetylation of Glo1 promoting its degradation; human Glo1 protein undergoes acetylation at K148 and likely de-acetylation by cytosolic sirtuin-2 (Lundby et al., 2012). In immunoprecipitation and proteomics studies, I found no evidence of increased Glo1 acetylation in HG cultures. In conventional cylcoheximide block of protein synthesis studies, I found evidence of decreased half-life of Glo1 protein and increased proteolysis in HG cultures. It therefore appears that hPDLFs in HG culture activates a process of increased proteolysis that exacerbates dicarbonyl stress by de-stabilising Glo1 to proteolysis. A possible mechanisms is activation of autophagy as this may be activated by expsosure of cells to high glucose concentration – e.g. endothelial cells (Panieri et al., 2010), and Glo1 degradation may be thereby enhanced (Kristensen et al., 2008).

4.4 Sensitivity of hPDLFs cells to toxicity of exogenous methylglyoxal *in vitro*

Primary hPDLFs were incubated with exogenous MG for 48 h and cell growth and viability assessed. The results show that at ≥ 50 μM MG there was a decrease in hPDLFs viable cell number without decrease in cell viability – indicative of growth arrest, and with ≥ 200 μM MG there was decrease in cell growth and viability. This suggested that with addition of exogenous MG of progressively increased concentration, there is initially growth arrest of hPDLFs and the both growth arrest and cytotoxicity at ≥ 200 μM MG. Addition of 200 μM MG decreased cell growth and viability to similar extent in both low and high glucose conditions.

These effects of exogenous MG show a similar concentration-response relationship to the effect of MG on other proliferating cells (Kang et al., 1996) but effective concentrations far exceed those achieved physiologically (Rabbani and Thornalley, 2014c). This concentration also exceeds the concentration of MG in many foods and beverages (Degen et al., 2012) but is found in particularly types of honey – e.g. Manuka honey (Mavric et al., 2008). Alternatively, the bacteriocidal activity of MG in Manuka honey has been investigated and found to decrease dental plaques; Manuka honey was applied to the gingival sulcus of all the teeth, 3 times and twice per day, leaving the honey in the mouth for 5 min. It is likely that short term topical application limits toxicity to the surface layer of the tooth-gum junction (Nayak et al., 2010).The study was also an open trial with subjects aware of the treatment. A similar study with a chewable "honey leather" also found decreased dental plaque and gingival bleeding scores with 3 daily, 10 min exposures for 21 days (English et al., 2004). Again, this was an open study. It would be of interest to compare high and low MG content honey of similar appearance to control for placebo effects**.** The high activity of Glo1 in hPDLFs and periodontal epithelial cells may provide host protection against MG toxicity where micro-organisms may be more vulnerable.

Increased physiological levels of MG may drive hPDLFs dysfunction and detachment from the extrecellular matrix – as found for vascular endothelial cells in high glucose cultures (Dobler et al., 2006). This may be particularly damaging for sustaining the periodontal ligament, secure attachement of teeth in the jaw socket and epithelial barrier to infection.

4.5 The effect of glyoxalase 1 inducers on glyoxalase system and MG metabolism in hPDLFs *in vitro*

tRSV has received much attention as a potential health beneficial dietary supplement for prevention and treatment of obesity, cardiovascular disease, cancer, diabetes and hypertension (Bradamante et al., 2004, Jang et al., 1997, Fröjdö et al., 2008, Baur and Sinclair, 2006). Whil benefits have been found in experimental models, clinical translation has been difficult to achieve – for example, see meta-analysis of benefit in obesity and diabetes (Liu et al., 2014). A contributary factor has been the use of concentrations of tRSV in *in vitro* studies that are readily translatable (Boocock et al., 2007) and high doses in animal models that unsafe and

toxic clinically. Recent review of tRSV safety by the European Food Safety Authority suggest an upper tolerable clinical dose of <14 mg/kg (*ca.* 1 g per day in an adult) (EFSA, 2016). tRSV has been claimed to function as a direct activator of SIRT1 but this is limited to concentrations of 50 – 100 μM not achieved (Milne et al., 2007). Lower concentrations of tRSV (3 - 10 μM) inhibit phosphodiesterases, increased cAMP and NAD+, increasing *in situ* activity of sirtuins (Park et al., 2012). In recent studies our team have identified tRSV as also an activator of Nrf2 and inducer of Glo1 with inducer activity in the range 1 – 10 μM. They also recognised that this concentraion of tRSV was difficult to achieve clinically with safe clinical doses, they discovered HSP was also an activator of Nrf2 and inducer of Glo1 at concentrations achieved clinically and highly safe doses - albeit with low maximal response, and they developed tRSV and HSP in synergistic combination as a potent Glo1 inducer at clinically translatable concentrations and highly safe doses (Xue et al., 2016). The effect of tRSV, HSP and tRSV-HSP combination on dicarbonyl stress and function of hPDLFs in LG and HG cultures was therefore investigated.

HepG2 cells stably transfected to express lucerifase under GLO-ARE promoter incubated with 0.625 - 20 μM tRSV showed induction of lucerifase expression whereas HepG2 cells stably transfected with a non-functional mutant GLO1-ARE showed no activity. HSP showed similar activity except with a lower EC_{50} and lower E_{max}. Combined together, tRSV and HSP were synergistic – inducing reporter activity with 5 μM HSP and 0.1 – 1 μM tRSV. These hits were validated by measuring increase of Glo1 protein in HepG 2 cells and human aortal endothelial cells and dermal BJ fibroblasts in primary culture (Xue et al., 2016). Other investigators had found corroborative evidence of induction of Glo1 expresion by tRSV in HepG2 cells *in vitro* (Cheng et al., 2012). Recent studies from our group (Xue et al., 2015a, Xue et al., 2015c) and of others (Yang et al., 2014) suggest tRSV activates Nrf2 by preventing nuclear acetylation and inactivation of Nrf2. HSP may activate Nrf2 through induction and activation of protein kinase A, upstream of Fyn kinase which drives Nrf2 translocational oscillations and ARE-linked gene expression (Xue et al., 2015c, Hwang et al., 2012). HSP is a partial agonist (which is likely due to inhibitory nuclear acetylation of Nrf2 blocking a high E_{max}). Combination with tRSV and HSP provides for faster nuclear translocation and decreased inactivation of Nrf2

and thereby a high transcriptional response at relatively low activator concentrations (Xue et al., 2015a, Xue et al., 2015c).

Glo1 inducers had interesting effects on Glo1 activity in hPDLFs in culture. Incubation of hPDLFs cells with tRSV, HSP and tRSV-HSP in combination in LG and HG conditions did not change cell growth and viability. In LG control cultures, HSP and tRSV-HSP combined increased Glo1 activity by 20 – 22% whereas tRSV alone did not, suggesting that HSP may be more effective in LG cultures. In HG cultures, tRSV, HSP and tRSV-HSP combined all prevented the decrease of Glo1 activity of the HG control. This was associated with prevention of a decrease in Glo1 protein in HG cultures and a classical cycloheximide protein half-life study with tRSV suggests the recovery of Glo1 protein was due to prevention of HG-induced increased Glo1 degradation. Cycloheximide protein half-life studies have problems of interpretation, however, as cycloheximide blocks all protein synthesis and hence may change the rate of Glo1 degradation as well as the intended blocking of Glo1 synthesis. The effect of HG culture and tRSV treatment on Glo1 turnover requires future corroboration with proteome dynamics studies.

tRSV treatment stabilized the Glo1 protein and increased the half-life of Glo1 protein. Low concentrations of tRSV have been claimed to inhibit cellular proteases at 2 – 10 μM (Qureshi et al., 2012). If tRSV is a general protease inhibitor, however, it is suprising that protein damage modifications in cell protein did not all increase. Further studies are required as to how tRSV stabilises Glo1.

No effects for tRSV, HSP and tRSV-HSP combined were found on Glo2 and MG reductase and MG dehydrogenase, suggesting an effect specific for Glo1. The effect of tRSV, HSP and tRSV-HSP combined on glucose metabolism, D- and L-lactate formation was also remarkable. HSP and tRSV-HSP combined decreased glucose consumption by hPDLFs in LG cultures whereas tRSV did not, suggesting a caloric restriction mimetic effect induced by HSP. In HG cultures, tRSV did not reverse increased glucose consumption compared to LG control whereas HSP partly corrected and tRSV-HSP combined totally corrected increased glucose consumption, suggesting a caloric restriction mimetic effect induced by HSP which is potentiated and synergised by tRSV. Flux of D-lactate showed similar effects suggesting that the flux of D-lactate and hence flux of MG formation is influenced by flux of glucose consumption and may be decreased by HSP and tRSV-HSP combined in LG cultures

and the HG-induced increase prevented partly by HSP and totally by tRSV-HSP combined.

Studies of dicarbonyls in cells and medium were performed only with tRSV and showed that tRSV reversed partly the HG-induced increase of MG in cells and culture medium and decreased glyoxal in cells and culture medium but did not affect HG-induced increases in 3-DG. This suggests that tRSV partly corrects dicarbonyl stress induced by HG in cultures of hPDLFs. Cellular dicarbonyls were also studied with HSP and tRSV-HSP combined and this showed that HSP alone and tRSV-HSP combined provided complete protection against dicarbonyl stress in HG conditions, the combination of prevention of decline in Glo1 activity and increased MG formation both likely contributing to this effect.

A further contributory factor to protection against dicarbonyl stress by tRSV was the effect on cellular GSH. Cellular GSH was increased by tRSV in both LG and HG cultures such that the HG-induced decrease in cellular GSH was corrected and indeed increased above LG control levels. Previously periodontitis is associated with elevated oxidative stress and poor glycemic status in patients with diabetes (Allen et al., 2011). tRSV was found to be an effective antioxidant to protect human gingival fibroblasts (HGFs) from damage under oxidative stress induced by H_2O_2 (Orihuela-Campos et al., 2015). tRSV antioxidant mechanisms may relate to its ability to stimulate synthesis of GSH. tRSV produced a small decrease in protein thiols in LG and HG cultures. The reason for this is unclear but as cellular GSH concentration was increased, it seems to relate to decreased activity of thiol transferases – such as glutaredoxin (Lillig et al., 2008).

I studied the effect of tRSV on protein damage markers in hPDLFs cell protein. There were no improvements in oxidative damage markers – DT, MetSO, NFK and 3-NT – induced by tRSV in either LG or HG conditions, suggesting any functional benefit of tRSV on hPDLFs are not mediated through correction of oxidative damage. There were improvements of glycation damage, however. For early glycation damage, cellular protein FL content increase in HG cultures was corrected by tRSV. This may relate to increased clearance of FL-modified protein as the flux of FL free adducts was not changed by tRSV. Decrease in FL by tRSV in HG cultures probably also explains the correction of HG-induced increase in CML as oxidative degradation of FL is the major source of formation of CML. tRSV

decreased AGE content of cell protein: decreasing CMA in LG and HG cultures and correcting increased MG-H1 in HG cultures. This is linked to the improvement of dicarbonyl stress by tRSV. Relatedly, increased flux of MG-H1 free adduct formation in HG cultures was prevented by tRSV. Increased flux of formation of 3-DG in HG cultures was not prevented and as there was not related increase of 3DG-H in cell protein, this may relate to increased 3DG-H formation in the culture medium. MetSO free adduct is metabolised by MetSO reductase and was increased in HG cultures and not corrected by tRSV. This may reflect decreased MetSO reductase activity in HG cultures which was not corrected by tRSV.

4.6 The effect of glyoxalase 1 inducers on hPDLFs function *in vitro*

To assess hPDLFs function and effects of Glo1 inducers, I assessed the effect of tRSV on ECM component expression by hPDLFs and binding of hPDLFs to ECM. The minor decrease in expression of COL1 in high glucose treatment was corrected by tRSV. tRSV also produced a minor increase in expression of COL3 and COL12. These may contribute to improved ECM deposition by hPDLFs. Hyperglycaemia significantly affects collagen homeostasis, synthesis and maturation. In patients with diabetes, there is a decrease in the collagen production with an increase in collagenase activity in gingival tissues (Mealey, 1999). tRSV was found to upregulate the production of collagen-I gene after 3 h of incubation post-induction of oxidative stress (Orihuela-Campos et al., 2015).

Previous studies have shown that MG targets functional RGD and GFOGER integrin binding sites in the ECM and stimulates cell detachment, as shown for endothelial cells and pancreatic beta-cells (Dobler et al., 2006, Tym et al., 2014). I therefore investigated effects of tRSV, HSP and tRSV-HSP combined on hPDLFs bidning to the ECM – using collagen-1 as the ECM target.

When hPDLFs were incubated in HG, there was a *ca.* 30% decrease in adhesion of the cells to collagen-I. Glo1 inducers both individually and combination increased adhesion of hPDLFs to collagen-I in LG and HG conditions. This suggests integrin expression was increased and/or MG modification and functional impairment of it was decreased. We previously showed that overexpression of Glo1 in endothelial cells corrected HG-induced decreased attachment to collagen-IV where MG modification of a function arg in integrins was implicated (Ahmed et al.,

2008). With respect to integrin-ECM binding, it has been claimed that there is a high affinity binding site of tRSV on integrin $\alpha_V\beta_3$ – based on binding to purified integrin fragments, and binding of tRSV to this induces extracellular-regulated kinases 1 and 2 (ERK1/2)- and serine-15-p53- dependent phosphorylation leading to apoptosis (Lin et al., 2006). Expresion of $\alpha_V\beta_3$ integrin has been found in hPDLFs *in vivo* (Steffensen et al., 1992). Effects of HSP on integrins are known. Integrins binding collagens on hPDLFs are a_1b_1, a_2b_1 and $a_{11}b_1$; only a_2b_1 and $a_{11}b_1$ have been shown, by immunohistochemistry, to be present in the periodontal ligament *in vivo*. *In vitro*, a_1b_1, a_2b_1 and $a_{11}b_1$ all contribute to cell attachment to collagens-I and -III, and cell migration on collagen-I (Popova et al., 2007, Barczyk et al., 2009). The role of integrins in hPDLFs function has been expertly reviewed by Barczyk *et al*. (Barczyk et al., 2013). It is likely, therefore, that tRSV and HSP have increased functionally of a_1b1, a_2b_1 and $a_{11}b_1$ integrins. In the previous work on this group, MG modification blocked functionally of a_1b_1 and a_2b_1 integrins (Dobler et al., 2006) and hence increasing the functionality of these integrin is suspected.

Studies of binding of hPDLFs to collagen-I modified with MG and conditioned medium with and without prior dicarbonyl scavenging with aminoguanidine suggested that MG modification of collagen-I, regardless of whether the source of the MG is exogenous or leaking from hPDLFs, impairs binding of hPDLFs and this is prevented by the Glo1 inducers. In collagen-I the major motif that is modified by MG is GFOGER (Barczyk et al., 2013, Dobler et al., 2006). MG modification of GFOGER likely causes detachment of hPDLFs, anoikis and decreased cell movements in wound healing. Independent previous studies have reported a tRSV, ferulic acid and tetrahydrocurcuminoid combination increased hPDLFs function in a model of wound healing (San Miguel et al., 2010). This may be linked to improved ECM function.

Impaired hPDLFs-ECM interaction in dicarbonyl stress may explain tissue breakdown of periodontium in periodontal diseases in hyperglycaemia. Recently, it was found that administration of tRSV to a rat model of periodontitis produced inhibition of periodontitis-mediated loss of alveolar bone and tissue breakdown in the periodontium (Bhattarai et al., 2016). As tRSV increases Glo1 activity and protein in hPDLFs incubated with high glucose, this decreases MG concentration and MG-H1 formation. This will minimise the MG modification of integrins and

integrin binding sites in the ECM and improve the cell binding. Tissue breakdown of the periodontium is thereby prevented and the attachment of the tooth to the periodontium will be improved.

4.7 AGE-RAGE axis as a potential source of dicarbonyl stress in hPDLFs *in vitro*

Hyperglycaemia increases AGEs accumulation in plasma and tissues by oxidation and non-enzymatic glycation of proteins. AGEs cause alteration of matrix molecules cross-linking, damage of the growth factors efficiency, elevation of oxidative stress in diabetic conditions, and exaggeration of inflammation – possibly through engagement of cellular RAGE (Chang et al., 2013). Glycation of collagen-I and fibronectin in hPDLFs modify cell function, including decrease in cell migration which causes alteration in periodontal wound healing in diabetic individuals (Murillo et al., 2008). There are modest increases of AGEs and RAGE without histologic destruction in periodontium of animals with diabetes and without periodontitis. However, periodontal breakdown in mice with diabetes and periodontitis was aggressive with evidence of increased AGEs and RAGE expression. Furthermore, in healthy animals with periodontitis, AGE accumulation and RAGE expression were found. The AGE-RAGE axis may contribute to inflammation (Chang et al., 2013) and RAGE was found to be expressed in hPDLFs (Hasegawa, 2008). RAGE may have a significant role in model periodontal disease (Lalla et al., 2000).

There is a preliminary evidence that activation of RAGE by proteins highly modified by AGEs decreased expression of Glo1 (Bierhaus, 2006). The mechanistic details are still unclear. The decrease in Glo1 activity may occur in hPDLFs when RAGE binds CML-HSA and AGE-HSA and activates NF-κB. Crosstalk between NF-κB and Nrf2 (Liu et al., 2008) is expected to downregulated basal and inducible expression of Glo1 (Xue et al., 2012a). Culture of hPDLFs for 3 days with highly glycated albumin derivatives, however, gain no indication of activation of NF-kB, as judged by nuclear concentration of p65-DNA binding, nor decrease in Glo1 mRNA or activity. This suggests that the AGE-RAGE axis in hPDLFs in culture is not functional for activation of NF-kB and down regulation of Glo1. Rather dicarbonyl stress in high glucose cultures was linked to increased proteolysis of Glo1 and decreased Glo1 activity, modest decrease in cellular GSH concentration and

increased formation of MG linked to increased glucose metabolism. This was corrected by Glo1 inducers.

4.8 The effect of high glucose concentration on the cytosolic proteome of hPDLFs *in vitro*

I examined the cytosolic proteome of hPDLFs incubated in LG and HG conditions by high resolution mass spectrometry proteomics analysis. This was the same type of extract as used in protein glycation, oxidation and nitration adduct residue analysis reported above where increased total MG-H1 residue content was found in HG cultures. This analysis detects modified and unmodified proteins but with limited total sequence coverage: the mean sequence coverage of proteins detected was 16.7%. Hence, some MG-H1 and FL residues sites are likely undetected.

There was 1105 proteins were identified in hPDLFs cytosolic extracts: 1077 proteins were found in extracts from LG and HG cultures; 16 proteins were only in LG extracts and 12 proteins only in HG extracts. Of the 1077 proteins common to LG and HG conditions, 21 were down regulated and 18 were up-regulated in HG conditions.

Actin-related protein 2/3 complex subunit 1B is one of down regulated proteins in hPDLFs with high glucose incubation. This protein involves in innate immune system specifically in Fc-gamma receptor (FCGR) dependent phagocytosis pathway which responsible about the process of phagocytosis to eliminate invading infectious agents. FCGR is specific types of phagocytic receptors (Nimmerjahn and Ravetch, 2006). Downregulation of actin-related protein 2/3 complex subunit 1B may affect the process of removing the infectious agent which could increase the inflammatory process in the periodontium and increase the tissue breakdown in hyperglycaemic condition.

High mobility group protein B1 was downregulated in hPDLFs incubated in high glucose. This protein involves in many pathways in the innate immune system and programmed cell death. The innate immune system pathways include toll-like receptors cascades, advanced glycosylation endproduct receptor signalling, TRAF6 mediated NF-kB activation and cytosolic sensors of pathogen-associated DNA. Toll-like receptors (TLR) family that identify exact components conserved among

microorganisms. TLRs activation leads to the initiation of inflammatory responses and to the development of antigen-specific adaptive immunity. The TLR-induced inflammatory response is dependent on a common signalling pathway that is facilitated by the adaptor molecule MyD88 (Takeda et al., 2003). Advanced glycosylation endproduct receptor signalling also known as receptor for advanced glycation end-products (RAGE). The major inflammatory pathway activated by RAGE activation is NF-κB (Bierhaus, 2006). High mobility group protein B1 also involves in programmed cell death pathway specifically in apoptosis induced DNA fragmentation. As HMGB1 involves in inflammation and found to be decreased in the hPDLFs cell lysate when cultured in high glucose concentration, this suggests leaking out of the cell and starting the inflammation signalling cascade via RAGE interaction.

The E3 ubiquitin-protein ligase HUWE1 was also down-regulated in high glucose incubation. This protein is involved in adaptive immune system specifically in Class I MHC mediated antigen processing and presentation pathway. This will affect the ability of identify and counter bacteria and viruses invading to periodontium tissues in hyperglycaemia, with decreased resistance to invading of infectious agents which may cause initiation of inflammatory process and tissue breakdown in the periodontium in hyperglycaemia.

Signal transducer and activator of transcription 1-alpha/beta protein was also downregulated in hPDLFs in high glucose incubations. Many pathways are affected by this protein - including FGFR1, interleukin-6, growth hormone receptor signalling, and PDGF and SCF-KIT. Alpha-enolase protein was down regulated with high glucose incubation in hPDLFs. Cytosolic enolase dimer catalyses the reversible reaction of phosphoenolpyruvate and to form 2-phosphoglycerate (Giallongo et al., 1986).

Aldo-keto reductase family 1 member C3 was up-regulated in hPDLFs when incubated in high glucose. This protein involves in the metabolism of lipids and lipoproteins, metabolism of vitamins and cofactors, visual phototransduction and signalling by retinoic acid.

Sixteen proteins were found only in hPDLFs in low glucose incubations and may have been down regulated and thereby undetectable in the HG cultures. The proteins included: glycogen synthase kinase-3β (isoform-2) – influencing NF-κB

binding and p53 signaling (Perkins, 2006); and NADP-dependent aldehyde dehydrogenase (Ko et al., 2012). Twelve proteins were detected only in HG cultures. Transcription changes in HG conditions may have increased their expression such that they became detectable. These proteins included: E3 ubiquitin-protein ligase (isoform 3); and glycogen debranching enzyme (isoform 5) – involved in glucose metabolism and glycogen breakdown.

Pathways analysis of proteins down-regulated and up-regulated by HG cultures indicate many and diverse pathways were changed. Mechanisms other than dicarbonyl stress and MG glycation may be involved.

4.9 Cytosolic dicarbonyl proteome in hPDLFs *in vitro*

To identify proteins that are susceptible to MG modification, I prepared a cell extract with increased modification with exogenous MG. This showed 173 proteins were modified by MG-H1. Protein modifications were also analysed in cytosolic extracts from LG and HG incubations. Only one of the 173 proteins modified in the positive control samples was found also modified in a cell extract: that was of actin cytoplasmic 2 protein or γ-actin in HG cultures. γ-Actin is a ubiquitous protein essential for the actin filament cytoskeleton in all non-muscle cells. It is required for reinforcement and long-term stability of F-actin–based structures (Belyantseva et al., 2009). This may disrupt actin polymerisation. Older studies suggest MG promotes or stabilises actin polymerisatioon (Fésüs et al., 1981).

In LG cell extracts there were 7 proteins detected with MG-H1 adduct residues. These were not detected in the positive control and so their modfication requires further confirmation. In HG cell extracts there were 7 proteins detected with MG-H1 adduct residues – incluing actin. These were not detected in the positive control and so their modfication requires further confirmation. As the related unmodified proteins were not detected in the cell extracts, it is conceivable that MG modification leads to their accumulation during the cell culture to a detectable level. Moesin was detected with MG-H1 adduct in the MG modification postive control and the unmodified protein was detected and decreased in the HG incubations. It is conceivable that MG modification of Moesin occurs in cells and increase of this leads to decreased half-life and lower concentration of unmodified moesin in HG cultures. Moesin was detected as MG-modified in human aorta and carotid arteries

of diabetic patients by immunohistochemistry and mass spectrometry (Lund et al., 2011).

From the incubations in LG and HG, evidence for some other modifications were found: FL, CML and CEL. Vimentin protein is found modified by FL in the positive control, LG and HG conditions. It was previously claimed that vimentin was selectively modified by CML residues (Kueper et al., 2007) but this is unlikely as CML originates mostly from FL degradation. It may be that in previous studies that FL residues in vimentin were degraded to CML residues in pre-analytic processing. Vimentin is structurally important for the mechanical integrity of cells and localization of intracellular components (Guo et al., 2013). Echinoderm microtubule-associated protein-like 1 was modified by MG-H1 in LG and HG conditions. This protein involves in regulation of microtubules in the cytoskeleton.

4.10 Characterisation of protein glycation, oxidation and nitration markers in plasma protein of healthy subject, subjects with chronic periodontitis and periodontitis patients with co-morbidities

Plasma protein was collected from patients with periodontitis and patients with periodontitis and other comorbid diseases such as diabetes and CKD. Plasma was analysed for protein damage markers using gold standard analytical technique LC-MS/MS with stable isotope dilution analysis. The result shows significant changes in the level of protein damage markers in the plasma of patients with periodontitis and patients with periodontitis, diabetes and CKD. The level of 3DG-H, MOLD, MetSO, NFK and 3-NT was increased significantly in patients with periodontitis and patients with periodontitis, diabetes and CKD as compared with healthy subjects. MetSO, NFK and 3-NT are oxidative markers and it was found that periodontitis is associated with oxidative stress and worsened by poor glycaemic status in patients with diabetes (Allen et al., 2011). The residue content of MetSO in plasma of diabetic, CKD and periodontitis was higher by 160% compared to patients with periodontitis only. This findings suggest the ability of local periodontal inflammation to cause potential systematic effects.

4.11 Potential impact of Glo1 inducers on the periodontal diseases

Manuka honey was claimed to decrease dental plaque around the tooth by its bacteriocidal activity of MG (Nayak et al., 2010). The level of MG in Manuka honey exceeds the concentration of MG in many foods and beverages (Degen et al., 2012). The bacteriocidal activity of Manuka honey depends on its content of sugar, H_2O_2, MG, and bee defensin-1. Indeed, elimination of MG alone from Manuka honey did not decrease its bacteriocidal activity (Kwakman et al., 2010).

In this project rather Glo1 inducers, decreasing dicarbonyl stress, improved the functionality of hPDLFs *in vitro*. Applying Glo1 inducers to dental tissues clinically may be achieved through tablets, mouth wash, tooth paste and chewing gum. This could improve prevention of the tissue breakdown at early stages of the disease and improve the outcome of clinical procedures such as teeth scaling and root planning and periodontal surgeries. In addition, Glo1 inducers could decrease the need of antibiotics in treatment of periodontitis and help decrease the development of antibiotic resistance. Also, in patients with diabetes Glo1 inducers could decrease the level of tissue breakdown and improve the periodontal health status. Periodontitis in patients was found to increase the levels of protein glycation, oxidation and nitration markers in plasma. This may impact on systemic health status in patient with and without diabetes, increasing the risk of impaired glycaemic control and related complications.

5. Conclusions and further work

5.1 Conclusion

Multiple aspects of hPDLFs function in periodontitis were studied in this PhD project:

(i) MG metabolism by the glyoxalase pathway in hPDLFs *in vitro* was studied for the first time and its dysfunction in high glucose concentration was characterised;

(ii) The effect of Glo1 inducers on the formation and metabolism of MG in hyperglycaemia and protein damage in hPDLFs *in vitro* was investigated;

(iii) The effect of dicarbonyl stress and its alleviation by Glo1 inducers on hPDLFs binding to collagen-1 was investigated;

(iv) The effect of high glucose concentration on the cytosolic proteome of hPDLFs *in vitro* was studied; and

(v) A pilot investigation of plasma protein glycation, oxidation and nitration in clinical periodontitis was completed.

Glyoxalase system, dicarbonyls, markers of protein damage and whole proteomics have, for the first time as far as I am aware, been comprehensively quantified in human periodontal ligament fibroblasts cells an in *in vitro* hyperglycaemic model. The findings have shown that there is a risk of dicarbonyl stress and increased protein damage in periodontal diseases whereby MG formation is increased and Glo1 is down-regulated by increased proteolysis. Glo1 induction may now be viewed as a future target for pharmacological therapies to treat and prevent periodontal diseases if the findings of the high glucose model of hPDLFs culture can be translated to mechanisms of periodontitis clinically.

hPDLFs cultured in medium containing a higher glucose concentration have an increased glucose consumption, increased flux of formation of D-lactate, decreased Glo1 activity and modestly decreased GSH content that imposes dicarbonyl stress. There was no evidence for increased oxidative stress and increased oxidative damage in high glucose concentration cultures. There was an increase in the cellular concentration of MG and 3-DG in high glucose, although there was no change in glyoxal. High glucose concentration associated decline in Glo1 activity was due to decreased Glo1 protein and decreased Glo1 protein half-life. Increase cellular content of MG cause an increased in MG-H1 free adduct and MG-H1

residue content of cells suggests that there is increased MG glycation of cellular protein in high glucose concentrations *in vitro*. In addition, impaired adhesion to collagen -I was found following MG-glycation of collagen and this was suggestive of altered hPDLFs function in cell-cell and cell-matrix interactions. Increased release of MG from hPDLFs and glycation of extracellular matrix proteins and increased turnover of cellular proteins via MG-H1 modification may contribute to breakdown of periodontium in hyperglycaemia.

Treatment of periodontal ligament fibroblasts model, hPDLFs, with Glo1 inducers protected the cells against decline in the Glo1 activity in high glucose concentrations *in vitro*. Furthermore, increased formation of MG and other dicarbonyls in high glucose concentrations were returned to control levels. Glo1 inducers prevented increased AGE adduct residues in cell protein and flux of formation in high glucose concentrations. In addition, the adhesion study shows that the Glo1 inducers not only prevent impaired collagen-I adhesion of hPDLFs in high glucose culture but even enhance the adhesion ability of the cells to collagen-1 in low glucose culture too, suggesting a remarkable ability to improve hPDLFs function in primary cultures in relatively low glucose concentrations. These findings, if they can be translated to mechanisms of periodontitis clinically, suggests that Glo1 inducer is a promising pharmacological agent which may improve protection from periodontal tissue breakdown in periodontal diseases. Stimulation of Glo1 expression may contribute to health benefits of Glo1 inducers and they may protect against the development of periodontal diseases in diabetes.

A limitation of this study has been that hPDLFs is a primary cell population and the cells used in this study were only from 3 different donors. However, the primary effects were found and validated in all 3 different donor hPDLFs samples. However, this thesis has shown that glycation occurs within cultured hPDLFs and that MG accumulates in high glucose exposure, driving dicarbonyl stress. Periodontitis is a further disease wherein dicarbonyl stress may be implicated as a pathological mechanism.

5.2 Further work

In this study I investigated the effect of high glucose concentration on periodontal ligament fibroblasts *in vitro* and beneficial role of Glo1 inducer in countering dicarbonyl stress. However I did not examine the possible mechanism related with the protecting effects of a Glo1 inducer against dicarbonyl stress. It would be of interest to silence Glo1 in control and tRSV, HSP and tRSV-HSP treated cells to assess if the benefits of tRSV, HSP and tRSV-HSP are Glo1 dependent. In activating Nrf2 and influencing other targets, tRSV, HSP and tRSV-HSP may have many other effects as well as Glo1 induction and stabilisation in hPDLFs. Previously, tRSV has received significant attention as either a potential therapy or preventive agent against chronic diseases such as diabetes, cardiovascular atherosclerosis, cancer and hypertension. However, the bioavailability of tRSV in human subjects is low after oral administration. This is mainly due to the rapid metabolism of tRSV and excretion of conjugates. HSP is also a Glo1 inducer and together with tRSV the synergism produces an effective binary formulation for induction of Glo1 and related effects – for example, caloric restriction mimetic effect seen herein. Deliberate design of synergistic pharmaceutical dose co-formulations of dietary bioactive compounds may be an effective strategy to achieve health benefits clinically in prevention and treatment of periodontitis and other disease. tRSV-HSP co-formulation could be a suitable treatment of periodontitis. This will explored in future.

The studies with hPDLFs cells require follow-up with more investigation about contribution of glycation on periodontal breakdown. Finally, it will be important to study glyoxalase system, dicarbonyl stress and glycation on other cell lines originated from oral tissues and study its effect on other oral diseases.

References

ABORDO, E. A., MINHAS, H. S. & THORNALLEY, P. J. 1999. Accumulation of alpha-oxoaldehydes during oxidative stress: a role in cytotoxicity. *Biochem Pharmacol,* 58**,** 641-8.

ADA 2015. 2. Classification and diagnosis of diabetes. *Diabetes Care,* 38**,** S8-S16.

AEBERSOLD, R. & MANN, M. 2003. Mass spectrometry-based proteomics. *Nature,* 422**,** 198-207.

AGALOU, S. 2005. Profound Mishandling of Protein Glycation Degradation Products in Uremia and Dialysis. *Journal of the American Society of Nephrology,* 16**,** 1471-1485.

AGARWAL, S., CHANDRA, C. S., PIESCO, N. P., LANGKAMP, H. H., BOWEN, L. & BARAN, C. 1998. Regulation of periodontal ligament cell functions by interleukin-1β. *Infection and immunity,* 66**,** 932-937.

AGGARWAL, B. B. & SHISHODIA, S. 2006. Resveratrol in health and disease. *Boca Raton, CRC Taylor & Francis*.

AHMAD, S. T., ARJUMAND, W., NAFEES, S., SETH, A., ALI, N., RASHID, S. & SULTANA, S. 2012. Hesperidin alleviates acetaminophen induced toxicity in Wistar rats by abrogation of oxidative stress, apoptosis and inflammation. *Toxicology letters,* 208**,** 149-161.

AHMED, M., BRINKMANN, F. E., DEGENHARDT, T., THORPE, S. & BAYNES, J. 1997. Nε-(Carboxyethyl) lysine, a product of the chemical modification of proteins by methylglyoxal, increases with age in human lens proteins. *Biochem. J,* 324**,** 565-570.

AHMED, N., ARGIROV, O., MINHAS, H., CORDEIRO, C. & THORNALLEY, P. 2002. Assay of advanced glycation endproducts (AGEs): surveying AGEs by chromatographic assay with derivatization by 6-aminoquinolyl-N-hydroxysuccinimidyl-carbamate and application to Nε-carboxymethyl-lysine-and Nε-(1-carboxyethyl) lysine-modified albumin. *Biochem. J,* 364**,** 1-14.

AHMED, N., BABAEI-JADIDI, R., HOWELL, S., BEISSWENGER, P. & THORNALLEY, P. 2005a. Degradation products of proteins damaged by glycation, oxidation and nitration in clinical type 1 diabetes. *Diabetologia,* 48**,** 1590-1603.

AHMED, N., BABAEI-JADIDI, R., HOWELL, S. K., BEISSWENGER, P. J. & THORNALLEY, P. J. 2005b. Degradation products of proteins damaged by

glycation, oxidation and nitration in clinical type 1 diabetes. *Diabetologia,* 48**,** 1590-1603.

AHMED, N., DOBLER, D., DEAN, M. & THORNALLEY, P. J. 2005c. Peptide mapping identifies hotspot site of modification in human serum albumin by methylglyoxal involved in ligand binding and esterase activity. *J Biol Chem,* 280**,** 5724-32.

AHMED, N. & THORNALLEY, P. J. 2002. Chromatographic assay of glycation adducts in human serum albumin glycated in vitro by derivatization with 6-aminoquinolyl-N-hydroxysuccinimidyl-carbamate and intrinsic fluorescence. *Biochemical Journal,* 364**,** 15-24.

AHMED, N. & THORNALLEY, P. J. 2007. Advanced glycation endproducts: what is their relevance to diabetic complications? *Diabetes Obesity & Metabolism,* 9**,** 233-245.

AHMED, N., THORNALLEY, P. J., DAWCZYNSKI, J., FRANKE, S., STROBEL, J., STEIN, G. & HAIK, G. M. 2003. Methylglyoxal-derived hydroimidazolone advanced glycation end-products of human lens proteins. *Invest Ophthalmol Vis Sci,* 44**,** 5287-92.

AHMED, N., THORNALLEY, P. J., LUTHEN, R., HAUSSINGER, D., SEBEKOVA, K., SCHINZEL, R., VOELKER, W. & HEIDLAND, A. 2004. Processing of protein glycation, oxidation and nitrosation adducts in the liver and the effect of cirrhosis. *J Hepatol,* 41**,** 913-9.

AHMED, U., DOBLER, D., LARKIN, S. J., RABBANI, N. & THORNALLEY, P. J. 2008. Reversal of hyperglycemia-induced angiogenesis deficit of human endothelial cells by overexpression of glyoxalase 1 in vitro. *Ann N Y Acad Sci,* 1126**,** 262-4.

ALI, O. 2010. Type 1 diabetes mellitus: epidemiology, genetics, pathogenesis, and clinical manifestations. *In:* PORETSKY, L. (ed.) *Principles of Diabetes Mellitus.* 2 ed. New York: Springer US.

ALLEN, D. W., SCHROEDER, W. & BALOG, J. 1958. Observations on the chromatographic heterogeneity of normal adult and fetal human hemoglobin: a study of the effects of crystallization and chromatography on the heterogeneity and isoleucine content. *Journal of the American Chemical Society,* 80**,** 1628-1634.

ALLEN, E. M., MATTHEWS, J. B., O' HALLORAN, D. J., GRIFFITHS, H. R. & CHAPPLE, I. L. 2011. Oxidative and inflammatory status in Type 2 diabetes patients with periodontitis. *Journal of Clinical Periodontology,* 38**,** 894-901.

ALLEN, R. E., LO, T. W. & THORNALLEY, P. J. 1993a. Purification and characterisation of glyoxalase II from human red blood cells. *Eur J Biochem,* 213**,** 1261-7.

ALLEN, R. E., LO, T. W. & THORNALLEY, P. J. 1993b. A simplified method for the purification of human red blood cell glyoxalase. I. Characteristics, immunoblotting, and inhibitor studies. *J Protein Chem,* 12**,** 111-9.

ALMASRI, A., WISITHPHROM, K., WINDSOR, L. J. & OLSON, B. 2007. Nicotine and Lipopolysaccharide Affect Cytokine Expression From Gingival Fibroblasts. *Journal of Periodontology,* 78**,** 533-541.

AMADORI, M. 1929a. The condensation product of glucose and p-anisidine. *Atti R Accad Naz Lincei,* 9**,** 226–230.

AMADORI, M. 1929b. The product of the condensation of glucose and p-phenetidine. *Atti R Accad Naz Lincei,* 9**,** 68–73.

ANDERSON, N. L. & ANDERSON, N. G. 1998. Proteome and proteomics: New technologies, new concepts, and new words. *ELECTROPHORESIS,* 19**,** 1853-1861.

ANET, E. 1960. Degradation of carbohydrates. I. Isolation of 3-deoxyhexosones. *Australian Journal of Chemistry,* 13**,** 396-403.

ANTHARAVALLY, B. S., MALLIA, K. A., ROSENBLATT, M. M., SALUNKHE, A. M., ROGERS, J. C., HANEY, P. & HAGHDOOST, N. 2011. Efficient removal of detergents from proteins and peptides in a spin column format. *Analytical Biochemistry,* 416**,** 39-44.

ARAFA, H., ALY, H., ABD-ELLAH, M. & EL-REFAEY, H. 2009. Hesperidin attenuates benzo [α] pyrene-induced testicular toxicity in rats via regulation of oxidant/antioxidant balance. *Toxicology and industrial health,* 25**,** 417-427.

ARAI, M., YUZAWA, H., NOHARA, I., OHNISHI, T., OBATA, N., IWAYAMA, Y., HAGA, S., TOYOTA, T., UJIKE, H. & ARAI, M. 2010. Enhanced carbonyl stress in a subpopulation of schizophrenia. *Archives of general psychiatry,* 67**,** 589.

ARRICK, D. M., SUN, H., PATEL, K. P. & MAYHAN, W. G. 2011. Chronic resveratrol treatment restores vascular responsiveness of cerebral arterioles in type 1 diabetic rats. *American Journal of Physiology-Heart and Circulatory Physiology,* 301**,** H696-H703.

ARRIETA-BLANCO, J., BARTOLOMÉ-VILLAR, B., JIMENEZ-MARTINEZ, E., SAAVEDRA-VALLEJO, P. & ARRIETA-BLANCO, F. 2002. Dental problems in patients with diabetes mellitus (II): gingival index and periodontal disease. *Medicina oral: organo oficial de la Sociedad Espanola de Medicina Oral y de la Academia Iberoamericana de Patologia y Medicina Bucal,* 8**,** 233-247.

ATKINS, T. & THORNALLY, P. 1989. Erythrocyte glyoxalase activity in genetically obese (ob/ob) and streptozotocin diabetic mice. *Diabetes research (Edinburgh, Scotland),* 11**,** 125-129.

AVERY, J. K. 2011. *Oral development and histology,* Thieme.

AYDIN, S. 2007. A comparison of ghrelin, glucose, alpha-amylase and protein levels in saliva from diabetics. *BMB Reports,* 40**,** 29-35.

BABA, S. P., BARSKI, O. A., AHMED, Y., O'TOOLE, T. E., CONKLIN, D. J., BHATNAGAR, A. & SRIVASTAVA, S. 2009. Reductive metabolism of AGE precursors: a metabolic route for preventing AGE accumulation in cardiovascular tissue. *Diabetes,* 58**,** 2486-2497.

BABAEI-JADIDI, R., KARACHALIAS, N., AHMED, N., BATTAH, S. & THORNALLEY, P. J. 2003. Prevention of incipient diabetic nephropathy by high-dose thiamine and benfotiamine. *Diabetes,* 52**,** 2110-20.

BAILEY, R., COOPER, J. D., ZEITELS, L., SMYTH, D. J., YANG, J. H., WALKER, N. M., HYPPONEN, E., DUNGER, D. B., RAMOS-LOPEZ, E., BADENHOOP, K., NEJENTSEV, S. & TODD, J. A. 2007. Association of the vitamin D metabolism gene CYP27B1 with type 1 diabetes. *Diabetes,* 56**,** 2616-21.

BAKER, P. J. 2000. The role of immune responses in bone loss during periodontal disease. *Microbes and Infection,* 2**,** 1181-1192.

BALAKRISHNAN, A. & MENON, V. P. 2007a. Effect of hesperidin on nicotine toxicity and histopathological studies. *Toxicology mechanisms and methods,* 17**,** 233-239.

BALAKRISHNAN, A. & MENON, V. P. 2007b. Protective effect of hesperidin on nicotine induced toxicity in rats. *Indian journal of experimental biology,* 45**,** 194.

BANTSCHEFF, M., LEMEER, S., SAVITSKI, M. M. & KUSTER, B. 2012. Quantitative mass spectrometry in proteomics: critical review update from 2007 to the present. *Analytical and bioanalytical chemistry,* 404**,** 939-965.

BANTSCHEFF, M., SCHIRLE, M., SWEETMAN, G., RICK, J. & KUSTER, B. 2007. Quantitative mass spectrometry in proteomics: a critical review. *Analytical and bioanalytical chemistry,* 389**,** 1017-1031.

BARCZYK, M., BOLSTAD, A. I. & GULLBERG, D. 2013. Role of integrins in the periodontal ligament: organizers and facilitators. *Periodontology 2000,* 63**,** 29-47.

BARCZYK, M., OLSEN, L.-H. B., DA FRANCA, P., LOOS, B., MUSTAFA, K., GULLBERG, D. & BOLSTAD, A. 2009. A role for α11β1 integrin in the human periodontal ligament. *Journal of dental research,* 88**,** 621-626.

BARGER, J. L., KAYO, T., VANN, J. M., ARIAS, E. B., WANG, J., HACKER, T. A., WANG, Y., RAEDERSTORFF, D., MORROW, J. D. & LEEUWENBURGH, C. 2008. A low dose of dietary resveratrol partially mimics caloric restriction and retards aging parameters in mice. *PloS one,* 3**,** e2264.

BARTOLD, P. M. 2006. Periodontal tissues in health and disease: introduction. *Periodontol 2000,* 40**,** 7-10.

BATTAH, S., AHMED, N. & THORNALLEY, P. J. Kinetics and mechanism of the reaction of metformin with methylglyoxal. International Congress Series, 2002. Elsevier, 355-356.

BAUR, J. A., PEARSON, K. J., PRICE, N. L., JAMIESON, H. A., LERIN, C., KALRA, A., PRABHU, V. V., ALLARD, J. S., LOPEZ-LLUCH, G. & LEWIS, K. 2006. Resveratrol improves health and survival of mice on a high-calorie diet. *Nature,* 444**,** 337-342.

BAUR, J. A. & SINCLAIR, D. A. 2006. Therapeutic potential of resveratrol: the in vivo evidence. *Nature reviews Drug discovery,* 5**,** 493-506.

BECK, J. D., SLADE, G. & OFFENBACHER, S. 2000. Oral disease, cardiovascular disease and systemic inflammation. *Periodontology 2000,* 23**,** 110-120.

BEERTSEN, W., MCCULLOCH, C. A. G. & SODEK, J. 1997. The periodontal ligament: a unique, multifunctional connective tissue. *Periodontol 2000,* 13**,** 20-40.

BEISSWENGER, P. J., HOWELL, S. K., NELSON, R. G., MAUER, M. & SZWERGOLD, B. S. 2003. Alpha-oxoaldehyde metabolism and diabetic complications. *Biochem Soc Trans,* 31**,** 1358-63.

BEISSWENGER, P. J., HOWELL, S. K., O'DELL, R. M., WOOD, M. E., TOUCHETTE, A. D. & SZWERGOLD, B. S. 2001. alpha-Dicarbonyls

increase in the postprandial period and reflect the degree of hyperglycemia. *Diabetes Care,* 24**,** 726-32.

BEISSWENGER, P. J., HOWELL, S. K., TOUCHETTE, A. D., LAL, S. & SZWERGOLD, B. S. 1999. Metformin reduces systemic methylglyoxal levels in type 2 diabetes. *Diabetes,* 48**,** 198-202.

BELYANTSEVA, I. A., PERRIN, B. J., SONNEMANN, K. J., ZHU, M., STEPANYAN, R., MCGEE, J., FROLENKOV, G. I., WALSH, E. J., FRIDERICI, K. H. & FRIEDMAN, T. B. 2009. γ-Actin is required for cytoskeletal maintenance but not development. *Proceedings of the National Academy of Sciences,* 106**,** 9703-9708.

BENER, A., SALEH, N. M. & AL-HAMAQ, A. 2011. Prevalence of gestational diabetes and associated maternal and neonatal complications in a fast-developing community: global comparisons. *Int J Womens Health,* 3**,** 367-73.

BENNETT, S. T. & TODD, J. A. 1996. Human type 1 diabetes and the insulin gene: principles of mapping polygenes. *Annu Rev Genet,* 30**,** 343-70.

BHATTARAI, G., POUDEL, S. B., KOOK, S.-H. & LEE, J.-C. 2016. Resveratrol prevents alveolar bone loss in an experimental rat model of periodontitis. *Acta biomaterialia,* 29**,** 398-408.

BIERHAUS, A., FLEMING, T., STOYANOV, S., LEFFLER, A., BABES, A., NEACSU, C., SAUER, S. K., EBERHARDT, M., SCHNÖLZER, M., LASISCHKA, F., NEUHUBER, W. L., KICHKO, T. I., KONRADE, I., ELVERT, R., MIER, W., PIRAGS, V., LUKIC, I. K., MORCOS, M., DEHMER, T., RABBANI, N., THORNALLEY, P. J., EDELSTEIN, D., NAU, C., FORBES, J., HUMPERT, P. M., SCHWANINGER, M., ZIEGLER, D., STERN, D. M., COOPER, M. E., HABERKORN, U., BROWNLEE, M., REEH, P. W. & NAWROTH, P. P. 2012. Methylglyoxal modification of Nav1.8 facilitates nociceptive neuron firing and causes hyperalgesia in diabetic neuropathy. *Nat Med,* 18**,** 926-933.

BIERHAUS, A., KONRADE, I., HAAG, G., HUMPERT, P., MORCOS, M., HAMMES, H., TEW, K. & NAWROTH, P. 2005a. The receptor RAGE regulates glyoxalase-1 transcription, expression and activity. *Diabetologia,* 48**,** A90–A90.

BIERHAUS, A., STOYANOV, S., HAAG, G. M., KONRADE, I. 2006. RAGE-deficiency reduces diabetes-associated impairment of glyoxalase-1 in neuronal cells. *Diabetes,* 55**,** A511-A511.

BIRKENMEIER, G., STEGEMANN, C., HOFFMANN, R., GÜNTHER, R., HUSE, K. & BIRKEMEYER, C. 2010. Posttranslational modification of human glyoxalase 1 indicates redox-dependent regulation. *PloS one,* 5**,** e10399.

BONDARENKO, P. V., CHELIUS, D. & SHALER, T. A. 2002. Identification and relative quantitation of protein mixtures by enzymatic digestion followed by capillary reversed-phase liquid chromatography-tandem mass spectrometry. *Analytical chemistry,* 74**,** 4741-4749.

BONSIGNORE, A., LEONCINI, G., SIRI, A. & RICCI, D. 1973. Kinetic behaviour of glyceraldehyde 3-phosphate conversion into methylglyoxal. *The Italian journal of biochemistry,* 22**,** 131.

BOOCOCK, D. J., FAUST, G. E., PATEL, K. R., SCHINAS, A. M., BROWN, V. A., DUCHARME, M. P., BOOTH, T. D., CROWELL, J. A., PERLOFF, M. & GESCHER, A. J. 2007. Phase I dose escalation pharmacokinetic study in healthy volunteers of resveratrol, a potential cancer chemopreventive agent. *Cancer Epidemiology Biomarkers & Prevention,* 16**,** 1246-1252.

BOOKCHIN, R. M. & GALLOP, P. M. 1968. Structure of hemoglobin AIc: Nature of the N-terminal β chain blocking group. *Biochemical and biophysical research communications,* 32**,** 86-93.

BORGNAKKE, W. S. & GENCO, R. J. 2015. Periodontal disease and diabetes mellitus. *International Textbook of Diabetes Mellitus, Fourth Edition, Fourth Edition***,** 988-1004.

BOTTINI, N., MUSUMECI, L., ALONSO, A., RAHMOUNI, S., NIKA, K., ROSTAMKHANI, M., MACMURRAY, J., MELONI, G. F., LUCARELLI, P., PELLECCHIA, M., EISENBARTH, G. S., COMINGS, D. & MUSTELIN, T. 2004. A functional variant of lymphoid tyrosine phosphatase is associated with type I diabetes. *Nat Genet,* 36**,** 337-8.

BRADAMANTE, S., BARENGHI, L. & VILLA, A. 2004. Cardiovascular protective effects of resveratrol. *Cardiovascular drug reviews,* 22**,** 169-188.

BRADFORD, M. 1976. A Rapid and Sensitive Method for the Quantitation of Microgram Quantities of Protein Utilizing the Principle of Protein-Dye Binding. *Analytical Biochemistry,* 72**,** 248-254.

BRANDT, R. B., SIEGEL, S. A., WATERS, M. G. & BLOCH, M. H. 1980. Spectrophotometric assay for D-(−)-lactate in plasma. *Analytical biochemistry,* 102**,** 39-46.

BREM, H. & TOMIC-CANIC, M. 2007. Cellular and molecular basis of wound healing in diabetes. *Journal of Clinical Investigation,* 117**,** 1219.

BROPHY, P., CROWLEY, P. & BARRETT, J. 1990. Relative distribution of glutathione transferase, glyoxalase I and glyoxalase II in helminths. *International journal for parasitology,* 20**,** 259-261.

BROUWERS, O., NIESSEN, P., HAENEN, G., MIYATA, T., BROWNLEE, M., STEHOUWER, C., DE MEY, J. & SCHALKWIJK, C. 2010. Hyperglycaemia-induced impairment of endothelium-dependent vasorelaxation in rat mesenteric arteries is mediated by intracellular methylglyoxal levels in a pathway dependent on oxidative stress. *Diabetologia,* 53**,** 989-1000.

BROUWERS, O., NIESSEN, P. M., FERREIRA, I., MIYATA, T., SCHEFFER, P. G., TEERLINK, T., SCHRAUWEN, P., BROWNLEE, M., STEHOUWER, C. D. & SCHALKWIJK, C. G. 2011. Overexpression of glyoxalase-I reduces hyperglycemia-induced levels of advanced glycation end products and oxidative stress in diabetic rats. *Journal of Biological Chemistry,* 286**,** 1374-1380.

BROWNLEE, M. 2001. Biochemistry and molecular cell biology of diabetic complications. *Nature,* 414**,** 813-20.

BROWNLEE, M. 2005. The pathobiology of diabetic complications: a unifying mechanism. *Diabetes,* 54**,** 1615-25.

BROWNLEE, M., VLASSARA, H., KOONEY, A., ULRICH, P. & CERAMI, A. 1986. Aminoguanidine prevents diabetes-induced arterial wall protein cross-linking. *Science,* 232**,** 1629-1632.

BRUCE, C. R., CAREY, A. L., HAWLEY, J. A. & FEBBRAIO, M. A. 2003. Intramuscular Heat Shock Protein 72 and Heme Oxygenase-1 mRNA Are Reduced in Patients With Type 2 Diabetes Evidence That Insulin Resistance Is Associated With a Disturbed Antioxidant Defense Mechanism. *Diabetes,* 52**,** 2338-2345.

BUETLER, T. M., LECLERC, E., BAUMEYER, A., LATADO, H., NEWELL, J., ADOLFSSON, O., PARISOD, V., RICHOZ, J., MAURER, S. & FOATA, F. 2008. Nε-carboxymethyllysine-modified proteins are unable to bind to RAGE and activate an inflammatory response. *Molecular nutrition & food research,* 52**,** 370-378.

BULLON, P., MORILLO, J., RAMIREZ-TORTOSA, M., QUILES, J., NEWMAN, H. & BATTINO, M. 2009. Metabolic syndrome and periodontitis: is oxidative stress a common link? *Journal of Dental Research,* 88**,** 503-518.

BULLON, P., NEWMAN, H. N. & BATTINO, M. 2014. Obesity, diabetes mellitus, atherosclerosis and chronic periodontitis: a shared pathology via oxidative stress and mitochondrial dysfunction? *Periodontology 2000,* 64**,** 139-153.

BUNN, H., HANEY, D., GABBAY, K. & GALLOP, P. 1975. Further identification of the nature and linkage of the carbohydrate in hemoglobin A1c. *Biochemical and biophysical research communications,* 67**,** 103.

BURKHART, J. M., PREMSLER, T. & SICKMANN, A. 2011. Quality control of nano-LC-MS systems using stable isotope-coded peptides. *Proteomics,* 11**,** 1049-1057.

BUSH, P. E. & NORTON, S. J. 1985. S-(Nitrocarbobenzoxy)glutathiones: potent competitive inhibitors of mammalian glyoxalase II. *J. Med. Chem.,* 28**,** 828-830.

BUXTON, T. & GUILBAULT, G. 1974. Fluorometric analysis for N'-formylkynurenine in plasma and urine. *Clinical Chemistry,* 20**,** 765-768.

CAHAN, P., LI, Y., IZUMI, M. & GRAUBERT, T. A. 2009. The impact of copy number variation on local gene expression in mouse hematopoietic stem and progenitor cells. *Nature genetics,* 41**,** 430-437.

CAMERON, A. D., OLIN, B., RIDDERSTRÖM, M., MANNERVIK, B. & JONES, T. A. 1997. Crystal structure of human glyoxalase I—evidence for gene duplication and 3D domain swapping. *The EMBO journal,* 16**,** 3386-3395.

CAMERON, A. D., RIDDERSTRÖM, M., OLIN, B., KAVARANA, M. J., CREIGHTON, D. J. & MANNERVIK, B. 1999a. Reaction mechanism of glyoxalase I explored by an X-ray crystallographic analysis of the human enzyme in complex with a transition state analogue. *Biochemistry,* 38**,** 13480-13490.

CAMERON, A. D., RIDDERSTROM, M., OLIN, B. & MANNERVIK, B. 1999b. Crystal structure of human glyoxalase II and its complex with a glutathione thiolester substrate analogue. *Structure,* 7**,** 1067-78.

CANI, P. D., AMAR, J., IGLESIAS, M. A., POGGI, M., KNAUF, C., BASTELICA, D., NEYRINCK, A. M., FAVA, F., TUOHY, K. M. & CHABO, C. 2007. Metabolic endotoxemia initiates obesity and insulin resistance. *Diabetes,* 56**,** 1761-1772.

CARDENAS-LEON, M., DÍAZ-DÍAZ, E., ARGÜELLES-MEDINA, R., SANCHEZ-CANALES, P., DIAZ-SANCHEZ, V. & LARREA, F. 2008. [Glycation and protein crosslinking in the diabetes and ageing pathogenesis].

Revista de investigacion clinica; organo del Hospital de Enfermedades de la Nutricion, 61**,** 505-520.

CASATI, M. Z., ALGAYER, C., CARDOSO DA CRUZ, G., RIBEIRO, F. V., CASARIN, R. C., PIMENTEL, S. P. & CIRANO, F. R. 2013. Resveratrol decreases periodontal breakdown and modulates local levels of cytokines during periodontitis in rats. *Journal of periodontology,* 84**,** e58-e64.

CERAMI, A. 1986. Aging of proteins and nucleic acids: what is the role of glucose? . *Trends in Biochemical Sciences,* 11**,** 311-314.

CERIELLO, A. 2000. Oxidative stress and glycemic regulation. *Metabolism-Clinical and Experimental,* 49**,** 27-29.

CHANG, P.-C., CHIEN, L.-Y., YEO, J. F., WANG, Y.-P., CHUNG, M.-C., CHONG, L. Y., KUO, M. Y.-P., CHEN, C.-H., CHIANG, H.-C., NG, B. N., LEE, Q. Q., PHAY, Y. K., NG, J. R. & ERK, K. Y. 2013. Progression of Periodontal Destruction and the Roles of Advanced Glycation End Products in Experimental Diabetes. *Journal of Periodontology,* 84**,** 379-388.

CHANG, P.-C. & LIM, L. P. 2012. Interrelationships of periodontitis and diabetes: A review of the current literature. *Journal of Dental Sciences,* 7**,** 272-282.

CHANG, Y. C., HSIEH, Y. S., LII, C. K., HUANG, F. M., TAI, K. W. & CHOU, M. Y. 2003. Induction of c-fos expression by nicotine in human periodontal ligament fibroblasts is related to cellular thiol levels. *Journal of periodontal research,* 38**,** 44-50.

CHAPPLE, I. L., MILWARD, M. R., LING-MOUNTFORD, N., WESTON, P., CARTER, K., ASKEY, K., DALLAL, G. E., DE SPIRT, S., SIES, H. & PATEL, D. 2012. Adjunctive daily supplementation with encapsulated fruit, vegetable and berry juice powder concentrates and clinical periodontal outcomes: a double-blind RCT. *Journal of clinical periodontology,* 39**,** 62-72.

CHAVAKIS, T., BIERHAUS, A., AL-FAKHRI, N., SCHNEIDER, D., WITTE, S., LINN, T., NAGASHIMA, M., MORSER, J., ARNOLD, B., PREISSNER, K. T. & NAWROTH, P. P. 2003. The pattern recognition receptor (RAGE) is a counterreceptor for leukocyte integrins: a novel pathway for inflammatory cell recruitment. *J Exp Med,* 198**,** 1507-15.

CHELIUS, D. & BONDARENKO, P. V. 2002. Quantitative profiling of proteins in complex mixtures using liquid chromatography and mass spectrometry. *Journal of proteome research,* 1**,** 317-323.

CHEN, F., WOLLMER, M. A., HOERNDLI, F., MUNCH, G., KUHLA, B., ROGAEV, E. I., TSOLAKI, M., PAPASSOTIROPOULOS, A. & GOTZ, J. 2004. Role for glyoxalase I in Alzheimer's disease. *Proceedings of the National Academy of Sciences,* 101**,** 7687-7692.

CHEN, M.-C., YE, Y.-Y., JI, G. & LIU, J.-W. 2010a. Hesperidin upregulates heme oxygenase-1 to attenuate hydrogen peroxide-induced cell damage in hepatic L02 cells. *Journal of agricultural and food chemistry,* 58**,** 3330-3335.

CHEN, M., GU, H., YE, Y., LIN, B., SUN, L., DENG, W., ZHANG, J. & LIU, J. 2010b. Protective effects of hesperidin against oxidative stress of tert-butyl hydroperoxide in human hepatocytes. *Food and Chemical Toxicology,* 48**,** 2980-2987.

CHEN, Q., FISCHER, A., REAGAN, J. D., YAN, L.-J. & AMES, B. N. 1995. Oxidative DNA damage and senescence of human diploid fibroblast cells. *Proceedings of the National Academy of Sciences,* 92**,** 4337-4341.

CHEN, S., LI, J., ZHANG, Z., LI, W., SUN, Y., ZHANG, Q., FENG, X. & ZHU, W. 2012. Effects of resveratrol on the amelioration of insulin resistance in KKAy mice. *Canadian journal of physiology and pharmacology,* 90**,** 237-242.

CHEN, Y.-T., SHIH, C.-J., OU, S.-M., HUNG, S.-C., LIN, C.-H., TARNG, D.-C. & GROUP, T. G. K. D. T. R. 2015. Periodontal Disease and Risks of Kidney Function Decline and Mortality in Older People: A Community-Based Cohort Study. *American Journal of Kidney Diseases*.

CHEN, Y., AHMED, N. & THORNALLEY, P. 2005. Peptide mapping of human hemoglobin modified minimally by methylglyoxal in vitro. *Annals of the New York Academy of Sciences,* 1043**,** 905-905.

CHENG, A.-S., CHENG, Y.-H., CHIOU, C.-H. & CHANG, T.-L. 2012. Resveratrol upregulates Nrf2 expression to attenuate methylglyoxal-induced insulin resistance in Hep G2 cells. *Journal of agricultural and food chemistry,* 60**,** 9180-9187.

CHENG, C., TSUNEYAMA, K., KOMINAMI, R., SHINOHARA, H., SAKURAI, S., YONEKURA, H., WATANABE, T., TAKANO, Y., YAMAMOTO, H. & YAMAMOTO, Y. 2005. Expression profiling of endogenous secretory receptor for advanced glycation end products in human organs. *Modern pathology,* 18**,** 1385-1396.

CHI, T.-C., CHEN, W.-P., CHI, T.-L., KUO, T.-F., LEE, S.-S., CHENG, J.-T. & SU, M.-J. 2007. Phosphatidylinositol-3-kinase is involved in the

antihyperglycemic effect induced by resveratrol in streptozotocin-induced diabetic rats. *Life Sciences,* 80**,** 1713-1720.

CHIBA, H., KIM, H., MATSUMOTO, A., AKIYAMA, S., ISHIMI, Y., SUZUKI, K. & UEHARA, M. 2014. Hesperidin Prevents Androgen Deficiency-induced Bone Loss in Male Mice. *Phytotherapy Research,* 28**,** 289-295.

CHIN, M. P., REISMAN, S. A., BAKRIS, G. L., O'GRADY, M., LINDE, P. G., MCCULLOUGH, P. A., PACKHAM, D., VAZIRI, N. D., WARD, K. W. & WARNOCK, D. G. 2014. Mechanisms contributing to adverse cardiovascular events in patients with type 2 diabetes mellitus and stage 4 chronic kidney disease treated with bardoxolone methyl. *American journal of nephrology,* 39**,** 499-508.

CHOI, E. J. 2008. Antioxidative effects of hesperetin against 7, 12-dimethylbenz (a) anthracene-induced oxidative stress in mice. *Life sciences,* 82**,** 1059-1064.

CHOI, E. J., KIM, G. D., CHEE, K.-M. & KIM, G.-H. 2006. Effects of hesperetin on vessel structure formation in mouse embryonic stem (mES) cells. *Nutrition,* 22**,** 947-951.

CHOI, I.-Y., KIM, S.-J., JEONG, H.-J., PARK, S.-H., SONG, Y.-S., LEE, J.-H., KANG, T.-H., PARK, J.-H., HWANG, G.-S. & LEE, E.-J. 2007. Hesperidin inhibits expression of hypoxia inducible factor-1 alpha and inflammatory cytokine production from mast cells. *Molecular and cellular biochemistry,* 305**,** 153-161.

CHOU, A. M., SAE-LIM, V., LIM, T. M., SCHANTZ, J. T., TEOH, S. H., CHEW, C. L. & HUTMACHER, D. W. 2002. Culturing and characterization of human periodontal ligament fibroblasts—a preliminary study. *Materials Science and Engineering: C,* 20**,** 77-83.

CHOUDHARY, C., KUMAR, C., GNAD, F., NIELSEN, M. L., REHMAN, M., WALTHER, T. C., OLSEN, J. V. & MANN, M. 2009. Lysine acetylation targets protein complexes and co-regulates major cellular functions. *Science,* 325**,** 834-40.

CIANCIOLA, L. J., PARK, B. H., BRUCK, E., MOSOVICH, L. & GENCO, R. J. 1982. Prevalence of Periodontal Disease in Insulin-Dependent Diabetes Mellitus (Juvenile Diabetes). *The Journal of the American Dental Association,* 104**,** 653-660.

CIDDI, V. & DODDA, D. 2014. Therapeutic potential of resveratrol in diabetic complications: In vitro and in vivo studies. *Pharmacological Reports,* 66**,** 799-803.

CLELLAND, J. D. & THORNALLEY, P. J. 1991. S-2-hydroxyacylglutathione-derivatives: enzymatic preparation, purification and characterisation. *J. Chem. Soc., Perkin Trans. 1***,** 3009-3015.

CLUGSTON, SUSAN L., YAJIMA, R. & HONEK, JOHN F. 2004. Investigation of metal binding and activation of Escherichia coli glyoxalase I: kinetic, thermodynamic and mutagenesis studies. *Biochem. J.,* 377**,** 309.

COHEN, J. 2002. The immunopathogenesis of sepsis. *Nature,* 420**,** 885-891.

COMPTON, S. J. & JONES, C. G. 1985. Mechanism of dye response and interference in the Bradford protein assay. *Anal Biochem,* 151**,** 369-74.

CONBOY, C. M., SPYROU, C., THORNE, N. P., WADE, E. J., BARBOSA-MORAIS, N. L., WILSON, M. D., BHATTACHARJEE, A., YOUNG, R. A., TAVARÉ, S. & LEES, J. A. 2007. Cell cycle genes are the evolutionarily conserved targets of the E2F4 transcription factor. *PLoS One,* 2**,** e1061.

CONNOR, H., WOODS, H. & LEDINGHAM, J. 1983. Comparison of the kinetics and utilisation of D (–)-and L (+)-sodium lactate in normal man. *Annals of nutrition and metabolism,* 27**,** 481-487.

CONSTANT, J. 1997. Alcohol, ischemic heart disease, and the French paradox. *Clinical cardiology,* 20**,** 420-424.

CORDELL, P. A., FUTERS, T. S., GRANT, P. J. & PEASE, R. J. 2004. The Human hydroxyacylglutathione hydrolase (HAGH) gene encodes both cytosolic and mitochondrial forms of glyoxalase II. *J Biol Chem,* 279**,** 28653-61.

COREY, L. A., NANCE, W. E., HOFSTEDE, P. & SCHENKEIN, H. A. 1993. Self-reported periodontal disease in a Virginia twin population. *Journal of periodontology,* 64**,** 1205-1208.

COVERT, M. W. 2005. Achieving Stability of Lipopolysaccharide-Induced NF- B Activation. *Science,* 309**,** 1854-1857.

CSISZAR, A., LABINSKYY, N., PINTO, J. T., BALLABH, P., ZHANG, H., LOSONCZY, G., PEARSON, K., DE CABO, R., PACHER, P. & ZHANG, C. 2009. Resveratrol induces mitochondrial biogenesis in endothelial cells. *American Journal of Physiology-Heart and Circulatory Physiology,* 297**,** H13-H20.

CUSI, K., MAEZONO, K., OSMAN, A., PENDERGRASS, M., PATTI, M. E., PRATIPANAWATR, T., DEFRONZO, R. A., KAHN, C. R. & MANDARINO, L. J. 2000. Insulin resistance differentially affects the PI 3-

kinase- and MAP kinase-mediated signaling in human muscle. *J Clin Invest,* 105**,** 311-20.

DA-CUNHA, M., JACQUEMIN, P., DELPIERRE, G., GODFRAIND, C., THÉATE, I., VERTOMMEN, D., CLOTMAN, F., LEMAIGRE, F., DEVUYST, O. & VAN SCHAFTINGEN, E. 2006. Increased protein glycation in fructosamine 3-kinase-deficient mice. *Biochem. J,* 399**,** 257-264.

DAKIN, H. & DUDLEY, H. 1913. An enzyme concerned with the formation of hydroxy acids from ketonic aldehydes. *Journal of Biological Chemistry,* 14**,** 155-157.

DANDONA, P. 2004. Inflammation: the link between insulin resistance, obesity and diabetes. *Trends in Immunology,* 25**,** 4-7.

DARLING, T. N. & BLUM, J. J. 1988. d-lactate production by< i> Leishmania braziliensis</i> through the glyoxalase pathway. *Molecular and biochemical parasitology,* 28**,** 121-127.

DAUPHINEE, S. M. & KARSAN, A. 2005. Lipopolysaccharide signaling in endothelial cells. *Lab Invest,* 86**,** 9-22.

DE HEMPTINNE, V., RONDAS, D., TOEPOEL, M. & VANCOMPERNOLLE, K. 2009. Phosphorylation on Thr-106 and NO-modification of glyoxalase I suppress the TNF-induced transcriptional activity of NF-κB. *Molecular and cellular biochemistry,* 325**,** 169-178.

DE HEMPTINNE, V., RONDAS, D., VANDEKERCKHOVE, J. & VANCOMPERNOLLE, K. 2007. Tumour necrosis factor induces phosphorylation primarily of the nitric-oxide-responsive form of glyoxalase I. *Biochem. J,* 407**,** 121-128.

DE VRESE, M. & BARTH, C. 1991. Postprandial plasma D-lactate concentrations after yogurt ingestion. *Zeitschrift für Ernährungswissenschaft,* 30**,** 131-137.

DEGEN, J., HELLWIG, M. & HENLE, T. 2012. 1, 2-Dicarbonyl compounds in commonly consumed foods. *Journal of agricultural and food chemistry,* 60**,** 7071-7079.

DELPIERRE, G., RIDER, M. H., COLLARD, F., STROOBANT, V., VANSTAPEL, F., SANTOS, H. & VAN SCHAFTINGEN, E. 2000. Identification, cloning, and heterologous expression of a mammalian fructosamine-3-kinase. *Diabetes,* 49**,** 1627-1634.

DOBLER, D., AHMED, N., SONG, L., EBOIGBODIN, K. E. & THORNALLEY, P. J. 2006. Increased dicarbonyl metabolism in endothelial cells in

hyperglycemia induces anoikis and impairs angiogenesis by RGD and GFOGER motif modification. *Diabetes,* 55**,** 1961-9.

DOLINSKY, V. W. & DYCK, J. R. 2011. Calorie restriction and resveratrol in cardiovascular health and disease. *Biochimica et Biophysica Acta (BBA)-Molecular Basis of Disease,* 1812**,** 1477-1489.

DONNELLY, R., EMSLIE-SMITH, A. M., GARDNER, I. D. & MORRIS, A. D. 2000. ABC of arterial and venous disease: vascular complications of diabetes. *BMJ,* 320**,** 1062-6.

DOWSETT, S., ARCHILA, L., SEGRETO, V., ECKERT, G. & KOWOLIK, M. 2001. Periodontal disease status of an indigenous population of Guatemala, Central America. *Journal of clinical periodontology,* 28**,** 663-671.

DRAGANI, B., COCCO, R., RIDDERSTROM, M., STENBERG, G., MANNERVIK, B. & ACETO, A. 1999. Unfolding and refolding of human glyoxalase II and its single-tryptophan mutants. *J Mol Biol,* 291**,** 481-90.

DU, J., ZENG, J., OU, X., REN, X. & CAI, S. 2006. Methylglyoxal downregulates Raf-1 protein through a ubiquitination-mediated mechanism. *The international journal of biochemistry & cell biology,* 38**,** 1084-1091.

DU, R., LONG, J., YAO, J., DONG, Y., YANG, X., TANG, S., ZUO, S., HE, Y. & CHEN, X. 2010. Subcellular quantitative proteomics reveals multiple pathway cross-talk that coordinates specific signaling and transcriptional regulation for the early host response to LPS. *Journal of proteome research,* 9**,** 1805-1821.

DUNN, J. A., MCCANCE, D. R., THORPE, S. R., LYONS, T. J. & BAYNES, J. W. 1991. Age-dependent accumulation of N. epsilon.-(carboxymethyl) lysine and N. epsilon.-(carboxymethyl) hydroxylysine in human skin collagen. *Biochemistry,* 30**,** 1205-1210.

DUNN, J. A., PATRICK, J. S., THORPE, S. R. & BAYNES, J. W. 1989. Oxidation of glycated proteins: age-dependent accumulation of N. epsilon.-(carboxymethyl) lysine in lens proteins. *Biochemistry,* 28**,** 9464-9468.

EDWARDS, L., CLELLAND, J. D. & THORNALLEY, P. J. 1993. Characteristics of the inhibition of human promyelocytic leukaemia HL60 cell growth by Sd-lactoylglutathione in vitro. *Leukemia research,* 17**,** 305-310.

EDWARDS, L. G., ADESIDA, A. & THORNALLEY, P. J. 1996. Inhibition of human leukaemia 60 cell growth by S-D-lactoylglutathione in vitro. Mediation by metabolism to N-D-lactoylcysteine and induction of apoptosis. *Leukemia research,* 20**,** 17-26.

EDWARDS, L. G. & THORNALLEY, P. J. 1994. Prevention of S-d-lactoylglutathione-induced inhibition of human leukaemia 60 cell growth by uridine. *Leukemia research,* 18**,** 717-722.

EFFROS, R. B. & WALFORD, R. L. 1984. T cell cultures and the Hayflick limit. *Human immunology,* 9**,** 49-65.

EFSA 2016. Safety of synthetic trans-resveratrol as a novel food pursuant to Regulation. *EFSA Journal 2016,* 14**,** 4368.

EISENBARTH, G. 1986. Type I diabetes mellitus. A chronic autoimmune disease. *The New England journal of medicine,* 314**,** 1360.

EKWALL, K. & MANNERVIK, B. 1973. The sterochemical configuration of the lactoyl group of< i> S</i>-lactoylglutathionine formed by the action of glyoxalase I from porcine erythrocytes and yeast. *Biochimica et Biophysica Acta (BBA)-General Subjects,* 297**,** 297-299.

EL-OSTA, A., BRASACCHIO, D., YAO, D., POCAI, A., JONES, P. L., ROEDER, R. G., COOPER, M. E. & BROWNLEE, M. 2008. Transient high glucose causes persistent epigenetic changes and altered gene expression during subsequent normoglycemia. *The Journal of experimental medicine,* 205**,** 2409-2417.

ELAVARASAN, J., VELUSAMY, P., GANESAN, T., RAMAKRISHNAN, S. K., RAJASEKARAN, D. & PERIANDAVAN, K. 2012. Hesperidin-mediated expression of Nrf2 and upregulation of antioxidant status in senescent rat heart. *Journal of Pharmacy and Pharmacology,* 64**,** 1472-1482.

ELDRED, G. E. & LASKY, M. R. 1993. Retinal age pigments generated by self-assembling lysosomotropic detergents.

EMRICH, L. J., SHLOSSMAN, M. & GENCO, R. J. 1991. Periodontal Disease in Non-Insulin-Dependent Diabetes Mellitus. *Journal of Periodontology,* 62**,** 123-131.

ENGEBRETSON, S. P., HEY-HADAVI, J., EHRHARDT, F. J., HSU, D., CELENTI, R. S., GRBIC, J. T. & LAMSTER, I. B. 2004. Gingival Crevicular Fluid Levels of Interleukin-1β and Glycemic Control in Patients With Chronic Periodontitis and Type 2 Diabetes. *Journal of Periodontology,* 75**,** 1203-1208.

ENGELGAU, M. M., HERMAN, W. H., SMITH, P. J., GERMAN, R. R. & AUBERT, R. E. 1995. The epidemiology of diabetes and pregnancy in the U.S., 1988. *Diabetes Care,* 18**,** 1029-33.

ENGELS-DEUTSCH, M., PINI, A., YAMASHITA, Y., SHIBATA, Y., HAIKEL, Y., SCHOLLER-GUINARD, M. & KLEIN, J. P. 2003. Insertional Inactivation of pac and rmlB Genes Reduces the Release of Tumor Necrosis Factor Alpha, Interleukin-6, and Interleukin-8 Induced by Streptococcus mutans in Monocytic, Dental Pulp, and Periodontal Ligament Cells. *Infection and Immunity,* 71**,** 5169-5177.

ENGLISH, H., PACK, A. & MOLAN, P. 2004. The effects of manuka honey on plaque and gingivitis: a pilot study. *Journal of the International Academy of Periodontology,* 6**,** 63-67.

ERIKSSON, U. J., WENTZEL, P., MINHAS, H. S. & THORNALLEY, P. J. 1998. Teratogenicity of 3-deoxyglucosone and diabetic embryopathy. *Diabetes,* 47**,** 1960-1966.

ERLUND, I., MERIRINNE, E., ALFTHAN, G. & ARO, A. 2001. Plasma kinetics and urinary excretion of the flavanones naringenin and hesperetin in humans after ingestion of orange juice and grapefruit juice. *The Journal of nutrition,* 131**,** 235-241.

EURODIAB, A. 2000. Variation and trends in incidence of childhood diabetes in Europe. *Lancet,* 355**,** 873-876.

EWASCHUK, J. B., NAYLOR, J. M. & ZELLO, G. A. 2005. D-lactate in human and ruminant metabolism. *The Journal of nutrition,* 135**,** 1619-1625.

FAJANS, S. S., BELL, G. I. & POLONSKY, K. S. 2001. Molecular mechanisms and clinical pathophysiology of maturity-onset diabetes of the young. *N Engl J Med,* 345**,** 971-80.

FANG, X., SCHUMMER, M., MAO, M., YU, S., TABASSAM, F. H., SWABY, R., HASEGAWA, Y., TANYI, J. L., LAPUSHIN, R., EDER, A., JAFFE, R., ERICKSON, J. & MILLS, G. B. 2002. Lysophosphatidic acid is a bioactive mediator in ovarian cancer. *Biochimica et Biophysica Acta (BBA) - Molecular and Cell Biology of Lipids,* 1582**,** 257-264.

FARIAS GOMES, SIMONE GUIMARÃES MELOTO, CAROLINA BERALDO CUSTODIO, WILLIAM RIZZATTI-BARBOSA & MARISA, C. 2010. Aging and the periodontium. *Brazilian Journal of Oral Sciences,* 9.

FERGUSON, G. P., VANPATTEN, S., BUCALA, R. & AL-ABED, Y. 1999. Detoxification of methylglyoxal by the nucleophilic bidentate, phenylacylthiazolium bromide. *Chemical research in toxicology,* 12**,** 617-622.

FÉSÜS, L., MUSZBEK, L. & LAKI, K. 1981. The effect of methylglyoxal on actin. *Biochemical and biophysical research communications,* 99**,** 617-622.

FINOT, P. & MAURON, J. 1969. Le blocage de la lysine par la réaction de MAILLARD. I. Synthèse de N-(désoxy-1-D-fructosyl-1)-et N-(désoxy-1-D-lactulosyl-1)-L-lysines. *Helvetica Chimica Acta,* 52**,** 1488-1495.

FLORENS, L., CAROZZA, M. J., SWANSON, S. K., FOURNIER, M., COLEMAN, M. K., WORKMAN, J. L. & WASHBURN, M. P. 2006. Analyzing chromatin remodeling complexes using shotgun proteomics and normalized spectral abundance factors. *Methods,* 40**,** 303-311.

FOKKEMA, S. 2012. Peripheral blood monocyte responses in periodontitis. *International journal of dental hygiene,* 10**,** 229-235.

FONSECA, V. & JOHN-KALARICKAL, J. 2010. Type 2 diabetes mellitus: epidemiology, genetics, pathogenesis, and clinical manifestations. *In:* PORETSKY, L. (ed.) *Principles of diabetes mullitus.* 2nd ed. New York: Springer.

FORRISTAL, C. E., CHRISTENSEN, D. R., CHINNERY, F. E., PETRUZZELLI, R., PARRY, K. L., SANCHEZ-ELSNER, T. & HOUGHTON, F. D. 2013. Environmental oxygen tension regulates the energy metabolism and self-renewal of human embryonic stem cells. *PloS one,* 8**,** e62507.

FROHLICH-REITERER, E. E., HOFER, S., KASPERS, S., HERBST, A., KORDONOURI, O., SCHWARZ, H. P., SCHOBER, E., GRABERT, M. & HOLL, R. W. 2008. Screening frequency for celiac disease and autoimmune thyroiditis in children and adolescents with type 1 diabetes mellitus--data from a German/Austrian multicentre survey. *Pediatr Diabetes,* 9**,** 546-53.

FRÖJDÖ, S., DURAND, C. & PIROLA, L. 2008. Metabolic effects of resveratrol in mammals—a link between improved insulin action and aging. *Curr Aging Sci,* 1**,** 145-51.

FUKUNAGA, Y., KATSURAGI, Y., IZUMI, T. & SAKIYAMA, F. 1982. Fluorescence Characteristics of Kynurenine and N′-Formylkynurenine, Their Use as Reporters of the Environment of Tryptophan 62 in Hen Egg-White Lysozyme. *Journal of biochemistry,* 92**,** 129-141.

FURUKAWA, T., WAKAI, K., YAMANOUCHI, K., OSHIDA, Y., MIYAO, M., WATANABE, T. & SATO, Y. 2007. Associations of periodontal damage and tooth loss with atherogenic factors among patients with type 2 diabetes mellitus. *Internal Medicine,* 46**,** 1359-1364.

GALE, C. P. & GRANT, P. J. 2004. The characterisation and functional analysis of the human glyoxalase-1 gene using methods of bioinformatics. *Gene,* 340**,** 251-260.

GALE, E. A. & GILLESPIE, K. M. 2001. Diabetes and gender. *Diabetologia,* 44**,** 3-15.

GALLAGHER, K. A., LIU, Z.-J., XIAO, M., CHEN, H., GOLDSTEIN, L. J., BUERK, D. G., NEDEAU, A., THOM, S. R. & VELAZQUEZ, O. C. 2007. Diabetic impairments in NO-mediated endothelial progenitor cell mobilization and homing are reversed by hyperoxia and SDF-1α. *Journal of Clinical Investigation,* 117**,** 1249.

GALLET, X., CHARLOTEAUX, B., THOMAS, A. & BRASSEUR, R. 2000. A fast method to predict protein interaction sites from sequences. *J Mol Biol,* 302**,** 917-26.

GANGADHARIAH, M. H., WANG, B., LINETSKY, M., HENNING, C., SPANNEBERG, R., GLOMB, M. A. & NAGARAJ, R. H. 2010. Hydroimidazolone modification of human αA-crystallin: Effect on the chaperone function and protein refolding ability. *Biochimica et Biophysica Acta (BBA)-Molecular Basis of Disease,* 1802**,** 432-441.

GARG, A., GARG, S., ZANEVELD, L. & SINGLA, A. 2001. Chemistry and pharmacology of the citrus bioflavonoid hesperidin. *Phytotherapy Research,* 15**,** 655-669.

GENCO, R. J., VAN DYKE, T., LEVINE, M., NELSON, R. & WILSON, M. 1986. 1985 Kreshover lecture. Molecular factors influencing neutrophil defects in periodontal disease. *Journal of dental research,* 65**,** 1379-1391.

GEPTS, W. & LECOMPTE, P. M. 1981. The pancreatic islets in diabetes. *Am J Med,* 70**,** 105-15.

GHOSH, S. & HAYDEN, M. S. 2008. New regulators of NF-κB in inflammation. *Nature Reviews Immunology,* 8**,** 837-848.

GIACCO, F., DU, X., D'AGATI, V. D., MILNE, R., SUI, G., GEOFFRION, M. & BROWNLEE, M. 2014. Knockdown of glyoxalase 1 mimics diabetic nephropathy in nondiabetic mice. *Diabetes,* 63**,** 291-9.

GIALLONGO, A., FEO, S., MOORE, R., CROCE, C. M. & SHOWE, L. C. 1986. Molecular cloning and nucleotide sequence of a full-length cDNA for human alpha enolase. *Proceedings of the National Academy of Sciences,* 83**,** 6741-6745.

GIARDINO, I., EDELSTEIN, D. & BROWNLEE, M. 1994. Nonenzymatic glycosylation in vitro and in bovine endothelial cells alters basic fibroblast growth factor activity. A model for intracellular glycosylation in diabetes. *J Clin Invest,* 94**,** 110-7.

GODFREY, L., YAMADA-FOWLER, N., SMITH, J., THORNALLEY, P. J. & RABBANI, N. 2014. Arginine-directed glycation and decreased HDL plasma concentration and functionality. *Nutrition & diabetes,* 4**,** e134.

GOLUB, L., LEE, H.-M., RYAN, M., GIANNOBILE, W., PAYNE, J. & SORSA, T. 1998. Tetracyclines inhibit connective tissue breakdown by multiple non-antimicrobial mechanisms. *Advances in dental research,* 12**,** 12-26.

GOLUB, L., LEE, H., LEHRER, G., NEMIROFF, A., MCNAMARA, T., KAPLAN, R. & RAMAMURTHY, N. 1983. Minocycline reduces gingival collagenolytic activity during diabetes. *Journal of periodontal research,* 18**,** 516-526.

GREEN, A. & PATTERSON, C. C. 2001. Trends in the incidence of childhood-onset diabetes in Europe 1989-1998. *Diabetologia,* 44 Suppl 3**,** B3-8.

GRIFFIN, N. M., YU, J., LONG, F., OH, P., SHORE, S., LI, Y., KOZIOL, J. A. & SCHNITZER, J. E. 2010. Label-free, normalized quantification of complex mass spectrometry data for proteomic analysis. *Nature biotechnology,* 28**,** 83-89.

GROOP, L. C. 1999. Insulin resistance: the fundamental trigger of type 2 diabetes. *Diabetes Obes Metab,* 1 Suppl 1**,** S1-7.

GRUNDY, S. M. 2000. Metabolic complications of obesity. *Endocrine,* 13**,** 155-65.

GUARENTE, L. 2013. Introduction: Sirtuins in Aging and Diseases. *In:* HIRSCHEY, D. M. (ed.) *Sirtuins: Methods and Protocols.* Totowa, NJ: Humana Press.

GUIGLIA, R., MUSCIOTTO, A., COMPILATO, D., PROCACCINI, M., RUSSO, L., CIAVARELLA, D., MUZIO, L., CANNONE, V., PEPE, I., D'ANGELO, M. & CAMPISI, G. 2010. Aging and Oral Health: Effects in Hard and Soft Tissues. *Current Pharmaceutical Design,* 16**,** 619-630.

GUO, M., EHRLICHER, A. J., MAHAMMAD, S., FABICH, H., JENSEN, M. H., MOORE, J. R., FREDBERG, J. J., GOLDMAN, R. D. & WEITZ, D. A. 2013. The role of vimentin intermediate filaments in cortical and cytoplasmic mechanics. *Biophysical journal,* 105**,** 1562-1568.

GUZMAN, S., KARIMA, M., WANG, H.-Y. & DYKE, T. E. V. 2003. Association between interleukin-1 genotype and periodontal disease in a diabetic population. *Journal of periodontology,* 74**,** 1183-1190.

HAIK JR, G. M., LO, T. W. & THORNALLEY, P. J. 1994. Methylglyoxal concentration and glyoxalase activities in the human lens. *Experimental eye research,* 59**,** 497-500.

HALLER, M. J., ATKINSON, M. A. & SCHATZ, D. 2005. Type 1 diabetes mellitus: etiology, presentation, and management. *Pediatr Clin North Am,* 52**,** 1553-78.

HAMBSCH, B., CHEN, B. G., BRENNDÖRFER, J., MEYER, M., AVRABOS, C., MACCARRONE, G., LIU, R. H., EDER, M., TURCK, C. W. & LANDGRAF, R. 2010. Methylglyoxal-mediated anxiolysis involves increased protein modification and elevated expression of glyoxalase 1 in the brain. *Journal of neurochemistry,* 113**,** 1240-1251.

HANNINEN, A., JALKANEN, S., SALMI, M., TOIKKANEN, S., NIKOLAKAROS, G. & SIMELL, O. 1992. Macrophages, T cell receptor usage, and endothelial cell activation in the pancreas at the onset of insulin-dependent diabetes mellitus. *J Clin Invest,* 90**,** 1901-10.

HANSEN, J. B., PO, G. A., BODVARSDOTTIR, T. B. & WAHL, P. 2004. Inhibition of insulin secretion as a new drug target in the treatment of metabolic disorders. *Current medicinal chemistry,* 11**,** 1595-1615.

HANSEN, R. E., ØSTERGAARD, H., NØRGAARD, P. & WINTHER, J. R. 2007. Quantification of protein thiols and dithiols in the picomolar range using sodium borohydride and 4,4′-dithiodipyridine. *Analytical Biochemistry,* 363**,** 77-82.

HANSEN, R. E. & WINTHER, J. R. 2009. An introduction to methods for analyzing thiols and disulfides: Reactions, reagents, and practical considerations. *Analytical Biochemistry,* 394**,** 147-158.

HARBORNE, J. B. & WILLIAMS, C. A. 2000. Advances in flavonoid research since 1992. *Phytochemistry,* 55**,** 481-504.

HASEGAWA, N. 2008. Effect of high mobility group box 1 (HMGB1) in cultured human periodontal ligament cells. *Kokubyo Gakkai zasshi. The Journal of the Stomatological Society, Japan,* 75**,** 155-161.

HASTINGS, P., LUPSKI, J. R., ROSENBERG, S. M. & IRA, G. 2009. Mechanisms of change in gene copy number. *Nature Reviews Genetics,* 10**,** 551-564.

HATIPOGLU, H., YAYLAK, F. & GUNGOR, Y. 2015. A brief review on the periodontal health in metabolic syndrome patients. *Diabetes & Metabolic Syndrome: Clinical Research & Reviews,* 9**,** 124-126.

HAUSENBLAS, H. A., SCHOULDA, J. A. & SMOLIGA, J. M. 2015. Resveratrol treatment as an adjunct to pharmacological management in type 2 diabetes mellitus—systematic review and meta-analysis. *Molecular nutrition & food research,* 59**,** 147-159.

HAYASHI, T. & NAMKI, M. 1980. Formation of two-carbon sugar fragment at an early stage of the browning reaction of sugar with amine. *Agricultural and Biological Chemistry,* 44**,** 2575-2580.

HENLE, T. & BACHMANN, A. 1996. Synthesis of pyrraline reference material. *Zeitschrift für Lebensmittel-Untersuchung und Forschung,* 202**,** 72-74.

HENLE, T., WALTER, A. W., HAEßNER, R. & KLOSTERMEYER, H. 1994. Detection and identification of a protein-bound imidazolone resulting from the reaction of arginine residues and methylglyoxal. *Zeitschrift für Lebensmittel-Untersuchung und Forschung,* 199**,** 55-58.

HENQUIN, J.-C. 2000. Triggering and amplifying pathways of regulation of insulin secretion by glucose. *Diabetes,* 49**,** 1751-1760.

HERNEBRING, M., BROLEN, G., AGUILANIU, H., SEMB, H. & NYSTROM, T. 2006. Elimination of damaged proteins during differentiation of embryonic stem cells. *Proceedings of the National Academy of Sciences,* 103**,** 7700-7705.

HIGHFIELD, J. 2009. Diagnosis and classification of periodontal disease. *Australian Dental Journal,* 54**,** S11-S26.

HIMO, F. & SIEGBAHN, P. E. 2001. Catalytic mechanism of glyoxalase I: a theoretical study. *Journal of the American Chemical Society,* 123**,** 10280-10289.

HODGE, J. E. 1953. Dehydrated foods, chemistry of browning reactions in model systems. *Journal of Agricultural and Food Chemistry,* 1**,** 928-943.

HOFMANN, M. A., DRURY, S., FU, C., QU, W., TAGUCHI, A., LU, Y., AVILA, C., KAMBHAM, N., BIERHAUS, A. & NAWROTH, P. 1999. RAGE mediates a novel proinflammatory axis: a central cell surface receptor for S100/calgranulin polypeptides. *Cell,* 97**,** 889-901.

HOLT, R. I., COCKRAM, C., FLYVBJERG, A. & GOLDSTEIN, B. J. 2011. *Textbook of diabetes,* John Wiley & Sons.

HORIUCHI, T. & KUROKAWA, T. 1991. Purification and properties of fructosylamine oxidase from Aspergillus sp. 1005. *Agricultural and biological chemistry,* 55**,** 333-338.

HOSSEINIMEHR, S. J., AHMADI, A., BEIKI, D., HABIBI, E. & MAHMOUDZADEH, A. 2009. Protective effects of hesperidin against genotoxicity induced by 99m Tc-MIBI in human cultured lymphocyte cells. *Nuclear medicine and biology,* 36**,** 863-867.

HOU, F. F., REN, H., OWEN, W. F., GUO, Z. J., CHEN, P. Y., SCHMIDT, A. M., MIYATA, T. & ZHANG, X. 2004. Enhanced expression of receptor for advanced glycation end products in chronic kidney disease. *Journal of the American Society of Nephrology,* 15**,** 1889-1896.

HOVE, H. 1998. Lactate and short chain fatty acid production in the human colon: implications for D-lactic acidosis, short-bowel syndrome, antibiotic-associated diarrhoea, colonic cancer, and inflammatory bowel disease. *Danish medical bulletin,* 45**,** 15.

HUGGINS, T. G., WELLS-KNECHT, M., DETORIE, N., BAYNES, J. & THORPE, S. 1993. Formation of o-tyrosine and dityrosine in proteins during radiolytic and metal-catalyzed oxidation. *Journal of Biological Chemistry,* 268**,** 12341-12347.

HWANG, S.-L., LIN, J.-A., SHIH, P.-H., YEH, C.-T. & YEN, G.-C. 2012. Pro-cellular survival and neuroprotection of citrus flavonoid: the actions of hesperetin in PC12 cells. *Food & function,* 3**,** 1082-1090.

IACOPINO, A. M. 2001. Periodontitis and Diabetes Interrelationships: Role of Inflammation. *Annals of Periodontology,* 6**,** 125-137.

IDF 2015. IDF Diabetes Atlas. 7th ed. Brussels, Belgium: International Diabetes Federation.

IGIC, M., KESIC, L., LEKOVIC, V., APOSTOLOVIC, M., MIHAILOVIC, D., KOSTADINOVIC, L. & MILASIN, J. 2012. Chronic gingivitis: the prevalence of periodontopathogens and therapy efficiency. *Eur J Clin Microbiol Infect Dis,* 31**,** 1911-1915.

IKEDA, K., HIGASHI, T., SANO, H., JINNOUCHI, Y., YOSHIDA, M., ARAKI, T., UEDA, S. & HORIUCHI, S. 1996. N ε-(carboxymethyl) lysine protein adduct is a major immunological epitope in proteins modified with advanced glycation end products of the Maillard reaction. *Biochemistry,* 35**,** 8075-8083.

INAGI, R., MIYATA, T., UEDA, Y., YOSHINO, A., NANGAKU, M., DE STRIHOU, C. V. Y. & KUROKAWA, K. 2002. Efficient in vitro lowering of carbonyl stress by the glyoxalase system in conventional glucose peritoneal dialysis fluid. *Kidney international,* 62**,** 679-687.

INOUE, Y. & KIMURA, A. 1992. Purification and characterization of glyoxalase II from Hansenula mrakii. *Journal of fermentation and bioengineering,* 73**,** 271-276.

IOANNIDOU, E. & SWEDE, H. 2011. Disparities in Periodontitis Prevalence among Chronic Kidney Disease Patients. *Journal of Dental Research,* 90**,** 730-734.

IOANNIDOU, E., SWEDE, H. & DONGARI-BAGTZOGLOU, A. 2011. Periodontitis Predicts Elevated C-reactive Protein Levels in Chronic Kidney Disease. *Journal of Dental Research,* 90**,** 1411-1415.

ISHIHAMA, Y., ODA, Y., TABATA, T., SATO, T., NAGASU, T., RAPPSILBER, J. & MANN, M. 2005. Exponentially modified protein abundance index (emPAI) for estimation of absolute protein amount in proteomics by the number of sequenced peptides per protein. *Molecular & Cellular Proteomics,* 4**,** 1265-1272.

ITAKURA, K., UCHIDA, K. & OSAWA, T. 1996. A novel fluorescent malondialdehyde-lysine adduct. *Chemistry and physics of lipids,* 84**,** 75-79.

ITAYA, T., KAGAMI, H., OKADA, K., YAMAWAKI, A., NARITA, Y., INOUE, M., SUMITA, Y. & UEDA, M. 2009. Characteristic changes of periodontal ligament-derived cells during passage. *Journal of periodontal research,* 44**,** 425-433.

IZAGUIRRE, G., KIKONYOGO, A. & PIETRUSZKO, R. 1998. Methylglyoxal as substrate and inhibitor of human aldehyde dehydrogenase: comparison of kinetic properties among the three isozymes. *Comp Biochem Physiol B Biochem Mol Biol,* 119**,** 747-54.

JAIN, M. & PARMAR, H. S. 2011. Evaluation of antioxidative and anti-inflammatory potential of hesperidin and naringin on the rat air pouch model of inflammation. *Inflammation Research,* 60**,** 483-491.

JANG, M., CAI, L., UDEANI, G. O., SLOWING, K. V., THOMAS, C. F., BEECHER, C. W., FONG, H. H., FARNSWORTH, N. R., KINGHORN, A. D. & MEHTA, R. G. 1997. Cancer chemopreventive activity of resveratrol, a natural product derived from grapes. *Science,* 275**,** 218-220.

JI, H., WU, L., MA, X., MA, X. & QIN, G. 2014. The effect of resveratrol on the expression of AdipoR1 in kidneys of diabetic nephropathy. *Molecular biology reports,* 41**,** 2151-2159.

JING, Y. H., CHEN, K. H., YANG, S. H., KUO, P. C. & CHEN, J. K. 2010. Resveratrol ameliorates vasculopathy in STZ-induced diabetic rats: role of AGE–RAGE signalling. *Diabetes/metabolism research and reviews,* 26**,** 212-222.

JOHNSON, R. N., EASDALE, R. W., TATNELL, M. & BAKER, J. R. 1991. Significance of variation in turnover of glycated albumin on indices of diabetic control. *Clinica Chimica Acta,* 198**,** 229-238.

JÖNSSON, D., AMISTEN, S., BRATTHALL, G., HOLM, A. & NILSSON, B.-O. 2009. LPS induces GROα chemokine production via NF-κB in oral fibroblasts. *Inflamm. Res.*, 58**,** 791-796.

JÖNSSON, D., NEBEL, D., BRATTHALL, G. & NILSSON, B.-O. 2008. LPS-induced MCP-1 and IL-6 production is not reversed by oestrogen in human periodontal ligament cells. *Archives of Oral Biology,* 53**,** 896-902.

JÖNSSON, D., NEBEL, D., BRATTHALL, G. & NILSSON, B. O. 2011. The human periodontal ligament cell: a fibroblast-like cell acting as an immune cell. *Journal of periodontal research,* 46**,** 153-157.

JÖNSSON, D., WAHLIN, Å., IDVALL, I., JOHNSSON, I., BRATTHALL, G. & NILSSON, B. O. 2005. Differential effects of estrogen on DNA synthesis in human periodontal ligament and breast cancer cells. *Journal of periodontal research,* 40**,** 401-406.

KALPANA, K., SRINIVASAN, M. & MENON, V. P. 2009. Evaluation of antioxidant activity of hesperidin and its protective effect on H2O2 induced oxidative damage on pBR322 DNA and RBC cellular membrane. *Molecular and cellular biochemistry,* 323**,** 21-29.

KAMARAJ, S., ANANDAKUMAR, P., JAGAN, S., RAMAKRISHNAN, G. & DEVAKI, T. 2010. Modulatory effect of hesperidin on benzo (a) pyrene induced experimental lung carcinogenesis with reference to COX-2, MMP-2 and MMP-9. *European journal of pharmacology,* 649**,** 320-327.

KANAZE, F., BOUNARTZI, M., GEORGARAKIS, M. & NIOPAS, I. 2007. Pharmacokinetics of the citrus flavanone aglycones hesperetin and naringenin after single oral administration in human subjects. *European journal of clinical nutrition,* 61**,** 472-477.

KANG, S. R., PARK, K. I., PARK, H. S., LEE, D. H., KIM, J. A., NAGAPPAN, A., KIM, E. H., LEE, W. S., SHIN, S. C. & PARK, M. K. 2011. Anti-inflammatory effect of flavonoids isolated from Korea Citrus aurantium L. on lipopolysaccharide-induced mouse macrophage RAW 264.7 cells by blocking of nuclear factor-kappa B (NF-κB) and mitogen-activated protein kinase (MAPK) signalling pathways. *Food Chemistry,* 129**,** 1721-1728.

KANG, Y., EDWARDS, L. G. & THORNALLEY, P. J. 1996. Effect of methylglyoxal on human leukaemia 60 cell growth: modification of DNA, G 1 growth arrest and induction of apoptosis. *Leukemia research,* 20**,** 397-405.

KAO, C.-L., CHEN, L.-K., CHANG, Y.-L., YUNG, M.-C., HSU, C.-C., CHEN, Y.-C., LO, W.-L., CHEN, S.-J., KU, H.-H. & HWANG, S.-J. 2010. Resveratrol protects human endothelium from H (2) O (2)-induced oxidative stress and senescence via SirT1 activation. *Journal of atherosclerosis and thrombosis,* 17**,** 970-979.

KARACHALIAS N, B.-J. R., AHMED N, BAYNES K, THORNALLEY PJ 2005. Urinary d-lactate as a marker of biochemical dysfunction linked to the development of diabetic microvascular complications. *Diabet Med,* 22(Suppl.2)**,** 21.

KARACHALIAS, N., BABAEI-JADIDI, R., RABBANI, N. & THORNALLEY, P. J. 2010. Increased protein damage in renal glomeruli, retina, nerve, plasma and urine and its prevention by thiamine and benfotiamine therapy in a rat model of diabetes. *Diabetologia,* 53**,** 1506-1516.

KARJALAINEN, J., KNIP, M., HYOTY, H., LEINIKKI, P., ILONEN, J., KAAR, M. L. & AKERBLOM, H. K. 1988. Relationship between serum insulin autoantibodies, islet cell antibodies and Coxsackie-B4 and mumps virus-specific antibodies at the clinical manifestation of type 1 (insulin-dependent) diabetes. *Diabetologia,* 31**,** 146-52.

KARVONEN, M., VIIK-KAJANDER, M., MOLTCHANOVA, E., LIBMAN, I., LAPORTE, R. & TUOMILEHTO, J. 2000. Incidence of childhood type 1 diabetes worldwide. Diabetes Mondiale (DiaMond) Project Group. *Diabetes care,* 23**,** 1516-1526.

KASAJ, A. & WILLERSHAUSEN, B. 2013. Periodontal diseases in children and adolescents. *MONATSSCHRIFT KINDERHEILKUNDE,* 161**,** 518-523.

KASHKET, S., MAIDEN, M., HAFFAJEE, A. & KASHKET, E. 2003. Accumulation of methylglyoxal in the gingival crevicular fluid of chronic periodontitis patients. *Journal of clinical periodontology,* 30**,** 364-367.

KATO, H. 1960. Studies on Browning Reactions between Sugars and Amino Compounds: Part V. Isolation and Characterization of New Carbonyl Compounds, 3-Deoxy-osones formed from N-Glycosides and their Significance for Browning Reaction. *Journal of the Agricultural Chemical Society of Japan,* 24**,** 1-12.

KATO, H., HAYASE, F., SHIN, D. B., OIMOMI, M. & BABA, S. 1988. 3-Deoxyglucosone, an intermediate product of the Maillard reaction. *Progress in clinical and biological research,* 304**,** 69-84.

KELLEY, D. E., MINTUN, M. A., WATKINS, S. C., SIMONEAU, J. A., JADALI, F., FREDRICKSON, A., BEATTIE, J. & THERIAULT, R. 1996. The effect of non-insulin-dependent diabetes mellitus and obesity on glucose transport and phosphorylation in skeletal muscle. *J Clin Invest,* 97**,** 2705-13.

KENNEDY, A., OVERMAN, A., LAPOINT, K., HOPKINS, R., WEST, T., CHUANG, C.-C., MARTINEZ, K., BELL, D. & MCINTOSH, M. 2009. Conjugated linoleic acid-mediated inflammation and insulin resistance in human adipocytes are attenuated by resveratrol. *Journal of lipid research,* 50**,** 225-232.

KESSNER, D., CHAMBERS, M., BURKE, R., AGUS, D. & MALLICK, P. 2008. ProteoWizard: open source software for rapid proteomics tools development. *Bioinformatics,* 24**,** 2534-2536.

KHAN, M. K. & DANGLES, O. 2014. A comprehensive review on flavanones, the major citrus polyphenols. *Journal of Food Composition and Analysis,* 33**,** 85-104.

KHOJASTEH, A. A., NIKBIN, S., BUERY, R. R. & OYONG, G. G. 2010. Establishment of Primary Cultured Human Fibroblasts from Periodontal Ligament.

KIDA, K., MIMURA, G., ITO, T., MURAKAMI, K., ASHKENAZI, I. & LARON, Z. 2000. Incidence of Type 1 diabetes mellitus in children aged 0-14 in Japan, 1986-1990, including an analysis for seasonality of onset and month of birth: JDS study. The Data Committee for Childhood Diabetes of the Japan Diabetes Society (JDS). *Diabet Med,* 17**,** 59-63.

KIHM, L. P., MULLER-KREBS, S., KLEIN, J., EHRLICH, G., MERTES, L., GROSS, M. L., ADAIKALAKOTESWARI, A., THORNALLEY, P. J., HAMMES, H. P., NAWROTH, P. P., ZEIER, M. & SCHWENGER, V. 2011. Benfotiamine protects against peritoneal and kidney damage in peritoneal dialysis. *J Am Soc Nephrol,* 22**,** 914-26.

KIM, H. Y., PARK, M., KIM, K., LEE, Y. M. & RHYU, M. R. 2013a. Hesperetin stimulates cholecystokinin secretion in enteroendocrine STC-1 cells. *Biomolecules and Therapeutics,* 21**,** 121-125.

KIM, J. & AMAR, S. 2006. Periodontal disease and systemic conditions: a bidirectional relationship. *Odontology,* 94**,** 10-21.

KIM, J. Y., JUNG, K. J., CHOI, J. S. & CHUNG, H. Y. 2004. Hesperetin: a potent antioxidant against peroxynitrite. *Free Radical Research,* 38**,** 761-769.

KIM, M., LIM, J., YOUN, H., HONG, Y., YANG, K., PARK, H., CHUNG, S., KOH, S., SHIN, S. & CHOI, B. 2013b. Resveratrol prevents renal lipotoxicity and inhibits mesangial cell glucotoxicity in a manner dependent on the AMPK–SIRT1–PGC1α axis in db/db mice. *Diabetologia,* 56**,** 204-217.

KIM, N.-S., SEKINE, S., KIUCHI, N. & KATO, S. 1995. cDNA cloning and characterization of human glyoxalase I isoforms from HT-1080 cells. *Journal of biochemistry,* 117**,** 359-361.

KIM, S.-H., KIM, B.-K. & LEE, Y.-C. 2011. Antiasthmatic effects of hesperidin, a potential Th2 cytokine antagonist, in a mouse model of allergic asthma. *Mediators of inflammation,* 2011.

KINANE, D. F., PRESHAW, P. M. & LOOS, B. G. 2011. Host-response: understanding the cellular and molecular mechanisms of host-microbial interactions - Consensus of the Seventh European Workshop on Periodontology. *Journal of Clinical Periodontology,* 38**,** 44-48.

KINSKY, O. R., HARGRAVES, T. L., ANUMOL, T., JACOBSEN, N. E., DAI, J., SNYDER, S. A., MONKS, T. J. & LAU, S. S. 2016. Metformin scavenges methylglyoxal to form a novel imidazolinone metabolite in humans. *Chemical Research in Toxicology*.

KIRK, J. 1960. The glyoxalase I activity of arterial tissue in individuals of various ages. *Journal of Gerontology,* 15**,** 139-141.

KISLINGER, T., FU, C., HUBER, B., QU, W., TAGUCHI, A., DU YAN, S., HOFMANN, M., YAN, S. F., PISCHETSRIEDER, M. & STERN, D. 1999. N ε-(carboxymethyl) lysine adducts of proteins are ligands for receptor for advanced glycation end products that activate cell signaling pathways and modulate gene expression. *Journal of Biological Chemistry,* 274**,** 31740-31749.

KISTINGER, T., FU, C., HUBER, B., QU, W., TAGUCHI, A., YAN, S., HOFMANN, M., YAN, A., PISCHETSRIEDER, M. & STERN, D. 1999. N'-

(carboxymethyl) lysine adducts of proteins are ligands for receptor for advanced glycation end products that activate cell signaling pathways and modulate gene expression. *J Biol Chem,* 274**,** 3l740.

KO, Y., ASHOK, S., ZHOU, S., KUMAR, V. & PARK, S. 2012. Aldehyde dehydrogenase activity is important to the production of 3-hydroxypropionic acid from glycerol by recombinant Klebsiella pneumoniae. *Process Biochemistry,* 47**,** 1135-1143.

KOITO, W., ARAKI, T., HORIUCHI, S. & NAGAI, R. 2004. Conventional antibody against Nε-(carboxymethyl) lysine (CML) shows cross-reaction to Nε-(carboxyethyl) lysine (CEL): immunochemical quantification of CML with a specific antibody. *Journal of biochemistry,* 136**,** 831-837.

KONDOH, Y., KAWASE, M., KAWAKAMI, Y. & OHMORI, S. 1992a. Concentrations ofd-lactate and its related metabolic intermediates in liver, blood, and muscle of diabetic and starved rats. *Research in experimental medicine,* 192**,** 407-414.

KONDOH, Y., KAWASE, M. & OHMORI, S. 1992b. D-Lactate concentrations in blood, urine and sweat before and after exercise. *European journal of applied physiology and occupational physiology,* 65**,** 88-93.

KORNMAN, K. S. 2008. Mapping the pathogenesis of periodontitis: a new look. *Journal of periodontology,* 79**,** 1560-1568.

KORNMAN, K. S., CRANE, A., WANG, H. Y., GIOVLNE, F. S. D., NEWMAN, M. G., PIRK, F. W., WILSON, T. G., HIGGINBOTTOM, F. L. & DUFF, G. W. 1997. The interleukin-1 genotype as a severity factor in adult periodontal disease. *Journal of clinical periodontology,* 24**,** 72-77.

KOSCHINSKY, T., HE, C. J., MITSUHASHI, T., BUCALA, R., LIU, C., BUENTING, C., HEITMANN, K. & VLASSARA, H. 1997. Orally absorbed reactive glycation products (glycotoxins): An environmental risk factor in diabetic nephropathy. *Proceedings of the National Academy of Sciences,* 94**,** 6474-6479.

KRISTENSEN, A. R., SCHANDORFF, S., HØYER-HANSEN, M., NIELSEN, M. O., JÄÄTTELÄ, M., DENGJEL, J. & ANDERSEN, J. S. 2008. Ordered organelle degradation during starvation-induced autophagy. *Molecular & Cellular Proteomics,* 7**,** 2419-2428.

KRUSZYNSKA, Y. T. & OLEFSKY, J. M. 1996. Cellular and molecular mechanisms of non-insulin dependent diabetes mellitus. *J Investig Med,* 44**,** 413-28.

KUEPER, T., GRUNE, T., PRAHL, S., LENZ, H., WELGE, V., BIERNOTH, T., VOGT, Y., MUHR, G.-M., GAEMLICH, A. & JUNG, T. 2007. Vimentin is the specific target in skin glycation structural prerequisites, functional consequences, and role in skin aging. *Journal of Biological Chemistry,* 282**,** 23427-23436.

KUHLA, B., LÜTH, H.-J., HAFERBURG, D., BOECK, K., ARENDT, T. & MÜNCH, G. 2005. Methylglyoxal, Glyoxal, and Their Detoxification in Alzheimer's Disease. *Annals of the New York Academy of Sciences,* 1043**,** 211-216.

KUHN R AND DANSI A 1936. A molecular rearrangement of N-glucosides. *Ber,* 69B**,** 1745–1754.

KUHN R, W. F. 1937. The Amadori rearrangement. *Ber.,* 70B**,** 769–772.

KUMAR, A., KAUNDAL, R. K., IYER, S. & SHARMA, S. S. 2007. Effects of resveratrol on nerve functions, oxidative stress and DNA fragmentation in experimental diabetic neuropathy. *Life Sciences,* 80**,** 1236-1244.

KUMAR, A. & SHARMA, S. S. 2010. NF-κB inhibitory action of resveratrol: A probable mechanism of neuroprotection in experimental diabetic neuropathy. *Biochemical and Biophysical Research Communications,* 394**,** 360-365.

KURZ, A., RABBANI, N., WALTER, M., BONIN, M., THORNALLEY, P., AUBURGER, G. & GISPERT, S. 2010. Alpha-synuclein deficiency leads to increased glyoxalase I expression and glycation stress. *Cellular and Molecular Life Sciences,* 68**,** 721-733.

KURZ, A., RABBANI, N., WALTER, M., BONIN, M., THORNALLEY, P., AUBURGER, G. & GISPERT, S. 2011. Alpha-synuclein deficiency leads to increased glyoxalase I expression and glycation stress. *Cellular and Molecular Life Sciences,* 68**,** 721-733.

KWAK, M.-K., WAKABAYASHI, N., ITOH, K., MOTOHASHI, H., YAMAMOTO, M. & KENSLER, T. W. 2003. Modulation of gene expression by cancer chemopreventive dithiolethiones through the Keap1-Nrf2 pathway Identification of novel gene clusters for cell survival. *Journal of Biological Chemistry,* 278**,** 8135-8145.

KWAKMAN, P. H., TE VELDE, A. A., DE BOER, L., SPEIJER, D., VANDENBROUCKE-GRAULS, C. M. & ZAAT, S. A. 2010. How honey kills bacteria. *The FASEB Journal,* 24**,** 2576-2582.

LAGOUGE, M., ARGMANN, C., GERHART-HINES, Z., MEZIANE, H., LERIN, C., DAUSSIN, F., MESSADEQ, N., MILNE, J., LAMBERT, P. &

ELLIOTT, P. 2006. Resveratrol improves mitochondrial function and protects against metabolic disease by activating SIRT1 and PGC-1α. *Cell,* 127**,** 1109-1122.

LAKSCHEVITZ, F., ABOODI, G., TENENBAUM, H. & GLOGAUER, M. 2011. Diabetes and Periodontal Diseases: Interplay and Links. *Current Diabetes Reviews,* 7**,** 433-439.

LAKSHMINARASIMHAN, M., RAUH, D., SCHUTKOWSKI, M. & STEEGBORN, C. 2013. Sirt1 activation by resveratrol is substrate sequence-selective. *Aging (Albany NY),* 5**,** 151-154.

LALLA, E., CHENG, B., LAL, S., KAPLAN, S., SOFTNESS, B., GREENBERG, E., GOLAND, R. S. & LAMSTER, I. B. 2007. Diabetes mellitus promotes periodontal destruction in children. *J Clin Periodontol,* 34**,** 294-298.

LALLA, E., LAMSTER, I. B., FEIT, M., HUANG, L., SPESSOT, A., QU, W., KISLINGER, T., LU, Y., STERN, D. M. & SCHMIDT, A. M. 2000. Blockade of RAGE suppresses periodontitis-associated bone loss in diabetic mice. *J Clin Invest,* 105**,** 1117-24.

LANG, N. P. & LINDHE, J. 2015. *Clinical periodontology and implant dentistry,* John Wiley & Sons.

LANG, N. P., SCHÄTZLE, M. A. & LÖE, H. 2009. Gingivitis as a risk factor in periodontal disease. *Journal of Clinical Periodontology,* 36**,** 3-8.

LAPP, A. & DUNN, M. 1955. DL-Methionine sulphoxide. *Biochem. Prep***,** 80-85.

LARSEN, K., ARONSSON, A.-C., MARMSTÅL, E. & MANNERVIK, B. 1985. Immunological comparison of glyoxalase I from yeast and mammals and quantitative determination of the enzyme in human tissues by radioimmunoassay. *Comparative Biochemistry and Physiology Part B: Comparative Biochemistry,* 82**,** 625-638.

LEBLANC, A. R. & REISZ, R. R. 2013. Periodontal ligament, cementum, and alveolar bone in the oldest herbivorous tetrapods, and their evolutionary significance. *PloS one,* 8.

LEE, J.-H., SONG, M.-Y., SONG, E.-K., KIM, E.-K., MOON, W. S., HAN, M.-K., PARK, J.-W., KWON, K.-B. & PARK, B.-H. 2009. Overexpression of SIRT1 protects pancreatic β-cells against cytokine toxicity by suppressing the nuclear factor-κB signaling pathway. *Diabetes,* 58**,** 344-351.

LEE, J. H. & KIM, G. H. 2010. Evaluation of antioxidant and inhibitory activities for different subclasses flavonoids on enzymes for rheumatoid arthritis. *Journal of food science,* 75**,** H212-H217.

LEE, M. K. 1993. Neurofilaments are obligate heteropolymers in vivo. *The Journal of Cell Biology,* 122**,** 1337-1350.

LEE, Y.-S., BAK, E. J., KIM, M., PARK, W., SEO, J. T. & YOO, Y.-J. 2008. Induction of IL-8 in periodontal ligament cells by H2O2. *The Journal of Microbiology,* 46**,** 579-584.

LEKLI, I., RAY, D. & DAS, D. K. 2010. Longevity nutrients resveratrol, wines and grapes. *Genes & nutrition,* 5**,** 55-60.

LEKLI, I., SZABO, G., JUHASZ, B., DAS, S., DAS, M., VARGA, E., SZENDREI, L., GESZTELYI, R., VARADI, J. & BAK, I. 2008. Protective mechanisms of resveratrol against ischemia-reperfusion-induced damage in hearts obtained from Zucker obese rats: the role of GLUT-4 and endothelin. *American Journal of Physiology-Heart and Circulatory Physiology,* 294**,** H859-H866.

LENZEN, S. 2008. Oxidative stress: the vulnerable beta-cell. *Biochemical Society Transactions,* 36**,** 343-347.

LEU, J. P. & ZONSZEIN, J. 2010. Diagnostic criteria and classification of diabetes. *In:* PORETSKY, L. (ed.) *Principles of diabetes mellitus.* 2nd ed. New York: Springer.

LÉVÈQUES, A., ACTIS-GORETTA, L., REIN, M. J., WILLIAMSON, G., DIONISI, F. & GIUFFRIDA, F. 2012. UPLC–MS/MS quantification of total hesperetin and hesperetin enantiomers in biological matrices. *Journal of pharmaceutical and biomedical analysis,* 57**,** 1-6.

LEVY-MARCHAL, C., PATTERSON, C. & GREEN, A. 1995. Variation by age group and seasonality at diagnosis of childhood IDDM in Europe. The EURODIAB ACE Study Group. *Diabetologia,* 38**,** 823-30.

LEWIS, E. J., GREENE, T., SPITALEWIZ, S., BLUMENTHAL, S., BERL, T., HUNSICKER, L. G., POHL, M. A., ROHDE, R. D., RAZ, I. & YERUSHALMY, Y. 2012. Pyridorin in type 2 diabetic nephropathy. *Journal of the American Society of Nephrology,* 23**,** 131-136.

LI, D., MITSUHASHI, S. & UBUKATA, M. 2012a. Protective effects of hesperidin derivatives and their stereoisomers against advanced glycation end-products formation. *Pharmaceutical biology,* 50**,** 1531-1535.

LI, G., LIAO, Y., WANG, X., SHENG, S. & YIN, D. 2006. In situ estimation of the entire color and spectra of age pigment-like materials: Application of a front-surface 3D-fluorescence technique. *Experimental gerontology,* 41**,** 328-336.

LI, R., CAI, L., REN, D.-Y., XIE, X.-F., HU, C.-M. & LI, J. 2012b. Therapeutic effect of 7, 3′-dimethoxy hesperetin on adjuvant arthritis in rats through inhibiting JAK2-STAT3 signal pathway. *International immunopharmacology,* 14**,** 157-163.

LI, R., CAI, L., XIE, X. F., YANG, F. & LI, J. 2010. Hesperidin suppresses adjuvant arthritis in rats by inhibiting synoviocyte activity. *Phytotherapy Research,* 24**,** S71-S76.

LI, R., LI, J., CAI, L., HU, C. M. & ZHANG, L. 2008. Suppression of adjuvant arthritis by hesperidin in rats and its mechanisms. *Journal of Pharmacy and Pharmacology,* 60**,** 221-228.

LI, T., DU, Y., WANG, L., HUANG, L., LI, W., LU, M., ZHANG, X. & ZHU, W.-G. 2012c. Characterization and prediction of lysine (K)-acetyl-transferase specific acetylation sites. *Molecular & Cellular Proteomics,* 11**,** M111. 011080.

LI, W., HUANG, B., LIU, K., HOU, J. & MENG, H. 2015. Up-Regulated Leptin in Periodontitis Promotes Inflammatory Cytokine Expression in Periodontal Ligament Cells. *Journal of periodontology***,** 1-18.

LILIENSIEK, B., WEIGAND, M. A., BIERHAUS, A., NICKLAS, W., KASPER, M., HOFER, S., PLACHKY, J., GRONE, H. J., KURSCHUS, F. C., SCHMIDT, A. M., YAN, S. D., MARTIN, E., SCHLEICHER, E., STERN, D. M., HAMMERLING, G. G., NAWROTH, P. P. & ARNOLD, B. 2004. Receptor for advanced glycation end products (RAGE) regulates sepsis but not the adaptive immune response. *J Clin Invest,* 113**,** 1641-50.

LILJENBERG, B., LINDHE, J., BERGLUNDH, T., DAHLEN, G. & JONSSON, R. 1994. Some microbiological, histopathological and immunohistochemical characteristics of progressive periodontal disease. *Journal of clinical periodontology,* 21**,** 720-727.

LILLIG, C. H., BERNDT, C. & HOLMGREN, A. 2008. Glutaredoxin systems. *Biochimica et Biophysica Acta (BBA)-General Subjects,* 1780**,** 1304-1317.

LIMPHONG, P., MCKINNEY, R. M., ADAMS, N. E., BENNETT, B., MAKAROFF, C. A., GUNASEKERA, T. & CROWDER, M. W. 2009. Human glyoxalase II contains an Fe(II)Zn(II) center but is active as a mononuclear Zn(II) enzyme. *Biochemistry,* 48**,** 5426-34.

LIN, H.-Y., LANSING, L., MERILLON, J.-M., DAVIS, F. B., TANG, H.-Y., SHIH, A., VITRAC, X., KRISA, S., KEATING, T. & CAO, H. J. 2006. Integrin αVβ3 contains a receptor site for resveratrol. *The FASEB Journal,* 20**,** 1742-1744.

LINDHE, J., HAMP, S. E. & LÖE, H. 1973. Experimental periodontitis in the beagle dog. *Journal of Periodontal Research,* 8**,** 1-10.

LINDHE, J., HAMP, S. E. & LÖE, H. 1975. Plaque induced periodontal disease in beagle dogs. *Journal of periodontal research,* 10**,** 243-255.

LING, A. R. 1908. Malting. *Journal of the Institute of Brewing,* 14**,** 494-521.

LIU, B., BHAT, M., PADIVAL, A. K., SMITH, D. G. & NAGARAJ, R. H. 2004a. Effect of dicarbonyl modification of fibronectin on retinal capillary pericytes. *Invest Ophthalmol Vis Sci,* 45**,** 1983-95.

LIU, G.-H., QU, J. & SHEN, X. 2008. NF-κB/p65 antagonizes Nrf2-ARE pathway by depriving CBP from Nrf2 and facilitating recruitment of HDAC3 to MafK. *Biochimica et Biophysica Acta (BBA) - Molecular Cell Research,* 1783**,** 713-727.

LIU, H., SADYGOV, R. G. & YATES, J. R. 2004b. A model for random sampling and estimation of relative protein abundance in shotgun proteomics. *Analytical chemistry,* 76**,** 4193-4201.

LIU, J., JIANG, Y., MAO, J., GU, B., LIU, H. & FANG, B. 2013. High Levels of Glucose Induces a Dose-Dependent Apoptosis in Human Periodontal Ligament Fibroblasts by Activating Caspase-3 Signaling Pathway. *Applied Biochemistry and Biotechnology,* 170**,** 1458-1471.

LIU, K., ZHOU, R., WANG, B. & MI, M.-T. 2014. Effect of resveratrol on glucose control and insulin sensitivity: a meta-analysis of 11 randomized controlled trials. *The American journal of clinical nutrition,* 99**,** 1510-1519.

LO, T. W., SELWOOD, T. & THORNALLEY, P. J. 1994a. The reaction of methylglyoxal with aminoguanidine under physiological conditions and prevention of methylglyoxal binding to plasma proteins. *Biochemical pharmacology,* 48**,** 1865-1870.

LO, T. W., WESTWOOD, M. E., MCLELLAN, A. C., SELWOOD, T. & THORNALLEY, P. J. 1994b. Binding and modification of proteins by methylglyoxal under physiological conditions. A kinetic and mechanistic study with N alpha-acetylarginine, N alpha-acetylcysteine, and N alpha-acetyllysine, and bovine serum albumin. *J Biol Chem,* 269**,** 32299-305.

LO, T. W. C. & THORNALLEY, P. J. 1992. Inhibition of proliferation of human leukaemia 60 cells by diethyl esters of glyoxalase inhibitors in vitro. *Biochemical Pharmacology,* 44**,** 2357-2363.

LOE, H., ANERUD, A., BOYSEN, H. & MORRISON, E. 1986. Natural history of periodontal disease in man. Rapid, moderate and no loss of attachment in Sri Lankan laborers 14 to 46 years of age. *J Clin Periodontol,* 13**,** 431-440.

LOE, H., ANERUD, A., BOYSEN, H. & SMITH, M. 1978. The natural history of periodontal disease in man. *J Periodontal Res,* 13**,** 550-562.

LÖE, H., ANERUD, A., BOYSEN, H. & SMITH, M. 1978. The Natural History of Periodontal Disease in Man: The Rate of Periodontal Destruction Before 40 Years of Age. *Journal of Periodontology,* 49**,** 607-620.

LONGO, N., BELL, G., SHUSTER, R., GRIFFIN, L., LANGLEY, S. & ELSAS, L. 1989. Human fibroblasts express the insulin-responsive glucose transporter (GLUT4). *Transactions of the Association of American Physicians,* 103**,** 202-213.

LONGO, N., WANG, Y., SMITH, S. A., LANGLEY, S. D., DIMEGLIO, L. A. & GIANNELLA-NETO, D. 2002. Genotype-phenotype correlation in inherited severe insulin resistance. *Hum Mol Genet,* 11**,** 1465-75.

LOWE, C. E., COOPER, J. D., BRUSKO, T., WALKER, N. M., SMYTH, D. J., BAILEY, R., BOURGET, K., PLAGNOL, V., FIELD, S., ATKINSON, M., CLAYTON, D. G., WICKER, L. S. & TODD, J. A. 2007. Large-scale genetic fine mapping and genotype-phenotype associations implicate polymorphism in the IL2RA region in type 1 diabetes. *Nat Genet,* 39**,** 1074-82.

LOWRY, O. H., ROSEBROUGH, N. J., FARR, A. L. & RANDALL, R. J. 1951. Protein measurement with the Folin phenol reagent. *J Biol Chem,* 193**,** 265-75.

LU, P., VOGEL, C., WANG, R., YAO, X. & MARCOTTE, E. M. 2007. Absolute protein expression profiling estimates the relative contributions of transcriptional and translational regulation. *Nature biotechnology,* 25**,** 117-124.

LU, R., ZHANG, J., SUN, W., DU, G. & ZHOU, G. 2015. Inflammation-related cytokines in oral lichen planus: an overview. *Journal of Oral Pathology & Medicine,* 44**,** 1-14.

LUND, T., SVINDLAND, A., PEPAJ, M., JENSEN, A.-B., BERG, J. P., KILHOVD, B. & HANSSEN, K. F. 2011. Fibrin (ogen) may be an important

target for methylglyoxal-derived AGE modification in elastic arteries of humans. *Diabetes and Vascular Disease Research***,** 1479164111416831.

LUNDBY, A., LAGE, K., WEINERT, B. T., BEKKER-JENSEN, D. B., SECHER, A., SKOVGAARD, T., KELSTRUP, C. D., DMYTRIYEV, A., CHOUDHARY, C. & LUNDBY, C. 2012. Proteomic analysis of lysine acetylation sites in rat tissues reveals organ specificity and subcellular patterns. *Cell reports,* 2**,** 419-431.

MACARULLA, M., ALBERDI, G., GÓMEZ, S., TUEROS, I., BALD, C., RODRIGUEZ, V., MARTÍNEZ, J. & PORTILLO, M. 2009. Effects of different doses of resveratrol on body fat and serum parameters in rats fed a hypercaloric diet. *Journal of physiology and biochemistry,* 65**,** 369-376.

MACLEOD, A. K., MCMAHON, M., PLUMMER, S. M., HIGGINS, L. G., PENNING, T. M., IGARASHI, K. & HAYES, J. D. 2009. Characterization of the cancer chemopreventive NRF2-dependent gene battery in human keratinocytes: demonstration that the KEAP1–NRF2 pathway, and not the BACH1–NRF2 pathway, controls cytoprotection against electrophiles as well as redox-cycling compounds. *Carcinogenesis,* 30**,** 1571-1580.

MADSON, M. A. & FEATHER, M. S. 1981. An improved preparation of 3-deoxy-D-erythro-hexos-2-ulose via the bis (benzoylhydrazone) and some related constitutional studies. *Carbohydrate Research,* 94**,** 183-191.

MAECHLER, P. 2002. Mitochondria as the conductor of metabolic signals for insulin exocytosis in pancreatic β-cells. *Cellular and Molecular Life Sciences CMLS,* 59**,** 1803-1818.

MAEDA, H., FUJII, S., MONNOUCHI, S., WADA, N. & AKAMINE, A. 2012. Differentiation of Periodontal Ligament Stem/Progenitor Cells: Roles of TGF-β1. *Stem Cells and Cancer Stem Cells,*. Springer.

MALLONE, R. & VAN ENDERT, P. 2008. T cells in the pathogenesis of type 1 diabetes. *Curr Diab Rep,* 8**,** 101-6.

MAO, L., HARTL, D., NOLDEN, T., KOPPELSTÄTTER, A., KLOSE, J., HIMMELBAUER, H. & ZABEL, C. 2008. Pronounced alterations of cellular metabolism and structure due to hyper-or hypo-osmosis. *Journal of proteome research,* 7**,** 3968-3983.

MARIOTTI, A. & COCHRAN, D. L. 1990. Characterization of fibroblasts derived from human periodontal ligament and gingiva. *Journal of periodontology,* 61**,** 103-111.

MARK, L., NIKFARDJAM, M. S. P., AVAR, P. & OHMACHT, R. 2005. A validated HPLC method for the quantitative analysis of trans-resveratrol and trans-piceid in Hungarian wines. *Journal of chromatographic science,* 43**,** 445-449.

MARTIN, S., PAWLOWSKI, B., GREULICH, B., ZIEGLER, A. G., MANDRUP-POULSEN, T. & MAHON, J. 1992. Natural course of remission in IDDM during 1st yr after diagnosis. *Diabetes Care,* 15**,** 66-74.

MATSUMOTO, K., SANO, H., NAGAI, R., SUZUKI, H., KODAMA, T., YOSHIDA, M., UEDA, S., SMEDSRØD, B. & HORIUCHI, S. 2000. Endocytic uptake of advanced glycation end products by mouse liver sinusoidal endothelial cells is mediated by a scavenger receptor distinct from the macrophage scavenger receptor class A. *Biochem. J.,* 352**,** 233.

MAVRIC, E., WITTMANN, S., BARTH, G. & HENLE, T. 2008. Identification and quantification of methylglyoxal as the dominant antibacterial constituent of Manuka (Leptospermum scoparium) honeys from New Zealand. *Molecular nutrition & food research,* 52**,** 483-489.

MCLELLAN, A., PHILIPS, S. & THORNALLEY, P. 1993. The assay of SD-lactoylglutathione in biological systems. *Analytical biochemistry,* 211**,** 37-43.

MCLELLAN, A. C., PHILLIPS, S. A. & THORNALLEY, P. J. 1992. Fluorimetric assay of D-lactate. *Anal Biochem,* 206**,** 12-6.

MCLELLAN, A. C. & THORNALLEY, P. J. 1989. Glyoxalase activity in human red blood cells fractioned by age. *Mech Ageing Dev,* 48**,** 63-71.

MCLELLAN, A. C. & THORNALLEY, P. J. 1991. Optimisation of non-denaturing polyacrylamide gel electrophoretic analysis of glyoxalase I phenotypes in clinical blood samples. *Clin Chim Acta,* 204**,** 137-43.

MCLELLAN, A. C. & THORNALLEY, P. J. 1992. Synthesis and chromatography of 1, 2-diamino-4, 5-dimethoxybenzene, 6, 7-dimethoxy-2-methylquinoxaline and 6, 7-dimethoxy-2, 3-dimethylquinoxaline for use in a liquid chromatographic fluorimetric assay of methylglyoxal. *Analytica chimica acta,* 263**,** 137-142.

MCLELLAN, A. C., THORNALLEY, P. J., BENN, J. & SONKSEN, P. H. 1994a. Glyoxalase system in clinical diabetes mellitus and correlation with diabetic complications. *Clin Sci (Lond),* 87**,** 21-9.

MCLELLAN, A. C., THORNALLEY, P. J., BENN, J. & SONKSEN, P. H. 1994b. Glyoxalase System in Clinical Diabetes Mellitus and Correlation with Diabetic Complications. *Clin. Sci.,* 87**,** 21-29.

MEALEY, B. 1999. Diabetes and periodontal diseases. *Journal of periodontology,* 70**,** 935-949.

MEALEY, B. 2000. Diabetes and periodontal disease: two sides of a coin. *Compendium of continuing education in dentistry (Jamesburg, NJ: 1995),* 21**,** 943-6, 948, 950, passim; quiz 956.

MEALEY, B. L. 2006. Periodontal disease and diabetes: A two-way street. *The Journal of the American Dental Association,* 137**,** S26-S31.

MEALEY, B. L. & OATES, T. W. 2006. Diabetes Mellitus and Periodontal Diseases. *Journal of Periodontology,* 77**,** 1289-1303.

MEALEY, B. L. & OCAMPO, G. L. 2007. Diabetes mellitus and periodontal disease. *Periodontol 2000,* 44**,** 127-153.

MEGGER, D. A., BRACHT, T., MEYER, H. E. & SITEK, B. 2013. Label-free quantification in clinical proteomics. *Biochimica et Biophysica Acta (BBA) - Proteins and Proteomics,* 1834**,** 1581-1590.

MEISEL, P., SIEGEMUND, A., DOMBROWA, S., SAWAF, H., FANGHAENEL, J. & KOCHER, T. 2002. Smoking and polymorphisms of the interleukin-1 gene cluster (IL-1β, IL-1α, and IL-1RN) in patients with periodontal disease. *Journal of periodontology,* 73**,** 27-32.

MEISEL, P., SIEGEMUND, A., GRIMM, R., HERRMANN, F., JOHN, U., SCHWAHN, C. & KOCHER, T. 2003. The interleukin-1 polymorphism, smoking, and the risk of periodontal disease in the population-based SHIP study. *Journal of dental research,* 82**,** 189-193.

MELDAL, M. & KINDTLER, J. 1986. Synthesis of a proposed antigenic hexapeptide from Escherichia coli K88 protein fimbriae. *Acta chemica Scandinavica. Series B: Organic chemistry and biochemistry,* 40**,** 235.

MENG, H.-X., LI, W., CHEN, Z.-B., SHI, D., LIU, Y.-Y., ZHANG, X., SUN, X.-J., XU, L. & ZHANG, L. 2015. Association between Plasma Leptin Level and Systemic Inflammatory Markers in Patients with Aggressive Periodontitis. *Chinese Medical Journal,* 128**,** 528.

MICHALOWICZ, B., AEPPLP, D., KUBA, R., BEREUTER, J., CONRY, J., SEGAL, N., BOUCHARD, T. & PIHLSTROM, B. 1991a. A twin study of genetic variation in proportional radiographic alveolar bone height. *Journal of dental research,* 70**,** 1431-1435.

MICHALOWICZ, B. S., AEPPLI, D., VIRAG, J. G., KLUMP, D. G., HINRICHS, E., SEGAL, N. L., BOUCHARD JR, T. J. & PIHLSTROM, B. L. 1991b. Periodontal findings in adult twins. *Journal of periodontology,* 62**,** 293-299.

MICHALOWICZ, B. S., DIEHL, S. R., GUNSOLLEY, J. C., SPARKS, B. S., BROOKS, C. N., KOERTGE, T. E., CALIFANO, J. V., BURMEISTER, J. A. & SCHENKEIN, H. A. 2000. Evidence of a substantial genetic basis for risk of adult periodontitis. *Journal of periodontology,* 71**,** 1699-1707.

MILLER, N. 2012. Ten Cate's oral histology, 8th edition. *Br Dent J,* 213**,** 194-194.

MILNE, J. C., LAMBERT, P. D., SCHENK, S., CARNEY, D. P., SMITH, J. J., GAGNE, D. J., JIN, L., BOSS, O., PERNI, R. B. & VU, C. B. 2007. Small molecule activators of SIRT1 as therapeutics for the treatment of type 2 diabetes. *Nature,* 450**,** 712-716.

MINGZHAN, X., NAILA, R., HIROSHI, M., PRECIOUS, I., NEIL, K., TOMOKAZU, S., TAKASHI, M., MASAYUKI, Y. & PAUL, J. T. 2012. Transcriptional control of glyoxalase 1 by Nrf2 provides a stress-responsive defence against dicarbonyl glycation. *Biochemical Journal,* 443**,** 213-222.

MITSUI, Y. & SCHNEIDER, E. L. 1976. Relationship between cell replication and volume in senescent human diploid fibroblasts. *Mechanisms of ageing and development,* 5**,** 45-56.

MIYATA, T., DE STRIHOU, C. V. Y., IMASAWA, T., YOSHINO, A., UEDA, Y., OGURA, H., KOMINAMI, K., ONOGI, H., INAGI, R. & NANGAKU, M. 2001. Glyoxalase I deficiency is associated with an unusual level of advanced glycation end products in a hemodialysis patient. *Kidney international,* 60**,** 2351-2359.

MOHR, S. B., GARLAND, C. F., GORHAM, E. D. & GARLAND, F. C. 2008. The association between ultraviolet B irradiance, vitamin D status and incidence rates of type 1 diabetes in 51 regions worldwide. *Diabetologia,* 51**,** 1391-8.

MONDER, C. 1967. α-Keto aldehyde dehydrogenase, an enzyme that catalyzes the enzymic oxidation of methylglyoxal to pyruvate. *Journal of Biological Chemistry,* 242**,** 4603-4609.

MONNIER, V. M., KOHN, R. R. & CERAMI, A. 1984. Accelerated age-related browning of human collagen in diabetes mellitus. *Proceedings of the National Academy of Sciences,* 81**,** 583-587.

MORANDINI, A. C. F., SIPERT, C. R., GASPAROTO, T. H., GREGHI, S. L. A., PASSANEZI, E., REZENDE, M. L. R., SANT'ANA, A. P., CAMPANELLI, A. P., GARLET, G. P. & SANTOS, C. F. 2010. Differential Production of

Macrophage Inflammatory Protein-1α, Stromal-Derived Factor-1, and IL-6 by Human Cultured Periodontal Ligament and Gingival Fibroblasts Challenged With Lipopolysaccharide From P. gingivalis. *Journal of Periodontology,* 81**,** 310-317.

MORCOS, M., DU, X., HUTTER, A., PFISTERER, F., THORNALLEY, P., BAYNES, J., THORPE, S., EL BAKI, R., AHMED, N. & MIFTARI, N. Life extension in Caenorhabditis elegans by overexpression of glyoxalase I-The connection to protein damage by glycation, oxidation and nitration. Free Radical Research, 2005. TAYLOR & FRANCIS LTD S43-S43.

MORCOS, M., DU, X., PFISTERER, F., HUTTER, H., SAYED, A. A., THORNALLEY, P., AHMED, N., BAYNES, J., THORPE, S. & KUKUDOV, G. 2008. Glyoxalase-1 prevents mitochondrial protein modification and enhances lifespan in Caenorhabditis elegans. *Aging cell,* 7**,** 260-269.

MORTENSEN, P. B., HOVE, H., CLAUSEN, M. R. & HOLTUG, K. 1991. Fermentation to short-chain fatty acids and lactate in human faecal batch cultures intra-and inter-individual variations versus variations caused by changes in fermented saccharides. *Scandinavian journal of gastroenterology,* 26**,** 1285-1294.

MORTUZA, R., CHEN, S., FENG, B., SEN, S. & CHAKRABARTI, S. 2013. High glucose induced alteration of SIRTs in endothelial cells causes rapid aging in a p300 and FOXO regulated pathway. *PloS one,* 8**,** e54514.

MURATA-KAMIYA, N., KAJI, H. & KASAI, H. 1999. Deficient nucleotide excision repair increases base-pair substitutions but decreases TGGC frameshifts induced by methylglyoxal in Escherichia coli. *Mutation Research/Genetic Toxicology and Environmental Mutagenesis,* 442**,** 19-28.

MURATA-KAMIYA, N., KAMIYA, H., KAJI, H. & KASAI, H. 1998. Nucleotide Excision Repair Proteins May Be Involved in the Fixation of Glyoxal-Induced Mutagenesis in Escherichia coli. *Biochemical and biophysical research communications,* 248**,** 412-417.

MURATA, K., INOUE, Y., SAIKUSA, T., WATANABE, K., FUKUDA, Y., MAKOTO, S. & KIMURA, A. 1986. Metabolism of α-ketoaldehydes in yeasts: Inducible formation of methyglyoxal reductase and its relation to growth arrest of Saccharomyces cerevisiae. *Journal of fermentation technology,* 64**,** 1-4.

MURILLO, J., WANG, Y., XU, X., KLEBE, R. J., CHEN, Z., ZARDENETA, G., PAL, S., MIKHAILOVA, M. & STEFFENSEN, B. 2008. Advanced Glycation of Type I Collagen and Fibronectin Modifies Periodontal Cell Behavior. *Journal of Periodontology,* 79**,** 2190-2199.

NAGUIB, G., AL-MASHAT, H., DESTA, T. & GRAVES, D. T. 2004. Diabetes Prolongs the Inflammatory Response to a Bacterial Stimulus Through Cytokine Dysregulation. *J Invest Dermatol,* 123**,** 87-92.

NAKAYAMA, T., HAYASE, F. & KATO, H. 1980. Formation of ε-(2-Formyl-5-hydroxy-methyl-pyrrol-1-yl)-l-norleucine in the Maillard Reaction between d-Glucose and l-Lysine. *Agricultural and Biological Chemistry,* 44**,** 1201-1202.

NANCI, A. & BOSSHARDT, D. D. 2006. Structure of periodontal tissues in health and disease. *Periodontol 2000,* 40**,** 11-28.

NANGIA-MAKKER, P., OCHIENG, J., CHRISTMAN, J. K. & RAZ, A. 1993. Regulation of the expression of galactoside-binding lectin during human monocytic differentiation. *Cancer Res,* 53**,** 5033-7.

NARAYAN, K. M., BOYLE, J. P., THOMPSON, T. J., GREGG, E. W. & WILLIAMSON, D. F. 2007. Effect of BMI on lifetime risk for diabetes in the U.S. *Diabetes Care,* 30**,** 1562-6.

NASS, N., BRÖMME, H.-J., HARTIG, R., KORKMAZ, S., SEL, S., HIRCHE, F., WARD, A., SIMM, A., WIEMANN, S. & LYKKESFELDT, A. E. 2014. Differential response to α-oxoaldehydes in tamoxifen resistant MCF-7 breast cancer cells.

NAYAK, P. A., NAYAK, U. A. & MYTHILI, R. 2010. Effect of Manuka honey, chlorhexidine gluconate and xylitol on the clinical levels of dental plaque. *Contemporary clinical dentistry,* 1**,** 214.

NEEPER, M., SCHMIDT, A. M., BRETT, J., YAN, S. D., WANG, F., PAN, Y. C., ELLISTON, K., STERN, D. & SHAW, A. 1992. Cloning and expression of a cell surface receptor for advanced glycosylation end products of proteins. *J Biol Chem,* 267**,** 14998-5004.

NEHER, B. D., MAZZAFERRO, L. S., KOTIK, M., OYHENART, J., HALADA, P., KŘEN, V. & BRECCIA, J. D. 2015. Bacteria as source of diglycosidase activity: Actinoplanes missouriensis produces 6-O-α-l-rhamnosyl-β-d-glucosidase active on flavonoids. *Applied microbiology and biotechnology***,** 1-10.

NELSON, R. G., SHLOSSMAN, M., BUDDING, L. M., PETTITT, D. J., SAAD, M. F., GENCO, R. J. & KNOWLER, W. C. 1990. Periodontal Disease and NIDDM in Pima Indians. *Diabetes Care,* 13**,** 836-840.

NEMET, I., VARGA-DEFTERDAROVIC, L. & TURK, Z. 2006. Methylglyoxal in food and living organisms. *Mol Nutr Food Res,* 50**,** 1105-17.

NESVIZHSKII, A. I., KELLER, A., KOLKER, E. & AEBERSOLD, R. 2003. A statistical model for identifying proteins by tandem mass spectrometry. *Analytical chemistry,* 75**,** 4646-4658.

NEUBERG, C. 1913. The destruction of lactic aldehyde and methylglyoxal by animal organs. *Biochem Z,* 49**,** 502-506.

NEWMAN, M. G., TAKEI, H., KLOKKEVOLD, P. R. & CARRANZA, F. A. 2011. *Carranza's clinical periodontology,* Elsevier health sciences.

NIEMIEC, B. A. 2012. *Veterinary periodontology,* John Wiley & Sons.

NIMMERJAHN, F. & RAVETCH, J. V. 2006. Fcγ Receptors: Old Friends and New Family Members. *Immunity,* 24**,** 19-28.

NISHIMURA, C., FURUE, M., ITO, T., OMORI, Y. & TANIMOTO, T. 1993. Quantitative determination of human aldose reductase by enzyme-linked immunosorbent assay: Immunoassay of human aldose reductase. *Biochemical pharmacology,* 46**,** 21-28.

NISHIMURA, F., TERRANOVA, V., FOO, H., KURIHARA, M., KURIHARA, H. & MURAYAMA, Y. 1996. Glucose-mediated alteration of cellular function in human periodontal ligament cells. *Journal of dental research,* 75**,** 1664-1671.

NISHINAKA, T. & YABE-NISHIMURA, C. 2005. Transcription factor Nrf2 regulates promoter activity of mouse aldose reductase (AKR1B3) gene. *Journal of pharmacological sciences***,** 0501140011.

NISTICO, L., BUZZETTI, R., PRITCHARD, L. E., VAN DER AUWERA, B., GIOVANNINI, C., BOSI, E., LARRAD, M. T., RIOS, M. S., CHOW, C. C., COCKRAM, C. S., JACOBS, K., MIJOVIC, C., BAIN, S. C., BARNETT, A. H., VANDEWALLE, C. L., SCHUIT, F., GORUS, F. K., TOSI, R., POZZILLI, P. & TODD, J. A. 1996. The CTLA-4 gene region of chromosome 2q33 is linked to, and associated with, type 1 diabetes. Belgian Diabetes Registry. *Hum Mol Genet,* 5**,** 1075-80.

NIWA, T., MIYAZAKI, T., KATSUZAKI, T., TATEMICHI, N. & TAKEI, Y. 1996. Serum levels of 3-deoxyglucosone and tissue contents of advanced glycation end products are increased in streptozotocin-induced diabetic rats with nephropathy. *Nephron,* 74**,** 580-5.

NIZAM, N., DISCIOGLU, F., SAYGUN, I., BAL, V., AVCU, F., OZKAN, C. K. & SERDAR, M. A. 2014. The Effect of α-Tocopherol and Selenium on Human Gingival Fibroblasts and Periodontal Ligament Fibroblasts In Vitro. *Journal of periodontology,* 85**,** 636-644.

NIZAMUTDINOVA, I. T., JEONG, J. J., XU, G. H., LEE, S.-H., KANG, S. S., KIM, Y. S., CHANG, K. C. & KIM, H. J. 2008. Hesperidin, hesperidin methyl chalone and phellopterin from Poncirus trifoliata (Rutaceae) differentially regulate the expression of adhesion molecules in tumor necrosis factor-α-stimulated human umbilical vein endothelial cells. *International immunopharmacology,* 8**,** 670-678.

O'CONNELL, P. A. A., TABA, M., NOMIZO, A., FOSS FREITAS, M. C., SUAID, F. A., UYEMURA, S. A., TREVISAN, G. L., NOVAES, A. B., SOUZA, S. L. S., PALIOTO, D. B. & GRISI, M. F. M. 2008. Effects of Periodontal Therapy on Glycemic Control and Inflammatory Markers. *Journal of Periodontology,* 79**,** 774-783.

O'DOWD, L. K., DURHAM, J., MCCRACKEN, G. I. & PRESHAW, P. M. 2010. Patients' experiences of the impact of periodontal disease. *Journal of Clinical Periodontology,* 37**,** 334-339.

OBAYASHI, H., NAKANO, K., SHIGETA, H., YAMAGUCHI, M., YOSHIMORI, K., FUKUI, M., FUJII, M., KITAGAWA, Y., NAKAMURA, N. & NAKAMURA, K. 1996. Formation of crossline as a fluorescent advanced glycation end productin vitroandin vivo. *Biochemical and biophysical research communications,* 226**,** 37-41.

OFFENBACHER, S. 1996. Periodontal diseases: pathogenesis. *Annals of periodontology/the American Academy of Periodontology,* 1**,** 821.

OGURA, N., SHIBATA, Y., KAMINO, Y., MATSUDA, U., HAYAKAWA, M., OIKAWA, T., TAKIGUCHI, H., IZUMI, H. & ABIKO, Y. 1994. Stimulation of Interleukin-6 Production of Periodontal Ligament Cells by Porphyromonas endodontalis Lipopolysaccharide. *Biochemical Medicine and Metabolic Biology,* 53**,** 130-136.

OH, M. S., URIBARRI, J., ALVERANGA, D., LAZAR, I., BAZILINSKI, N. & CARROLL, H. J. 1985. Metabolic utilization and renal handling of D-lactate in men. *Metabolism,* 34**,** 621-625.

OHGI, S. & JOHNSON, P. 1996. Glucose modulates growth of gingival fibroblasts and periodontal ligament cells: correlation with expression of basic fibroblast growth factor. *Journal of periodontal research,* 31**,** 579-588.

OHMORI, S. & IWAMOTO, T. 1988. Sensitive determination of D-lactic acid in biological samples by high-performance liquid chromatography. *Journal of Chromatography B: Biomedical Sciences and Applications,* 431**,** 239-247.

OHMORI, S., NOSE, Y., OGAWA, H., TSUYAMA, K., HIROTA, T., GOTO, H., YANO, Y., KONDOH, Y., NAKATA, K. & TSUBOI, S. 1991. Fluorimetric

and high-performance liquid chromatographic determination of D-lactate in biological samples. *Journal of Chromatography B: Biomedical Sciences and Applications,* 566**,** 1-8.

OKA, K., MOROKUMA, M., IMANAKA-YOSHIDA, K., SAWA, Y., ISOKAWA, K. & HONDA, M. J. 2012. Cellular turnover in epithelial rests of Malassez in the periodontal ligament of the mouse molar. *European Journal of Oral Sciences,* 120**,** 484-494.

OKADA, N., KOBAYASHI, M., MUGIKURA, K., OKAMATSU, Y., HANAZAWA, S., KITANO, S. & HASEGAWA, K. 1997. Interleukin-6 production in human fibroblasts derived from periodontal tissues is differentially regulated by cytokines and a glucocorticoid. *Journal of Periodontal Research,* 32**,** 559-569.

ONG, S.-E. & MANN, M. 2005. Mass spectrometry-based proteomics turns quantitative. *Nat Chem Biol,* 1**,** 252-262.

OORTGIESEN, D. A. W., PLACHOKOVA, A. S., GEENEN, C., MEIJER, G. J., WALBOOMERS, X. F., VAN DEN BEUCKEN, J. J. J. P. & JANSEN, J. A. 2012. Alkaline phosphatase immobilization onto Bio-Gide ® and Bio-Oss ® for periodontal and bone regeneration. *J Clin Periodontol,* 39**,** 546-555.

ORIHUELA-CAMPOS, R. C., TAMAKI, N., MUKAI, R., FUKUI, M., MIKI, K., TERAO, J. & ITO, H.-O. 2015. Biological impacts of resveratrol, quercetin, and N-acetylcysteine on oxidative stress in human gingival fibroblasts. *Journal of Clinical Biochemistry and Nutrition,* 56**,** 220-227.

OZAKI, K., HANAZAWA, S., TAKESHITA, A., CHEN, Y., WATANABE, A., NISHIDA, K., MIYATA, Y. & KITANO, S. 1996. interleukin-1β and tumor necrosis factor-α stimulate synergistically the expression of monocyte chemoattractant protein-1 in fibroblastic cells derived from human periodontal ligament. *Oral Microbiology and Immunology,* 11**,** 109-114.

ÖZDEMIR, B., SHI, B., BANTLEON, H. P., MORITZ, A., RAUSCH-FAN, X. & ANDRUKHOV, O. 2014. Endocannabinoids and Inflammatory Response in Periodontal Ligament Cells.

PACHOLEC, M., BLEASDALE, J. E., CHRUNYK, B., CUNNINGHAM, D., FLYNN, D., GAROFALO, R. S., GRIFFITH, D., GRIFFOR, M., LOULAKIS, P. & PABST, B. 2010. SRT1720, SRT2183, SRT1460, and resveratrol are not direct activators of SIRT1. *Journal of Biological Chemistry,* 285**,** 8340-8351.

PACIOS, S., KANG, J., GALICIA, J., GLUCK, K., PATEL, H., OVAYDI-MANDEL, A., PETROV, S., ALAWI, F. & GRAVES, D. T. 2012. Diabetes

aggravates periodontitis by limiting repair through enhanced inflammation. *The FASEB Journal,* 26**,** 1423-1430.

PAGE, R. C. & EKE, P. I. 2007. Case definitions for use in population-based surveillance of periodontitis. *Journal of periodontology,* 78**,** 1387-1399.

PAGE, R. C. & KORNMAN, K. S. 1997. The pathogenesis of human periodontitis: an introduction. *Periodontology 2000,* 14**,** 9-11.

PAK, C. Y., EUN, H. M., MCARTHUR, R. G. & YOON, J. W. 1988. Association of cytomegalovirus infection with autoimmune type 1 diabetes. *Lancet,* 2**,** 1-4.

PALSAMY, P. & SUBRAMANIAN, S. 2008. s. *Biomedicine & Pharmacotherapy,* 62**,** 598-605.

PALSAMY, P. & SUBRAMANIAN, S. 2009. Modulatory effects of resveratrol on attenuating the key enzymes activities of carbohydrate metabolism in streptozotocin–nicotinamide-induced diabetic rats. *Chemico-biological interactions,* 179**,** 356-362.

PALSAMY, P. & SUBRAMANIAN, S. 2010. Ameliorative potential of resveratrol on proinflammatory cytokines, hyperglycemia mediated oxidative stress, and pancreatic β-cell dysfunction in streptozotocin-nicotinamide-induced diabetic rats. *Journal of cellular physiology,* 224**,** 423-432.

PALSAMY, P. & SUBRAMANIAN, S. 2011. Resveratrol protects diabetic kidney by attenuating hyperglycemia-mediated oxidative stress and renal inflammatory cytokines via Nrf2–Keap1 signaling. *Biochimica et Biophysica Acta (BBA)-Molecular Basis of Disease,* 1812**,** 719-731.

PALUMBO, A. 2011. The Anatomy and Physiology of the Healthy Periodontium. *Gingival Diseases - Their Aetiology, Prevention and Treatment.* InTech.

PAMPLONA, R., PORTERO-OTÍN, M., BELLMUNT, M. J., GREDILLA, R. & BARJA, G. 2002. Aging increases N epsilon-(Carboxymethyl) lysine and caloric restriction decreases N epsilon-(Carboxyethyl) lysine and N epsilon-(Malondialdehyde) lysine in rat heart mitochondrial proteins. *Free radical research,* 36**,** 47-54.

PANCHAUD, A., AFFOLTER, M., MOREILLON, P. & KUSSMANN, M. 2008. Experimental and computational approaches to quantitative proteomics: status quo and outlook. *Journal of proteomics,* 71**,** 19-33.

PANIERI, E., TOIETTA, G., MELE, M., LABATE, V., RANIERI, S. C., FUSCO, S., TESORI, V., ANTONINI, A., MAULUCCI, G. & DE SPIRITO, M.

2010. Nutrient withdrawal rescues growth factor-deprived cells from mTOR-dependent damage. *Aging,* 2**,** 487-503.

PAPAPANOU, P. N. 1996. Periodontal Diseases: Epidemiology. *Annals of Periodontology,* 1**,** 1-36.

PARASKEVAS, S., HUIZINGA, J. D. & LOOS, B. G. 2008. A systematic review and meta-analyses on C-reactive protein in relation to periodontitis. *J Clin Periodontol,* 35**,** 277-290.

PARHIZ, H., ROOHBAKHSH, A., SOLTANI, F., REZAEE, R. & IRANSHAHI, M. 2015. Antioxidant and Anti-Inflammatory Properties of the Citrus Flavonoids Hesperidin and Hesperetin: An Updated Review of their Molecular Mechanisms and Experimental Models. *Phytotherapy Research,* 29**,** 323-331.

PARK, L., RAMAN, K. G., LEE, K. J., LU, Y., FERRAN, L. J., CHOW, W. S., STERN, D. & SCHMIDT, A. M. 1998. Suppression of accelerated diabetic atherosclerosis by the soluble receptor for advanced glycation endproducts. *Nature medicine,* 4**,** 1025-1031.

PARK, S.-J., AHMAD, F., PHILP, A., BAAR, K., WILLIAMS, T., LUO, H., KE, H., REHMANN, H., TAUSSIG, R. & BROWN, A. L. 2012. Resveratrol ameliorates aging-related metabolic phenotypes by inhibiting cAMP phosphodiesterases. *Cell,* 148**,** 421-433.

PASCAL, S. M. A., VEIGA-DA-CUNHA, M., GILON, P., VAN SCHAFTINGEN, E. & JONAS, J. C. 2009. Effects of fructosamine-3-kinase deficiency on function and survival of mouse pancreatic islets after prolonged culture in high glucose or ribose concentrations. *AJP: Endocrinology and Metabolism,* 298**,** E586-E596.

PATIL, C., ROSSA, C. & KIRKWOOD, K. L. 2006. Actinobacillus actinomycetemcomitans lipopolysaccharide induces interleukin-6 expression through multiple mitogen-activated protein kinase pathways in periodontal ligament fibroblasts. *Oral Microbiology and Immunology,* 21**,** 392-398.

PEARSON, K. J., BAUR, J. A., LEWIS, K. N., PESHKIN, L., PRICE, N. L., LABINSKYY, N., SWINDELL, W. R., KAMARA, D., MINOR, R. K. & PEREZ, E. 2008. Resveratrol delays age-related deterioration and mimics transcriptional aspects of dietary restriction without extending life span. *Cell metabolism,* 8**,** 157-168.

PEMBERTON, K. & BARRETT, J. 1989. The detoxification of xenobiotic compounds by Onchocerca gutturosa (Nematoda: Filarioidea). *International journal for parasitology,* 19**,** 875-878.

PENUMATHSA, S. V., THIRUNAVUKKARASU, M., ZHAN, L., MAULIK, G., MENON, V., BAGCHI, D. & MAULIK, N. 2008. Resveratrol enhances GLUT-4 translocation to the caveolar lipid raft fractions through AMPK/Akt/eNOS signalling pathway in diabetic myocardium. *Journal of cellular and molecular medicine,* 12**,** 2350-2361.

PERCHE, O., VERGNAUD-GAUDUCHON, J., MORAND, C., DUBRAY, C., MAZUR, A. & VASSON, M.-P. 2014. Orange juice and its major polyphenol hesperidin consumption do not induce immunomodulation in healthy well-nourished humans. *Clinical Nutrition,* 33**,** 130-135.

PERGOLA, P. E., RASKIN, P., TOTO, R. D., MEYER, C. J., HUFF, J. W., GROSSMAN, E. B., KRAUTH, M., RUIZ, S., AUDHYA, P. & CHRIST-SCHMIDT, H. 2011. Bardoxolone methyl and kidney function in CKD with type 2 diabetes. *New England Journal of Medicine,* 365**,** 327-336.

PERKINS, N. D. 2006. Post-translational modifications regulating the activity and function of the nuclear factor kappa B pathway. *Oncogene,* 25**,** 6717-6730.

PERRY, G. H., YANG, F., MARQUES-BONET, T., MURPHY, C., FITZGERALD, T., LEE, A. S., HYLAND, C., STONE, A. C., HURLES, M. E. & TYLER-SMITH, C. 2008. Copy number variation and evolution in humans and chimpanzees. *Genome research,* 18**,** 1698-1710.

PERVAIZ, S. 2003. Resveratrol: from grapevines to mammalian biology. *The FASEB journal,* 17**,** 1975-1985.

PETERS, T., JR. 1962. The biosynthesis of rat serum albumin. I. Properties of rat albumin and its occurrence in liver cell fractions. *J Biol Chem,* 237**,** 1181-5.

PETERSON, C. M., KOENIG, R. J., JONES, R. L., SAUDEK, C. D. & CERAMI, A. 1977. Correlation of serum triglyceride levels and hemoglobin AIc concentrations in diabetes mellitus. *Diabetes,* 26**,** 507-509.

PHILIPS, S. A. & THORNALLEY, P. J. 1993. The formation of methylglyoxal from triose phosphates. *European Journal of Biochemistry,* 212**,** 101-105.

PHILLIPS, S. 2012. Oral embryology, histology and anatomy.

PHILLIPS, S. A., MIRRLEES, D. O. N. & THORNALLEY, P. J. 1993. Modification of the glyoxalase system in streptozotocin-Induced diabetic rats and the effect of the aldose reductase Inhibitor Statil. *Biochm. Soc. Trans.,* 21**,** 162S-162S.

PHILLIPS, S. A. & THORNALLEY, P. J. 1993. The formation of methylglyoxal from triose phosphates. Investigation using a specific assay for methylglyoxal. *Eur J Biochem,* 212**,** 101-5.

PICONI, L., QUAGLIARO, L. & CERIELLO, A. 2003. Oxidative stress in diabetes. *Clinical Chemistry and Laboratory Medicine,* 41**,** 1144-1149.

PIETTA, P.-G. 2000. Flavonoids as antioxidants. *Journal of natural products,* 63**,** 1035-1042.

PIHLSTROM, B. L., MICHALOWICZ, B. S. & JOHNSON, N. W. 2005. Periodontal diseases. *The Lancet,* 366**,** 1809-1820.

PISCHETSRIEDER, M., SEIDEL, W., MÜNCH, G. & SCHINZEL, R. 1999. N 2-(1-Carboxyethyl) deoxyguanosine, a nonenzymatic glycation adduct of DNA, induces single-strand breaks and increases mutation frequencies. *Biochemical and biophysical research communications,* 264**,** 544-549.

PONGOR, S., ULRICH, P. C., BENCSATH, F. A. & CERAMI, A. 1984. Aging of proteins: isolation and identification of a fluorescent chromophore from the reaction of polypeptides with glucose. *Proceedings of the National Academy of Sciences,* 81**,** 2684-2688.

POPADIAK, K., POTEMPA, J., RIESBECK, K. & BLOM, A. M. 2007. Biphasic effect of gingipains from Porphyromonas gingivalis on the human complement system. *The Journal of Immunology,* 178**,** 7242-7250.

POPOV, N., SCHMITT, M., SCHULZECK, S. & MATTHIES, H. 1974. [Reliable micromethod for determination of the protein content in tissue homogenates]. *Acta biologica et medica Germanica,* 34**,** 1441-1446.

POPOVA, S., LUNDGREN-ÅKERLUND, E., WIIG, H. & GULLBERG, D. 2007. Physiology and pathology of collagen receptors. *Acta physiologica,* 190**,** 179-187.

PRESHAW, P. M., ALBA, A. L., HERRERA, D., JEPSEN, S., KONSTANTINIDIS, A., MAKRILAKIS, K. & TAYLOR, R. 2013. Periodontitis and diabetes: a two-way relationship. *Diabetologia,* 55**,** 21-31.

PRESHAW, P. M., FOSTER, N. & TAYLOR, J. J. 2007. Cross-susceptibility between periodontal disease and type 2 diabetes mellitus: an immunobiological perspective. *Periodontol 2000,* 45**,** 138-157.

PRESHAW, P. M. & TAYLOR, J. J. 2011. How has research into cytokine interactions and their role in driving immune responses impacted our

understanding of periodontitis? *Journal of Clinical Periodontology*, 38**,** 60-84.

PRICE, D. L., RHETT, P. M., THORPE, S. R. & BAYNES, J. W. 2001. Chelating activity of advanced glycation end-product inhibitors. *Journal of Biological Chemistry*, 276**,** 48967-48972.

PROCTOR, R., KUMAR, N., STEIN, A., MOLES, D. & PORTER, S. 2005. Oral and Dental Aspects of Chronic Renal Failure. *Journal of Dental Research,* 84**,** 199-208.

QUEISSER, M. A., YAO, D., GEISLER, S., HAMMES, H. P., LOCHNIT, G., SCHLEICHER, E. D., BROWNLEE, M. & PREISSNER, K. T. 2010. Hyperglycemia impairs proteasome function by methylglyoxal. *Diabetes,* 59**,** 670-8.

QURESHI, N., MORRISON, D. C. & REIS, J. 2012. Proteasome protease mediated regulation of cytokine induction and inflammation. *Biochimica et Biophysica Acta (BBA)-Molecular Cell Research,* 1823**,** 2087-2093.

RABBANI, N., ALAM, S. S., RIAZ, S., LARKIN, J. R., AKHTAR, M. W., SHAFI, T. & THORNALLEY, P. J. 2009. High-dose thiamine therapy for patients with type 2 diabetes and microalbuminuria: a randomised, double-blind placebo-controlled pilot study. *Diabetologia,* 52**,** 208-12.

RABBANI, N., CHITTARI, M. V., BODMER, C. W., ZEHNDER, D., CERIELLO, A. & THORNALLEY, P. J. 2010. Increased glycation and oxidative damage to apolipoprotein B100 of LDL cholesterol in patients with type 2 diabetes and effect of metformin. *Diabetes,* 59**,** 1038-1045.

RABBANI, N., GODFREY, L., XUE, M., SHAHEEN, F., GEOFFRION, M., MILNE, R. & THORNALLEY, P. J. 2011. Glycation of LDL by Methylglyoxal Increases Arterial Atherogenicity A Possible Contributor to Increased Risk of Cardiovascular Disease in Diabetes. *Diabetes,* 60**,** 1973-1980.

RABBANI, N., SHAHEEN, F., ANWAR, A., MASANIA, J. & THORNALLEY, P. J. 2014a. Assay of methylglyoxal-derived protein and nucleotide AGEs. *Biochem. Soc. Trans,* 42**,** 511-517.

RABBANI, N. & THORNALLEY, P. 2008a. Dicarbonyls linked to damage in the powerhouse: glycation of mitochondrial proteins and oxidative stress. *Biochem Soc Trans,* 36**,** 1045-50.

RABBANI, N. & THORNALLEY, P. J. 2008b. The Dicarbonyl Proteome. *Annals of the New York Academy of Sciences,* 1126**,** 124-127.

RABBANI, N. & THORNALLEY, P. J. 2009. Quantitation of markers of protein damage by glycation, oxidation, and nitration in peritoneal dialysis. *Perit Dial Int,* 29 Suppl 2**,** S51-6.

RABBANI, N. & THORNALLEY, P. J. 2012a. Dicarbonyls (Glyoxal, Methylglyoxal, and 3-Deoxyglucosone). *Uremic Toxins***,** 177-192.

RABBANI, N. & THORNALLEY, P. J. 2012b. Glycation research in amino acids: a place to call home. *Amino Acids,* 42**,** 1087-96.

RABBANI, N. & THORNALLEY, P. J. 2012c. Methylglyoxal, glyoxalase 1 and the dicarbonyl proteome. *Amino Acids,* 42**,** 1133-42.

RABBANI, N. & THORNALLEY, P. J. 2014a. Dicarbonyl proteome and genome damage in metabolic and vascular disease. *Biochem. Soc. Trans,* 42**,** 425-432.

RABBANI, N. & THORNALLEY, P. J. 2014b. Glyoxalase Centennial: 100 Years of Glyoxalase Research and Emergence of Dicarbonyl Stress. *Biochemical Society Transactions,* 42.

RABBANI, N. & THORNALLEY, P. J. 2014c. Measurement of methylglyoxal by stable isotopic dilution analysis LC-MS/MS with corroborative prediction in physiological samples. *Nature protocols,* 9**,** 1969-1979.

RABBANI, N. & THORNALLEY, P. J. 2015. Dicarbonyl stress in cell and tissue dysfunction contributing to ageing and disease. *Biochemical and biophysical research communications,* 458**,** 221-226.

RABBANI, N., XUE, M. & THORNALLEY, P. J. 2014b. Activity, regulation, copy number and function in the glyoxalase system. *Biochem Soc Trans,* 42**,** 419-424.

RACKER, E. 1951. The mechanism of action of glyoxalase. *J Biol Chem,* 190**,** 685-96.

RACKER, E. Glutathione as a coenzyme in intermediary metabolism. Glutathione, a symposium, 1954. 165-183.

RAGNARSSON, B., CARR, G. & DANIEL, J. 1985. Basic Biological Sciences Isolation and Growth of Human Periodontal Ligament Cells in vitro. *Journal of dental research,* 64**,** 1026-1030.

RAMELET, A. A. 2001. Clinical benefits of Daflon 500 mg in the most severe stages of chronic venous insufficiency. *Angiology,* 52**,** S49-S56.

RANGANATHAN, S., CIACCIO, P. J., WALSH, E. S. & TEW, K. D. 1999. Genomic sequence of human glyoxalase-I: analysis of promoter activity and its regulation. *Gene,* 240**,** 149-155.

RAPPSILBER, J., RYDER, U., LAMOND, A. I. & MANN, M. 2002. Large-scale proteomic analysis of the human spliceosome. *Genome research,* 12**,** 1231-1245.

RAUH, D., FISCHER, F., GERTZ, M., LAKSHMINARASIMHAN, M., BERGBREDE, T., ALADINI, F., KAMBACH, C., BECKER, C. F. W., ZERWECK, J., SCHUTKOWSKI, M. & STEEGBORN, C. 2013. An acetylome peptide microarray reveals specificities and deacetylation substrates for all human sirtuin isoforms. *Nat Commun,* 4.

REDON, R., ISHIKAWA, S., FITCH, K. R., FEUK, L., PERRY, G. H., ANDREWS, T. D., FIEGLER, H., SHAPERO, M. H., CARSON, A. R. & CHEN, W. 2006. Global variation in copy number in the human genome. *nature,* 444**,** 444-454.

REINIGER, N., LAU, K., MCCALLA, D., EBY, B., CHENG, B., LU, Y., QU, W., QUADRI, N., ANANTHAKRISHNAN, R. & FURMANSKY, M. 2010. Deletion of the receptor for advanced glycation end products reduces glomerulosclerosis and preserves renal function in the diabetic OVE26 mouse. *Diabetes,* 59**,** 2043-2054.

RIBOULET-CHAVEY, A., PIERRON, A., DURAND, I., MURDACA, J., GIUDICELLI, J. & VAN OBBERGHEN, E. 2006. Methylglyoxal impairs the insulin signaling pathways independently of the formation of intracellular reactive oxygen species. *Diabetes,* 55**,** 1289-1299.

RIDDERSTROM, M., SACCUCCI, F., HELLMAN, U., BERGMAN, T., PRINCIPATO, G. & MANNERVIK, B. 1996. Molecular cloning, heterologous expression, and characterization of human glyoxalase II. *J Biol Chem,* 271**,** 319-23.

RIVERA, L., MORÓN, R., ZARZUELO, A. & GALISTEO, M. 2009. Long-term resveratrol administration reduces metabolic disturbances and lowers blood pressure in obese Zucker rats. *Biochemical pharmacology,* 77**,** 1053-1063.

RIZZA, S., MUNIYAPPA, R., IANTORNO, M., KIM, J.-A., CHEN, H., PULLIKOTIL, P., SENESE, N., TESAURO, M., LAURO, D. & CARDILLO, C. 2011. Citrus polyphenol hesperidin stimulates production of nitric oxide in endothelial cells while improving endothelial function and reducing inflammatory markers in patients with metabolic syndrome. *The Journal of Clinical Endocrinology & Metabolism,* 96**,** E782-E792.

ROBERTSON, R. P. 2006. Oxidative stress and impaired insulin secretion in type 2 diabetes. *Current opinion in pharmacology,* 6**,** 615-619.

ROCHA, K., SOUZA, G., EBAID, G., SEIVA, F., CATANEO, A. & NOVELLI, E. 2009. Resveratrol toxicity: effects on risk factors for atherosclerosis and hepatic oxidative stress in standard and high-fat diets. *Food and Chemical Toxicology,* 47**,** 1362-1367.

ROCHE, E. F., MENON, A., GILL, D. & HOEY, H. 2005. Clinical presentation of type 1 diabetes. *Pediatric Diabetes,* 6**,** 75-78.

ROMANO, B., PAGANO, E., MONTANARO, V., FORTUNATO, A. L., MILIC, N. & BORRELLI, F. 2013. Novel insights into the pharmacology of flavonoids. *Phytotherapy research,* 27**,** 1588-1596.

ROMERO-PÉREZ, A. I., IBERN-GÓMEZ, M., LAMUELA-RAVENTÓS, R. M. & DE LA TORRE-BORONAT, M. C. 1999. Piceid, the major resveratrol derivative in grape juices. *Journal of Agricultural and Food Chemistry,* 47**,** 1533-1536.

RONDEROS, M., PIHLSTROM, B. L. & HODGES, J. S. 2001. Periodontal disease among indigenous people in the Amazon rain forest. *Journal of clinical periodontology,* 28**,** 995-1003.

RÖPER, H., RÖPER, S., HEYNS, K. & MEYER, B. 1983. N.m.r. spectroscopy of N-(1-deoxy-d-fructos-1-yl)-l-amino acids ("fructose-amino acids"). *Carbohydrate Research,* 116**,** 183-195.

ROSCA, M. G., MUSTATA, T. G., KINTER, M. T., OZDEMIR, A. M., KERN, T. S., SZWEDA, L. I., BROWNLEE, M., MONNIER, V. M. & WEISS, M. F. 2005. Glycation of mitochondrial proteins from diabetic rat kidney is associated with excess superoxide formation. *Am J Physiol Renal Physiol,* 289**,** F420-30.

ROTELLI, A. E., GUARDIA, T., JUÁREZ, A. O., DE LA ROCHA, N. E. & PELZER, L. E. 2003. Comparative study of flavonoids in experimental models of inflammation. *Pharmacological research,* 48**,** 601-606.

RUGGIERO-LOPEZ, D., LECOMTE, M., MOINET, G., PATEREAU, G., LAGARDE, M. & WIERNSPERGER, N. 1999. Reaction of metformin with dicarbonyl compounds. Possible implication in the inhibition of advanced glycation end product formation. *Biochemical pharmacology,* 58**,** 1765-1773.

RYAN, M. E., CARNU, O. & KAMER, A. 2003. The influence of diabetes on the periodontal tissues. *The Journal of the American Dental Association,* 134**,** 34S-40S.

SADYGOV, R. G., COCIORVA, D. & YATES, J. R. 2004. Large-scale database searching using tandem mass spectra: Looking up the answer in the back of the book. *Nat Meth,* 1**,** 195-202.

SAHU, B. D., KUNCHA, M., SINDHURA, G. J. & SISTLA, R. 2013. Hesperidin attenuates cisplatin-induced acute renal injury by decreasing oxidative stress, inflammation and DNA damage. *Phytomedicine,* 20**,** 453-460.

SAKAGUCHI, T., YAN, S. F., YAN, S. D., BELOV, D., RONG, L. L., SOUSA, M., ANDRASSY, M., MARSO, S. P., DUDA, S., ARNOLD, B., LILIENSIEK, B., NAWROTH, P. P., STERN, D. M., SCHMIDT, A. M. & NAKA, Y. 2003. Central role of RAGE-dependent neointimal expansion in arterial restenosis. *J Clin Invest,* 111**,** 959-72.

SAKATA, K., HIROSE, Y., QIAO, Z., TANAKA, T. & MORI, H. 2003. Inhibition of inducible isoforms of cyclooxygenase and nitric oxide synthase by flavonoid hesperidin in mouse macrophage cell line. *Cancer letters,* 199**,** 139-145.

SALVI, G. E., CAROLLO-BITTEL, B. & LANG, N. P. 2008. Effects of diabetes mellitus on periodontal and peri-implant conditions: update on associations and risks. *Journal of Clinical Periodontology,* 35**,** 398-409.

SALVI, G. E., YALDA, B., COLLINS, J. G., JONES, B. H., SMITH, F. W., ARNOLD, R. R. & OFFENBACHER, S. 1997. Inflammatory Mediator Response as a Potential Risk Marker for Periodontal Diseases in Insulin-Dependent Diabetes Mellitus Patients. *Journal of Periodontology,* 68**,** 127-135.

SAN MIGUEL, S. M., OPPERMAN, L. A., ALLEN, E. P., ZIELINSKI, J. & SVOBODA, K. K. 2010. Antioxidants counteract nicotine and promote migration via RacGTP in oral fibroblast cells. *Journal of periodontology,* 81**,** 1675-1690.

SANDBERG, G. E., SUNDBERG, H. E., FJELLSTROM, C. A. & WIKBLAD, K. F. 2000. Type 2 diabetes and oral health. *Diabetes Research and Clinical Practice,* 50**,** 27-34.

SANDERS, S. L., JENNINGS, J., CANUTESCU, A., LINK, A. J. & WEIL, P. A. 2002. Proteomics of the eukaryotic transcription machinery: identification of proteins associated with components of yeast TFIID by multidimensional mass spectrometry. *Molecular and cellular biology,* 22**,** 4723-4738.

SANTARIUS, T., BIGNELL, G. R., GREENMAN, C. D., WIDAA, S., CHEN, L., MAHONEY, C. L., BUTLER, A., EDKINS, S., WARIS, S., THORNALLEY, P. J., FUTREAL, P. A. & STRATTON, M. R. 2010.

GLO1-A novel amplified gene in human cancer. *Genes, Chromosomes and Cancer,* 49**,** 711-725.

SANTOS, V. R., LIMA, J. A., GONÇALVES, T. E. D., BASTOS, M. F., FIGUEIREDO, L. C., SHIBLI, J. A. & DUARTE, P. M. 2010. Receptor activator of nuclear factor-kappa B ligand/osteoprotegerin ratio in sites of chronic periodontitis of subjects with poorly and well-controlled type 2 diabetes. *Journal of periodontology,* 81**,** 1455-1465.

SASAKI, N. A., GARCIA-ALVAREZ, M. C., WANG, Q., ERMOLENKO, L., FRANCK, G., NHIRI, N., MARTIN, M.-T., AUDIC, N. & POTIER, P. 2009. N-Terminal 2, 3-diaminopropionic acid (Dap) peptides as efficient methylglyoxal scavengers to inhibit advanced glycation endproduct (AGE) formation. *Bioorganic & medicinal chemistry,* 17**,** 2310-2320.

SAVELIEV, S., BRATZ, M., ZUBAREV, R., SZAPACS, M., BUDAMGUNTA, H. & URH, M. 2013. Trypsin/Lys-C protease mix for enhanced protein mass spectrometry analysis. *Nature Methods,* 10.

SCHIMANDLE, C. M. & VANDER JAGT, D. L. 1979. Isolation and kinetic analysis of the multiple forms of glyoxalase-I from human erythrocytes. *Archives of biochemistry and biophysics,* 195**,** 261-268.

SCHMATZ, R., MAZZANTI, C. M., SPANEVELLO, R., STEFANELLO, N., GUTIERRES, J., MALDONADO, P. A., CORRÊA, M., DA ROSA, C. S., BECKER, L. & BAGATINI, M. 2009a. Ectonucleotidase and acetylcholinesterase activities in synaptosomes from the cerebral cortex of streptozotocin-induced diabetic rats and treated with resveratrol. *Brain research bulletin,* 80**,** 371-376.

SCHMATZ, R., SCHETINGER, M. R. C., SPANEVELLO, R. M., MAZZANTI, C. M., STEFANELLO, N., MALDONADO, P. A., GUTIERRES, J., CORRÊA, M. D. C., GIROTTO, E. & MORETTO, M. B. 2009b. Effects of resveratrol on nucleotide degrading enzymes in streptozotocin-induced diabetic rats. *Life Sciences,* 84**,** 345-350.

SCHMIDT, A. M., HORI, O., CHEN, J. X., LI, J. F., CRANDALL, J., ZHANG, J., CAO, R., YAN, S. D., BRETT, J. & STERN, D. 1995. Advanced glycation endproducts interacting with their endothelial receptor induce expression of vascular cell adhesion molecule-1 (VCAM-1) in cultured human endothelial cells and in mice. A potential mechanism for the accelerated vasculopathy of diabetes. *J Clin Invest,* 96**,** 1395-403.

SCHMIDT, A. M., VIANNA, M., GERLACH, M., BRETT, J., RYAN, J., KAO, J., ESPOSITO, C., HEGARTY, H., HURLEY, W. & CLAUSS, M. 1992. Isolation and characterization of two binding proteins for advanced

glycosylation end products from bovine lung which are present on the endothelial cell surface. *Journal of Biological Chemistry,* 267**,** 14987-14997.

SCHMIDT, R., BÖHME, D., SINGER, D. & FROLOV, A. 2015. Specific tandem mass spectrometric detection of AGE-modified arginine residues in peptides. *Journal of Mass Spectrometry,* 50**,** 613-624.

SCHNIDER, S. L. & KOHN, R. R. 1981. Effects of age and diabetes mellitus on the solubility and nonenzymatic glucosylation of human skin collagen. *Journal of Clinical Investigation,* 67**,** 1630-1635.

SEARLE, B. C. 2010. Scaffold: a bioinformatic tool for validating MS/MS-based proteomic studies. *Proteomics,* 10**,** 1265-1269.

ŠEBEKOVÁ, K., KRAJČOVIČOVÁ-KUDLÁČKOVÁ, M., SCHINZEL, R., FAIST, V., KLVANOVÁ, J. & HEIDLAND, A. 2001. Plasma levels of advanced glycation end products in healthy, long-term vegetarians and subjects on a western mixed diet. *European journal of nutrition,* 40**,** 275-281.

SEINO, Y., NANJO, K., TAJIMA, N., KADOWAKI, T., KASHIWAGI, A., ARAKI, E., ITO, C., INAGAKI, N., IWAMOTO, Y., KASUGA, M., HANAFUSA, T., HANEDA, M. & UEKI, K. 2010. Report of the Committee on the Classification and Diagnostic Criteria of Diabetes Mellitus. *Journal of Diabetes Investigation,* 1**,** 212-228.

SEITZ, C. T. & WINGARD JR, R. E. 1978. An improved conversion of hesperidin into hesperetin including purity determination by gradient-elution, high-pressure liquid chromatography. *Journal of Agricultural and Food Chemistry,* 26**,** 278-280.

SELL, D. & MONNIER, V. 1989. Structure elucidation of a senescence cross-link from human extracellular matrix. Implication of pentoses in the aging process. *Journal of Biological Chemistry,* 264**,** 21597-21602.

SELWITZ, R. H., ISMAIL, A. I. & PITTS, N. B. 2007. Dental caries. *The Lancet,* 369**,** 51-59.

SESSA, L., GATTI, E., ZENI, F., ANTONELLI, A., CATUCCI, A., KOCH, M., POMPILIO, G., FRITZ, G., RAUCCI, A. & BIANCHI, M. E. 2014. The receptor for advanced glycation end-products (RAGE) is only present in mammals, and belongs to a family of cell adhesion molecules (CAMs). *PloS one,* 9**,** e86903.

SEYMOUR, G. 1987. Invited review: Possible mechanisms involved in the immunoregulation of chronic inflammatory periodontal disease. *Journal of dental research,* 66**,** 2-9.

SHAKIBAEI, M., HARIKUMAR, K. B. & AGGARWAL, B. B. 2009. Resveratrol addiction: to die or not to die. *Molecular nutrition & food research,* 53**,** 115-128.

SHANG, J., SUN, H. & XIAO, H. 2008. Resveratrol improves non-alcoholic fatty liver disease by activating AMP-activated protein kinase1. *Acta Pharmacologica Sinica,* 29**,** 698-706.

SHARMA-LUTHRA, R. & KALE, R. 1994. Age related changes in the activity of the glyoxalase system. *Mechanisms of ageing and development,* 73**,** 39-45.

SHARMA, S., MISRA, C. S., ARUMUGAM, S., ROY, S., SHAH, V., DAVIS, J. A., SHIRUMALLA, R. K. & RAY, A. 2011. Antidiabetic activity of resveratrol, a known SIRT1 activator in a genetic model for type-2 diabetes. *Phytotherapy Research,* 25**,** 67-73.

SHARMA, S. S., KUMAR, A., ARORA, M. & KAUNDAL, R. K. 2009. Neuroprotective potential of combination of resveratrol and 4-amino 1, 8 naphthalimide in experimental diabetic neuropathy: focus on functional, sensorimotor and biochemical changes. *Free radical research,* 43**,** 400-408.

SHEVCHENKO, G., MUSUNURI, S., WETTERHALL, M. & BERGQUIST, J. 2012. Comparison of extraction methods for the comprehensive analysis of mouse brain proteome using shotgun-based mass spectrometry. *Journal of proteome research,* 11**,** 2441-2451.

SHIBATA, M., SHINTAKU, Y., MATSUZAKI, K. & UEMATSU, S. 2014. The effect of IL-17 on the production of proinflammatory cytokines and matrix metalloproteinase-1 by human periodontal ligament fibroblasts. *Orthodontics & Craniofacial Research,* 17**,** 60-68.

SHIMASAKI, H. 1994. Assay of fluorescent lipid peroxidation products. *Methods in enzymology,* 233**,** 338.

SHINOHARA, M., THORNALLEY, P. J., GIARDINO, I., BEISSWENGER, P., THORPE, S. R., ONORATO, J. & BROWNLEE, M. 1998. Overexpression of glyoxalase-I in bovine endothelial cells inhibits intracellular advanced glycation endproduct formation and prevents hyperglycemia-induced increases in macromolecular endocytosis. *J Clin Invest,* 101**,** 1142-7.

SHIPANOVA, I. N., GLOMB, M. A. & NAGARAJ, R. H. 1997. Protein modification by methylglyoxal: chemical nature and synthetic mechanism of a major fluorescent adduct. *Archives of biochemistry and biophysics,* 344**,** 29-36.

SHRIVASTAVA, M., KAR, V. & SHRIVASTAVA, S. 2013. Cyclophosphamide altered the myocardial marker enzymes: Protection provoked by Hesperidin in Rats. *International Journal of Phytomedicine,* 5**,** 141.

SHU, L., GUAN, S. M., FU, S. M., GUO, T., CAO, M. & DING, Y. 2008. Estrogen Modulates Cytokine Expression in Human Periodontal Ligament Cells. *Journal of Dental Research,* 87**,** 142-147.

SIEMANN, E. & CREASY, L. 1992. Concentration of the phytoalexin resveratrol in wine. *American Journal of Enology and Viticulture,* 43**,** 49-52.

SILAN, C. 2008. The effects of chronic resveratrol treatment on vascular responsiveness of streptozotocin-induced diabetic rats. *Biological and Pharmaceutical Bulletin,* 31**,** 897-902.

SINGH, A. P., ARORA, S., BHARDWAJ, A., SRIVASTAVA, S. K., KADAKIA, M. P., WANG, B., GRIZZLE, W. E., OWEN, L. B. & SINGH, S. 2012. CXCL12/CXCR4 Protein Signaling Axis Induces Sonic Hedgehog Expression in Pancreatic Cancer Cells via Extracellular Regulated Kinase- and Akt Kinase-mediated Activation of Nuclear Factor κB Implications For Bidirectional Tumor-Stromal Interactions. *Journal of Biological Chemistry,* 287**,** 39115-39124.

SITTE, N., MERKER, K., VON ZGLINICKI, T., GRUNE, T. & DAVIES, K. J. 2000. Protein oxidation and degradation during cellular senescence of human BJ fibroblasts: part I—effects of proliferative senescence. *The FASEB Journal,* 14**,** 2495-2502.

SLOTS, J. 1979. Subgingival microflora and periodontal disease. *Journal of clinical periodontology,* 6**,** 351-382.

SMITH, M., SEYMOUR, G. J. & CULLINAN, M. P. 2010. Histopathological features of chronic and aggressive periodontitis. *Periodontology 2000,* 53**,** 45-54.

SMITH, P. K., KROHN, R. I., HERMANSON, G. T., MALLIA, A. K., GARTNER, F. H., PROVENZANO, M. D., FUJIMOTO, E. K., GOEKE, N. M., OLSON, B. J. & KLENK, D. C. 1985. Measurement of protein using bicinchoninic acid. *Analytical Biochemistry,* 150**,** 76-85.

SMYTH, D. J., COOPER, J. D., BAILEY, R., FIELD, S., BURREN, O., SMINK, L. J., GUJA, C., IONESCU-TIRGOVISTE, C., WIDMER, B., DUNGER, D. B., SAVAGE, D. A., WALKER, N. M., CLAYTON, D. G. & TODD, J. A. 2006. A genome-wide association study of nonsynonymous SNPs identifies a type 1 diabetes locus in the interferon-induced helicase (IFIH1) region. *Nat Genet,* 38**,** 617-9.

SOCRANSKY, S., HAFFAJEE, A., CUGINI, M., SMITH, C. & KENT, R. 1998. Microbial complexes in subgingival plaque. *Journal of clinical periodontology,* 25**,** 134-144.

SOCRANSKY, S., HAFFAJEE, A., SMITH, C. & DUFF, G. 2000. Microbiological parameters associated with IL-1 gene polymorphisms in periodontitis patients. *Journal of clinical periodontology,* 27**,** 810-818.

SOHAL, R. 1981. *Age pigments,* Elsevier/North-Holland Biomedical Press Amsterdam.

SOKOLOVSKY, M., RIORDAN, J. F. & VALLEE, B. L. 1966. Tetranitromethane. A Reagent for the Nitration of Tyrosyl Residues in Proteins*. *Biochemistry,* 5**,** 3582-3589.

SOLÍS-CALERO, C., ORTEGA-CASTRO, J., FRAU, J. & MUÑOZ, F. 2015. Scavenger mechanism of methylglyoxal by metformin. A DFT study. *Theoretical Chemistry Accounts,* 134**,** 1-14.

SOMERMAN, M. J., YOUNG, M. F., FOSTER, R. A., MOEHRING, J. M., IMM, G. & SAUK, J. J. 1990. Characteristics of human periodontal ligament cells in vitro. *Archives of Oral Biology,* 35**,** 241-247.

SOMMER, A., FISCHER, P., KRAUSE, K., BOETTCHER, K., BROPHY, P. M., WALTER, R. D. & LIEBAU, E. 2001. A stress-responsive glyoxalase I from the parasitic nematode Onchocerca volvulus. *Biochem J,* 353**,** 445-52.

SOUFI, F. G., MOHAMMAD-NEJAD, D. & AHMADIEH, H. 2012. Resveratrol improves diabetic retinopathy possibly through oxidative stress–nuclear factor κB–apoptosis pathway. *Pharmacological Reports,* 64**,** 1505-1514.

SOUTHERLAND, J. H., TAYLOR, G. W., MOSS, K., BECK, J. D. & OFFENBACHER, S. 2006. Commonality in chronic inflammatory diseases: periodontitis, diabetes, and coronary artery disease. *Periodontology 2000,* 40**,** 130-143.

SOUZA, P. P. C., PALMQVIST, P., LUNDGREN, I., LIE, A., COSTA-NETO, C. M., LUNDBERG, P. & LERNER, U. H. 2010. Stimulation of IL-6 Cytokines in Fibroblasts by Toll-like Receptors 2. *Journal of Dental Research,* 89**,** 802-807.

SPARROW, J. R., PARISH, C. A., HASHIMOTO, M. & NAKANISHI, K. 1999. A2E, a lipofuscin fluorophore, in human retinal pigmented epithelial cells in culture. *Investigative ophthalmology & visual science,* 40**,** 2988-2995.

SPARVERO, L. J., ASAFU-ADJEI, D., KANG, R., TANG, D., AMIN, N., IM, J., RUTLEDGE, R., LIN, B., AMOSCATO, A. A., ZEH, H. J. & LOTZE, M. T. 2009. RAGE (Receptor for Advanced Glycation Endproducts), RAGE Ligands, and their role in Cancer and Inflammation. *J Transl Med,* 7**,** 17.

STEFFENSEN, B., DUONG, A. H., MILAM, S. B., POTEMPA, C. L., WINBORN, W. B., MAGNUSON, V. L., CHEN, D., ZARDENETA, G. & KLEBE, R. J. 1992. Immunohistological localization of cell adhesion proteins and integrins in the periodontium. *Journal of periodontology,* 63**,** 584-592.

STOYANOV, S., KONRADE, I., HAAG, G., LUKIC, I., HUMPERT, P., RABBANI, N., THORNALLEY, P., NAWROTH, P. & BIERHAUS, A. 2007. RAGE-dependent glyoxalase-1 impairment mediates functional deficits in diabetic neuropathy. *Diabetologie und Stoffwechsel,* 2**,** P99.

STUMVOLL, M., GOLDSTEIN, B. J. & VAN HAEFTEN, T. W. 2005. Type 2 diabetes: principles of pathogenesis and therapy. *Lancet,* 365**,** 1333-46.

SU, H.-C., HUNG, L.-M. & CHEN, J.-K. 2006. Resveratrol, a red wine antioxidant, possesses an insulin-like effect in streptozotocin-induced diabetic rats. *American Journal of Physiology-Endocrinology And Metabolism,* 290**,** E1339-E1346.

SULAIMAN, M., MATTA, M. J., SUNDERESAN, N., GUPTA, M. P., PERIASAMY, M. & GUPTA, M. 2010. Resveratrol, an activator of SIRT1, upregulates sarcoplasmic calcium ATPase and improves cardiac function in diabetic cardiomyopathy. *American Journal of Physiology-Heart and Circulatory Physiology,* 298**,** H833-H843.

SUN, C., ZHANG, F., GE, X., YAN, T., CHEN, X., SHI, X. & ZHAI, Q. 2007. SIRT1 improves insulin sensitivity under insulin-resistant conditions by repressing PTP1B. *Cell metabolism,* 6**,** 307-319.

SUN, H., DONG, T., ZHANG, A., YANG, J., YAN, G., SAKURAI, T., WU, X., HAN, Y. & WANG, X. 2013. Pharmacokinetics of hesperetin and naringenin in the Zhi Zhu Wan, a traditional Chinese medicinal formulae, and its pharmacodynamics study. *Phytotherapy Research,* 27**,** 1345-1351.

SUVAN, J. E., PETRIE, A., NIBALI, L., DARBAR, U., RAKMANEE, T., DONOS, N. & D'AIUTO, F. 2015. Association between overweight/obesity and increased risk of periodontitis. *Journal of clinical periodontology,* 42**,** 733-739.

SVENSSON, J., LYNGAAE-JORGENSEN, A., CARSTENSEN, B., SIMONSEN, L. B. & MORTENSEN, H. B. 2009. Long-term trends in the incidence of

type 1 diabetes in Denmark: the seasonal variation changes over time. *Pediatr Diabetes,* 10**,** 248-54.

SZKUDELSKA, K., NOGOWSKI, L. & SZKUDELSKI, T. 2009. Resveratrol, a naturally occurring diphenolic compound, affects lipogenesis, lipolysis and the antilipolytic action of insulin in isolated rat adipocytes. *The Journal of steroid biochemistry and molecular biology,* 113**,** 17-24.

SZKUDELSKA, K., NOGOWSKI, L. & SZKUDELSKI, T. 2011. Resveratrol and genistein as adenosine triphosphate–depleting agents in fat cells. *Metabolism,* 60**,** 720-729.

SZKUDELSKI, T. 2006. Resveratrol inhibits insulin secretion from rat pancreatic islets. *European journal of pharmacology,* 552**,** 176-181.

SZKUDELSKI, T. 2007. Resveratrol-induced inhibition of insulin secretion from rat pancreatic islets: evidence for pivotal role of metabolic disturbances. *American Journal of Physiology-Endocrinology And Metabolism,* 293**,** E901-E907.

TAKAHASHI, K. 1977. Further studies on the reactions of phenylglyoxal and related reagents with proteins. *Journal of biochemistry,* 81**,** 403-414.

TAKAOKA, M. 1940. Of the phenolic substances of white hellebore (Veratrum grandiflorum Loes. fil.). *Journal of Faculty of Sciences Hokkaido Imperial University,* 3**,** 1-16.

TAKEDA, K., KAISHO, T. & AKIRA, S. 2003. Toll-like receptors. *Annual review of immunology,* 21**,** 335-376.

TAKUMI, H., NAKAMURA, H., SIMIZU, T., HARADA, R., KOMETANI, T., NADAMOTO, T., MUKAI, R., MUROTA, K., KAWAI, Y. & TERAO, J. 2012. Bioavailability of orally administered water-dispersible hesperetin and its effect on peripheral vasodilatation in human subjects: implication of endothelial functions of plasma conjugated metabolites. *Food & function,* 3**,** 389-398.

TALESA, V., ROSI, G., BISTONI, F., MARCONI, P., NORTON, S. & PRINCIPATO, G. 1989. Presence of a plant-like glyoxalase II in Candida albicans. *Biochemistry international,* 21**,** 397-403.

TAMAKI, N., CRISTINA ORIHUELA-CAMPOS, R., INAGAKI, Y., FUKUI, M., NAGATA, T. & ITO, H.-O. 2014. Resveratrol improves oxidative stress and prevents the progression of periodontitis via the activation of the Sirt1/AMPK and the Nrf2/antioxidant defense pathways in a rat periodontitis model. *Free Radical Biology and Medicine,* 75**,** 222-229.

TANAKA, M., GROSSNIKLAUS, U., HERR, W. & HERNANDEZ, N. 1988. Activation of the U2 snRNA promoter by the octamer motif defines a new class of RNA polymerase II enhancer elements. *Genes & Development,* 2**,** 1764-1778.

TATE, S. S. 1975. Interaction of γ/-glutamyl transpeptidase with S-acyl derivatives of glutathione. *FEBS Lett.,* 54**,** 319-322.

TAYLOR, G. W. & BORGNAKKE, W. S. 2008. Periodontal disease: associations with diabetes, glycemic control and complications. *Oral Diseases,* 14**,** 191-203.

TAYLOR, G. W., BURT, B. A., BECKER, M. P., GENCO, R. J. & SHLOSSMAN, M. 1998. Glycemic Control and Alveolar Bone Loss Progression in Type 2 Diabetes. *Annals of Periodontology,* 3**,** 30-39.

TAYLOR, J. J., PRESHAW, P. M. & LALLA, E. 2015. A review of the evidence for pathogenic mechanisms that may link periodontitis and diabetes. *Journal of clinical periodontology,* 40**,** S113-S134.

TELES, R., SAKELLARI, D., TELES, F., KONSTANTINIDIS, A., KENT, R., SOCRANSKY, S. & HAFFAJEE, A. 2010. Relationships among gingival crevicular fluid biomarkers, clinical parameters of periodontal disease, and the subgingival microbiota. *Journal of periodontology,* 81**,** 89-98.

TESSIER, F., OBRENOVICH, M. & MONNIER, V. M. 1999. Structure and mechanism of formation of human lens fluorophore LM-1 relationship to vesperlysine A and the advanced Maillard reaction in aging, diabetes, and cataractogenesis. *Journal of Biological Chemistry,* 274**,** 20796-20804.

THANGARAJAH, H., YAO, D., CHANG, E. I., SHI, Y., JAZAYERI, L., VIAL, I. N., GALIANO, R. D., DU, X.-L., GROGAN, R. & GALVEZ, M. G. 2009. The molecular basis for impaired hypoxia-induced VEGF expression in diabetic tissues. *Proceedings of the National Academy of Sciences,* 106**,** 13505-13510.

THEILADE, E. 1986. The non-specific theory in microbial etiology of inflammatory periodontal diseases. *Journal of clinical periodontology,* 13**,** 905-911.

THIES, R. S., MOLINA, J. M., CIARALDI, T. P., FREIDENBERG, G. R. & OLEFSKY, J. M. 1990. Insulin-receptor autophosphorylation and endogenous substrate phosphorylation in human adipocytes from control, obese, and NIDDM subjects. *Diabetes,* 39**,** 250-9.

THIMMULAPPA, R. K., MAI, K. H., SRISUMA, S., KENSLER, T. W., YAMAMOTO, M. & BISWAL, S. 2002. Identification of Nrf2-regulated

genes induced by the chemopreventive agent sulforaphane by oligonucleotide microarray. *Cancer research,* 62**,** 5196-5203.

THIRUNAVUKKARASU, M., PENUMATHSA, S. V., KONERU, S., JUHASZ, B., ZHAN, L., OTANI, H., BAGCHI, D., DAS, D. K. & MAULIK, N. 2007. Resveratrol alleviates cardiac dysfunction in streptozotocin-induced diabetes: Role of nitric oxide, thioredoxin, and heme oxygenase. *Free Radical Biology and Medicine,* 43**,** 720-729.

THOMAS, M. C., TIKELLIS, C., KANTHARIDIS, P., BURNS, W. C., COOPER, M. E. & FORBES, J. M. 2004. The role of advanced glycation in reduced organic cation transport associated with experimental diabetes. *Journal of Pharmacology and Experimental Therapeutics,* 311**,** 456-466.

THOMSON, W. M., BROADBENT, J. M., WELCH, D., BECK, J. D. & POULTON, R. 2007. Cigarette smoking and periodontal disease among 32-year-olds: a prospective study of a representative birth cohort. *Journal of clinical periodontology,* 34**,** 828-834.

THORNALLEY, J. D. C. A. P. J. 1991. S-2-hydroxyacylglutathione-derivatives: enzymatic preparation, purification and characterisation *Journal of the Chemical Society, Perkin Transactions 1***,** 3009-3015.

THORNALLEY, P. 1998a. Cell activation by glycated proteins. AGE receptors, receptor recognition factors and functional classification of AGEs. *Cellular and molecular biology (Noisy-le-Grand, France),* 44**,** 1013-1023.

THORNALLEY, P. 1999. The clinical significance of glycation. *Clinical laboratory,* 45**,** 263-273.

THORNALLEY, P. 2008. Protein and nucleotide damage by glyoxal and methylglyoxal in physiological systems--role in ageing and disease. *Drug Metabol Drug Interact,* 23**,** 125-50.

THORNALLEY, P., BATTAH, S., AHMED, N., KARACHALIAS, N., AGALOU, S., BABAEI-JADIDI, R. & DAWNAY, A. 2003a. Quantitative screening of advanced glycation endproducts in cellular and extracellular proteins by tandem mass spectrometry. *Biochem. J,* 375**,** 581-592.

THORNALLEY, P., GRESKOWIAK, M. & DELLA BIANCA, V. 1990. Potentiation of secretion from neutrophils by S-d-lactoylglutathione. *Med. Sci. Res,* 18**,** 813.

THORNALLEY, P., HOOPER, N., JENNINGS, P., FLORKOWSKI, C., JONES, A., LUNEC, J. & BARNETT, A. 1989. The human red blood cell glyoxalase

system in diabetes mellitus. *Diabetes research and clinical practice,* 7**,** 115-120.

THORNALLEY, P. & TISDALE, M. 1988. Inhibition of proliferation of human promyelocytic leukaemia HL60 cells by SD-lactoylglutathione in vitro. *Leukemia research,* 12**,** 897.

THORNALLEY, P. J. 1988. Modification of the glyoxalase system in human red blood cells by glucose in vitro. *Biochem. J,* 254**,** 751-755.

THORNALLEY, P. J. 1993. The glyoxalase system in health and disease. *Mol Aspects Med,* 14**,** 287-371.

THORNALLEY, P. J. 1998b. Cell activation by glycated proteins. AGE receptors, receptor recognition factors and functional classification of AGEs. *Cell Mol Biol (Noisy-le-grand),* 44**,** 1013-23.

THORNALLEY, P. J. 1998c. Glutathione-dependent detoxification of alpha-oxoaldehydes by the glyoxalase system: involvement in disease mechanisms and antiproliferative activity of glyoxalase I inhibitors. *Chem Biol Interact,* 111-112**,** 137-51.

THORNALLEY, P. J. 2003a. The enzymatic defence against glycation in health, disease and therapeutics: a symposium to examine the concept. *Biochem Soc Trans,* 31**,** 1341-2.

THORNALLEY, P. J. 2003b. Glyoxalase I--structure, function and a critical role in the enzymatic defence against glycation. *Biochem Soc Trans,* 31**,** 1343-8.

THORNALLEY, P. J. 2003c. Use of aminoguanidine (Pimagedine) to prevent the formation of advanced glycation endproducts. *Archives of Biochemistry and Biophysics,* 419**,** 31-40.

THORNALLEY, P. J. 2005. Dicarbonyl intermediates in the maillard reaction. *Ann N Y Acad Sci,* 1043**,** 111-7.

THORNALLEY, P. J. 2007. Dietary AGEs and ALEs and risk to human health by their interaction with the receptor for advanced glycation endproducts (RAGE)--an introduction. *Mol Nutr Food Res,* 51**,** 1107-10.

THORNALLEY, P. J., BATTAH, S., AHMED, N., KARACHALIAS, N., AGALOU, S., BABAEI-JADIDI, R. & DAWNAY, A. 2003b. Quantitative screening of advanced glycation endproducts in cellular and extracellular proteins by tandem mass spectrometry. *Biochem J,* 375**,** 581-92.

THORNALLEY, P. J., EDWARDS, L. G., KANG, Y., WYATT, C., DAVIES, N., LADAN, M. J. & DOUBLE, J. 1996. Antitumour activity of S-p-bromobenzylglutathione cyclopentyl diester in vitro and in vivo. Inhibition of glyoxalase I and induction of apoptosis. *Biochem Pharmacol,* 51**,** 1365-72.

THORNALLEY, P. J., IRSHAD, Z., XUE, M. & RABBANI, N. Disturbance of the Glyoxalase System in Human Vascular Endothelial Cells by High Glucose In Vitro and Reversal by trans-Resveratrol. DIABETES, 2014. AMER DIABETES ASSOC 1701 N BEAUREGARD ST, ALEXANDRIA, VA 22311-1717 USA, A10-A10.

THORNALLEY, P. J. & MINHAS, H. S. 1999. Rapid hydrolysis and slow α,β-dicarbonyl cleavage of an agent proposed to cleave glucose-derived protein cross-links. *Biochemical Pharmacology,* 57**,** 303-307.

THORNALLEY, P. J. & RABBANI, N. Glyoxalase in tumourigenesis and multidrug resistance. Seminars in cell & developmental biology, 2011a. Elsevier, 318-325.

THORNALLEY, P. J. & RABBANI, N. 2011b. Protein damage in diabetes and uremia-identifying hotspots of proteome damage where minimal modification is amplified to marked pathophysiological effect. *Free Radical Research,* 45**,** 89-100.

THORNALLEY, P. J. & RABBANI, N. 2014. Detection of oxidized and glycated proteins in clinical samples using mass spectrometry — A user's perspective. *Biochimica et Biophysica Acta (BBA) - General Subjects,* 1840**,** 818-829.

THORNALLEY, P. J., WARIS, S., FLEMING, T., SANTARIUS, T., LARKIN, S. J., WINKLHOFER-ROOB, B. M., STRATTON, M. R. & RABBANI, N. 2010. Imidazopurinones are markers of physiological genomic damage linked to DNA instability and glyoxalase 1-associated tumour multidrug resistance. *Nucleic Acids Res*.

THORNALLEY, P. J., YUREK-GEORGE, A. & ARGIROV, O. K. 2000. Kinetics and mechanism of the reaction of aminoguanidine with the α-oxoaldehydes glyoxal, methylglyoxal, and 3-deoxyglucosone under physiological conditions. *Biochemical pharmacology,* 60**,** 55-65.

THORPE, S. R. & BAYNES, J. W. CML: a brief history. International Congress Series, 2002. Elsevier, 91-99.

TOMOKIYO, A., MAEDA, H., FUJII, S., WADA, N., SHIMA, K. & AKAMINE, A. 2008. Development of a multipotent clonal human periodontal ligament cell line. *Differentiation,* 76**,** 337-347.

TRIPLITT, C., SOLIS-HERRERA, C., REASNER, C., DEFRONZO, R. A. & CERSOSIMO, E. 2015. Classification of Diabetes Mellitus.

TROMBELLI, L., FARINA, R., MARZOLA, A., BOZZI, L., LILJENBERG, B. & LINDHE, J. 2008. Modeling and remodeling of human extraction sockets. *J Clin Periodontol,* 35**,** 630-639.

TSAI, C., HAYES, C. & TAYLOR, G. W. 2002. Glycemic control of type 2 diabetes and severe periodontal disease in the US adult population. *Commun Dent Oral Epidemiol,* 30**,** 182-192.

TSURUGA, E., NAKASHIMA, K., ISHIKAWA, H., YAJIMA, T. & SAWA, Y. 2009. Stretching modulates oxytalan fibers in human periodontal ligament cells. *Journal of Periodontal Research,* 44**,** 170-174.

TURIÁK, L., OZOHANICS, O., MARINO, F., DRAHOS, L. & VÉKEY, K. 2011. Digestion protocol for small protein amounts for nano-HPLC-MS (MS) analysis. *Journal of proteomics,* 74**,** 942-947.

TYLER, M. I. 2000. Amino acid analysis. *Amino Acid Analysis Protocols.* Springer.

UM, J.-H., PARK, S.-J., KANG, H., YANG, S., FORETZ, M., MCBURNEY, M. W., KIM, M. K., VIOLLET, B. & CHUNG, J. H. 2010. AMP-activated protein kinase–deficient mice are resistant to the metabolic effects of resveratrol. *Diabetes,* 59**,** 554-563.

UNGER, R. E., PETERS, K., SARTORIS, A., FREESE, C. & KIRKPATRICK, C. J. 2014. Human endothelial cell-based assay for endotoxin as sensitive as the conventional Limulus Amebocyte Lysate assay. *Biomaterials,* 35**,** 3180-3187.

UNGVARI, Z., LABINSKYY, N., MUKHOPADHYAY, P., PINTO, J. T., BAGI, Z., BALLABH, P., ZHANG, C., PACHER, P. & CSISZAR, A. 2009. Resveratrol attenuates mitochondrial oxidative stress in coronary arterial endothelial cells. *American Journal of Physiology-Heart and Circulatory Physiology,* 297**,** H1876-H1881.

UOTILA, L. 1973. Purification and characterization of S-2-hydroxyacylglutathione hydrolase (glyoxalase II) from human liver. *Biochemistry,* 12**,** 3944-3951.

VAETH, A. 2006. Phloretin acute oral toxicity study in the rat. *Unpublished report submitted by European Flavour and Fragrance Association to FLAVIS Secretariat. Frey-tox, Germany Lab no. 02809.*

VALENCIA, J. V., WELDON, S. C., QUINN, D., KIERS, G. H., DEGROOT, J., TEKOPPELE, J. M. & HUGHES, T. E. 2004. Advanced glycation end

product ligands for the receptor for advanced glycation end products: biochemical characterization and formation kinetics. *Analytical biochemistry,* 324**,** 68-78.

VAN BELLE, T. L., COPPIETERS, K. T. & VON HERRATH, M. G. 2011. Type 1 diabetes: etiology, immunology, and therapeutic strategies. *Physiological reviews,* 91**,** 79-118.

VAN DER VELDEN, U. 2005. Purpose and problems of periodontal disease classification. *Periodontol 2000,* 39**,** 13-21.

VAN DYKE, T. & SERHAN, C. 2003. Resolution of inflammation: a new paradigm for the pathogenesis of periodontal diseases. *Journal of Dental Research,* 82**,** 82-90.

VAN DYKE, T. E. & DAVE, S. 2005. Risk factors for periodontitis. *Journal of the International Academy of Periodontology,* 7**,** 3.

VANDER JAGT, D. 1993. Glyoxalase II: molecular characteristics, kinetics and mechanism. *Biochemical Society transactions,* 21**,** 522.

VANDER JAGT, D. L., HASSEBROOK, R. K., HUNSAKER, L. A., BROWN, W. M. & ROYER, R. E. 2001. Metabolism of the 2-oxoaldehyde methylglyoxal by aldose reductase and by glyoxalase-I: roles for glutathione in both enzymes and implications for diabetic complications. *Chem Biol Interact,* 130-132**,** 549-62.

VANDER JAGT, D. L. & HUNSAKER, L. A. 2003. Methylglyoxal metabolism and diabetic complications: roles of aldose reductase, glyoxalase-I, betaine aldehyde dehydrogenase and 2-oxoaldehyde dehydrogenase. *Chem Biol Interact,* 143-144**,** 341-51.

VANG, O., AHMAD, N., BAILE, C. A., BAUR, J. A., BROWN, K., CSISZAR, A., DAS, D. K., DELMAS, D., GOTTFRIED, C. & LIN, H.-Y. 2011. What is new for an old molecule? Systematic review and recommendations on the use of resveratrol. *PL o S One*.

VASAN, S., ZHANG, X., ZHANG, X., KAPURNIOTU, A., BERNHAGEN, J., TEICHBERG, S., BASGEN, J., WAGLE, D., SHIH, D., TERLECKY, I., BUCALA, R., CERAMI, A., EGAN, J. & ULRICH, P. 1996. An agent cleaving glucose-derived protein crosslinks in vitro and in vivo. *Nature,* 382**,** 275-278.

VAZZANA, N., SANTILLI, F., CUCCURULLO, C. & DAVÌ, G. 2009. Soluble forms of RAGE in internal medicine. *Intern Emerg Med,* 4**,** 389-401.

VIEIRA RIBEIRO, F., DE MENDONÇA, A. C., SANTOS, V. R., BASTOS, M. F., FIGUEIREDO, L. C. & DUARTE, P. M. 2011. Cytokines and bone-related factors in systemically healthy patients with chronic periodontitis and patients with type 2 diabetes and chronic periodontitis. *Journal of periodontology,* 82**,** 1187-1196.

VINCE, R. & DALUGE, S. 1971. Glyoxalase inhibitors. A possible approach to anticancer agents. *J. Med. Chem.,* 14**,** 35-37.

VINCE, R., DALUGE, S. & WADD, W. B. 1971. Inhibition of glyoxalase I by S-substituted glutathiones. *J. Med. Chem.,* 14**,** 402-404.

VINIK, A. I. 2008. Diabetic neuropathies. *Controversies in Treating Diabetes.* Springer.

VISHWANATH, V., FRANK, K. E., ELMETS, C. A., DAUCHOT, P. J. & MONNIER, V. M. 1986. Glycation of skin collagen in type I diabetes mellitus: correlation with long-term complications. *Diabetes,* 35**,** 916-921.

WADA, N., MAEDA, H., YOSHIMINE, Y. & AKAMINE, A. 2004. Lipopolysaccharide stimulates expression of osteoprotegerin and receptor activator of NF-kappa B ligand in periodontal ligament fibroblasts through the induction of interleukin-1 beta and tumor necrosis factor-alpha. *Bone,* 35**,** 629-635.

WEI, D., CI, X., CHU, X., WEI, M., HUA, S. & DENG, X. 2012. Hesperidin suppresses ovalbumin-induced airway inflammation in a mouse allergic asthma model. *Inflammation,* 35**,** 114-121.

WEINBERG, M., WESTPHAL, C., FROUM, S., PALAT, M. & SCHOOR, R. 2014. *Comprehensive periodontics for the dental hygienist,* Pearson Higher Ed.

WESTWOOD, M. E. & THORNALLEY, P. J. 1995. Molecular characteristics of methylglyoxal-modified bovine and human serum albumins. Comparison with glucose-derived advanced glycation endproduct-modified serum albumins. *J Protein Chem,* 14**,** 359-372.

WIEBE, C. B. & PUTNINS, E. E. 2000. The periodontal disease classification system of the American Academy of Periodontology-an update. *JOURNAL-CANADIAN DENTAL ASSOCIATION,* 66**,** 594-599.

WILLERSHAUSEN-ZÖNNCHEN, B., LEMMEN, C. & HAMN, G. 1991. Influence of high glucose concentrations on glycosaminoglycan and collagen synthesis in cultured human gingival fibroblasts. *Journal of clinical periodontology,* 18**,** 190-195.

WILLIAMS IV, R., LIM, J. E., HARR, B., WING, C., WALTERS, R., DISTLER, M. G., TESCHKE, M., WU, C., WILTSHIRE, T. & SU, A. I. 2009. A common and unstable copy number variant is associated with differences in Glo1 expression and anxiety-like behavior. *PLoS One,* 4**,** e4649.

WILLIS, J. A., SCOTT, R. S., DARLOW, B. A., LEWY, H., ASHKENAZI, I. & LARON, Z. 2002. Seasonality of birth and onset of clinical disease in children and adolescents (0-19 years) with type 1 diabetes mellitus in Canterbury, New Zealand. *J Pediatr Endocrinol Metab,* 15**,** 645-7.

WILMSEN, P. K., SPADA, D. S. & SALVADOR, M. 2005. Antioxidant activity of the flavonoid hesperidin in chemical and biological systems. *Journal of agricultural and food chemistry,* 53**,** 4757-4761.

WILSON, A., ELSTON, R., TRAN, L. & SIERVOGEL, R. 1991. Use of the robust sib-pair method to screen for single-locus, multiple-locus, and pleiotropic effects: application to traits related to hypertension. *American journal of human genetics,* 48**,** 862.

WIŚNIEWSKI, J. R., ZOUGMAN, A., NAGARAJ, N. & MANN, M. 2009. Universal sample preparation method for proteome analysis. *Nature methods,* 6**,** 359-362.

WOLFF, S., CRABBE, M. & THORNALLEY, P. 1984. The autoxidation of glyceraldehyde and other simple monosaccharides. *Experientia,* 40**,** 244-246.

WONDRAK, G. T., CERVANTES-LAUREAN, D., ROBERTS, M. J., QASEM, J. G., KIM, M., JACOBSON, E. L. & JACOBSON, M. K. 2002. Identification of α-dicarbonyl scavengers for cellular protection against carbonyl stress. *Biochemical pharmacology,* 63**,** 361-373.

WONG, J. H. & CAGNEY, G. 2010. An Overview of Label-Free Quantitation Methods in Proteomics by Mass Spectrometry. *In:* HUBBARD, S. J. & JONES, A. R. (eds.) *Proteome Bioinformatics.* Humana Press.

WONG, K. K., DELEEUW, R. J., DOSANJH, N. S., KIMM, L. R., CHENG, Z., HORSMAN, D. E., MACAULAY, C., NG, R. T., BROWN, C. J. & EICHLER, E. E. 2007. A comprehensive analysis of common copy-number variations in the human genome. *The American Journal of Human Genetics,* 80**,** 91-104.

WRIGHT, E., SCISM-BACON, J. L. & GLASS, L. C. 2006. Oxidative stress in type 2 diabetes: the role of fasting and postprandial glycaemia. *International Journal of Clinical Practice,* 60**,** 308-314.

WRÓBEL, K., WRÓBEL, K., GARAY-SEVILLA, M. E., NAVA, L. E. & MALACARA, J. M. 1997. Novel analytical approach to monitoring advanced glycosylation end products in human serum with on-line spectrophotometric and spectrofluorometric detection in a flow system. *Clinical chemistry,* 43**,** 1563-1569.

WU, L., ZHANG, Y., MA, X., ZHANG, N. & QIN, G. 2012. The effect of resveratrol on FoxO1 expression in kidneys of diabetic nephropathy rats. *Molecular biology reports,* 39**,** 9085-9093.

WU, V.-Y. & STEWARD, L. A. 1991. Purification of glycated hemoglobin free of hemoglobin A1c and its use to produce monoclonal antibodies specific for deoxyfructosyllsine residues in glycohemoglobin. *Biochemical and biophysical research communications,* 176**,** 207-212.

XIMÉNEZ-FYVIE, L. A., HAFFAJEE, A. D. & SOCRANSKY, S. S. 2000. Comparison of the microbiota of supra-and subgingival plaque in health and periodontitis. *Journal of clinical periodontology,* 27**,** 648-657.

XIONG, J., MROZIK, K., GRONTHOS, S. & BARTOLD, P. M. 2012. Epithelial Cell Rests of Malassez Contain Unique Stem Cell Populations Capable of Undergoing Epithelial–Mesenchymal Transition. *Stem Cells and Development,* 21**,** 2012-2025.

XIONG, Y. & GUAN, K.-L. 2012. Mechanistic insights into the regulation of metabolic enzymes by acetylation. *The Journal of cell biology,* 198**,** 155-164.

XU, D., YOUNG, J. H., KRAHN, J. M., SONG, D., CORBETT, K. D., CHAZIN, W. J., PEDERSEN, L. C. & ESKO, J. D. 2013. Stable RAGE-heparan sulfate complexes are essential for signal transduction. *ACS chemical biology,* 8**,** 1611-1620.

XU, L., YANG, Z.-L., LI, P. & ZHOU, Y.-Q. 2009. Modulating effect of Hesperidin on experimental murine colitis induced by dextran sulfate sodium. *Phytomedicine,* 16**,** 989-995.

XUE, J., RAY, R., SINGER, D., BÖHME, D., BURZ, D. S., RAI, V., HOFFMANN, R. & SHEKHTMAN, A. 2014. The receptor for advanced glycation end products (RAGE) specifically recognizes methylglyoxal-derived AGEs. *Biochemistry,* 53**,** 3327-3335.

XUE, M., ANTONYSUNIL, A., RABBANI, NAILA AND THORNALLEY, PAUL J 2009. Protein damage in the ageing process : advances in quantitation and the importance of enzymatic defences. *Redox metabolism and longevity relationships in animals and plants.* New York ; Abingdon [England]: Taylor & Francis Group.

XUE, M., MOMIJI, H., RABBANI, N., BARKER, G., BRETSCHNEIDER, T., SHMYGOL, A., RAND, D. A. & THORNALLEY, P. J. 2015a. Frequency modulated translocational oscillations of Nrf2 mediate the antioxidant response element cytoprotective transcriptional response. *Antioxidants & redox signaling,* 23**,** 613-629.

XUE, M., MOMIJI, H., RABBANI, N., BARKER, G., BRETSCHNEIDER, T., SHMYGOL, A., RAND, D. A. & THORNALLEY, P. J. 2015b. Frequency modulated translocational oscillations of Nrf2 mediate the ARE cytoprotective transcriptional response *Antioxidants & Redox Signaling,* 23**,** 613 - 629.

XUE, M., MOMIJI, H., RABBANI, N., BRETSCHNEIDER, T., RAND, D. A. & THORNALLEY, P. J. 2015c. Frequency modulated translocational oscillations of Nrf2, a transcription factor functioning like a wireless sensor. *Biochemical Society Transactions,* 43**,** 669-673.

XUE, M., RABBANI, N., MOMIJI, H., IMBASI, P., ANWAR, M. M., KITTERINGHAM, N., PARK, B. K., SOUMA, T., MORIGUCHI, T., YAMAMOTO, M. & THORNALLEY, P. J. 2012a. Transcriptional control of glyoxalase 1 by Nrf2 provides a stress-responsive defence against dicarbonyl glycation. *Biochem J,* 443**,** 213-22.

XUE, M., RABBANI, N., MOMIJI, H., IMBASI, P., ANWAR, M. M., KITTERINGHAM, N. R., PARK, B. K., SOUMA, T., MORIGUCHI, T., YAMAMOTO, M. & THORNALLEY, P. J. 2012b. Transcriptional control of glyoxalase 1 by Nrf2 provides a stress responsive defence against dicarbonyl glycation. *Biochem J,* 443**,** 213-222.

XUE, M., RABBANI, N. & THORNALLEY, P. J. Glyoxalase in ageing. Seminars in cell & developmental biology, 2011. Elsevier, 293-301.

XUE, M., WEICKERT, M. O., QURESHI, S., NGIANGA-BAKWIN, K., ANWAR, A., WALDRON, M., MESSENGER, D., FOWLER, M., JENKINS, G., RABBANI, N. & THORNALLEY, P. J. 2016. Improved glycemic control and vascular function in overweight and obese subjects by glyoxalase 1 inducer formulation *Diabetes,* in revision.

YAMADA, S., KUMAZAWA, S., ISHII, T., NAKAYAMA, T., ITAKURA, K., SHIBATA, N., KOBAYASHI, M., SAKAI, K., OSAWA, T. & UCHIDA, K. 2001. Immunochemical detection of a lipofuscin-like fluorophore derived from malondialdehyde and lysine. *Journal of lipid research,* 42**,** 1187-1196.

YAMAGISHI, S.-I., NAKAMURA, K. & IMAIZUMI, T. 2005. Advanced Glycation End Products (AGEs) and Diabetic Vascular Complications. *Current Diabetes Reviews,* 1**,** 93-106.

YAMAJI, Y., KUBOTA, T., SASAGURI, K., SATO, S., SUZUKI, Y., KUMADA, H. & UMEMOTO, T. 1995. Inflammatory cytokine gene expression in human periodontal ligament fibroblasts stimulated with bacterial lipopolysaccharides. *Infection and immunity,* 63**,** 3576-3581.

YAMAMOTO, M., IZUHARA, Y., KAKUTA, T., TAKIZAWA, S., FUJITA, A., HIGAKI, T., VAN YPERSELE DE STRIHOU, C. & MIYATA, T. 2007. Carbonyl stress reduction in peritoneal dialysis fluid: development of a novel high-affinity adsorption bead. *Perit Dial Int,* 27**,** 300-8.

YAMAMOTO, M., JOKURA, H., HASHIZUME, K., OMINAMI, H., SHIBUYA, Y., SUZUKI, A., HASE, T. & SHIMOTOYODOME, A. 2013. Hesperidin metabolite hesperetin-7-O-glucuronide, but not hesperetin-3′-O-glucuronide, exerts hypotensive, vasodilatory, and anti-inflammatory activities. *Food & function,* 4**,** 1346-1351.

YAMAMOTO, T., KITA, M., OSEKO, F., NAKAMURA, T., IMANISHI, J. & KANAMURA, N. 2006. Cytokine production in human periodontal ligament cells stimulated with Porphyromonas gingivalis. *Journal of Periodontal Research,* 41**,** 554-559.

YAMAMOTO, Y., TAHARA, Y., CHA, T., NOMA, Y., FUKUDA, M., YAMATO, E., YONEDA, H., HASHIMOTO, F., OHBOSHI, C. & HIROTA, M. 1989. Radioimmunoassay of glycated serum protein using monoclonal antibody to glucitollysine and coomassie-brilliant-blue-coated polystyrene beads. *Diabetes research (Edinburgh, Scotland),* 11**,** 45.

YAMAZAKI, K., OHSAWA, Y. & YOSHIE, H. 2001. Elevated proportion of natural killer T cells in periodontitis lesions: a common feature of chronic inflammatory diseases. *The American journal of pathology,* 158**,** 1391-1398.

YAN, S. F., RAMASAMY, R. & SCHMIDT, A. M. 2009. Receptor for AGE (RAGE) and its ligands—cast into leading roles in diabetes and the inflammatory response. *Journal of Molecular Medicine,* 87**,** 235-247.

YANG, H.-L., CHEN, S.-C., SENTHIL KUMAR, K., YU, K.-N., LEE CHAO, P.-D., TSAI, S.-Y., HOU, Y.-C. & HSEU, Y.-C. 2011. Antioxidant and anti-inflammatory potential of hesperetin metabolites obtained from hesperetin-administered rat serum: an ex vivo approach. *Journal of agricultural and food chemistry,* 60**,** 522-532.

YANG, Y., LI, W., LIU, Y., SUN, Y., LI, Y., YAO, Q., LI, J., ZHANG, Q., GAO, Y. & GAO, L. 2014. Alpha-lipoic acid improves high-fat diet-induced hepatic steatosis by modulating the transcription factors SREBP-1, FoxO1 and Nrf2 via the SIRT1/LKB1/AMPK pathway. *The Journal of nutritional biochemistry,* 25**,** 1207-1217.

YAO, D., TAGUCHI, T., MATSUMURA, T., PESTELL, R., EDELSTEIN, D., GIARDINO, I., SUSKE, G., RABBANI, N., THORNALLEY, P. J. & SARTHY, V. P. 2007. High glucose increases angiopoietin-2 transcription in microvascular endothelial cells through methylglyoxal modification of mSin3A. *Journal of Biological Chemistry,* 282**,** 31038-31045.

YASAKA, T., ICHISAKA, S., KATSUMOTO, T., MAKI, H., SAJI, M., KIMURA, G. & OHNO, K. 1996. Apoptosis involved in density-dependent regulation of rat fibroblastic 3Y1 cell culture. *Cell structure and function,* 21**,** 483-489.

YE, J., CHEN, R. G., ASHKENAZI, I. & LARON, Z. 1998. Lack of seasonality in the month of onset of childhood IDDM (0.7-15 years) in Shanghai, China. *J Pediatr Endocrinol Metab,* 11**,** 461-4.

YEH, C.-C., KAO, S.-J., LIN, C.-C., WANG, S.-D., LIU, C.-J. & KAO, S.-T. 2007. The immunomodulation of endotoxin-induced acute lung injury by hesperidin in vivo and in vitro. *Life sciences,* 80**,** 1821-1831.

YONEKURA, H., YAMAMOTO, Y., SAKURAI, S., PETROVA, R., ABEDIN, M., LI, H., YASUI, K., TAKEUCHI, M., MAKITA, Z. & TAKASAWA, S. 2003. Novel splice variants of the receptor for advanced glycation end-products expressed in human vascular endothelial cells and pericytes, and their putative roles in diabetes-induced vascular injury. *Biochem. J,* 370**,** 1097-1109.

YU, W., FU, Y. C. & WANG, W. 2012. Cellular and molecular effects of resveratrol in health and disease. *Journal of cellular biochemistry,* 113**,** 752-759.

ZEE, K. Y. 2009. Smoking and periodontal disease. *Australian Dental Journal,* 54**,** S44-S50.

ZENDER, L., XUE, W., ZUBER, J., SEMIGHINI, C. P., KRASNITZ, A., MA, B., ZENDER, P., KUBICKA, S., LUK, J. M. & SCHIRMACHER, P. 2008. An oncogenomics-based in vivo RNAi screen identifies tumor suppressors in liver cancer. *Cell,* 135**,** 852-864.

ZHANG, H., MORGAN, B., POTTER, B. J., MA, L., DELLSPERGER, K. C., UNGVARI, Z. & ZHANG, C. 2010. Resveratrol improves left ventricular diastolic relaxation in type 2 diabetes by inhibiting oxidative/nitrative stress: in vivo demonstration with magnetic resonance imaging. *American Journal of Physiology-Heart and Circulatory Physiology,* 299**,** H985-H994.

ZHANG, L., PANG, S., DENG, B., QIAN, L., CHEN, J., ZOU, J., ZHENG, J., YANG, L., ZHANG, C. & CHEN, X. 2012. High glucose induces renal mesangial cell proliferation and fibronectin expression through JNK/NF-

κB/NADPH oxidase/ROS pathway, which is inhibited by resveratrol. *The international journal of biochemistry & cell biology,* 44**,** 629-638.

ZHANG, Q., TANG, N., BROCK, J. W., MOTTAZ, H. M., AMES, J. M., BAYNES, J. W., SMITH, R. D. & METZ, T. O. 2007. Enrichment and analysis of nonenzymatically glycated peptides: boronate affinity chromatography coupled with electron-transfer dissociation mass spectrometry. *Journal of proteome research,* 6**,** 2323-2330.

ZIMMERMANN, G. S., BASTOS, M. F., DIAS GONÇALVES, T. E., CHAMBRONE, L. & DUARTE, P. M. 2013. Local and Circulating Levels of Adipocytokines in Obese and Normal Weight Individuals With Chronic Periodontitis. *Journal of Periodontology,* 84**,** 624-633.

ZYBAILOV, B., MOSLEY, A. L., SARDIU, M. E., COLEMAN, M. K., FLORENS, L. & WASHBURN, M. P. 2006. Statistical Analysis of Membrane Proteome Expression Changes in Saccharomyces c erevisiae. *Journal of proteome research,* 5**,** 2339-2347.

Appendix I – Table of total identified cytosolic proteins in hPDLFs

Table 57: Total identified cytosolic proteins in hPDLFs

Protein accession numbers	Protein name	Gene accession numbers
P43034	Platelet-activating factor acetylhydrolase	PAFAH1B1
Q9Y281	Cofilin-2	CFL2
Q12873-3	Isoform 3 of Chromodomain-helicase-DNA-binding protein 3	CHD3
A0A087X0S5	Collagen alpha-1(VI) chain	COL6A1
P26038	Moesin	MSN
Q9BZK7	F-box-like/WD repeat-containing protein	TBL1XR1
P61221	ATP-binding cassette sub-family E member 1	ABCE1
Q9NX08	COMM domain-containing protein 8	COMMD8
Q9UHD9	Ubiquilin-2	UBQLN2
Q9BRP8-2	Isoform 2 of Partner of Y14 and mago	WIBG
Q99707	Methionine synthase	MTR
Q15021	Condensin complex subunit 1	NCAPD2
P63241-2	Isoform 2 of Eukaryotic translation initiation factor 5A-1	EIF5A
E5RIH5	TELO2-interacting protein 2	TTI2
O15143	Actin-related protein 2/3 complex subunit 1B	ARPC1B
O95816	BAG family molecular chaperone regulator 2	BAG2
P09429	High mobility group protein B1	HMGB1
Q7Z6Z7	E3 ubiquitin-protein ligase	HUWE1
P38117-2	Isoform 2 of Electron transfer flavoprotein subunit beta	ETFB
P35241-5	Isoform 5 of Radixin	RDX
P42224	Signal transducer and activator of transcription 1-alpha/beta	STAT1
Q96BJ3	Axin interactor, dorsalization-associated protein	AIDA
Q96HC4|	PDZ and LIM domain protein 5	PDLIM5
H0YBD7	Heterogeneous nuclear ribonucleoprotein H (Fragment)	HNRNPH1
A0A0B4J269	Tubulin beta-3 chain	TUBB3
P06733	Alpha-enolase	ENO1
G3XAI2	Laminin subunit beta-1	LAMB1
A8MTY9	Down syndrome critical region protein 3	DSCR3
O95372	Acyl-protein thioesterase 2	LYPLA2
Q9H3H3-2	Isoform 2 of UPF0696 protein C11orf68	C11orf68

Q05519-2	Isoform 2 of Serine/arginine-rich splicing factor 11	SRSF11
Q32Q12	Nucleoside diphosphate kinase	NME1-NME2
C9J0J7	Profilin-2	PFN2
O15085-2	Isoform 2 of Rho guanine nucleotide exchange factor 11	ARHGEF11
Q9NUQ8-2	Isoform 2 of ATP-binding cassette sub-family F member 3	ABCF3
P42330	Aldo-keto reductase family 1 member C3	AKR1C3
O14617-5	Isoform 5 of AP-3 complex subunit delta-1	AP3D1
Q86VS8	Protein Hook homolog 3	HOOK3
Q9UHD8-2	Isoform 2 of Septin-9	SPET9
P98082-3	Isoform 3 of Disabled homolog 2	DAB2
P48507	Glutamate--cysteine ligase regulatory subunit	GCLM
P78371	T-complex protein 1 subunit beta	CCT2
A0A0A0MR50	Cullin-4A	CUL4
A0A0C4DGQ5	Calpain small subunit 1	CAPNS1
Q14157-5	Isoform 5 of Ubiquitin-associated protein 2-like	UBAP2L
Q9Y680-2	Isoform 2 of Peptidyl-prolyl cis-trans isomerase	FKBP7
P29401-2	Isoform 2 of Transketolase	TKT
Q13045-2	Isoform 2 of Protein flightless-1 homolog	FLII
P20042	Eukaryotic translation initiation factor 2 subunit 2	EIF2S2
Q16822	Phosphoenolpyruvate carboxykinase [GTP], mitochondrial	PCK2
P22059	Oxysterol-binding protein 1	OSBP
P08708	40S ribosomal protein S17-like	RPS17L
E7EMW7	E3 ubiquitin-protein ligase UBR5	UBR5
Q96PU8-3	Isoform 2 of Protein quaking	QKI
P35241	Ezrin	EZR
P26885	Peptidyl-prolyl cis-trans isomerase FKBP2	FKBP2
P28074-3	Isoform 3 of Proteasome subunit beta type-5	PSMB5
P68371	Tubulin beta-4B chain	TUBB4B
Q9Y6M1	Insulin-like growth factor 2 mRNA-binding protein 2	IGF2BP2
F8VXU5	Vacuolar protein sorting-associated protein 29	VPS29
P41091	Eukaryotic translation initiation factor 2 subunit 3	EIF2S3
Q99832	T-complex protein 1 subunit eta	CCT7
Q8TEX9-2	Isoform 2 of Importin-4	IPO4
P18085	ADP-ribosylation factor 4	ARF4
P07437	Tubulin beta chain	TUBB
O75083	WD repeat-containing protein 1	WDR1

E7EQV9	Ribosomal protein L15 (Fragment)	RPL15
Q9NT62-2	Isoform 2 of Ubiquitin-like-conjugating enzyme	ATG3
Q13885	Tubulin beta-2A chain	TUBB2A
B5MCX3	Septin-2	Sep-02
Q9NQZ2	Something about silencing protein 10	UTP3
P31942-2	Isoform 2 of Heterogeneous nuclear ribonucleoprotein H3	HNRNPH3
Q13347	Eukaryotic translation initiation factor 3 subunit I	EIF3
Q12906	Isoform 2 of Interleukin enhancer-binding factor 3	ILF3
P12956	X-ray repair cross-complementing protein 6	XRCC6
P19784	Casein kinase II subunit alpha	CSNK2A2
P42677	40S ribosomal protein S27	RPS27
Q9Y617	Phosphoserine aminotransferase	PSAT1
P04040	Catalase	CAT
Q96EP0-3	Isoform 3 of E3 ubiquitin-protein ligase	RNF31
H0Y804	Aldo-keto reductase family 1 member C1 (Fragment)	AKR1C1
F8VPD4	CAD protein	CAD
P05387	60S acidic ribosomal protein P2	RPLP2
O43264	Centromere/kinetochore protein zw10 homolog	ZW10
P35580-3	Isoform 3 of Myosin-10	MYH10
P35579	Myosin-9	MYH9
P52597	Heterogeneous nuclear ribonucleoprotein F	HNRNPF
A0A0A0MRE5	Arf-GAP with SH3 domain, ANK repeat and PH domain-containing protein 1	ASAP1
Q9BS26	Endoplasmic reticulum resident protein 44	ERP44
H7C0A4	Vigilin (Fragment)	HDLBP
P49773	Histidine triad nucleotide-binding protein 1	HINT1
D6REX3	Protein transport protein	SEC31A
Q9Y4G6	Talin-2	TLN2
P62937	Peptidyl-prolyl cis-trans isomerase A	PPIA
A0A0A0MRJ6	Protein-L-isoaspartate(D-aspartate) O-methyltransferase	PCMT1
Q8N122-3	Isoform 3 of Regulatory-associated protein of mTOR	RPTOR
Q9NR28	Diablo homolog, mitochondrial	DIABLO
Q8TD19	Serine/threonine-protein kinase	NEK9
Q9UDY2-3	Isoform C1 of Tight junction protein ZO-2	TJP2
J3QRS3	Myosin regulatory light chain 12A	MYL12A
Q93008-1	Isoform 2 of Probable ubiquitin carboxyl-terminal hydrolase FAF-X	USP9X
Q9UKV8-2	Isoform 2 of Protein argonaute-2	AGO2

Q9UNE7-2	Isoform 2 of E3 ubiquitin-protein ligase CHIP	STUB1
Q9BRK5	45 kDa calcium-binding protein	SDF4
O00754-2	Isoform 2 of Lysosomal alpha-mannosidase	MAN2B1
P36507	Dual specificity mitogen-activated protein kinase kinase 2	MAP2K2
Q06830	Peroxiredoxin-1	PRDX1
P50454	Serpin H1	SERPINH1
Q13642-1	Isoform 1 of Four and a half LIM domains protein 1	FHL1
P24844	Myosin regulatory light polypeptide 9	MYL9
P49915	GMP synthase [glutamine-hydrolyzing]	GMPS
J3KND3	Myosin light polypeptide 6	MYL6
P04075	Fructose-bisphosphate aldolase A	ALDOA
Q02750	Dual specificity mitogen-activated protein kinase kinase 1	MAP2K1
Q9HAU0-2	Isoform 2 of Pleckstrin homology domain-containing family A member 5	PLEKHA5
P22626	Heterogeneous nuclear ribonucleoproteins A2/B1	HNRNPA2B1
P17931	Galectin-3	LGALS3
Q86VP6	Cullin-associated NEDD8-dissociated protein 1	CAND1
J3KNL6	Protein transport protein Sec16A	SEC16A
Q9NXG2	THUMP domain-containing protein 1	THUMPD1
Q6XQN6-3	Isoform 3 of Nicotinate phosphoribosyltransferase	NAPRT
O60664-2	Isoform 2 of Perilipin-3	PLIN3
O43252	Bifunctional 3'-phosphoadenosine 5'-phosphosulfate synthase 1	PAPSS1
Q9Y3I0	tRNA-splicing ligase RtcB homolog	RTCB
A0A087X0I4	Coatomer subunit epsilon	COPE
Q9NYU2-2	Isoform 2 of UDP-glucose:glycoprotein glucosyltransferase 1	UGGT1
Q8TDZ2-4	Isoform 4 of Protein-methionine sulfoxide oxidase MICAL1	MICAL1
P26196	Probable ATP-dependent RNA helicase	DDX6
P35222	Catenin beta-1	CTNNB1
Q15008-4	Isoform 4 of 26S proteasome non-ATPase regulatory subunit 6	PSMD6
P49721	Proteasome subunit beta type-2	PSMB2
Q9Y6G9	Cytoplasmic dynein 1 light intermediate chain 1	DYNC1LI1
J3KTN0	Eukaryotic initiation factor 4A-I	EIF4
V9GYM8	Rho guanine nucleotide exchange factor 2	ARHGEF2
Q92900-2	Isoform 2 of Regulator of nonsense transcripts 1	UPF1
O94903	Proline synthase co-transcribed bacterial homolog protein	PROSC

P53618	Coatomer subunit beta	COPB1
Q16531	DNA damage-binding protein 1	DDB1
Q96AC1-3	Isoform 3 of Fermitin family homolog 2	FERMT2
Q9UHB9	Signal recognition particle subunit SRP68	SRP68
Q13325-2	Isoform 2 of Interferon-induced protein with tetratricopeptide repeats 5	IFIT5
P20700	Lamin-B1	LMNB1
Q92905	COP9 signalosome complex subunit 5	COPS5
O00154-6	Isoform 6 of Cytosolic acyl coenzyme A thioester hydrolase	ACOT7
Q5T9B7	Adenylate kinase isoenzyme 1	AK1
Q00341-2	Isoform 2 of Vigilin	HDLBP
Q14155-5	Isoform 5 of Rho guanine nucleotide exchange factor 7	ARHGEF7
Q13177	Serine/threonine-protein kinase PAK 2	PAK2
Q14258	E3 ubiquitin/ISG15 ligase	TRIM25
Q9Y230	RuvB-like 2	RUVBL2
P53004	Biliverdin reductase A	BLVRA
P55010	Eukaryotic translation initiation factor 5	EIF5
P40222	Alpha-taxilin	TXLNA
A0A075B6Q0	Ras-related protein Rap-1A (Fragment)	RAP1A
Q99471	Prefoldin subunit 5	PFDN5
P58004	Sestrin-2	SESN2
A0A0A0MRI2	Sorting nexin 6, isoform CRA_b	SNX6
Q92841	Probable ATP-dependent RNA helicase	DDX17
Q92616	Translational activator GCN1	GCN1L1
A0A0A0MQS9	Laminin subunit alpha-4	LAMA4
Q9UK76	Hematological and neurological expressed 1 protein	HN1
P04792	Heat shock protein beta-1	HSPB1
P00813	Adenosine deaminase	ADA
Q9UHD1	Cysteine and histidine-rich domain-containing protein 1	CHORDC1
Q08211	ATP-dependent RNA helicase A	DHX9
Q9P2R3-4	Isoform 4 of Rabankyrin-5	ANKFY1
P31946-2	Isoform Short of 14-3-3 protein beta/alpha	YWHAB
P38919	Eukaryotic initiation factor 4A-III	EIF4
P28070	Proteasome subunit beta type-4	PSMB4
Q96ST2	Protein IWS1 homolog	IWS1
P15880	40S ribosomal protein S2	RPS2
O94832	Unconventional myosin-Id	MYO1D

RABP2	Cellular retinoic acid-binding protein 2	CRABP2
P60842	Eukaryotic initiation factor 4A-I (Fragment)	EIF4
F5GX11	Proteasome subunit alpha type-1	PSMA1
P40121	Macrophage-capping protein	CAPG
P53621	Coatomer subunit alpha	COPA
P07355-2	Isoform 2 of Annexin A2	ANXA2
P13489	Ribonuclease inhibitor	RNH1
P55060-3	Isoform 3 of Exportin-2	CSE1L
Q99961	Endophilin-A2	SH3
P40763-3	Isoform 3 of Signal transducer and activator of transcription 3	STAT3
P06737	Glycogen phosphorylase, brain form	PYGB
A5YKK6-2	Isoform 2 of CCR4-NOT transcription complex subunit 1	CNOT1
Q13418	Integrin-linked protein kinase	ILK
Q9NVA2-2|	Isoform 2 of Septin-11	SPET11
P55145	Mesencephalic astrocyte-derived neurotrophic factor	MANF
F8WAE5	Eukaryotic translation initiation factor 2A	EIF2A
O14908	PDZ domain-containing protein	GIPC1
E7EU96	Casein kinase II subunit alpha'	CSNK2A1
Q9NZL4-3	Isoform 3 of Hsp70-binding protein 1	HSPBP1
P61163	Alpha-centractin	ACTR1A
O00273	DNA fragmentation factor subunit alpha	DFFA
O43488	Aflatoxin B1 aldehyde reductase member 2	AKR7A2
Q13557-10	Isoform Delta 10 of Calcium/calmodulin-dependent protein kinase type II subunit delta	CAMK2D
E9PLK3	Puromycin-sensitive aminopeptidase	NPEPPS
Q9NZI8-2	Isoform 2 of Insulin-like growth factor 2 mRNA-binding protein 1	IGF2BP1
O14818	Proteasome subunit alpha type-7	PSMA7
O00203-3	Isoform 2 of AP-3 complex subunit beta-1	AP3B1
Q5SSJ5	Heterochromatin protein 1-binding protein 3	HP1BP3
Q8NBF2	NHL repeat-containing protein 2	NHLRC2
P55263-2	Isoform 2 of Adenosine kinase	ADK
P49593	Protein phosphatase 1F	PPM1F
P25789	Proteasome subunit alpha type-4	PSMA4
C9JLV4	Apoptotic protease-activating factor 1	APAF1
B8ZZZ7	DNA polymerase-transactivated protein 6, isoform CRA_b	SPATS2L
P09104	Gamma-enolase	ENO2
P09960	Leukotriene A-4 hydrolase	LTA4H

B4E0K5	Mitogen-activated protein kinase 14	MAPK14
Q9NRS6	Sorting nexin-15	SNX15
P54727	UV excision repair protein RAD23 homolog B	RAD23B
O43390	Heterogeneous nuclear ribonucleoprotein R	HNRNPR
Q9Y224	UPF0568 protein C14orf166	C14orf166
Q6DKJ4	Nucleoredoxin	NXN
P53602	Diphosphomevalonate decarboxylase	MVD
Q9Y5P6-2	Isoform 2 of Mannose-1-phosphate guanyltransferase beta	GMPPB
Q13242	Serine/arginine-rich splicing factor 9	SRSF9
Q9NQG5	Regulation of nuclear pre-mRNA domain-containing protein 1B	RPRD1B
O95340-2	Isoform B of Bifunctional 3'-phosphoadenosine 5'-phosphosulfate synthase 2	PAPSS2
Q06210-2	Isoform 2 of Glutamine--fructose-6-phosphate aminotransferase [isomerizing] 1	GFPT1
Q8NEU8	DCC-interacting protein 13-beta	APPL2
P68104	Elongation factor 1-alpha 1	EEF1A1
P29218-3	Isoform 3 of Inositol monophosphatase 1	IMPA1
F5H5D3	Tubulin alpha-1C chain	TUBA1C
Q3SY69	Mitochondrial 10-formyltetrahydrofolate dehydrogenase	ALDH1L2
O15144	Actin-related protein 2/3 complex subunit 2	ARPC2
O95793-3	Isoform 3 of Double-stranded RNA-binding protein Staufen homolog 1	STAU1
P49407-2	Isoform 1B of Beta-arrestin-1	ARRB1
Q99879	Histone H2B type 1-M	HIST1H2BM
P58546	Myotrophin	MTPN
E9PDF6	Unconventional myosin-Ib	MYO1B
Q07954	Prolow-density lipoprotein receptor-related protein 1	LRP1
Q9NTX5	Ethylmalonyl-CoA decarboxylase	ECHDC1
O00505	Importin subunit alpha-4	KPNA3
O00267-2	Isoform 2 of Transcription elongation factor SPT5	SUPT5H
H3BP20	Beta-hexosaminidase	HEXA
F8W9J4	Dystonin	DST
Q9UBS4	DnaJ homolog subfamily B member 11	DNAJB11
Q6WCQ1-2	Isoform 2 of Myosin phosphatase Rho-interacting protein	MPRIP
Q9Y285-2	Isoform 2 of Phenylalanine--tRNA ligase alpha subunit	FARSA
A6PVN5	Serine/threonine-protein phosphatase 2A activator	PPP2R4
O14841	5-oxoprolinase	OPLAH
P48163	NADP-dependent malic enzyme	ME1

P68363	Tubulin alpha-1B chain	TUBA1B
Q12797	Aspartyl/asparaginyl beta-hydroxylase	ASPH
J3KR97	Tubulin-specific chaperone D	TBCD
H7BZT7	S-formylglutathione hydrolase (Fragment)	ESD
O4317	D-3-phosphoglycerate dehydrogenase	PHGDH
H3BR70	Pyruvate kinase	PKM
P26639-2	Isoform 2 of Threonine--tRNA ligase, cytoplasmic	TARS
Q12874	Splicing factor 3A subunit 3	SF3A3
Q96HE7	ERO1-like protein alpha	ERO1
Q9NS86	LanC-like protein 2	LANCL2
P30043	Flavin reductase (NADPH)	BLVRB
P23246	Splicing factor, proline- and glutamine-rich	SFPQ
O14974-3	Isoform 3 of Protein phosphatase 1 regulatory subunit 12A	PPP1R12A
P61201	COP9 signalosome complex subunit 2	COPS2
Q92783-2|	Isoform 2 of Signal transducing adapter molecule 1	STAM
Q9BR76	Coronin-1B	CORO1
P13010	X-ray repair cross-complementing protein 5	XRCC5
P33991	DNA replication licensing factor	MCM4
O95433-2	Isoform 2 of Activator of 90 kDa heat shock protein ATPase homolog 1	AHSA1
A0A087WUK2	Heterogeneous nuclear ribonucleoprotein D-like	HNRNPDL
A0A0C4DGG9	Isoform 2 of Chromodomain-helicase-DNA-binding protein 4	CHD4
P19838-2	Isoform 2 of Nuclear factor NF-kappa-B p105 subunit	NFKB1
P54725-3	Isoform 3 of UV excision repair protein RAD23 homolog A	RAD23A
P61764-2	Isoform 2 of Syntaxin-binding protein 1	STXBP1
Q15056-2	Isoform Short of Eukaryotic translation initiation factor 4H	EIF4H
Q9H267	Vacuolar protein sorting-associated protein 33B	VPS33B
Q9UKG1	DCC-interacting protein 13-alpha	APPL1
F8VYY9	5'-AMP-activated protein kinase subunit gamma-1	PRKAG1
J3KNQ4	Alpha-parvin	PARVA
F6TLX2	Glyoxalase domain-containing protein 4	GLOD4
B7WPG3	Heterogeneous nuclear ribonucleoprotein L-like	HNRNPLL
P07602-3	Isoform Sap-mu-9 of Prosaposin	PSAP
U3C7B4	UPF0364 protein C6orf211	C6orf211
P46108-2	Isoform Crk-I of Adapter molecule crk	CRK
O60664-3	Isoform 3 of Perilipin-3	PLIN3
Q13439-4	Isoform 4 of Golgin subfamily A member 4	GOLGA4

D6RBV2	Vesicular integral-membrane protein VIP36	LMAN2
Q9Y678	Coatomer subunit gamma-1	COPG1
Q14103-3	Isoform 3 of Heterogeneous nuclear ribonucleoprotein D0	HNRNPD
P49756	RNA-binding protein 25	RBM25
O75165	DnaJ homolog subfamily C member 13	DNAJC13
P40227	T-complex protein 1 subunit zeta	CCT6A
Q7Z4V5	Hepatoma-derived growth factor-related protein 2	HDGFRP2
P00441	Superoxide dismutase [Cu-Zn]	SOD1
Q9Y305	Acyl-coenzyme A thioesterase 9, mitochondrial	ACOT9
P62280	40S ribosomal protein S11	RPS11
B0QZ18	Copine-1	CPNE1
Q12792	Twinfilin-1	TWF1
Q13185	Chromobox protein homolog 3	CBX3
O75368	SH3 domain-binding glutamic acid-rich-like protein	SH3BGRL
P46940	Ras GTPase-activating-like protein	IQGAP1
Q6P2E9	Enhancer of mRNA-decapping protein 4	EDC4
A0A0D9SFS3	2-oxoglutarate dehydrogenase, mitochondrial	OGDH
H9KV75	Alpha-actinin-1	ACTN1
P50579-3	Isoform 3 of Methionine aminopeptidase 2	METAP2
P19367-2	Isoform 2 of Hexokinase-1	HK1
B0YIW6	Archain 1, isoform CRA_a	ARCN1
Q8N8S7-2	Isoform 2 of Protein enabled homolog	ENAH
O75592-2	Isoform 2 of E3 ubiquitin-protein ligase	MYCBP2
P25788-2	Isoform 2 of Proteasome subunit alpha type-3	PSMA3
E9PNN6	Aldehyde dehydrogenase, dimeric NADP-preferring	ALDH3A1
P08758	Annexin A1	ANXA5
Q15942	Zyxin	ZYX
Q02809-2	Isoform 2 of Procollagen-lysine,2-oxoglutarate 5-dioxygenase 1	PLOD1
Q9NQW7-3	Isoform 3 of Xaa-Pro aminopeptidase 1	XPNPEP1
A0A0B4J1W3	N-alpha-acetyltransferase 15, NatA auxiliary subunit	NAA15
P62195-2	Isoform 2 of 26S protease regulatory subunit 8	PSMC5
Q96QK1	Vacuolar protein sorting-associated protein 35	VPS35
Q9Y570-4	Isoform 4 of Protein phosphatase methylesterase 1	PPME1
Q14315	Filamin-C	FLNC
P32119	Peroxiredoxin-2	PRDX2
P02769	Serum albumin	ALB
A0A087WUT6	Eukaryotic translation initiation factor 5B	EIF5B

P12814-3	Isoform 3 of Alpha-actinin-1	ACTN1
O94855-2	Isoform 2 of Protein transport protein Sec24D	SEC24D
B4DJV2	Citrate synthase	CS
Q99459	Cell division cycle 5-like protein	CDC5
Q14764	Major vault protein	MVP
P06737-2	Isoform 2 of Glycogen phosphorylase, liver form	PYGL
O43707	Alpha-actinin-4	ACTN4
P36578	60S ribosomal protein L4	RPL4
Q8IYI6	Exocyst complex component 8	EXOC8
M0R061	Coatomer subunit epsilon	COPE
P62424	60S ribosomal protein L7a	RPL7A
P18124	60S ribosomal protein L7	RPL7
Q12768	WASH complex subunit strumpellin	KIAA0196
P21964-2	Isoform Soluble of Catechol O-methyltransferase	COMT
P61088	Ubiquitin-conjugating enzyme E2 N	UBE2N
J3KTA4	Probable ATP-dependent RNA helicase	DDX5
P06733-2	Isoform MBP-1 of Alpha-enolase	ENO1
O43615	Mitochondrial import inner membrane translocase subunit	TIMM44
O00425	Insulin-like growth factor 2 mRNA-binding protein 3	IGF2BP3
P00760	Cationic trypsin	TRY1
Q6ZVM7-5	Isoform 5 of TOM1-like protein 2	TOM1L2
P10253	Lysosomal alpha-glucosidase	GAA
P62906	60S ribosomal protein L10a	RPL10A
Q9HC35	Echinoderm microtubule-associated protein-like 4	EML4
E5RK69	Annexin A6	ANXA6
P04406-2	Isoform 2 of Glyceraldehyde-3-phosphate dehydrogenase	GAPDH
P04083	Annexin	ANXA1
P30086	Phosphatidylethanolamine-binding protein 1	PEBP1
H0Y449	Nuclease-sensitive element-binding protein 1 (Fragment)	YBX1
P23526	Adenosylhomocysteinase	AHCY
A0A0D9SF53	ATP-dependent RNA helicase	DDX3X
A0A0B4J2B4	40S ribosomal protein S15	RPS15
P04406	Glyceraldehyde-3-phosphate dehydrogenase	GAPDH
Q92499	ATP-dependent RNA helicase	DDX1
P10809	60 kDa heat shock protein, mitochondrial	HSPD1
P55884-2	Isoform 2 of Eukaryotic translation initiation factor 3 subunit B	EIF3B
Q9BUF5	Tubulin beta-6 chain	TUBB6

P48735	Isocitrate dehydrogenase [NADP], mitochondrial	IDH2
P30085	UMP-CMP kinase	CMPK1
Q16576	Histone-binding protein	RBBP7
P35573-2	Isoform 5 of Glycogen debranching enzyme	AGL
P62753	40S ribosomal protein S6	RPS6
B4DWR3	Prefoldin subunit 3	VBP1
Q6ZN40	Tropomyosin 1 (Alpha), isoform CRA_f	TPM1
Q96I99-2	Isoform 2 of Succinyl-CoA ligase [GDP-forming] subunit beta, mitochondrial	SUCLG2
P23396-2	Isoform 2 of 40S ribosomal protein S3	RPS3
Q9Y3P9	Rab GTPase-activating protein 1	RABGAP1
H0YL52	Tropomyosin alpha-1 chain (Fragment)	TPM1
Q92734-2	Isoform 2 of Protein TFG	TFG
P49419-2	Isoform 2 of Alpha-aminoadipic semialdehyde dehydrogenase	ALDH7A1
P00966	Argininosuccinate synthase	ASS1
P78527	DNA-dependent protein kinase catalytic subunit	PRKDC
Q9Y6D6	Brefeldin A-inhibited guanine nucleotide-exchange protein 1	ARFGEF1
K7EN08	Nuclear factor 1	NFIX
O00487	26S proteasome non-ATPase regulatory subunit 14	PSMD14
Q8TDQ7-4	Isoform 4 of Glucosamine-6-phosphate isomerase 2	GNPDA2
Q07666	KH domain-containing, RNA-binding, signal transduction-associated protein 1	KHDRBS1
O60341-2	Isoform 2 of Lysine-specific histone demethylase 1A	KDM1A
Q96P70	Importin-9	IPO9
P00761	Trypsin	TRYP
Q14697-2	Isoform 2 of Neutral alpha-glucosidase AB	GANAB
Q14204	Cytoplasmic dynein 1 heavy chain 1	DYNC1H1
P21796	Voltage-dependent anion-selective channel protein 1	VDAC1
Q8N1G4	Leucine-rich repeat-containing protein 47	LRRC47
O75828	Carbonyl reductase [NADPH] 3	CBR3
D6RF62	Multifunctional protein ADE2	PAICS
Q60FE5	Filamin A	FLNA
P13639	Elongation factor 2	EEF2
A0A087X020	Ribosome maturation protein SBDS	SBDS
P07737	Profilin-1	PFN1
Q6NZI2	Polymerase I and transcript release factor	PTRF
P62158	Calmodulin	CALM1
P47755	F-actin-capping protein subunit alpha-2	CAPZA2
P17812	CTP synthase 1	CTPS1

A0A0A0MRM8	Unconventional myosin-VI	MYO6
A0A087WWE2	DNA-directed RNA polymerase	POLR2A
W4VSQ9	Cdc42-interacting protein 4	TRIP10
Q9BT78	COP9 signalosome complex subunit 4	COPS4
E9PB90	Hexokinase	HK2
G5E972	Lamina-associated polypeptide 2, isoform alpha	TMPO
Q14697	Neutral alpha-glucosidase AB	GANAB
O43583	Density-regulated protein	DENR
H7C2E7	Filamin-A	FLNA
P52594-2	Isoform 2 of Arf-GAP domain and FG repeat-containing protein 1	AGFG1
D6RGG3	Collagen alpha-1(XII) chain	COL12
P24534	Elongation factor 1-beta	EEF1
Q9NZB2-6	Isoform F of Constitutive coactivator of PPAR-gamma-like protein 1	FAM120A
Q15293	Reticulocalbin-1	RCN1
O15145	Actin-related protein 2/3 complex subunit 3	ARPC3
M0QZR4	Rho guanine nucleotide exchange factor 1	ARHGEF1
Q8TCT9-5	Isoform 5 of Minor histocompatibility antigen H13	HM13
Q96K76-4	Isoform 4 of Ubiquitin carboxyl-terminal hydrolase 47	USP47
P49589-3	Isoform 3 of Cysteine--tRNA ligase, cytoplasmic	CARS
P23634-6	Isoform XB of Plasma membrane calcium-transporting ATPase 4	ATP2B4
Q92804-2	Isoform Short of TATA-binding protein-associated factor 2N	TAF15
Q8WUM4-2	Isoform 2 of Programmed cell death 6-interacting protein	PDCD6IP
K7EMW4	Nicalin	NCLN
O75643	U5 small nuclear ribonucleoprotein 200 kDa helicase	SNRNP200
Q9NRV9	Heme-binding protein 1	HEBP1
O95817	BAG family molecular chaperone regulator 3	BAG3
A6NMH6	Septin-8	Sep-08
P05023-4	Isoform 4 of Sodium/potassium-transporting ATPase subunit alpha-1	ATP1A1
Q96A49	Synapse-associated protein 1	SYAP1
Q9UG63-2	Isoform 2 of ATP-binding cassette sub-family F member 2	ABCF2
O60784	Target of Myb protein 1	TOM1
F8W7C6	60S ribosomal protein L10	RPL10
Q16658	Fascin	FSCN1
A0A087WZZ	Splicing factor 3B subunit 2 (Fragment)	SF3B2

5		
Q14257-2	Isoform 2 of Reticulocalbin-2	RCN2
P10599	Thioredoxin domain-containing protein 17	TXN
Q9HB07	UPF0160 protein MYG1, mitochondrial	C12orf10
Q9H0U4	Ras-related protein Rab-1B	RAB1B
E9PIE3	Protein kinase C delta-binding protein	PRKCDBP
P00558	Phosphoglycerate kinase 1	PGK1
P55268	Laminin subunit beta-2	LAMB2
O94760	N(G),N(G)-dimethylarginine dimethylaminohydrolase 1	DDAH1
H0Y5F5	Polyadenylate-binding protein	PABPC4
Q09028-3	Isoform 3 of Histone-binding protein	RBBP4
F5GZ78	Paxillin	PXN
A8K7Q2	Heat shock cognate 71 kDa protein (Fragment)	HSPA8
Q96G03	Phosphoglucomutase-2	PGM2
C9JFV4	Proline-, glutamic acid- and leucine-rich protein 1	PELP1
FKBP3	Peptidyl-prolyl cis-trans isomerase	FKBP3
P17612-2	Isoform 2 of cAMP-dependent protein kinase catalytic subunit alpha	PRKACA
P25787	Proteasome subunit alpha type-2	PSMA2
E9PCA1	T-complex protein 1 subunit epsilon	CCT5
P62917	60S ribosomal protein L8	RPL8
O94992	Protein HEXIM1	HEXIM1
Q9Y265	RuvB-like 1	RUVBL1
P62701	40S ribosomal protein S4, X isoform	RPS4X
Q13409-6	Isoform 2F of Cytoplasmic dynein 1 intermediate chain 2	DYNC1I2
Q05639	Elongation factor 1-alpha 2	EEF1A2
P35606	Coatomer subunit beta'	COPB2
Q8TBA6-2	Isoform 2 of Golgin subfamily A member 5	GOLGA5
Q5H909	Melanoma-associated antigen D2	MAGED2
D3YTB1	60S ribosomal protein L32 (Fragment)	RPL32
Q13523	Serine/threonine-protein kinase PRP4 homolog	PRPF4B
P68366-2	Isoform 2 of Tubulin alpha-4A chain	TUBA4A
Q9HCN8	Stromal cell-derived factor 2-like protein 1	SDF2L1
Q92973	Transportin-1	TNPO1
P15121	Aldose reductase	AKR1B1
Q9UBC2-2	Isoform 2 of Epidermal growth factor receptor substrate 15-like 1	EPS15L1
P29590	Protein PML	PML
P54652	Heat shock-related 70 kDa protein 2	HSPA2

P20908	Collagen alpha-1(V) chain	COL5
Q6IBS0	Twinfilin-2	TWF2
P62241	40S ribosomal protein S8	RPS8
P50570-2	Isoform 2 of Dynamin-2	DNM2
H7BYY1	Tropomyosin 1 (Alpha), isoform CRA_m	TPM1
O00148	ATP-dependent RNA helicase	DDX39
P07951-3	Isoform 3 of Tropomyosin beta chain	TPM2
O95394-4	Isoform 3 of Phosphoacetylglucosamine mutase	PGM3
O00231	26S proteasome non-ATPase regulatory subunit 11	PSMD11
O95782-2	Isoform B of AP-2 complex subunit alpha-1	AP2A1
Q5JRA6-2	Isoform 2 of Melanoma inhibitory activity protein 3	MIA3
P25398	40S ribosomal protein S12	RPS12
P50991	T-complex protein 1 subunit delta	CCT4
J3KR44	Ubiquitin thioesterase	OTUB1
HNRH2	Heterogeneous nuclear ribonucleoprotein H2	HNRNPH2
Q16762	Thiosulfate sulfurtransferase	TST
Q12931-2	Isoform 2 of Heat shock protein 75 kDa, mitochondrial	TRAP1
B8ZZU8	Transcription elongation factor B (SIII), polypeptide 2 (18kDa, elongin B), isoform CRA_b	TCEB2
A0A0D9SGF6	A0A0D9SGF6_HUMAN Spectrin alpha chain, non-erythrocytic 1	SPTAN1
A0A087WXM6	60S ribosomal protein L17 (Fragment)	RPL17
P30050	60S ribosomal protein L12	RPL12
P23284	Peptidyl-prolyl cis-trans isomerase B	PPIB
Q08209-2	Isoform 2 of Serine/threonine-protein phosphatase 2B catalytic subunit alpha isoform	PPP3CA
Q9Y2J2-2	Isoform 2 of Band 4.1-like protein 3	EPB41L3
Q92538-2	Isoform 2 of Golgi-specific brefeldin A-resistance guanine nucleotide exchange factor 1	GBF1
P54886	Delta-1-pyrroline-5-carboxylate synthase	ALDH18A1
P30101	Protein disulfide-isomerase	PDIA3
O75533	Splicing factor 3B subunit 1	SF3B1
P49411	Elongation factor Tu, mitochondrial	TUFM
Q04760	Lactoylglutathione lyase	GLO1
Q9UQ80	Proliferation-associated protein 2G4	PA2G4
P23142	Fibulin-1	FBLN1
Q9P2J5	Leucine--tRNA ligase, cytoplasmic	LARS
A0A0C4DG17	40S ribosomal protein SA (Fragment)	RPSA
P27348	14-3-3 protein theta	YWHAQ
Q8IVL6-2	Isoform 2 of Prolyl 3-hydroxylase 3	LEPREL2

O43143	Putative pre-mRNA-splicing factor ATP-dependent RNA helicase	DHX15
A0A0C4DGS5	Golgin subfamily A member 2	GOLGA2
O60645-3	Isoform 3 of Exocyst complex component 3	EXOC3
Q96KP4	Cytosolic non-specific dipeptidase	CNDP2
Q13247-3	Isoform SRP55-3 of Serine/arginine-rich splicing factor 6	SRSF6
P63104	14-3-3 protein zeta/delta	YWHAZ
E9PK25	Cofilin-1	CFL1
P17655	Calpain-2 catalytic subunit	CAPN2
Q96D15	Reticulocalbin-3	RCN3
Q13464	Rho-associated protein kinase 1	ROCK1
Q13813-3	Isoform 3 of Spectrin alpha chain, non-erythrocytic 1	SPTAN1
E5RJR5	S-phase kinase-associated protein 1	SKP1
O43396	Thioredoxin-like protein 1	TXNL1
Q14008-3	Isoform 3 of Cytoskeleton-associated protein 5	CKAP5
Q4J6C6-4	Isoform 4 of Prolyl endopeptidase-like	PREPL
P23219-2	Isoform 2 of Prostaglandin G/H synthase 1	PTGS1
Q969E4	Transcription elongation factor A protein-like 3	TCEAL3
Q13564-2	Isoform 2 of NEDD8-activating enzyme E1 regulatory subunit	NAE1
P08133	Annexin A5	ANXA6
H0Y3Y9	26S proteasome non-ATPase regulatory subunit 4 (Fragment)	PSMD4
Q9UMX0	Ubiquilin-1	UBQLN1
P62495	Eukaryotic peptide chain release factor subunit 1	ETF1
P06753-3	Isoform 3 of Tropomyosin alpha-3 chain	TPM3
P17987	T-complex protein 1 subunit alpha	TCP1
O43242	26S proteasome non-ATPase regulatory subunit 3	PSMD3
P52735-2	Isoform 2 of Guanine nucleotide exchange factor VAV2	VAV2
P18669	Phosphoglycerate mutase 1	PGAM1
A0A0A0MTN3	Glutathione S-transferase Mu 3	GSTM3
P14550	Alcohol dehydrogenase [NADP(+)]	AKR1A1
Q8WWM7-2	Isoform 2 of Ataxin-2-like protein	ATXN2L
Q9UBT2-2	Isoform 2 of SUMO-activating enzyme subunit 2	UBA2
Q15233-2	Isoform 2 of Non-POU domain-containing octamer-binding protein	NONO
Q06124-2	Isoform 2 of Tyrosine-protein phosphatase non-receptor type 11	PTPN11
P30622-2	Isoform 3 of CAP-Gly domain-containing linker	CLIP1

	protein 1	
O15344-2	Isoform 2 of E3 ubiquitin-protein ligase Midline-1	MID1
P08621	U1 small nuclear ribonucleoprotein 70 kDa	SNRNP70
D3DQV9	Eukaryotic translation initiation factor 4 gamma 2 (Fragment)	EIF4G2
Q9Y2Z0	Suppressor of G2 allele of SKP1 homolog	SUGT1
Q9NR45	Sialic acid synthase	NANS
B4DLR8	NAD(P)H dehydrogenase [quinone] 1	NQO1
Q02878	60S ribosomal protein L6	RPL6
Q15365	Poly(rC)-binding protein 1	PCBP1
P16152	Carbonyl reductase [NADPH] 1	CBR1
P63267	Actin, gamma-enteric smooth muscle	ACTG2
H3BQZ7	HCG2044799	HNRNPUL2
Q9UEW8-2	Isoform 2 of STE20/SPS1-related proline-alanine-rich protein kinase	STK39
P12270	Nucleoprotein TPR	TPR
P42704	Leucine-rich PPR motif-containing protein, mitochondrial	LRPPRC
Q9UHV9	Prefoldin subunit 2	PFDN2
P68133	Actin, alpha skeletal muscle	ACTA1
P02545-2	Isoform C of Prelamin-A/C	LMNA
E9PHV5	Sperm-specific antigen 2	SSFA2
Q96CV9-2	Isoform 2 of Optineurin	OPTN
O14964	Hepatocyte growth factor-regulated tyrosine kinase substrate	HGS
J3KN67	Tropomyosin alpha-3 chain	TPM3
P31689	DnaJ homolog subfamily A member 1	DNAJA1
Q12888-2	Isoform 2 of Tumor suppressor p53-binding protein 1	TP53BP1
P33176	Kinesin-1 heavy chain	KIF5B
P22102	Trifunctional purine biosynthetic protein adenosine-3	GART
Q02252-2	Isoform 2 of Methylmalonate-semialdehyde dehydrogenase [acylating], mitochondrial	ALDH6A1
Q9NZ56	Formin-2	FMN2
P04899-4	Isoform sGi2 of Guanine nucleotide-binding protein G(i) subunit alpha-2	GNAI2
P26640	Valine--tRNA ligase	VARS
P08243-3	Isoform 3 of Asparagine synthetase [glutamine-hydrolyzing]	ASNS
P46100-2	Isoform 1 of Transcriptional regulator ATRX	ATRX
O60884	DnaJ homolog subfamily A member 2	DNAJA2
Q7Z3J2	UPF0505 protein C16orf62	C16orf62
F2Z2Y4	Pyridoxal kinase	PDXK

P05388	60S acidic ribosomal protein P0	RPLP0
P49189|	4-trimethylaminobutyraldehyde dehydrogenase	ALDH9
Q9NUY8-2	Isoform 2 of TBC1 domain family member 23	TBC1D23
P02461	Collagen alpha-1(III) chain	COL3
P62258	14-3-3 protein epsilon	YWHAE
Q63HN8-4	Isoform 2 of E3 ubiquitin-protein ligase RNF213	RNF213
P24752	Acetyl-CoA acetyltransferase, mitochondrial	ACAT1
Q9UMS4	Pre-mRNA-processing factor 19	PRPF19
Q15477	Helicase SKI2W	SKIV2
D6RBW1	Eukaryotic translation initiation factor 4E	EIF4
C9JEJ2	Choline-phosphate cytidylyltransferase A	PCYT1A
A0A0C4DGS1	Isoform 3 of Dolichyl-diphosphooligosaccharide--protein glycosyltransferase 48 kDa subunit	DDOST
F5H6E2	Unconventional myosin-Ic	MYO1C
Q9NSD9	Phenylalanine--tRNA ligase beta subunit	FARSB
P61158	Actin-related protein 3	ACTR3
P35637-2	Isoform Short of RNA-binding protein FUS	FUS
P14735	Insulin-degrading enzyme	IDE
A0A024R571	EH domain-containing protein 1	EHD1
P07686	Beta-hexosaminidase subunit beta	HEXB
Q08378	Golgin subfamily A member 3	GOLGA3
Q9H1B7	Interferon regulatory factor 2-binding protein-like	IRF2BP
Q92896-2	Isoform 2 of Golgi apparatus protein 1	GLG1
P46063	ATP-dependent DNA helicase Q1	RECQL
Q05707-2	Isoform 2 of Collagen alpha-1(XIV) chain	COEA1
Q14152	Eukaryotic translation initiation factor 3 subunit A	EIF3
P42765	3-ketoacyl-CoA thiolase, mitochondrial	ACAA2
Q86WN1	F-BAR and double SH3 domains protein 1	FCHSD1
P49902-2	Isoform 2 of Cytosolic purine 5'-nucleotidase	NT5C2
H3BN57	Protein BLOC1S5-TXNDC5	TXNDC5
A0A087WUZ3	Spectrin beta chain, non-erythrocytic 1	SPTBN1
P63261	Actin, cytoplasmic 2	ACTG1
P13797	Plastin-3	PLS3
E7ESC6	Exportin-7	XPO7
P09972	Fructose-bisphosphate aldolase C	ALDOC
B4DXZ6	Fragile X mental retardation syndrome-related protein 1	FXR1
O76003	Glutaredoxin-3	GLRX3
B4DDD6	Drebrin-like protein	DBNL
O15305	Phosphomannomutase 2	PMM2

O14744	Protein arginine N-methyltransferase 5	PRMT5
P36957	Dihydrolipoyllysine-residue succinyltransferase component of 2-oxoglutarate dehydrogenase complex, mitochondrial	DLST
O43852-3	Isoform 3 of Calumenin	CALU
O43237	Cytoplasmic dynein 1 light intermediate chain 2	DYNC1LI2
P36543	V-type proton ATPase subunit E 1	ATP6V1E1
A0A087WTA8	Collagen alpha-2(I) chain	COL1A2
P26599-2	Isoform 2 of Polypyrimidine tract-binding protein 1	PTBP1
O75874	Isocitrate dehydrogenase [NADP] cytoplasmic	IDH1
P07339	Cathepsin D	CTSD
Q5SW79-2	Isoform 2 of Centrosomal protein of 170 kDa	CEP170
H3BMS0	RNA-binding protein with serine-rich domain 1	RNPS1
Q96M27	Protein PRRC1	PRRC1
P52630-4	Isoform 2 of Signal transducer and activator of transcription 2	STAT2
Q13561-2	Isoform 2 of Dynactin subunit 2	DCTN2
P02452	Collagen alpha-1(I) chain	COL1
P12111	Collagen alpha-3(VI) chain	COL6
Q32P28	Prolyl 3-hydroxylase 1	LEPRE1
A0A0A0MSA7	Eukaryotic translation initiation factor 4 gamma 3	EIF4G3
Q9H4L5-2	Isoform 1b of Oxysterol-binding protein-related protein 3	OSBPL3
A0A087WYT3	Prostaglandin E synthase 3	PTGES3
P48739-3	Isoform 3 of Phosphatidylinositol transfer protein beta isoform	PITPNB
P07195	L-lactate dehydrogenase B chain	LDHB
Q9NYL9	Tropomodulin-3	TMOD3
C9JFR7	Cytochrome c (Fragment)	CYCS
O14558	Heat shock protein beta-6	HSPB6
P49321	Nuclear autoantigenic sperm protein	NASP
Q9H444	Charged multivesicular body protein 4b	CHMP4
O14980	Exportin-1	XPO1
Q01518	Adenylyl cyclase-associated protein 1	CAP1
C9J7E5	Transportin-3	TNPO3
P47897-2	Isoform 2 of Glutamine--tRNA ligase	QARS
P46777	60S ribosomal protein L5	RPL5
Q5JSL3	Dedicator of cytokinesis protein 11	DOCK11
Q99714	3-hydroxyacyl-CoA dehydrogenase type-2	HSD17B10

Q14789-2	Isoform 2 of Golgin subfamily B member 1	GOLGB1
O95671-2	Isoform 2 of N-acetylserotonin	ASMTL
K7ELL7	Glucosidase 2 subunit beta	PRKCSH
Q15393	Splicing factor 3B subunit 3	SF3B3
P18206-2	Isoform 1 of Vinculin	VCL
P38606	V-type proton ATPase catalytic subunit A	ATP6V1A
P62805	Histone H4	HIST1H4A
Q01082-3	Isoform 2 of Spectrin beta chain, non-erythrocytic 1	SPTBN1
P78318	Immunoglobulin-binding protein 1	IGBP1
Q8IWE2-2	Isoform 2 of Protein NOXP20	FAM114A1
A0A087WYV8	Fibrillin-2	FBN2
B4DFG0	Protein DEK	DEK
Q9H788	SH2 domain-containing protein 4A	SH2D4A
Q5HY54	Filamin-A (Fragment)	FLNA
Q9NYF8-2	Isoform 2 of Bcl-2-associated transcription factor 1	BCLF1
P78559	Microtubule-associated protein 1A	MAP1B
Q02790	Peptidyl-prolyl cis-trans isomerase	FKBP4
Q9UNZ2-5	Isoform 3 of NSFL1 cofactor p47	NSFL1C
H7C0E5	Zinc finger protein ZPR1 (Fragment)	ZPR1
A0A087X1Z3	Proteasome activator complex subunit 2	PSME2
Q9NX46	Poly(ADP-ribose) glycohydrolase ARH3	ADPRHL2
I3L0K2	Thioredoxin	TXNDC17
P28838-2	Isoform 2 of Cytosol aminopeptidase	LAP3
Q15459	Splicing factor 3A subunit 1	SF3A1
Q04917	14-3-3 protein eta	YWHAH
P78417	Glutathione S-transferase omega-1	GSTO1
Q14160-3	Isoform 3 of Protein scribble homolog	SCRIB
P09936	Ubiquitin carboxyl-terminal hydrolase isozyme L1	UCHL1
P28482	Mitogen-activated protein kinase 1	MAPK1
P26641-2	Isoform 2 of Elongation factor 1-gamma	EEF1G
Q96AE4-2	Isoform 2 of Far upstream element-binding protein 1	FUBP1
Q92945	Far upstream element-binding protein 2	KHSRP
A0A087WZH7	Myristoylated alanine-rich C-kinase substrate	MARCKS
Q7L5N1	COP9 signalosome complex subunit 6	COPS6
Q8WVM8-2	Isoform 2 of Sec1 family domain-containing protein 1	SCFD1
P11021	78 kDa glucose-regulated protein	HSPA5
Q14974	Importin subunit beta-1	KPNB1
O00232	26S proteasome non-ATPase regulatory subunit 12	PSMD12

A0A087WWM0	Trafficking protein particle complex subunit 3	TRAPPC3
1433G	14-3-3 protein gamma	YWHAG
Q15435	Protein phosphatase 1 regulatory subunit 7	PPP1R7
P49792	E3 SUMO-protein ligase RanBP2	RANBP2
P35221	Catenin alpha-1	CTNNA1
Q9BTT0	Acidic leucine-rich nuclear phosphoprotein 32 family member E	ANP32E
P27824-2	Isoform 2 of Calnexin	CANX
P63010-2	Isoform 2 of AP-2 complex subunit beta	AP2B1
P39019	40S ribosomal protein S19	RPS19
P43487-2	Isoform 2 of Ran-specific GTPase-activating protein	RANBP1
Q10567-2	Isoform B of AP-1 complex subunit beta-1	AP1B1
Q9ULV4-2	Isoform 2 of Coronin-1C	CORO1C
Q9Y2X3	Nucleolar protein 58	NOP58
Q15436	Protein transport protein Sec23A	SEC23A
Q06323	Proteasome activator complex subunit 1	PSME1
P15586	N-acetylglucosamine-6-sulfatase	GNS
E7ETU9	Procollagen-lysine,2-oxoglutarate 5-dioxygenase 2	PLOD2
H3BPE1	Microtubule-actin cross-linking factor 1, isoforms 1/2/3/5	MACF1
P45974-2	Isoform Short of Ubiquitin carboxyl-terminal hydrolase 5	USP5
A0A087WXS7	ATPase ASNA1	ASNA1
O14776-2	Isoform 2 of Transcription elongation regulator 1	TCERG1
Q15084-5	Isoform 5 of Protein disulfide-isomerase A6	PDIA6
Q96FQ6	Protein S100-A16	S100A16
Q93009-3	Isoform 3 of Ubiquitin carboxyl-terminal hydrolase 7	USP7
P12081	Isoform 4 of Histidine--tRNA ligase, cytoplasmic	HARS
Q9HB71	Calcyclin-binding protein	CACYBP
Q86UU1-2	Isoform 2 of Pleckstrin homology-like domain family B member 1	PHLDB1
P80303-2	Isoform 2 of Nucleobindin-2	NUCB2
Q2M389	WASH complex subunit 7	KIAA1033
O60701-3	Isoform 3 of UDP-glucose 6-dehydrogenase	UGDH
Q7KZF4	Staphylococcal nuclease domain-containing protein 1	SND1
P62314	Small nuclear ribonucleoprotein Sm D1	SNRPD1
P09601	Heme oxygenase 1	HMOX1
P50395	Rab GDP dissociation inhibitor beta	GDI2
O94804	Serine/threonine-protein kinase 10	STK10
P09496-2	Isoform Non-brain of Clathrin light chain A	CLTA

P38646	Stress-70 protein, mitochondrial	HSPA9
B4DDF4	Calponin	CNN2
P14866	Heterogeneous nuclear ribonucleoprotein L	HNRNPL
Q8TAT6-2	Isoform 2 of Nuclear protein localization protein 4 homolog	NPLOC4
H0Y9H6	Calpastatin (Fragment)	CAST
Q9Y490	Talin-1	TLN1
Q93052	Lipoma-preferred partner	LPP
P67936-2	Isoform 2 of Tropomyosin alpha-4 chain	TPM4
Q12906-4	Isoform 4 of Interleukin enhancer-binding factor 3	ILF3
A0A0C4DG89	Probable ATP-dependent RNA helicase	DDX46
E9PKF6	Serine/threonine-protein phosphatase 6 regulatory subunit 3	PPP6R3
P54578	Ubiquitin carboxyl-terminal hydrolase 14	USP14
P53992	Protein transport protein Sec24C	SEC24C
Q86UP2	Kinectin	KTN1
O95373	Importin-7	IPO7
Q9UBR2	Cathepsin Z	CTSZ
P08670	Vimentin	VIM
F5H4R6	Nucleosome assembly protein 1-like 1	NAP1L1
Q9UDT6-2	Isoform 2 of CAP-Gly domain-containing linker protein 2	CLIP2
H0YFY6	Nuclear mitotic apparatus protein 1	NUMA1
A0A087X2H1	E3 ubiquitin-protein ligase	HECTD1
A0A087WVC1	ATP-dependent RNA helicase	DDX50
Q14914	Prostaglandin reductase 1	PTGR1
Q8N0X7	Spartin	SPG20
Q9BZQ8	Protein Niban	FAM129A
G3V0E4	Mitochondrial-processing peptidase subunit beta	PMPCB
E5RGA2	Eukaryotic translation initiation factor 3 subunit E	EIF3
Q9UEW8	Serine/threonine-protein kinase OSR1	OXSR1
Q13895	Bystin	BYSL
Q8IX12-2	Isoform 2 of Cell division cycle and apoptosis regulator protein 1	CCAR1
Q9H2G2	STE20-like serine/threonine-protein kinase	SLK
P07951	Tropomyosin beta chain	TPM2
Q6P2Q9	Pre-mRNA-processing-splicing factor 8	PRPF8
E7EQT4	Apoptotic chromatin condensation inducer in the nucleus	ACIN1
P05997	Collagen alpha-2(V) chain	COL5

P07954	Fumarate hydratase, mitochondrial	FH
P49368	T-complex protein 1 subunit gamma	CCT3
H9KV28	Protein diaphanous homolog 1	DIAPH1
A0A0B4J2C3	Translationally-controlled tumor protein	TPT1
P27797	Calreticulin	CALR
Q07960	Rho GTPase-activating protein 1	ARHGAP1
Q9BSJ8-2	Isoform 2 of Extended synaptotagmin-1	ESYT1
Q16204	Coiled-coil domain-containing protein 6	CCDC6
Q9H3S7	Tyrosine-protein phosphatase non-receptor type 23	PTPN23
P36776-3	Isoform 3 of Lon protease homolog, mitochondrial	LONP1
O15460-2	Isoform IIa of Prolyl 4-hydroxylase subunit alpha-2	P4HA2
O43665-3	Isoform 3 of Regulator of G-protein signaling 10	RGS10
O75410-2	Isoform 2 of Transforming acidic coiled-coil-containing protein 1	TACC1
P49257	Protein ERGIC-53	LMAN1
P30084	Enoyl-CoA hydratase, mitochondrial	ECHS1
P25705	ATP synthase subunit alpha, mitochondrial	ATP5A1
P67936	Tropomyosin alpha-4 chain	TPM4
E9PGM4	1,4-alpha-glucan-branching enzyme	GBE1
Q9UJ70-2	Isoform 2 of N-acetyl-D-glucosamine kinase	NAGK
P06396-2	Isoform 2 of Gelsolin	GSN
P05455	Lupus La protein	SSB
Q9BWD1	Acetyl-CoA acetyltransferase, cytosolic	ACAT2
Q9Y3X0	Coiled-coil domain-containing protein 9	CCDC9
P54577	Tyrosine--tRNA ligase, cytoplasmic	YARS
P07237	Protein disulfide-isomerase A4	P4HB
P06132	Uroporphyrinogen decarboxylase	UROD
P12110	Collagen alpha-2(VI) chain	COL6
G3V5R9	Kinesin light chain 1	KLC1
Q15643	Thyroid receptor-interacting protein 11	TRIP11
Q12904-2	Isoform 2 of Aminoacyl tRNA synthase complex-interacting multifunctional protein 1	AIMP1
G3V180	Dipeptidyl peptidase 3	DPP3
O43776	Asparagine--tRNA ligase, cytoplasmic	NARS
H0YB24	Cell cycle and apoptosis regulator protein 2 (Fragment)	CCAR2
Q4G0J3-3	Isoform 3 of La-related protein 7	LARP7
Q16555	Dihydropyrimidinase-related protein 2	DPYSL2
P53999	Activated RNA polymerase II transcriptional coactivator p15	SUB1
X6RJP6	Transgelin-2 (Fragment)	TAGLN2

Q16543	Hsp90 co-chaperone Cdc37	CDC37
P37837	Transaldolase	TALDO1
P36871	Phosphoglucomutase-1	PGM1
G8JLD3	ELKS/Rab6-interacting/CAST family member 1	ERC1
O60763-2	Isoform 2 of General vesicular transport factor p115	USO1
O75534-4	Isoform 4 of Cold shock domain-containing protein E1	CSDE1
H3BRE8	RNA polymerase II-associated protein 1	RPAP1
P17174	Aspartate aminotransferase, cytoplasmic	GOT1
A0A087WVQ6	Clathrin heavy chain	CLTC
Q14240-2	Isoform 2 of Eukaryotic initiation factor 4A-II	EIF4A2
Q9H1E3	Nuclear ubiquitous casein and cyclin-dependent kinase substrate 1	NUCKS1
P41250	Glycine--tRNA ligase	GARS
P30041	Peroxiredoxin-6	PRDX6
P17661	Desmin	DES
O43852-7	Isoform 7 of Calumenin	CALU
P43490	Nicotinamide phosphoribosyltransferase	NAMPT
Q8NC51-2	Isoform 2 of Plasminogen activator inhibitor 1 RNA-binding protein	SERBP1
Q02818	Nucleobindin-1	NUCB1
P00338-3	Isoform 3 of L-lactate dehydrogenase A chain	LDHA
E7EX17	Eukaryotic translation initiation factor 4B	EIF4B
Q9P0K7-2	Isoform 2 of Ankycorbin	RAI14
Q5T4S7-2	Isoform 2 of E3 ubiquitin-protein ligase	UBR4
J3KR24	Isoleucine--tRNA ligase, cytoplasmic	IARS
P07996	Thrombospondin-1	THBS1
P62714	Serine/threonine-protein phosphatase 2A catalytic subunit beta isoform	PPP2CB
A0A087X2I1	26S protease regulatory subunit 10B	PSMC6
O95336	6-phosphogluconolactonase	PGLS
P09874	Poly [ADP-ribose] polymerase 1	PARP1
Q14166	Tubulin--tyrosine ligase-like protein 12	TTLL12
Q9Y5S2	Serine/threonine-protein kinase MRCK beta	CDC42BPB
Q15717-2	Isoform 2 of ELAV-like protein 1	ELAV1
I3L459	Phosphatidylinositol transfer protein alpha isoform	PITPNA
O43399	Tumor protein D54	TPD52L2
Q14694-2	Isoform 2 of Ubiquitin carboxyl-terminal hydrolase 10	USP10
Q63ZY3-3	Isoform 3 of KN motif and ankyrin repeat domain-containing protein 2	KANK2
Q9Y520-5	Isoform 5 of Protein PRRC2C	PRRC2C

Q02952-2	Isoform 2 of A-kinase anchor protein 12	AKAP12
Q15046-2	Isoform Mitochondrial of Lysine--tRNA ligase	KARS
Q14566	DNA replication licensing factor MCM6	MCM6
Q8WU90	Zinc finger CCCH domain-containing protein 15	ZC3H15
H7C456	Microtubule-associated protein 1B	MAP4
G3V1L9	Tight junction protein 1 (Zona occludens 1), isoform CRA_a	TJP1
P61978-2	Isoform 2 of Heterogeneous nuclear ribonucleoprotein K	HNRNPK
P55072	Transitional endoplasmic reticulum ATPase	VCP
Q13200	26S proteasome non-ATPase regulatory subunit 2	PSMD2
Q05682	Caldesmon	CALD1
P04844-2	Isoform 2 of Dolichyl-diphosphooligosaccharide--protein glycosyltransferase subunit 2	RPN2
Q96AY3	Peptidyl-prolyl cis-trans isomerase FKBP10	FKBP10
Q9UNS2-2	Isoform 2 of COP9 signalosome complex subunit 3	COPS3
A0AVT1	Ubiquitin-like modifier-activating enzyme 6	UBA6
F8WCF6	Protein ARPC4-TTLL3	ARPC4-TTLL3
P34931	Heat shock 70 kDa protein 1-like	HSPA1L
Q99497	Protein deglycase DJ-1	PARK7
Q01995	Transgelin	TAGLN
Q15811-8	Isoform 8 of Intersectin-1	ITSN1
P07814	Bifunctional glutamate/proline--tRNA ligase	EPRS
Q9ULZ3-2	Isoform 2 of Apoptosis-associated speck-like protein containing a CARD	PYCARD
Q9NSE4	Isoleucine--tRNA ligase, mitochondrial	IARS2
Q9Y6Y8	SEC23-interacting protein	SEC23IP
F8W031	Uncharacterized protein (Fragment)	F8W031
Q08J23-2	Isoform 2 of tRNA (cytosine(34)-C(5))-methyltransferase	NSUN2
Q99873-4	Isoform 4 of Protein arginine N-methyltransferase 1	PRMT1
M0R0P8	Unconventional myosin-IXb	MYO9B
P46939-2	Isoform 2 of Utrophin	UTRN
Q9UHB6-4	Isoform 4 of LIM domain and actin-binding protein 1	LIMA1
P53396-2	Isoform 2 of ATP-citrate synthase	ACLY
Q9NZN4	EH domain-containing protein 2	EHD2
P13674	Prolyl 4-hydroxylase subunit alpha-1	P4HA1
Q9Y450	HBS1-like protein	HBS1
Q13263	Transcription intermediary factor 1-beta	TRIM28
Q96TA1-2	Isoform 2 of Niban-like protein 1	FAM129B
Q02543	60S ribosomal protein L18a	RPL18A

Q8WVC0-2	Isoform 2 of RNA polymerase-associated protein LEO1	LEO1
Q16222-3	Isoform 3 of UDP-N-acetylhexosamine pyrophosphorylase	UAP1
Q9Y696	Chloride intracellular channel protein 4	CLIC4
Q09666	Neuroblast differentiation-associated protein	AHNAK
P35998	26S protease regulatory subunit 7	PSMC2
P51812	Ribosomal protein S6 kinase alpha-3	RPS6KA3
O95302-3	Isoform 3 of Peptidyl-prolyl cis-trans isomerase	FKBP9
P53985	Monocarboxylate transporter 1	SLC16A1
Q01105-2	Isoform 2 of Protein SET	SET
P14618	Pyruvate kinase PKM	PKM
Q9UBB4	Ataxin-10	ATXN10
Q05682-5	Isoform 5 of Caldesmon	CALD1
P28161	Glutathione S-transferase Mu 2	GSTM2
A0A0C4DFR6	Isoform 2 of Protein SEC13 homolog	SEC13
E9PM90	Vacuolar protein sorting-associated protein 28 homolog (Fragment)	VPS28
O15067	Phosphoribosylformylglycinamidine synthase	PFAS
Q9H2M9	Rab3 GTPase-activating protein non-catalytic subunit	RAB3GAP2
A0A087WTT1	Polyadenylate-binding protein (Fragment)	PABPC1
Q9H4A4	Aminopeptidase B	RNPEP
P09211	Glutathione S-transferase P	GSTP1
A2A274	Aconitate hydratase, mitochondrial	ACO2
P13667	Protein disulfide-isomerase A3	PDIA4
P0DMV8	Heat shock 70 kDa protein 1A	HSPA1A
Q52LW3	Rho GTPase-activating protein 29	ARHGAP29
J3KN16	Proteasome-associated protein ECM29 homolog	KIAA0368
Q9NQC3	Reticulon-4	RTN4
Q13547	Histone deacetylase 1	HDAC1
P63279	SUMO-conjugating enzyme UBC9	UBE2I
Q96I24	Far upstream element-binding protein 3	FUBP3
Q6UXH1-5	Isoform 5 of Cysteine-rich with EGF-like domain protein 2	CRELD2
Q9UQE7	Structural maintenance of chromosomes protein 3	SMC3
P52788	Spermine synthase	SMS
O60506-3	Isoform 3 of Heterogeneous nuclear ribonucleoprotein Q	SYNCRIP
Q13501-2	Isoform 2 of Sequestosome-1	SQSTM1
P52209-2	Isoform 2 of 6-phosphogluconate dehydrogenase,	PGD

	decarboxylating	
Q99536	Synaptic vesicle membrane protein VAT-1 homolog	VAT1
Q7KZ85	Transcription elongation factor SPT6	SUPT6H
Q01813	ATP-dependent 6-phosphofructokinase, platelet type	PFKP
Q8IZ07	Ankyrin repeat domain-containing protein 13A	ANKRD13
H7C2U0	T-complex protein 1 subunit theta (Fragment)	CCT8
Q9H3U1-2	Isoform 2 of Protein unc-45 homolog A	UNC45A
E9PM69	26S protease regulatory subunit 6A	PSMC3
P23381	Tryptophan--tRNA ligase, cytoplasmic	WARS
P07858	Cathepsin B	CTSB
P49841-2	Isoform 2 of Glycogen synthase kinase-3 beta	GSK3B
P11047	Laminin subunit gamma-1	LAMC1
Q9Y295	Developmentally-regulated GTP-binding protein 1	DRG1
Q9NTI5-2	Isoform 2 of Sister chromatid cohesion protein PDS5 homolog B	PDS5B
Q9HCE1	Putative helicase MOV-10	MOV10
O15355	Protein phosphatase 1G	PPM1G
F8W1A4	Adenylate kinase 2, mitochondrial	AK2
O15371-2	Isoform 2 of Eukaryotic translation initiation factor 3 subunit D	EIF3D
Q9C0C9	E2/E3 hybrid ubiquitin-protein ligase	UBE2O
Q9UBQ7	Glyoxylate reductase/hydroxypyruvate reductase	GRHPR
G3V2Q1	Heterogeneous nuclear ribonucleoproteins C1/C2	HNRNPC
P40123	Adenylyl cyclase-associated protein 2	CAP2
Q9BQS8-4	Isoform 4 of FYVE and coiled-coil domain-containing protein 1	FYCO1
P46060	Ran GTPase-activating protein 1	RANGAP1
Q99613	Eukaryotic translation initiation factor 3 subunit C	EIF3
O75116	Rho-associated protein kinase 2	ROCK2
C9J0I9	Nuclear-interacting partner of ALK	ZC3HC1
Q9Y3Z3	Deoxynucleoside triphosphate triphosphohydrolase	SAMHD1
E5RIW3	Tubulin-specific chaperone A	TBCA
O00429-2	Isoform 4 of Dynamin-1-like protein	DNM1L
Q07065	Cytoskeleton-associated protein 4	CKAP4
Q8WX93	Palladin	PALLD
O75369-2	Isoform 2 of Filamin-B	FLNB
O14745	Na(+)/H(+) exchange regulatory cofactor NHE-RF1	SLC9A3R1
P31749	RAC-alpha serine/threonine-protein kinase	AKT1
Q96T76-8	Isoform 5 of MMS19 nucleotide excision repair protein homolog	MMS19
P42785	Lysosomal Pro-X carboxypeptidase	PRCP

P06576	ATP synthase subunit beta, mitochondrial	ATP5B
E9PGC8	Microtubule-associated protein	MAP1A
P16615-5	Isoform 5 of Sarcoplasmic/endoplasmic reticulum calcium ATPase 2	ATP2A2
P15374	Ubiquitin carboxyl-terminal hydrolase isozyme L3	UCHL3
P17096-2	Isoform HMG-Y of High mobility group protein HMG-I/HMG-Y	HMGA1
Q9UH65	Switch-associated protein 70	SWAP70
Q9BXS5	AP-1 complex subunit mu-1	AP1M1
Q9Y4E8	Ubiquitin carboxyl-terminal hydrolase 15	USP15
Q9C0C2	182 kDa tankyrase-1-binding protein	TNKS1BP1
P80723	Brain acid soluble protein 1	BASP1
P30419	Glycylpeptide N-tetradecanoyltransferase 1	NMT1
P21399	Cytoplasmic aconitate hydratase	ACO1
Q27J81-2	Isoform 2 of Inverted formin-2	INF2
A0A0C4DGX4	Cullin-1	CUL1
A0A087WX08	Gamma-adducin	ADD3
E7EVA0	Microtubule-associated protein 4 (Fragment)	MAP4
P35555	Fibrillin-1	FBN1
P20073-2	Isoform 2 of Annexin A7	ANXA7
Q4V328	GRIP1-associated protein 1	GRIPAP1
GCP60	Golgi resident protein GCP60	ACBD3
Q5T5C7	Serine--tRNA ligase, cytoplasmic	SARS
Q8NC51-3	Isoform 3 of Plasminogen activator inhibitor 1 RNA-binding protein	SERBP1
Q70UQ0	Inhibitor of nuclear factor kappa-B kinase-interacting protein	IKBIP
Q01518-2	Isoform 2 of Adenylyl cyclase-associated protein 1	CAP1
Q15075	Early endosome antigen 1	EEA1
Q9UMX5	Neudesin	NENF
P21980	Protein-glutamine gamma-glutamyltransferase 2	TGM2
Q12765-2	Isoform 2 of Secernin-1	SCRN1
P43155-2	Isoform 2 of Carnitine O-acetyltransferase	CART
Q9BU89	Deoxyhypusine hydroxylase	DOHH
P39748	Flap endonuclease 1	FEN1
E9PRQ7	UBX domain-containing protein 1	UBXN1
P0CG38	POTE ankyrin domain family member I	POTEI
P17096	High mobility group protein HMG-I/HMG-Y	HMGA1
Q99460	26S proteasome non-ATPase regulatory subunit 1	PSMD1

P22314-2	Isoform 2 of Ubiquitin-like modifier-activating enzyme 1	UBA1
P20810-10	Isoform 10 of Calpastatin	CAST
P19174-2	Isoform 2 of 1-phosphatidylinositol 4,5-bisphosphate phosphodiesterase gamma-1	PLCG1
P27361-2	Isoform 2 of Mitogen-activated protein kinase 3	MAPK3
Q14696	LDLR chaperone MESD	MESDC2
J3KQ32	Obg-like ATPase 1	OLA1
Q8NF91	Nesprin-1	SYNE1
P11586	C-1-tetrahydrofolate synthase, cytoplasmic	MTHFD1
P50552	Vasodilator-stimulated phosphoprotein	VASP
Q9NRY4	Rho GTPase-activating protein 35	ARHGAP35
P50502	Hsc70-interacting protein	ST13
P04080	Cystatin-B	CSTB
P29692-3	Isoform 3 of Elongation factor 1-delta	EEF1D
O14933	Ubiquitin/ISG15-conjugating enzyme E2 L6	UBE2L6
E7EX90	Dynactin subunit 1	DCTN1
Q68E01-2	Isoform 2 of Integrator complex subunit 3	INTS3
P54687	Branched-chain-amino-acid aminotransferase, cytosolic	BCAT1
P31948-2	Isoform 2 of Stress-induced-phosphoprotein 1	STIP1
P43686	26S protease regulatory subunit 6B	PSMC4
Q9P0J1-2	Isoform 2 of [Pyruvate dehydrogenase [acetyl-transferring]]-phosphatase 1, mitochondrial	PDP1
Q14247-2	Isoform 2 of Src substrate cortactin	CTTN
A0A087WV05	Protein GJA9-MYCBP	GJA9-MYCBP
Q9Y4L1	Hypoxia up-regulated protein 1	HYOU1
P04843	Dolichyl-diphosphooligosaccharide--protein glycosyltransferase subunit 1	RPN1
B0QY89	Eukaryotic translation initiation factor 3 subunit L	EIF3
Q92598	Heat shock protein 105 kDa	HSPH1
Q13492-2	Isoform 2 of Phosphatidylinositol-binding clathrin assembly protein	PICALM
P49327	Fatty acid synthase	FASN
Q5JSH3-2	Isoform 2 of WD repeat-containing protein 44	WDR44
Q13308-6	Isoform 6 of Inactive tyrosine-protein kinase 7	PTK7
Q15029-3	Isoform 3 of 116 kDa U5 small nuclear ribonucleoprotein component	EFTUD2
Q9NVS9-3	Isoform 3 of Pyridoxine-5'-phosphate oxidase	PNPO
Q14847	LIM and SH3 domain protein 1	LASP1
P62328	Thymosin beta-4	TMSB4X

O43592	Exportin-T	XPOT
P11766	Alcohol dehydrogenase class-3	ADH5
P46937-5	Isoform 5 of Transcriptional coactivator YAP1	YAP1
Q15149-3	Isoform 3 of Plectin	PLEC
Q32MZ4-3	Isoform 3 of Leucine-rich repeat flightless-interacting protein 1	LRRFIP1
Q15149-4	Isoform 4 of Plectin	PLEC
P35658-2	Isoform 2 of Nuclear pore complex protein	NUP214
P49588	Alanine--tRNA ligase, cytoplasmic	AARS
Q15149	Plectin	PLEC
P78357	Contactin-associated protein 1	CNTNAP1
Q8IWV7	E3 ubiquitin-protein ligase	UBR1
E9PGC0	Ras GTPase-activating protein 1	RASA1
Q9UGI8-2	Isoform 2 of Testin	TES
Q15181	Inorganic pyrophosphatase	PPA1
B3KS98	Eukaryotic translation initiation factor 3 subunit H	EIF3
D6R9B6	40S ribosomal protein S3a	RPS3A
P05091	Aldehyde dehydrogenase, mitochondrial	ALDH2
P06748-2	Isoform 2 of Nucleophosmin	NPM1
O95352	Ubiquitin-like modifier-activating enzyme	ATG7
Q8IVF2-3	Isoform 3 of Protein AHNAK2	AHNAK2
P56537	Eukaryotic translation initiation factor 6	EIF6
P14625	Endoplasmin	HSP90B1
Q53EL6-2	Isoform 2 of Programmed cell death protein 4	PDCD4
Q9Y2Q3	Glutathione S-transferase kappa 1	GSTK1
Q9Y3F4-2	Isoform 2 of Serine-threonine kinase receptor-associated protein	STRAP
O00410-3	Isoform 3 of Importin-5	IPO5
A8MXH2	Nucleosome assembly protein 1-like 4 (Fragment)	NAP1L4
P30040	Endoplasmic reticulum resident protein 29	ERP29
P16278-3	Isoform 3 of Beta-galactosidase	GLB1
Q00839	Heterogeneous nuclear ribonucleoprotein U	HNRNPU
P49441	Inositol polyphosphate 1-phosphatase	INPP1
P30520	Adenylosuccinate synthetase isozyme 2	ADSS
O96019	Actin-like protein 6A	ACTL6
E5RHG8	Transcription elongation factor B polypeptide 1 (Fragment)	TCEB1
B5MDF5	GTP-binding nuclear protein Ran	RAN
J9JID7	Lamin B2, isoform CRA_a	LMNB2
O94973-2	Isoform 2 of AP-2 complex subunit alpha-2	AP2A2
RAB9A	Ras-related protein Rab-9A	RAB9A

E9PAV3	Nascent polypeptide-associated complex subunit alpha, muscle-specific form	NACA
A0A087WY61	Nuclear mitotic apparatus protein 1 (Fragment)	NUMA1
P30533	Alpha-2-macroglobulin receptor-associated protein	LRPAP1
P07900-2	Isoform 2 of Heat shock protein HSP 90-alpha	HSP90AA1
Q5VZU9	Tripeptidyl-peptidase 2	TPP2
PSMD7	26S proteasome non-ATPase regulatory subunit 7	PSMD7
E9PHY5	Band 4.1-like protein 2	EPB41L2
Q04637-9	Isoform 9 of Eukaryotic translation initiation factor 4 gamma 1	EIF4G1
E9PJ04	Splicing factor 3B subunit 2	SF3B2
P60983	Glia maturation factor beta	GMFB
R4GN77	Ubiquitin-conjugating enzyme E2 E3 (Fragment)	UBE2E3
Q15654	Thyroid receptor-interacting protein 6	TRIP6
O75436	Vacuolar protein sorting-associated protein 26A	VPS26A
P08238	Heat shock protein HSP 90-beta	HSP90
Q9Y2D5-4	Isoform 2 of A-kinase anchor protein 2	AKAP2
A8MXP9	Matrin-3	MATR3
P19338	Nucleolin	NCL
O43149	Zinc finger ZZ-type and EF-hand domain-containing protein 1	ZZEF1
F8W6I7	Heterogeneous nuclear ribonucleoprotein A1	HNRNPA1
P51991	Heterogeneous nuclear ribonucleoprotein A3	HNRNPA3
F5GWE5	Phosphatidylinositol transfer protein alpha isoform (Fragment)	PITPNA
Q9NZ08-2	Isoform 2 of Endoplasmic reticulum aminopeptidase 1	ERAP1
P78347-2	Isoform 2 of General transcription factor II-I	GTF2I
Q6PGP7	Tetratricopeptide repeat protein 37	TTC37
P52907	F-actin-capping protein subunit alpha-1	CAPZA1
P48681	Nestin	NES
A0A087WYS1	UTP--glucose-1-phosphate uridylyltransferase	UGP2
Q9UHX1-2	Isoform 2 of Poly(U)-binding-splicing factor PUF60	PUF60
J3KRC4	5'(3')-deoxyribonucleotidase, cytosolic type	NT5C
Q9HC07	Transmembrane protein 165	TMEM165
Q9UKY7	Protein CDV3 homolog	CDV3
Q9NRY5	Protein FAM114A2	FAM114A2
O43865	Putative adenosylhomocysteinase 2	AHCYL1
P54136	Arginine--tRNA ligase, cytoplasmic	RARS
O76094	Signal recognition particle subunit	SRP72
P49750-4	Isoform 4 of YLP motif-containing protein 1	YLPM1

F5H6I7	Atlastin-3	ATL3
Q9P2E9	Ribosome-binding protein 1	RRBP1
Q9Y2W1	Thyroid hormone receptor-associated protein 3	THRAP3
Q5JRX3-2	Isoform 2 of Presequence protease, mitochondrial	PITRM1
O00151	PDZ and LIM domain protein 1	PDLIM1
P21589-2	Isoform 2 of 5'-nucleotidase	NT5E
Q5LJA9	Ubiquitin carboxyl-terminal hydrolase (Fragment)	UCHL5
P52306-5	Isoform 5 of Rap1 GTPase-GDP dissociation stimulator 1	RAP1GDS1
P55084-2	Isoform 2 of Trifunctional enzyme subunit beta, mitochondrial	HADHB
Q9UQ35	Serine/arginine repetitive matrix protein 2	SRRM2
P00367	Glutamate dehydrogenase 1, mitochondrial	GLUD1
P56192	Methionine--tRNA ligase, cytoplasmic	MARS
P34932	Heat shock 70 kDa protein 4	HSPA4
Q16666-2	Isoform 2 of Gamma-interferon-inducible protein 16	IFI16
B4DY09	Interleukin enhancer-binding factor 2	ILF2
Q9NUQ9	Protein FAM49B	FAM49B
P50990-2	Isoform 2 of T-complex protein 1 subunit theta	CCT8
P31939-2	Isoform 2 of Bifunctional purine biosynthesis protein PURH	PUR9
Q9NZT2-2	Isoform 2 of Opioid growth factor receptor	OGFR
Q96RF0-2	Isoform 2 of Sorting nexin-18	SNX18
Q15691	Microtubule-associated protein RP/EB family member 1	MAPRE1
Q9UHD2	Serine/threonine-protein kinase TBK1	TBK1
Q9Y263	Phospholipase A-2-activating protein	PLAA
Q14195-2	Isoform LCRMP-4 of Dihydropyrimidinase-related protein 3	DPYSL3
J3KS95	Mitotic spindle-associated MMXD complex subunit MIP18 (Fragment)	FAM96B
P51149	Ras-related protein Rab-7a	RAB7A
B7Z7F3	Ran-binding protein 3	RANBP3
P14868	Aspartate--tRNA ligase, cytoplasmic	DARS
P00387-2	Isoform 2 of NADH-cytochrome b5 reductase 3	CYB5R3
Q92934	Bcl2-associated agonist of cell death	BAD
P30153	Serine/threonine-protein phosphatase 2A 65 kDa regulatory subunit A alpha isoform	PPP2R1A
Q15020	Squamous cell carcinoma antigen recognized by T-cells 3	SART3
B1AK87	Capping protein (Actin filament) muscle Z-line, beta, isoform CRA_a	CAPZB
P62191	26S protease regulatory subunit 4	PSMC1

O00299	Chloride intracellular channel protein 1	CLIC1
E9PK54	Heat shock cognate 71 kDa protein	HSPA8
Q58FG1	Putative heat shock protein HSP 90-alpha A4	HSP90AA4P

Appendix II – Submitted manuscript

Manuscript was submitted to Glycoconjugate journal (in press, 2016)

Mass spectrometric determination of advanced glycation in biology

Naila Rabbani,[1] Amal Ashour[2] and Paul J Thornalley[1,2]

[1]Warwick Systems Biology Centre, Senate House, University of Warwick, Coventry CV4 7AL, U.K. and [2]Clinical Sciences Research Laboratories, Warwick Medical School, University of Warwick, University Hospital, Coventry CV2 2DX, U.K.

Corresponding author: Dr Naila Rabbani Tel +44 2476968593 Email: N.Rabbani@warwick.ac.uk

Keywords: glycation; mass spectrometry; proteomics; glucose; methylglyoxal, fructosamine; hydroimidazolone; bioinformatics; Orbitrap.

Word count: 3447.

Appendix III – Conference abstract

1. Glyoxalase centennial conference (Coventry 2013 - Poster)

Dicarbonyl Stress and the Glyoxalase System in Periodontal Ligament Fibroblasts *in vitro*

Amal Ashour, Paul J Thornalley and Naila Rabbani

Periodontal ligament (PDL) inflammation or periodontitis is a common disease characterized by gradual destruction of connective tissue fibres that attach a tooth to the alveolar bone within which it sits. Diabetes and inflammation enhances periodontal bone loss through enhanced resorption and diminished bone formation. PDL fibroblast attachment and function to type 1 collagen is impaired by methylglyoxal (MG) modification *in vitro.* We hypothesise that increased PDL detachment and dysfunction by MG may occur in biochemical dysfunction in hyperglycaemia and by increased exposure to exogenous MG by ingestion of high MG content food and beverages. The aim of this study was to evaluate the effects of low and high glucose concentrations and exogenous MG on the glyoxalase system in human periodontal ligament fibroblasts (hPDLFs) *in vitro*.

Primary hPDLFs were purchased from ScienCell (Carlsbad, USA) and cultured for three days with high glucose (25 mM) and low (8 mM) glucose to mimic hyperglycaemic conditions. There was a 37% decrease of glyoxalase 1 activity ($p<0.01$) in hPDLFs incubated in high glucose compared to control. The flux of MG formation, as judged by increase in D-lactate, was increased 42% ($P<0.012$). We conclude that the exposure of PDL cells to high glucose down regulate Glo1 which may increase MG glycation to collagen and playing a role in PDL dysfunction.

2. 7th Saudi Student Conference UK (Edinburgh 2014 - Poster)

Dicarbonyl Stress and the Glyoxalase System in Periodontal Ligament Fibroblasts *in vitro*

Amal Ashour, Paul J Thornalley and Naila Rabbani

Periodontal ligament (PDL) inflammation or periodontitis is a common disease characterized by gradual destruction of connective tissue fibres that attach a tooth to the alveolar bone. Diabetes and inflammation enhances periodontal bone loss through enhanced resorption and diminished bone formation. PDL fibroblast attachment and function to type 1 collagen is impaired by methylglyoxal (MG) modification *in vitro.* Glyoxalase 1 (Glo1) is the main enzyme catalysing the metabolism of MG in PDL fibroblasts. it is hypothesised that increased PDL detachment and dysfunction by MG may occur in biochemical dysfunction in hyperglycaemia and by increased exposure to exogenous MG by ingestion of high MG content food and beverages.

The aim of this study was to evaluate the effects of low and high glucose concentrations and exogenous MG on the glyoxalase system in human periodontal ligament fibroblasts (hPDLFs) *in vitro*.

Primary hPDLFs were cultured for three days with high glucose (25 mM) and low (8 mM) glucose to mimic hyperglycaemic conditions. Glo1 activity was determined by measuring the initial rate of formation of S-D-lactoyl-glutathione from the hemithioacetal substrate formed non-enzymatically from methylglyoxal and reduced glutathione (GSH).The reaction is followed spectrophotometrically at 240 nm; $\Delta\varepsilon_{240}$ = 2.86 mM^{-1} cm^{-1}. D-glucose consumption and D-lactate formation were determined using end-point enzymatic assay spectrophotometrically at 340 nm and ($\lambda_{excitation}$ 340 and $\lambda_{emission}$ 460 nm) respectively. Dicarbonyl content and protein damage markers of medium and cell protein were determined by stable isotopic dilution analysis using LC-MS/MS.

There was a 49% decrease of glyoxalase 1 activity ($p<0.0001$) in hPDLFs incubated in high glucose compared to control. The flux of MG formation, as judged by increase in D-lactate, was increased 42% ($P<0.01$).

To conclude, the exposure of PDL cells to high glucose down regulate Glo1 which may increase MG glycation to collagen and playing a role in PDL dysfunction.

3. European Association for the Study of Diabetes. (Vienna 2014 - Poster)

Resveratrol corrects dicarbonyl stress in periodontal ligament fibroblasts in model hyperglycaemia *in vitro*.

Amal Ashour, Paul J Thornalley and Naila Rabbani

Background and aim
Diabetes and inflammation enhances periodontal bone loss through enhanced resorption and diminished bone formation. It has been shown that human PDL fibroblast (hPDLF) attachment and function to type 1 collagen was impaired by methylglyoxal (MG) modification *in vitro.* We found that increased hPDLFsdetachment and dysfunction was partly mediated by increased exposure to high glucose concentration with increased formation of MG, decreased metabolism of MG by glyoxalase 1 (Glo1) and increased formation of MG-derived advanced glycation endproducts (AGEs). The aim of this study was to evaluate the effect of resveratrol (RES) on MG metabolism in hPDLFs *in vitro* in high and low glucose concentration.
Materials and methods
hPDLFs were cultured for three days in medium containing low glucose concentration (LG, 8 mM) and also high glucose concentration (HG, 25 mM) to model hyperglycaemic conditions. The effect of addition of Res (10 μM) was studied. The activity of Glo1, D-glucose consumption and D-lactate formation were measured. The concentrations of MG and MG-derived AGE, MG-H1, were quantified by stable isotopic dilution analysis using LC-MS/MS.
Results
There was a significant decrease in Glo1 activity in HG (527 ± 97 versus 930 ± 85 mU/mg protein, $p<0.001$). In HG there was an increase in D-lactate flux (4.71 ± 0.47 versus 3.88 ± 0.47 nmol per million cells per day, $p<0.012$) and an increase in cellular concentration of MG (10.7 ± 1.5 versus 7.6 ± 0.5 pmol per million cells, $p<0.002$). The concentration of MG was increased in HG culture medium (448 ± 37 nM versus 276 ± 82 nM; $p<0.01$). Decreased Glo1 activity in HG was corrected by RES treatment (964 ± 87 mU/mg protein, $p<0.001$ with respect to HG control). RES also decreased MG content of cells (6.74 ± 1.26 pmol per million cells; $P< 0.023$) and medium (351 ± 36 nM; $P<0.018$) with respect to corresponding HG control.
Conclusion
We conclude that hPDLFs suffer dicarbonyl stress and MG accumulation in high glucose concentration *in vitro* that may be corrected by treatment with RES.

4. 8th Saudi Student Conference UK (London 2015 - Poster)

Dicarbonyls stress in periodontal ligament fibroblasts is corrected by Resveratrol in model hyperglycaemia *in vitro*.

Amal Ashour[1], Paul J Thornalley and Naila Rabbani

Background and aim
Diabetes and inflammation enhances periodontal bone loss through enhanced resorption and diminished bone formation. It has been shown that human PDL fibroblast (hPDLF) attachment and function to type1 collagen was impaired by methylglyoxal (MG) modification *in vitro.* We found that increased hPDLFsdetachment and dysfunction was partly mediated by increased exposure to high glucose concentration with increased formation of MG, decreased metabolism of MG by glyoxalase1(Glo1) and increased formation of advanced glycation endproducts(AGEs). The aim of this study was to evaluate the effect of resveratrol (RES) on MG metabolism in hPDLFs *in vitro* in high and low glucose concentration.
Materials and methods
hPDLFs were cultured for three days in medium containing low glucose concentration(LG, 8mM) and also high glucose concentration (HG, 25 mM) to model hyperglycaemic conditions. The effect of addition of RES (10 μM) was studied. The activity of Glo1, D-glucose consumption and D-lactate formation were measured. The concentrations of MG and MG-derived AGE, MG-H1, were quantified by stable isotopic dilution analysis LC-MS/MS.
Results
There was a significant decrease in Glo1 activity in HG (527±97 versus 930 ± 85 mU/mg protein, $P<0.001$). In HG there was an increase in D-lactate flux (4.71±0.47 versus 3.88 ± 0.47 nmol/million cells/day, $P<0.012$) and an increase in cellular concentration of MG (10.7±1.5 versus 7.6 ± 0.5 pmol/million cells, $P<0.002$). The concentration of MG was increased in HG culture medium (448±37 versus 276 ± 82 nM; $P<0.01$). Decreased Glo1 activity in HG was corrected by RES treatment (964 ± 87 mU/mg protein, $P<0.001$ with respect to HG control). RES decreased MG content of cells (6.74 ± 1.26 pmol /million cells; $P<0.023$) and medium (351 ± 36 nM; $P<0.018$) with respect to corresponding HG control.
Conclusion
We conclude that hPDLFs suffer dicarbonyl stress and MG accumulation in high glucose concentration *in vitro* that may be corrected by RES treatment.

5. EuroPerio 8 conference (London 2015 - Poster)

Resveratrol corrects dicarbonyl stress in periodontal ligament fibroblasts in model hyperglycaemia *in vitro*.

Amal Ashour, Paul J Thornalley and Naila Rabbani

Aim: The aim of this study was to evaluate the effect of resveratrol (RES) on glyoxalase1 (Glo1) activity and methylglyoxal (MG) metabolism in human PDL fibroblast (hPDLFs) in vitro in high and low glucose concentration.
Material and Methods: hPDLFs were cultured for three days in medium containing low glucose concentration (LG, 8mM) and also high glucose concentration (HG, 25mM) to model hyperglycaemic conditions. The effect of addition of Res (10μM) was studied. The activity of Glo1, D-glucose consumption and D-lactate formation were measured. The concentrations of MG and MG-derived AGE, MG-H1, were quantified by stable isotopic dilution analysis using LC-MS/MS.
Results: There was a significant decrease in Glo1 activity in HG (529 ± 106 versus 930 ± 84 mU/mg protein, $p<0.001$). In HG there was an increase in D-lactate flux (4.95 ± 0.42 versus 3.48 ± 0.52 nmol per million cells per day, $p<0.003$) and an increase in cellular concentration of MG (8.66 ± 1.51 versus 3.98 ± 1.00 pmol per million cells, $p<0.003$). The concentration of MG was increased in HG culture medium (449 ± 38 nM versus 276 ± 82 nM; $p<0.05$). Decreased Glo1 activity in HG was corrected by RES treatment (996 ± 55 mU/mg protein, $p<0.0007$ with respect to HG control). RES also decreased MG content of cells (6.74 ± 2.34 pmol per million cells; $P<0.024$) and medium (351 ± 36 nM; $P<0.018$) with respect to corresponding HG control.
Conclusion: hPDLFs suffer dicarbonyl stress and MG accumulation in high glucose concentration in vitro that may be corrected by RES treatment.

6. Warwick Medical School Student Symposium (Coventry 2015 - Talk)

Resveratrol corrects dicarbonyl stress in periodontal ligament fibroblasts in model hyperglycaemia *in vitro*.

Amal Ashour, Paul J Thornalley and Naila Rabbani

Background and aim

Periodontal ligament inflammation (periodontitis) is a common disease characterized by gradual destruction of connective tissue fibres that attach a tooth to the alveolar bone within which it sits. Diabetes and inflammation enhances periodontal bone loss through enhanced resorption and diminished bone formation. It has been shown that PDL fibroblast attachment and function to type 1 collagen was impaired by methylglyoxal (MG) modification *in vitro*. We hypothesise that increased PDL detachment and dysfunction by MG may be mediated by increased exposure to not only endogenous MG but also by exogenous MG by ingestion of high MG content food and beverages. The aim of this study was to evaluate the effects of high and low glucose concentrations on MG metabolism in human periodontal ligament fibroblasts (hPDLFs) with and without resveratrol (RSV) treatment

Materials and methods

Primary hPDLFs were cultured for three days in medium containing low glucose concentration (LG, 8 mM) and also high glucose concentration (HG, 25 mM) to model hyperglycaemic conditions. The effect of addition of RSV (10 µM) was studied. The activity of Glo1, D-glucose consumption and D-lactate formation were measured. The concentrations of MG and MG-derived AGE, MG-H1, were quantified by stable isotopic dilution analysis using LC-MS/MS. The efficiency of hPDLFsadhesion to collagen type 1 was tested by colorimetric cell adhesion assay.

Results

There was a significant decrease in Glo1 activity and increase in D-lactate flux and cellular concentration of MG and MG-H1 in HG compare to LG and this was corrected with RSV treatment. The table below summarises the results of the study.

Assay	Low glucose (control)	High glucose (control)	High glucose +RSV (10µM)
Glo1 activity mU/mg protein	928 ± 84	529 ± 109**	964 ± 87^{ooo}
D-Lactate nmol per million cells per day	7.00 ± 0.36	9.90 ± 1.08**	9.78± 078 ***
MG pmol per million cells	3.98 ± 1.00	10.6 ± 1.07	6.98 ± 0.89^{oo}
MG-H1(mmol/mol Arg)	0.431 ± 0.061	0.806 ± 0.184 *	0.560 ± 0.088^{oo}

Data are mean ± SD, n = 4. Significance: **, P<0.01 and ***, P<0.001 with respect to low glucose (control) (8mM) (*t*-test). Significance: ^{oo}, P<0.01 and ^{ooo}, P<0.001 with respect to high glucose (control) (25mM) (*t*-test).

The efficiency of hPDLFsadhesion to collagen type 1 was decreased by 37% in HG. This was also corrected by RSV.

Conclusion

We conclude that hPDLFs suffer dicarbonyl stress increasing MG levels in model hyperglycaemia *in vitro* that was corrected by RSV treatment. Functional impairment of hPDLFswas also reversed by RSV.

7. 12th International Symposium on the Maillard Reaction (Tokyo 2015 – Poster)

DICARBONYL STRESS IMPAIRS FUNCTION OF PERIODONTAL LIGAMENT FIBROBLASTS IN MODEL HYPERGLYCAEMIA

Amal Ashour, Paul J Thornalley and Naila Rabbani

Background and aim

Periodontal ligament inflammation (periodontitis) is a common disease characterized by gradual destruction of connective tissue fibres that attach a tooth to the alveolar bone within which it sits. Diabetes and inflammation enhances periodontal bone loss through enhanced resorption and diminished bone formation. PDL fibroblast attachment to type 1 collagen and function was impaired by methylglyoxal (MG) modification *in vitro.* We hypothesise that increased PDL detachment and dysfunction may be exacerbated by increased endogenous MG in hyperglycemia associated with diabetes. The aim of this study was to evaluate the effects of high and low glucose concentrations on MG metabolism in human periodontal ligament fibroblasts (hPDLFs) with and without resveratrol (RSV) treatment

Materials and methods

Primary hPDLFs were cultured for three days in medium containing low glucose (LG, 8 mM) and high glucose concentration (HG, 25 mM) to model hyperglycaemic conditions with and without RSV (10 μM). The activity of Glo1, D-glucose consumption and D-lactate formation were measured. The concentrations of MG and MG-derived AGE, MG-H1, were quantified by stable isotopic dilution analysis using LC-MS/MS. The efficiency of hPDLFsadhesion to collagen type 1 was tested by colorimetric cell adhesion assay.

Results

In hPDLFs incubated with HG there was a significant decrease in Glo1 activity, increase in D-lactate flux, increase in cellular concentration of MG and increase in MG-H1 residue content of cell protein, compared to LG control. Decrease of Glo1 activity and increase in MG and MG-G1 residue content of cell protein was corrected with RSV treatment. The results are summarised in the table below.

Analyte	Low glucose (8 mM)	High glucose (25 mM)	High glucose +RSV (10μM)
Glo1 activity (mU/mg protein)	928 ± 84	529 ± 109**	964 ± 87^{ooo}
D-Lactate (nmol per million cells / day)	7.00 ± 0.36	9.90 ± 1.08**	9.78 ± 0.78 ***
MG (pmol / million cells)	3.98 ± 1.00	10.6 ± 1.07	6.98 ± 0.89^{oo}
MG-H1 (mmol/mol arg)	0.431 ± 0.061	0.806 ± 0.184 *	0.560 ± 0.088^{oo}

Data are mean ± SD, n = 4. Significance: *, ** and ***, P<0.05, P<0.01 and P<0.001, respectively, compared to LG; ^{oo} and ^{ooo}, P<0.01 and P<0.001 compared to HG.

The efficiency of hPDLFsadhesion to collagen type 1 was decreased by 37% in HG and was corrected by RSV.

Conclusion

We conclude that hPDLFs suffer dicarbonyl stress and functional impairment in model hyperglycaemia *in vitro* which is corrected by RSV treatment.

8. 1st Reunion Meeting of BIOCLAIMS and 5th International Symposium of the Human Nutrition & Metabolism Research and Training Centre (Graz 2015, Talk)

Resveratrol corrects dicarbonyl stress in periodontal ligament fibroblasts in model hyperglycaemia *in vitro*.

Amal Ashour, Paul J Thornalley and Naila Rabbani

Background and aim

Periodontal ligament inflammation (periodontitis) is a common disease characterized by gradual destruction of connective tissue fibres that attach a tooth to the alveolar bone within which it sits. Diabetes and inflammation enhances periodontal bone loss through enhanced resorption and diminished bone formation. PDL fibroblast attachment to type 1 collagen and function was impaired by methylglyoxal (MG) modification *in vitro*. We hypothesise that increased PDL detachment and dysfunction may be exacerbated by increased endogenous MG in hyperglycemia associated with diabetes. The aim of this study was to evaluate the effects of high and low glucose concentrations on MG metabolism in human periodontal ligament fibroblasts (hPDLFs) with and without resveratrol (RSV) treatment

Materials and methods

Primary hPDLFs were cultured for three days in medium containing low glucose (LG, 8 mM) and high glucose concentration (HG, 25 mM) to model hyperglycaemic conditions with and without RSV (10 μM). The activity of Glo1, D-glucose consumption and D-lactate formation were measured. The concentrations of MG and MG-derived AGE, MG-H1, were quantified by stable isotopic dilution analysis using LC-MS/MS. The efficiency of hPDLFsadhesion to collagen type 1 was tested by colorimetric cell adhesion assay.

Results

In hPDLFs incubated with HG there was a significant decrease in Glo1 activity, increase in D-lactate flux, increase in cellular concentration of MG and increase in MG-H1 residue content of cell protein, compared to LG control. Decrease of Glo1 activity and increase in MG and MG-G1 residue content of cell protein was corrected with RSV treatment. The results are summarised in the table below.

Analyte	Low glucose (8 mM)	High glucose (25 mM)	High glucose +RSV (10μM)
Glo1 activity (mU/mg protein)	928 ± 84	529 ± 109**	964 ± 87^{ooo}
D-Lactate (nmol per million cells / day)	7.00 ± 0.36	9.90 ± 1.08**	9.78 ± 0.78 ***
MG (pmol / million cells)	3.98 ± 1.00	10.6 ± 1.07	6.98 ± 0.89^{oo}
MG-H1 (mmol/mol arg)	0.431 ± 0.061	0.806 ± 0.184 *	0.560 ± 0.088^{oo}

Data are mean ± SD, n = 4. Significance: *, ** and ***, P<0.05, P<0.01 and P<0.001, respectively, compared to LG; ^{oo} and ^{ooo}, P<0.01 and P<0.001 compared to HG.

The efficiency of hPDLFsadhesion to collagen type 1 was decreased by 37% in HG and was corrected by RSV.

Conclusion

We conclude that hPDLFs suffer dicarbonyl stress and functional impairment in model hyperglycaemia *in vitro* which is corrected by RSV treatment.

9. 9th Saudi Student Conference UK (Birmingham 2016 - Poster)

The effect of resveratrol on dicarbonyl stress in periodontal ligament fibroblasts in model hyperglycaemia. An *in vitro* study

Amal Ashour[1], Paul J Thornalley[1] and Naila Rabbani[1]

Background and aim

Periodontal ligament inflammation (periodontitis) is a common disease characterized by gradual destruction of connective tissue fibres that attach a tooth to the alveolar bone within which it sits. Diabetes and inflammation enhances periodontal bone loss through enhanced resorption and diminished bone formation. PDL fibroblast attachment to type 1 collagen and function was impaired by methylglyoxal (MG) modification *in vitro.* We hypothesise that increased PDL detachment and dysfunction may be exacerbated by increased endogenous MG in hyperglycemia associated with diabetes. The aim of this study was to evaluate the effects of high and low glucose concentrations on MG metabolism in human periodontal ligament fibroblasts (hPDLFs) function with and without resveratrol (RSV) treatment

Materials and methods

Primary hPDLFs were cultured for three days in medium containing low glucose (LG, 8 mM) and high glucose concentration (HG, 25 mM) to model hyperglycaemic conditions with and without RSV (10 µM). The activity of Glo1, D-glucose consumption and D-lactate formation were measured. The concentrations of MG and MG-derived AGE, MG-H1, were quantified by stable isotopic dilution analysis using LC-MS/MS. The efficiency of hPDLFsadhesion to collagen type 1 was tested by colorimetric cell adhesion assay.

Results

In hPDLFs incubated with HG there was a significant decrease in Glo1 activity, increase in D-lactate flux, increase in cellular concentration of MG and increase in MG-H1 residue content of cell protein, compared to LG control. Decrease of Glo1 activity and increase in MG and MG-G1 residue content of cell protein was corrected with RSV treatment. The results are summarised in the table below.

Analyte	Low glucose (8 mM)	High glucose (25 mM)	High glucose +RSV (10µM)
Glo1 activity (mU/mg protein)	928 ± 84	529 ± 109**	964 ± 87^{ooo}
D-Lactate (nmol per million cells / day)	7.00 ± 0.36	9.90 ± 1.08**	9.78 ± 0.78 ***
MG (pmol / million cells)	3.98 ± 1.00	10.6 ± 1.07	6.98 ± 0.89^{oo}
MG-H1 (mmol/mol arg)	0.431 ± 0.061	0.806 ± 0.184 *	0.560 ± 0.088^{oo}

Data are mean ± SD, n = 4. Significance: *, ** and ***, P<0.05, P<0.01 and P<0.001, respectively, compared to LG; ^{oo} and ^{ooo}, P<0.01 and P<0.001 compared to HG.

The efficiency of hPDLFsadhesion to collagen type 1 was decreased by 37% in HG and was corrected by RSV.

Conclusion

We conclude that hPDLFs suffer dicarbonyl stress and functional impairment in model hyperglycaemia *in vitro* which is corrected by RSV treatment.

10. Midlands Academy of Medical Sciences Festival (Birmingham 2016 – Talk)

Resveratrol corrects dicarbonyl stress in periodontal ligament fibroblasts in model hyperglycaemia *in vitro*.

AA Ashour, PJ Thornalley and N Rabbani

Periodontal ligament inflammation (periodontitis) is a common disease characterized by gradual destruction of connective fibres that attach a tooth to the alveolar bone. Diabetes and inflammation enhances periodontal bone loss through enhanced resorption and diminished bone formation. Periodontal ligament (PDL) fibroblast attachment to type1 collagen and function were impaired by methylglyoxal (MG) modification *in vitro*[1]. We hypothesise that increased PDL detachment and dysfunction may be exacerbated by increased endogenous MG in hyperglycaemia associated with diabetes. The aim of this study was to evaluate the effects of high and low glucose concentrations on MG metabolism in human PDL fibroblasts (hPDLFs) with and without resveratrol (RSV) treatment.

Primary hPDLFs were cultured for three days in medium containing low glucose (LG,8mM) and high glucose concentration (HG, 25mM) to model hyperglycaemic conditions with and without RSV (10 μM). The activity of Glo1, D-glucose consumption and D-lactate formation were measured. The concentrations of MG and MG-derived AGE, MG-H1, were quantified by stable isotopic dilution analysis using LC-MS/MS. The efficiency of hPDLFsadhesion to collagen type 1 was tested by colorimetric cell adhesion assay.

In hPDLFs incubated with HG there was a significant decrease in Glo1 activity, increase in D-lactate flux, increase in cellular concentration of MG and increase in MG-H1 residue content of cell protein, compared to LG control. Decrease of Glo1 activity and increase in MG and MG-H1 residue content of cell protein was corrected with RSV treatment. The results are summarised in the table below.

Analyte	LG	HG	HG+RSV
Glo1 activity (mU/mg protein)	928±84	529±109**	964±87^{ooo}
D-Lactate (nmol per million cells/day)	7.00±0.36	9.90±1.08**	9.78±0.78***
MG (pmol/million cells)	3.98±1.00	10.6±1.07	6.98±0.89^{oo}
MG-H1 (mmol/mol arg)	0.431±0.061	0.806±0.184*****	0.560±0.088^{oo}

Data are mean±SD, n=4. Significance: *,**and***, P<0.05, P<0.01 and P<0.001, respectively, compared to LG; ^{oo}and^{ooo}, P<0.01 and P<0.001 compared to HG.

The efficiency of hPDLFsadhesion to collagen type1 was decreased by 37% in HG and was corrected by RSV.
We conclude that hPDLFs suffer dicarbonyl stress and functional impairment in model hyperglycaemia *in vitro* which is corrected by RSV treatment.

Reference:

1. Murillo, J., et al., Advanced Glycation of Type I Collagen and Fibronectin Modifies Periodontal Cell Behavior. Journal of Periodontology, 2008. 79(11): p. 2190-2199.